VOLUME II

TABLE OF CONTENTS

II.1 CHARACTERIZATION OF WASTEWATER DISCHARGES FROM THE FOOD PROCESSING INDUSTRY IN THE SAN JOAQUIN VALLEY 27

A. Data Acquisition 27

B. Publicly Owned Treatment Works (POTWs) 42

C. Salinity Loads in the Central Valley 45

1. Nitrate and Ammonium Loads 62
2. Specific Industry Analyses – Tomato, Wine and Meat Industries 67
3. Screening analysis of the wastewater's chemical composition 69
4. Criteria Selection 69
5. Results 71

D. Other Industries in the Central Valley 76

a) The Dairy Industry in the Central Valley 76

II.2 SEP STUDY MANAGEMENT OF SALINITY IN WASTEWATER FROM THE CALIFORNIA FOOD PROCESSING INDUSTRY – UNSATURATED ZONE MODELING 79

A. Introduction 79

1. Problem Definition 79
2. Conceptual Model 81

B. Case-based Modeling Approach 85

1. Case 1: Limited NH3 and FDS attenuation, high FDS loading 86
2. Case 2: Limited NO3 and FDS attenuation, high FDS loading 87
3. Case 3: Significant N attenuation (NH3 and NO3), moderate to high FDS loading 87
4. Summary of scenarios 87
5. Support for case-based approach in groundwater data 88

C. Numerical Modeling – Input Parameters 92

1. Numerical Modeling Code – MIN3P 93
2. Model Setting 95
3. Spatial and Temporal Discretization 96
4. Flow boundary conditions and water balance 96
5. Background Chemical Composition 99
6. Transport Boundary Conditions 101
7. Transport parameters 102
8. Root Solute Uptake 103
9. Biogeochemical Reaction Network and Reaction Parameters 108
   a) Biogeochemical Reactions 108
   b) Mineral dissolution-precipitation reactions 111
   c) Ion Exchange Reactions 112

D. Numerical Modeling – Case-specific Input Parameters 112
1. Case-Specific Soil Properties 112
2. Waste Water Application Rates 113

E. Industry Specific Modeling Inputs 115
1. Case- and Industry-Specific Parameters 116
   a) Tomato Processing Facilities 116
   b) Wineries and Grape Processing Facilities 121
   c) Milk Processing Facilities 127
   d) Meat Packing Plants 132
   e) Modesto POTW 138

II.3 MODEL APPLICATION AND RESULTS 143

A. Baseline Scenario Results 143
1. Overview of Baseline Results – All Industries 143
2. Detailed Discussion of Baseline Simulation Results 148
   a) Wineries Case 1 – Limited NH3 and Salinity Attenuation 148
   b) Wineries Case 2 – Limited Nitrate and Salinity Attenuation 153
   c) Wineries Case 3 – Significant Nitrogen Attenuation, Limited Salinity Attenuation 157
3. Effectiveness of the Attenuation Processes 161
   a) Wine and Grape Processors 161
   b) All Industries 162

B. Comparison of Baseline Results and Available Groundwater Data 163

C. Modesto POTW Scenario 165

D. Model Sensitivity Analysis 168
1. Water Table Fluctuations 169
2. Salinity Buildup in the Root Zone 175
   a) Leaching Fraction 175
   b) Soil Salinity and Crop Yield 178
   c) SAR and Hydraulic Conductivity 183
3. Salinity Toxicity to Crops and Microbes 185
4. Summary of Model Sensitivity Analysis 190

E. Discharge Management Scenarios 191
1. Waste Application Management 191
   a) BOD Loading Rate 191
   b) NaCl Loading Rate 194
   c) Increased Application Area 196
   d) Summary of Loading Rate Experiments 197
2. Waste Stream Management 198
   a) BOD Concentration 198
   b) FDS Concentration 202
   c) In-Plant Chemical Substitution 204
   d) Summary of Waste Stream Management Scenarios 206
3. Site Selection 206
   a) Depth to Water Table 207
   b) Soil Calcite Concentration 212

c) Soil Gypsum Concentration....215
d) Soil Cation Exchange Capacity....217
e) Site Precipitation....221
f) Site Evapotranspiration....221
4. Summary of Management and Site Scenario Results....222

F. Demonstration Case (Improved Management Scenario)....223

G. Summary....227

II.4 SATURATED ZONE ANALYSIS....236

A. Introduction....236
1. Food Processors in the Area....239

B. Hydrogeologic Setting....239
1. Regional Hydrology....242

C. Water Recharge and Pumping....245

D. Numerical Modeling of the Study Area....247
1. Spatial Discretization....248
2. Boundary Conditions....250
a) Pumping Wells....251
b) Evapotranspiration....253
c) Ground-Water / Surface Water Interactions....253
3. Hydrogeologic Parameters....253
4. The Effects of Spatial Variability....256

E. Results of Flow Model....266

F. Salinity Transport Modeling....270
1. Numerical Model....270
2. Solute Transport Parameters....270
3. Initial and Recharge Concentrations....271
4. Food Processor Land Discharge Concentrations....273

G. Sensitivity Analysis....277

H. Monte Carlo Simulations....281
1. Monte Carlo simulation Results....283
2. An alternative Monte Carlo analysis....295

I. Summary....302

II.5 ENVIRONMENTALLY IMPACTED SITES ANALYSIS....306

A. Introduction....306

B. Sensitive Sites....306

C. Potential Impacts.....307
1. Endangered Species Critical Habitats 315

II.6 APPENDICES..... 319

A. Appendix A: List of Dischargers Included in the Screening Analysis (Names and WDID) 319

B. Appendix B: Environmentally Sensitive Areas 320
1. List of Codes for Potential Impacts 320
2. List of Environmental Sensitive Areas near Food Processing Facilities 321
3. Potentially Environmentally Sensitive Areas Near POTWs.....357

C. Appendix C: SEP Study Management of Salinity in Wastewater from the California Food Processing Industry – Unsaturated Zone Modeling 371
1. Tomato Canning Baseline Simulations 371
2. Wineries and Grape Processing Baseline Simulations 380
3. Daily Processing Baseline Simulations 389
4. Meat Packing Baseline Simulations 398
5. POTW Baseline Simulation 407

Tables

TABLE 1: CENTRAL VALLEY FOOD PROCESSORS 28
TABLE 2: COUNTS OF FOOD PROCESSING FACILITIES AND POTWS SURVEYED BY INDUSTRY AND COUNTY. TEMPLATES WERE NOT CREATED FOR 24 POTWS, SEE TABLE 3 38
TABLE 3: CENTRAL VALLEY POTWS 42
TABLE 4: FIXED DISSOLVED SOLIDS (FDS) LOADS IN METRIC TONS, SOME FDS DATA FROM EC CORRELATION, GAP FILLING AS DESCRIBED IN TEXT WAS USED FOR TOTAL LOAD COLUMNS. SEE FIGURE 2 FOR MAP OF AREAS IN TABLE. 61 PERCENT OF PROCESSORS REPORTED EC OR FDS MEASUREMENTS 46
TABLE 5: FIXED DISSOLVED SOLIDS (FDS) LOADS IN METRIC TONS, 61% OF PROCESSORS REPORTING EC OF FDS VALUES 47
TABLE 6 60
TABLE 7: AMMONIUM (NH4) LOADS IN METRIC TONS, GAP FILLING AS DESCRIBED IN TEXT WAS USED FOR TOTAL LOAD COLUMNS. SEE FIGURE 2 FOR MAP OF AREAS IN TABLE. 21% OF PROCESSORS REPORTED NH4 63
TABLE 8: AMMONIUM (NH4) LOADS IN METRIC TONS, 21% OF PROCESSORS REPORTED NH4 64
TABLE 9: NITRATE (NO3) LOADS IN METRIC TONS, GAP FILLING AS DESCRIBED IN TEXT WAS USED FOR TOTAL LOAD COLUMNS. SEE FIGURE 2 FOR MAP OF AREAS IN TABLE. 55% OF PROCESSORS REPORTED NO3 65
TABLE 10: NITRATE (NO3) LOADS IN METRIC TONS, 55% OF PROCESSORS REPORTED NO3 66
TABLE 11: OVERVIEW OF CASES 88
TABLE 12: DECEMBER 2005 GROUNDWATER DATA FROM FOOD PROCESSING LAND APPLICATION SITE 89
TABLE 13: CRITERIA FOR CLASSIFYING GROUNDWATER DATA INTO THE THREE CASES 90
TABLE 14: WATER BALANCE AT THE DISCHARGE SITE 98
TABLE 15: BACKGROUND CHEMICAL COMPOSITION 100
TABLE 16: RAINWATER CHEMICAL COMPOSITION 101
TABLE 17: ACTIVE ROOT UPTAKE PARAMETERS 104
TABLE 18: SUMMARY OF UPTAKE FACTORS 108
TABLE 19: RATE PARAMETERS FOR BIOGEOCHEMICAL REACTIONS INVOLVING NITROGEN COMPOUNDS 110
TABLE 20: RATE PARAMETERS FOR ADDITIONAL BIOGEOCHEMICAL REACTIONS 111
TABLE 21: MODESTO SOIL HYDRAULIC CONDUCTIVITY PARAMETERS 113
TABLE 22: INDUSTRY-SPECIFIC LAND APPLICATION RATES FOR TOMATO PROCESSORS 117
TABLE 23: CONCENTRATIONS OF MAIN COMPONENTS OF CONCERN IN TOMATO WASTEWATER 118
TABLE 24: INDUSTRY-SPECIFIC FDS COMPONENT FACTORS FOR TOMATO PROCESSORS 119
TABLE 25: INDUSTRY-SPECIFIC EFFLUENT CHEMICAL COMPOSITION FOR TOMATO PROCESSORS 120
TABLE 26: MIXING RATIOS FOR TOMATO PROCESSOR SCENARIOS 121
TABLE 27: INDUSTRY-SPECIFIC LAND APPLICATION RATES FOR WINERIES AND GRAPE PROCESSORS 122
TABLE 28: MIXING RATIOS FOR WINERY SCENARIOS 123
TABLE 29: CONCENTRATIONS OF MAIN COMPONENTS OF CONCERN IN WINERY AND GRAPE PROCESSING WASTEWATER 124
TABLE 30: INDUSTRY-SPECIFIC FDS COMPONENT FACTORS FOR WINERIES AND GRAPE PROCESSORS 125
TABLE 31: EFFLUENT CHEMICAL COMPOSITION FOR WINERY CASES 126
TABLE 32: CONCENTRATIONS OF MAIN COMPONENTS OF CONCERN IN MILK PROCESSING DISCHARGE 128
TABLE 33: EFFLUENT CHEMICAL COMPOSITION FOR MILK PROCESSOR CASES 130

TABLE 34: INDUSTRY-SPECIFIC LAND APPLICATION RATES FOR MILK PROCESSORS 131
TABLE 35: MIXING RATIOS FOR DAIRY SCENARIOS.....132
TABLE 36: INDUSTRY-SPECIFIC LAND APPLICATION RATES FOR MEAT PACKERS 133
TABLE 37: CONCENTRATIONS OF MAIN COMPONENTS OF CONCERN IN MEAT PACKING WASTEWATER.....134
TABLE 38: INDUSTRY-SPECIFIC FDS COMPONENT FACTORS FOR MEAT PACKERS 135
TABLE 39: EFFLUENT CHEMICAL COMPOSITION FOR MEAT PACKER CASES.....137
TABLE 40: MIXING RATIOS FOR MEAT PACKERS 138
TABLE 41: LAND APPLICATION RATES FOR MODESTO POTW 140
TABLE 42: MIXING RATIOS FOR MODESTO POTW.....141
TABLE 43: EFFLUENT CHEMICAL COMPOSITION FOR MODESTO POTW 142
TABLE 44: CASE 1 WASTEWATER APPLICATION RATE, WASTEWATER CONCENTRATIONS AND BREAKTHROUGH CONCENTRATIONS AT THE WATER TABLE.....146
TABLE 45: CASE 2 WASTEWATER APPLICATION RATE, WASTEWATER CONCENTRATIONS AND BREAKTHROUGH CONCENTRATIONS AT THE WATER TABLE.....147
TABLE 46: CASE 3 WASTEWATER APPLICATION RATE, WASTEWATER CONCENTRATIONS AND BREAKTHROUGH CONCENTRATIONS AT THE WATER TABLE.....148
TABLE 47: MASS BALANCE OF COMPONENTS - WINERY CASE 1 152
TABLE 48: MASS BALANCE OF COMPONENTS - WINERY CASE 2 156
TABLE 49: MASS BALANCE OF COMPONENTS - WINERY CASE 3 160
TABLE 50: MASS BALANCE FOR MODESTO POTW 167
TABLE 51: ECW AND SAR FOR WINERY SIMULATIONS.....185
TABLE 52: SUMMARY OF NUMERICAL EXPERIMENTS ON SITE AND MANAGEMENT OPTIONS.....223
TABLE 53: TABLE LISTING THE HARMONIC, K_H, GEOMETRIC, K_G, AND ARITHMETIC,K_A, MEANS OF THE FOUR LITHOLOGIC REGIONS SHOWN IN FIGURES 148 AND 149, AS WELL AS THE RATIO OF HORIZONTAL TO VERTICAL HYDRAULIC CONDUCTIVITIES (K_{HOR}/K_{VERT}).....256
TABLE 54: TABLE SHOWING STATISTICS OF THE CONCENTRATION DIFFERENCES FOR EACH THE THREE SCENARIOS OF DISPERSIVITY RATIOS.....279
TABLE 55: TABLE SHOWING THE PARAMETER VALUES USED IN THE MONTE CARLOS SIMULATIONS.....282
TABLE 56: THIS TABLE SHOWS SUMMARY STATISTICS FOR THE VALUES OF THE ENSEMBLE MIN, MEAN, MAX AND STANDARD DEVIATION OF THE CONCENTRATION GENERATED IN THE MONTE CARLO SIMULATIONS 283
TABLE 57: THIS TABLE SHOWS SUMMARY STATISTICS FOR THE VALUES OF THE ENSEMBLE MIN, MEAN, MAX AND STANDARD DEVIATION OF THE CONCENTRATION DIFFERENCES (ΔC) 297
TABLE 58: CENTRAL VALLEY FOOD PROCESSORS AND POTWS IN CLOSE PROXIMITY TO ENDANGERED SPECIES CRITICAL HABITATS. [1]LABELS SHOWN IN APPENDIX II.6.B AND ON FIGURES 187-192.....315
TABLE 59: NAICS INDUSTRY CLASSIFICATION MAP LABELS. NUMBERS CORRESPOND TO MAP LABELS IN FIGURES 187-192 ABOVE AND APPENDICES B.2 AND B.3 IN SECTION II.6.B. 318

Figures

FIGURE 1....36
FIGURE 2....37
FIGURE 3....39
FIGURE 4....40
FIGURE 5....41
FIGURE 6....44
FIGURE 7....49
FIGURE 8....49
FIGURE 9....50
FIGURE 10....50
FIGURE 11....51
FIGURE 12....51
FIGURE 13....52
FIGURE 14....52
FIGURE 15....53
FIGURE 16....53
FIGURE 17....54
FIGURE 18....55
FIGURE 19....56
FIGURE 20....57
FIGURE 21....58
FIGURE 22....61
FIGURE 23....62
FIGURE 24....67
FIGURE 25....68
FIGURE 26....68
FIGURE 27....69
FIGURE 28....70
FIGURE 29....72
FIGURE 30....73
FIGURE 31....74
FIGURE 32....77
FIGURE 33....78
FIGURE 34....82
FIGURE 35....91
FIGURE 36....91
FIGURE 37....92
FIGURE 38....95
FIGURE 39....96
FIGURE 40....105
FIGURE 41....106
FIGURE 42....107
FIGURE 43....121
FIGURE 44....127
FIGURE 45....129
FIGURE 46....136
FIGURE 47....139
FIGURE 48....145
FIGURE 49....146

FIGURE 50 147
FIGURE 51 150
FIGURE 52 151
FIGURE 53 154
FIGURE 54 155
FIGURE 55 158
FIGURE 56 159
FIGURE 57 162
FIGURE 58 162
FIGURE 59 164
FIGURE 60 165
FIGURE 61 166
FIGURE 62 168
FIGURE 63 170
FIGURE 64 170
FIGURE 65 171
FIGURE 66 172
FIGURE 67 172
FIGURE 68 173
FIGURE 69 174
FIGURE 70 174
FIGURE 71 175
FIGURE 72 176
FIGURE 73 177
FIGURE 74 177
FIGURE 75 178
FIGURE 76 179
FIGURE 77 180
FIGURE 78 181
FIGURE 79 181
FIGURE 80 182
FIGURE 81 183
FIGURE 82 184
FIGURE 83 184
FIGURE 84 186
FIGURE 85 187
FIGURE 86 188
FIGURE 87 189
FIGURE 88 190
FIGURE 89 192
FIGURE 90 192
FIGURE 91 193
FIGURE 92 194
FIGURE 93 194
FIGURE 94 195
FIGURE 95 196
FIGURE 96 196
FIGURE 97 197
FIGURE 98 199
FIGURE 99 200
FIGURE 100 200

FIGURE 101....201
FIGURE 102....202
FIGURE 103....203
FIGURE 104....203
FIGURE 105....204
FIGURE 106....205
FIGURE 107....205
FIGURE 108....206
FIGURE 109....207
FIGURE 110....208
FIGURE 111....209
FIGURE 112....209
FIGURE 113....210
FIGURE 114....211
FIGURE 115....211
FIGURE 116....213
FIGURE 117....213
FIGURE 118....214
FIGURE 119....214
FIGURE 120....215
FIGURE 121....216
FIGURE 122....216
FIGURE 123....218
FIGURE 124....218
FIGURE 125....219
FIGURE 126....219
FIGURE 127....220
FIGURE 128....220
FIGURE 129....221
FIGURE 130....222
FIGURE 131....225
FIGURE 132....226
FIGURE 133....226
FIGURE 134....239
FIGURE 135....240
FIGURE 136....241
FIGURE 137....242
FIGURE 138....243
FIGURE 139....244
FIGURE 140....245
FIGURE 141....246
FIGURE 142....247
FIGURE 143....249
FIGURE 144....250
FIGURE 145....251
FIGURE 146....252
FIGURE 147....252
FIGURE 148....254
FIGURE 149....255
FIGURE 150....258
FIGURE 151....259

FIGURE 152....260
FIGURE 153....261
FIGURE 154....262
FIGURE 155....263
FIGURE 156....264
FIGURE 157....265
FIGURE 158....266
FIGURE 159....267
FIGURE 160....268
FIGURE 161....269
FIGURE 162....270
FIGURE 163....273
FIGURE 164....274
FIGURE 165....275
FIGURE 166....276
FIGURE 167....277
FIGURE 168....280
FIGURE 169....281
FIGURE 170....284
FIGURE 171....285
FIGURE 172....286
FIGURE 173....287
FIGURE 174....288
FIGURE 175....289
FIGURE 176....290
FIGURE 177....291
FIGURE 178....292
FIGURE 179....293
FIGURE 180....294
FIGURE 181....295
FIGURE 182....298
FIGURE 183....299
FIGURE 184....300
FIGURE 185....301
FIGURE 186....302
FIGURE 187....309
FIGURE 188....310
FIGURE 189....311
FIGURE 190....312
FIGURE 191....313
FIGURE 192....314

II.1 Characterization of Wastewater Discharges from the Food Processing Industry in the San Joaquin Valley

This section provides a review of food processor discharges (volumes, loads and concentrations) in the Central Valley. It provides information about the data acquisition campaign, the data acquired, and summary statistics by industry, by hydrologic region and by county and its variability over time. The focus of this section is on salinity and nitrogen (N) compounds, although numerous other chemicals of concern such as Fe, Mn, SO_4 and BOD, were also surveyed and recorded.

Loads of salinity and N compounds (nitrate and ammonium) are the focus of our study. A detailed discussion of the rationale for focusing on this mix from a modeling perspective is provided in subsequent sections. In addition, evaluation of the major contributors to groundwater quality degradation identifies FDS and N compounds as the most frequently recorded causes of degradation (e.g., Staff report presented on January 2005 to the Board of the Central Valley Water Quality Control Board).

Information is also provided here on publicly-owned treatment works (POTWs) having significant food-processing related operations. However, this information is not very well developed because in many cases it is difficult to separate food-processing related activity from other types of activity. We set as a limited goal for this study to identify those POTWs that have relevance to the food processing industry, and serve as a starting point for additional work. Sub-Section A discusses our data acquisition methods and provides general background information. Sub-Section B provides information on the POTWs covered in our study. Sub-Section C provides a detailed analysis of salinity and N compounds discharged by processors in various industries and geographies. Sub-Section D analyzes the food processing wastewater streams from a chemical perspective. Three high-impact industrial groups are analyzed in this section in order to identify characteristic discharges by these industries.

A. Data Acquisition

Our survey of the food-processing industry included detailed analyses of nearly 200 Central Valley facilities. We analyzed and recorded the Waste Discharge Requirements (WDR) and monthly discharges and concentrations reported in each facility's files. This data is stored in individual templates created for each processor. In developing our data acquisition campaign, we considered formats for data reporting and analysis that can be useful for future data acquisition and reporting.

Waste Discharge Requirements (WDRs) issued by the Central Valley Regional Water Quality Control Board to the food processing facilities and periodical monitoring reports for California Central Valley food processors were obtained from the Regional Water Quality Control Board offices in Fresno and Sacramento. The files were copied and subsequently scanned for use on the project. Monitoring reports were gathered for 2003, 2004 and 2005 for reporting processors, shown in Table 1. These reports were condensed to create templates recording all chemical constituents reported by the food processors, as shown for a winery in Figure 1. Templates made

for each processor contain all available effluent concentration data and volume data for 2003, 2004 and 2005.

Table 1: Central Valley Food Processors

	Agency/File Name	WDID[1]	County	Industry by NAICS (4)	NAICS Code
1	ALPINE PACKING COMPANY	5B392048001	San Joaquin	Animal slaughtering & processing	31161
2	AMERICAN YEAST CORPORATION	5D152011001 and 5D152011002	Kern	Fruit and Vegetable Canning, Pickling, and Drying	31142
3	AZTECA MILLING/VALLEY GRAIN	5C202008001	Madera	Fruit & vegetable canning	311421
4	BAKER COMMODITIES, INC	5D102015001	Fresno	Fat and Oils Refining and Blending	311225
5	BALLANTINE PRODUCE CO, INC	5D102100001	Fresno	Fruit and Vegetable Canning, Pickling, and Drying	31142
6	BARREL TEN QTR CIR LAND CO INC	5B392030001	San Joaquin	Wineries	31213
7	BEEF PACKERS INC	5D102040001	Fresno	Animal slaughtering & processing	31161
8	BELL-CARTER OLIVE COMPANY	5D102068001	Fresno	Fruit & vegetable canning	311421
9	BOGHOSIAN RAISIN PACKING CO	5D101115001	Fresno	Dried & dehydrated food mfg	311423
10	BOLTHOUSE, W M	5D152211001	Kern	Fruit and Vegetable Canning, Pickling, and Drying	31142
11	BOLTHOUSE, W M	5D151194001	Kern	Fruit and Vegetable Canning, Pickling, and Drying	31142
12	BOOTH RANCHES, LLC	5D542122001	Fresno	Fruit & vegetable canning	311421
13	BRONCO WINE COMPANY, INC.	5C502025001	Stanislaus	Wineries	31213
14	CACCIATORE FINE WINES & OLIVE	5D542127001	Tulare	Wineries	31213
15	CAG 45 INC	5C502036001	Stanislaus	Fruit and Vegetable Canning, Pickling, and Drying	31142
16	CALIF CONCENTRATE COMPANY	5B392035001	San Joaquin	Fruit and Vegetable Canning, Pickling, and Drying	31142

17	CALIFORNIA DAIRIES, INC, Canal	5D541067001	Tulare	Dairy Product Manufacturing	3115
18	CALIFORNIA DAIRIES, INC, Farm	5D541067001	Tulare	Dairy Product Manufacturing	3115
19	CALIFORNIA OLIVE GROWERS	5C202010001	Madera	Fruit & vegetable canning	311421
20	CALIFORNIA PISTACHIO ORCHARDS	5D162021001	Kings	Roasted Nuts and Peanut Butter Manufacturing	311911
21	CALIFORNIA DAIRIES, INC	5C245017001	Merced	Dairy Product Manufacturing	3115
22	CALIFORNIA NATURAL PRODUCTS	5B391079001	San Joaquin	Fruit & vegetable canning	311421
23	CANANDAIGUA WINE CO, INC	5C202012001	Madera	Wineries	31213
24	CANANDAIGUA WINE COMPANY, INC	5C202007001	Madera	Wineries	31213
25	CANANDAIGUA WINE COMPANY	5B392033001	San Joaquin	Wineries	31213
26	CERUTTI BROS, INC.	5C502043001	Stanislaus	Frozen Food Manufacturing	31141
27	CHEROKEE FREIGHT LINES	5B392105001	San Joaquin	Waste & Miscellaneous	N/A
28	CHINCHIOLO FRUIT COMPANY	5B392093001	San Joaquin	Fruit and Vegetable Canning, Pickling, and Drying	31142
29	CHOOLJIAN BROS PACKING CO	5D102012002	Fresno	Dried & dehydrated food mfg	311423
30	CHOWCHILLA PISTACHIO COMPANY	5C202026001	Madera	Roasted Nuts and Peanut Butter Manufacturing	311911
31	CLAUSEN MEAT PACKING CO, INC	5C242003001	Merced	Animal slaughtering & processing	31161
32	COELHO MEAT COMPANY	5D541021001	Tulare	Animal slaughtering & processing	31161
33	CONAGRA GROCERY PRODUCTS CO.	5D102111001	Fresno	Fruit & vegetable canning	311421
34	CONAGRA GROCERY PRODUCTS CO	5B50NC00011	Stanislaus	Fruit & vegetable canning	311421
35	CONOPCO DBA UNILEVER BFNA	5C242022001	Merced	Fruit & vegetable canning	311421
36	DAIRYMAN'S MEAT PROCESSING	5C242014001	Merced	Animal slaughtering & processing	31161
37	DARLING INTERNATIONAL	5C502027001	Stanislaus	Rendering and Meat Byproduct Processing	311613

	INC				
38	DEL MONTE CORPORATION	5D162009001	Kings	Fruit and Vegetable Canning, Pickling, and Drying	31142
39	DEL MONTE CORPORATION	5D102057002	Fresno	Fruit and Vegetable Canning, Pickling, and Drying	31142
40	DEL REY JUICE COMPANY	5D101108001	Fresno	Fruit and Vegetable Canning, Pickling, and Drying	31142
41	DEL REY PACKING COMPANY	5D101125001	Fresno	Fruit and Vegetable Canning, Pickling, and Drying	31142
42	DELANO GROWERS GRAPE PRODUCTS	5D152072001	Kern	Wineries	31213
43	DELICATO VINEYARDS	5B392039001	San Joaquin	Wineries	31213
44	DICKER, WILLIAM	5C201003001	Madera	Roasted Nuts and Peanut Butter Manufacturing	311911
45	GALLO, E & J	5C202017001	Madera	Wineries	31213
46	GALLO, E & J	5C242004001	Merced	Wineries	31213
47	EXETER DEHYDRATOR INC	5D542002001	Tulare	Dried & dehydrated food mfg	311423
48	FAMILY TREE	5D542119001	Fresno	Fruit and Vegetable Canning, Pickling, and Drying	31142
49	FIG GARDEN PACKING, INC.	5D102097001	Fresno	Fruit and Vegetable Canning, Pickling, and Drying	31142
50	FOSTER FARMS	5C241006001	Merced	Waste & Miscellaneous	N/A
51	FOUR BAR C FARMS, INC	5D101113001	Fresno	Dried & dehydrated food mfg	311423
52	FOWLER PACKING COMPANY, INC	5D101088001	Fresno	Dried & dehydrated food mfg	311423
53	RECOT, INC	5D152033001	Kern	Fruit & vegetable canning	311421
54	GALLO E & J CRUSHER	5D102022001	Fresno	Wineries	31213
55	GALLO E & J STILLAGE	5D102022001	Fresno	Wineries	31213
56	SUN GARDEN GANGI CANNING CO.	5C241003002	Merced	Fruit & vegetable canning	311421
57	GILLETTE CITRUS COMPANY	5D101130001	Tulare	Fruit & vegetable canning	311421
58	GIUMARRA VINEYARDS CORP	5D152006001	Kern	Wineries	31213

59	GOLD COAST PISTACHIO, INC	5D102134001	Fresno	Roasted Nuts and Peanut Butter Manufacturing	311911
60	GOLDEN STATE CITRUS PACKERS	5D542003001	Tulare	Fruit & vegetable canning	311421
61	GOLDEN STATE VINTNERS - CUTLER	5D542006001	Tulare	Wineries	31213
62	GOLDEN STATE VINTNERS	5D102133001	Fresno	Wineries	31213
63	GOLDEN VALLEY GRAPE JUICE/WINE	5C202033001	Madera	Wineries	31213
64	GOLDSTONE LAND CO	5B392004003	San Joaquin	Wineries	31213
65	GRIMMWAY ENTERPRISES	5C15NC00025	Kern	Fruit and Vegetable Canning, Pickling, and Drying	31142
66	GRIMMWAY ENTERPRISES, INC	5D152210002	Kern	Fruit and Vegetable Canning, Pickling, and Drying	31142
67	GRIMMWAY FROZEN FOODS	5D152209001	Kern	Frozen Food Manufacturing	31141
68	GRIMWAYS	5D152209002	Kern	Fruit and Vegetable Canning, Pickling, and Drying	31142
69	HARRIS FARMS, INC	5D102019001	Fresno	Animal slaughtering & processing	31161
70	HECK CELLARS	5D152038001	Kern	Wineries	31213
71	HERSHEY FOODS CORP	5C502003001	Stanislaus	Fruit & vegetable canning	311421
72	HILMAR	5C242018001	Merced	Dairy Product Manufacturing	3115
73	HMC GROUP COLD STORAGE, INC	5D102108001	Fresno	Frozen Food Manufacturing	31141
74	HUGHSON NUT COMPANY	5C502044001	Stanislaus	Roasted Nuts and Peanut Butter Manufacturing	311911
75	INGOMAR	5C241010001	Merced	Fruit & vegetable canning	311421
76	ITO PACKING CO, INC	5D101063001	Fresno	Fruit and Vegetable Canning, Pickling, and Drying	31142
77	DOLE PACKAGE FROZEN FOODS, INC	5C242002001	Merced	Frozen Food Manufacturing	31141
78	JUE, JEFF & VELVET	5D101133001	Fresno	Dried & dehydrated food mfg	311423
79	KAUTZ VINEYARDS INC	5B051019001	Calaveras	Wineries	31213
80	KEENAN FARMS, INC	5D162022001	Kings	Roasted Nuts and Peanut Butter Manufacturing	311911

81	KERN RIDGE GROWERS, LLC	5D152078001	Kern	Fruit & vegetable canning	311421
82	KRAFT FOODS, INC	5D542010001	Tulare	Dairy Product Manufacturing	3115
83	LAMANUZZI & PANTALEO	5D102005002	Fresno	Dried & dehydrated food mfg	311423
84	LAMANUZZI & PANTALEO	5D102005003	Fresno	Dried & dehydrated food mfg	311423
85	LAMANUZZI & PANTALEO	5D202025001	Madera	Dried & dehydrated food mfg	311423
86	LIBERTY PACKING COMPANY	5C242010001	Merced	Fruit & vegetable canning	311421
87	LION RAISINS, INC.	5D102027001	Fresno	Dried & dehydrated food mfg	311423
88	LOBUE BROS, INC	5D542013001	Tulare	Fruit & vegetable canning	311421
89	LODI VINTNERS, INC.	5B392040001	San Joaquin	Wineries	31213
90	LONG RANCH, INC.	5B395278001	San Joaquin	Animal slaughtering & processing	31161
91	LOS GATOS TOMATO PRODUCTS	5D102109001	Fresno	Fruit & vegetable canning	311421
92	MADERA ENTERPRISES, INC	5C201025001	Madera	Dried & dehydrated food mfg	311423
93	MANNA PRO CORPORATION	5D102064001	Fresno	Fruit & vegetable canning	311421
94	MODERN DEVELOPMENT COMPANY	5D102119001	Fresno	Wineries	31213
95	MONARCH NUT COMPANY	5D541070001	Kern	Roasted Nuts and Peanut Butter Manufacturing	311911
96	MORADA PRODUCE COMPANY	5B39NC00019	San Joaquin	Fruit and Vegetable Canning, Pickling, and Drying	31142
97	MORNING STAR PACKING COMPANY	5C241011001	Merced	Fruit & vegetable canning	311421
98	MOUA YAVA, GALLO CHEESE	5B24NC00009	Merced	Dairy Product Manufacturing	3115
99	MUSCO FAMILY OLIVE COMPANY	5B392059002	San Joaquin	Waste & Miscellaneous	N/A
100	MUSCO FAMILY OLIVE COMPANY	5B392059001	San Joaquin	Fruit & vegetable canning	311421
101	NICHOLS PISTACHIO	5D161023001	Kings	Roasted Nuts and Peanut Butter Manufacturing	311911
102	NONINI, A WINERY	5D102050001	Fresno	Wineries	31213
103	NORDMAN OF CALIFORNIA	5D102069001	Fresno	Wineries	31213

104	NT GARGIULO & DERRICK ASSOC	5C201027002	Fresno	Fruit & vegetable canning	311421
105	OAK RIDGE WINERY, LLC	5B392001001	San Joaquin	Wineries	31213
106	OASIS FOODS, INC	5C242013001	Merced	Fruit and Vegetable Canning, Pickling, and Drying	31142
107	O'NEILLS VINTNERS & DISTILLERS	5D102031001	Fresno	Wineries	31213
108	PARAMOUNT FARMS, INC	5D152207001	Kern	Roasted Nuts and Peanut Butter Manufacturing	311911
109	PARAMOUNT FARMS, INC.	5D151170001	Kern	Roasted Nuts and Peanut Butter Manufacturing	311911
110	PATTERSON FROZEN FOODS, INC.	5C502033001	Stanislaus	Fruit and Vegetable Canning, Pickling, and Drying	31142
111	DUREY LIBBY WEST PISTACHIO PLANT	5C201003001	Madera	Roasted Nuts and Peanut Butter Manufacturing	311911
112	PORTERVILLE CITRUS	5D542008001	Tulare	Fruit & vegetable canning	311421
113	RICHWOOD MEAT COMPANY	5C242026001	Merced	Animal slaughtering & processing	31161
114	RJM ENTERPRISES	5B392108001	San Joaquin	Wineries	31213
115	ROBERT MONDAVI CORPORATION	5B392068001	San Joaquin	Wineries	31213
116	SALWASSER, INC	5D102099001	Fresno	Dried & dehydrated food mfg	311423
117	SALWASSER, INC	5D102099002	Fresno	Dried & dehydrated food mfg	311423
118	SAN JOAQUIN VALLEY EXPRESS	5D102024002	Fresno	Wineries	31213
119	SCHATZ, RODNEY & GAYLA	5B39NC00011	San Joaquin	Wineries	31213
120	SCHENONE, ERNIE & MARY	5B39NC00037	San Joaquin	Fruit & vegetable canning	311421
121	SENSIENT TECHNOLOGIES CORP.	5C242005001	Merced	Fruit & vegetable canning	311421
122	SEQUOIA ORANGE COMPANY, INC	5D542036001	Tulare	Fruit & vegetable canning	311421
123	SETTON PROPERTIES, INC.	5D541071001	Tulare	Roasted Nuts and Peanut Butter Manufacturing	311911
124	SK FOODS INC & CITY OF LEMOORE	5D161024001	Kings	Fruit & vegetable canning	311421
125	S.M.S. BRINERS INC.	5B391066001	San Joaquin	Fruit and Vegetable Canning, Pickling, and	31142

				Drying	
126	SPENKER RANCH INC	5B39NC00017	San Joaquin	Wineries	31213
127	SPRECKLES SUGAR COMPANY, INC	5D102041001	Fresno	Beet Sugar Manufacturing	311313
128	SUN PACIFIC SHIPPERS	5D542016001	Tulare	Fruit & vegetable canning	311421
129	SUN PACIFIC SHIPPERS	5D151197001	Kern	Fruit & vegetable canning	311421
130	SUN PACIFIC SHIPPERS	5D541028001	Tulare	Fruit & vegetable canning	311421
131	SUN WORLD, INC	5D155000001	Kern	Fruit and Vegetable Canning, Pickling, and Drying	31142
132	SUNKIST GROWERS, INC	5D542044001	Tulare	Fruit & vegetable canning	311421
133	SUNLAND PACKINGHOUSE CO	5D542032001	Tulare	Fruit & vegetable canning	311421
134	SUN-MAID RAISIN GROWERS	5D102053001	Fresno	Dried & dehydrated food mfg	311423
135	SUN-MAID RAISIN GROWERS	5D102042003	Fresno	Dried & dehydrated food mfg	311423
136	SUNSHINE RAISIN CORP DBA	5D102142001	Fresno	Dried & dehydrated food mfg	311423
137	SUNSWEET DRYERS	5C202029001	Madera	Dried & dehydrated food mfg	311423
138	SURABIAN PACKING CO, INC	5D102137001	Fresno	Fruit and Vegetable Canning, Pickling, and Drying	31142
139	SUTTER HOME WINERY, INC.	5B39NC00012	San Joaquin	Wineries	31213
140	SWORLCO, A LIMITED PRTNSHIP	5D540131001	Tulare	Fruit & vegetable canning	311421
141	TARTARIC MANUFACTURING CORP.	5C502051001	Stanislaus	Fruit & vegetable canning	311421
142	TELLES, JESS P	5D542015001	Tulare	Fruit & vegetable canning	311421
143	THE WINE GROUP LLC	5D152039001	Kern	Wineries	31213
144	TOMATEK INC & CTY OF FIREBAUGH	5C100107001	Fresno	Fruit & vegetable canning	311421
145	TREEHOUSE CA ALMONDS, LLC	5D541089001	Tulare	Roasted Nuts and Peanut Butter Manufacturing	311911
146	TRI-COUNTY CITRUS PACKERS	5D542031001	Tulare	Fruit & vegetable canning	311421
147	TRIPLE E PRODUCE	5B392077001	San	Fruit & vegetable	311421

	CORPORATION		Joaquin	canning	
148	VALLEY GOLD, LLC	5C242033002	Merced	Dairy Product Manufacturing	3115
149	VALLEY SUN DRIED PRODUCTS	5C502046001	Stanislaus	Dried & dehydrated food mfg	311423
150	VAN RUITEN-TAYLOR RANCH LTD	5B39NC00036	San Joaquin	Wineries	31213
151	VENTURA COASTAL CORPORATION	5D542014001	Tulare	Fruit & vegetable canning	311421
152	VICTOR PACKING CO	5C202013001	Madera	Dried & dehydrated food mfg	311423
153	VIE-DEL COMPANY	5D102047001	Fresno	Wineries	31213
154	VISALIA CITRUS PACKING GROUP	5D542019001	Tulare	Fruit & vegetable canning	311421
155	VITA-PAKT CITRUS PRODUCTS CO.	5D101128001	Fresno	Dried & dehydrated food mfg	311423
156	WINE GROUP, INC.	5D542026001	Tulare	Wineries	31213
157	WINE GROUP, THE	5B392003001	San Joaquin	Wineries	31213
158	WINE GROUP, INC.	5D102044002	Fresno	Wineries	31213
159	WOODBRIDGE PARTNERS INC	5B392043001	San Joaquin	Animal slaughtering & processing	31161
160	ZORIA FARMS, INC	5B20NC00003	Madera	Dried & dehydrated food mfg	311423

Central Valley food processors surveyed in study, numbers correspond to labels in Figures 3 and 4. [1]Unique processor identification number used by the Regional Water Quality Boards. The distribution of these facilities in the Central Valley is further discussed below.

Month		Jan	Feb	Mar	Apr	May	Jun	Jul	Aug	Sep	Oct	Nov	Dec
Volume	kgal	6510	5880	7750	10470	11,501	9,270	7,440	9,641	10,020	12,214	11,340	10,478
Flow	kgal/day												
pH		7.4	7.7	6.2	7.6	7.5	7.9	7.6	6.3	5.0	4.5	5.0	9.4
Conductivity	mic-S/cm												
Fixed Dissolved Solids (FDS)	mg/L	310	440	515	800	490	1300	520	1570	1400	3575	1000	96
Volatile Dissolved Solids (VDS)	mg/L												
Total Dissolved Solids (TDS)	mg/L	960	1100	1790	1300	1000	1600	1200	2765	4600	8800	2441.667	1300
Total Suspended Solids (TSS)	mg/L	1600	1200	985	1200	310	260	190	1340	1100	5725	5050	210
Total COD or COD	mg/L												
Total BOD5 or BOD5	mg/L	2300	1500	2750	740	1700	930	1700	4900	11000	12250	4533.333	1200
Total Organic Carbon (TOC)	mg/L												
Soluble BOD	mg/L												
Soluble COD	mg/L												
Soluble Organic Carbon	mg/L												
NH4-N	mg/L												
NO3-N	mg/L	4.4	4.4	4.95	4.5	5	4	5.1	2.55	5.5	5.325	5.333333	5
NO2-N	mg/L												
(NO3 + NO2)-N	mg/L												
TKN	mg/L	59	20	28	12	5.5	14	22	64.65	72	376	177.6667	14
Total Nitrogen	mg/L												
Total P	mg/L												
Alkalinity as CaCO3	mg/L	140	120	105	280	190	290	160	105	0	0	65	81
Hardness as CaCO3	mg/L	160	180	250	200	190	270	190	240	230	322.5	268.3333	230
Chloride Cl	mg/L	70	99	65	180	240	550	150	62.5	42	88.25	154.1667	330
Sulfate SO4	mg/L	21	21	46	120	22	28	21	56	50	78	105	23
Carbonate CO3	mg/L												
Bicorbonate HCO3	mg/L												
Boron	mic-g/L												
Sulfide	mic-g/L												
Calcium Ca	mg/L	39	43	58.5	49	47	68	48	56	53	74.75	62.16667	56
Magnesium Mg	mg/L	15	18	25.5	19	18	25	18	24.5	24	33.5	25.33333	22
Potassium K	mg/L												
Sodium Na	mg/L	64	81	65	230	200	420	110	149	41	163	116.1667	330
Aluminum	mic-g/L												
Arsenic As	mic-g/L												
Cadmium Cd	mic-g/L												
Copper Cu	mic-g/L												
Iron Fe	mic-g/L												
Lead Pb	mic-g/L												
Manganese Mn	mic-g/L												
Nickel Ni	mic-g/L												
Selenium Se	mic-g/L												
Zinc Zn	mic-g/L												

Figure 1

Sample Template of Effluent Data for a Central Valley Winery

Each of the food processing facilities and some POTWs surveyed are represented through a template (example: Figure 1) in our data base. Data is recorded for each facility for the 3 years, 2003 to 2005. Figure 1 represents only a part of the complete file, which includes additional background information, as well as additional information on water supply quality parameters for several facilities. Many of the processors report only a partial list of the parameters shown in Figure 1.

A total of 160 food-processing facilities were surveyed, including some facilities with multiple effluent discharge sites. The few facilities not included in the survey are located in the Sacramento River Basin, where the salinity problem is minor. Out of the 160 food processing facilities, 68 facilities are in the San Joaquin River Basin (Region 5B) and 92 facilities are in the Tulare Lake Basin (Region 5C), see Figure 2. Additionally, 47 POTWs were considered and templates were created for 23 of these facilities, covering those POTWs with food-processing related activities. POTWs surveyed include 22 in the San Joaquin River Basin, 19 in the Tulare Lake Basin and 6 in the Sacramento River Basin (Region 5A). The food processors in our survey fall into 12 industrial groups using the definitions employed by the North American

Industry Classification System (NAICS) (4). Counts of food processors and POTWs by industrial group and county are shown in Table 2. Table 3 provides a complete list of POTWs considered in the survey.

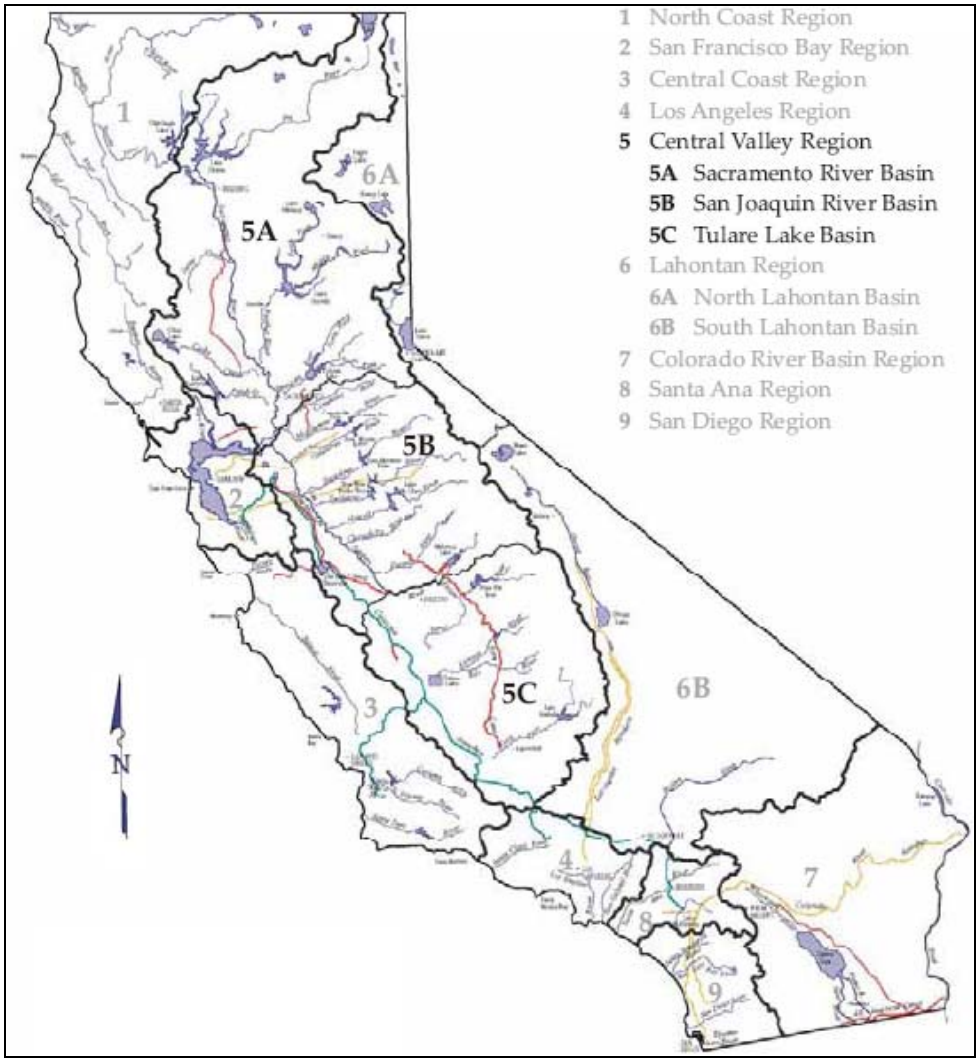

Figure 2

California Hydrologic Regions, the Central Valley covers the regions marked by 5A, 5B and 5C. Our survey primarily covers Regions 5B and 5C which are generally recognized as being more threatened by salinity than Region 5A.

Table 2: Counts of food processing facilities and POTWs surveyed by industry and county. Templates were not created for 24 POTWs, see Table 3

Industry	NAICS Code	Butte	Calaveras	Fresno	Kern	Kings	Madera	Merced	San Joaquin	Solano	Stanislaus	Sutter	Tehama	Tulare	Yolo	Grand Total
Animal slaughtering & processing	31161			2				3	3					1		9
Beet Sugar Manufacturing	311313			1												1
Dairy Product Manufacturing	3115							4						3		7
Dried & dehydrated food mfg	311423			14			5				1			1		21
Fat and Oils Refining and Blending	311225			1												1
Frozen Food Manufacturing	31141			1	1			1			1					4
Fruit & vegetable canning	311421			7	3	1	2	6	4		3			14		40
Fruit and Vegetable Canning, Pickling, and Drying	31142			8	7	1		1	4		2					23
Rendering and Meat Byproduct Processing	311613										1					1
Roasted Nuts and Peanut Butter Manufacturing	311911			1	3	3	3				1			2		13
Waste & Miscellaneous	unknown							1	2							3
Wineries	31213		1	10	4		4	1	13		1			3		37
POTWs	NA	2		3	6	3	1	6	6	1	9	1	1	7	1	47
Grand Total		**2**	**1**	**48**	**24**	**8**	**15**	**23**	**32**	**1**	**19**	**1**	**1**	**31**	**1**	**207**

Locations of food processing facilities covered in our survey are shown for the northern, middle and southern portions of the Central Valley in Figures 3, 4 and 5 respectively. Color codes and symbols are used to identify the various industrial groups and the numbered labels correspond to entries in Table 1.

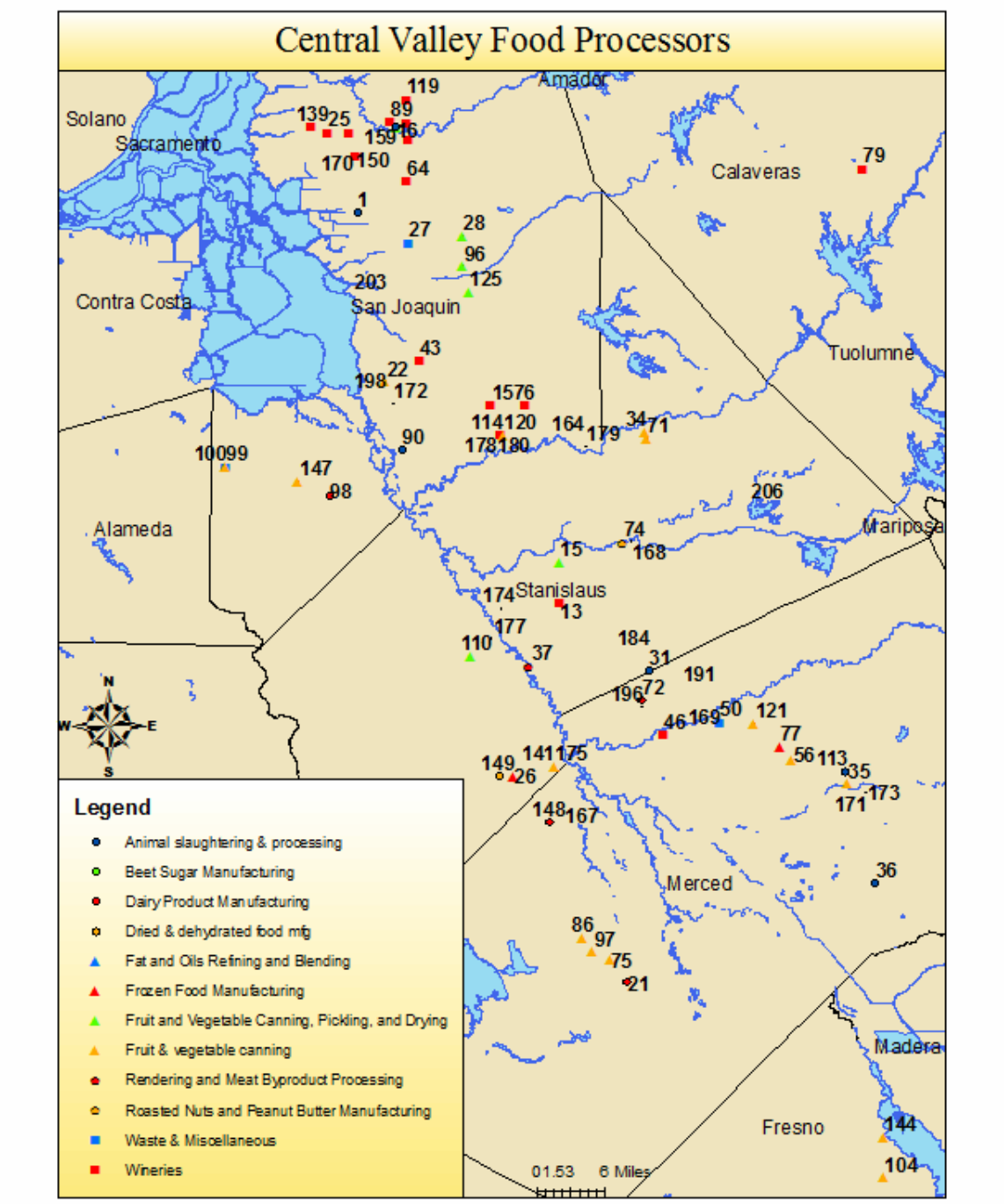

Figure 3

Locations of the food processing facilities in the northern part of the Central Valley, primarily the San Joaquin River Basin (Region 5B). Shown in blue are surface water bodies and river basins. Numbered labels correspond to entries in Table 1.

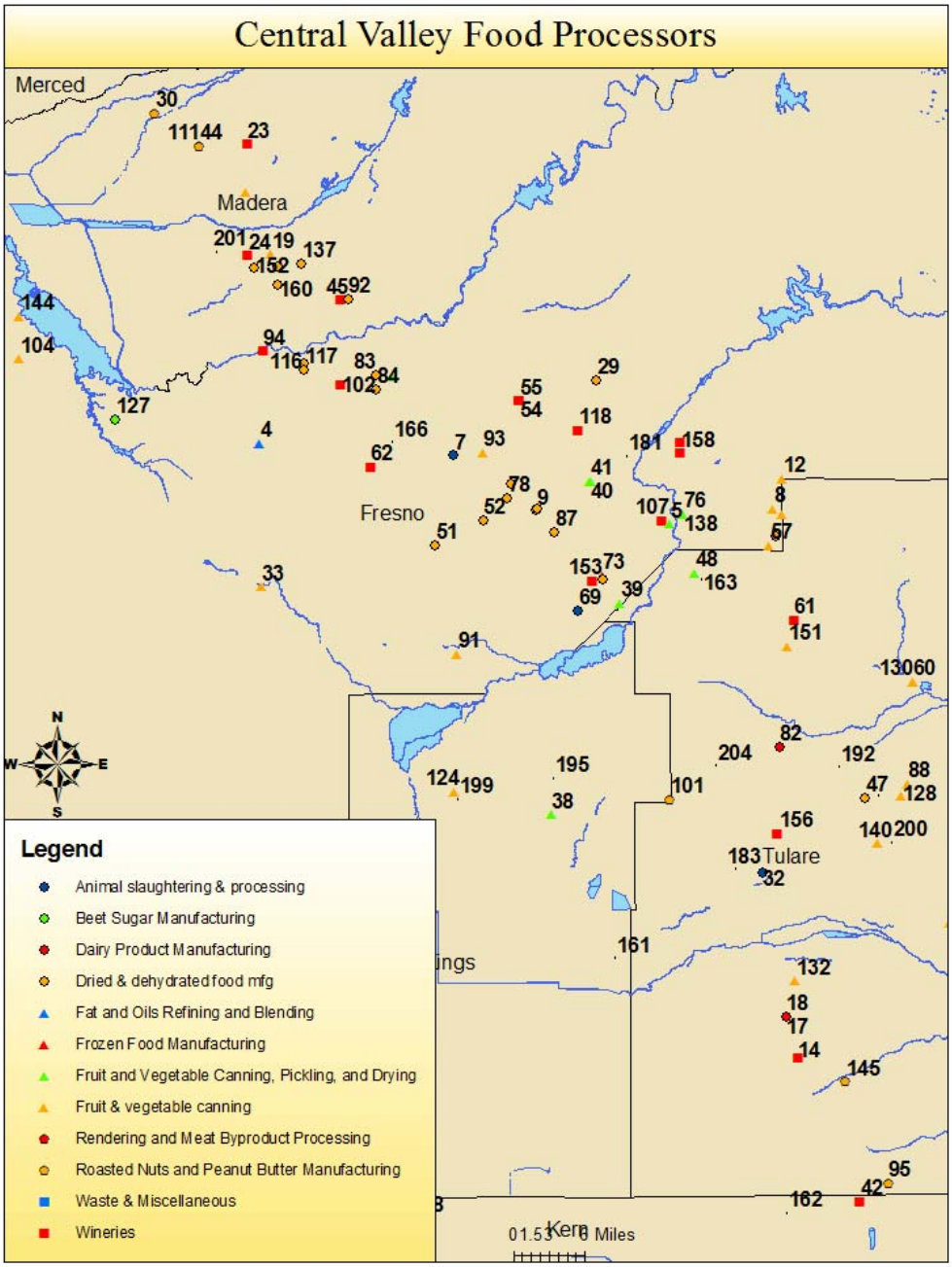

Figure 4

Locations of the food processing facilities in the middle of the Central Valley, which contains portions of the San Joaquin River Basin (Region 5B) and the Tulare Lake Basin (Region 5C). Shown in blue are surface water bodies and river basins, numbered labels correspond to entries in Table 1.

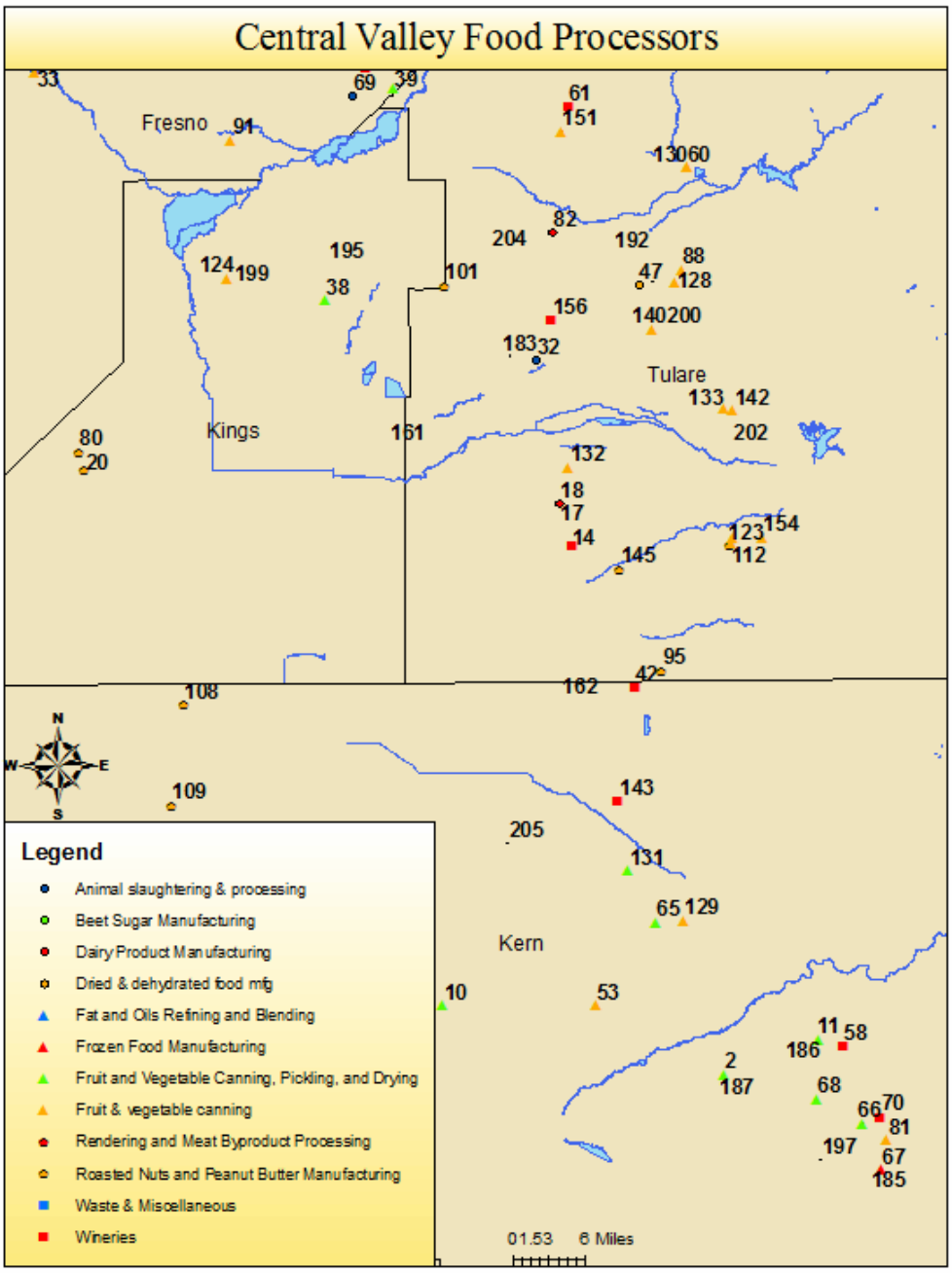

Figure 5

Locations of the food processing facilities in the southern part of the Central Valley, which is comprised primarily of the Tulare Lake Basin (Region 5C). Shown in blue are surface water bodies and river basins, numbered labels correspond to entries in Table 1.

B. Publicly Owned Treatment Works (POTWs)

POTWs accepting waste water from food processing related activity were also included in the survey. POTWs surveyed are listed in Table 3 and their locations are shown in Figure 6. Templates similar to Figure 1 were created for major POTWs within the regional study area and for some other POTWs.

Table 3: Central Valley POTWs

Central Valley Publicly Owned Treatment Works (POTWs)			
	POTWs	Food %[a]	Template
185	City of Arvin		N
186	City of Bakersfield (#2)		N
187	City of Bakersfield (#3)		N
188	City of Ceres	0	N
189	City of Chico		N
161	City of Corcoran		Y
190	City of Corning		N
162	City of Delano		Y
191	City of Delhi	0	N
163	City of Dinuba		Y
164	City of Escalon	56	Y
165	City of Exeter		Y
192	City of Farmersville		N
166	City of Fresno		Y
193	City of Gibson Canyon		N
194	City of Gridley		N
167	City of Gustine	55	Y
195	City of Hanford		N
196	City of Hilmar	0	N
168	City of Hughson	50	Y
197	City of Lamont		N
198	City of Lathrop		N
199	City of Lemoore		N
200	City of Lindsay		N
169	City of Livingston	100	Y
170	City of Lodi		Y
171	City of Los Banos		Y
201	City of Madera		N
172	City of Manteca		Y
173	City of Merced		Y
174	City of Modesto	24	Y

175	City of Newman	60	Y
176	City of Oakdale	19	Y
177	City of Patterson	0	Y
202	City of Porterville		N
178	City of Ripon	12	Y
179	City of Riverbank	16	Y
180	City of Salida	3	Y
181	City of Sanger		Y
182	City of Selma-Kingsburg-Fowler		Y
203	City of Stockton		N
183	City of Tulare		Y
184	City of Turlock	44	Y
204	City of Visalia		N
205	City of Wasco		N
206	City of Waterford	0	N
207	City of Woodland		N
208	City of Yuba City		N

Central Valley POTWs. [a]Percent of water treated coming from food processors. Data was not available for blank entries.

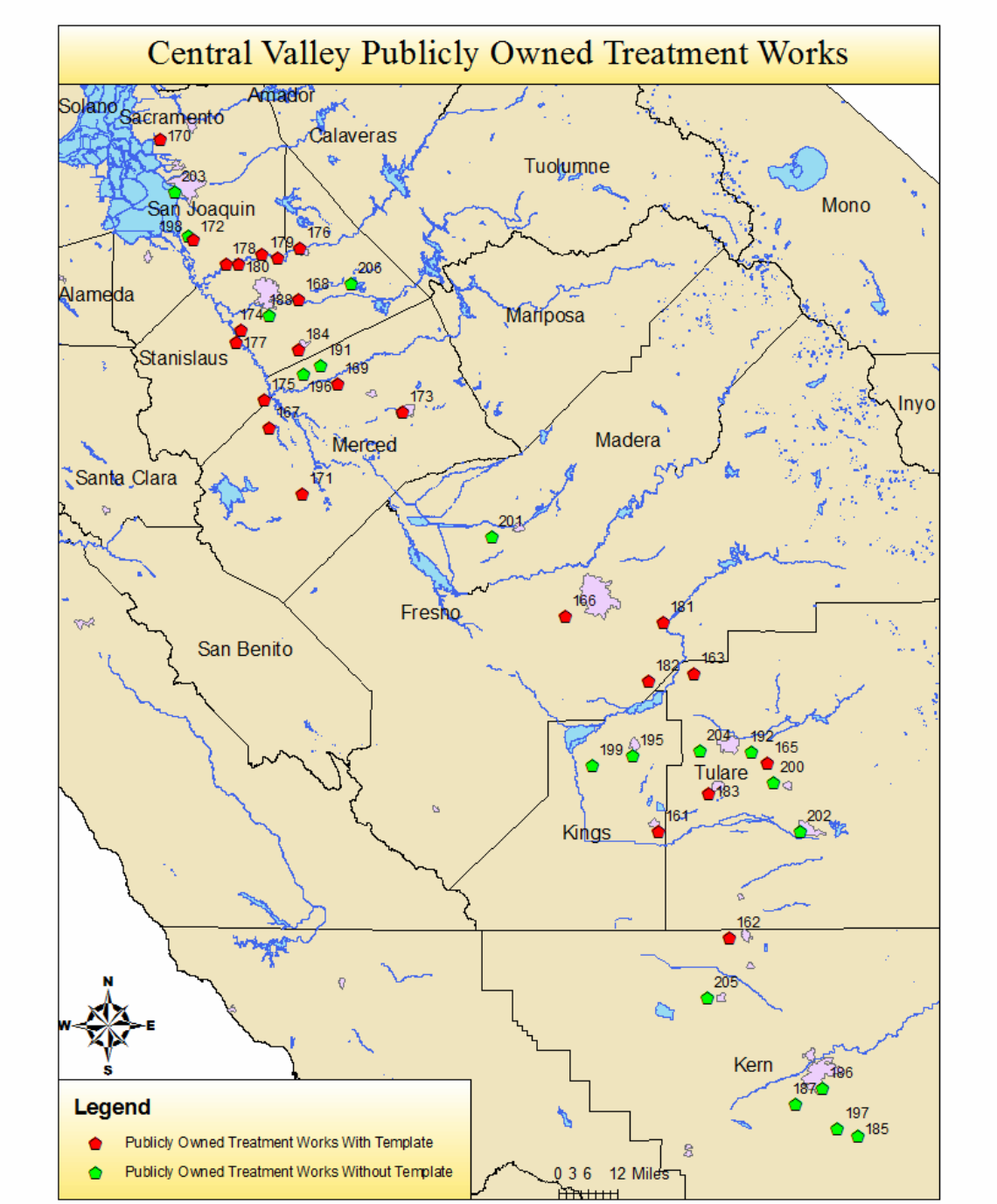

Figure 6

Central Valley POTWs, numbered labels correspond to entries in Table 4. POTWs in the cities of Gibson Canyon, Woodland, Yuba City, Gridley, Chico and Corning are not shown because they are north of the area shown. Urban areas are shown as purple and surface water as blue.

C. Salinity Loads in the Central Valley

This section provides estimates of loads of salinity and N compounds (nitrate and ammonium) in wastewater discharges from the food industry for the various hydrologic regions and counties in the Central Valley. As discussed earlier, fixed dissolved solids (FDS) will be used as the primary measure of salinity. Data reported directly by processors were used for this analysis whenever possible. Where FDS concentrations were not reported, they were estimated from measurements of electrical conductivity (EC), following correlation analysis and discussion provided in Subsection 4. Reported FDS data and FDS values derived by correlation with EC, FDS (mg/L) = 0.6 x EC (umhos/cm), were used to estimate salinity loads as the product of volume discharged and salinity concentration, see Equation 1.

(1) $$FDS\left(\frac{mg}{L}\right) \times Volume\,(kgal) \times \frac{3.785\times10^{3}\,(L)}{(kgal)} \times \frac{metric\ ton}{10^{9}mg} = FDS\ Load\ (metric\ tons)$$

Total FDS loads and FDS loads broken into hydraulic region and industry are shown in Table 4 and by county and industry in Table 5.

Gap filling was used to compensate for months processors reported an effluent volume, but not a FDS or EC measurement. A volume weighted average effluent salinity concentration for each processor was calculated from months the processor reported salinity data, as shown in Equation 2.

(2) $$\frac{\Sigma(Volume\times Concentration)}{\Sigma(Volume)} = Volume\ weighted\ effluent\ concentration\ (mg/L)$$

A processor's volume weighted effluent salinity concentration is multiplied by the processor's total discharge volume for months with and without salinity measurements to estimate the total FDS load for that processor by Equation 1. Salinity loads for years with no reporting available is estimated either as the equivalents of the single reported year or as the average of the two reported years. A third form of gap filling will be discussed and added later. Gap filling is an attempt to compensate for incomplete data. There is no unique method of gap filling, making it somewhat speculative, and as such it is subject to uncertainty. In order to account for this uncertainty, we report below loads computed from reported data as well as loads augmented through gap-filling. Tables 4 and 5 show both the actual reported loads and the total loads including the gap-filling described here for 2003, 2004 and 2005.

Table 4: Fixed Dissolved Solids (FDS) loads in metric tons, some FDS data from EC correlation, gap filling as described in text was used for total load columns. See Figure 2 for map of areas in table. 61 percent of processors reported EC or FDS measurements

		FDS Loads (metric tons)					
	Industry	Reported 2003 Load	Total 2003 Load With Gap Filling	Reported 2004 Load	Total 2004 Load With Gap Filling	Reported 2005 Load	Total 2005 Load With Gap Filling
Total For Central Valley	Total	34300	56700	36400	58300	55000	59700
	Animal slaughtering & processing	3	560	270	570	540	540
	Beet Sugar Manufacturing	0	0	0	0	0	0
	Dairy Product Manufacturing	3230	3230	5090	5110	4260	4540
	Dried & dehydrated food mfg	160	190	100	160	90	130
	Fat and Oils Refining and Blending	33	112	27	92	16	57
	Frozen Food Manufacturing	1510	1510	1630	1630	1820	1820
	Fruit & vegetable canning	12100	30900	9400	28400	26600	28200
	Fruit and Vegetable Canning, Pickling, and Drying	11000	11100	10100	10100	9900	9900
	Rendering and Meat Byproduct Processing	0	0	0	0	0	0
	Roasted Nuts and Peanut Butter Manufacturing	340	820	3780	4390	5600	6300
	Waste & Miscellaneous	2090	3440	2180	3820	2360	4050
	Wineries	3780	4950	3810	3990	3730	4080
San Joaquin River Basin	Total	20700	41100	20600	41200	34900	38200
	Animal slaughtering & processing	3	10	10	10	10	10
	Beet Sugar Manufacturing	0	0	0	0	0	0
	Dairy Product Manufacturing	2770	2770	4570	4580	3570	3590
	Dried & dehydrated food mfg	80	100	20	80	20	50
	Fat and Oils Refining and Blending	0	0	0	0	0	0
	Frozen Food Manufacturing	530	530	800	800	680	680
	Fruit & vegetable canning	9400	27500	6800	25600	22800	24300
	Fruit and Vegetable Canning, Pickling, and Drying	3360	3360	2960	2960	2900	2910
	Rendering and Meat Byproduct Processing	0	0	0	0	0	0
	Roasted Nuts and Peanut Butter Manufacturing	0	20	10	10	30	30
	Waste & Miscellaneous	2090	3440	2180	3820	2360	4050
	Wineries	2450	3390	3310	3370	2510	2520
Tulare Lake Basin	Total	13700	15600	15800	17100	20000	21500
	Animal slaughtering & processing	0	550	260	560	530	530
	Beet Sugar Manufacturing	0	0	0	0	0	0
	Dairy Product Manufacturing	450	450	520	520	690	950
	Dried & dehydrated food mfg	82	90	82	84	67	74
	Fat and Oils Refining and Blending	33	112	27	92	16	57
	Frozen Food Manufacturing	990	990	840	840	1140	1140
	Fruit & vegetable canning	2800	3400	2700	2800	3800	3900
	Fruit and Vegetable Canning, Pickling, and Drying	7690	7690	7130	7170	7010	7020
	Rendering and Meat Byproduct Processing	0	0	0	0	0	0
	Roasted Nuts and Peanut Butter Manufacturing	340	800	3770	4380	5600	6300
	Waste & Miscellaneous	0	0	0	0	0	0
	Wineries	1330	1560	500	610	1220	1560

Table 5: Fixed Dissolved Solids (FDS) loads in metric tons, 61% of processors reporting EC of FDS values

	Calaveras	Fresno	Kern	Kings	Madera	Merced	San Joaquin	Stanislaus	Tulare	Total
Animal slaughtering & processing										
Reported 2003 Load	0	0	0	0	0	3	0	0	0	0
Total 2003 Load With Gap Filling	0	550	0	0	0	12	0	0	0	560
Reported 2004 Load	0	260	0	0	0	11	0	0	0	270
Total 2004 Load With Gap Filling	0	560	0	0	0	14	0	0	0	570
Reported 2005 Load	0	530	0	0	0	10	0	0	0	540
Total 2005 Load With Gap Filling	0	530	0	0	0	10	0	0	0	540
Beet Sugar Manufacturing										
Reported 2003 Load	0	0	0	0	0	0	0	0	0	0
Total 2003 Load With Gap Filling	0	0	0	0	0	0	0	0	0	0
Reported 2004 Load	0	0	0	0	0	0	0	0	0	0
Total 2004 Load With Gap Filling	0	0	0	0	0	0	0	0	0	0
Reported 2005 Load	0	0	0	0	0	0	0	0	0	0
Total 2005 Load With Gap Filling	0	0	0	0	0	0	0	0	0	0
Dairy Product Manufacturing										
Reported 2003 Load	0	0	0	0	0	2770	0	0	450	3230
Total 2003 Load With Gap Filling	0	0	0	0	0	2770	0	0	450	3230
Reported 2004 Load	0	0	0	0	0	4570	0	0	520	5090
Total 2004 Load With Gap Filling	0	0	0	0	0	4580	0	0	520	5110
Reported 2005 Load	0	0	0	0	0	3570	0	0	690	4260
Total 2005 Load With Gap Filling	0	0	0	0	0	3590	0	0	950	4540
Dried & dehydrated food mfg										
Reported 2003 Load	0	82	0	0	31	0	0	49	0	163
Total 2003 Load With Gap Filling	0	90	0	0	47	0	0	49	0	186
Reported 2004 Load	0	82	0	0	20	0	0	0	0	102
Total 2004 Load With Gap Filling	0	84	0	0	50	0	0	29	0	163
Reported 2005 Load	0	67	0	0	13	0	0	8	0	89
Total 2005 Load With Gap Filling	0	74	0	0	46	0	0	8	0	128
Fat and Oils Refining and Blending										
Reported 2003 Load	0	33	0	0	0	0	0	0	0	33
Total 2003 Load With Gap Filling	0	112	0	0	0	0	0	0	0	112
Reported 2004 Load	0	27	0	0	0	0	0	0	0	27
Total 2004 Load With Gap Filling	0	92	0	0	0	0	0	0	0	92
Reported 2005 Load	0	16	0	0	0	0	0	0	0	16
Total 2005 Load With Gap Filling	0	57	0	0	0	0	0	0	0	57
Frozen Food Manufacturing										
Reported 2003 Load	0	2	990	0	0	359	0	166	0	1513
Total 2003 Load With Gap Filling	0	2	990	0	0	359	0	166	0	1513
Reported 2004 Load	0	2	840	0	0	522	0	273	0	1635
Total 2004 Load With Gap Filling	0	2	840	0	0	522	0	273	0	1635
Reported 2005 Load	0	3	1140	0	0	525	0	157	0	1820
Total 2005 Load With Gap Filling	0	3	1140	0	0	525	0	157	0	1820
Fruit & vegetable canning										
Reported 2003 Load	0	1010	1090	358	0	8200	295	917	297	12100
Total 2003 Load With Gap Filling	0	1300	1090	358	3	8200	295	19000	640	30900
Reported 2004 Load	0	700	1020	370	3	6500	247	0	571	9400
Total 2004 Load With Gap Filling	0	700	1020	370	3	6500	247	18800	711	28400
Reported 2005 Load	0	1230	930	433	0	4000	182	18600	1212	26600
Total 2005 Load With Gap Filling	0	1230	930	433	3	5500	182	18600	1290	28200
Fruit and Vegetable Canning, Pickling, and Drying										
Reported 2003 Load	0	529	4530	2630	0	0	2	3360	0	11000
Total 2003 Load With Gap Filling	0	533	4530	2630	0	0	2	3360	0	11100
Reported 2004 Load	0	520	4690	1920	0	0	11	2950	0	10100
Total 2004 Load With Gap Filling	0	560	4690	1920	0	0	11	2950	0	10100
Reported 2005 Load	0	349	4410	2250	0	0	2	2900	0	9900
Total 2005 Load With Gap Filling	0	350	4410	2250	0	0	13	2900	0	9900
Rendering and Meat Byproduct Processing										
Reported 2003 Load	0	0	0	0	0	0	0	0	0	0
Total 2003 Load With Gap Filling	0	0	0	0	0	0	0	0	0	0
Reported 2004 Load	0	0	0	0	0	0	0	0	0	0
Total 2004 Load With Gap Filling	0	0	0	0	0	0	0	0	0	0
Reported 2005 Load	0	0	0	0	0	0	0	0	0	0
Total 2005 Load With Gap Filling	0	0	0	0	0	0	0	0	0	0
Roasted Nuts and Peanut Butter Manufacturing										
Reported 2003 Load	0	8	129	93	0	0	0	0	114	344
Total 2003 Load With Gap Filling	0	8	532	141	0	0	0	22	114	820
Reported 2004 Load	0	0	1750	112	0	0	0	11	1910	3780
Total 2004 Load With Gap Filling	0	8	2350	112	0	0	0	11	1910	4400
Reported 2005 Load	0	0	3640	265	0	0	0	34	1660	5600
Total 2005 Load With Gap Filling	0	8	4330	269	0	0	0	34	1660	6300
Waste & Miscellaneous										
Reported 2003 Load	0	0	0	0	0	1790	297	0	0	2090
Total 2003 Load With Gap Filling	0	0	0	0	0	1790	1650	0	0	3440
Reported 2004 Load	0	0	0	0	0	2020	158	0	0	2180
Total 2004 Load With Gap Filling	0	0	0	0	0	2020	1800	0	0	3820
Reported 2005 Load	0	0	0	0	0	2320	44	0	0	2360
Total 2005 Load With Gap Filling	0	0	0	0	0	2320	1732	0	0	4050
Wineries										
Reported 2003 Load	0	970	264	0	1310	0	584	560	93	3780
Total 2003 Load With Gap Filling	0	1210	264	0	1310	930	587	560	93	4950
Reported 2004 Load	0	285	109	0	1290	905	649	470	103	3810
Total 2004 Load With Gap Filling	0	399	113	0	1350	905	653	470	103	3990
Reported 2005 Load	0	392	795	0	354	955	821	382	35	3730
Total 2005 Load With Gap Filling	0	690	830	0	358	955	821	382	35	4080
Totals										
Reported 2003 Load	0	2630	7000	3080	1343	13100	1180	5000	960	34300
Total 2003 Load With Gap Filling	0	3800	7400	3130	1364	14000	2540	23200	1300	56700
Reported 2004 Load	0	1880	8400	2410	1313	14500	1070	3700	3100	36400
Total 2004 Load With Gap Filling	0	2410	9000	2410	1400	14600	2710	22600	3250	58300
Reported 2005 Load	0	2590	10900	2950	367	11400	1050	22100	3600	55000
Total 2005 Load With Gap Filling	0	2950	11600	2950	407	12900	2750	22100	3930	59700

The total salinity loads for the counties in the Central Valley are shown in Figure 20. This Figure should be read in conjunction with Figures 21 and 22 which show the division between the total

per county load among reported loads and estimated (gap-filled) loads for study years. Note that gap-filling is an attempt to overcome unreported data, and may be subject to large error. If one accepts these numbers, Stansilaus County contains the largest salinity discharge from the food processing industry, followed by Merced County, with Kern County a far third. Considering the relatively small area of Stanislaus County compared to the other counties, its leadership in terms of salinity load is even more significant. The largest salinity discharge is occuring over a relatively small area, and in turn can suggest a higher concentration of salinity per volume of available groundwater or per pumping well.

Figures 18 and 19 show the food processors in the Central Valley as bubbles that are proprtional in size to the processor's 3-year total salinity load. These Figures allow the identification of potential hot spots of salinity loading It should be noted that there is a high degree of uncertainity associated with gap filling. For example, using the one year of available data from Hershey Foods to estimate the loads in 2003 and 2004 accounts for the disparity between actual and estimated loads for Stanislaus County shown in Figure 22.

Figure 7 provides the distrubutions of the total salinity loads in the Central Valley among the various industrial groups, for the years 2003 to 2005. This figure can, in principle, provide an idea about the trends among the various industries, however it covers a relatively short period of time, and most changes may be reflective of seasonal variations in weather rather than long term trends. Most industries seem to provide similar contributions over this period.

Figures 8 to 17 provide the distributions of the total salinity loads in the San Joaquin River Basin, Tulare Lake Basin and the counties that comprise the Central Valley among the various industrial groups, for the years 2003, 2004 and 2005. These Figures show which industries are the dominant sources of salinity in each county in the Central Valley. For example, salinity loading in Madera county is dominated by the wine industry, whereas salinity loading in Kings County is dominated by the fruit and vegitable canning, pickling and drying industry.

Trends in the relative salinity discharges among industries may provide some insight. The relative contribution of the roasted nuts and peanut butter manufacuring industry has increased significantly in Tulare County (Figure 17) and Kern County (Figure 11) as well as the Tulare Lake Basin (Figure 9) as a whole. The increases in these areas partially accounts for the overall increase in whole Central Valley (Figure 9). The relative contributions among industries appears to be more consistant in the San Joaquin River Basin (Figure 8) than the Tulare Lake Basin (Figure 9).

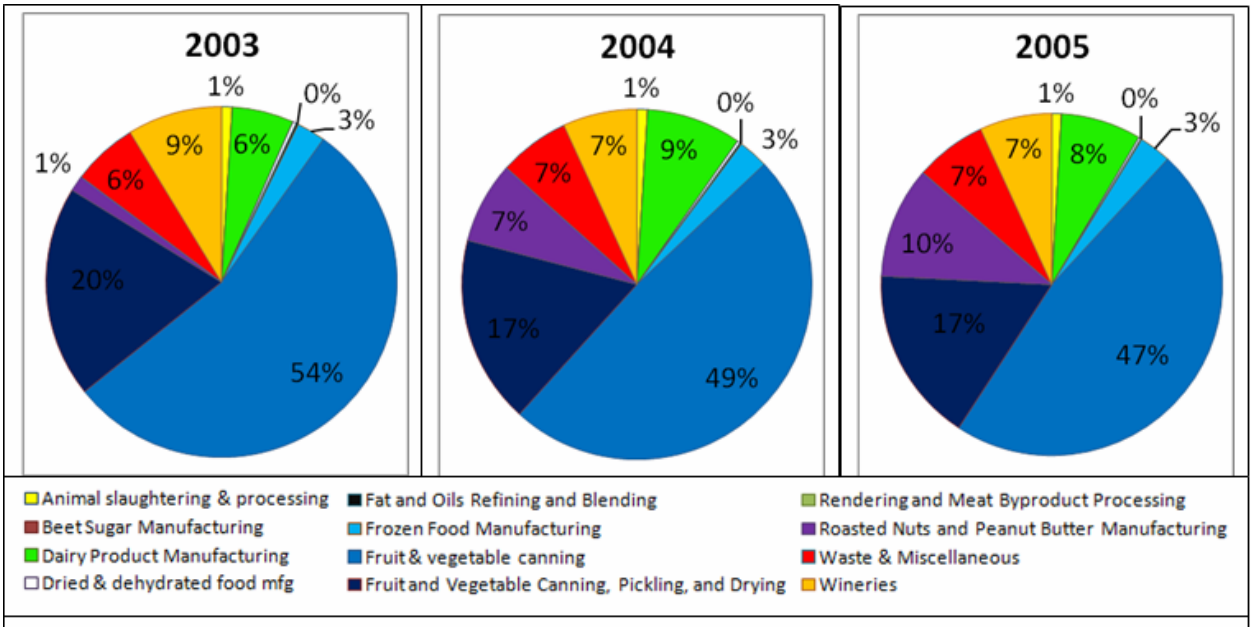

Figure 7

Percent of total FDS loads (metric tons) for the Central Valley by industry

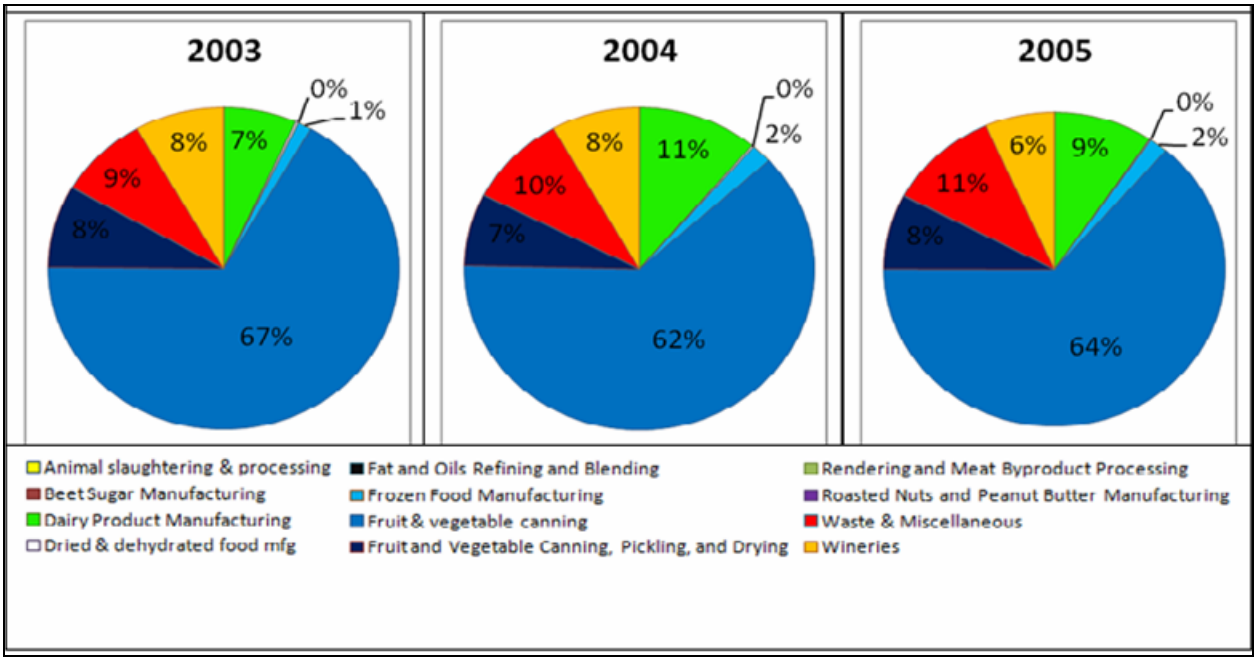

Figure 8

Percent of total FDS loads (metric tons) for San Joaquin River Basin by industry

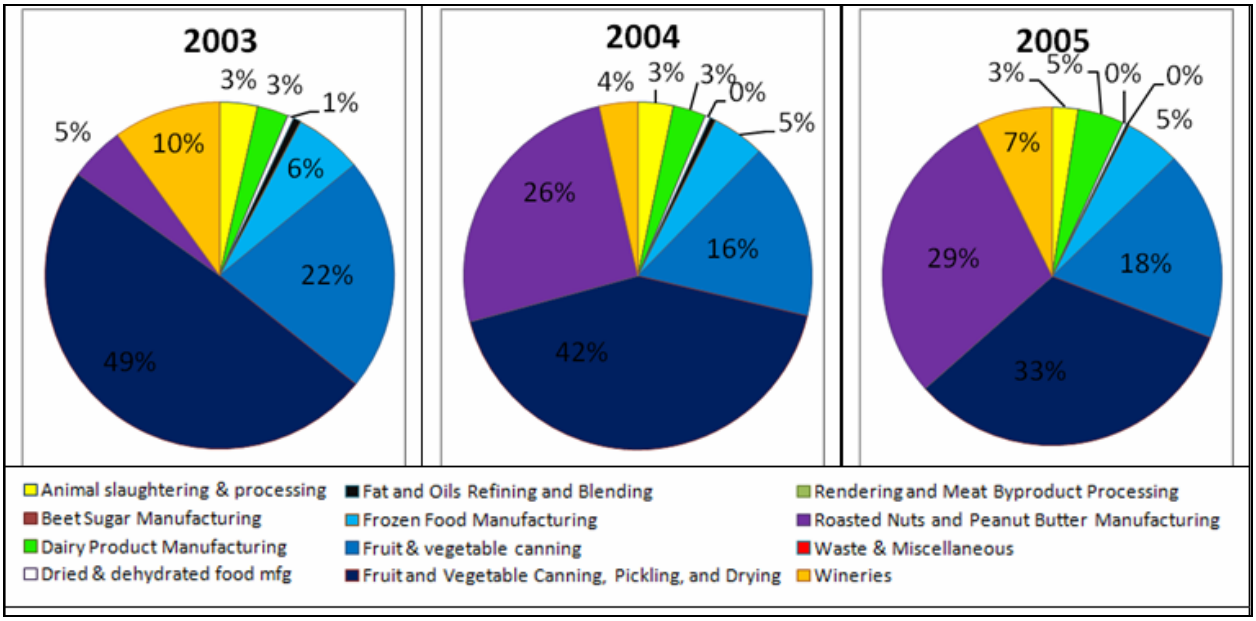

Figure 9

Percent of total FDS loads (metric tons) for Tulare Lake Basin by industry

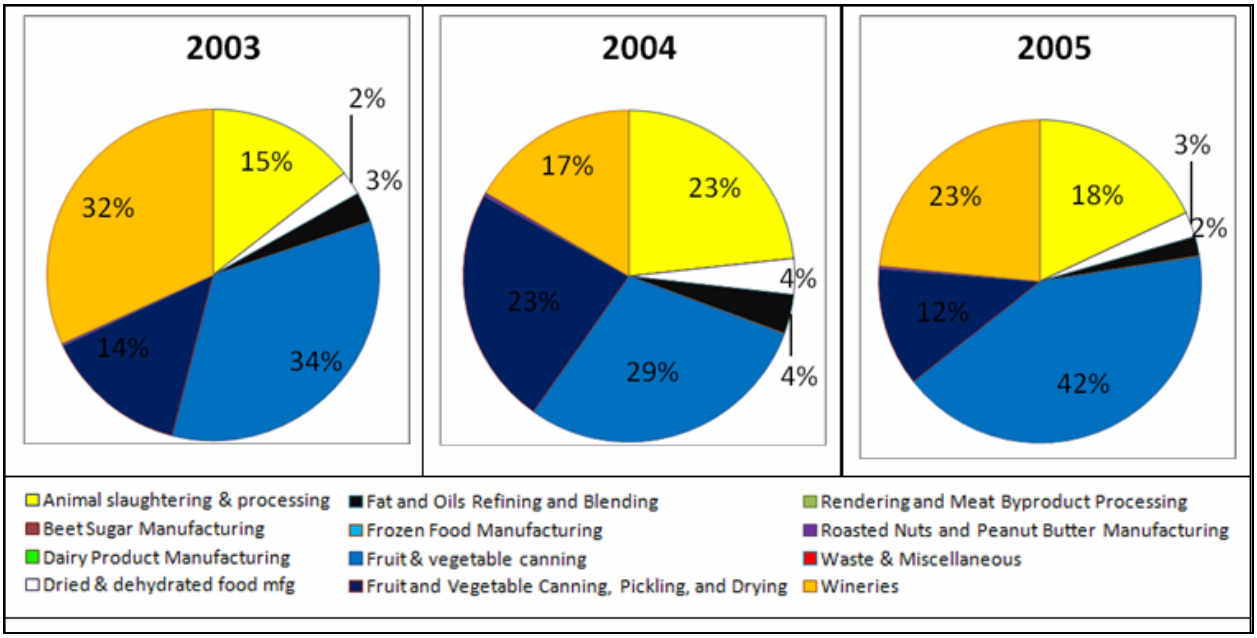

Figure 10

Percent of total FDS loads (metric tons) for Fresno County by industry

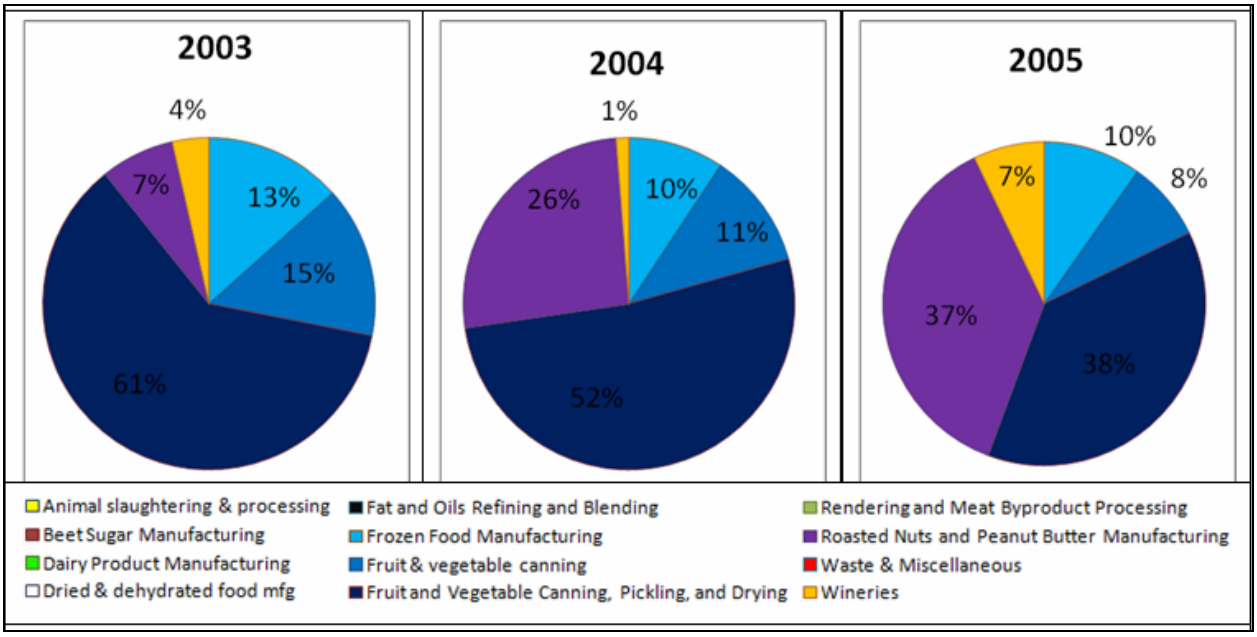

Figure 11

Percent of total FDS loads (metric tons) for Kern County by industry

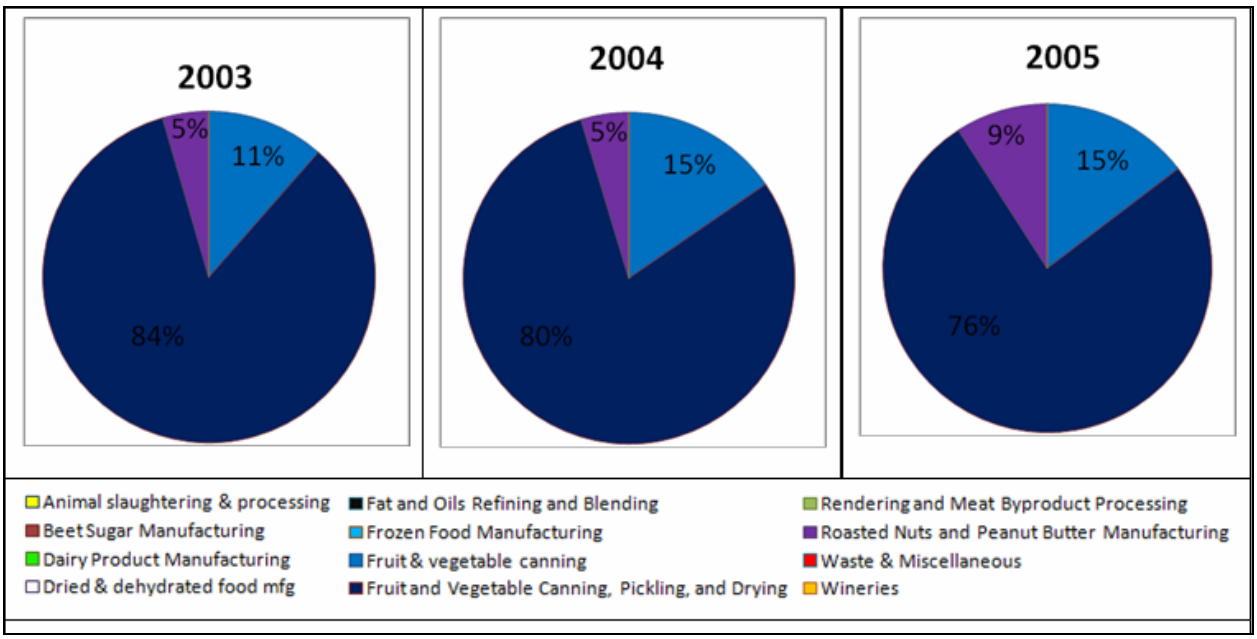

Figure 12

Percent of total FDS loads (metric tons) for Kings County by industry

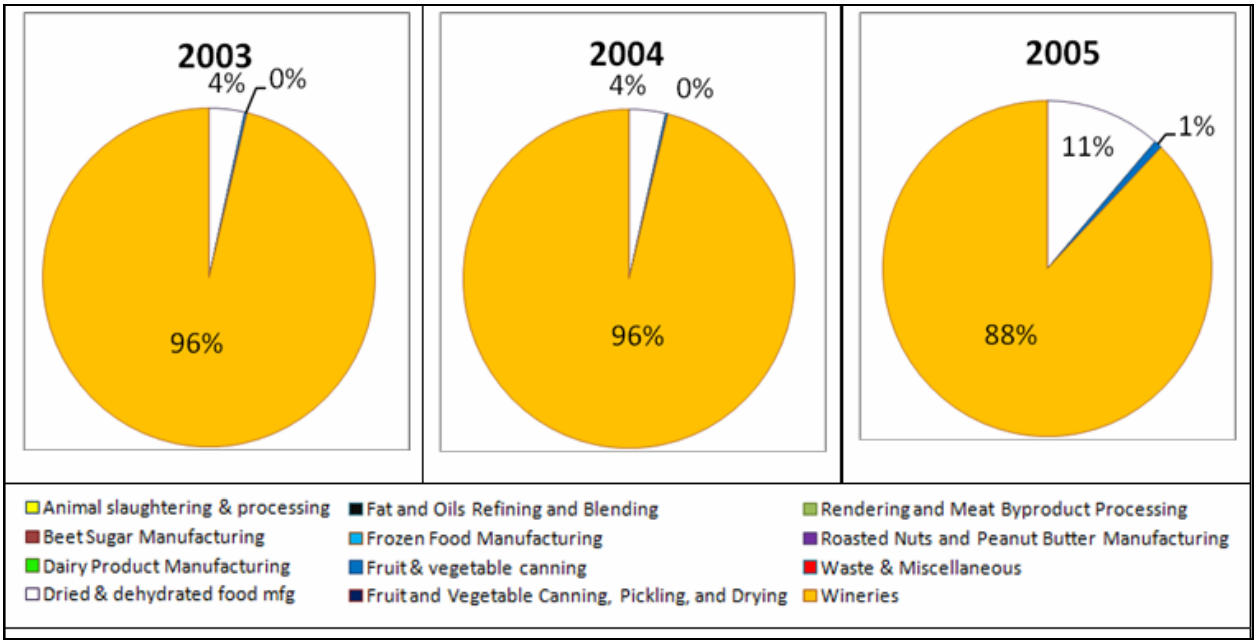

Figure 13

Percent of total FDS loads (metric tons) for Madera County by industry

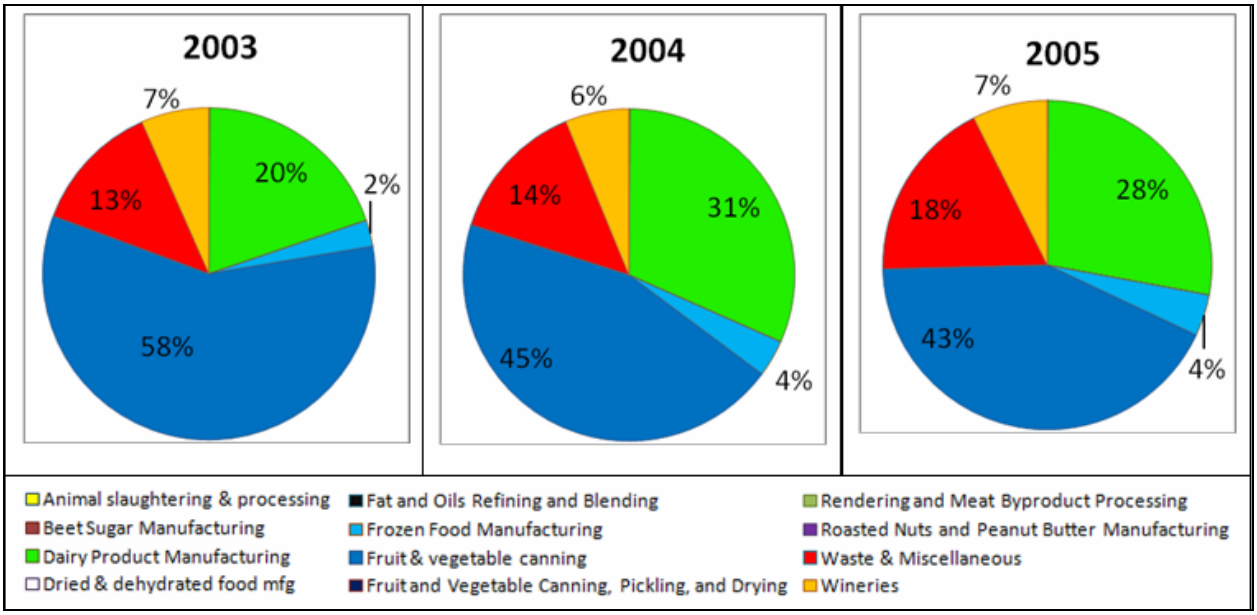

Figure 14

Percent of total FDS loads (metric tons) for Merced County by industry

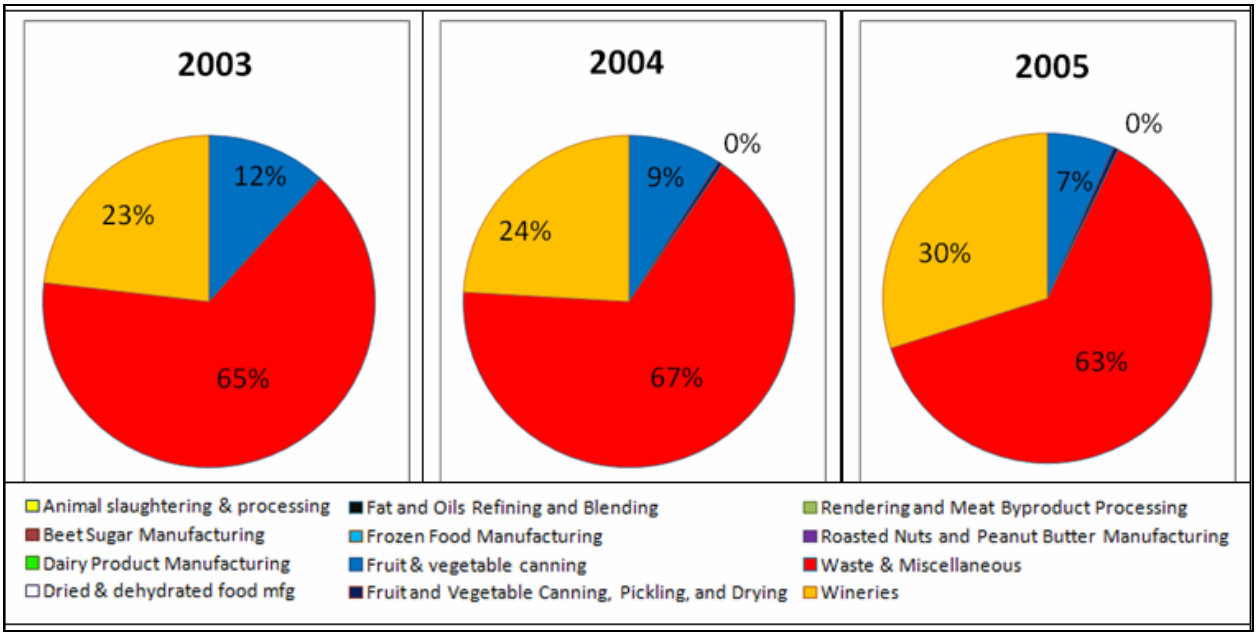

Figure 15

Percent of total FDS loads (metric tons) for San Joaquin County by industry

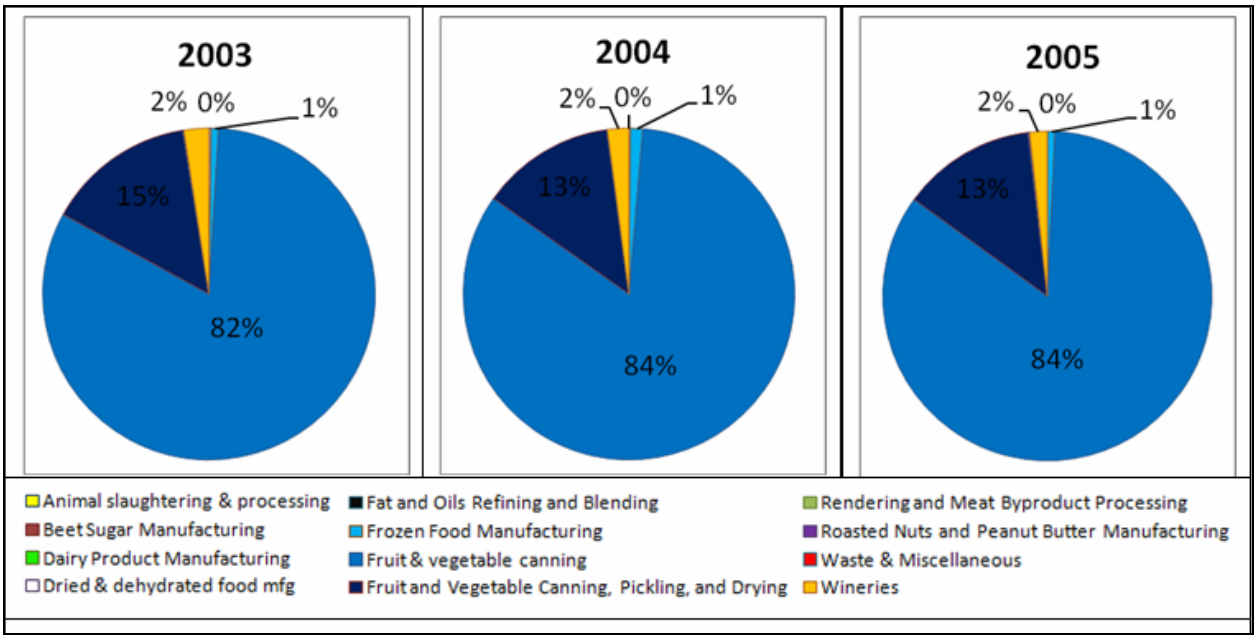

Figure 16

Percent of total FDS loads (metric tons) for Stanislaus County by industry

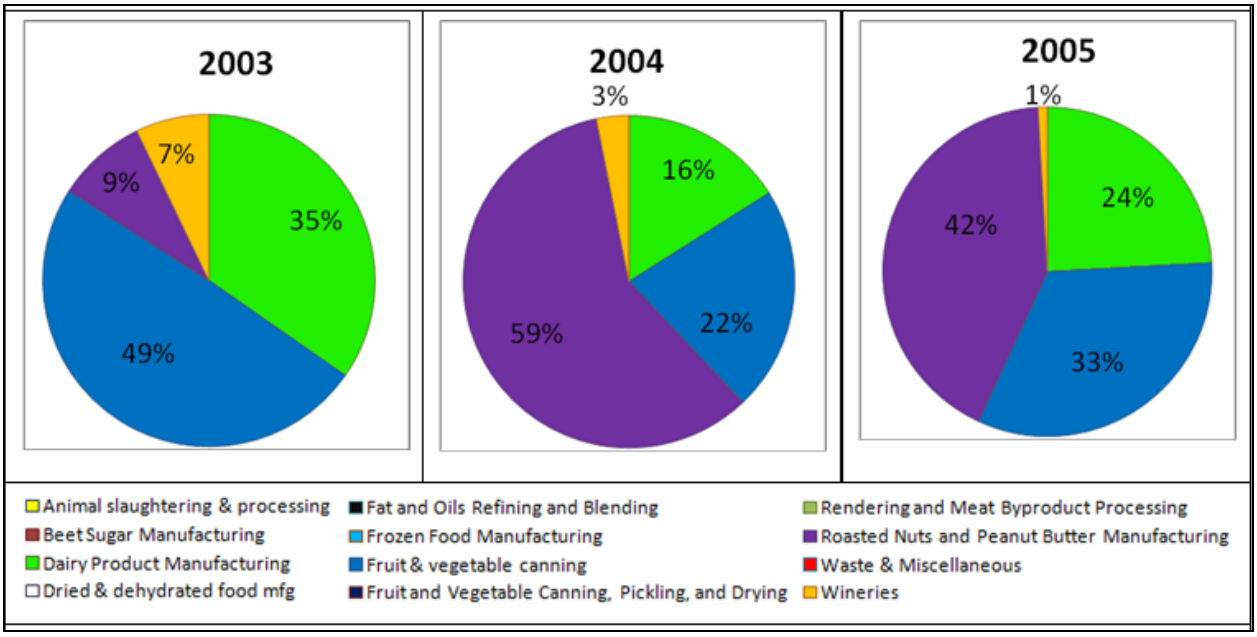

Figure 17

Percent of total FDS loads (metric tons) for Tulare County by industry

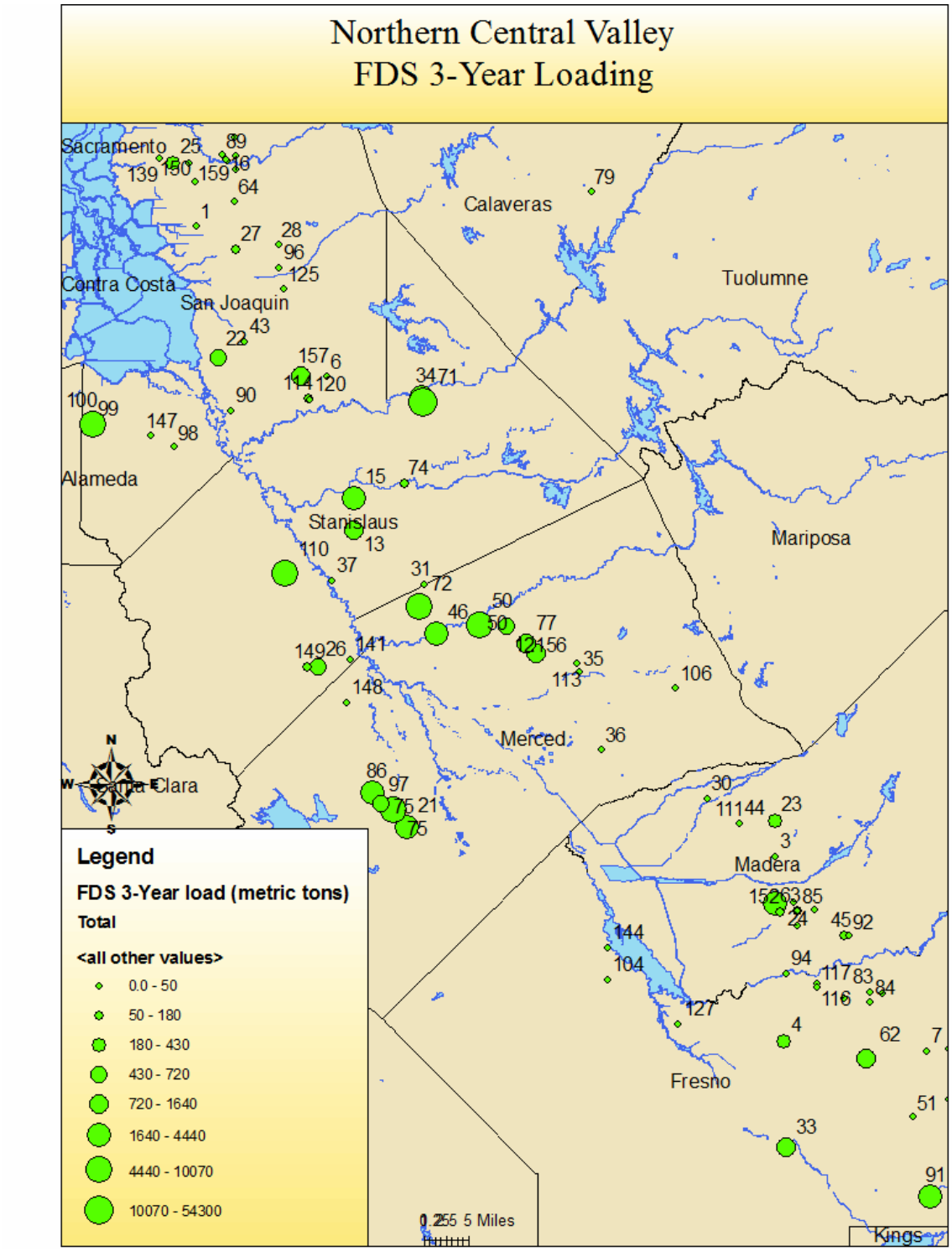

Figure 18

FDS 3-year load for northern Central Valley processors (metric tons). Gap filling as described in text was used. Numbers correspond to entries in Table 1.

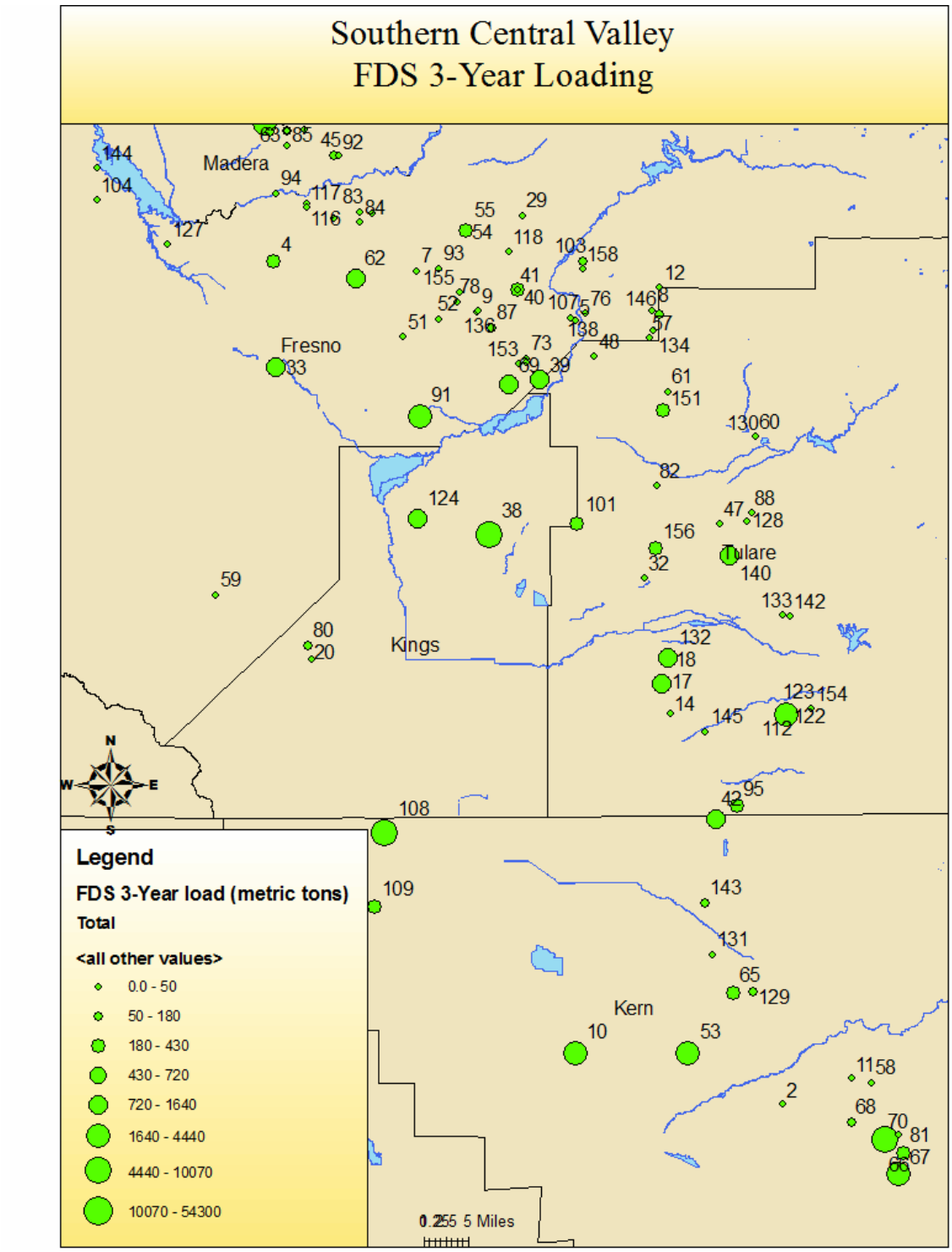

Figure 19

FDS 3-year load for southern Central Valley processors (metric tons). Gap filling as described in text was used. Numbers correspond to entries in Table 1.

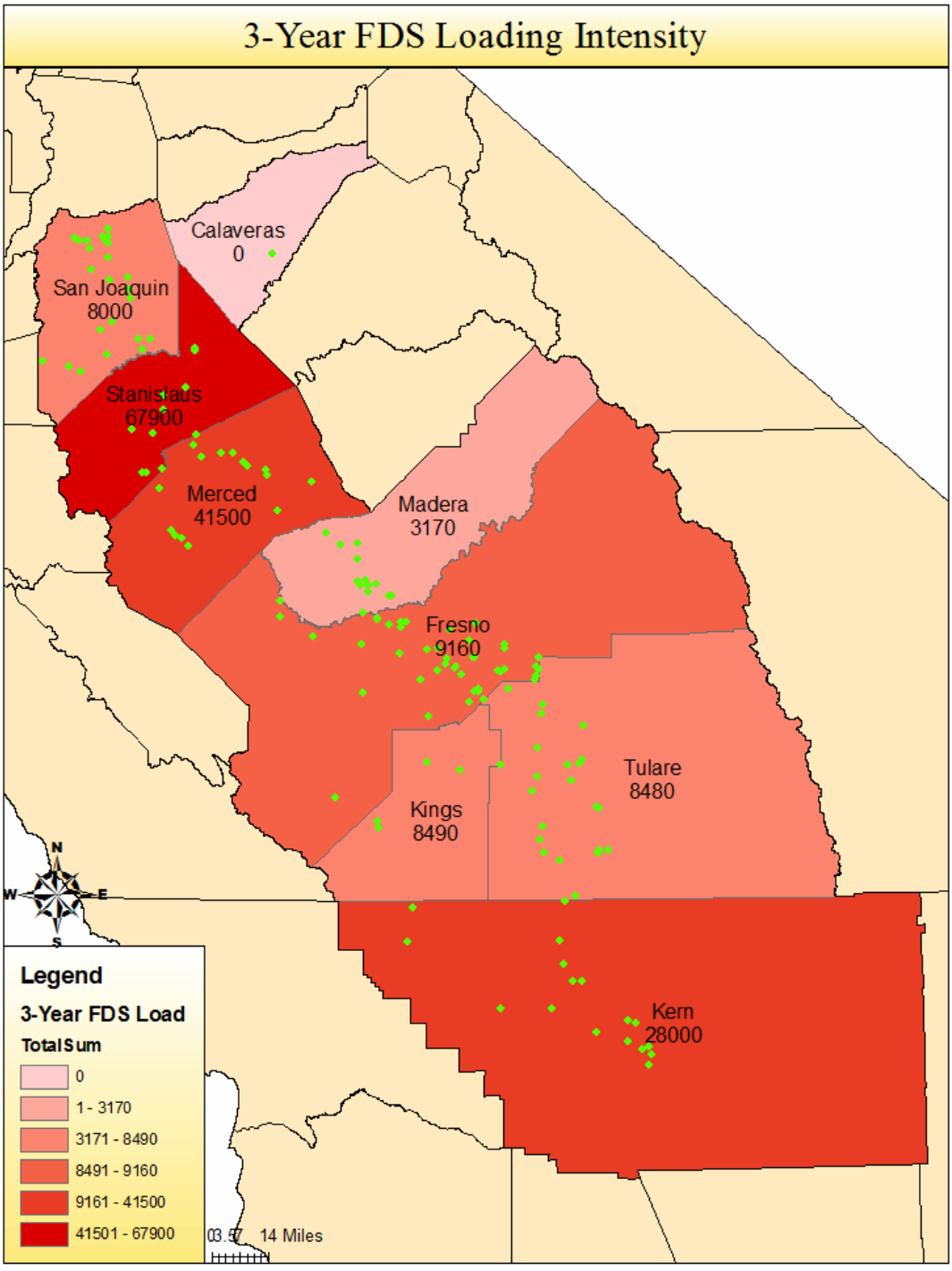

Figure 20

FDS 3-year total loading intensity (metric tons). Gap filling as described in text was used, 61% of processors reporting.

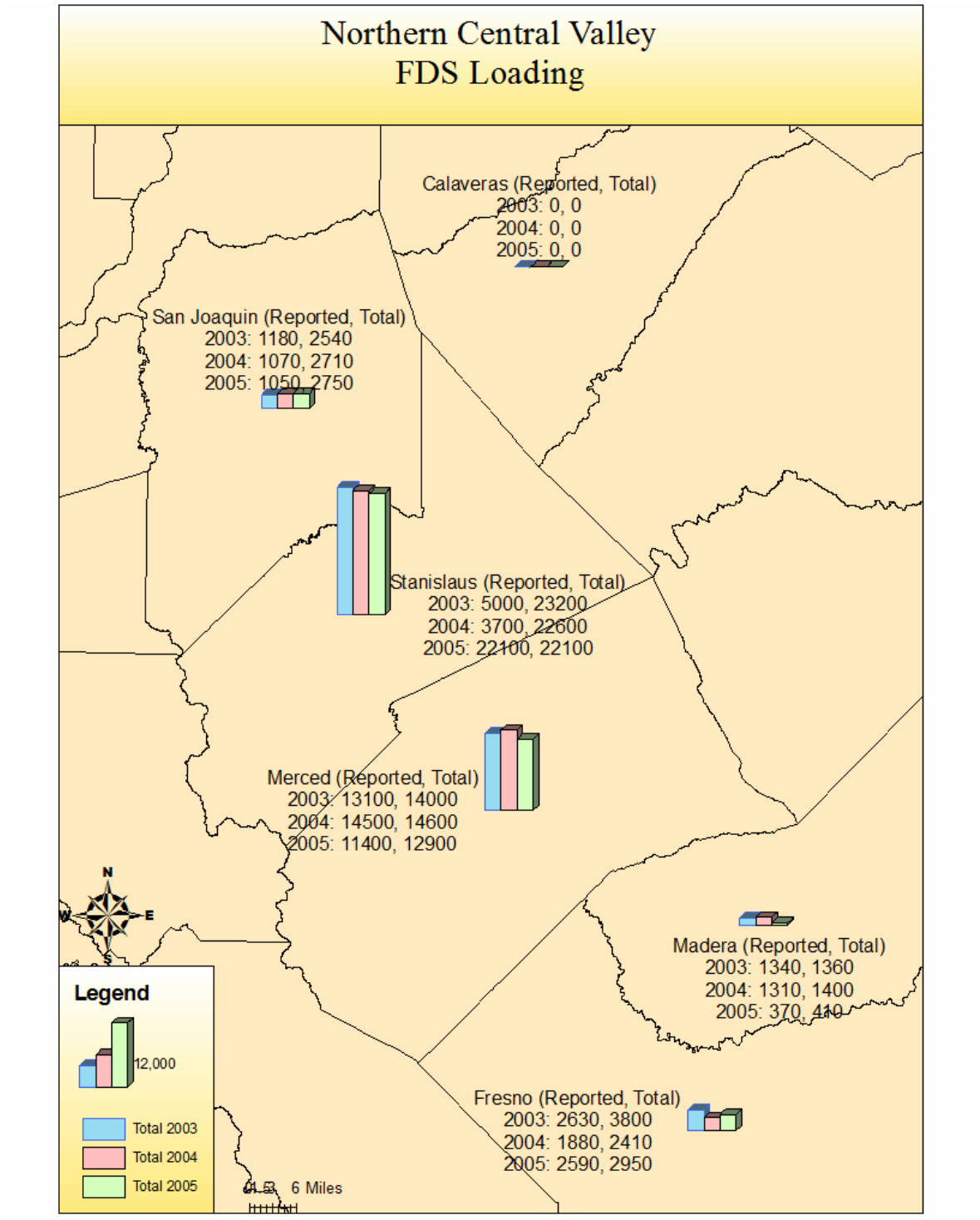

Figure 21A

Southern Central Valley FDS loading for 2003, 2004 and 2005 (metric tons), bars include gap filling as described in text. Actual reported loads and total with gap filling shown in labels, 61% of processors reporting.

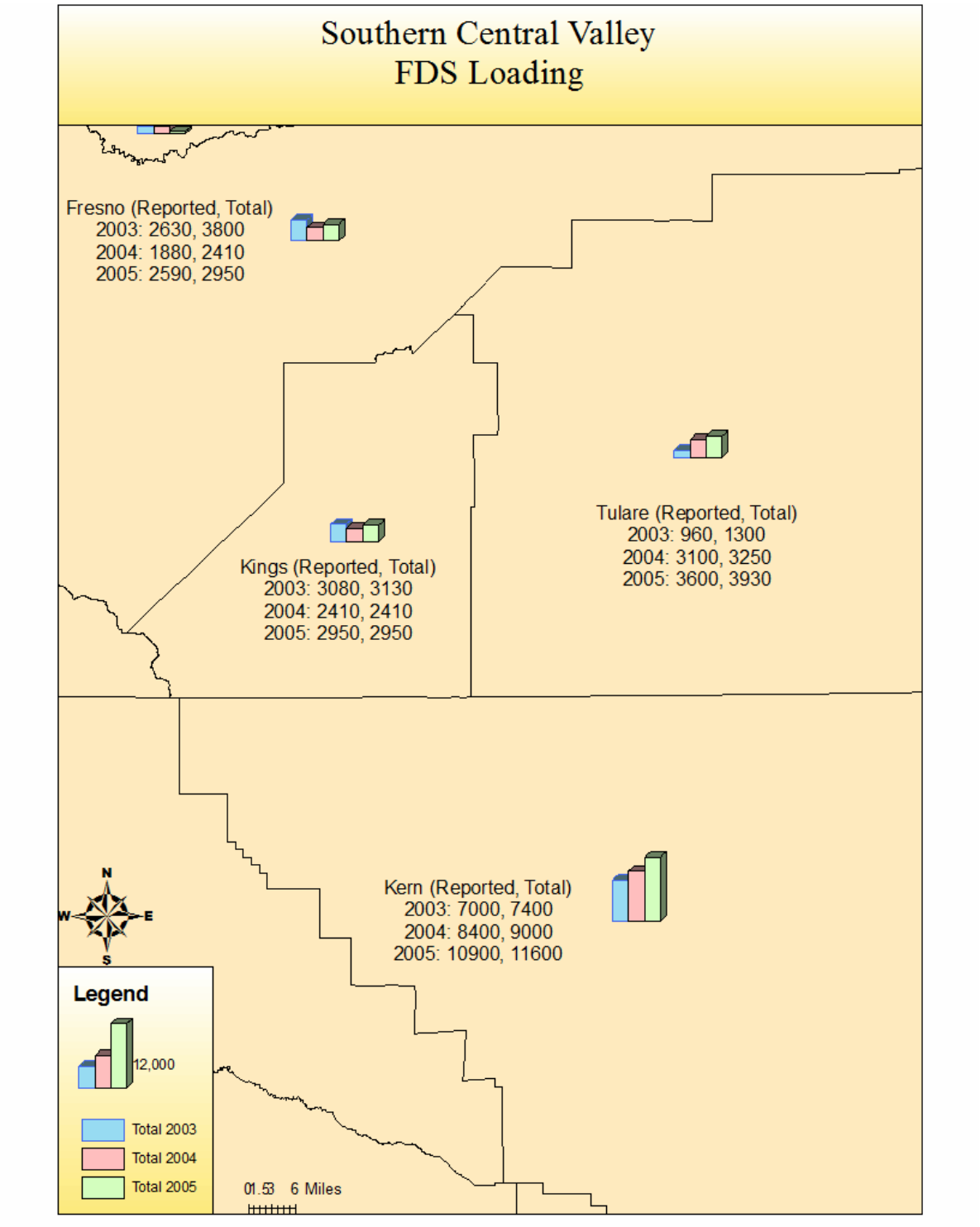

Figure 21B

Northern Central Valley FDS loading for 2003, 2004 and 2005 (metric tons), bars include gap filling as described in text. Actual reported loads and total with gap filling shown in labels, 61% of processors reporting.

Gap-filled loads shown in the Figures above represent the use of data from 61% of processors, those which report effluent volume as well as FDS or EC. Loads from processors reporting only volume data can be estimated from the industry volume weighted effluent salinity concentration observed in processors reporting salinity parameters. Industry volume weighted concentrations calculated by Equation 2 used for this gap-filling are shown in Table 6. This final form of gap-filling is also speculative in nature because it assumes the applicability of industrial averages for those processors with unreported FDS and EC measurements. However the contribution from this class of non-reporting facilities is relatively small because generally the smaller processors are those not reporting salinity parameters. Figure 23 and 24 are similar to Figures 21A and 21B except estimates of loads from processors reporting only volume have been included. 74% of processors reported at least volume data and are included in these Figures. The additional estimates of loads for processors reporting only volume data accounted for under 2% of the total Central Valley FDS load.

Table 6

NAICS Code	Industry Volume Weighted Average FDS Concentration (mg/L)	
31161	Animal slaughtering & processing	685
311313	Beet Sugar Manufacturing	No Data
3115	Dairy Product Manufacturing	943
311423	Dried & dehydrated food mfg	465
311225	Fat and Oils Refining and Blending	722
31141	Frozen Food Manufacturing	701
311421	Fruit & vegetable canning	312
31142	Fruit and Vegetable Canning, Pickling, and Drying	747
311613	Rendering and Meat Byproduct Processing	No Data
311911	Roasted Nuts and Peanut Butter Manufacturing	2400
unknown	Waste & Miscellaneous	1070
31213	Wineries	976

Industry volume weighted average FDS concentrations calculated from Equation 2 using data from processors reporting effluent volume and salinity concentrations. These concentrations are used to estimate loads for processors reporting only effluent volume data.

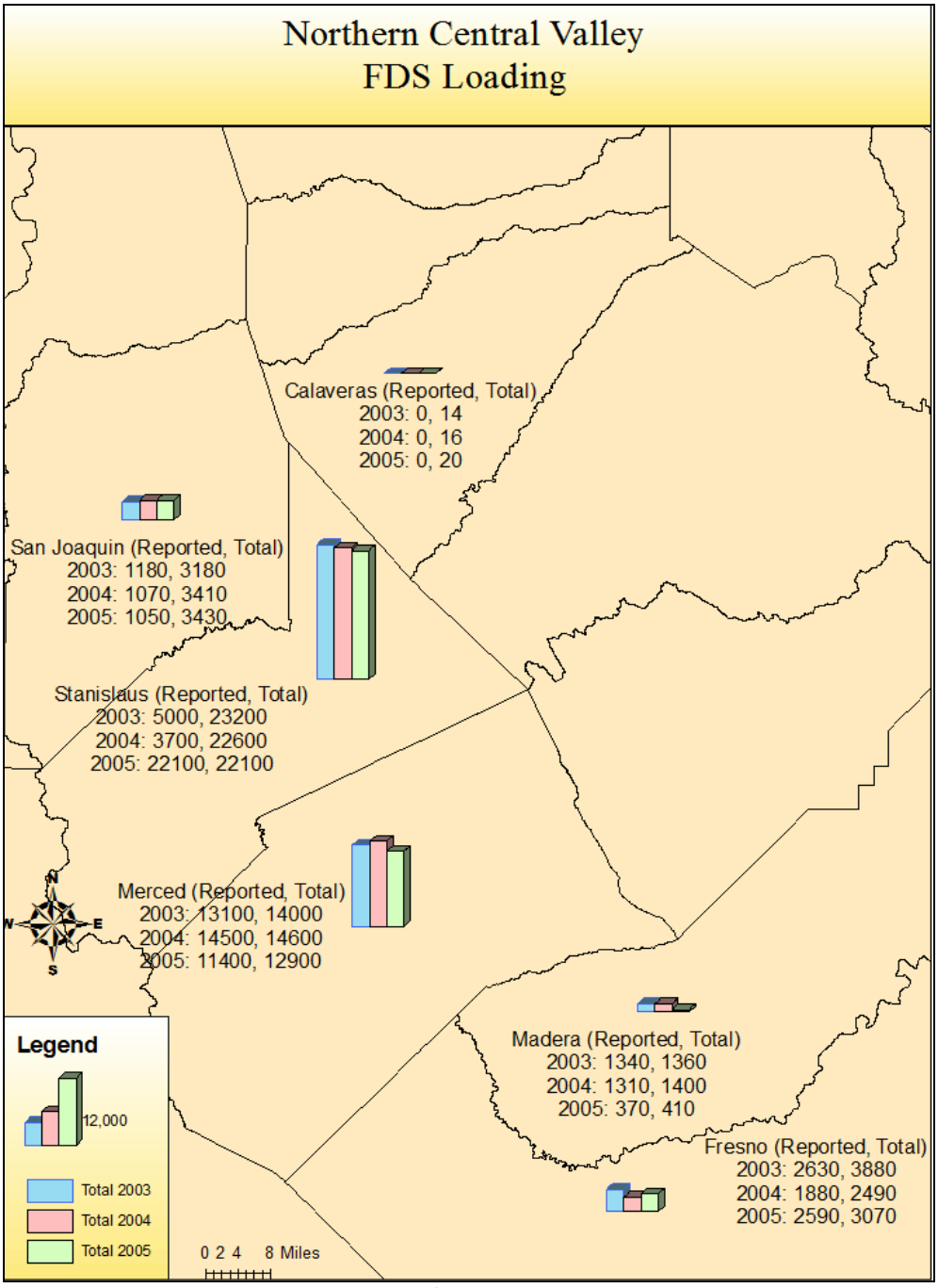

Figure 22

Northern Central Valley FDS loading for 2003, 2004 and 2005 (metric tons), bars include gap filling as described in text. Actual reported loads and total with gap filling shown in labels. 74% of processors reporting.

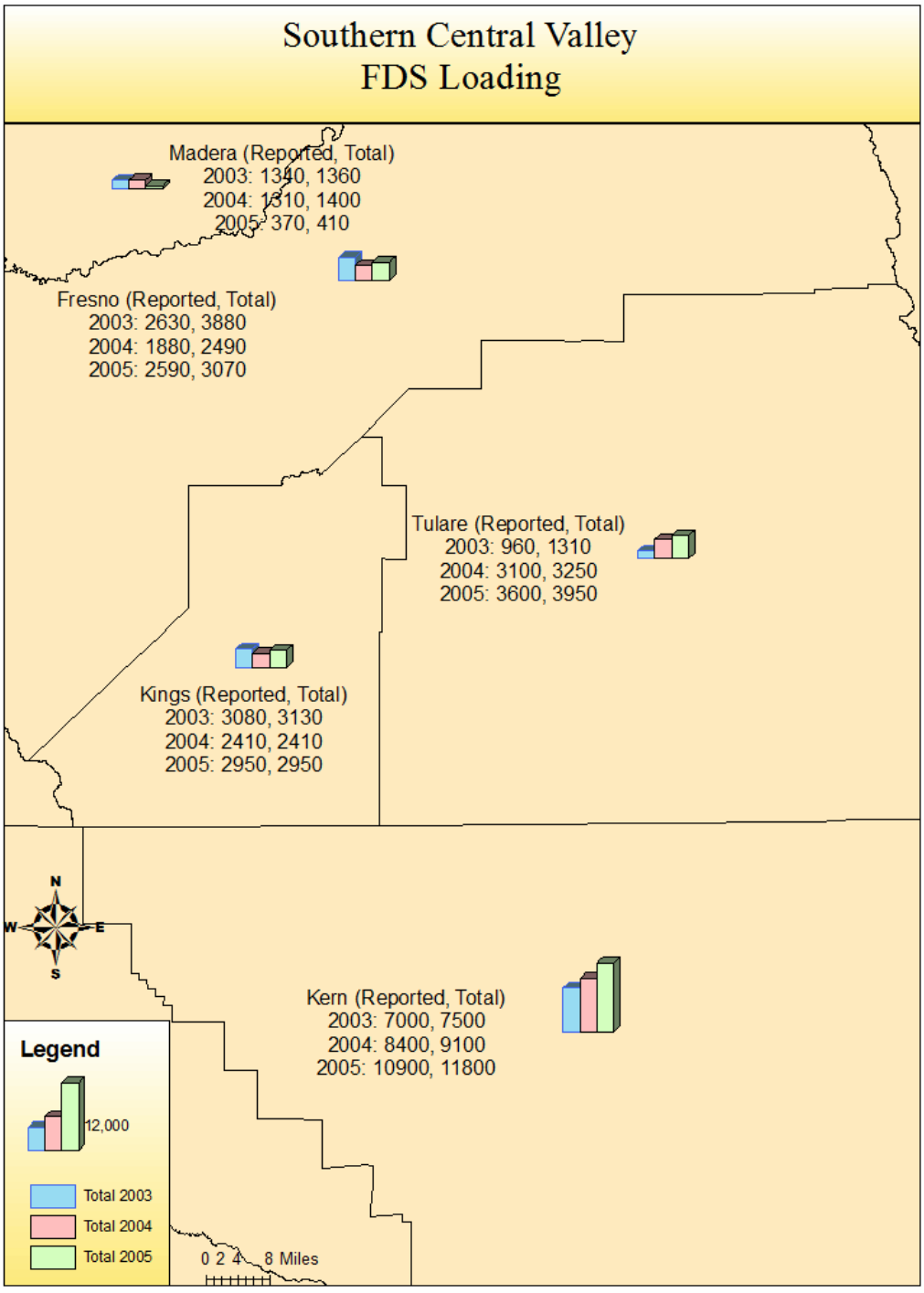

Figure 23

Southern Central Valley FDS loading for 2003, 2004 and 2005 (metric tons), bars include gap filling as described in text. Actual reported loads and total with gap filling shown in labels. 74% of processors reporting.

1. Nitrate and Ammonium Loads

In addition to FDS loads, Nitrate (NO_3^-) and Ammonium (NH_4^+) loads were also computed across the central valley. Ammonium loads in metric tons are reported in Tables 7 and 8 and nitrate loads are reported in Tables 9 and 10.

Table 7: Ammonium (NH4) loads in metric tons, gap filling as described in text was used for total load columns. See Figure 2 for map of areas in table. 21% of processors reported NH4

		NH4 Loads (metric tons)					
	Industry	Reported 2003 Load	Total 2003 Load With Gap Filling	Reported 2004 Load	Total 2004 Load With Gap Filling	Reported 2005 Load	Total 2005 Load With Gap Filling
Total For C	Total	157	160	180	201	244	255
	Animal slaughtering & processing	0	0.5	0.52	0.55	0.44	0.44
	Beet Sugar Manufacturing	0	0	0	0	0	0
	Dairy Product Manufacturing	52.6	52.9	38.9	57.7	89	90.1
	Dried & dehydrated food mfg	0.36	0.76	0.27	0.7	0.26	0.69
	Fat and Oils Refining and Blending	0	0	0	0	0	0
	Frozen Food Manufacturing	1.04	1.04	1.48	1.48	1.88	1.88
	Fruit & vegetable canning	30.6	30.9	22.7	22.9	20.6	20.8
	Fruit and Vegetable Canning, Pickling, and Drying	5.63	5.63	5.05	5.45	13.4	13.5
	Rendering and Meat Byproduct Processing	0	0	0	0	0	0
	Roasted Nuts and Peanut Butter Manufacturing	1.13	1.23	2.57	3.19	0	2.21
	Waste & Miscellaneous	44.7	44.7	74.2	74	104	104
	Wineries	21.3	22	34.4	35	15	21
San Joaqu	Total	134	135	159	178	215	216
	Animal slaughtering & processing	0	0.5	0.52	0.55	0.44	0.44
	Beet Sugar Manufacturing	0	0	0	0	0	0
	Dairy Product Manufacturing	52.6	52.9	38.9	57.7	89	90.1
	Dried & dehydrated food mfg	0	0	0	0	0	0
	Fat and Oils Refining and Blending	0	0	0	0	0	0
	Frozen Food Manufacturing	0	0	0	0	0	0
	Fruit & vegetable canning	15.9	16	12.3	12.4	10	10.1
	Fruit and Vegetable Canning, Pickling, and Drying	0	0	0	0	0	0
	Rendering and Meat Byproduct Processing	0	0	0	0	0	0
	Roasted Nuts and Peanut Butter Manufacturing	0	0	0	0	0	0
	Waste & Miscellaneous	44.7	44.7	74.2	74.2	104	104
	Wineries	20.5	20.5	33	33.1	11.2	11.3
Tulare Lak	Total	23.7	25	21.1	23.2	29.6	38.6
	Animal slaughtering & processing	0	0	0	0	0	0
	Beet Sugar Manufacturing	0	0	0	0	0	0
	Dairy Product Manufacturing	0	0	0	0	0	0
	Dried & dehydrated food mfg	0.36	0.76	0.27	0.7	0.26	0.69
	Fat and Oils Refining and Blending	0	0	0	0	0	0
	Frozen Food Manufacturing	1.04	1.04	1.48	1.48	1.88	1.88
	Fruit & vegetable canning	14.7	14.8	10.3	10.4	10.6	10.7
	Fruit and Vegetable Canning, Pickling, and Drying	5.63	5.63	5.05	5.45	13.4	13.5
	Rendering and Meat Byproduct Processing	0	0	0	0	0	0
	Roasted Nuts and Peanut Butter Manufacturing	1.13	1.23	2.57	3.19	0	2.21
	Waste & Miscellaneous	0	0	0	0	0	0
	Wineries	0.82	1.47	1.42	1.96	3.42	9.61

Table 8: Ammonium (NH4) loads in metric tons, 21% of processors reported NH4

NH4 Loads	Calaveras	Fresno	Kern	Kings	Madera	Merced	San Joaquin	Stanislaus	Tulare	Total
Animal slaughtering & processing										
Reported 2003 Load	0	0	0	0	0	0	0	0	0	0
Total 2003 Load With Gap Filling	0	0	0	0	0	0.5	0	0	0	0.5
Reported 2004 Load	0	0	0	0	0	0.52	0	0	0	0.52
Total 2004 Load With Gap Filling	0	0	0	0	0	0.55	0	0	0	0.55
Reported 2005 Load	0	0	0	0	0	0.44	0	0	0	0.44
Total 2005 Load With Gap Filling	0	0	0	0	0	0.44	0	0	0	0.44
Beet Sugar Manufacturing										
Reported 2003 Load	0	0	0	0	0	0	0	0	0	0
Total 2003 Load With Gap Filling	0	0	0	0	0	0	0	0	0	0
Reported 2004 Load	0	0	0	0	0	0	0	0	0	0
Total 2004 Load With Gap Filling	0	0	0	0	0	0	0	0	0	0
Reported 2005 Load	0	0	0	0	0	0	0	0	0	0
Total 2005 Load With Gap Filling	0	0	0	0	0	0	0	0	0	0
Dairy Product Manufacturing										
Reported 2003 Load	0	0	0	0	0	52.6	0	0	0	52.6
Total 2003 Load With Gap Filling	0	0	0	0	0	52.9	0	0	0	52.9
Reported 2004 Load	0	0	0	0	0	38.9	0	0	0	38.9
Total 2004 Load With Gap Filling	0	0	0	0	0	57.7	0	0	0	57.7
Reported 2005 Load	0	0	0	0	0	89	0	0	0	89
Total 2005 Load With Gap Filling	0	0	0	0	0	90.1	0	0	0	90.1
Dried & dehydrated food mfg										
Reported 2003 Load	0	0.36	0	0	0	0	0	0	0	0.36
Total 2003 Load With Gap Filling	0	0.76	0	0	0	0	0	0	0	0.76
Reported 2004 Load	0	0.27	0	0	0	0	0	0	0	0.27
Total 2004 Load With Gap Filling	0	0.7	0	0	0	0	0	0	0	0.7
Reported 2005 Load	0	0.26	0	0	0	0	0	0	0	0.26
Total 2005 Load With Gap Filling	0	0.69	0	0	0	0	0	0	0	0.69
Fat and Oils Refining and Blending										
Reported 2003 Load	0	0	0	0	0	0	0	0	0	0
Total 2003 Load With Gap Filling	0	0	0	0	0	0	0	0	0	0
Reported 2004 Load	0	0	0	0	0	0	0	0	0	0
Total 2004 Load With Gap Filling	0	0	0	0	0	0	0	0	0	0
Reported 2005 Load	0	0	0	0	0	0	0	0	0	0
Total 2005 Load With Gap Filling	0	0	0	0	0	0	0	0	0	0
Frozen Food Manufacturing										
Reported 2003 Load	0	0	1.04	0	0	0	0	0	0	1.04
Total 2003 Load With Gap Filling	0	0	1.04	0	0	0	0	0	0	1.04
Reported 2004 Load	0	0	1.48	0	0	0	0	0	0	1.48
Total 2004 Load With Gap Filling	0	0	1.48	0	0	0	0	0	0	1.48
Reported 2005 Load	0	0	1.88	0	0	0	0	0	0	1.88
Total 2005 Load With Gap Filling	0	0	1.88	0	0	0	0	0	0	1.88
Fruit & vegetable canning										
Reported 2003 Load	0	10.7	0	4	0	15.8	0.11	0	0	30.6
Total 2003 Load With Gap Filling	0	10.7	0	4	0.14	15.8	0.11	0	0.1	30.9
Reported 2004 Load	0	4.08	0	6.23	0.04	10.8	1.44	0	0.01	22.7
Total 2004 Load With Gap Filling	0	4.08	0	6.23	0.14	10.8	1.44	0	0.1	22.9
Reported 2005 Load	0	7.57	0	3.04	0	9.3	0.68	0	0	20.6
Total 2005 Load With Gap Filling	0	7.57	0	3.04	0.14	9.3	0.68	0	0.1	20.8
Fruit and Vegetable Canning, Pickling, and Drying										
Reported 2003 Load	0	0.39	5.24	0	0	0	0	0	0	5.63
Total 2003 Load With Gap Filling	0	0.39	5.24	0	0	0	0	0	0	5.63
Reported 2004 Load	0	0	5.05	0	0	0	0	0	0	5.05
Total 2004 Load With Gap Filling	0	0.26	5.19	0	0	0	0	0	0	5.45
Reported 2005 Load	0	0.13	13.3	0	0	0	0	0	0	13.4
Total 2005 Load With Gap Filling	0	0.13	13.4	0	0	0	0	0	0	13.5
Rendering and Meat Byproduct Processing										
Reported 2003 Load	0	0	0	0	0	0	0	0	0	0
Total 2003 Load With Gap Filling	0	0	0	0	0	0	0	0	0	0
Reported 2004 Load	0	0	0	0	0	0	0	0	0	0
Total 2004 Load With Gap Filling	0	0	0	0	0	0	0	0	0	0
Reported 2005 Load	0	0	0	0	0	0	0	0	0	0
Total 2005 Load With Gap Filling	0	0	0	0	0	0	0	0	0	0
Roasted Nuts and Peanut Butter Manufacturing										
Reported 2003 Load	0	0.06	0	0.04	0	0	0	0	1.03	1.13
Total 2003 Load With Gap Filling	0	0.06	0	0.14	0	0	0	0	1.03	1.23
Reported 2004 Load	0	0	0	0	0	0	0	0	2.57	2.57
Total 2004 Load With Gap Filling	0	0.06	0	0.14	0	0	0	0	2.98	3.19
Reported 2005 Load	0	0	0	0	0	0	0	0	0	0
Total 2005 Load With Gap Filling	0	0.06	0	0.14	0	0	0	0	2	2.21
Waste & Miscellaneous										
Reported 2003 Load	0	0	0	0	0	44.7	0	0	0	44.7
Total 2003 Load With Gap Filling	0	0	0	0	0	44.7	0	0	0	44.7
Reported 2004 Load	0	0	0	0	0	74.2	0	0	0	74.2
Total 2004 Load With Gap Filling	0	0	0	0	0	74.2	0	0	0	74.2
Reported 2005 Load	0	0	0	0	0	104.2	0	0	0	104
Total 2005 Load With Gap Filling	0	0	0	0	0	104.2	0	0	0	104
Wineries										
Reported 2003 Load	0	0.22	0.04	0	0.09	20.4	0.01	0	0.55	21.3
Total 2003 Load With Gap Filling	0	0.88	0.04	0	0.12	20.4	0.02	0	0.55	22
Reported 2004 Load	0	0.03	1.25	0	0.03	32.9	0.04	0	0.13	34.4
Total 2004 Load With Gap Filling	0	0.11	1.25	0	0.13	32.9	0.07	0	0.6	35.1
Reported 2005 Load	0	2.36	0	0	0.12	11.1	0.06	0	1.06	14.7
Total 2005 Load With Gap Filling	0	7.36	0.65	0	0.13	11.1	0.1	0	1.6	20.9
Totals										
Reported 2003 Load	0	11.8	6	4	0.1	133	0.1	0	1.6	157
Total 2003 Load With Gap Filling	0	12.8	6	4.1	0.3	134	0.1	0	1.7	160
Reported 2004 Load	0	4.4	8	6.2	0.1	157	1.5	0	2.7	180
Total 2004 Load With Gap Filling	0	5.2	8	6.4	0.3	176	1.5	0	3.7	201
Reported 2005 Load	0	10.3	15	3	0.1	214	0.7	0	1.1	244
Total 2005 Load With Gap Filling	0	15.8	16	3.2	0.3	215	0.8	0	3.7	255

Table 9: Nitrate (NO3) loads in metric tons, gap filling as described in text was used for total load columns. See Figure 2 for map of areas in table. 55% of processors reported NO3

		NO3 Loads (metric tons)					
	Industry	Reported 2003 Load	Total 2003 Load With Gap Filling	Reported 2004 Load	Total 2004 Load With Gap Filling	Reported 2005 Load	Total 2005 Load With Gap Filling
Total For Central Valley	Total	167	424	157	428	113	362
	Animal slaughtering & processing	0	0	0	0	0	0
	Beet Sugar Manufacturing	0	0	0	0	0	0
	Dairy Product Manufacturing	87	90	54	58	6.4	10
	Dried & dehydrated food mfg	1.9	2.3	1	1.7	0.9	1.2
	Fat and Oils Refining and Blending	0	0	0	0	0	0
	Frozen Food Manufacturing	12	12	17	17	8.1	8.1
	Fruit & vegetable canning	14	254	15	253	26	253
	Fruit and Vegetable Canning, Pickling, and Drying	24	26	26	47	56	61
	Rendering and Meat Byproduct Processing	0.1	0.1	0	0	0	0
	Roasted Nuts and Peanut Butter Manufacturing	0	6.5	3.4	6.9	3.2	7.5
	Waste & Miscellaneous	5.3	7.3	5.2	5.4	1.2	3.3
	Wineries	23	25	36	40	11	18
San Joaquin River Basin	Total	127	373	88	350	74	309
	Animal slaughtering & processing	0	0	0	0	0	0
	Beet Sugar Manufacturing	0	0	0	0	0	0
	Dairy Product Manufacturing	87	90	54	58	6	10
	Dried & dehydrated food mfg	0.8	1	0.3	0.7	0.1	0.1
	Fat and Oils Refining and Blending	0	0	0	0	0	0
	Frozen Food Manufacturing	3.9	3.9	7.9	7.9	1.7	1.7
	Fruit & vegetable canning	8.2	248	6.5	244	19	245
	Fruit and Vegetable Canning, Pickling, and Drying	3.1	3.1	1.6	19.9	36.8	36.8
	Rendering and Meat Byproduct Processing	0.1	0.1	0	0	0	0
	Roasted Nuts and Peanut Butter Manufacturing	0	0	0	0	0	0
	Waste & Miscellaneous	5.3	7.3	5.2	5.4	1.2	3.3
	Wineries	19	20	13	14	8.4	12
Tulare Lake Basin	Total	40	51	69	79	39	52
	Animal slaughtering & processing	0	0	0	0	0	0
	Beet Sugar Manufacturing	0	0	0	0	0	0
	Dairy Product Manufacturing	0	0	0	0	0	0
	Dried & dehydrated food mfg	1.1	1.3	0.7	1	0.8	1.1
	Fat and Oils Refining and Blending	0	0	0	0	0	0
	Frozen Food Manufacturing	8	8	8.7	8.7	6.4	6.4
	Fruit & vegetable canning	6	6.8	8.5	9.1	6.9	7.6
	Fruit and Vegetable Canning, Pickling, and Drying	21	23	25	27	19	24
	Rendering and Meat Byproduct Processing	0	0	0	0	0	0
	Roasted Nuts and Peanut Butter Manufacturing	0	6.5	3.4	6.9	3.2	7.5
	Waste & Miscellaneous	0	0	0	0	0	0
	Wineries	4	5.6	23	26	2.7	5.5

Table 10: Nitrate (NO3) loads in metric tons, 55% of processors reported NO3

	Calaveras	Fresno	Kern	Kings	Madera	Merced	San Joaquin	Stanislaus	Tulare	Total
Animal slaughtering & processing										
Reported 2003 Load	0	0	0	0	0	0.02	0.01	0	0	0.02
Total 2003 Load With Gap Filling	0	0	0	0	0	0.02	0.01	0	0	0.02
Reported 2004 Load	0	0	0	0	0	0.01	0.01	0	0	0.02
Total 2004 Load With Gap Filling	0	0	0	0	0	0.01	0.01	0	0	0.02
Reported 2005 Load	0	0	0	0	0	0.01	0	0	0	0.01
Total 2005 Load With Gap Filling	0	0	0	0	0	0.01	0	0	0	0.01
Beet Sugar Manufacturing										
Reported 2003 Load	0	0	0	0	0	0	0	0	0	0
Total 2003 Load With Gap Filling	0	0	0	0	0	0	0	0	0	0
Reported 2004 Load	0	0	0	0	0	0	0	0	0	0
Total 2004 Load With Gap Filling	0	0	0	0	0	0	0	0	0	0
Reported 2005 Load	0	0	0	0	0	0	0	0	0	0
Total 2005 Load With Gap Filling	0	0	0	0	0	0	0	0	0	0
Dairy Product Manufacturing										
Reported 2003 Load	0	0	0	0	0	86.9	0	0	0	86.9
Total 2003 Load With Gap Filling	0	0	0	0	0	90.5	0	0	0	90.5
Reported 2004 Load	0	0	0	0	0	53.9	0	0	0	53.9
Total 2004 Load With Gap Filling	0	0	0	0	0	58	0	0	0	58
Reported 2005 Load	0	0	0	0	0	6.4	0	0	0	6.4
Total 2005 Load With Gap Filling	0	0	0	0	0	10.2	0	0	0	10.2
Dried & dehydrated food mfg										
Reported 2003 Load	0	1.05	0	0	0.32	0	0	0.49	0	1.85
Total 2003 Load With Gap Filling	0	1.27	0	0	0.53	0	0	0.49	0	2.28
Reported 2004 Load	0	0.73	0	0	0.32	0	0	0	0	1.05
Total 2004 Load With Gap Filling	0	0.99	0	0	0.46	0	0	0.27	0	1.72
Reported 2005 Load	0	0.83	0	0	0.03	0	0	0.06	0	0.91
Total 2005 Load With Gap Filling	0	1.07	0	0	0.08	0	0	0.06	0	1.21
Fat and Oils Refining and Blending										
Reported 2003 Load	0	0	0	0	0	0	0	0	0	0
Total 2003 Load With Gap Filling	0	0	0	0	0	0	0	0	0	0
Reported 2004 Load	0	0	0	0	0	0	0	0	0	0
Total 2004 Load With Gap Filling	0	0	0	0	0	0	0	0	0	0
Reported 2005 Load	0	0	0	0	0	0	0	0	0	0
Total 2005 Load With Gap Filling	0	0	0	0	0	0	0	0	0	0
Frozen Food Manufacturing										
Reported 2003 Load	0	0	8.01	0	0	3.44	0	0.48	0	11.9
Total 2003 Load With Gap Filling	0	0	8.01	0	0	3.44	0	0.48	0	11.9
Reported 2004 Load	0	0	8.66	0	0	7.12	0	0.73	0	16.5
Total 2004 Load With Gap Filling	0	0	8.66	0	0	7.12	0	0.73	0	16.5
Reported 2005 Load	0	0	6.36	0	0	1.57	0	0.16	0	8.1
Total 2005 Load With Gap Filling	0	0	6.36	0	0	1.57	0	0.16	0	8.1
Fruit & vegetable canning										
Reported 2003 Load	0	0.43	4.72	0.19	0	7.83	0.36	0	0.62	14.2
Total 2003 Load With Gap Filling	0	0.44	4.96	0.29	0	7.83	0.36	239	1.13	254
Reported 2004 Load	0	0.52	7.17	0.42	0	5.42	0.76	0.3	0.41	15
Total 2004 Load With Gap Filling	0	0.52	7.25	0.42	0	5.42	0.76	238	0.96	253
Reported 2005 Load	0	1.59	4.43	0.37	0	2.75	0.43	16.3	0.48	26.3
Total 2005 Load With Gap Filling	0	1.59	4.53	0.37	0	3.41	0.44	241	1.13	253
Fruit and Vegetable Canning, Pickling, and Drying										
Reported 2003 Load	0	0.04	20.5	0.4	0	0	0	3.06	0	24
Total 2003 Load With Gap Filling	0	0.05	22.1	0.44	0	0	0.06	3.06	0	25.7
Reported 2004 Load	0	0	24.2	0.5	0	0	0	1.59	0	26.3
Total 2004 Load With Gap Filling	0	0.1	26.4	0.55	0	0	0.06	19.8	0	47
Reported 2005 Load	0	0.11	18.7	0.36	0	0	0.06	36.7	0	56
Total 2005 Load With Gap Filling	0	0.14	23.8	0.38	0	0	0.07	36.7	0	61.1
Rendering and Meat Byproduct Processing										
Reported 2003 Load	0	0	0	0	0	0	0	0.07	0	0.07
Total 2003 Load With Gap Filling	0	0	0	0	0	0	0	0.07	0	0.07
Reported 2004 Load	0	0	0	0	0	0	0	0.02	0	0.02
Total 2004 Load With Gap Filling	0	0	0	0	0	0	0	0.02	0	0.02
Reported 2005 Load	0	0	0	0	0	0	0	0.02	0	0.02
Total 2005 Load With Gap Filling	0	0	0	0	0	0	0	0.02	0	0.02
Roasted Nuts and Peanut Butter Manufacturing										
Reported 2003 Load	0	0	0	0	0	0	0	0	0.01	0.01
Total 2003 Load With Gap Filling	0	3.76	2.26	0.51	0	0	0	0	0.01	6.55
Reported 2004 Load	0	3.01	0.03	0.41	0	0	0	0	0	3.44
Total 2004 Load With Gap Filling	0	3.76	2.26	0.42	0	0	0	0	0.43	6.88
Reported 2005 Load	0	0	1.72	0.6	0	0	0	0	0.85	3.17
Total 2005 Load With Gap Filling	0	3.76	2.26	0.6	0	0	0	0	0.85	7.47
Waste & Miscellaneous										
Reported 2003 Load	0	0	0	0	0	5.26	0.01	0	0	5.27
Total 2003 Load With Gap Filling	0	0	0	0	0	7.32	0.01	0	0	7.32
Reported 2004 Load	0	0	0	0	0	5.18	0.01	0	0	5.19
Total 2004 Load With Gap Filling	0	0	0	0	0	5.39	0.01	0	0	5.4
Reported 2005 Load	0	0	0	0	0	1.17	0.03	0	0	1.2
Total 2005 Load With Gap Filling	0	0	0	0	0	3.28	0.03	0	0	3.31
Wineries										
Reported 2003 Load	0	1.44	2.06	0	5.24	2.47	3.18	7.65	0.51	22.5
Total 2003 Load With Gap Filling	0	2.21	2.83	0	5.61	2.47	3.87	7.65	0.58	25.2
Reported 2004 Load	0	1.56	21	0	2.36	2.39	4.22	3.99	0.05	35.6
Total 2004 Load With Gap Filling	0	2.97	22.9	0	2.66	2.39	4.82	3.99	0.28	40
Reported 2005 Load	0	1.3	1.09	0	0.19	0.89	3.7	3.61	0.3	11.1
Total 2005 Load With Gap Filling	0	2.53	2.53	0	3.49	0.89	4.19	3.61	0.41	17.7
Totals										
Reported 2003 Load	0	3	35	0.6	5.6	106	3.6	11.7	1.1	167
Total 2003 Load With Gap Filling	0	7.7	40	1.2	6.1	112	4.3	251	1.7	424
Reported 2004 Load	0	5.8	61	1.3	2.7	74	5	7	0.5	157
Total 2004 Load With Gap Filling	0	8.3	67	1.4	3.1	78.3	5.7	262	1.7	428
Reported 2005 Load	0	3.8	32	1.3	0.2	12.8	4.2	56.8	1.6	113
Total 2005 Load With Gap Filling	0	9.1	39	1.3	3.6	19.4	4.7	282	2.4	362

2. Specific Industry Analyses – Tomato, Wine and Meat Industries

Salinity loads within the highest impact industries were compared for seasonal variablity and chemical composition.

Figures 24-26 show the monthly FDS load variations over a period of 3 years for processors in the wine, tomato and vegetable canning and meat industries. Figure 27 shows these industries totals. Tomato and vegetables processors and wineries show strong seasonal variations, with peak discharges occuring in the summer and early fall months. When considering industry totals, the seasonality of the wineries appears minor compared to the tomato and vegetable processors.

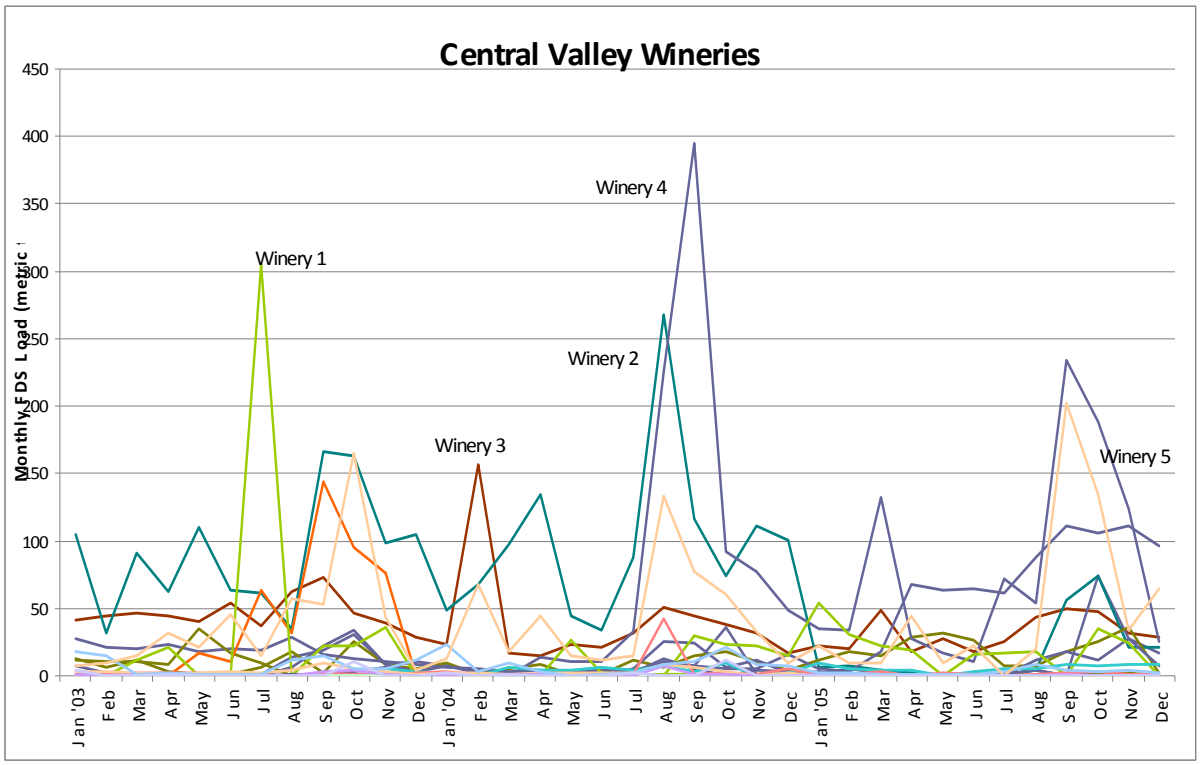

Figure 24

Monthly FDS loads for Central Valley wineries (metric tons). No gap filling was used

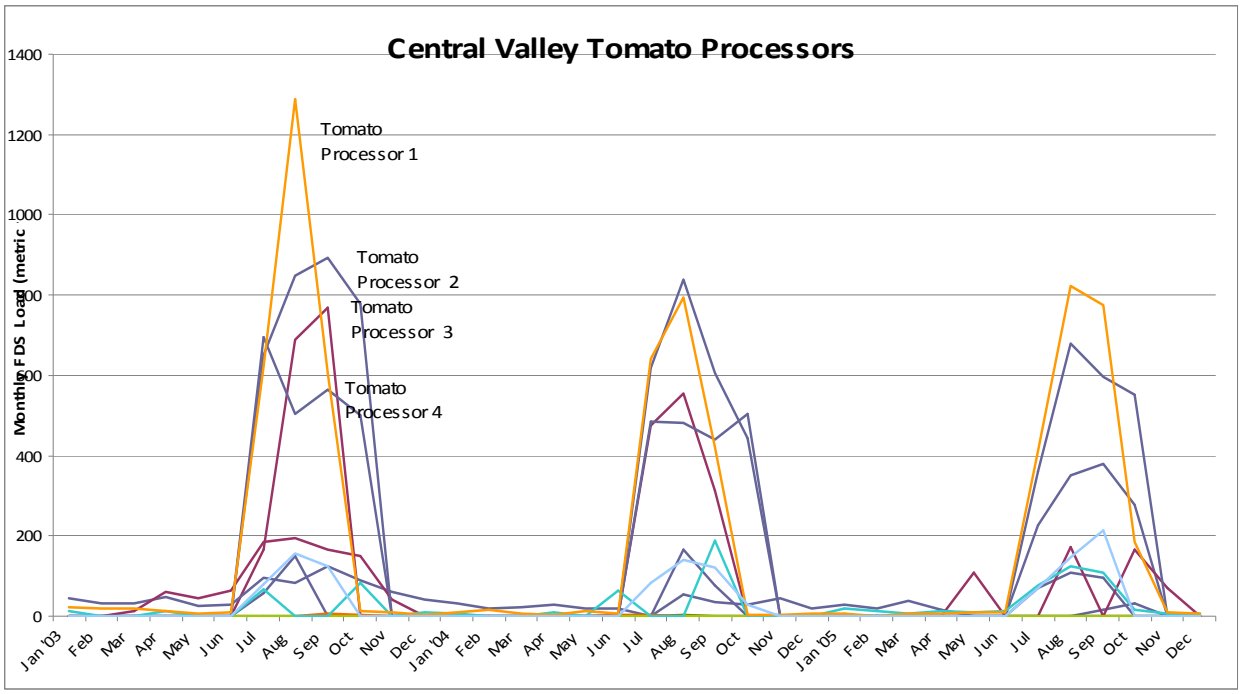

Figure 25

Monthly FDS loads for Central Valley tomato and vegetable processors (metric tons). No gap filling was used

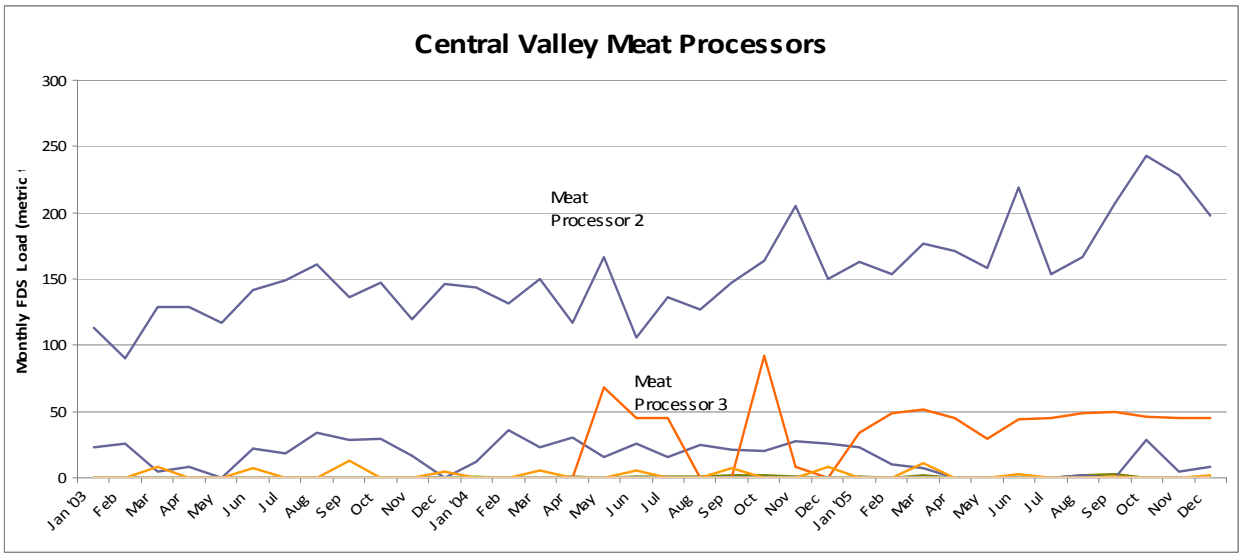

Figure 26

Monthly FDS loads for Central Valley meat processors (metric tons). No gap filling was used

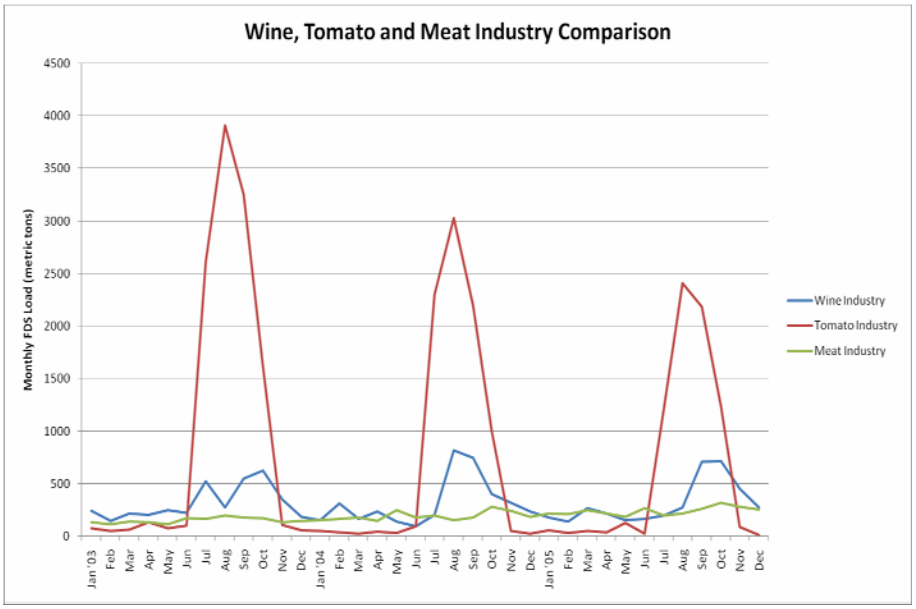

Figure 27

Monthly FDS loads for central valley wine, tomato and meat industries (metric tons). No gap filling was used

3. Screening analysis of the wastewater's chemical composition

The goal of the screening analysis was to develop a methodology for a preliminary evaluation of potential to impact the environment due to waste disposal by individual dischargers. The initial screening identified over 200 dischargers in 18 industrial categories. Three categories of dischargers were selected for further analysis: wineries (30 plants), tomato processors (11 plants), and meat packing plants (10 plants). The list of dischargers is attached as Section II Appendices: Appendix A. This selection was based partially on the number of dischargers in each category and their economic impact. In this preliminary screening there was a need to focus on groups of dischargers that were more likely to have a significant impact. It was assumed that the level of economic activity is a reasonable starting point for assessing the production levels and discharges. Excluding dairy processing, the three categories selected for further analysis were dominant both in value of shipment and payroll.

The screening analysis was focused on comparing potential impacts due to cumulative discharges within the selected group (i.e., identifying large, medium and small dischargers) rather than assessing the actual damage to the environment, if any, caused by the discharge.

4. Criteria Selection

The selection process of food producers discharging to land for further analysis must be multifaceted with the goal of identification of significant pollution sources or unique discharge patterns. For this purpose, the following parameters were considered:

- annual Total Dissolved Solids (TDS) load
- annual Fixed Dissolved Solids (FDS) load
- annual Biochemical Oxygen Demand load

- annual Total Kjeldahl Nitrogen (TKN) load
- annual (NO_2+NO_3)-N (oxidized nitrogen) load

For fixed dissolved solids (FDS) actual reported data for this analyte were used whenever possible. Where the FDS concentrations were not reported, they were estimated from the values of electrical conductivity (EC). The typical values of the FDS/EC ratio vary from 0.45 to 0.7 (Gustafson and Behrman 1939; Walton 1989; McPherson 1995; Atekwana et al. 2004). This relation is shown in Figure 28 based on the available data of 680 measurements of FDS and corresponding EC. Excluding the outliers from three dischargers (open symbols in Fig. A), a reasonable correlation was obtained with the FDS/EC ratio of 0.5537. In the following analysis, a rounded-off value was used and the FDS concentrations (expressed in mg/L) were calculated as 0.6 x EC (expressed in µS/cm).

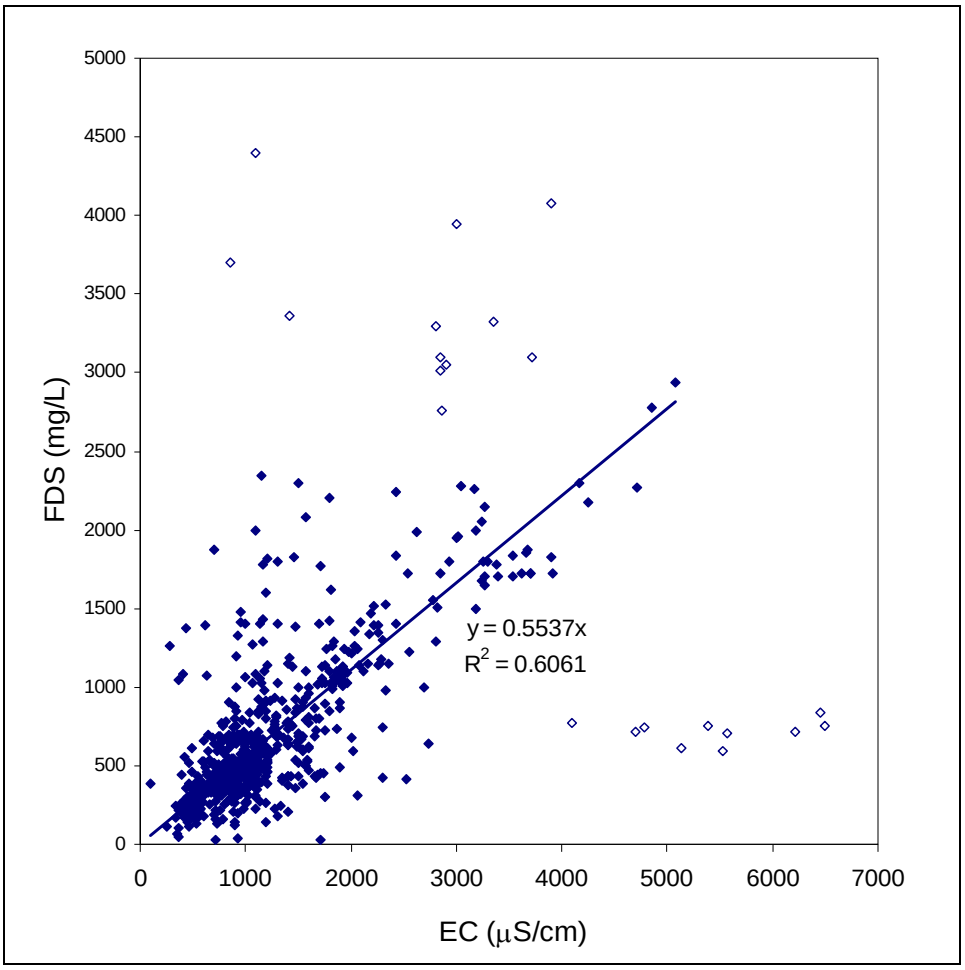

Figure 28

Regression of FDS on EC

In addition to FDS and TDS, three additional parameters (Biochemical Oxygen Demand - BOD, Total Kjeldahl Nitrogen - TKN and the sum of nitrite and nitrate - NO_2+NO_3-N) were chosen to create the footprint. These parameters were selected because their discharge to the environment is currently regulated or maybe regulated in the future. From the environmental point of view these constituents have direct impact on the aquatic environment.

The selection of water quality parameters was based on the availability of data and in full recognition that some important quality parameter (e.g., chloride or boron) are not considered as they are only sparsely recorded. Annual loads of these species were chosen as selection criteria in the screening analysis because they best represent the potential for water quality degradation. While high concentrations or short-term loads may create adverse effects at the point of discharge or in its immediate vicinity, the quality of a larger body of water is more affected by long-term trends.

In addition to these five loads, the ratios of TKN/BOD and oxidized nitrogen/BOD were also considered. These ratios provide indications of possible nitrogen transformation and oxygen demand in the soil. If the application rate of organics is large, oxygen may be depleted in the subsurface environment. Under such circumstances, microbial conversion of ammonia to nitrate may be inhibited and ammonia or nitrate may accumulate in groundwater. Conversely, if nitrate is applied to an anoxic environment together with biodegradable organics (BOD), nitrate will be utilized by microbes and converted to nitrogen gas thus alleviating nitrogen pollution potential. The exact values of organic application rates and nitrogen-to-organics ratios that will trigger such scenarios cannot be generally prescribed as it depends on site-specific conditions (see Section 6).

For each water quality parameter, the annual load was calculated from the reported monthly discharge volumes and concentrations for the last three years for which data were available (2003-2005). Annual loads are good indices of potential impacts on the environment (see Section 5) and especially for groundwater quality. While short-term variations of discharged volumes and concentrations of pollutants are important in evaluating the actual fate of these pollutants on each specific site, they obscure longer trends that are important in this screening analysis. The TKN/BOD and (NO_2+NO_3)-N/BOD ratios were also calculated from the annual loads neglecting any seasonal variations.

The purpose of this screening analysis is to compare individual producers within the chosen population rather than to assess the actual potential for water quality degradation that may vary significantly from site to site even for identical loads. Hence, the annual loads from all analyzed dischargers were normalized by the respective three-year maximum. As a result all normalized loads vary between zero and one.

5. Results

The results of the screening analysis are shown in the figures below for year 2003 through year 2005. For clarity, only those dischargers with loads larger than 5% of the respective maximum loads of the studied dischargers group were included in the graphs. “Radar” plots were chosen to visualize and compare distinct discharge footprints. Tomato processors are shown in red, wineries in green and meat packers in purple.

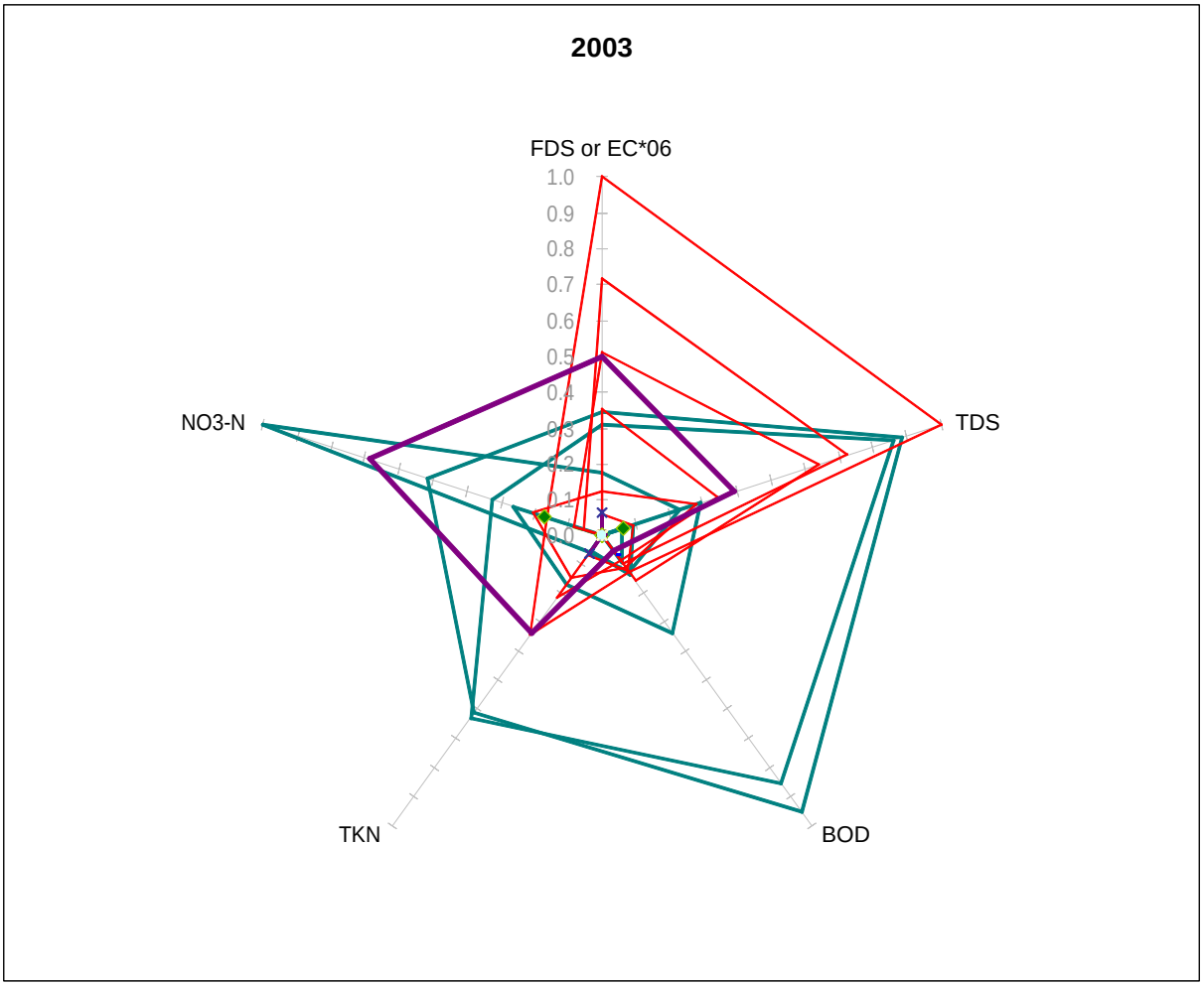

Figure 29

Normalized Annual Loadings for Tomato Processors (red), Wineries (green) and Meat Packers (purple) in 2003

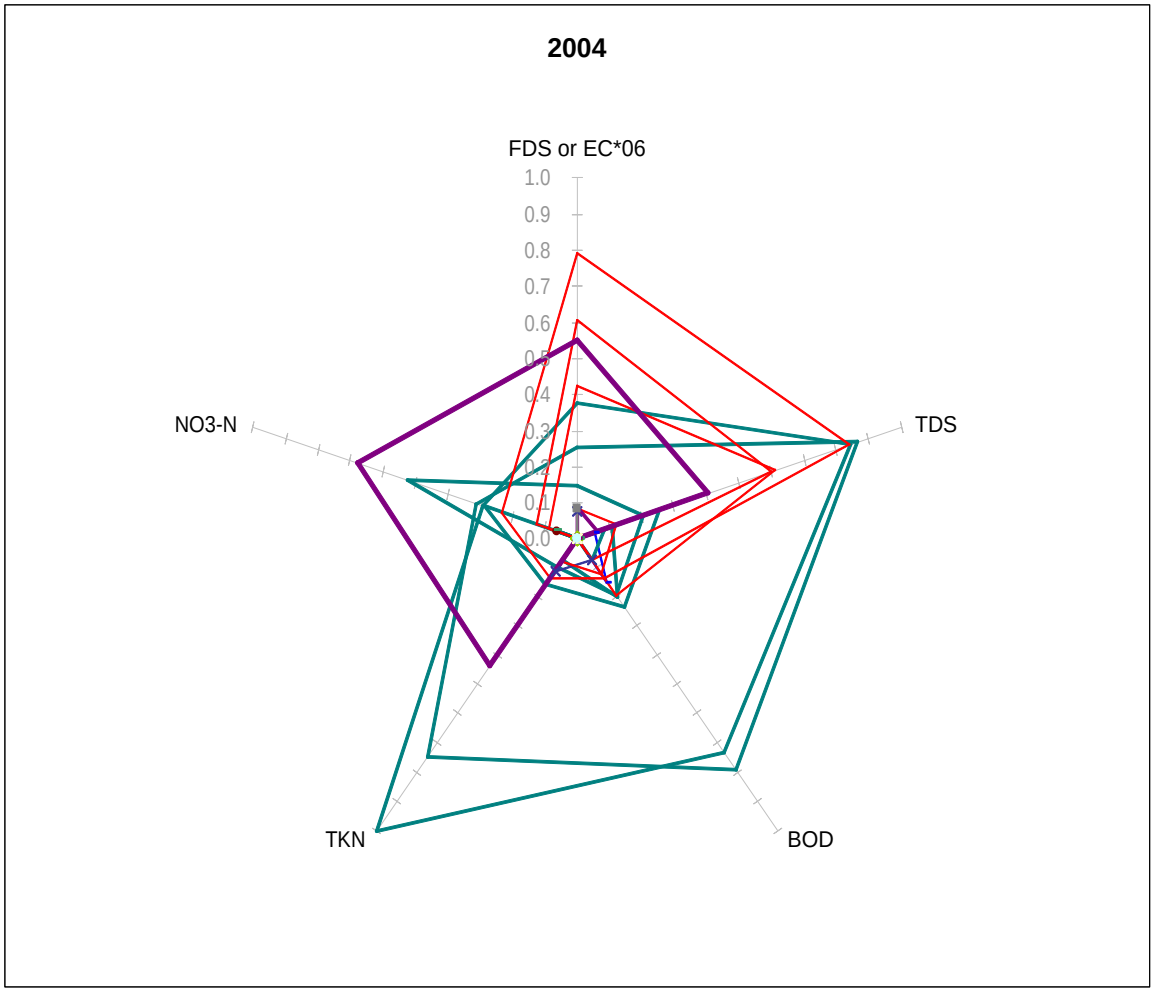

Figure 30

Normalized Annual Loadings for Tomato Processors (red), Wineries (green) and Meat Packers (purple) in 2004

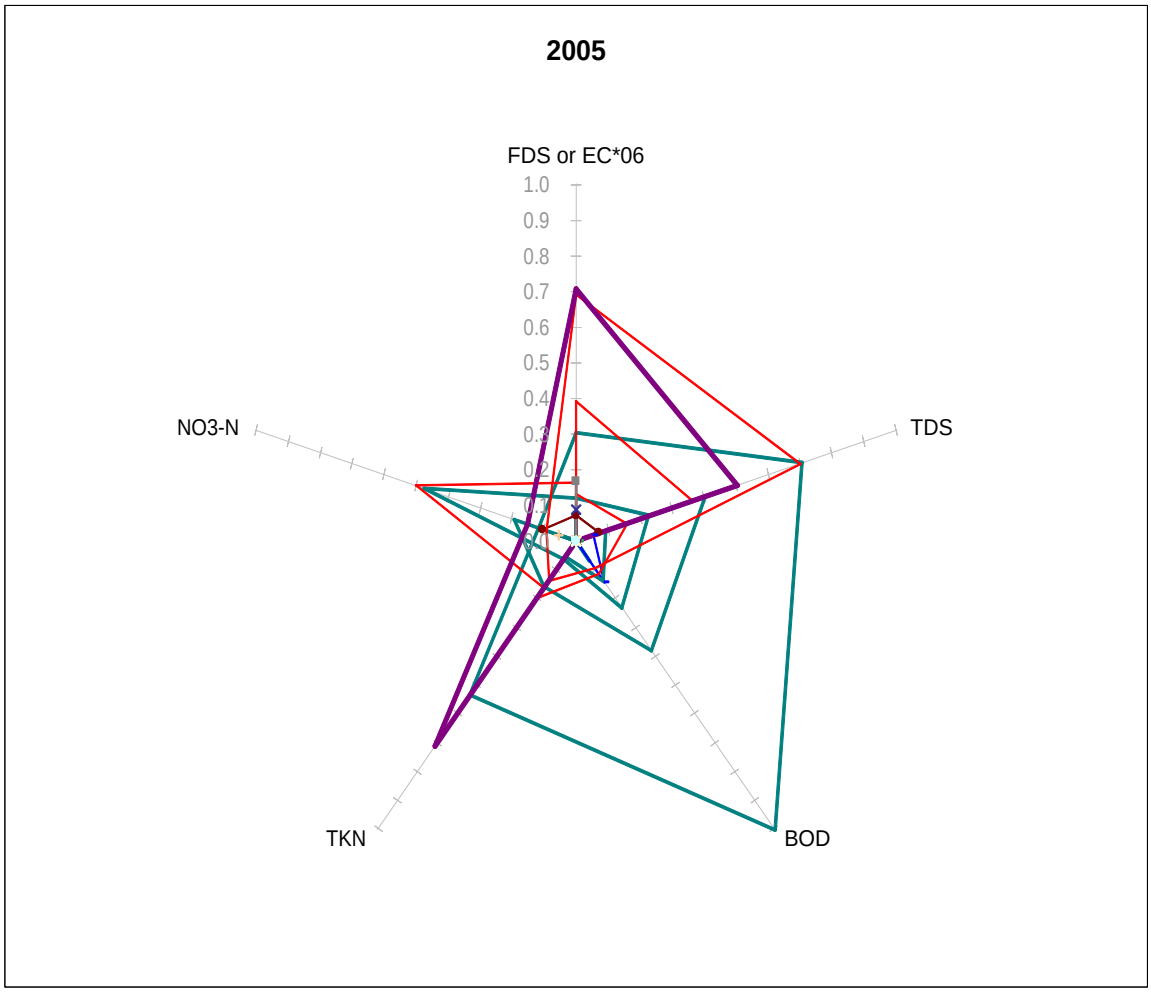

Figure 31

Normalized Annual Loadings for Tomato Processors (red), Wineries (green) and Meat Packers (purple) in 2005

Several observations can be drawn from the results presented in the last three graphs. First, only a few discharges (among 51 analyzed) dominate the loadings: three or four tomato processors, three or four wineries and one meat packer. These dischargers remain dominant through the three years with only minor changes to their discharge "footprints".

It further appears that the "footprints" are quite similar within each category. The contributions of all tomato processors differ in size but not in shape indicating similar compositions of waste. In the same fashion, both largest wineries have virtually identical "footprints". However, one of the other large wineries is unique as it contributes large loads of nitrate, possibly due to elevated nitrate concentrations in water withdrawn from its wells and used in production processes.

Each type of food processors has also a quite unique footprint related to the composition of discharged waste. Tomato processors discharge high loads of fixed dissolved solids (FDS representing inorganics) but much smaller organics (BOD) and nitrogenous compounds (TKN and NO_2+NO_3). In contrast, the discharges from wineries seem to be rich in organics (thus also in total dissolved solids but only moderate in fixed dissolved solids) and in reduced nitrogenous compound (TKN). Their discharges of nitrates vary as mentioned in the preceding paragraph.

The contributions of meat packers are more difficult to generalize as only a single source was large enough to exceed the 5% threshold. This discharger produced a significant load of fixed dissolved solids although not as large as the largest tomato processors. It also generated sizeable loads of reduced and oxidized nitrogen (TKN and NO_3-N) but again not as large as other sources (wineries in this case). Its contribution to the organic load was much smaller than any of the other sources.

The pattern of discharge loads from the biggest tomato processors with high FDS content suggests that they may have a significant impact on water salinity if discharged to groundwater or surface waters with low dilution. In contrast, the contributions to salinity from the largest wineries and meat processors are likely to be moderate (but still potentially significant depending on local conditions).

However, both wineries and meat processors can be identified as potentially large contributors to nitrate contamination in groundwater as their waste contain highest loads of reduced and oxidized nitrogenous species. Besides the nitrogenous species, the wineries also discharge significant loads of organics (shown as BOD) and also salts as noted in the preceding paragraph. Depending on the local conditions at the discharge site and time sequence of discharges, this waste composition pattern may be beneficial or detrimental. In principle, higher organic content may serve as an energy source for denitrifying bacteria that would convert objectionable nitrate into innocuous nitrogen gas. On the other hand, for such a transformation to occur, its site must remain anoxic (anaerobic) and the kinetics of denitrification fast enough to remove at least some nitrate. Depending on the location of this anoxic zone (river, lake, subsurface), such conditions may or may not be objectionable. Hence, the discharges from sites with a similar footprint should be closely examined. Additionally, if such wastewater is discharged to the land creating a significant anoxic zone, it is possible that ammonia present in the discharge or formed during decomposition of organics will not have a chance to be nitrified. Under such conditions, ammonia will penetrate into the underlying aquifer and contaminate groundwater.

D. Other Industries in the Central Valley

This brief section intends to provide a quick perspective on the previous discussion by considering any other industry that it is important in the context of Central Valley salinity analysis. This discussion is not meant to be comprehensive. Ample work is done in this context and is referenced amply throughout this report.

a) The Dairy Industry in the Central Valley

In addition to the food processing industry, the Central Valley dairy industry provides a significant salinity source. Data on locations and counts of adult cows for dairies in Madera, Fresno, Kings, Tulare and Kern counties were obtained from the Central Valley Regional Water Quality Control Board. The Board estimates a 1,000 cow dairy produces 770,000 pounds of salts, as FDS, per year [9]. Salinity loads from Central Valley food processors for 2005 are compared to Central Valley dairies in Figures 32 and 33. The total annual estimated salinity load from the dairies in Madera, Fresno, Kings, Tulare and Kern counties is 350,000 metric tons, compared to 22,000 metric tons for the food processing industry in the same counties in 2005.

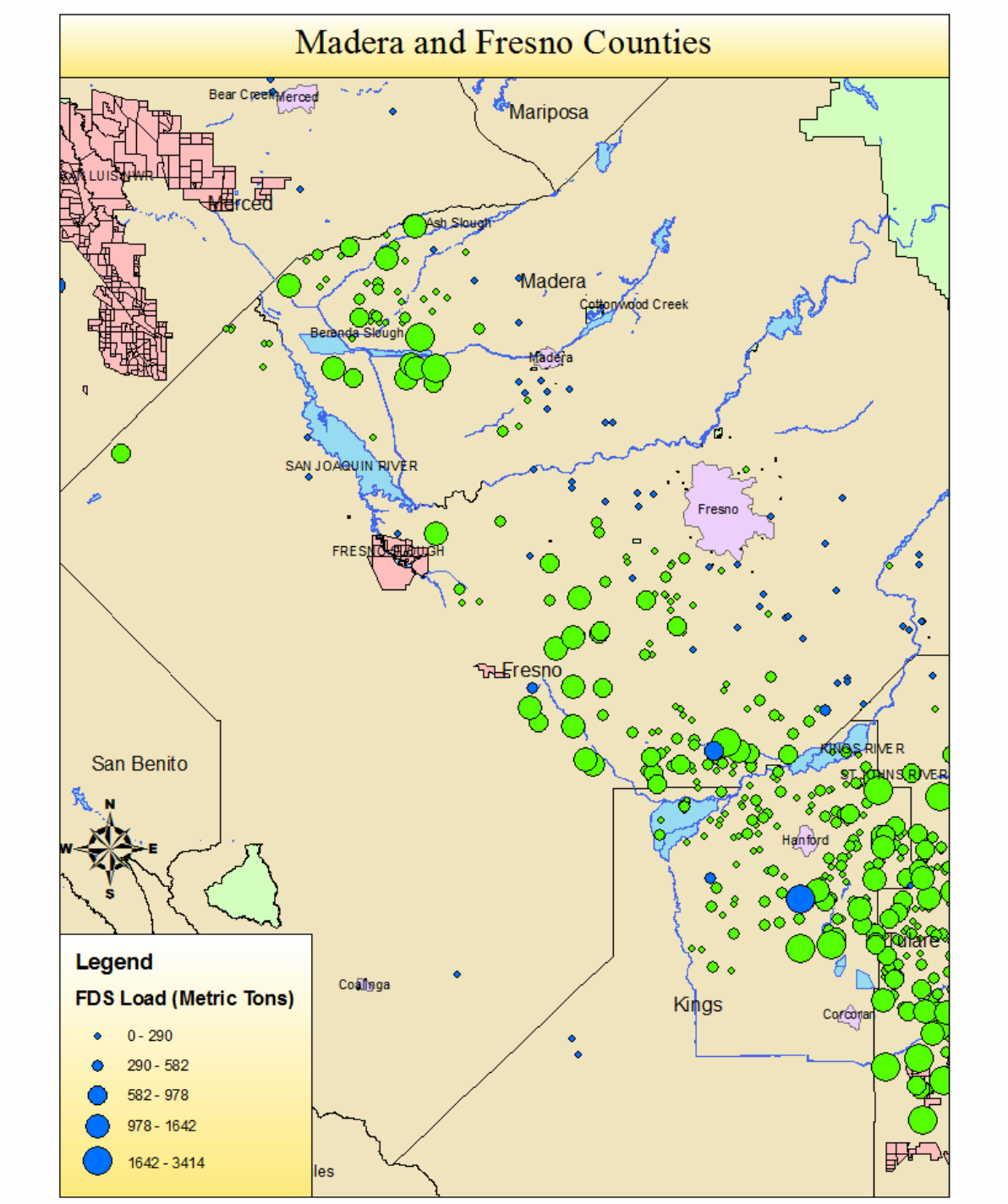

Figure 32

FDS loads for Central Valley dairies (green) and food processors (blue) in Madera and Fresno counties. Loads for dairies were estimated from facility size. The 2005 FDS loads were used for food processors.

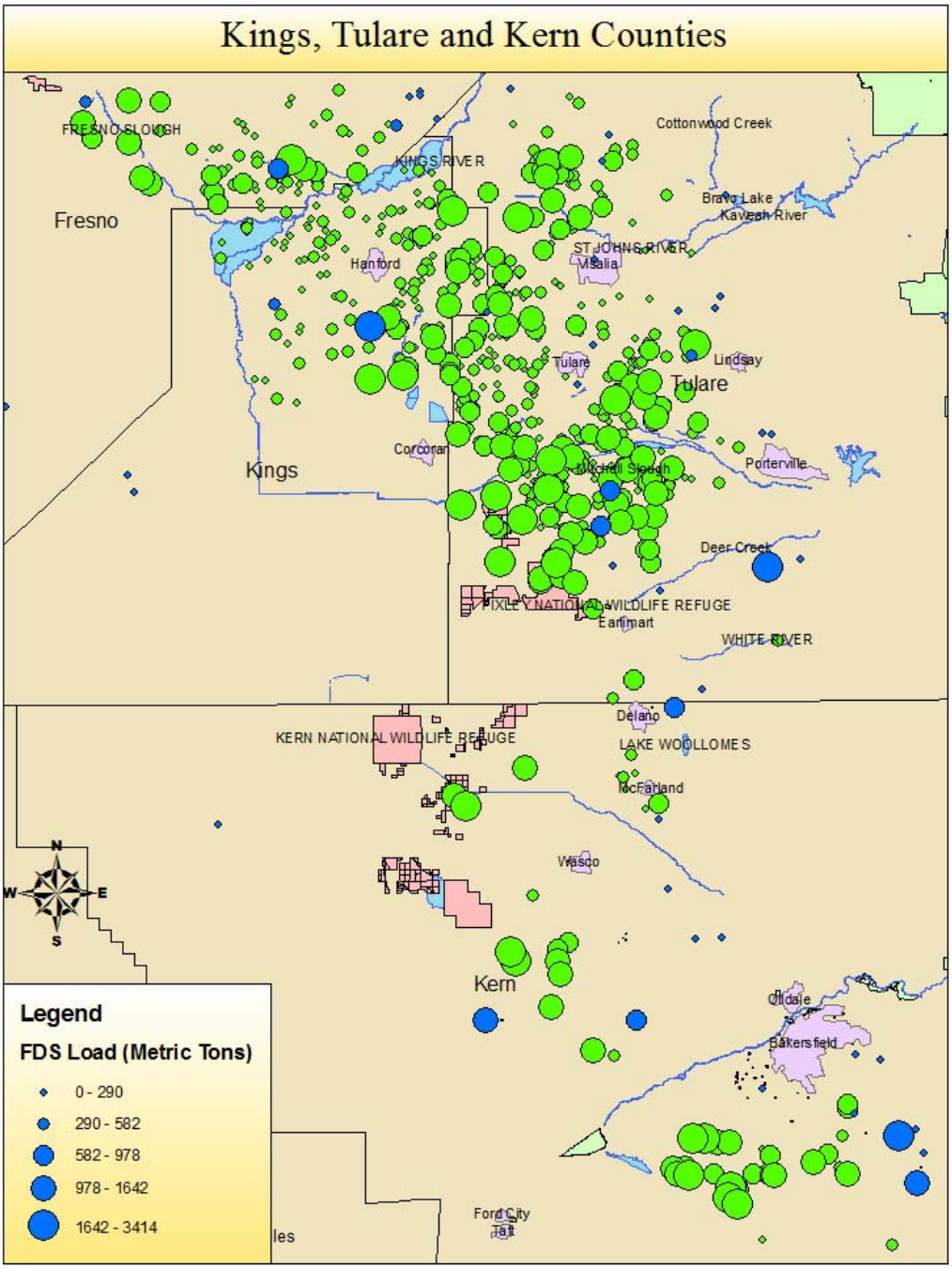

Figure 33

FDS loads for Central Valley dairies (green) and food processors (blue) in Kings, Tulare and Kern counties. Loads for dairies were estimated from facility size. The 2005 FDS loads were used for food processors.

II.2 SEP Study Management of Salinity in Wastewater from the California Food Processing Industry – Unsaturated Zone Modeling

A. Introduction

The vadose zone study in this report contains 2 parts. The first part, included in Section II.2, is devoted to studying of the flow and transport processes in the vadose zone, and to integrating these processes into a numerical model. It contains a detailed description of the concepts and assumptions that were employed in developing our model. The second part, which appears in Section II.3, describes applications of the numerical model through analysis and discussion of various scenarios. These scenarios represent various combinations of geological, hydrological and biogeochemical conditions. They intend to highlight various perspectives of the land application process, and to bracket the expected impacts of salinity discharge in terms of negative and positive scenarios. A summary of the unsaturated zone study is provided at the end of Section II.3.

The analysis of the flow and transport processes in the unsaturated zone precedes an analysis of these processes in the saturated zone, which is included in Section II.4. Section II.4 characterizes the migration of the solute fluxes from the land discharge areas, which are obtained from the analysis provided in Sections II.2 and II.3, once they reach the saturated zone. It models the evolution of the concentrations in groundwater in space and over time.

The analyses of the process taking place in the saturated and unsaturated zones are integrated through the concept of Representative Area (RA), which is the Lower San Joaquin River Basin. The RA analysis, which is described in Section II.4, encompasses a diverse range of food processing and land discharge activities, and it intends to capture the range of impacts to groundwater that is representative of the food processing activity over the entire Central Valley.

1. Problem Definition

As part of the SEP program, the purpose of this study is to evaluate unsaturated zone attenuation in response to land discharge of waste water from the food processing industry in the Central Valley, CA. The main objectives of this work are as follows. The first is to assess the geochemical and hydrological processes affecting the transport of chemicals in the shallow subsurface below the land discharge sites. Specifically, we will focus on the capacity of the root zone and the underlying unsaturated sediments to mitigate potential negative impacts of waste water application on water quality and to identify parameters that have a significant influence on the attenuation processes. The second objective is to identify a range of waste water fluxes infiltrating the groundwater from the land discharge areas. This range of fluxes will be used in our regional analysis. It can also be used as a benchmark for testing management alternatives for the land discharge sites. In the broader picture, information gained from this work is anticipated to provide guidance for improving current practices and policies to minimize the impact of waste water derived contamination on the groundwater resources of the Central Valley.

These objectives are addressed here through a series of multi-component reactive transport numerical simulations which are guided, as much as possible, by field and literature data. Numerical simulations of alternative scenarios are conducted for various industries (e.g. tomato processing facilities, wineries, meat packaging plants, etc.) to account for the effect of industry-specific waste water composition and application practices. For each industry, a number of scenarios are identified and simulated to cover a broad spectrum of waste water chemical compositions, soil conditions and parameters and their effect on the attenuation processes.

Part I of this document outlines the conceptual model development and the modeling strategy to determine recharge rates, concentrations, and mass loadings at the water table as a result of waste water land application. The first section introduces the conceptual model and general aspects of the modeling approach, which are applicable to all industries to be considered with the SEP study. The second section describes the "case-based" approach to bracketing variability in site conditions. The third through fifth sections describe model input parameters, from those used in all simulations, to those which are case and industry specific. Part II analyses the results of these simulations and subsequent numerical experiments designed to both test the sensitivity of the model to parameter changes and test multiple land application management scenarios.

This study will address the following questions:

- What is the capacity of the root zone and the underlying unsaturated sediments to mitigate potential negative impacts of waste water application on groundwater quality? What are the relative contributions of various waste attenuation mechanisms?
- What is the range of expected, near-source environmental impacts in terms of changes in concentrations of various chemicals at the interface between the saturated and unsaturated zones?
- What is the effect of site conditions on this attenuation? How does the soil's content of naturally-occurring gypsum and calcite minerals impact attenuation?
- What is the worth of discharge management practices? Can careful site selection, in regards to local geological and hydrological conditions, help mitigate environmental impacts? Can controls on discharge rate or area improve attenuation? When designing pre-application source controls for wastewater, what are the most important components to remove from the waste stream?
- What are industry-specific issues to consider (e.g., wineries, cheese manufacturers, olive producers, tomato canneries)?
- Is there a scientific basis for a deterministic "safe agronomic rate" of application of salinity and nitrogen compounds? In determining "safe rates", should we look only at concentrations or also at the loading rate of applications? Is current industry guidance appropriate?

These questions will be addressed through detailed numerical analyses of several case studies using "processes-based" modeling designed to account for interactions between biological and

chemical reactions and transport processes. Thus, this analysis examines attenuation in a dynamic manner using fundamental geochemical principles.

Ideally, we would have liked to explore all the sites and conditions experienced at the Central Valley, including hydrologic conditions, concentration profiles, discharge patterns, industries, soil parameters, land cover, etc. Since this is obviously not possible to do in a study of limited scope and budget, we will narrow down the range of conditions and locales that we will explore to a relatively small number of case studies, covering a diverse range of locales that will allow us to bracket the range of expected impacts from land discharge. These conditions will be designed to representing various industries. Looking at various industries operating in a diverse range of conditions will allow us to develop criteria for site selection. The model predictions will then be compared to observed groundwater conditions at discharge sites, in order to demonstrate their feasibility.

2. Conceptual Model

A review of available groundwater monitoring data from various food processors in the Central Valley (see Appendix B, Staff Report, 2006) reveals that the main concerns are associated with salinity and nitrate, and to a lesser degree ammonia (NH_3) and to a lesser degree Fe, Mn, SO_4, BOD. (Central Valley Regional Water Quality Control Board, 2005; Central Valley Regional Water Quality Control Board, 2006).

The term "salinity" encompasses multiple individual ion species and is commonly represented as either electrical conductivity (EC) or fixed dissolved solids (FDS). FDS is a direct measure of the concentrations of ionic species in the waste, while EC measures their charge. The major ions compromising salinity are: chloride (Cl^-), calcium (Ca^{2+}), magnesium (Mg^{2+}), potassium (K^+), sodium (Na^+), ammonium (NH_4^+), nitrate (NO_3^-), sulfate (SO_4^{2-}), and phosphate (PO_4^{3-}). Two carbonate species (CO_3^{2-} and HCO_3^-) are also significant contributors. (The relative predominance of the species is pH dependant, and in the subsequent text, they will be collectively referred to as carbonate for simplicity.) The trace elements aluminum (Al^{3+}), manganese (Mn^{2+}), zinc (Zn^{2+}), copper (Cu^{2+}), and iron (Fe^{2+}) can also contribute to FDS (Appelo and Postma, 2005; Hillel, 2000). (In the remainder of this document, the subscripts on these ions are dropped for convenience, and the ammonium ion will be referred to as its non-protenated form, ammonia (NH_3).)

A similar metric, total dissolved solids (TDS), measures both organic and inorganic compounds. In wastewater, which contains high levels of organic matter, TDS overestimates the actual inorganic salinity concentration. In groundwater, two measures are essentially equivalent, since it is typically very low in organic matter. Confining all analysis and discussion of salinity to FDS or EC measurements allowed us to avoid this potential problem. However, when we discuss actual groundwater measurements, we will report them in the form they were collected, either TDS or FDS, as appropriate.

Based on these observations, our unsaturated zone analysis focuses on salinity and on the fate of

N in its main oxidation states (NH_3 and NO_3). Although salinity is the primary topic of this study, the analysis of salinity concentrations should not be separated from the analysis of other chemicals of concern, because they are cross-linked. Nitrate and ammonia appear in solution as dissolved inorganic substance; these have an influence on FDS concentrations, albeit a small one due to the relative magnitude of their concentrations (10^1 to 10^2 mg L^{-1} for NH_3 and NO_3 versus 10^3mg L^{-1} for FDS). Additionally, salinity can interact with nitrogen attenuation processes; for instance, high salinity levels toxic to bacteria vital for nitrification and de-nitrification. Hence, our analysis will consider salinity and nitrogen compounds jointly.

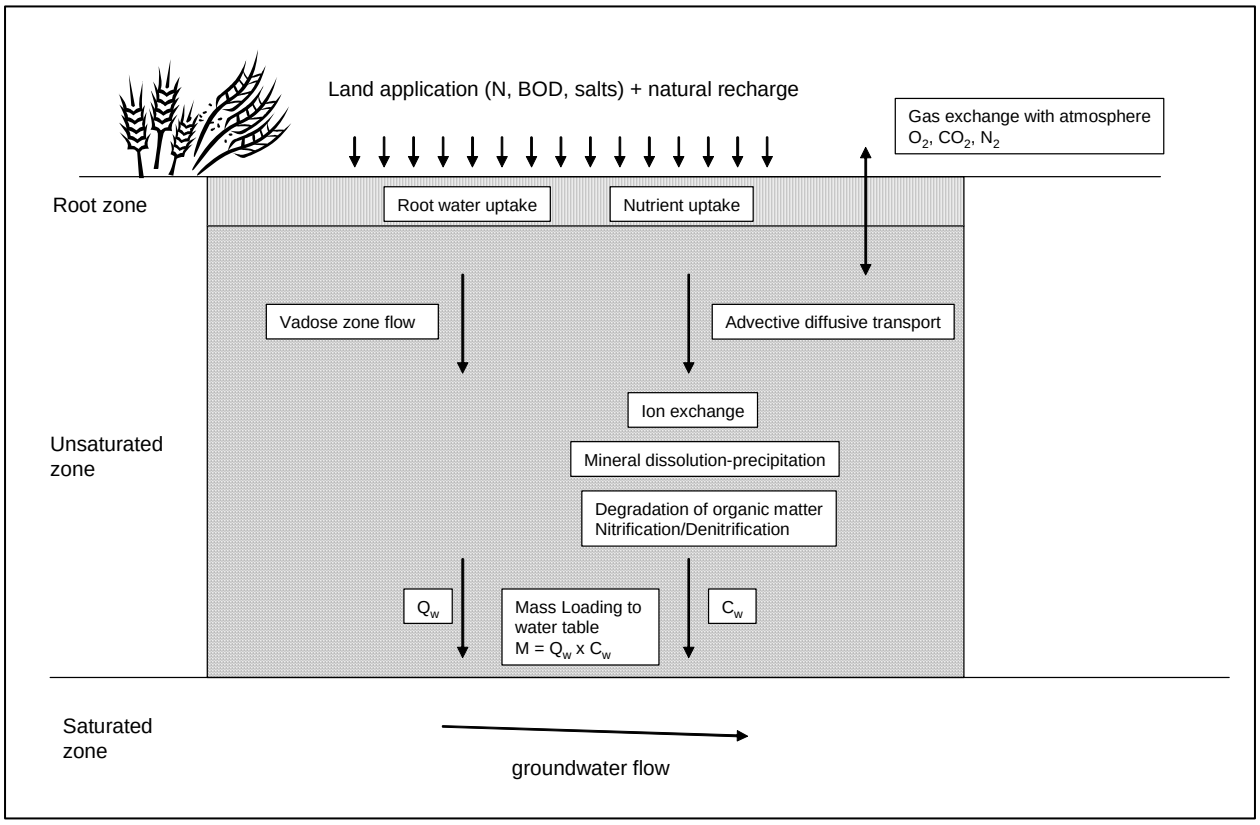

Figure 34

Conceptual model of attenuation processes, as discussed in Section II.2. Wastewater potentially containing high amounts of salinity, organic matter, and nitrogen compounds is applied at the ground surface. Soil processes such as plant nutrient uptake, soil sorption, and biodegradation attenuate the waste before it reaches the groundwater.

Figure 34 summarizes the key processes that constitute our conceptual model for land application sites in the Central Valley. Waste water is applied at the ground surface and infiltrates downwards towards the groundwater table. In the rooting zone, plant and soil evapotranspiration may remove a substantial portion of the water. These can reduce the flow rates and concentrate various components in the pore water, potentially leading to higher solute concentrations.

The applied wastewater typically contains nutrients, biodegradable organic carbon and dissolved salts. Thus the conceptual mode consists of two chemical subsystems: a) the N-C-O system describing the cycling of nitrogen and carbon compounds in the unsaturated zones, and b) major ions (Cl, Ca, Mg, K, Na, PO_4, CO_3, SO_4) contributing to salinity. Together these compounds provide the basic constituents needed to describe the major ion and redox chemistry at land application sites.

The two systems (salinity and NCO) are loosely coupled though the ammonia, iron, and manganese ions (NH_4, Fe, Mn), which sorb to soil and participate in the redox reactions. Root solute uptake within the top 1 m of soil also affects both systems, by removing essential plant nutrients (K, NH_3, NO_3, PO_4, SO_4, Ca, Mg, Zn) and releasing carbonate (CO_3^{2-}) as a byproduct of respiration and nutrient uptake (Tinker and Nye, 2000).

Gas exchange and soil saturation also couple the systems. The presence of oxygen (O_2) promotes the transformation of ammonia to nitrate (nitrification) and inhibits the transformation of nitrate to nitrogen gas (de-nitrification). Anoxic conditions can develop if microbial reactions consume the available oxygen more quickly than it can be replaced through diffusion. Additionally, the carbonate created as a byproduct of microbe mitigated redox reactions (Table 2) and plant nutrient uptake will, through equilibrium reactions, produce carbon dioxide (CO_2) gas. If this gas can readily escape the system, carbonate levels will decrease, also decreasing the total FDS concentration. The water content of the soil determines the ease at which these gases can diffuse to and from the atmosphere, necessitating vadose zone modeling.

The fate of other contaminants such as boron, selenium, and trace metals is expected to have little effect on the overall evolution of salinity concentration and redox conditions, although these compounds may still be of environmental concern due to low MCLs and toxicity at low concentrations. These compounds are not considered here, because the focus of the modeling is on major ion and redox chemistry. Once insight has been gained into major ion and redox chemistry, the fate of trace compounds can be inferred based on simulated geochemical conditions along the flow-path from ground surface to the water table, or if deemed necessary, additional modeling studies can be undertaken.

Attenuation of the major ions and NCO components starts with nutrients such as N, P, and K, which may be taken up by plants that are grown on the site. Additional attenuation of nitrogen, organic matter, and positively charged dissolved species may also occur below the root zone, before the waste water arrives at the water table. These attenuation processes include ion exchange, mineral dissolution-precipitation reactions, and microbially mediated conversion reactions.

Cation exchange processes can affect both salinity and ammonia. Ammonia, in its ionized NH_4^+ state, can sorb to soil particles, displacing other cations. In the same manner, other positively charged ions (K, Mg, N) contributing to FDS can be removed from the soil pore water. However, while the overall composition of salinity may be affected significantly by cation exchange, the total fixed dissolved solids will not be reduced unless an ion with a large molecular weight (K at

39.10 g mol^{-1}) replaces a lighter one (Na at 22.99 g mol^{-1}). The finite number of sorption sites on the soil capable of retaining cations limits the amount of salinity that may be removed. Once all sites are occupied, the total number of cations immobilized will remain constant, but stronger cations may replace weaker ones (e.g. magnesium replaces sodium), depending on the water composition (Appelo and Postma, 2005).

Mineral dissolution and precipitation reactions may have a significant effect on salinity due to removal or addition of dissolved components to the pore water, particularly carbonate. However, in terms of attenuation, the relevance of these reactions is limited for most other major ions such as Na, K, Mg, Cl, and SO_4 and for the nitrogen compounds. Generally, dissolution/precipitation reactions can have a positive effect on groundwater quality, for example due to the dissolution of the mineral calcite ($CaCO_3$), which buffers the pH to near neutral values. It may also have a negative effect, for example, due to the dissolution of native gypsum ($CaSO_4 \cdot 2H_2O$), which increases salinity.

Most waste streams contain a significant fraction of highly labile organic carbon (e.g. sugars), which readily undergoes microbially mediated degradation reactions. Organic carbon acts as the electron donor (ED) in these degradation reactions; however, for the reaction to go forward, a suitable electron acceptor (EA) is also required. Possible electron acceptors are foremost oxygen, which facilitates the aerobic degradation of dissolved organic carbon. The high oxygen demand of the waste water and the low solubility of O_2 limit oxygen ingress in dissolved form. However, in the unsaturated zone, oxygen can also be supplied in significant quantities through unsaturated zone gas transport, mostly by diffusion In this zone, biodegradation of NH_3 into NO_3 (nitrification) occurs. Additionally, carbonate can be removed through conversion to carbon dioxide and escape through gaseous diffusion, lowering salinity levels.

It is possible, though, for anaerobic conditions to develop in soils as well, particularly in fairly impermeable soils with high moisture content, which inhibit O_2 ingress and CO_2 egress. In this case, alternative compounds can serve as electron acceptors for microbial reactions, namely, NO_3, Fe(III), Mn(IV), and SO_4. NO_3 and SO_4 are often supplied with the waste water, while Fe(III) and Mn(IV) are typically present in the soil matrix in form of Fe and Mn-oxides. In this context, biodegradation of organic matter may cause additional attenuation of NO_3. It must be emphasized that de-nitrification only occurs under anaerobic conditions, which implies that this process is inhibited in the presence of oxygen. Similarly, NH_4 may be used as an alternative electron donor, providing an additional attenuation mechanism for ammonia. This process is mostly restricted to aerobic conditions (i.e. O_2 acts as the electron acceptor), although recent research suggests that anaerobic degradation of ammonia is also possible through the anammox process (Jetten, 2001).

The role of electron acceptors other than NO_3 or O_2 has been excluded from the analysis to minimize the number of scenarios under investigation. Under some circumstances, the presence of these electron acceptors in the sediments (e.g Mn or Fe oxides) or the waste water stream (e.g. sulfate) may also affect the overall evolution of salinity in the pore water as it moves through the soil. Here we only vary parameters that dominate the cycling of N. This can be justified, because

nitrification will occur under aerobic conditions. Under these conditions, the alternative EAs are stable. Furthermore, de-nitrification has a higher energy yield compared to reactions involving the alternative EA's and the effect of the alternative EAs on de-nitrification is negligible. It may be possible that alternative electron acceptors (EA) affect the persistence of ammonia under anaerobic conditions through the (annamox) process; however, neglecting this process will provide conservative estimates in terms of NH_3 loading to the aquifer.

Based on these processes, it can be expected that soils hold significant and long-term (renewable) attenuation potential for nitrogen compounds. On the other hand, the attenuation of overall salinity is typically limited. While root uptake, biodegradation, mineral dissolution and precipitation, and cation exchange are certain to lead to attenuation of waste, their combined effectiveness is unstudied, especially in regards to food-waste application. Previous estimates of attenuation have not taken into account the interactions of these processes, specifically how alterations to the waste stream made by one process (such as pH changes) will dynamically impact the others.

The conceptual model described in Figure 34 is quite common for modeling subsurface flows (cf., Delleur, 1999). However, it does not allow for subsurface heterogeneity, in the form of macropores or high-velocity flow channels. These effects are important primarily for small scale simulations, for example, for horizontal sections of the order of one or a few meters. The land discharge sites, however, are spatially large, with a spatial extent of the order of hundreds of meters, which is much larger that the scales of heterogeneity, and under such conditions it is reasonable to homogenize the flow domain (Rubin, 2003), which implies representing it through average properties, which are known as effective properties. The use of effective properties is justified for estimating impacts at the scale of the land application site which is of the order of hundreds of meters horizontally. Local responses, at the scale of a few meters or less, can deviate largely from the average response.

B. Case-based Modeling Approach

Differences in soil profiles, chemical compositions of the waste stream and in hydrologic conditions will alter the significance of and ranking between the various processes. For example:

- Soils richer in clay have larger sorption capacity, and thus larger capacity to reduce salinity loads over limited periods of time.
- Waste-water low in salinity discharged over gypsum-rich soils will show increase in salinity due to the dissolution of gypsum.
- In the absence of other sources, ammonia concentrations in the waste stream will decrease in soils characterized by low saturation and well-connected pore-space.
- Increased organic matter content in the waste stream increases oxygen demand, which will decrease the oxygen available for nitrification.
- Waste streams with low organic matter but high nitrogen concentrations will have a reduced capacity for microbially mediated nitrogen removal.

The large number of simultaneously-occurring processes taking place under a wide range of site conditions suggests that hundreds of site-specific analyses may be required in order to quantify the complete range of expected impacts. This task can be simplified, however, if instead of focusing on characterizing the entire range of impacts we will bracket it, by looking at conditions that lead to responses that define the extremes of this range. Following this reasoning, we will look at the combination of conditions that lead to largest and smallest loads of salinity and N-compounds, as well as to those situations that are most favorable in terms of minimization of environmental impacts.

The selection of these scenarios intends to investigate adverse as well as favorable conditions in terms of water quality degradation. Under ideal conditions, basically meaning if one is able to identify the most adversarial and favorable conditions, such an analysis can bracket the uncertainty associated with predicting the impact of the salinity discharge. Such an "extreme case" analysis is just one of many methods known to investigate uncertainty. For example, one could consider a Monte Carlo type of analysis. We gave this option a serious consideration and decided to avoid it at this stage for several reasons:

1. A Monte Carlo analysis would be appropriate after the important processes are identified, the parameters defined, and there's a good data base to define the distribution of the parameters.
2. Monte Carlo simulations are good to investigate conditions around the median, and it is very costly to investigate extreme conditions
3. Our trials indicated a 4 hours CPU time for s ingle realization. A complete set of Monte Carlo simulations, where the extremes are well defined, will require thousands of realizations and many sets of realizations. This is a very costly solution, especially for the vadose zone analysis, and not justified at such an early stage of the investigation.

Our numerical model simulates unsaturated flow and multi-component reactive transport of solute and gases, implying that the interactions between the various dissolved species, mineral phases and soil gases are considered explicitly. Based on the discussion above, a multitude of scenarios can be developed to estimate possible ranges of mass loadings at the water table. Two possible "worst case" scenarios are simulated. Case 1 is designed to demonstrate the effects of anoxic conditions and provides a worst case scenario for ammonia loading to the aquifer. Case 2 is structured to show the effect of aerobic conditions throughout the unsaturated zone, and provides a worst case for nitrate loading to the aquifer. Case 3 was created to demonstrate the conditions under which optimum nitrogen removal could be achieved. For each case, ion exchange and mineral dissolution precipitation were also included to evaluate the effect on salt attenuation and release.

1. Case 1: Limited NH3 and FDS attenuation, high FDS loading

Under conditions of high NH_3, BOD, and FDS loading, this scenario assumes that nitrification is

limited by anoxic conditions, i.e. high water saturations inhibit oxygen ingress. High pore water saturations may be due to low soil hydraulic conductivity and/or high application rates. Solute uptake and ion exchange remain as the main mechanisms for ammonia attenuation. Under these conditions, denitrification is likely and the fraction of NO_3 that is not removed by solute uptake is converted to benign N_2. This case constitutes a "worst case" in terms of ammonia and FDS loading to the water table for sites with high ammonia concentration, high BOD and high soil saturation.

2. Case 2: Limited NO3 and FDS attenuation, high FDS loading

This case assumes that pore water saturations in the unsaturated zone are low due to low application rates and/or high soil hydraulic conductivity. As a result, conditions remain aerobic throughout the unsaturated zone. This scenario allows for the conversion of ammonia to nitrate (nitrification), while nitrate remains stable. This scenario is a worst case scenario for sites with high FDS and N loading (independent of its form, i.e. NO_3, or NH_3), relatively low BOD loading (which still may be significant), and relatively high conductivity. The main mechanism for nitrate attenuation is solute uptake. This case constitutes the worst case in terms of nitrate loading to the water table.

3. Case 3: Significant N attenuation (NH3 and NO3), moderate to high FDS loading

This scenario is an intermediate case between Case 1 and Case 2. It assumes that conditions become anaerobic in the unsaturated zone, implying that denitrification can take place deep in the unsaturated zone, following the nitrification of ammonia in the shallow zone. This case is a best case scenario for N-loading, because all N that is not taken up by plants, is ultimately converted to N_2. However, it is highly dependent on the completion of nitrification before anaerobic conditions develop, and completion of de-nitrification before the waste water reaches the saturated zone. Furthermore, it is also assumed that FDS loading is relatively low. This case constitutes an ideal scenario for N attenuation, but may be difficult to design to minimize environmental impact.

4. Summary of scenarios

Table 11 summarizes the defining characteristics for each case. It includes the desired saturation conditions and the ratio of the hydraulic conductivity to the waste water application rate that is necessary to create these conditions. The K_{sat} values and applications rates are discussed further in Sections D.1 and D.2 of this document.

Table 11: Overview of Cases

Case	Saturation Conditions	Ratio of K_{sat} to Waste Water Application Rate	Waste water composition
1	High (0.9 – 0.99)	~1	High: NH_3, CH_2O, FDS Low: NO_3
2	Low (0.4 – 0.5)	~ 10,000	High: NO_3+NH_3, FDS Low: CH_2O
3	Moderate (0.8 – 0.9)	~10	Low: CH_2O, FDS, NH_3 and NO_3 (NO_3 low relative to CH_2O)

"High" and "low" values in Table 11 are relatively to the other dischargers in the industry. Tables 25, 31, 33, and 39 provide specific inputs for the various cases, and Figures 43-46 summarize the various industry footprints.

5. Support for case-based approach in groundwater data

The three potential cases are based on the possible effect of site conditions and wastewater composition on the loadings of nitrate, ammonia, and salinity to the groundwater table. To demonstrate that these are valid cases, we examined the records of suspected and recorded groundwater contamination found in Appendix B of the Central Valley Water Quality Control Staff Report (2005). Among the 223 processors discharging to land, 105 reported groundwater data. Of those 105 reporting, 30 were known to be causing groundwater degradation through salinity discharge, and 40 were suspected of it (nearly 70%). Nitrate degradation occurred less frequently (13 cases known, 25 cases suspected), as did ammonia degradation (3 known cases, 0 suspected).

Examples of all the cases were present in the data. A winery presented a clear Case 1 scenario, with degradation due to high salinity, ammonia, iron, manganese, organic matter, and carbonate. Another winery was found to be a good Case 2 example, with salinity, nitrate, and sulfate impacts. Any of the multiple plants with salinity problems but no nitrate or ammonia could be good examples of Case 3 processors.

The groundwater data from a food processor presents evidence for all cases. Monitoring wells there record groundwater data in the upper aquifer throughout and down-gradient of the land application area. Table 12 shows the concentrations in three wells in December 2005. All wells are within 1 mile of each other. In the groundwater data, organic matter is reported as biological oxygen demand (BOD), and ammonia is represented as total Kjehldahl nitrogen (TKN), a measure of organic nitrogen and ammonia in a water sample.

Table 12: December 2005 groundwater data from food processing land application site

	Monitoring Well #1 (Case 1)	Monitoring Well #19 (Case 2)	Monitoring Well #5 (Case 3)
Biological Oxygen Demand (BOD) (mg L^{-1})	7	2	5
NO_3 (mg L^{-1})	0.05	43	0.05
Total Kjeldahl Nitrogen (TKN) (mg L^{-1})	43	0.5	1.7
TDS (mg L^{-1})	2700	750	1600

To determine the frequency of occurrence of each case, the winery groundwater data from the most recent year was analyzed. (Other industries were lacking comprehensive datasets and could not be included.) Up-gradient wells were eliminated from consideration, leaving only those wells down-gradient from land application sites. Based on the range of concentrations detected and the criteria given in, each well was classified as either Case 1, Case 2, Case 3, or Other. The criteria were based on the water quality goals put forth by the California Water Quality Control Board (Marshack, 2003).

Table 13: Criteria for classifying groundwater data into the three cases

	Total Dissolved Solids ($mg\ L^{-1}$)	Total Kjeldahl Nitrogen ($mg\text{-}N\ L^{-1}$)	NO3 ($mg\text{-}N\ L^{-1}$)	Organic Matter	Fe, Mn
Case 1	>500	>30	<10	Present	Present
Case 2	>500	<30	>10	Absent	Absent to low
Case 3	>500	<30	<10	Absent	-

Of the 19 processors examined, 89% had salinity levels above the water quality objectives as stated in Marshack, 2003. Based on nitrogen compound concentrations, 5% were classified as Case 1, 58% as Case 2, 26% as Case 3, and 11% as other. Most cases classified as "Other" had salinity levels lower than 500 mg L^{-1}. The nitrate levels in the groundwater under the majority of land-application sites were elevated, leading to the high number of Case 2 classifications. It should be noted that no corrections for background levels were made, so ambient groundwater conditions may have caused some wells to be improperly classified. Additionally, because the cut-off criteria for each case was based on the groundwater quality objectives, the classifications should not be interpreted as "58% of wells demonstrated a worst-case scenario" but rather than "58% of wells showed a combined nitrate and salinity problem."

Histograms of the concentration of nitrate (Figure 35), TKN (Figure 36), and FDS (Figure 37) in the wastewater of the analyzed wineries were created to demonstrate that differences detected in the groundwater beneath a certain case classification could be observed in the applied waste. Despite the fact that little or no nitrate or TKN was detected for Case 3 wineries, the histogram showed that many of these processors had significant levels of nitrogen in their waste. This finding indicates that "best-case" scenarios for nitrogen do exist; conditions at these sites must favor its removal, otherwise the groundwater would show elevated nitrate and TKN.

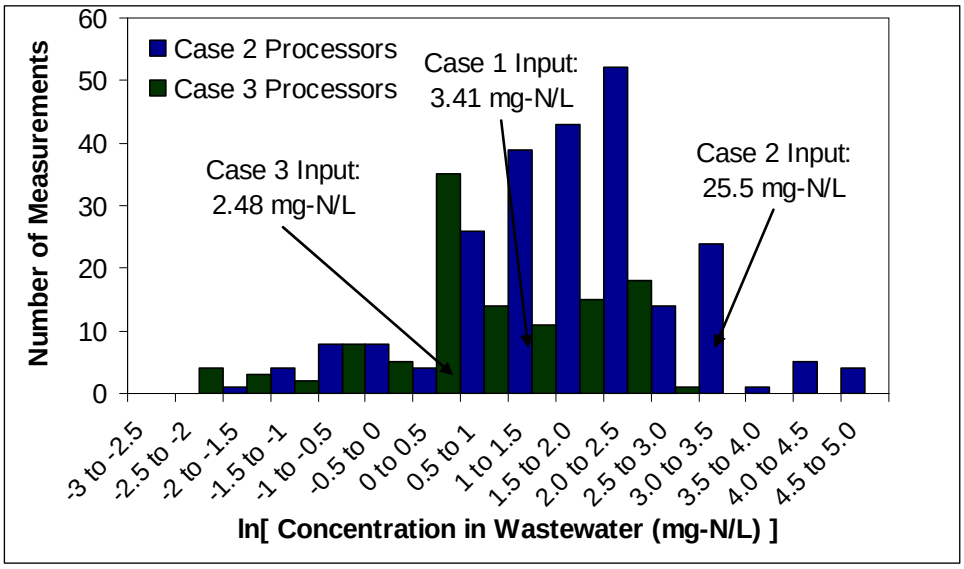

Figure 35

Nitrate concentrations in waste water by groundwater case. Case 2 processors tend to apply waste higher in nitrate to the land. However, all Case 3 processors have some nitrate in their waste, indicating that site conditions must be reducing the nitrate before it reaches the groundwater table. Case 1 is not included on the histogram due to the relatively low number of processors meeting this criterion.

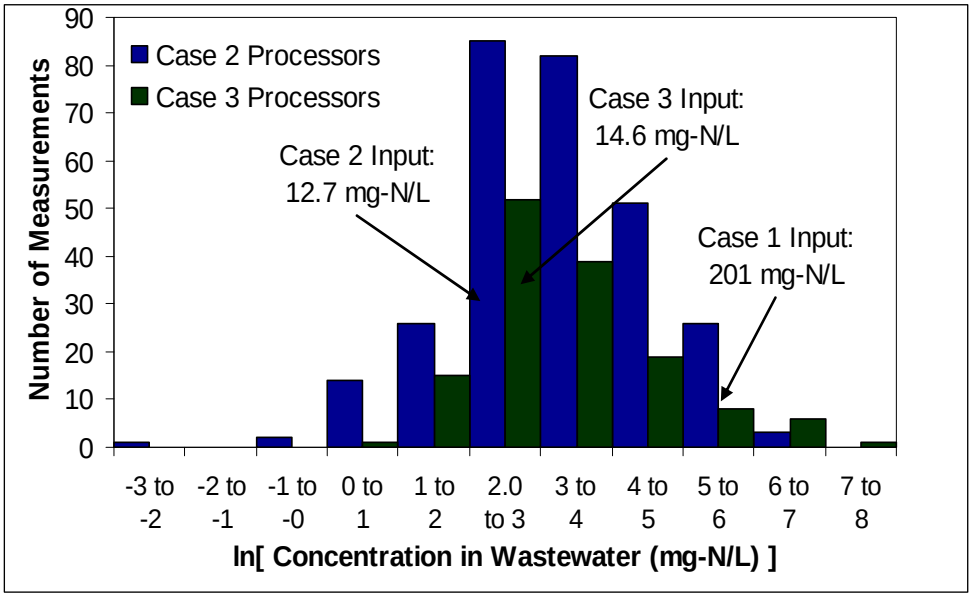

Figure 36

TKN concentrations in waste water by groundwater case. Case 2 and Case 3 processors apply waste with very similar TKN concentrations; however, they have very different amounts present in the underlying groundwater. Case 1 is not included on the histogram due to the relatively low number of processors meeting this criterion.

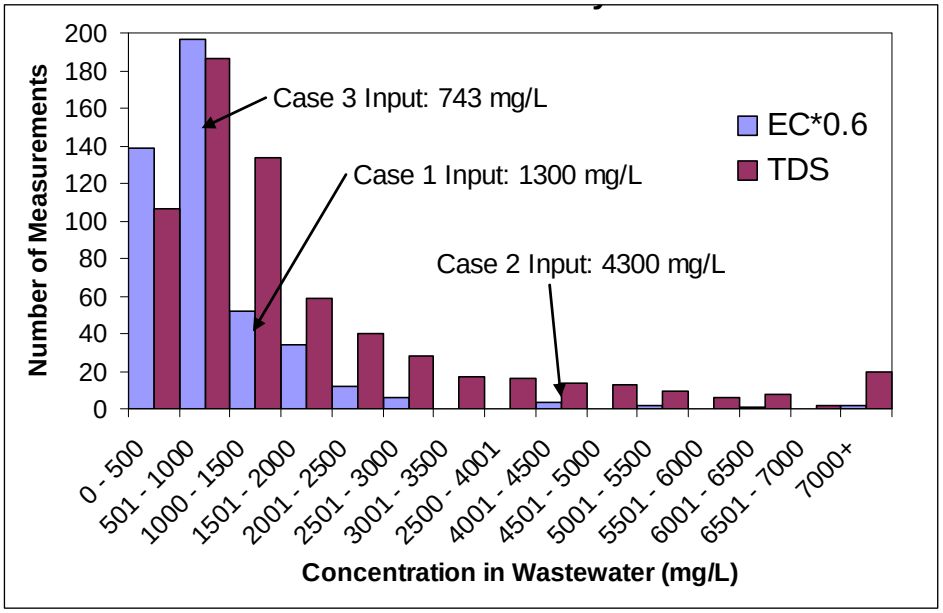

Figure 37

C. Numerical Modeling – Input Parameters

The numerical model MIN3P (Mayer et al., 2002) is used to simulate both the vadose zone water flow and chemistry. MIN3P is a general purpose flow and reactive transport code for variably saturated media providing a high degree of flexibility with respect to the definition of the reaction network. Advective-diffusive transport in the water phase and diffusive transport in the gas phase are included. Equilibrium reactions considered are aqueous complexation, gas partitioning between phases, oxidation-reduction, ion exchange, and surface complexation. The reaction network is designed to handle kinetically controlled intra-aqueous and dissolution-precipitation reactions, and the uptake of nutrients and other solutes by plants. All reactions can be defined through a database of chemical rate expressions, not requiring external code generation by the user. Three types of parameters are needed for input into MIN3P: numerical parameters describing the numerical representation of the physical domain and its discretization, flow and transport parameters describing medium's hydrologic properties, initial and boundary conditions, and chemical reaction parameters describing the sediment composition, reaction network and solute uptake.

Although the simulations presented are process-oriented and consider a significant degree of complexity, several potentially important processes had to be neglected to provide manageability, both in terms of study focus and computational demands. These simplifications are described below, and the implications of these on the modeling results are discussed in Part II:

- Soil is homogenous with respect to hydraulic conductivity and its related parameters, with no preferential flow paths present.
- Gas advection, namely in ingress of O_2 and the egress of N_2 and CO_2, is not considered. All transport of gasses is assumed to occur through diffusion.
- The fate and transport of trace elements (e.g. boron, selenium) are not modeled, as it is outside the scope of this study.
- No gypsum is present in the soil. While the Modesto area soil survey (USDA, 2006) shows no gypsum present, this assumption would not be appropriate if the model were extended to other areas of the central valley.
- Oxygen is the only electron acceptor used in the nitrification process.
- No provisions have been made for future alterations to the annual water budget due to climate change. The water budget modeled is consistent with the average monthly values for the time-period between 1986 – 2006.
- Transport is advective (pore-scale dispersion negligible).
- The microbial community is at steady-state; no growth or decay is incorporated. Additionally, bioclogging due to microbial mass is not modeled.
- Salinity may breakdown the soil structure in the presence of expanding clays, altering the conductivity of soils. However, we assume that most discharge sites will have been chosen so that they promote infiltration, i.e. they have low clay levels and are not subject to this problem.
- Organic matter in the wastewater was represented as a simple sugar (denoted CH_2O) in the numerical modeling and was assumed to be easily degradable. The BOD concentration (in mg-O_2 L^{-1}) was converted to mol L^{-1}, and this value was assumed to be equal to the concentration of CH_2O in the wastewater.

Additionally, several considerations are addressed in Part II:

- The toxicity of high salinity levels to microbes and crops is not directly modeled in the baseline simulations. These will be considered in the "best/worst" case framework by performing several model runs that eliminate nutrient and water uptake by plants and redox reactions performed by microbes.
- If the groundwater contains a significant amount of salinity, periodic water table fluctuations may exacerbate soil salinity problems. This issue is addressed using a simplified 2-D version of the model.

1. Numerical Modeling Code – MIN3P

The multi-component reactive flow and transport code, MIN3P (Mayer et al., 2002), was used to conduct the simulations. The program was selected for use here because it had two necessary attributes not found in other subsurface geochemistry codes: the ability to model partially saturated media in multiple dimensions and a flexible database system/reaction network to which additional equations could be added by the user.

MIN3P has been verified in comparison to other existing reactive transport models such as PHREEQC, PHAST, and MULTIFLO (Valocchi et al., 1981). In addition, simulation results have been compared to literature data. Specific verification examples include:

- Equilibrium redox mixing (comparison to PHAST)
- Biodegradation of toluene (comparison to PHAST)
- Dedolomitization (comparison with PHAST)
- Ion exchange (Valocchi et al., 1981)
- Acid mine drainage generation and attenuation (Lichtner, 1996)
- Copper leaching from a five spot well pattern (Lichtner, 1996)

Numerous applications of MIN3P have been reported in the literature, including: an assessment of suitability of reactive transport modeling for the evaluation of mine closure options (Bain et al., 2001), modeling kinetic processes controlling hydrogen and acetate concentrations in an aquifer-derived microcosm (Watson et al., 2003.), and a process-oriented description of the natural attenuation of petroleum hydrocarbons in an unconfined, partially saturated aquifer (Mayer et al., 2002).

MIN3P is one of the most advanced codes for modeling flow and transport in the vadose zone. Since its inception, it has undergone revisions and updates, and it is constantly under maintenance by it development team. There are other codes addressing flow and transport in the vadose zone, such as UNSATCHEM (Simunek et al., 1996; Suarez and Simunek, 1997). To explain our selection of MIN3P, we will benchmark it against UNSATCHEM.

The first thing to be said is that UNSATCHEM was published in 1996, and to the best of our knowledge, it has undergone only minimal upgrades and revisions since the late 1990's. Next, when selecting a code for a problem as complex such as ours, it was important for us to be able to work together with the code development team, and be able to implement code modifications where and when needed, and expediently. This option was provided to us amply by the MIN3P team, and in particular by the code primary developer, Dr. U. Mayer.

The next thing is to consider the range of processes covered by each of the codes. There may be particular processes that are covered better by one code or the other. In selecting a code, we considered the complete range of processes addressed by each code. Our investigation suggested the following:

- Processes included in both models: complexation, cation exchange, dissolution and precipitation, root water uptake, diffusion of CO_2.
- Processes included in UNSATCHEM only: Root water uptake as a function of osmotic stress, variable crop yield, root growth, changes in conductivity with changes in salinity.
- Processes included in MIN3P only: Chemical uptake by plants, bioghemical degradation reaction (nitrification and denitrification, sulfate reduction and respiration), and fate of the following chemicals: NH_4, CH_2O, Cu, Zn, Mn, Mn, Fe, PO_4, and diffusion of N_2, NH_3 and O_2.

It is clear that MIN3P is suited to cover a larger selection of processes which are relevant in the context of this project. Our strategy then is to adopt MIN3P, while taking measures to evaluate

the significance of those processes which are not modeled.

2. Model Setting

The simulations described below are set with conditions typical to the Modesto Study Area, shown in Figure 38. This area was selected for compatibility with the current saturated zone modeling efforts which are based on a United States Geological Survey investigation of the area's hydrogeology (Burow et al., 2004). The selection of unsaturated zone modeling parameters attempts to capture the soil types, precipitation, crop transpiration, and background groundwater chemistry found in this region. By considering a specific area within the Central Valley, it was possible to better constrain the values for these critical parameters.

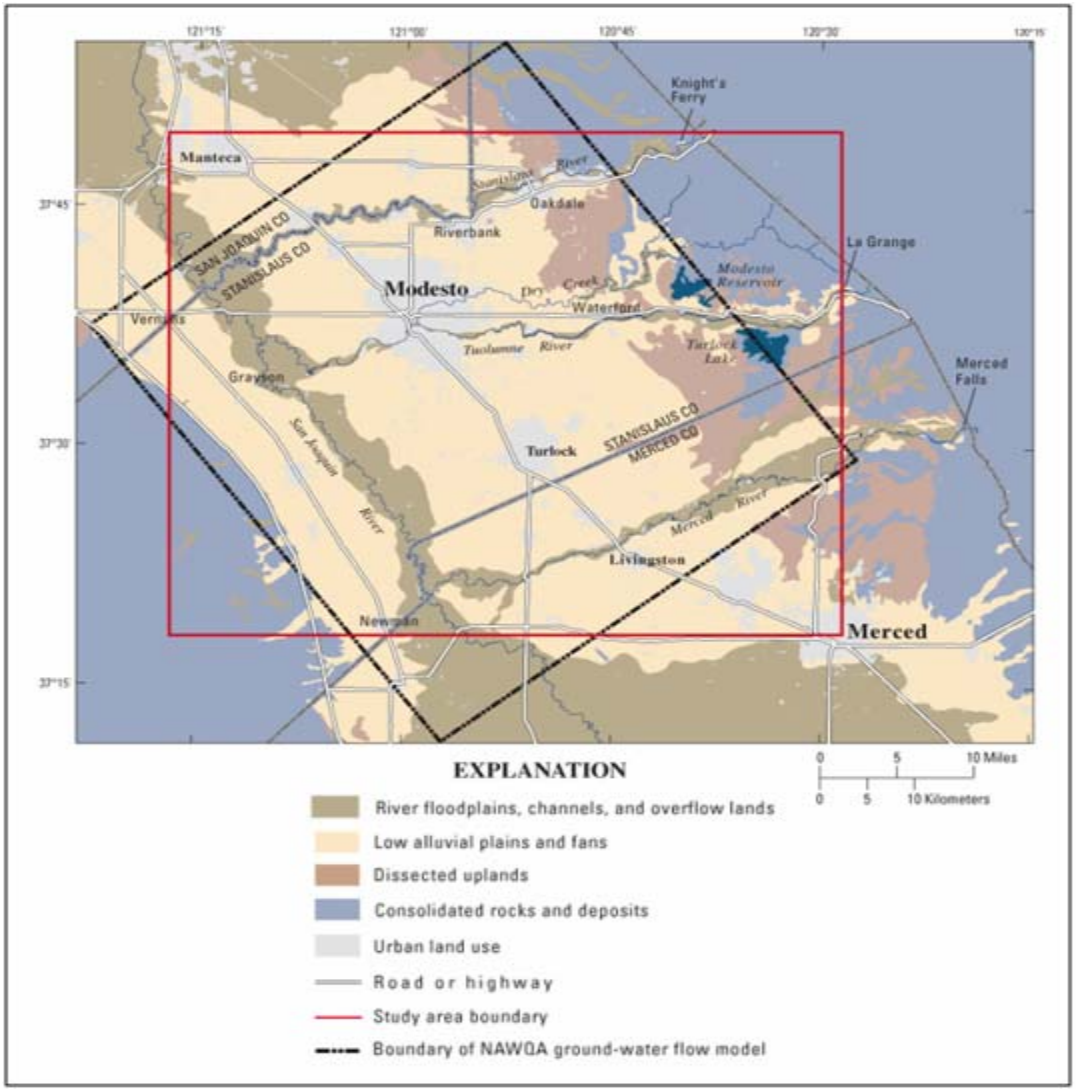

Figure 38

Modesto study area (Burow et al., 2004). The ranges of soil and hydrology parameters used in the simulations were designed to be representative of this area.

3. Spatial and Temporal Discretization

The 1-D model domain consists of a 15 m vertical column of soil with 1 m x 1 m lateral extents. This configuration is commonly used to analyze conditions where flow is primarily one-dimensional in the vertical direction, such as that in the vadose zone under a large source of infiltrating water.

The column was divided vertically into 151 cells; all with vertical dimension of 0.1 m except the top and bottom cells, which measured 0.05 m. The time-step was dynamically controlled by MIN3P during simulations, and the maximum time step was determined by the frequency of changes to the inflow boundary condition. The total time simulated was 30 years, chosen for consistency with the Hilmar SEP economic impact analysis.

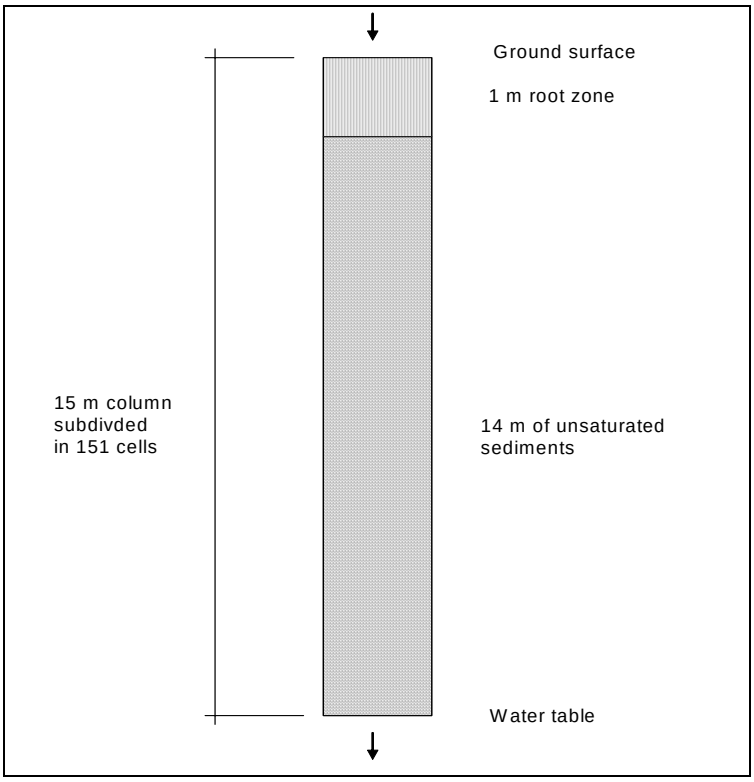

Figure 39

1-D simulation domain. The 15 m soil column is divided into 151 grid cells, each 0.1 m thick. Soil type is consistent throughout the column, and plant roots are present in the top 1 m.

4. Flow boundary conditions and water balance

The average annual precipitation in Modesto for the years 1931 to 2005 is 314 mm, with a maximum of 695 mm and a minimum of 109 mm (NOAA Western Regional Climate Center, 2006). Precipitation follows the annual trend common to most Central Valley locations: wet winters and dry summers. To determine the input to the simulations, the average monthly

precipitation rates were calculated using the 1986-2006 data from the National Oceanic and Atmospheric Administration's (NOAA) Western Regional Climate Center data(NOAA Western Regional Climate Center, 2006). All precipitation was assumed to infiltrate the soil; no corrections for run-off were performed.

Root water uptake was set equal to evapotranspiration (ET). The monthly averages of reference evapotranspiration (ET_0) for Modesto were calculated from the California Irrigation Management system data (Cal. Dep. of Water Resour., 2006) for 1987 – 2006. When designing the simulations, it was assumed that corn was grown from mid-June to mid-October and that winter wheat was grown for the remainder of the year, a typical pattern for the Central Valley. Kang et al. (Kang et al., 2003) measured the average monthly crop coefficients for corn and winter wheat in a semi-arid area. These values were used to predict the crop specific, average monthly evapotranspiration (ET_c) in Modesto by multiplying monthly crop coefficients (k_c) and monthly average reference evapotranspiration (ET_0). For example, the average ET_c for January was found using Eq 1.

Eq 1:
$$ET_{c,Jan} = k_{c,Jan} \frac{1}{19} \sum_{i=1987}^{2006} ET_{0,Jan,i}$$

Root water uptake, equal to ET_c, was limited to the first 1 meter of soil and assumed to be uniform throughout the root zone.

Table 14 shows the theoretical water balance for a field in Modesto, as calculated from the NOAA precipitation data and the ET_c values discussed previously. In the simulations, this cycle is repeated yearly over the course of 30 modeled years. During the spring and summer months, precipitation does not supply enough water to the crops. During times when waste water is applied at a site, it serves to meet part or this entire water deficit. When the combined precipitation and waste water application rates fall below the root water uptake, additional irrigation is applied to meet this deficit. The actual scenario-specific irrigation and waste water application rates are outlined in Section II.2.E.1.

Table 14: Water Balance at the Discharge Site

Month	Precipitation ($m\ s^{-1}$)	Root Water Uptake (ET_c) ($m\ s^{-1}$)	Water Needed from Waste Application or Irrigation ($m\ s^{-1}$)
January	2.54×10^{-8}	4.69×10^{-9}	-
February	2.53×10^{-8}	1.17×10^{-8}	-
March	1.83×10^{-8}	2.98×10^{-8}	1.15×10^{-8}
April	8.35×10^{-9}	6.63×10^{-8}	5.79×10^{-8}
May	7.22×10^{-9}	7.30×10^{-8}	6.58×10^{-8}
Early June	1.47×10^{-9}	4.04×10^{-8}	3.89×10^{-8}
Late June	1.47×10^{-9}	3.16×10^{-8}	3.02×10^{-8}
July	1.81×10^{-11}	7.57×10^{-8}	7.57×10^{-8}
August	1.54×10^{-10}	9.14×10^{-8}	9.13×10^{-8}
September	1.45×10^{-9}	5.35×10^{-8}	5.21×10^{-8}
Early October	4.51×10^{-9}	2.96×10^{-8}	2.51×10^{-8}
Late October	4.51×10^{-9}	1.35×10^{-8}	8.99×10^{-9}
November	8.31×10^{-9}	9.92×10^{-9}	1.61×10^{-9}
December	1.89×10^{-8}	4.55×10^{-9}	-

To obtain initial flow conditions in the subsurface representative of the area prior to land discharge of waste water from food-processing, a steady state simulation of flow was conducted using a recharge rate representative of average annual precipitation and necessary irrigation ($3.8 \times 10^{-8}\ m\ s^{-1}$). The transient simulations were then initialized with this pre-application flow pattern. A constant flux (second type) boundary condition was set at the top cell representing the total input from the combined precipitation, waste application, and irrigation. These values were varied on a monthly basis throughout most of the year, with biweekly variation in the June and October, which had crop coefficients that changed mid-month. A constant head (first type) boundary is specified at the bottom cell to represent the presence of the water table. The 1-D simulation required that the lateral boundaries be specified as no-flow. Root uptake was specified as a sink throughout the cells in the top 1 m of the soil profile.

5. Background Chemical Composition

Detailed, pre-waste application concentrations of the modeled chemicals are not available for the vadose zone. Instead, chemical concentrations in nearby groundwater are used as surrogates. The United States Geological Survey (USGS) collected a suite of water quality data from over 100 San Joaquin Valley wells between 1987 and 1988 (Shelton and Miller, 1991). To estimate background levels of most chemicals, typical concentrations from a subset of this data (six Modesto wells) were used. While the pore water initially present is likely to be displaced from the system quickly, its composition will determine the ions initially present on the exchange sites. If most of the exchange sites are occupied by easily displaceable ions (Mg, Ca), then ions present in the waste stream (K, NH_4, and Na) can readily replace them, affecting the composition of FDS, if not necessarily the concentration.

Some values not included in the USGS study (Shelton and Miller, 1991) were necessary to run the simulations: concentrations of ammonia and carbonate and partial pressures or aqueous concentrations of the gaseous species (oxygen, nitrogen, carbon dioxide, methane, and hydrogen sulfide). The main components (O_2, N_2) of the background gas in the vadose zone were assumed to be in equilibrium with the atmosphere for the high hydraulic conductivity cases. For low conductivity cases, a suboxic initial condition was specified. Carbon dioxide and carbonate were assumed in equilibrium with calcite present in the soil. The remaining components (those lacking data support) were assumed to be below their detection limits.

The background values were input into PHREEQC (Parkhurst and Appelo, 1999), along with a pH of 8.0 and were equilibrated with calcite. The equilibrated concentrations, shown in Table 15, were used for the MIN3P simulations as the initial concentrations throughout the vadose zone. The programs use the same database for equilibrium reaction parameters, and the initial mineral saturation indices were 0 in the MIN3P runs.

Table 15: Background Chemical Composition

Component	Initial Concentration (mg L^{-1})	Initial Concentration (mol L^{-1})	Source
Calcium (Ca^{2+})	46.9	1.17×10^{-3}	a
Magnesium (Mg^{2+})	17.7	7.30×10^{-4}	a
Potassium (K^{+})	4.3	1.10×10^{-4}	a
Sodium (Na^{+})	31.2	1.36×10^{-3}	a
Ammonium $\left(NH_4^+\right)$	1.81×10^{-6}	1.00×10^{-10}	b
Aluminum (Al^{3+})	1.34×10^{-12}	4.98×10^{-17}	a
Manganese (Mn^{2+})	7.50×10^{-4}	1.37×10^{-8}	a
Zinc (Zn^{2+})	1.09×10^{-3}	1.67×10^{-8}	a
Copper (Cu^{2+})	3.62×10^{-6}	5.70×10^{-11}	a
Iron (Fe^{2+})	1.01×10^{-13}	1.81×10^{-18}	a
Silicic acid (H_4SiO_4)	85.4	8.89×10^{-4}	a
Carbonate $\left(CO_3^{2-}\right)$	107	1.78×10^{-3}	b
Phosphate $\left(PO_4^{3-}\right)$	9.88×10^{-6}	1.04×10^{-10}	a
Sulfate $\left(SO_4^{2-}\right)$	25.1	2.61×10^{-4}	a
Chloride (Cl^{-})	18.9	5.33×10^{-4}	a
Nitrate (NO_3^{-})	5.81	9.37×10^{-5}	a
pH	8		a
Oxygen gas (O_2)	0.21 atm or 0.0021atm		b
Organic Matter (CH_2O)	0.83	2.76×10^{-5}	a
Dissolved hydrogen sulfide (HS^{-})	3.30×10^{-6}	1.00×10^{-10}	b

Dissolved methane (CH_4)	1.60×10^{-6}	1.00×10^{-10}	b
Nitrogen gas (N_2)	0.79 atm		b
Boric acid (H_3BO_3)	3.17	5.12×10^{-5}	a
a: Shelton (Shelton and Miller, 1991), b: assumed			

6. Transport Boundary Conditions

To represent the influent mass flux due to waste water application, a constant concentration boundary condition is specified at the top cell. The specified concentrations have two modes: waste water application and rain water application. During times of waste application, the concentrations for this boundary are set to match the industry-specific waste water concentrations (see Section II.2.E). During the non-operating season, the concentrations are set to resemble rainwater (Table 16). In the absence of alkalinity measurements, PHREEQC (Parkhurst and Appelo, 1999) was used to calculate the carbonate concentration necessary to ensure that the solution is charge balanced.

Table 16: Rainwater Chemical Composition

Component	Initial Concentration (mg L^{-1})	Initial Concentration (mol L^{-1})	Source
Calcium (Ca^{2+})	0.178	4.45×10^{-6}	A
Magnesium (Mg^{2+})	4.25×10^{-2}	1.75×10^{-6}	A
Potassium (K^{+})	0.276	1.20×10^{-5}	A
Sodium (Na^{+})	0.227	5.8×10^{-6}	A
Ammonium $\left(NH_4^+\right)$	18.2	1.01×10^{-3}	A
Aluminum (Al^{3+})	2.70×10^{-6}	1.00×10^{-10}	B
Manganese (Mn^{2+})	1.27×10^{-4}	2.31×10^{-9}	A
Zinc (Zn^{2+})	6.54×10^{-6}	1.00×10^{-10}	B
Copper (Cu^{2+})	6.35×10^{-6}	1.00×10^{-10}	B
Iron (Fe^{2+})	3.39×10^{-5}	6.07×10^{-10}	B

Silicic acid (H_4SiO_4)	9.61 x 10^{-6}	1.00 x 10^{-10}	B
Carbonate $\left(CO_3^{2-}\right)$	10.6	2.7 x 10^{-4}	C
Phosphate $\left(PO_4^{3-}\right)$	9.50 x 10^{-6}	1.00 x 10^{-10}	B
Sulfate $\left(SO_4^{2-}\right)$	0.132	1.375 x 10^{-6}	A
Chloride (Cl^-)	0.518	1.46 x 10^{-5}	A
Nitrate $\left(NO_3^-\right)$	29.9	4.83 x 10^{-4}	A
pH	6.49		A
Oxygen gas (O_2)	0.21 atm		B
Organic Matter (CH_2O)	0.61	1.9 x 10^{-5}	A
Dissolved hydrogen sulfide (HS^-)	3.31 x 10^{-6}	1.00 x 10^{-10}	B
Dissolved methane (CH_4)	1.61 x 10^{-6}	1.00 x 10^{-10}	B
Nitrogen gas (N_2)	0.79 atm		B
Boric acid (H_3BO_3)	6.10 x 10^{-6}	1.00 x 10^{-10}	B
A: (Collett et al., 1999); B: assumed (Appelo and Postma, 2005); C: calculated			

The second type outflow boundary in the bottom cell allowed for mass to be transported out of the system by advection.

7. Transport parameters

Transport is assumed to be advection controlled, eliminating pore-scale dispersion. This leads to a conservative approach in terms of modeled concentrations. Tests were conducted that included dispersion and differences in overall system behavior were found to be insignificant. Aqueous diffusion is neglected and the effective diffusion coefficient for the transport of gasses is estimated using the equation: $D_{eff} = D_g \phi^{4/3} S_g^{10/3}$, where D_g is the free diffusion coefficient in the soil gas phase (2.07 x 10^{-5} m^2 s^{-1} for all gases) ϕ is porosity (0.35 for all soil types), and S_g is the saturation of the gas phase (Millington, 1959).

8. Root Solute Uptake

Two types of models for root solute uptake are available in MIN3P: passive uptake and active uptake. When water carrying dissolved, non-ionic species moves into a plant's root system, uptake of these chemicals occurs. Alternately, when plants use respiration energy to transport ionic species across a membrane barrier, active uptake occurs (Barber, 1995). Passive uptake is assumed negligible for the model. The majority of the species considered are ionic, and experimental runs using passive uptake showed that only a small fraction of non-ionic species were removed. Active uptake is modeled using the Michaelis-Menten formulation (Barber, 1995):

Eq 2: $$I_x(t) = I_{x,\max} \frac{C_x(t)}{K_x + C_x(t)}$$

where $I_x(t)$ (μmol cm^{-2} s^{-1}) is the total uptake rate of species x at simulation time t, $I_{x,max}$ (μmol cm^{-2} s^{-1}) is the maximum ion uptake rate, C_x is the species concentration, and K_x is the concentration for which the reaction rate is $0.5*I_{max}$ (mol cm^{-3}). The crops are assumed to have the summer corn and winter wheat rotation discussed previously. The uptake parameters used are shown in Table 17 along with their source. Some unit conversions required the relationship between the dry weight of wheat and its root surface area, 0.15 m^2 g^{-1} (Smolders et al., 1996). To maintain electrical neutrality, an appropriate number of HCO_3^- or H^+ ions are released when an ion is absorbed (Tinker and Nye, 2000).

Table 17: Active Root Uptake Parameters

Nutrient	Corn			Wheat		
	$I_{x,max}$ (mol cm^{-2} s^{-1})	K_x (mol/L^{-1})	Ref.	$I_{x,max}$ (mol cm^{-2} s^{-1})	K_x (mol/L)	Ref.
Nitrate $\left(NO_3^-\right)$	10^{-12}	10^{-5}	a	4.81 x 10^{-13}	2.7 x10^{-5}	d
Ammonium $\left(NH_4^+\right)$	10^{-12}	10^{-5}	a	6.48 x 10^{-13}	5 x 10^{-5}	d
Potassium (K)	1.1 x 10^{-12}	1.4 x 10^{-5}	b, c	1.9 x 10^{-13}	7 x 10^{-6}	b, a
Sulfur (S)	3 x 10^{-13}	10^{-5}	c	-	-	-
Phosphorus (P)	3.26 x 10^{-12}	5.8 x 10^{-6}	c	1.4 x 10^{-13}	6 x 10^{-6}	a
Magnesium (Mg)	4 x 10^{-12}	1.5 x 10^{-4}	c	4.0 x 10^{-14}	1 x 10^{-6}	a
Calcium (Ca)	10^{-12}	4.0 x 10^{-3}	c	1.6 x 10^{-13}	5 x 10^{-6}	a
Zinc (Zn)	-	-	-	5.5 x 10^{-14}	8.9 x10^{-7}	e
A: (Barber, 1995); B: (Corwin, 2007); C: (Roose et al., 2001); D:(Goyal and Huffaker, 1986); E: (Rengel and Wheal, 1997)						

For corn, Coelho and Or (1998) report an average rooting depth of 0.84 m, with a root length density of 0.55 cm cm^{-3} and a root diameter of 0.036 cm. For wheat, Robinson et al. (1994) reported a root length density of approximately 50 km m^{-3} (5.0 cm cm^{-3}). Winter wheat has a maximum depth of penetration of 50 to100 cm from December through March and 125 to 200 cm during April and May (Gregory et al., 1978), and an average root diameter of 0.015 cm (Gahoonia et al., 1997). Based on these rooting lengths, both active solute uptake and root water uptake are specified to occur within the top 100 cm of the model.

Considerable uncertainty is associated with the root uptake parameters given in Table 17. The value of I_{max} is known to vary with plant age, cultivar, and temperature (Barber, 1984). To ensure that the solute uptake parameters selected were consistent with conditions in the Central Valley, preliminary simulation results were compared to known agronomic rates, as found in the *Western Fertilizer Handbook* (Ludwick et al., 2002) and determined by expert opinion (Corwin, 2007), and used to constrain I_{max}.

Additionally, most literature addresses only one set of these conditions, ignoring changes in I_{max} during the growing season. Although I_{max} is typically given as a constant, the total nutrient uptake as a function of time is often reported. Barraclough (1986) measured the cumulative

uptake of nitrogen, phosphorus, potassium, calcium, and magnesium in high-yielding winter wheat crops and modeled the pattern over time using logistic functions (Eq 3 through Eq 7, as given by the general form shown in Eq 8):

Eq 3: $$y_N = 0.95 + \frac{20.0}{1 + \exp(-0.055(t - 209))}$$

Eq 4: $$y_P = 0.13 + \frac{3.9}{1 + \exp(-0.048(t - 227))}$$

Eq 5: $$y_K = 0.41 + \frac{34.9}{1 + \exp(-0.039(t - 229))}$$

Eq 6: $$y_{Ca} = 0.019 + \frac{7.0}{1 + \exp(-0.035(t - 249))}$$

Eq 7: $$y_{Mg} = 0.017 + \frac{1.4}{1 + \exp(-0.049(t - 232))}$$

Eq 8: $$y_{nutrient} = a + \frac{c}{1 + \exp(-b(t - m))}$$

where $y_{nutrient}$ is the cumulative uptake in g m^{-2} and t is the time in number of days from sowing. These functions are expressed graphically in Figure 40.

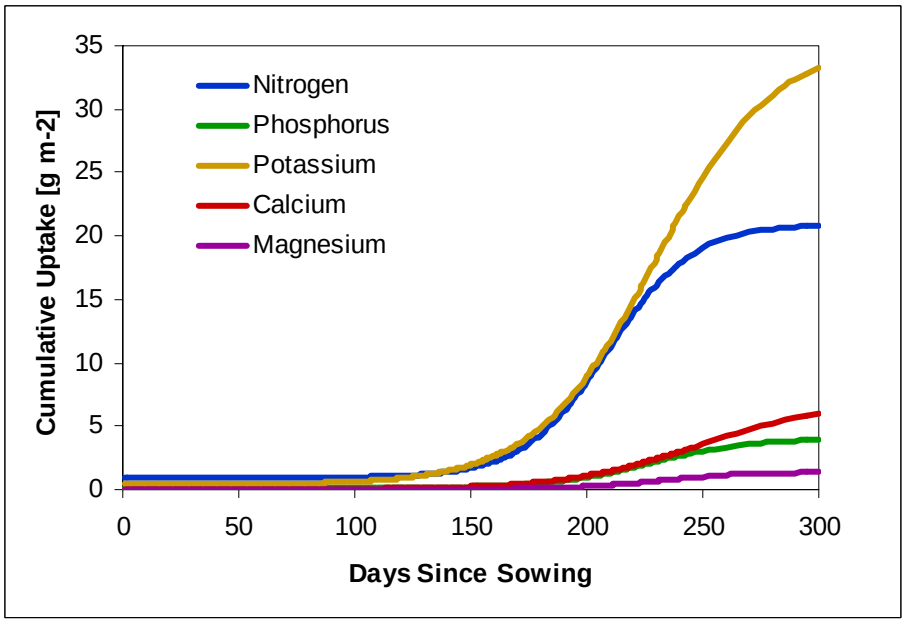

Figure 40

Cumulative uptake curves for winter wheat. The seedlings have low uptake levels immediately after planting in the fall, and these increase as the plant matures, until harvested in the spring at

around 250 to 300 days.

To calculate the uptake rate at any given period of time, the derivative of these exponential functions was found. It is shown in Eq 9, in its generalized form:

Eq 9:
$$R_{nutrient}(t) = \frac{dy_{nutrient}}{dt} = cb\frac{\exp(-b(t-m))}{[1+\exp(-b(t-m))]^2}$$

where $R_{nutrient}(t)$ is the nutrient uptake rate in g m^{-2} d^{-1}. For each nutrient, the uptake rate was calculated for Days 0 to 300, and the maximum uptake rate ($R_{nutrient,\,max}$) was found. The uptake factor at a given point in time was then obtained by dividing the two: $f_{nutrient,norm}(t) = R_{nutrient}(t) / R_{nutrient,\,max}$.

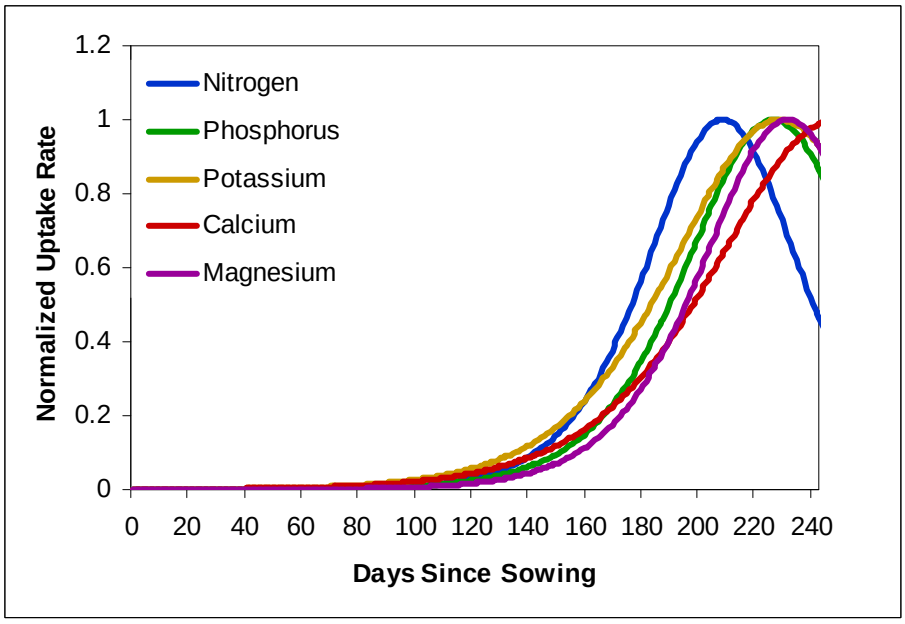

Figure 41

Uptake factors for wheat. These curves, derived from the cumulative uptake curves in Figure 40, show the overall uptake rate normalized by the maximum uptake rate, I_{max}.

The uptake factor curves were discretized into monthly time-steps in order to input them into MIN3P (Figure 42). The growing season was from sowing on October 15 to harvesting on June 15. For each month, the discretized $f_{nutrient,norm}(t)$ (Table 8) was multiplied by I_{max} to supply a time-variable uptake rate. In this manner, the uptake that MIN3P calculates at a given time-step is shown in Eq 10.

Eq 10:
$$I(t) = f_{norm}(t)\ I_{max}\frac{C_1(t)}{K_m + C_1(t)}$$

This procedure has two inherent assumptions: that I_{max} varies in time in the same manner as the

overall nutrient uptake and that the literature values for I_{max} are measured at the peak of the growing season, making them the highest possible.

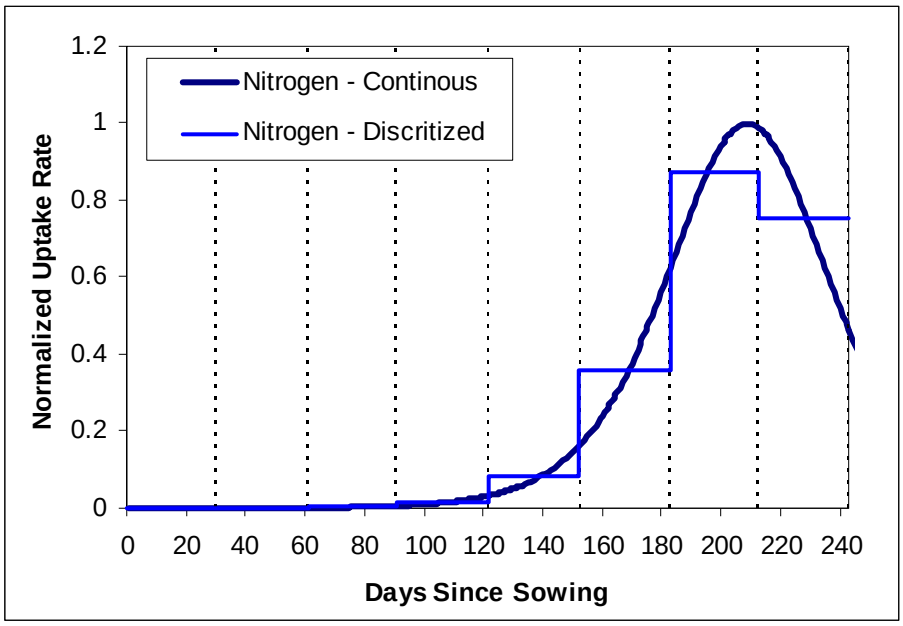

Figure 42

Discretized nitrogen uptake factors for wheat. The nitrogen uptake rate curve is shown here, broken down into monthly increments for input into the numerical model. The area under both the smooth and the step curves is consistent.

The same procedure was repeated for corn after generating logistic functions using data from Karlen et al. (1987) (Eq 11 to Eq 13). It was assumed that $f_{SO4,norm}(t) = f_{PO4,norm}(t)$ and $f_{K,norm}(t) = f_{Ca,norm}(t) = f_{Mg,norm}(t)$. The growing season was given as June 15 through October 15.

Eq 11: $$y_N = -0.002 + \frac{2.71}{1 + \exp(-0.124(x - 58))}$$

Eq 12: $$y_P = -0.0004 + \frac{0.423}{1 + \exp(-0.117(x - 60.1))}$$

Eq 13: $$y_K = -0.00024 + \frac{3.73}{1 + \exp(-0.187(x - 53.2))}$$

Table 18 summarizes the $R_{nutrient,norm}$ values for both corn and winter wheat.

Table 18: Summary of Uptake Factors

Time Period	Ca	K	NO_3	NH_4	Mg	PO_4	SO_4	Zn
Corn Uptake Factors								
June 15 – July 15	0.0363	0.0363	0.0750	0.0750	0.0363	0.0736	0.0736	-
July 15 – Aug 15	0.6052	0.6052	0.7250	0.7250	0.6052	0.7145	0.7145	-
Aug 15 - Sept 15	0.0444	0.0444	0.2423	0.2423	0.0444	0.3159	0.3159	-
Sept 15 - Oct 15	0.0002	0.0002	0.0093	0.0093	0.0002	0.0163	0.0163	-
Wheat Uptake Factors								
Oct 15 - Nov 15	0.0017	0.0015	0.0002	0.0002	0.0002	0.0003	-	0.0002
Nov 15 - Dec 15	0.0048	0.0049	0.0010	0.0010	0.0008	0.0012	-	0.0008
Dec 15 - Jan 15	0.0139	0.0159	0.0052	0.0052	0.0034	0.0050	-	0.0034
Jan 15 - Feb 15	0.0399	0.0515	0.0275	0.0275	0.0153	0.0216	-	0.0153
Feb 15 - Mar 15	0.1110	0.1579	0.1361	0.1361	0.0656	0.0891	-	0.0656
Mar 15 - Apr 15	0.2883	0.4270	0.5240	0.5240	0.2577	0.3269	-	0.2577
Apr 15 - May 15	0.6233	0.8353	0.9430	0.9430	0.7142	0.8006	-	0.7142
May 15 - June 15	0.8861	0.8378	0.4973	0.4973	0.8099	0.7793	-	0.8099

9. Biogeochemical Reaction Network and Reaction Parameters

a) Biogeochemical Reactions

Seven oxidation-reduction (redox) reactions are included in the simulations to describe the decay of organic matter, nitrate, and ammonia (Hunter et al., 1998; Langergraber and Simunek, 2005; MacQuarrie and Sudicky, 2001). The appropriate redox sequence is shown below, with anaerobic reactions occurring below the dotted line:

Eq 14: Nitrification

$$a: NH_3 + 2O_2 \rightarrow NO_2^- + 3H^+ + 2e^-$$
$$b: NO_2^- + H_2O \rightarrow NO_3^- + 2H^+ + 2e^-$$

Eq 15: Respiration

$$CH_2O + O_2 \rightarrow CO_3^{2-} + 2H^+$$

Eq 16: Methane oxidation $$CH_4 + 2O_2 \rightarrow CO_3^{2-} + 2H^+ + H_2O$$

Eq 17: Denitrification $$CH_2O + \frac{4}{5}NO_3^- \rightarrow \frac{2}{5}N_2 + CO_3^- + \frac{6}{5}H^+ + \frac{2}{5}H_20$$

Eq 18: Manganese reduction $$CH_2O + 2MnO_2 + 2H^+ \rightarrow CO_3^{2-} + 2Mn^{2+} + 2H_2O$$

Eq 19: Iron reduction $$CH_2O + 4FeOOH + 6H^+ \rightarrow CO_3^{2-} + 4Fe^{2+} + 6H_2O$$

Eq 20: Sulfate Reduction $$CH_2O + \frac{1}{2}SO_4^{2-} \rightarrow CO_3^{2-} + \frac{1}{2}HS^- + \frac{3}{2}H^+$$

Eq 21: Fermentation $$CH_2O + \frac{1}{2}H_2O \rightarrow \frac{1}{2}CO_3^{2-} + \frac{1}{2}CH_4 + H^+$$

While all of the possible key reactions are included in the modeling, the simulated model conditions determine which of the reactions are active at any given time. For instance, if simulation conditions show that the vadose zone remains oxygenated, only the top three reactions will be activated. Then if methane is not present, only nitrification and respiration will occur.

The rates of progress of these reactions are determined by Monod-type rate expressions. For example, the equation to determine the rate of de-nitrification is shown below:

Eq 22:
$$R = k\left(\frac{\left[NO_3^-\right]}{\left[NO_3^-\right] + K_{NO_3^-}}\right)\left(\frac{\left[CH_2O\right]}{\left[CH_2O\right] + K_{CH_2O}}\right)\left(\frac{K_i}{\left[H^+\right] + K_i}\right)$$

where k is the overall rate, K_i's are inhibition constants, and K_x's are the half-saturation constants, and the component concentrations are denoted by square brackets, except for $[H^+]$ (species concentration). The parameter values for the redox reactions involving nitrogen are shown in Table 19, and those for the remaining reactions are shown in Table 20. All rate constants for reactions involving organic carbon are normalized to the consumption of CH_2O.

Table 19: Rate Parameters for Biogeochemical Reactions Involving Nitrogen Compounds

	Nitrification	Denitrification	CH_2O Oxidation
Overall Rate, k (mol L^{-1} s^{-1})	2.00 x 10^{-9}	5.00 x 10^{-10}	2.00 x 10^{-10}
Half-sat CH_2O, K_{CH_2O} (mol L^{-1})	-	1.56 x 10^{-4}	1.88 x 10^{-4}
Half-sat O_2, K_{O_2} (mol L^{-1})	1.72 x 10^{-5}	-	4.69 x 10^{-6}
Half-sat NO_3, K_{NO_3} (mol L^{-1})	-	2.26 x 10^{-5}	-
Half-sat NH_4, K_{NH_4} (mol L^{-1})	1.88 x 10^{-4}	-	-
O_2 inhibition, $K_{inhibit,O_2}$ (mol L^{-1})	-	1.59 x 10^{-5}	-
pH inhibition, $K_{inhibit,H+}$ (mol L^{-1})	1.0 x 10^{-6}	1.0 x 10^{-6}	1.0 x 10^{-6}
Sources: (MacQuarrie and Sudicky, 2001), (Langergraber and Simunek, 2005), (Mailloux et al., 2002), (Dincer and Kargi, 2000)			

Table 20: Rate Parameters for Additional Biogeochemical Reactions

	Sulfate Reduction	Manganese reduction	Iron Reduction	Fermentation	Methane Oxidation
Overall Rate k (mol L^{-1} s^{-1})	5.00×10^{-10}	5.0×10^{12}	2.0×10^{-12}	1.00×10^{-11}	1.00×10^{-9}
Half-sat CH_2O, K_{CH_2O} (mol L^{-1})	1.06×10^{-4}	1.00×10^{-5}	5.00×10^{-3}	1.00×10^{-3}	-
Half-sat CH_4 K_{CH_4} (mol L^{-1})	-	-	-	-	1.00×10^{-5}
Half-sat O_2 K_{O_2} (mol L^{-1})	-	-	-	-	3.13×10^{-6}
Half-sat SO_4 K_{SO_4} (mol L^{-1})	1.60×10^{-3}	-	-	1.00×10^{-5}	-
NO_3 inhibition $K_{inhibit,NO_3}$ (mol L^{-1})	1.60×10^{-5}	5.00×10^{-8}	3.13×10^{-6}	1.60×10^{-5}	-
O_2 inhibition $K_{inhibit,O_2}$ (mol L^{-1})	3.13×10^{-5}	5.00×10^{-8}	3.13×10^{-6}	3.13×10^{-5}	-
pH inhibition $K_{inhibit,H+}$ (mol L^{-1})	1.0×10^{-6}	-	-	1.0×10^{-6}	-
Sources: (Mayer et al., 2001) and references therein					

These rates were selected based on a review of available literature data, as discussed in Mayer et al. (2001).

b) Mineral dissolution-precipitation reactions

Goldberg et al. (2005) measured manganese and iron oxide contents of 0.05 and 0.66 percent, respectively, for a selection of Central Valley soils. For the simulations, it is assumed that approximately 10% of these oxides are bio available and that these mineral phases are

reductively dissolved by Mn and Fe-reduction (see section C.9.a)

The soils also have a low to moderate calcite ($CaCO_3$) content (0 to 5 percent), are characterized by a wide range of salinity values (0 – 16 mmhos cm^{-1}), and gypsum ($CaSO_4 \cdot 2H_2O$) ranging from 0 to 5% (USDA, 2006). For the simulations, it was assumed that the sediments contain calcite at 1% and gypsum at 0%, by volume. (The effects of these assumptions are explored in Part II). The formation of secondary minerals was also included to control the concentrations of relevant aqueous components. Phases included are the carbonate containing minerals siderite ($FeCO_3$) and rhodochrosite ($MnCO_3$), and the sulfur containing minerals mackinawite (FeS) and gypsum ($CaSO_4 \cdot 2H_2O$). These phases should be viewed as solubility controls for Fe (II), H_2S, Mn(II) and SO_4. Dissolution and precipitation of calcite and the secondary phases are described as quasi-equilibrium reactions.

c) Ion Exchange Reactions

Within the Modesto area, the soil's cation exchange capacity (CEC) ranges from 1.0 meq $100g^{-1}$ for the Delhi soil series to 40 meq $100g^{-1}$ for the Meikle soil series, as reported by U.S. Department of Agriculture's Web Soil Survey (USDA, 2006). For the simulations, a cation exchange capacity of 3 meq/100g, and a dry bulk density of 1.5 g cm^{-3} was selected.

D. Numerical Modeling – Case-specific Input Parameters

The key variable parameters in this study include the soil hydraulic conductivity, waste water application rates, and waste water composition. These parameters were varied on both a case specific and industry specific basis. This section discusses how the soil parameters and application rates were selected to yield soil saturations representative of aerobic (case 1), anaerobic (Case 2), and mixed (Case 3) vadose zone conditions. Section E describes how these cases were coupled with industry specific inputs.

1. Case-Specific Soil Properties

Soil conductivity plays an important role in controlling moisture content and redox conditions and was therefore chosen as a sensitivity parameter. This parameter was determined based on published data. The Eastern Stanislaus County Soil Survey (Arkley, 1964), as published through the U.S. Department of Agriculture's Web Soil Survey (USDA, 2006), contains generalized information about the physical and chemical parameters of the soils in the Modesto area. These soils are predominantly alluvium, consisting of recent flood plain deposits and granitic alluvial fans. Their saturated hydraulic conductivity ranges from 4.2×10^{-7} m s^{-1} for Modesto Loam to 1.4×10^{-4} m s^{-1} for Delhi Sand. In the absence of more detailed data, Rosetta (Schaap et al., 2001) was used to estimate the van Genuchten-Mualem (Mualem, 1976; van Genuchten, 1980) parameters of these soils; the results are displayed in Table 21.

Table 21: Modesto Soil Hydraulic Conductivity Parameters

	Low (Modesto loam)	High (Dehli sand)
Saturated Conductivity (K_s)	4.2 x 10^{-7} m s^{-1}	1.41 x 10^{-4} m s^{-1}
Residual Saturation (S_r)	0.17	0.13
Air-entry parameter (α))	1.11 m^{-1}	3.53 m^{-1}
Pore-size distribution parameter (n)	1.47	1.47
Empirical curve fitting exponent (L)	0.5	0.5
Air Entry Pressure (P_a)	0 atm	0 atm

For the simulations, hydraulic conductivities have been defined as 9 x 10^{-8} m s^{-1} (case 1) , 1.4 x 10^{-4} m s^{-1} (case 2), and 2 x 10^{-7} m s^{-1} (case 3) to cover conditions of high, low and intermediate water saturations. The lower conductivities are slightly lower than the minimum observed value. However, this choice is justified by observed ponding in some land application areas and accounts for the possibility of clogging through organic matter deposition and/or excessive microbial growth (bioclogging). For low conductivity soils, the soil hydraulic function parameters for Modesto loam are used, while the Dehli sand hydraulic function parameters are employed for high conductivity media.

2. Waste Water Application Rates

In practice, waste water application rates for individual dischargers are limited by the WDRs issued by the Water Quality Board. These permits specify the application area ($A_{\text{permitted}}$ in acres) and maximum volumetric flow rate ($Q_{\text{permitted}}$ in gallons per day, or gal d^{-1}), and these values were used to calculate the permitted waste water application rate, q_{permit} (m s^{-1}), for each case (Eq 23):

Eq 23:
$$q_{\text{permit}} = \frac{Q_{\text{permit}}}{A_{\text{permit}}} b$$

where b is a factor converting gallons per acre per day (gal $acre^{-1}$ d^{-1}) to meters per second (m s^{-1}).

The rates permitted by the Water Quality Board are determined based upon the estimated waste stream concentrations, the application area, and the applicable loading limits for nitrogen, salt, and/or BOD. For example, in 2002, one tomato processor proposed (and was permitted) to discharge 5.3 million gal d^{-1} during July to October and 1.3 million gal d^{-1} during the rest of the

year to 1612 acres. This results in application rates of 3.6 x 10^{-8} m s^{-1} and 8.8 x 10^{-9} m s^{-1}. The permit specified that the following conditions were to be met:

> "a. Nutrient mass loading rates shall neither exceed agronomic rates for the crop to be planted nor cause groundwater degradation;
>
> b. Degradable organic (BOD) mass loading rates shall not create a nuisance and shall notdegrade groundwater quality; and
>
> c. Mass loading rates for nutrients and degradable organic compounds shall be based on the character of the wastewater, crop, soil, climate, other nutrient sources, and irrigation management system."

According to information provided in the WDR, at these rates and acreages, approximately 97 lb $acre^{-1}$ yr^{-1} of nitrogen, 2915 lb $acre^{-1}$ yr^{-1} of TDS, and 1383 lb $acre^{-1}$ yr^{-1} of BOD would be applied.

Another tomato processor was permitted to discharge up to 40,000 gal d^{-1} over an area of 13 acres (3.3 x 10^{-8} m s^{-1}) from July to October, not to exceed 4.8 million gal total. The WDR states that this would result in an application of approximately 154 lb $acre^{-1}$ d^{-1} of nitrogen, 2102 lb $acre^{-1}$ yr^{-1} of salts, and 199 lb $acre^{-1}$ d^{-1} of BOD.

A survey of WDRs showed that the typical BOD loading limits were 100 lbs $acre^{-1}$ d^{-1} on average and 300 lbs $acre^{-1}$ daily maximum. . To ensure that the waste streams being modeled were compliant with these regulations, the maximum permitted volumetric flux based on the concentration, $Q_{maximum}$, was calculated (Eq 24):

Eq 24:
$$Q_{\text{maximum}} = \frac{M_{\text{BOD,max}} A_{\text{modeled}}}{C_{\text{modeled}}} b$$

where $M_{BOD,max}$ is the maximum mass loading rate for BOD (100 lb $acre^{-1}$ d^{-1}), $C_{modeled}$ is case specific BOD concentration (mg L^{-1}), $A_{modeled}$ is the cross-sectional area of the column model (1 m^2), and b is a conversion factor. To find the specific flux: $q_{maximum} = Q_{maximum}/A_{modeled}$.

The modeled flux, $q_{modeled}$, was selected as the lower of the two values $q_{maximum}$ and q_{permit} (Table 22, Table 27). Selecting application rates in agreement with the WDRs, and not necessarily equal to the actual rates observed, ensured that the scenarios modeled were indicative of processors compliant with both the waste flow rate and BOD loading regulations. This method also produced the "worst case" scenario still within the regulations.

For most processors, the permissible application rates ranged from 1 x 10^{-8} to 9 x 10^{-8} m s^{-1}. These rates, coupled with the hydraulic conductivities discussed in Section 1, result in representative saturation levels for each case: 0.9 – 0.99 for Case 1, 0.4 – 0.5 for Case 2, and 0.8

– 0.9 for Case 3. Table 11summarizes the defining characteristics for each case. It includes the desired saturation conditions and the ratio of the hydraulic conductivity to the waste water application rate that is necessary to create these conditions. The K_{sat} values and application rates are discussed further in Sections 1 and 2 of this document.

E. Industry Specific Modeling Inputs

As discussed previously, the main components of concern in the wastewater have been identified as nitrate, ammonia, and organic matter. Salinity levels, as measured by the fixed dissolved solids (FDS) or electrical conductivity (EC), are also of primary concern. Salinity is created by the presence of ionic species, including sodium, calcium, magnesium, and potassium. Additionally, pH may play an important role in the solution chemistry; however, the waste discharge permits indicate that if pH is too low, lime must be applied to the soil surface to act as a buffer. It is therefore assumed that applied water has a pH no lower than approximately 6.5. The minimum and maximum values for each of these five important components are collected for each industry type and provide the full range of observed concentrations (Table 22, Table 29, Table 32, Table 37).

Since few processors provide ammonia concentrations, total Kjeldahl nitrogen (TKN) is used as a surrogate measure for ammonia. TKN measures the total organic and ammonia nitrogen. This assumption is conservative, because it assumes that all urea (organic nitrogen) present will be converted to ammonia relatively rapidly (as compared to nitrification rates). In saturated soil, Ma et al. (1999) estimated first order rates at 0.6032 h^{-1} for hydrolysis and 0.0169 h^{-1} for nitrification, noting that all urea was converted within the first 1 cm of a silty loam soil column. In unsaturated soils, Savant et al. (1987) report rates of hydrolysis, up to 2.5 mg h^{-1}, with almost 90% of urea being decayed within the top 0.5 cm. These studies support the assumption that hydrolysis is completed within the top soil layer (represented by a single element in MIN3P), and that it occurs much more rapidly than nitrification.

For several of the dischargers, the individual concentrations of the components contributing to salinity are not reported, and salinity was measured as either EC or FDS. To determine the individual concentrations necessary for the MIN3P simulations, the following equation is used (Eaton, 2005):

Eq 25:

$$(a) \quad FDS = 0.6 * EC$$

$$(b) \quad FDS = \left[Na^{+}\right] + \left[K^{+}\right] + \left[NH_4^{+}\right] + \left[Ca^{2+}\right] + \left[Mg^{2+}\right] + \left[Mn^{2+}\right] + \left[Zn^{2+}\right] + \left[Cu^{2+}\right] + \left[Fe^{2+}\right] + \left[Al^{3+}\right] + \left[Cl-\right] + \left[NO_3^{-}\right] + \left[CO_3^{2-}\right] + \left[SO_4^{2-}\right] + \left[PO_4^{3-}\right]$$

Using data from processors with complete records, the average fraction of FDS contributed by

each component is determined on an industry-specific basis (Table 24, Table 30, Table 38. To fill in gaps in the concentration records, a processor's average FDS concentration (or 0.6*EC) was multiplied by the average fraction for each component, to obtain an approximate component concentration.

At the flow rates modeled, waste water application had to be supplemented in some cases with irrigation and rainwater to meet the requirements for plant root water uptake. To determine the concentrations of the various components in the mixed water, the following formula is used:

Eq 26: $$[\mathrm{x}]_{simulated} = r[x]_{waste} + (1-r)[x]_{rainwater}$$

where $[x]$ is the concentration of any particular component and *r* is the mixing ratio. Monthly mixing ratios are determined on a case-specific basis (Table 16, Table 18, Table 25 and Table 30).

1. Case- and Industry-Specific Parameters

A total of twelve simulations were conducted, one of each case and industry combination. Based on the case-specific waste composition criteria discussed in Sections B.1through B.4 one processor was selected as representative of each case/industry combination. The application rate for each simulation was calculated using the permitted discharge area and volumetric flow rates found in that processor's WDRs, by the methods described in Section D.2. Processors were randomly assigned codes (eg, Tomato Processor B), and these codes are used to refer to them. Additionally, a simulation of the application of treated wastewater at the Modesto Publicly Owned Treatment Works (POTW) was conducted.

For reference, the groundwater quality objectives set by the Central Valley Water Quality Control Board are included (Marshack, 2003) in the figures and charts describing the simulation input parameters. These recommendations do not apply to the waste stream itself, but instead to the groundwater below and around the land application area. If the effluent concentrations exceed these limits, and sufficient attenuation does not occur, degradation of the groundwater will result.

The results of these simulations can be found in Part II of this document. They are listed as "Baseline Scenarios" and are used as the basis for further modeling work.

a) Tomato Processing Facilities

This section summarizes the industry and case-specific parameters for simulations focusing on the tomato-processing industry. Tomato processors typically discharge waste during the months of July, August, September, and October, the tomato harvest season. Although several tomato

processors discharge a small amount throughout the year due to the production of additional product lines, this assumption of summer-only discharge has been selected because it is the most representative of the industry as a whole. During the non-application periods, the flow rates were set to equal the precipitation rate plus the irrigation rate needed to meet root uptake demand. Table 22 presents the land application rates for the various cases. Case 1 was based on the rates permitted for "Tomato Plant B", Case 2 on the "Tomato Plant I" rates, and Case 3 on the "Tomato Plant L" rates.

Table 22: Industry-Specific Land Application Rates for Tomato Processors

Month	Case 1 ($m\ s^{-1}$)		Case 2 ($m\ s^{-1}$)		Case 3 ($m\ s^{-1}$)	
	Waste Water	Irrigation + Precip.	Waste Water	Irrigation + Precip.	Waste Water	Irrigation + Precip.
January	0	2.54×10^{-8}	0	2.54×10^{-8}	0	2.54×10^{-8}
February	0	2.53×10^{-8}	0	2.53×10^{-8}	0	2.53×10^{-8}
March	0	2.98×10^{-8}	0	2.98×10^{-8}	0	2.98×10^{-8}
April	0	6.63×10^{-8}	0	6.63×10^{-8}	0	6.63×10^{-8}
May	0	7.30×10^{-8}	0	7.30×10^{-8}	0	7.30×10^{-8}
Early June	0	4.04×10^{-8}	0	4.04×10^{-8}	0	4.04×10^{-8}
Late June	0	3.16×10^{-8}	0	3.16×10^{-8}	0	3.16×10^{-8}
July	9.81×10^{-8}	1.81×10^{-11}	5.5×10^{-8}	2.07×10^{-8}	1.3×10^{-8}	6.22×10^{-8}
August	9.81×10^{-8}	1.54×10^{-10}	5.5×10^{-8}	3.64×10^{-8}	1.3×10^{-8}	7.79×10^{-8}
September	9.81×10^{-8}	1.45×10^{-9}	5.5×10^{-8}	1.45×10^{-9}	1.3×10^{-8}	4.00×10^{-8}
Early October	9.81×10^{-8}	4.51×10^{-9}	5.5×10^{-8}	4.51×10^{-9}	1.3×10^{-8}	1.61×10^{-8}
Late October	9.81×10^{-8}	4.51×10^{-9}	5.5×10^{-8}	4.51×10^{-9}	1.3×10^{-8}	4.51×10^{-9}
November	0	9.92×10^{-9}	0	9.92×10^{-9}	0	9.92×10^{-9}
December	0	1.89×10^{-8}	0	1.89×10^{-8}	0	1.89×10^{-8}

Minimum and maximum values for each of the five key components (BOD, NO_3, TKN/NH_3, EC and pH) are presented in Table 23. Component factors to estimate industry-typical individual component concentrations from FDS are provided in Table 24.

Table 23: Concentrations of Main Components Of Concern In Tomato Wastewater

	Minimum Concentration	Maximum Concentration
Organic Matter as BOD (mg/L)	0	10000
Nitrate (mg-N/L)	0	14
Ammonium as Total Kjeldahl Nitrogen (mg-N/L)	0	745
Ammonium direct (mg-N/L)	0.5	8.6
EC (µS/cm)	0	15200
pH	4.2	8.2

Table 24: Industry-Specific FDS Component Factors For Tomato Processors

Species	Proportion of FDS Tomato Processors
Calcium (Ca^{2+})	0.037
Magnesium (Mg^{2+})	0.020
Potassium (K^{+})	0.088
Sodium (Na^{+})	0.25
Ammonium $\left(NH_4^+\right)$	0.042
Aluminum (Al^{3+})	0.0035
Manganese (Mn^{2+})	0.00028
Zinc (Zn^{2+})	0.00027
Copper (Cu^{2+})	0.00013
Iron (Fe^{2+})	0.0099
Carbonate $\left(CO_3^{2-}\right)$	0.21
Phosphate $\left(PO_4^{3-}\right)$	0.0062
Sulfate $\left(SO_4^{2-}\right)$	0.035
Chloride (Cl^{-})	0.27
Nitrate $\left(NO_3^-\right)$	0.0013

Table 23 summarizes the full concentration range for the primary components of concern and includes extreme values. However, the waste water composition for the individual cases was obtained by matching the effluent concentrations of selected tomato processors with contaminant concentrations that meet the case-specific criteria for the primary components of concern. The waste water concentrations of all modeled chemical components are shown in Table 25. The concentrations of the key components for the selected cases and the other tomato processors are shown graphically in Figure 43. The concentrations are normalized to the highest average value found in any industry-specific waste stream. Concentrations in Table 25 are modified to obtain

model input concentrations based on mixing ratios between waste water and rain/irrigation water (Table 26) as described in Section E.

Table 25: Industry-Specific Effluent Chemical Composition for Tomato Processors

Component	Groundwater WQ Objective (mg L^{-1}) (Marshack, 2003)	Case 1 Concentration (mg L^{-1}) [as mg-N L^{-1}]	Case 2 Concentration (mg L^{-1}) [as mg-N L^{-1}]	Case 3 Concentration (mg L^{-1}) [as mg-N L^{-1}]
Calcium (Ca^{2+})	N/A	62.2 (a)	29.2	33.5
Magnesium (Mg^{2+})	N/A	33.9 (a)	13.7	20.1
Potassium (K^{+})	N/A	148 (a)	74.8	74.7
Sodium (Na^{+})	20 – 69	417 (a)	211	211
Ammonium (NH_4^{+})	1.93 – 38.7 [1.5 – 30.0]	61.7 [47.9]	47.1 [36.5]	44.7 [34.69]
Aluminum (Al^{3+})	0.2 – 5.0	5.90 (a)	3.27	2.75
Manganese (Mn^{2+})	0.05 – 0.2	0.460 (a)	0.181	0.277
Zinc (Zn^{2+})	2.0 – 5.0	0.449 (a)	0.249 (a)	0.209
Copper (Cu^{2+})	0.17 – 1.3	0.225 (a)	0.125 (a)	0.105
Iron (Fe^{3+})	0.3 – 5.0	16.5 (a)	3.96	0.0121
Silicic acid (H_4SiO_4)	N/A	85 (c)	85 (c)	85 (c)
Carbonate (CO_3^{2-})	N/A	354.8 (a)	282	88.5
Phosphate (PO_4^{3-})	N/A	31.6 (a)	23.3	9.84
Sulfate (SO_4^{2-})	250 - 500	59.1 (a)	11.3	45.5
Chloride (Cl^{-})	106 - 250	447 (a)	197	251
Nitrate (NO_3^{-})	44.3 [10]	2.97 [0.67]	10.45 [2.43]	0.177 [0.040]
pH	6.5 – 8.5	5.38*	N/A*	6.4*
Oxygen gas (O_2)	N/A	0.21 atm (b)	0.21 atm (b)	0.21 atm (b)
Organic Matter (CH_2O)	200 – 500 (d)	824	122	746
Dissolved hydrogen sulfide (HS^{-})	N/A	3.31×10^{-4} (b)	3.31×10^{-4} (b)	3.31×10^{-4} (c)
Dissolved methane (CH_4)	N/A	1.61×10^{-4} (b)	1.61×10^{-4} (b)	1.61×10^{-4} (b)
Nitrogen gas (N_2)	N/A	0.79 atm (b)	0.79 atm (b)	0.79 atm (b)
Boric acid (H_3BO_3)	0.7 – 0.1	0.545 (a)	0.454	0.127
TDS/FDS	450 - 500	1674	930	780
a: ratio from FDS, b: assumed, c: background, d: from recent WDRs * pH assumed to equal 6.4 after buffering, as required in recent WDRs				

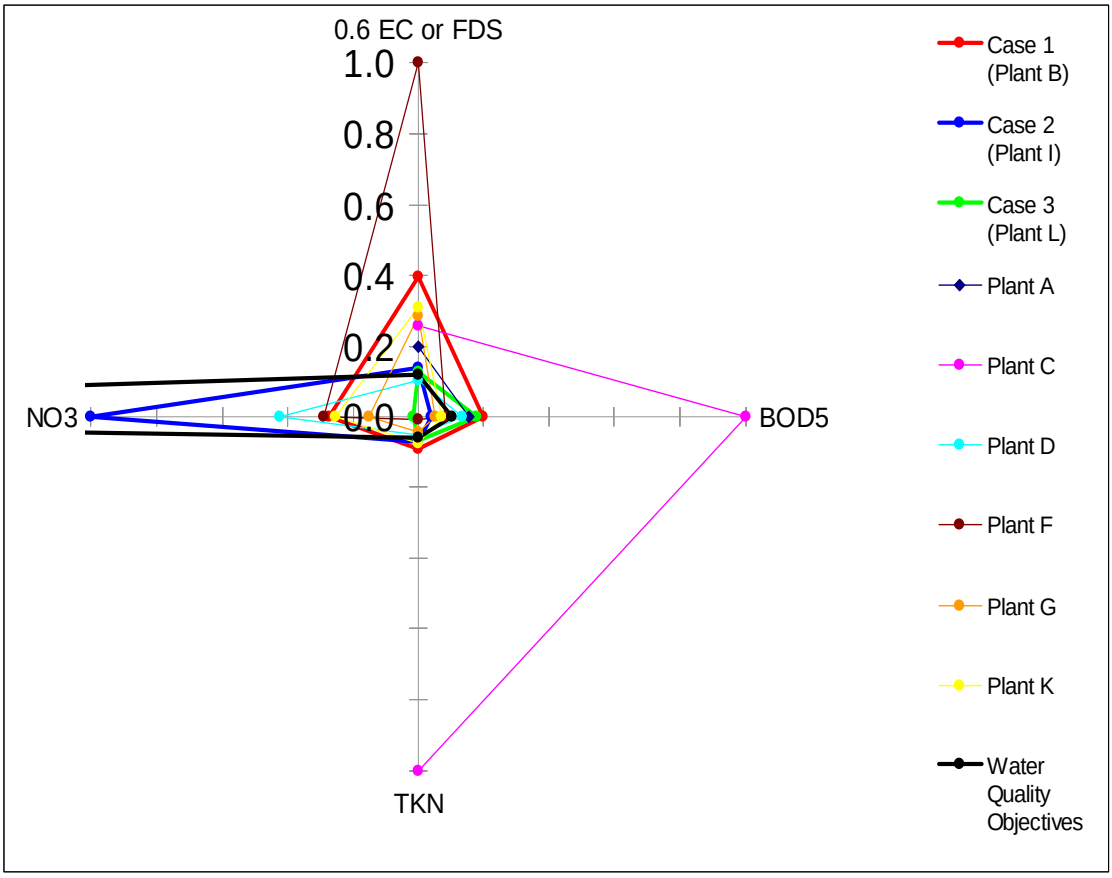

Figure 43

Concentration profile for tomato processors. The flow-weighted average concentration of each of the four components of interest was normalized by the highest average value found in all tomato processor waste-streams.

Table 26: Mixing Ratios for Tomato Processor Scenarios

Month	Case 1	Case 2	Case 3
July	1.00	0.73	0.18
August	1.00	0.60	0.15
September	0.99	0.97	0.25
Early October	0.96	0.92	0.46
Late October	0.96	0.92	0.75

b) Wineries and Grape Processing Facilities

This section summarizes the industry- and case-specific parameters for simulations focusing on

wineries and grape processing facilities. Wineries and grape processors typically discharge waste year-round. These rates fluctuate throughout the year, with high discharge occurring during the "crush" season and low discharge occurring during bottling. Table 27 presents the land application rates for the various cases. Case 1 was based on the rates permitted for "Winery E", Case 2 on the "Winery R" rates, and Case 3 on the "Winery J" rates.

Table 27: Industry-Specific Land Application Rates for Wineries and Grape Processors

Month	Case 1 ($m\ s^{-1}$)		Case 2 ($m\ s^{-1}$)		Case 3 ($m\ s^{-1}$)	
	Waste Water	Irrigation + Precip.	Waste Water	Irrigation + Precip.	Waste Water	Irrigation + Precip.
January	8.70×10^{-9}	2.54×10^{-8}	6.98×10^{-9}	2.54×10^{-8}	5.03×10^{-9}	2.54×10^{-8}
February	8.70×10^{-9}	2.53×10^{-8}	6.98×10^{-9}	2.53×10^{-8}	3.87×10^{-10}	2.53×10^{-8}
March	8.70×10^{-9}	2.12×10^{-8}	6.98×10^{-9}	2.43×10^{-8}	3.87×10^{-10}	2.97×10^{-8}
April	8.70×10^{-9}	5.88×10^{-8}	6.98×10^{-9}	6.44×10^{-8}	3.87×10^{-10}	6.73×10^{-8}
May	2.58×10^{-8}	4.83×10^{-8}	1.12×10^{-8}	6.32×10^{-8}	3.87×10^{-10}	7.43×10^{-8}
Early June	2.58×10^{-8}	1.50×10^{-8}	1.12×10^{-8}	2.99×10^{-8}	3.87×10^{-10}	4.10×10^{-8}
Late June	2.58×10^{-8}	5.99×10^{-9}	1.12×10^{-8}	2.09×10^{-8}	3.87×10^{-10}	3.20×10^{-8}
July	2.58×10^{-8}	5.12×10^{-8}	1.12×10^{-8}	6.61×10^{-8}	3.87×10^{-10}	7.72×10^{-8}
August	2.58×10^{-8}	6.73×10^{-8}	1.12×10^{-8}	8.23×10^{-8}	1.24×10^{-8}	8.10×10^{-8}
September	2.58×10^{-8}	2.84×10^{-8}	1.12×10^{-8}	4.34×10^{-8}	1.24×10^{-8}	4.22×10^{-8}
Early October	1.45×10^{-8}	1.53×10^{-8}	1.12×10^{-8}	1.87×10^{-8}	1.24×10^{-8}	1.75×10^{-8}
Late October	1.45×10^{-8}	4.51×10^{-9}	1.12×10^{-8}	4.51×10^{-9}	1.24×10^{-8}	4.51×10^{-9}
November	1.45×10^{-8}	8.31×10^{-9}	6.98×10^{-9}	8.31×10^{-9}	5.03×10^{-9}	8.31×10^{-9}
December	8.70×10^{-9}	1.89×10^{-8}	6.98×10^{-9}	1.89×10^{-8}	5.03×10^{-9}	1.89×10^{-8}

Table 28: Mixing Ratios for Winery Scenarios

Month	Case 1	Case 2	Case 3
January	0.26	0.22	0.17
February	0.26	0.22	0.02
March	0.29	0.22	0.01
April	0.13	0.10	0.01
May	0.35	0.15	0.01
Early June	0.63	0.27	0.01
Late June	0.81	0.35	0.01
July	0.33	0.14	0.005
August	0.28	0.12	0.13
September	0.48	0.20	0.23
Early October	0.49	0.37	0.41
Late October	0.76	0.71	0.73
November	0.64	0.46	0.38
December	0.32	0.27	0.21

Minimum and maximum values for each of the five key components (BOD, NO_3, TKN/NH_3, EC and pH) are presented in Table 29. Component factors to estimate industry-typical individual component concentrations from FDS are provided in Table 30.

Table 29: Concentrations of Main Components of Concern in Winery and Grape Processing Wastewater

	Minimum Concentration	Maximum Concentration
Organic Matter as BOD (mg/L)	0	29700
Nitrate (mg-N/L)	0	140
Ammonia as Total Kjeldahl Nitrogen (mg-N/L)	0	880
Ammonia direct (mg-N/L)	0	184
EC (µS/cm)	0	38400
pH	2.5	12.2

Table 30: Industry-Specific FDS Component Factors for Wineries and Grape Processors

Species	Proportion of FDS
Calcium (Ca^{2+})	0.059
Magnesium (Mg^{2+})	0.022
Potassium (K^{+})	0.14
Sodium (Na^{+})	0.14
Ammonium $\left(NH_4^+\right)$	0.062
Aluminum (Al^{3+})	N/A
Manganese (Mn^{2+})	0.00037
Zinc (Zn^{2+})	0.00057
Copper (Cu^{2+})	0.00011
Iron (Fe^{2+})	0.00186
Carbonate $\left(CO_3^{2-}\right)$	0.41
Phosphate $\left(PO_4^{3-}\right)$	0.012
Sulfate $\left(SO_4^{2-}\right)$	0.086
Chloride (Cl^{-})	0.13
Nitrate $\left(NO_3^-\right)$	0.0048

Table 29 summarizes the full concentration range for the primary components of concern and includes extreme values. The waste water concentrations of all modeled chemical components are shown in Table 31. The concentrations of the key components for the selected cases and the other wineries and grape processors are shown graphically in Figure 44. The concentrations are normalized to the highest average value found in any industry-specific waste stream. Concentrations in Table 31 are modified to obtain model input concentrations based on mixing ratios between waste water and rain/irrigation water (Table 28) as described in Section E.

Table 31: Effluent Chemical Composition for Winery Cases

Component	Groundwater WQ Objective ($mg\ L^{-1}$) (Marshack, 2003)	Case 1 Concentration ($mg\ L^{-1}$) [as mg-N L^{-1}]	Case 2 Concentration ($mg\ L^{-1}$) [as mg-N L^{-1}]	Case 3 Concentration ($mg\ L^{-1}$) [as mg-N L^{-1}]
Calcium (Ca^{2+})	N/A	77.0 (a)	254	39.4
Magnesium (Mg^{2+})	N/A	28.9 (a)	95.4	8.45
Potassium (K^{+})	N/A	184 (a)	606	55.2
Sodium (Na^{+})	20 – 69	188 (a)	621	156
Ammonium (NH_4^{+})	1.93 – 38.7 [1.5 – 30.0]	259 [201]	16.4 [12.7]	18.8 [14.6]
Aluminum (Al^{3+})	0.2 – 5.0	1.34×10^{-12} (c)	1.34×10^{-12} (c)	1.34×10^{-12} (c)
Manganese (Mn^{2+})	0.05 – 0.2	0.480 (a)	1.59 (a)	0.1066
Zinc (Zn^{2+})	2.0 – 5.0	0.740 (a)	2.44 (a)	0.6583
Copper (Cu^{2+})	0.17 – 1.3	0.150 (a)	0.480 (a)	0.1602
Iron (Fe^{2+})	0.3 – 5.0	2.43 (a)	8.00 (a)	3.5646
Silicic acid (H_4SiO_4)	N/A	85.4 (c)	85.4 (c)	85.4 (c)
Carbonate (CO_3^{2-})	N/A	533	1757	304 (a)
Phosphate (PO_4^{3-})	N/A	46.2	152	16.7
Sulfate (SO_4^{2-})	250 - 500	112 (a)	7.47	40.3
Chloride (Cl^{-})	106 - 250	136	538 (a)	41.2000
Nitrate (NO_3^{-})	44.3 [10]	15.1 [3.41]	112 [25.5]	11.0 [2.48]
pH	6.5 – 8.5	5.75*	8.73*	6.36
Oxygen gas (O_2)	N/A	0.21 atm (b)	0.21 atm (b)	0.21 atm (b)
Organic Matter (CH_2O)	200 – 500 (d)	4120	182	1206
Dissolved hydrogen sulfide (HS^{-})	N/A	3.31×10^{-4} (b)	3.31×10^{-4} (b)	3.31×10^{-4} (c)
Dissolved methane (CH_4)	N/A	1.61×10^{-4} (b)	1.61×10^{-4} (b)	1.61×10^{-4} (b)
Nitrogen gas (N_2)	N/A	0.79 atm (b)	0.79 atm (b)	0.79 atm (b)
Boric acid (H_3BO_3)	0.7 – 0.1	7.38	24.4 (a)	7.38
TDS/FDS	450 - 500	1300	4300	743

a: ratio from FDS, b: assumed, c: background, d: from recent WDRs
* pH assumed to equal 6.4 after buffering, as required in recent WDRs

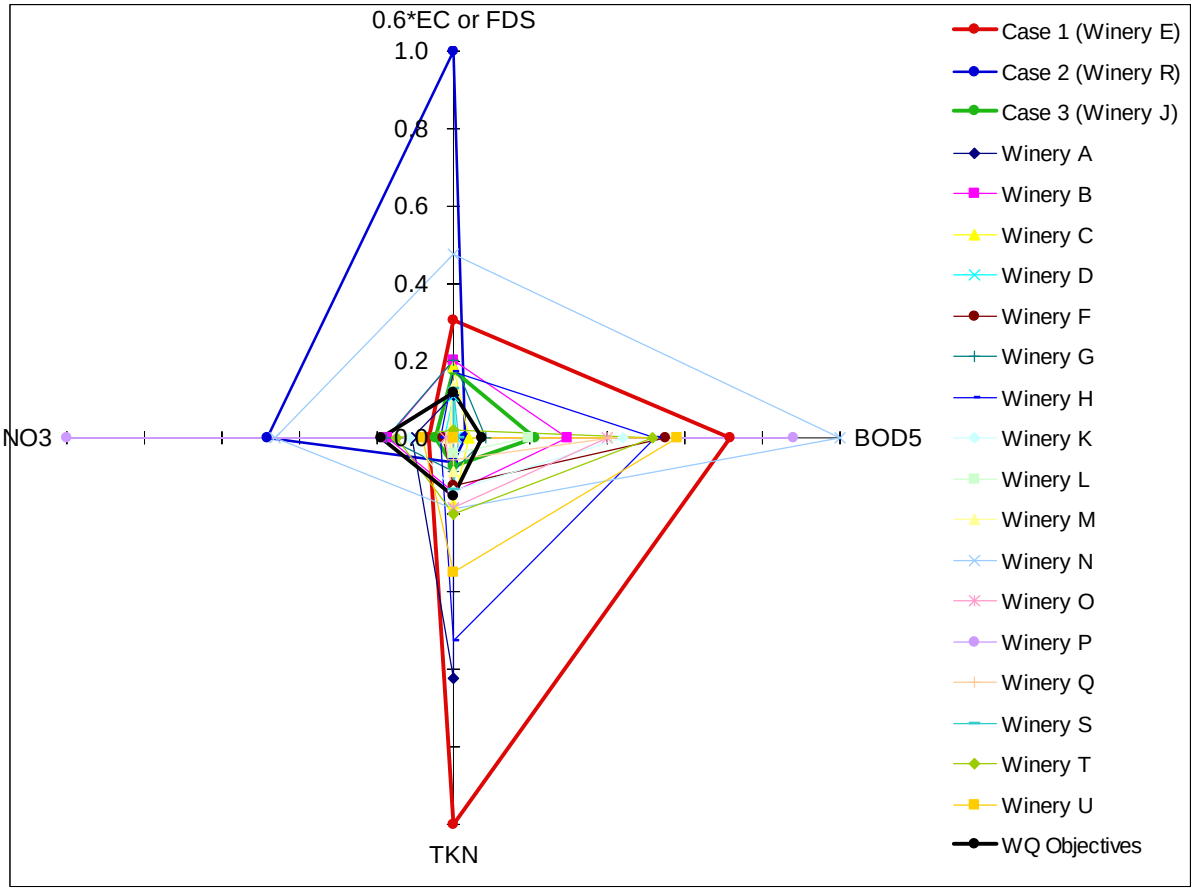

Figure 44

c) Milk Processing Facilities

This section summarizes the industry- and case-specific parameters for simulations focusing on facilities that process milk into cheese and whey. These facilities do not raise or house cattle on-site; they process milk and milk products obtained elsewhere. Due to the limited number of dairy processors, dairy waste-water characteristics were not derived from Central Valley data. Instead, literature sources were used to obtain FDS, organic matter, and species concentrations as wells as overall flow rates. Danalewich et al. (1998) provided a detailed summary of the waste-streams of 14 milk processors. Of these plants, 12 produced cheese, 1 plant sliced and packed cheese, and 1 plant canned dairy products; 7 of the plants also produced whey as a secondary product. Britz et al. (2005) summaries the characteristics of dairy waste described in multiple studies, but does not provide plant specific data.

Table 33 displays the full concentration range for the primary components of concern (BOD, NO_3, TKN/NH_3, EC and pH), including extreme values. The concentrations of the key components for the selected cases and the other dairy processors are shown graphically in Figure 45. The concentrations are normalized to the highest average value found in any industry-specific waste stream.

Table 32: Concentrations of Main Components of Concern in Milk Processing Discharge

	Minimum Concentration	Maximum Concentration	Processor Type 1 (Min)	Processor Type 2 (Max)	Source
Organic Matter as BOD (mg/L)	565	35,000	Cheese	Whey	a
Nitrate (mg-N/L)	0.6	80	Milk	Milk	b
Ammonium as Total Kjeldahl Nitrogen (mg-N/L)	14	1462	Cheese	Whey	a
Ammonium direct (mg-N/L)	0.7	64.3	Cheese	Whey	a
FDS	Non-detect	4762	Cheese	Cheese	b
pH	3.38	11.3	Cheese	Cheese	a
Sources: a, Britz et al. (2005); b, Danalewich et al. (1998); FDS = total dissolved solids – volatile dissolved solids					

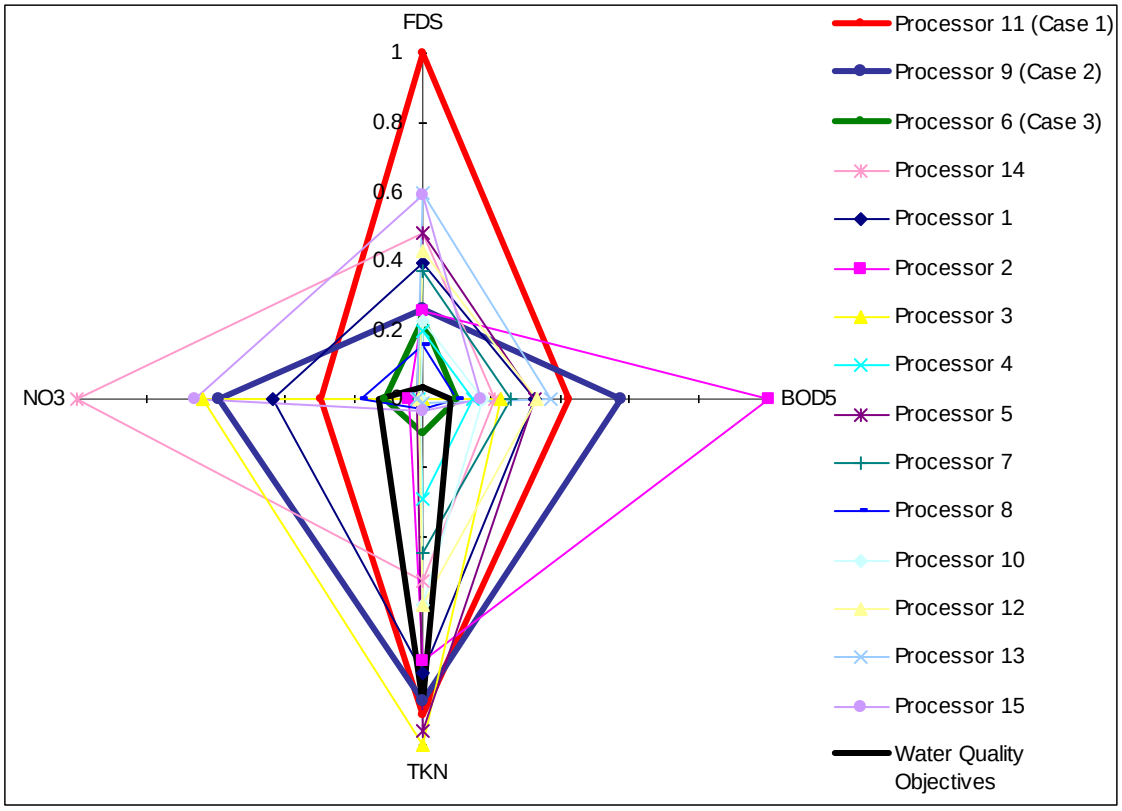

Figure 45

Concentration profile for dairy processors (Danalewich et al., 1998). The flow-weighted average concentration of each of the four components of interest was normalized by the highest average value found in all dairy processor waste-streams.

The waste water composition for the individual cases was obtained by examining the effluent concentrations of the processors described in Danalewich et al. (1998) and selecting three that met the case-specific criteria for the primary components of concern. Case 1 was based on the average effluents from "Plant 11", a cheese producer; Case 2 on "Plant 14", a cheese producer that also generates alcohol derived from milk products; and Case 3 on "Plant 6", which cans dairy products, particularly cheese dips.

The waste water concentrations of all modeled chemical components are shown in Table 33. It was assumed that waste in the concentrations described would be directly applied to land. (Unlike the data used for other modeled industries, these data are not specific to land dischargers.) This assumption could lead to the modeling of higher values for nitrogen and organic matter than would occur in reality. Dairy processors commonly add a waste pre-treatment step, such as filtering or activated sludge (Britz et al., 2005), that reduces these constituents but does little for the overall salinity levels.

Table 33: Effluent Chemical Composition for Milk Processor Cases

Component	Groundwater WQ Objective (mg L^{-1}) (Marshack, 2003)	Case 1 Concentration (mg L^{-1}) [as mg-N L^{-1}]	Case 2 Concentration (mg L^{-1}) [as mg-N L^{-1}]	Case 3 Concentration (mg L^{-1}) [as mg-N L^{-1}]
Calcium (Ca^{2+})	N/A	54.20	54.30	33.60
Magnesium (Mg^{2+})	N/A	11.80	8.30	16.90
Potassium (K^{+})	N/A	58.50	41.20	8.60
Sodium (Na^{+})	20 – 69	734	423	453
Ammonium (NH_4^{+})	1.93 – 38.7 [1.5 – 30.0]	165 [128]	95.3 [74.0]	18.0 [14.0]
Aluminum (Al^{3+})	0.2 – 5.0	0.257	0.100	0.071
Manganese (Mn^{2+})	0.05 – 0.2	0.327	0.009	0.001
Zinc (Zn^{2+})	2.0 – 5.0	6.54×10^{-4} (a)	6.54×10^{-4} (a)	6.54×10^{-4} (a)
Copper (Cu^{2+})	0.17 – 1.3	0.001	0.030	0.010
Iron (Fe^{2+})	0.3 – 5.0	4.33	0.247	0.091
Silicic acid (H_4SiO_4)	N/A	85.4 (b)	85.4 (b)	85.4 (b)
Carbonate (CO_3^{2-})	N/A	305	274	320
Phosphate (PO_4^{3-})	N/A	107.27	159	199
Sulfate (SO_4^{2-})	250 - 500	1649 (c)	574 (c)	25.0 (c)
Chloride (Cl^{-})	106 - 250	1649 (c)	574 (c)	25.0 (c)
Nitrate (NO_3^{-})	44.3 [10]	105 [23.7]	354 [80.0]	38 [8.60]
pH	6.5 – 8.5	6.9	8.5*	6.800
Oxygen gas (O_2)	N/A	0.21 atm (a)	0.21 atm (a)	0.21 atm (a)
Organic Matter (CH_2O)	200 – 500 (d)	2260	1103	533
Dissolved hydrogen sulfide (HS^{-})	N/A	3.31×10^{-4} (a)	3.31×10^{-4} (a)	3.31×10^{-4} (a)
Dissolved methane (CH_4)	N/A	1.61×10^{-4} (a)	1.61×10^{-4} (a)	1.61×10^{-4} (a)
Nitrogen gas (N_2)	N/A	0.79 atm (a)	0.79 atm (a)	0.79 atm (a)
Boric acid (H_3BO_3)	0.7 – 0.1	6.10×10^{-4} (a)	6.10×10^{-4} (a)	6.10×10^{-4} (a)
FDS	450 - 500	4762	2285	1108
a: assumed, b: background, c: from FDS not accounted for by other ions, * pH assumed to equal 8.5 after buffering, as required in recent WDRs				

The reported flow rates for the three processors were as follows: 132 to 257 m^3 d^{-1} for Processor 11 (Case 1), 1703 to 2650 m^3 d^{-1} for Processor 14 (Case 2), and 49 to 237 m^3 d^{-1} for Processor 6 (Case 3). Since no information was available about the area over which discharge would occur, the minimum permissible discharge area was found using the following equation:

Eq 27:
$$a = \frac{Q * C_{BOD}}{M_{\max}}$$

where a is the minimum area [m^2], Q is the maximum reported flow rate [m^3 s^{-1}] , C_{BOD} is the BOD concentration [mg m^3], and M_{max} is the USEPA recommended loading limit, 100 lb $acre^{-1}$ yr^{-1} (1.3×10^{-7} mg m^{-2} s^{-1}).

To obtain the land application rate, q [m s^{-1}], the flow rates given above were divided by the

calculated minimum area, *a*. Dairies typically have high flow rates during the summer months and lower rates during the winter (Danalewich et al., 1998). The high end of the flow range was used to calculate the summer application rate, while the lower end was used for the winter. Table 34 lists the resulting application rates along with the precipitation and necessary irrigation.

Table 34: Industry-Specific Land Application Rates For Milk Processors

Month	Case 1 ($m\ s^{-1}$)		Case 2 ($m\ s^{-1}$)		Case 3 ($m\ s^{-1}$)	
	Waste Water	Irrigation + Precip.	Waste Water	Irrigation + Precip.	Waste Water	Irrigation + Precip.
January	2.77×10^{-8}	2.54×10^{-8}	7.09×10^{-8}	2.54×10^{-8}	4.72×10^{-8}	2.54×10^{-8}
February	2.77×10^{-8}	2.53×10^{-8}	7.09×10^{-8}	2.53×10^{-8}	4.72×10^{-8}	2.53×10^{-8}
March	2.77×10^{-8}	1.83×10^{-8}	7.09×10^{-8}	1.83×10^{-8}	4.72×10^{-8}	1.83×10^{-8}
April	5.39×10^{-8}	1.23×10^{-8}	1.10×10^{-7}	8.35×10^{-9}	2.28×10^{-7}	8.35×10^{-9}
May	5.39×10^{-8}	1.91×10^{-8}	1.10×10^{-7}	7.22×10^{-9}	2.28×10^{-7}	7.22×10^{-9}
Early June	5.39×10^{-8}	1.47×10^{-9}	1.10×10^{-7}	1.47×10^{-9}	2.28×10^{-7}	1.47×10^{-9}
Late June	5.39×10^{-8}	1.47×10^{-9}	1.10×10^{-7}	1.47×10^{-9}	2.28×10^{-7}	1.47×10^{-9}
July	5.39×10^{-8}	2.18×10^{-8}	1.10×10^{-7}	1.81×10^{-11}	2.28×10^{-7}	1.81×10^{-11}
August	5.39×10^{-8}	3.75×10^{-8}	1.10×10^{-7}	1.54×10^{-10}	2.28×10^{-7}	1.54×10^{-10}
September	5.39×10^{-8}	1.45×10^{-9}	1.10×10^{-7}	1.45×10^{-9}	2.28×10^{-7}	1.45×10^{-9}
Early October	2.77×10^{-8}	4.51×10^{-9}	7.09×10^{-8}	4.51×10^{-9}	4.72×10^{-8}	4.51×10^{-9}
Late October	2.77×10^{-8}	4.51×10^{-9}	7.09×10^{-8}	4.51×10^{-9}	4.72×10^{-8}	4.51×10^{-9}
November	2.77×10^{-8}	8.31×10^{-9}	7.09×10^{-8}	8.31×10^{-9}	4.72×10^{-8}	8.31×10^{-9}
December	2.77×10^{-8}	1.89×10^{-8}	7.09×10^{-8}	1.89×10^{-8}	4.72×10^{-8}	1.89×10^{-8}

The concentrations in Table 33 were modified to obtain model input concentrations based on mixing ratios between waste water and rain/irrigation water (Table 35) as described in Section E.

Table 35: Mixing Ratios For Dairy Scenarios

Month	Case 1	Case 2	Case 3
January	0.52	0.74	0.65
February	0.52	0.74	0.65
March	0.60	0.79	0.72
April	0.81	0.93	0.96
May	0.74	0.94	0.97
Early June	0.97	0.99	0.99
Late June	0.97	0.99	0.99
July	0.71	1.00	1.00
August	0.59	1.00	1.00
September	0.97	0.99	0.99
Early October	0.86	0.94	0.91
Late October	0.86	0.94	0.91
November	0.77	0.90	0.85
December	0.59	0.79	0.71

d) Meat Packing Plants

This section summarizes the industry and case-specific parameters for simulations focusing on the meat packing industry. Meat packers typically discharge year-round, with peaks during the summer. Table 36 presents the land application rates for the various cases. Case 1 was based on the rates permitted for "Meat Packer B", Case 2 on the "Meat Packer D" rates, and Case 3 on the "Meat Packer A" rates.

Table 36: Industry-Specific Land Application Rates for Meat Packers

Month	Case 1 ($m\ s^{-1}$)		Case 2 ($m\ s^{-1}$)		Case 3 ($m\ s^{-1}$)	
	Waste Water	Irrigation + Precip.	Waste Water	Irrigation + Precip.	Waste Water	Irrigation + Precip.
January	1.82×10^{-8}	2.54×10^{-8}	6.98×10^{-9}	2.54×10^{-8}	2.60×10^{-8}	2.54×10^{-8}
February	1.82×10^{-8}	2.53×10^{-8}	6.98×10^{-9}	2.53×10^{-8}	2.60×10^{-8}	2.53×10^{-8}
March	1.82×10^{-8}	1.83×10^{-8}	6.98×10^{-9}	1.83×10^{-8}	2.60×10^{-8}	1.83×10^{-8}
April	1.82×10^{-8}	4.90×10^{-8}	6.98×10^{-9}	8.35×10^{-9}	2.60×10^{-8}	4.11×10^{-8}
May	1.82×10^{-8}	5.60×10^{-8}	1.12×10^{-8}	7.22×10^{-9}	2.60×10^{-8}	4.80×10^{-8}
Early June	1.82×10^{-8}	2.27×10^{-8}	1.12×10^{-8}	1.47×10^{-9}	2.60×10^{-8}	1.48×10^{-8}
Late June	1.82×10^{-8}	1.37×10^{-8}	1.12×10^{-8}	1.47×10^{-9}	2.60×10^{-8}	5.76×10^{-9}
July	1.82×10^{-8}	5.89×10^{-8}	1.12×10^{-8}	1.81×10^{-11}	2.60×10^{-8}	5.09×10^{-8}
August	1.82×10^{-8}	7.51×10^{-8}	1.12×10^{-8}	1.54×10^{-10}	2.60×10^{-8}	6.71×10^{-8}
September	1.82×10^{-8}	3.62×10^{-8}	1.12×10^{-8}	1.45×10^{-9}	2.60×10^{-8}	2.82×10^{-8}
Early October	1.82×10^{-8}	1.15×10^{-8}	1.12×10^{-8}	4.51×10^{-9}	2.60×10^{-8}	4.51×10^{-9}
Late October	1.82×10^{-8}	4.51×10^{-9}	1.12×10^{-8}	4.51×10^{-9}	2.60×10^{-8}	4.51×10^{-9}
November	1.82×10^{-8}	8.31×10^{-9}	6.98×10^{-9}	8.31×10^{-9}	2.60×10^{-8}	8.31×10^{-9}
December	1.82×10^{-8}	1.89×10^{-8}	6.98×10^{-9}	1.89×10^{-8}	2.60×10^{-8}	1.89×10^{-8}

Minimum and maximum values for each of the five key components (BOD, NO_3, TKN/NH_3, EC and pH) are presented in Table 37. Component factors to estimate industry-typical individual component concentrations from FDS are provided in Table 38.

Table 37: Concentrations of Main Components of Concern in Meat Packing Wastewater

	Minimum Concentration	Maximum Concentration
Organic Matter as BOD (mg/L)	18	1700
Nitrate (mg-N/L)	0	2.31
Ammonium as Total Kjeldahl Nitrogen (mg-N/L)	22	1700
Ammonium direct (mg-N/L)	24	58
EC (µS/cm)	530	3300
pH	7.2	7.9

Table 38: Industry-Specific FDS Component Factors for Meat Packers

Species	Proportion of FDS
Calcium (Ca^{2+})	0.0391
Magnesium (Mg^{2+})	0.0147
Potassium (K^{+})	0.0546
Sodium (Na^{+})	0.26
Ammonium $\left(NH_4^+\right)$	0.146
Aluminum (Al^{3+})	0
Manganese (Mn^{2+})	0.00012
Zinc (Zn^{2+})	0.000167
Copper (Cu^{2+})	0
Iron (Fe^{2+})	0.00753
Carbonate $\left(CO_3^{2-}\right)$	0.299
Phosphate $\left(PO_4^{3-}\right)$	0.0294
Sulfate $\left(SO_4^{2-}\right)$	0.112
Chloride (Cl^{-})	0.03
Nitrate $\left(NO_3^-\right)$	0.0103

The waste water concentrations of all modeled chemical components are shown in Table 39. The concentrations of the key components for the selected cases and the other wineries and grape processors are shown graphically in Figure 46. The concentrations are normalized to the highest average value found in any industry-specific waste stream. Concentrations in Table 39 are modified to obtain model input concentrations based on mixing ratios between waste water and rain/irrigation water as described in Section E.

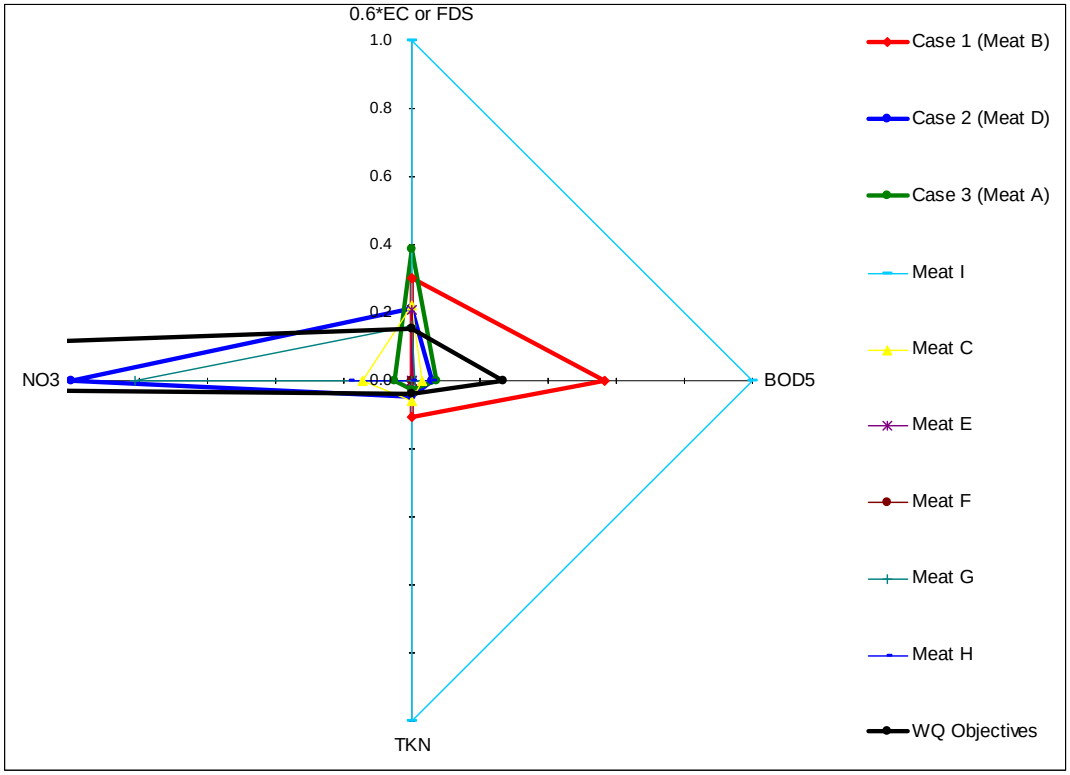

Figure 46

Concentration profile for meat packers. The flow-weighted average concentration of each of the four components of interest was normalized by the highest average value found in all meat packer waste-streams.

Table 39: Effluent Chemical Composition for Meat Packer Cases

Component	Groundwater WQ Objective (mg L^{-1}) (Marshack, 2003)	Case 1 Concentration (mg L^{-1}) [as mg-N L^{-1}]	Case 2 Concentration (mg L^{-1}) [as mg-N L^{-1}]	Case 3 Concentration (mg L^{-1}) [as mg-N L^{-1}]
Calcium (Ca^{2+})	N/A	36.7	27.3	49.5
Magnesium (Mg^{2+})	N/A	13.8	10.3	18.7
Potassium (K^{+})	N/A	51	38.1	69.1
Sodium (Na^{+})	20 – 69	243	181	329
Ammonium (NH_4^{+})	1.93 – 38.7 [1.5 – 30.0]	106 [82]	49.5 [38.4]	28.1 [21.8]
Aluminum (Al^{3+})	0.2 – 5.0	0	0	0
Manganese (Mn^{2+})	0.05 – 0.2	0.11	0.08398	0.152
Zinc (Zn^{2+})	2.0 – 5.0	0.16	0.117	0.212
Copper (Cu^{2+})	0.17 – 1.3	0	0	0
Iron (Fe^{2+})	0.3 – 5.0	7.1	5.25	9.52
Silicic acid (H_4SiO_4)	N/A	85.4 (b)	85.4 (b)	85.4 (b)
Carbonate (CO_3^{-})	N/A	280	209	379
Phosphate (PO_4^{-})	N/A	27.6	20.5	37.2
Sulfate (SO_4^{-})	250 - 500	105	77.9	141
Chloride (Cl^{-})	106 - 250	28.1	20.9	38.0
Nitrate (NO_3^{-})	44.3 [10]	0 [0]	2.82 [0.637]	0.650 [0.136]
pH	6.5 – 8.5	7.5	7.30	7.9
Oxygen gas (O_2)	N/A	0.21 (a)	0.21 (a)	0.21 (a)
Organic Matter (CH_2O)	200 – 500 (d)	779	97.0	120
Dissolved hydrogen sulfide (HS^{-})	N/A	3.31×10^{-4} (a)	3.31×10^{-4} (a)	3.31×10^{-4} (a)
Dissolved methane (CH_4)	N/A	1.61×10^{-4} (a)	1.61×10^{-4} (a)	1.61×10^{-4} (a)
Nitrogen gas (N_2)	N/A	0.79 atm (a)	0.79 atm (a)	0.79 atm (a)
Boric acid (H_3BO_3)	0.7 – 0.1	6.10×10^{-4} (a)	6.10×10^{-4} (a)	6.10×10^{-4} (a)
FDS	450 - 500	936	698	1270
a: assumed, b: background, c: from FDS not accounted for by other ions, * pH assumed to equal 8.5 after buffering, as required in recent WDRs				

Table 40: Mixing Ratios for Meat Packers

Month	Case 1	Case 2	Case 3
January	0.42	0.82	0.51
February	0.42	0.82	0.51
March	0.50	0.86	0.59
April	0.27	0.93	0.39
May	0.25	0.94	0.35
Early June	0.44	0.99	0.64
Late June	0.57	0.99	0.82
July	0.24	1.00	0.34
August	0.20	1.00	0.28
September	0.33	0.99	0.48
Early October	0.61	0.96	0.85
Late October	0.80	0.96	0.85
November	0.69	0.93	0.76
December	0.49	0.86	0.58

e) Modesto POTW

The POTW simulation was intended to model a particular application and geologic setting, in order to serve their intended purpose. Thus, it was constructed differently than the case/industry simulations, in that it was focused on matching the parameters found at a particular location.

The Modesto POTW applies two waste streams to irrigated land near its 2350 acre site bordering the San Joaquin River. One waste stream contains municipal wastewater after secondary treatment and is relatively low in salinity and organic matter. The second waste stream comes from nearby tomato processors and is applied directly to the land surface. This waste has similar characteristics to that of other tomato processors (Section E.1.a) and its application only occurs during the tomato canning season, from June to October. When the tomato waste stream is insufficient to irrigate the site, the first waste stream (the secondary treatment effluent) is used to

supplement it. The resulting mixing ratios are shown in Table 42.The flow-averaged concentrations for each waste stream were used as input to the POTW model.

Due to its proximity to the river, the depth to the water table at the discharge site (3.5 m) is much lower than the average value used for the other simulations (15 m). Additionally, the soil texture is predominantly sand loam (USDA, 2006), estimated to have a K_{sat} value of 1.45×10^{-5} m s^{-1}, a residual saturation of 0.039, and porosity of 0.39 with the van-Genuchten parameters N = 1.45 and $\alpha = 2.67 \times 10^{-2}$ (Schaap et al., 2001).

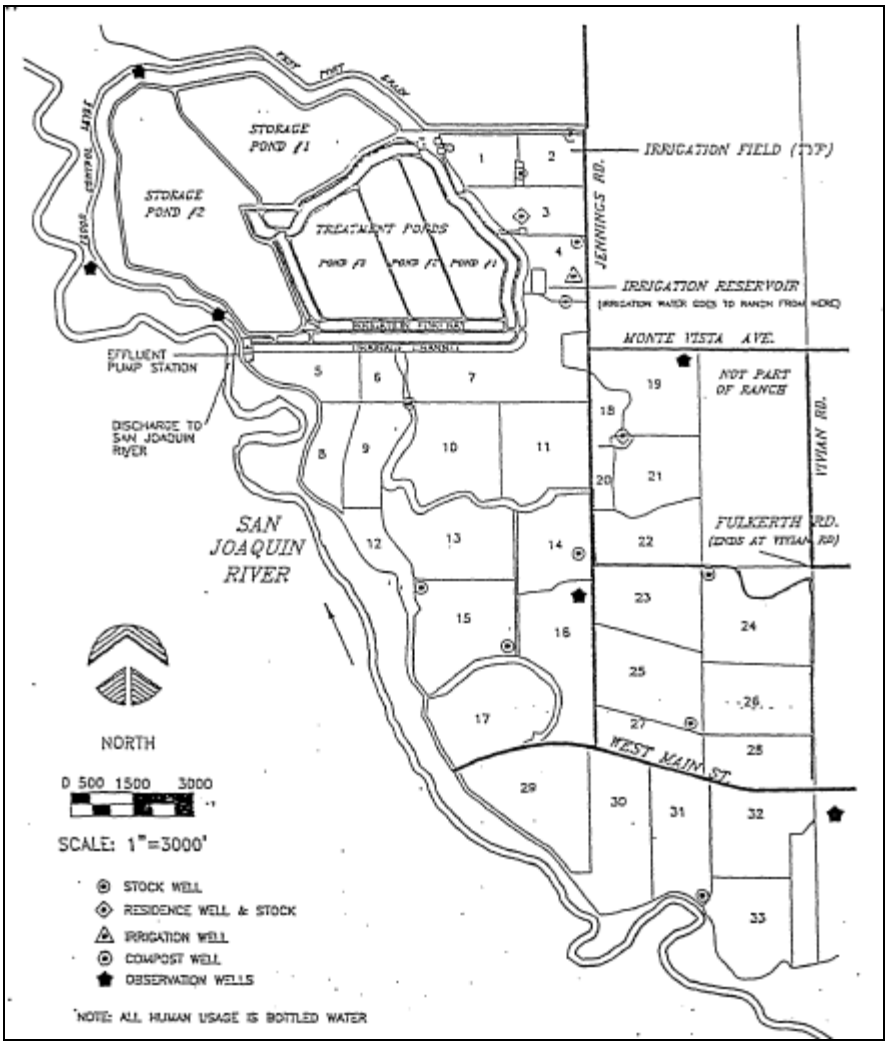

Figure 47

Discharge Locations for Modesto POTW, from WDR for City of Modesto Water Quality Control Facility (California Water Quality Control Board - Central Valley Region, 2001).

Table 41: Land Application Rates for Modesto POTW

Month	Segregated Cannery Waste Water	Treated Municipal Wastewater	Precipitation
January	0	3.69×10^{-9}	2.54×10^{-8}
February	0	2.69×10^{-9}	2.53×10^{-8}
March	0	1.18×10^{-8}	1.83×10^{-8}
April	0	5.93×10^{-8}	8.35×10^{-9}
May	0	6.75×10^{-8}	7.22×10^{-9}
Early June	0	3.99×10^{-8}	1.47×10^{-9}
Late June	0	3.09×10^{-8}	1.47×10^{-9}
July	9.31×10^{-8}	8.25×10^{-9}	1.81×10^{-11}
August	1.07×10^{-7}	1.82×10^{-8}	1.54×10^{-10}
September	1.03×10^{-7}	1.96×10^{-9}	1.45×10^{-9}
Early October	0	2.57×10^{-8}	4.51×10^{-9}
Late October	0	1.56×10^{-8}	4.51×10^{-9}
November	0	1.23×10^{-8}	8.31×10^{-9}
December	0	4.36×10^{-9}	1.89×10^{-8}

Table 42: Mixing Ratios for Modesto POTW

Month	Segregated Cannery Waste Water	Treated Municipal Wastewater	Precipitation
January	0	0.13	0.87
February	0	0.10	0.90
March	0	0.39	0.61
April	0	0.88	0.12
May	0	0.90	0.10
Early June	0	0.96	0.04
Late June	0	0.95	0.05
July	0.92	0.08	0
August	0.85	0.15	0
September	0.97	0.02	0.01
Early October	0	0.85	0.15
Late October	0	0.78	0.22
November	0	0.60	0.40
December	0	0.19	0.81

Table 43: Effluent Chemical Composition for Modesto POTW

Component	Cannery Waste Concentration (mg L^{-1}), [as mg-N L^{-1}]	Treated Municipal Waste Concentration (mg L^{-1}), [as mg-N L^{-1}]
Calcium (Ca^{2+})	64.4	38
Magnesium (Mg^{2+})	21.7	31.9
Potassium (K^{+})	102	24
Sodium (Na^{+})	190	150
Ammonium (NH_4^{+})	34.53	6.91
Aluminum (Al^{3+})	2.97	0.05
Manganese (Mn^{2+})	0.23	0.637
Zinc (Zn^{2+})	0.12	0.00226
Copper (Cu^{2+})	0.04	0.00110
Iron (Fe^{2+})	8.27	0.0637
Silicic acid (H_4SiO_4)	0	0
Carbonate (CO_3^{2-})	180	220
Phosphate (PO_4^{3-})	16.0	4.63
Sulfate (SO_4^{2-})	29.5	60.0
Chloride (Cl^{-})	298	90.0
Nitrate (NO_3^{-})	0.14	21.0
pH	5.10	7
Oxygen gas (O_2)	0.21 (a)	0.21 (a)
Organic Matter (CH_2O)	1149	45
Dissolved hydrogen sulfide (HS^{-})	3.31×10^{-4} (a)	3.31×10^{-4} (a)
Dissolved methane (CH_4)	1.61×10^{-4} (a)	1.61×10^{-4} (a)
Nitrogen gas (N_2)	0.79 atm (a)	0.79 atm (a)
Boric acid (H_3BO_3)	0.27	6.10×10^{-4} (a)
FDS	852	0.28
a: assumed, b: background, c: from FDS not accounted for by other ions, * pH assumed to equal 8.5 after buffering, as required in recent WDRs		

II.3 Model Application and Results

This Section discusses application of the flow and transport model MIN3P to various scenarios. An extended discussion of what is implied by a scenario, which are the elements included in the design of a scenario and how to interpret it is provided in Section II.2. The outcome of the scenario investigation is a series of fluxes representing mass transfer from the unsaturated to the saturated zone. These fluxes will be implemented in our Representative Area analysis in Section II.4. Model Application and Results

A. Baseline Scenario Results

The "baseline" scenarios, discussed in Section II.2, represent the model inputs and parameters. These baseline cases are intended to provide estimates of salinity, as well as concentrations of nitrogen, and organic matter, that are representative of each industry, and three sets of wastewater application conditions, referred to as cases. Graphics representing the breakthrough concentration curves of these four components are shown in Section A.1 for each industry. More detailed discussion and graphics, including breakthrough curves of each FDS component (e.g. Ca, Na, Cl), may be found in Section A.2. In order to focus the discussion, this section describes only the wine and grape industry results, chosen as an example because of the comprehensive groundwater data set available. Detailed graphs depicting the results for the other industries may be found in Section II.6: Appendix C. In subsequent sections of this report, alternate scenarios will be discussed. These alternates were designed to explore multiple permutations on the baseline scenarios.

1. Overview of Baseline Results – All Industries

The magnitude of the concentration reaching the groundwater varied depending on the input wastewater composition, and the site conditions. The breakthrough curves for fixed dissolved solids (FDS), nitrate (NO_3), ammonium (NH_4), and organic matter (OM), the primary contaminants of concern, are shown in Figure 1 for Case 1, Figure 2 for Case 2, and Figure 3 for Case 3. For reference, the concentrations of each of these COCs in the applied waste water are listed in the accompanying tables (Table 44-46).

All cases and industries showed FDS breakthrough above the 500 mg L^{-1} water quality objective, some up to 16 times higher. FDS concentrations ranged from 1400 to 9800 mg L^{-1} in Case 1, 1400 to 3600 mg L^{-1}, and 1300 to 1900 mg L^{-1} in Case 3. FDS breakthrough concentration was most strongly dependent on that of the applied waste. However, its composition, particularly the relative proportion of carbonate, was highly influenced by the modeled pore water saturation level. In Case 2, where saturations remained low, degassing of carbon dioxide was significant. This process allowed more carbonate and bicarbonate (CO_3^- and HCO_3^{2-}), which must remain in equilibrium with CO_2 gas, to escape from the system.

For nitrogen compounds, the concentrations at the water table were dependent on the characteristics of the waste stream combined with the saturation levels depicted in each case. For Case 1 (Figure 48), after initial flushing of the pore water, no nitrate breakthrough occurred due to prevailing anaerobic conditions which facilitate denitrification, i.e. the reduction of nitrate into nitrogen gas. While ammonia was highly retarded by ion exchange reactions, breakthrough eventually occurred for all industries, time dependent on the loading rate. For tomato and dairy processors, the concentrations at 30 years exceed the 30 mg-N L^{-1} groundwater quality objective. If the simulations were to continue past 30 years, other industries would also produce concentrations exceeding the limit. This is supported by the high concentrations of ammonia present in the 5 to 10 m zone, shown in the profiles in the Appendix. For Case 2 (Figure 49), no ammonia breakthrough was noted, due to prevailing aerobic conditions throughout the vadose zone. However, simulated nitrate levels exceeded the USEPA maximum recommended limit of 10 mg-N L^{-1} (USEPA, 2003; Marshak, 2003), and ranged from 80 to 1200 mg-NO3 L^{-1}. The EPA states that the regulations of nitrates in groundwater are centered on preventing blue baby syndrome (USEPA 2007): "The U.S. EPA Oral Reference Dose (RfD) and the Maximum Contaminant Level (MCL) for drinking water ... are set to prevent methemoglobinemia in infants, the most sensitive health endpoint in children...The MCL is 1 mg L^{-1} for nitrites and 10 mg L^{-1} for nitrates in drinking water. As a potential health effect, the U.S. EPA states that, 'Infants below the age of six months who drink water containing nitrate in excess of the MCL could become seriously ill and, if untreated, may die.'" Additional information is available from IRIS, the main database used for risk assessment information (http://www.epa.gov/iris/subst/0076.htm) and at the EPA's page for MCLs (http://www.epa.gov/safewater/mcl.html#mcls.)

A review article by Walton (1951) the most commonly cited source for information on nitrate heath effects on infants. Pg. 992-993 of the article discusses some aspects of nitrates and well water in this context. "High nitrate waters have been found most frequently in private wells serving rural homes...In many cases farm wells, and particularly dug wells, are inadequately protected against contamination by surface water or water percolating but a short distance through the soil…the principal sources of nitrogenous matter in the soil are the decomposition products of plants, animals and microorganisms; the liquid and solid wastes of animal metabolism; and fertilizers added to enrich the soil."

In Case 3 (Figure 50), which was designed for optimal nitrogen removal, only one instance of breakthrough of nitrate or ammonia was noted. For the dairy simulation, ammonia breakthrough at concentrations of 16 mg L^{-1} was predicted. If the waste application rate was slightly adjusted for this simulation, breakthrough could likely be prevented.

In the majority of simulations, organic matter reached the water table, despite the restriction of its application to 100 lb $acre^{-1}$ d^{-1}. Since there are no water quality guidelines for organic material, it is difficult to estimate the negative impact this may have on the groundwater. It is also important to realize that the predictions are strongly dependent on the rates of both aerobic and anaerobic organic matter degradation. The simulations were constrained by rates reported in the literature data; however, reported values do vary widely.

The majority of simulated breakthrough curves, particularly for Case 2 (Figure 49) depict concentrations that oscillate between two values over a short time increment. These rapid changes in concentration are directly due to the transient waste loading, which is altered seasonally for all industries and cases. In some cases, these oscillations are less apparent due to dampening along the flowpath, a less transient nature of the input function, and also the plotting scale. The concentration fluctuations are most notable for those simulations with low saturation levels or higher flow rates, since these conditions lead to stronger seasonal changes and weaker dampening of the input signal.

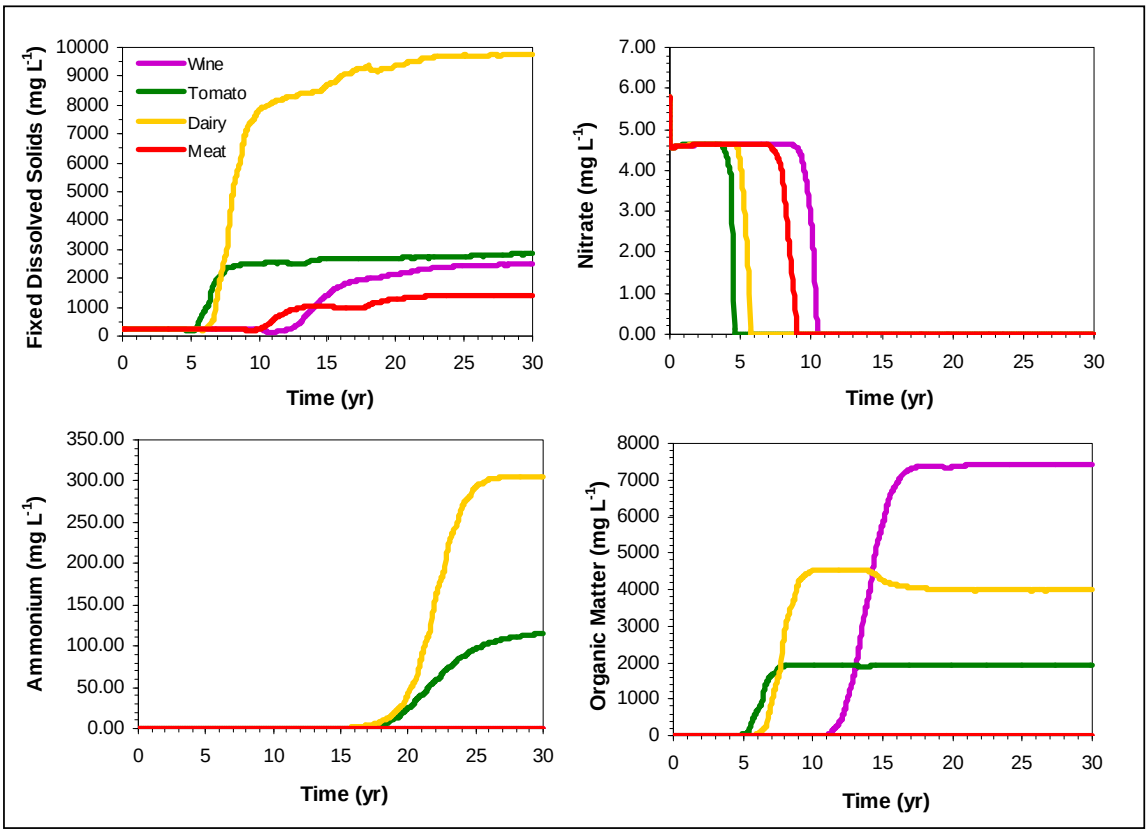

Figure 48

Case 1 Breakthrough Curves

Table 44: Case 1 Wastewater Application Rate, Wastewater Concentrations and Breakthrough Concentrations at the Water Table

	$Q_{applied}$	FDS		NO_3		NH_4		OM	
	$m\ s^{-1}$	C_{waste}	C_{out}	C_{waste}	C_{out}	C_{waste}	C_{out}	C_{waste}	C_{out}
Tomato	$9.81x10^{-8}$	1674	2852	2.97	nd	61.7	115	824	1935
Winery	$2.58x10^{-8}$	1300	2480	15.1	nd	259	0.174	4120	7442
Dairy	$5.39x10^{-8}$	4762	9774	105	nd	165	305	2260	3996
Meat	$1.82x10^{-8}$	936	1406	0	nd	106	nd	779	788

$Q_{applied}$ is maximum rate of wastewater application. Concentration in mg L^{-1}. nd = below detectable value.
C_{out} is the effluent concentration at 30 years.

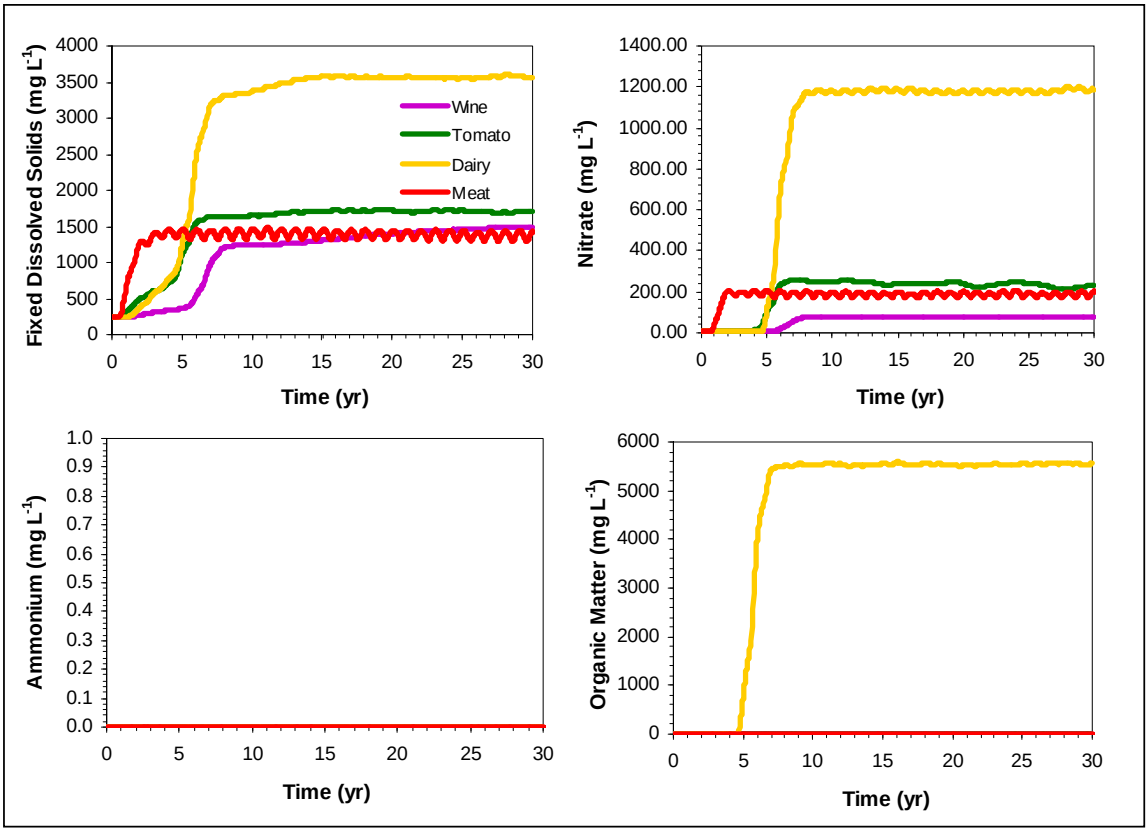

Figure 49

Case 2 Breakthrough Curves

Table 45: Case 2 Wastewater Application Rate, Wastewater Concentrations and Breakthrough Concentrations at the Water Table

	$Q_{applied}$	FDS		NO_3		NH_4		OM	
	m s^{-1}	C_{waste}	C_{out}	C_{waste}	C_{out}	C_{waste}	C_{out}	C_{waste}	C_{out}
Tomato	$5.50x10^{-8}$	930	1718	10.5	231	47.1	nd	122	nd
Winery	$1.12x10^{-8}$	4300	1493	112	78.5	16.4	nd	182	nd
Dairy	$1.10x10^{-7}$	2285	3570	354	1188	95.3	nd	1103	5559
Meat	$1.12x10^{-8}$	698	1432	2.82	202	49.5	nd	97.0	0.207

$Q_{applied}$ is maximum rate of wastewater application. Concentration in mg L^{-1}. nd = below detectable value.
C_{out} is the effluent concentration at 30 years.

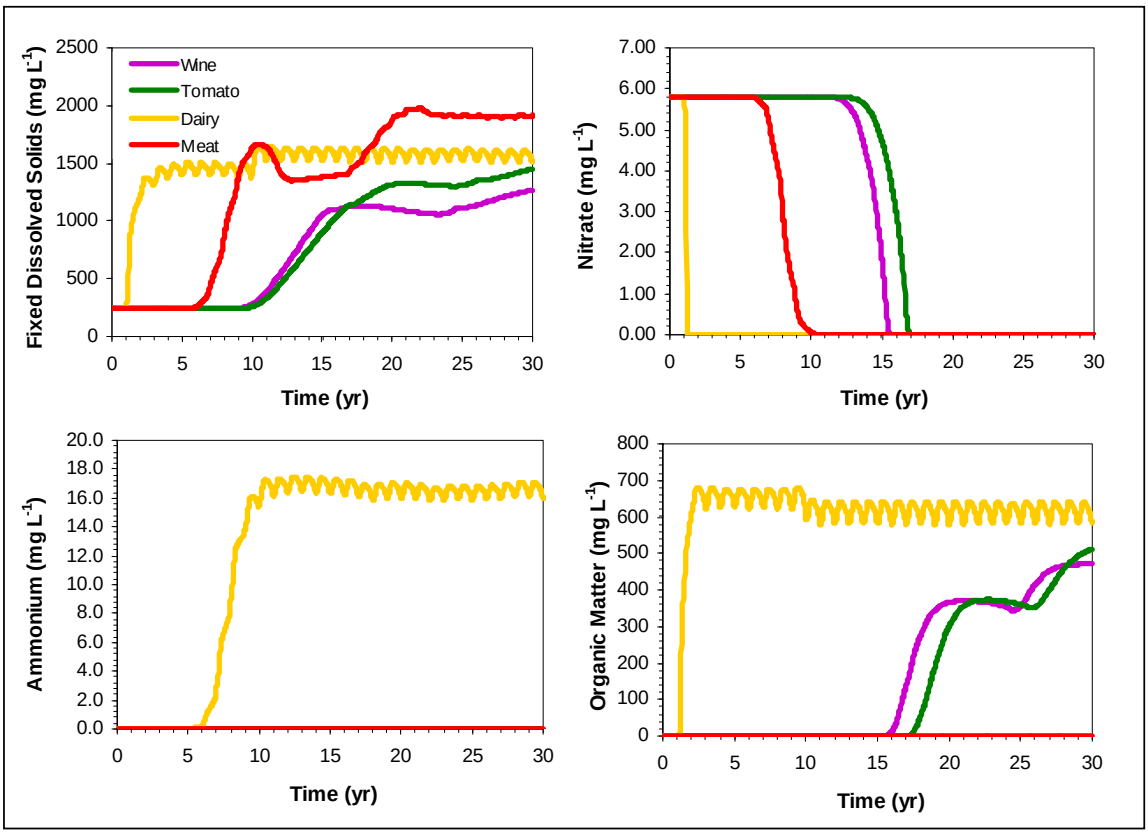

Figure 50

Case 3 Breakthrough Curves

Table 46: Case 3 Wastewater Application Rate, Wastewater Concentrations and Breakthrough Concentrations at the Water Table

	$Q_{applied}$	FDS		NO3		NH4		OM	
	m s^{-1}	C_{waste}	C_{out}	C_{waste}	C_{out}	C_{waste}	C_{out}	Cw_{aste}	C_{out}
Tomato	$1.30x10^{-8}$	780	1452	0.177	nd	44.7	nd	746	512
Winery	$1.24x10^{-8}$	743	1266	11.0	nd	18.8	nd	1206	473
Dairy	$2.28x10^{-7}$	1108	1508	38	nd	18.0	16.0	533	581
Meat	$2.60x10^{-8}$	1270	1915	0.65	nd	28.1	0.025	120	nd

$Q_{applied}$ is maximum rate of wastewater application. Concentration in mg L^{-1}. nd = below detectable value. C_{out} is the effluent concentration at 30 years.

2. Detailed Discussion of Baseline Simulation Results

The following sections more thoroughly discuss the processes which control breakthrough of the four main contaminants, as well as the individual components (Mg, Na, Cl, etc.) that contribute to salinity. In order to streamline the discussion, only the simulation results from the wine and grape industry are included. These results are intended to demonstrate how the model functions and how the main contaminants of concern are attenuated, while noting that very similar behavior is noted for the other industry scenarios. The wine and grape industry was singled out for discussion not because of any underlying characteristics of its wastewater or of the predicted results, but because it had the most comprehensive set of groundwater data available to act as a comparison to the model results (Section B). Several detailed graphs and tables for the wine industry are presented in the following sections; the corresponding figures for the other industries can be found in II.6 Appendix C.

a) Wineries Case 1 – Limited NH3 and Salinity Attenuation

This scenario represents conditions of relatively impermeable soils with high application rates that result in high average moisture contents. Temporal changes in application rates allow the temporary development of unsaturated conditions; however, anaerobic conditions prevail through most of the soil profile. These conditions result in limited degradation of organic carbon (Figure 51). Any nitrate that enters the system is either reduced rapidly (58%: Table 47) or taken up by roots (44%: Table 47). (In this case, the amount attenuated in this manner sums to 112% of the mass applied because additional nitrate mass enters the system through the degradation of ammonia). The nitrate reaching the water table originates from pore water present in the soil column prior to land application (Figure 51). Only a relatively small fraction of ammonia

entering the system is oxidized (4%: Table 47) due to the predominately anaerobic conditions. However, the simulations suggest that a significant fraction of ammonia is removed by active root uptake (12%: Table 47). The largest contribution of ammonia attenuation is by sorption (57%: Table 47), leading to significant retardation of ammonia at the water table relative to conservative components such as Cl (Figure 51). For the simulated time period, less than 0.01% of ammonia applied at the ground surface arrives at the water table. These results suggest that soil sorption is the dominant factor for ammonia attenuation in this system. Ultimately, however, this is unsustainable, and the minor breakthrough noted near Year 30 (Figure 51) would sharply increase if the simulation were allowed to continue beyond that limit. Between 5 and 10 m below ground surface, the ammonium concentration is over 300 mg L^{-1} (Figure 52) and the ultimate breakthrough concentration is likely to be in this range. Earlier breakthrough occurs for the tomato and dairy industries (Figure 48) as a result of higher mass loading rates. Chloride is assumed to be transported conservatively and breakthrough occurs around 15 years (Figure 51). Na transport is slightly retarded due to ion exchange reactions (Figure 51).

However, over the 30 year simulation period, 36% of Na and 66% of Cl applied at the ground surface is predicted to reach the water table (Figure 51). As expected, these results suggest that the attenuation potential for Na and Cl is limited. On the other hand, potassium removal is significant, with attenuation attributable both to ion exchange (58%) and root uptake (14%, Table 47). The slightly acidic nature of the recharge water and biodegradation reactions leads to significant calcite dissolution, increasing the Ca-content of the pore water. The simulations suggest that these processes (Na and K loading, calcite dissolution) lead to the displacement of Mg from the exchange sites. As a result, both Mg and Ca loadings at the water table are significantly higher than applied at the ground surface (Ca: 148%, Mg: 154%, Table 47). Overall, this scenario shows effectively no retardation of the FDS breakthrough curve (Figure 51); the initial breakthrough of both the FDS and Cl curves is at approximately 12 years. Over the 30-year simulated time-span, only 43% of the FDS applied at the surface reaches the groundwater, indicating significant attenuation (Table 47). While a significant amount of the total FDS is removed, the plume was predicted to move through the soil at the same rate as a conservative tracer.

In this scenario, carbonate composes almost half of the total FDS reaching the water table, 1734 lb acre-1 yr^{-1} CO3 to 3782 lb $acre^{-1}$ yr^{-1} FDS, but only 40% of that applied, 3520 lb $acre^{-1}$ yr^{-1} CO3 to 8729 lb $acre^{-1}$ yr^{-1} FDS (Table 47). Additional carbonate is generated as a result of biodegradation processes (92 mol m^{-2}) and root release (8 mol m^{-2}), but most (76 mol m^{-2}) is lost to precipitation of calcite, due to favorable pH conditions during years 10 to 15.

Under anaerobic conditions, alternative electron acceptors such as MnO2, FeOOH and SO4 are utilized in biodegradation reactions, leading to the precipitation of secondary phases such as siderite ($FeCO_3$), rhodochrosite ($MnCO_3$), and mackinawite (FeS) and the release of Mn and Fe to the saturated zone (Figure 51). (Note: the biodegradation of organic matter using the soil minerals MnO_2 and FeOOH as electron acceptors is listed in Table 47 as "Biodegradation (mineral)" while the biodegradation of organic matter using SO_4, NO_3, and O_2 as electron acceptors is listed as "Biodegradation (aqueous)". The mass balance results suggest that Mn and

Fe are mostly cycled internally (by reductive dissolution and re-precipitation); however, loadings of these ions increase in comparison to application with the waste water (Table 47). Sulfate reduction is initially inhibited due to the presence of Mn-oxides; but is rapidly consumed after depletion of this mineral phase. Attenuation processes of Zn and Cu were not simulated considering that these processes are poorly constrained.

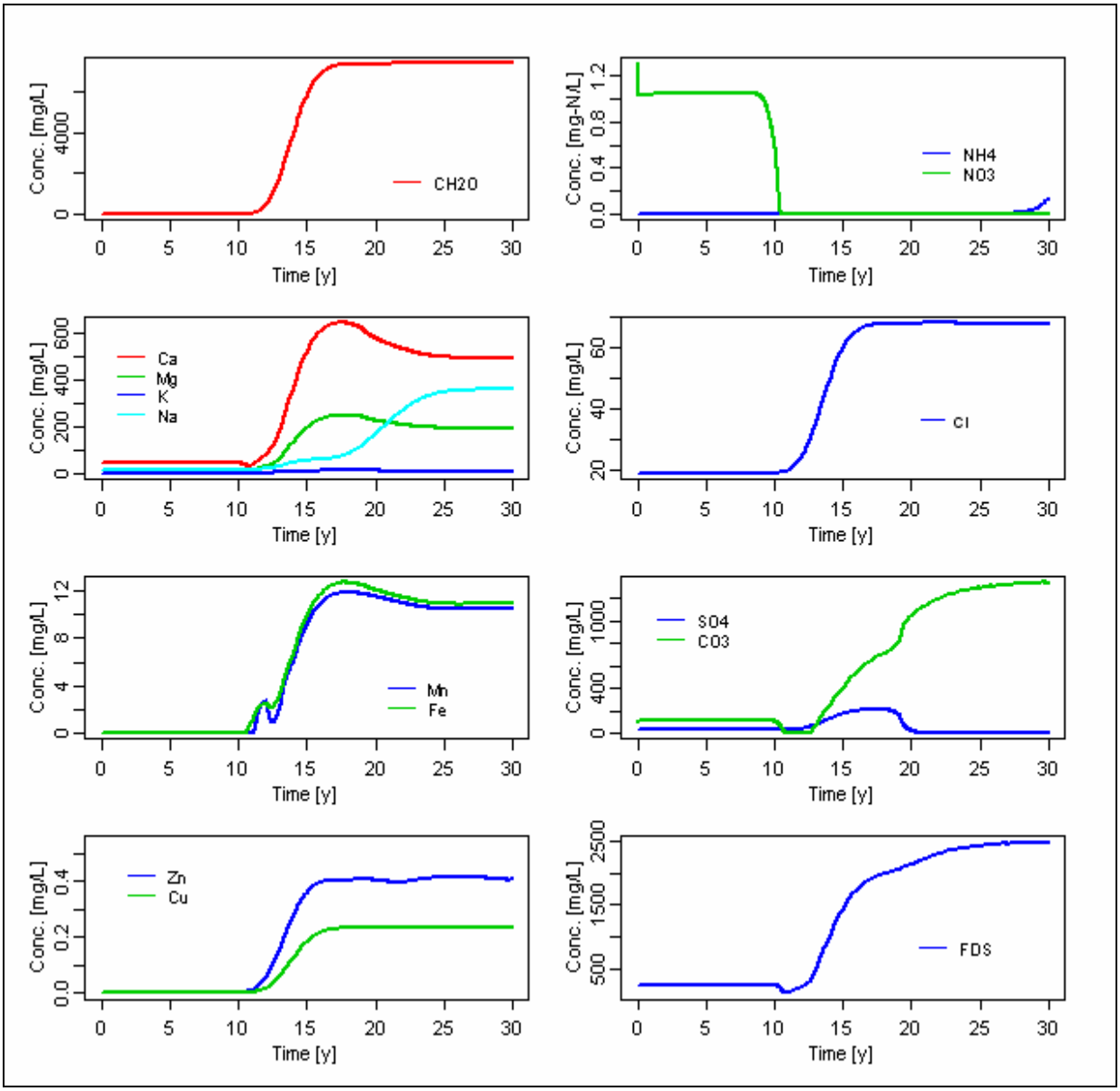

Figure 51

Breakthrough Curves for Wine Case 1

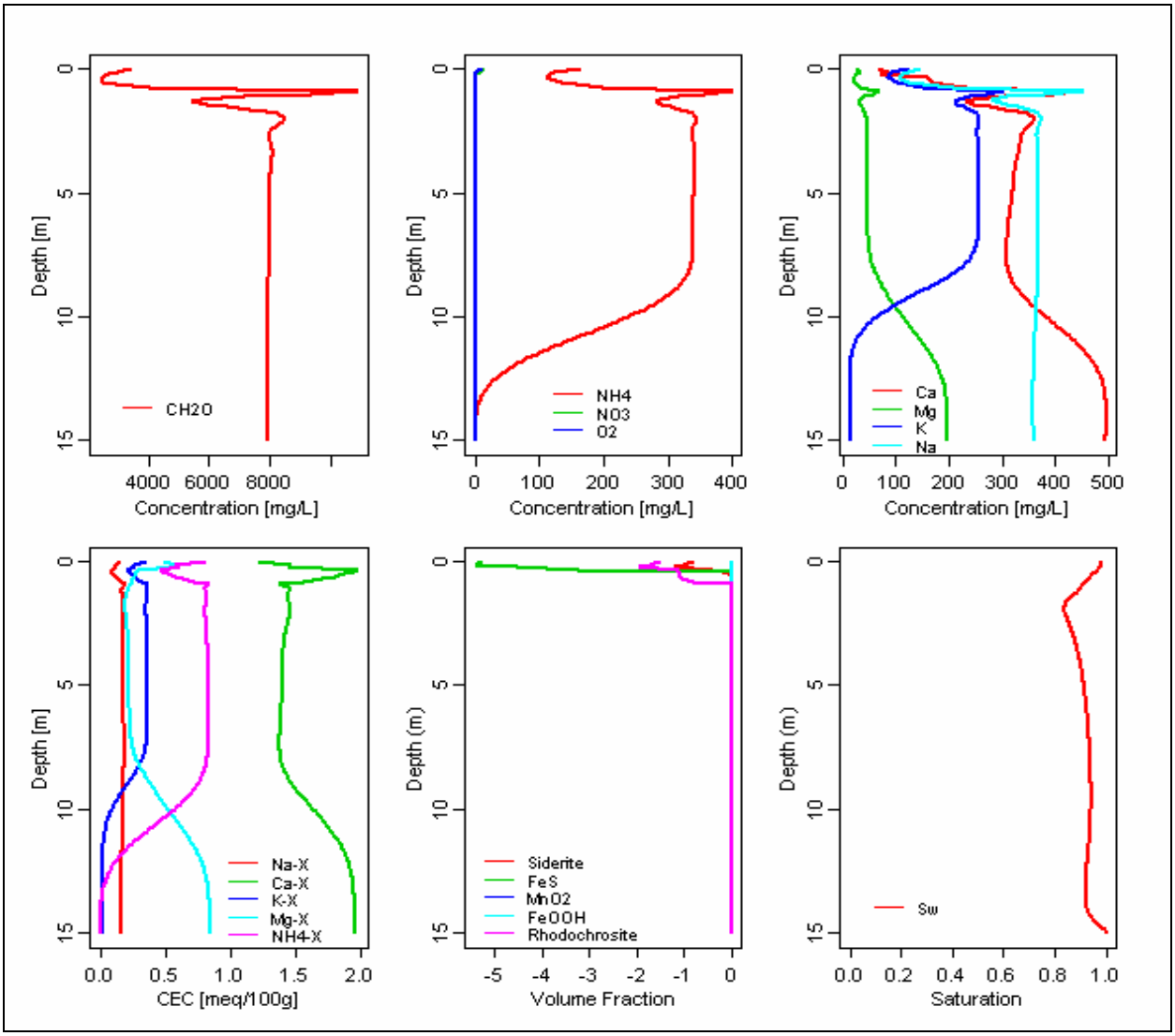

Figure 52

Profile for Wine Case 1, Year 30

Table 47: Mass Balance of Components - Winery Case 1

	Surface Loading	Storage	Degassing	Biodegredation (Aqueous)	Biodegredation (Mineral)	Root Uptake	Precipitation	Adsorption	Water Table	Mass Error
CH_2O	22865	-10269	0	-473	-337	0	0	0	-11750	37.27
	100%	-45%	0%	-2%	-1%	0%	0%	0%	-51%	0%
NH_4	1203	-325	0	-45	0	-146	0	-685	0	1.97
	100%	-27%	0%	-4%	0%	-12%	0%	-57%	0%	0.2%
NO_3	187	7	0	-108	0	-82	0	0	-4	0.16
	100%	4%	0%	-58%	0%	-44%	0%	0%	-2%	0.1%
O_2	110	0	70	-180	0	0	0	0	0	-0.02
	100%	0%	64%	-164%	0%	0%	0%	0%	0%	0.0%
K^+	895	-208	0	0	0	-132	0	-526	-28	1.42
	100%	-23%	0%	0%	0%	-15%	0%	-59%	-3%	0.2%
Ca^{2+}	633	-462	0	0	0	-85	165	689	-940	0.08
	100%	-73%	0%	0%	0%	-14%	26%	109%	-148%	0.0%
Mg^{2+}	239	-112	0	0	0	-97	0	339	-368	0.02
	100%	-47%	0%	0%	0%	-41%	0%	142%	-154%	0.0%
Na^+	1093	-477	0	0	0	0	0	-222	-392	1.44
	100%	-44%	0%	0%	0%	0%	0%	-20%	-36%	0.1%
Fe^{2+}	11	-12	0	0	1180	0	-1147	-14	-18	0.85
	100%	-101%	0%	0%	10269%	0%	-9986%	-121%	-154%	7.4%
Mn^{2+}	2	-12	0	0	652	0	-609	-17	-19	-1.84
	100%	-518%	0%	0%	28558%	0%	-26654%	-744%	-822%	-80.6%
CO_3^{2-}	3520	-2041	-137	945	678	134	-1361	0	-1734	4.03
	100%	-58%	-4%	27%	19%	4%	-39%	0%	-49%	0.1%
SO_4^{2-}	673	-11	0	-472	0	-46	0	0	-145	-1.13
	100%	-2%	0%	-70%	0%	-7%	0%	0%	-22%	-0.2%
Cl-	202	-70	0	0	0	0	0	0	-133	-0.06
	100%	-34%	0%	0%	0%	0%	0%	0%	-66%	0.0%
PO_4^{3-}	71	-1	0	0	0	-69	0	0	-1	0.12
	100%	-1%	0%	0%	0%	-97%	0%	0%	-2%	0.2%
FDS	8729	-3722	-137	321	2510	-524	-2952	-435	-3782	7.06
	100%	-43%	-2%	4%	29%	-6%	-34%	-5%	-43%	0.1%

Mass balance in pounds per acre per year and percent of total component loading.

b) Wineries Case 2 – Limited Nitrate and Salinity Attenuation

This scenario is characterized by low organic carbon loading and permeable sediments with relatively significant N-loading. These conditions facilitate O_2 ingress and CO_2 egress through the unsaturated pore space (Figure 54) and the vadose zone remains aerobic throughout facilitating rapid degradation of organic carbon, and nitrification of ammonia,. The simulations suggest that organic carbon is completely depleted prior to reaching the water table (Table 48). The calculated mass balance for NH_3 suggests that 81% of the ammonia loading is removed by biodegradation reactions (nitrification), while the remaining ammonia mass is removed by plant uptake (Table 48). Although nitrification of ammonia increases NO_3 concentrations to values above inflow concentrations (corresponding to a gain of 45% of the inflow mass loading), total N loading to the aquifer is moderate (47 % of NO_3 and 0% of NH_3, Table 48). The mass balance also suggests that most (86%) of the NO_3 applied at the surface is taken up by plants (Table 48), however, the conversion of ammonia to nitrate increases the total nitrate mass by 45%, leading to breakthrough at the water table. NO_3 loading to the aquifer reaches concentrations of 20 mg L^{-1} (Table 48).

Despite the lower flow rates, arrival times at the water table are shorter than for scenario 1 due to higher permeability and lower moisture contents. This is evidenced by the Cl breakthrough curve (6-8 years, Table 48). Similar to Case 1, ion exchange tends to retard the transport of Na; however, this effect is limited due to the low affinity of Na for ion exchange sites. The simulations suggest that 42% of Na and 83% of Cl applied at the ground surface arrive at the water table. Results indicate that Mg and Ca are displaced from exchange sites (7% and 121% of surface application, respectively), but that Ca is removed by precipitation (135%). K is removed by root uptake and ion exchange (8% and 82 % of surface application, respectively). These processes lead to around 75% of applied Mg and Ca reaching the water table, while K is effectively attenuated (Table 48).

Attenuation of salinity represented by FDS is fairly high, with only 31% of that applied reaching the water table. Nearly 80% of the carbonate applied escaped from the system through carbon dioxide degassing. This process allowed the levels of carbonate dissolved into solution to remain much lower than in the other cases, in turn lowering the overall salinity level.

In contrast to Case 1, the electron acceptors SO_4, MnO_2, and FeOOH are not consumed, because conditions in the domain remain aerobic. A significant amount of oxygen is supplied through the gas phase replenishing the electron acceptor demand in the system (Table 48). Some sulfate attenuation takes place through root uptake (4%). Overall, this scenario causes little retardation, but significant attenuation of the salinity front and yields to a fairly high nitrate loading of the aquifer.

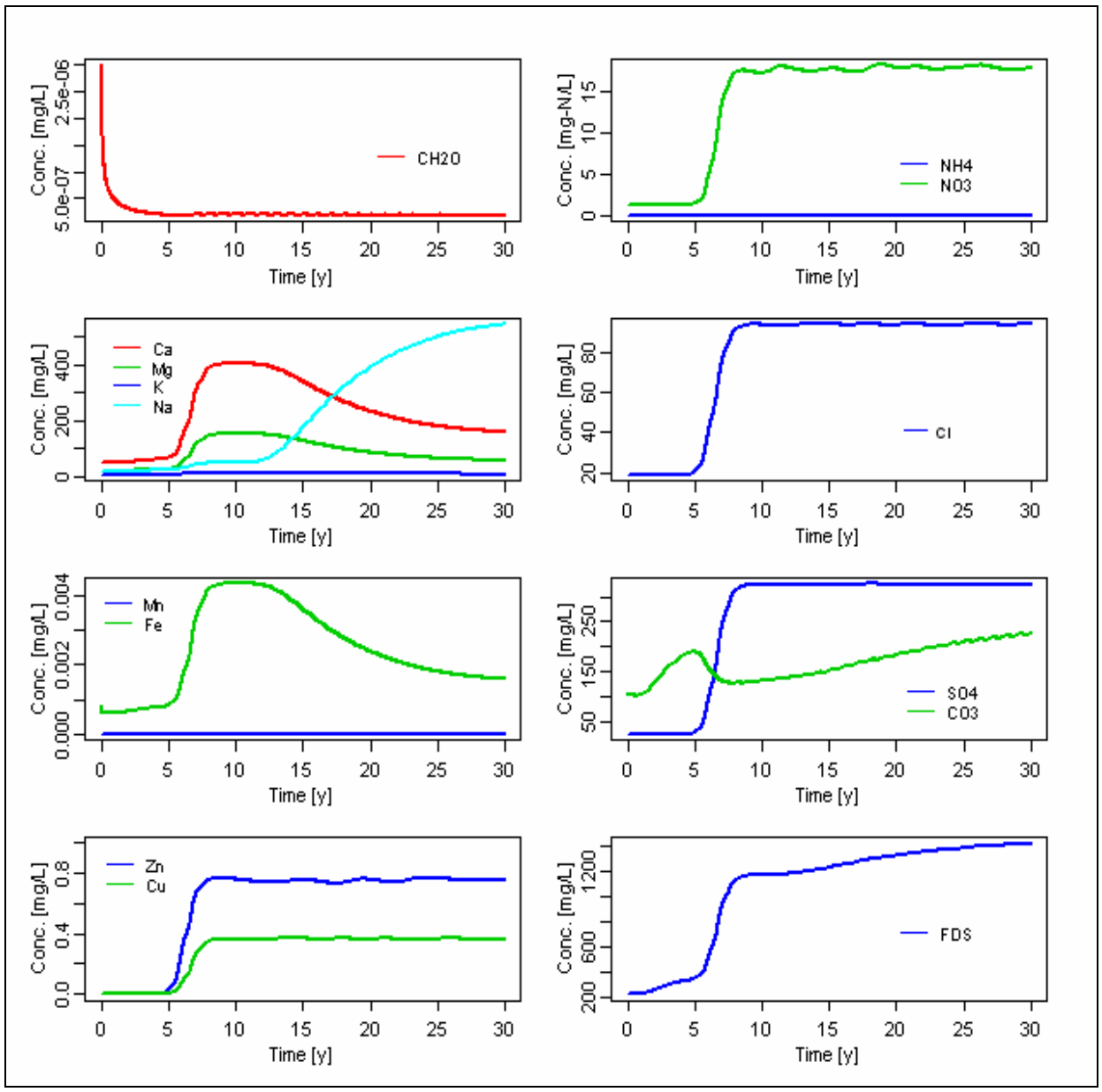

Figure 53

Breakthrough Curves for Wine Case 2

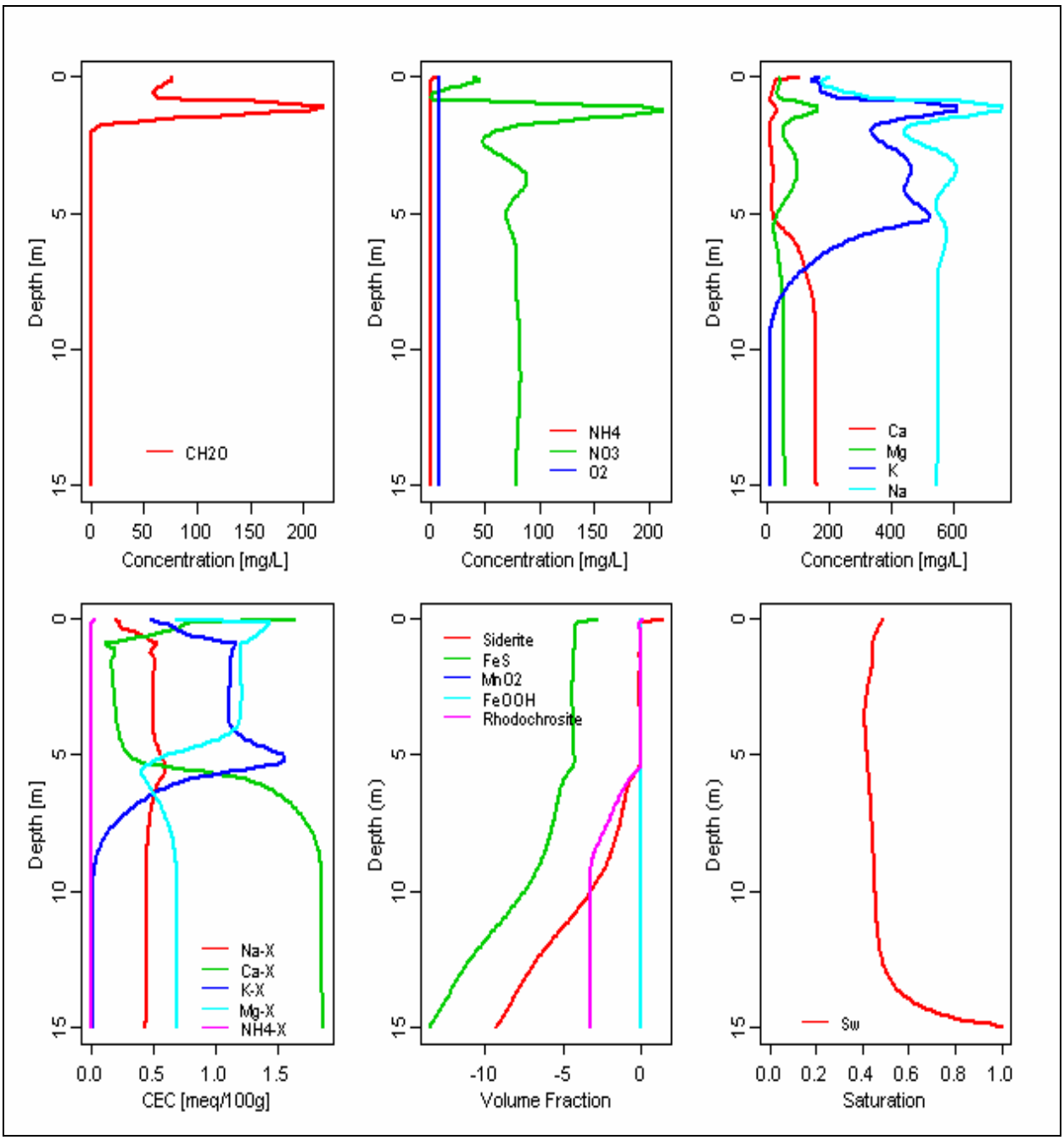

Figure 54

Profiles for Wine Case 2, Year 30

Table 48: Mass Balance of Components - Winery Case 2

	Surface Loading	Storage	Degassing	Biodegredation (Aqueous)	Biodegredation (Mineral)	Root Uptake	Precipitation	Adsorption	Water Table	Mass Error
CH_2O	654	-6	0	-647	0	0	0	0	0	1.77
	100%	-1%	0%	-99%	0%	0%	0%	0%	0%	0%
NH_4	92	0	0	-74	0	-18	0	0	0	0.22
	100%	0%	0%	-81%	0%	-19%	0%	0%	0%	0.2%
NO_3	435	-53	0	195	0	-373	0	0	-203	0.94
	100%	-12%	0%	45%	0%	-86%	0%	0%	-47%	0.2%
O_2	109	0	832	-915	0	0	0	0	-27	-0.03
	100%	0%	761%	-836%	0%	0%	0%	0%	-25%	0.0%
K^+	1528	-115	0	0	0	-129	0	-1252	-26	4.08
	100%	-8%	0%	0%	0%	-8%	0%	-82%	-2%	0.3%
Ca^{2+}	985	-39	0	0	0	-66	-1328	1194	-745	1.23
	100%	-4%	0%	0%	0%	-7%	-135%	121%	-76%	0.1%
Mg^{2+}	371	-28	0	0	0	-95	0	27	-275	0.43
	100%	-8%	0%	0%	0%	-26%	0%	7%	-74%	0.1%
Na^+	1839	-379	0	0	0	0	0	-684	-772	4.49
	100%	-21%	0%	0%	0%	0%	0%	-37%	-42%	0.2%
Fe^{2+}	20	0	0	0	0	0	-19	-1	0	-0.01
	100%	0%	0%	0%	0%	0%	-94%	-5%	0%	0.0%
Mn^{2+}	4	0	0	0	0	0	-3	-1	0	-0.15
	100%	-3%	0%	0%	0%	0%	-70%	-31%	0%	-3.8%
CO_3^{2-}	5139	-166	-4008	1293	0	312	-2010	0	-549	10.38
	100%	-3%	-78%	25%	0%	6%	-39%	0%	-11%	0.2%
SO_4^{2-}	1101	-211	0	0	0	-44	0	0	-843	2.21
	100%	-19%	0%	0%	0%	-4%	0%	0%	-77%	0.2%
Cl-	305	-53	0	0	0	0	0	0	-253	0.20
	100%	-17%	0%	0%	0%	0%	0%	0%	-83%	0.1%
PO_4^{3-}	123	-3	0	0	0	-109	0	0	-10	0.34
	100%	-2%	0%	0%	0%	-89%	0%	0%	-9%	0.3%
FDS	11942	-1047	-4008	1415	0	-523	-3359	-717	-3677	24.38
	100%	-9%	-34%	12%	0%	-4%	-28%	-6%	-31%	0.2%

Mass balance in pounds per acre per year and percent of total component loading.

c) Wineries Case 3 – Significant Nitrogen Attenuation, Limited Salinity Attenuation

This case is characterized by a lower loading rate than Case 1 and a higher hydraulic conductivity, which results in lower soil saturations (Figure 56). These conditions promote nitrification of ammonia under unsaturated conditions in the shallow sediments, where conditions remain aerobic (77% of NH_3 is oxidized). The remainder of ammonia is removed by root uptake (23%) and NH_3 loading to the groundwater is averted (Table 49). Although NO3 is produced by nitrification, root uptake removes nitrate (>107% of surface application) and avoids NO_3-loading to the groundwater. Note that removal rates larger than 100% occur due to contributions from sources additional to the land application, such as transformations. Low concentrations present at the water table originate from background water present prior to land application (Figure 55). As simulated, root uptake is the primary removal mechanism of nitrate; however, conditions lower in the vadose zone are also favorable for nitrate attenuation, which provides an additional protection against NO_3 breakthrough.

Although this case demonstrates that it is theoretically possible to avoid N-loading to the aquifer completely through a combination of root uptake and microbially mediated conversion to N_2, it confirms that salinity attenuation is limited, with 58% of the applied FDS, 61% of Cl, and 29% of Na applied at the ground surface arriving at the water table (Table 49). Salinity breakthrough occurs in a non-retarded fashion, although the composition of the pore water has been altered significantly. Carbonate, a byproduct of biodegradation and root uptake, again composes a large portion of FDS (>50%), as it cannot escape the system as CO_2 gas due to high moisture contents.

Mass loadings of Ca and Mg are only slightly lower than that applied, around 80%. Fe and Mn are much increased in comparison to loadings applied at the ground surface (by 267% for Fe and over 3 orders of magnitude for Mn). These limited reductions are due to calcite dissolution, and the release of Mg from exchange sites. Increases are due to the reductive dissolution of Fe and Mn-oxides under anaerobic conditions.

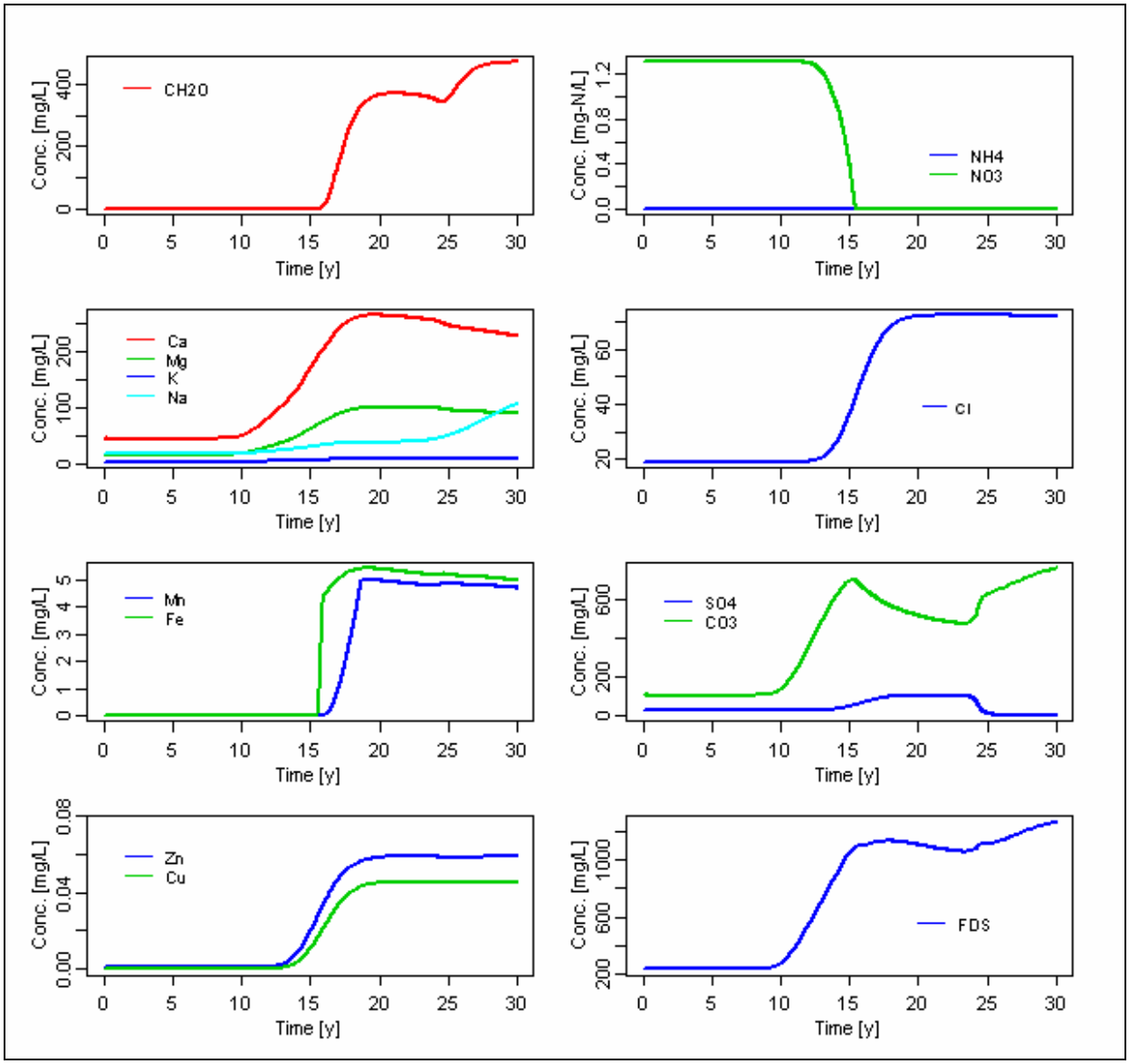

Figure 55

Breakthrough Curves for Wine Case 3

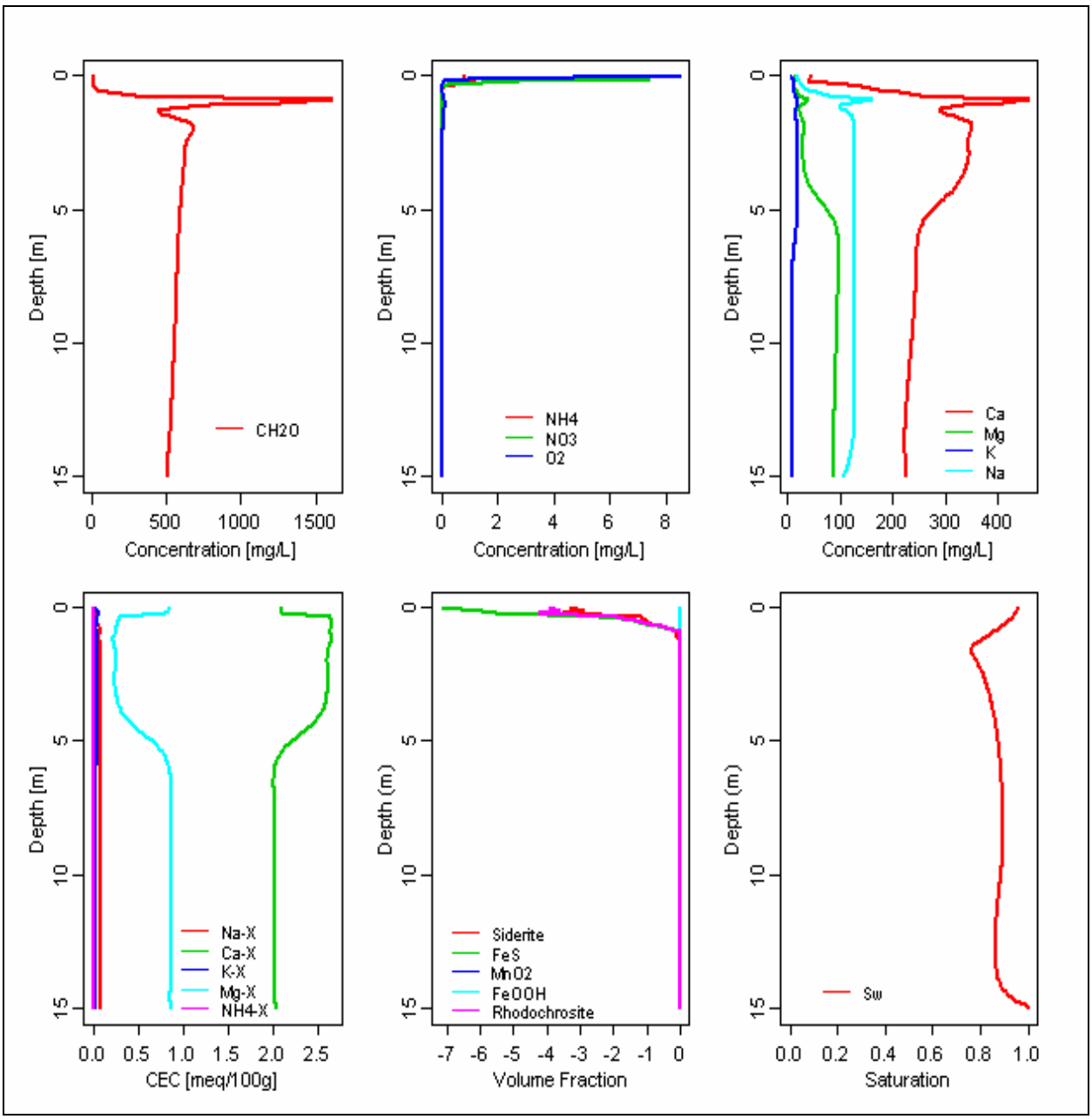

Figure 56

Profiles for Wine Case 3, Year 30

Table 49: Mass Balance of Components - Winery Case 3

	Surface Loading	Storage	Degassing	Biodegredation (Aqueous)	Biodegredation (Mineral)	Root Uptake	Precipitation	Adsorption	Water Table	Mass Error
CH_2O	1880	-700	0	-501	-266	0	0	0	-405	7.40
	100%	-37%	0%	-27%	-14%	0%	0%	0%	-22%	0%
NH_4	74	0	0	-57	0	-17	0	0	0	0.17
	100%	0%	0%	-77%	0%	-23%	0%	0%	0%	0.2%
NO_3	144	8	0	9	0	-154	0	0	-7	0.11
	100%	5%	0%	7%	0%	-107%	0%	0%	-5%	0.1%
O_2	105	11	396	-505	0	0	0	0	-8	0.00
	100%	11%	376%	-480%	0%	0%	0%	0%	-7%	0.0%
K^+	176	-11	0	0	0	-128	0	-19	-17	0.57
	100%	-6%	0%	0%	0%	-73%	0%	-11%	-10%	0.3%
Ca^{2+}	457	-286	0	0	0	-85	403	-115	-375	-0.17
	100%	-63%	0%	0%	0%	-19%	88%	-25%	-82%	0.0%
Mg^{2+}	172	-76	0	0	0	-90	0	138	-144	-0.06
	100%	-44%	0%	0%	0%	-52%	0%	80%	-83%	0.0%
Na^+	313	-141	0	0	0	0	0	-83	-89	0.52
	100%	-45%	0%	0%	0%	0%	0%	-26%	-29%	0.2%
Fe^{2+}	2	-7	0	0	673	0	-644	-18	-5	0.73
	100%	-396%	0%	0%	36771%	0%	-35169%	-1000%	-267%	39.7%
Mn^{2+}	0	-8	0	0	642	0	-607	-23	-6	-1.54
	100%	-2079%	0%	0%	173663%	0%	-164153%	-6324%	-1624%	-416.2%
CO_3^{2-}	1352	-1176	-191	1001	533	113	-649	0	-982	1.79
	100%	-87%	-14%	74%	39%	8%	-48%	0%	-73%	0.1%
SO_4^{2-}	297	17	0	-167	0	-44	0	0	-104	-0.94
	100%	6%	0%	-56%	0%	-15%	0%	0%	-35%	-0.3%
Cl-	177	-69	0	0	0	0	0	0	-108	-0.10
	100%	-39%	0%	0%	0%	0%	0%	0%	-61%	-0.1%
PO_4^{3-}	11	0	0	0	0	-11	0	0	0	0.05
	100%	-1%	0%	0%	0%	-98%	0%	0%	-1%	0.4%
FDS	3176	-1749	-191	787	1848	-416	-1496	-121	-1838	1.13
	100%	-55%	-6%	25%	58%	-13%	-47%	-4%	-58%	0.0%

Mass balance in pounds per acre per year and percent of total component loading.

3. Effectiveness of the Attenuation Processes

a) Wine and Grape Processors

For the winery and grape processor scenarios, between 30 to 60% of the applied FDS over the 30 year period reached the water table (Figure 57). Attenuation by plant uptake and soil adsorption was low; for Case 1, 2, and 3, the total removal of FDS by these processes was 6, 4, and 13% of that applied, respectively. By producing carbonate, biodegradation acted as a strong source of FDS in Cases 1 and 3, with approximately 1500 and 1600 lbs $acre^{-1}$ yr^{-1} being produced. Mineral precipitation acted to counterbalance some of these additions.

The percent of applied FDS reaching the water table was not static throughout the simulations. When two five-year increments were examined (years 15 to 20 versus years 25 to 30), the FDS loading to the water table went from 63 to 80% in Case 1, 35 to 37% in Case 2, and 85 to 90% in Case 3. The increase was primarily due to the steady increase in the carbonate concentration from years 15 to 30 in Case 1 and years 20 to 30 in Case 3. Precipitation of calcium and carbonate into calcite delays breakthrough, acting as a buffer.

The fate of nitrogen compounds in the system, shown in Figure 58, indicates the strong influence attenuation processes have over ammonia and nitrate concentrations. Plant nutrient uptake removed between 12 and 17% of the applied ammonia and 45 to 110% of the nitrate (100% of that applied at the surface plus a portion of that converted from ammonia). Biodegradation typically played a larger role; in Case 2 and 3, it converted 81 and 77% of ammonia to nitrate. In Case 2, this nitrate remained in the system, due to aerobic conditions, causing the overall nitrate reaching the water table to be 47% of that applied at the surface. In Case 3, the conditions were more favorable for denitrification. A large portion of the nitrate was either extracted by roots or converted to nitrogen gas, and only 5% of the nitrate applied reached the groundwater. Ammonia sorption had a small influence on Cases 2 and 3 because nitrification acted as the dominant sink. In Case 1, where nitrification was inhibited, 57% of the ammonia was removed via sorption.

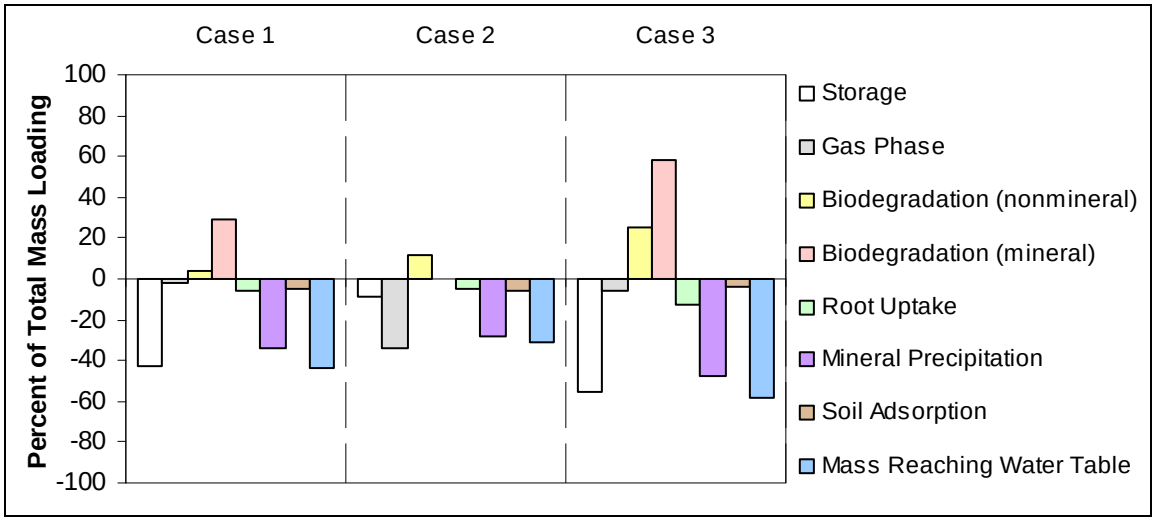

Figure 57

FDS Mass Balance for Winery Cases over the 30-year Simulation Period

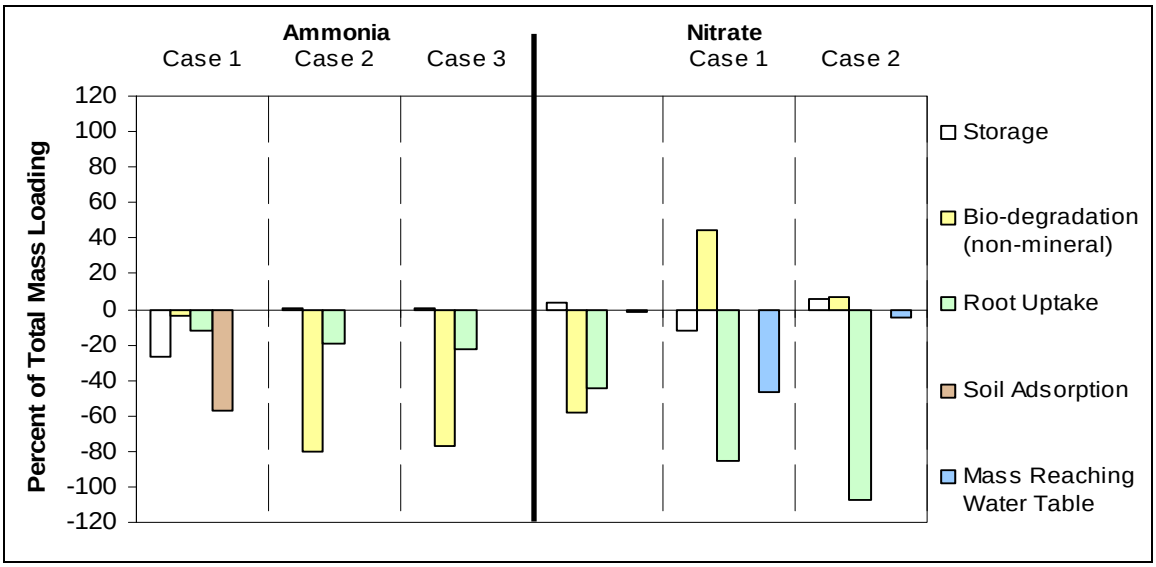

Figure 58

Nitrogen Mass Balance for Winery Cases over the 30-year Simulation Period

b) All Industries

For tomato processors, 53 to 100% of FDS applied reached the groundwater, depending on the case. For dairy processors, this range was 71 to 110%, and for the meat packaging industry, it was 67 to 140%. The FDS mass loading was increased by the dissolution of soil minerals. The wine and grape industry had lower percentages (30 to 60%) due to the characteristics of its waste. For tomato and dairy processors, between 18 to 49% of the FDS concentration was attributable to sodium or chloride, while for wineries and meat packaging, between 11 and 28%

was contributed by these ions. Instead, potassium and carbonate were present in higher fractions.

For Case 2, dairy, tomato, and meat processors had higher mass loadings of nitrate appearing at the water table than were added via the wastewater: 216, 396, and 913%, respectively. The additional nitrate was produced through the conversion of ammonia. In Case 2 for meat packers, the ammonia concentration was approximately ten times that of nitrate, leading to its nine-fold increase between the surface and the water table.

B. Comparison of Baseline Results and Available Groundwater Data

Available groundwater data sets included several years of nitrate, TKN, BOD, and TDS measurements from wells located in and around waste application sites. The majority of this data was from wineries and grape producers, limiting the comparison to only these cases. Since the modeling work aimed at providing a range of possible outcomes rather than predicting concentrations at any particular land application site, this comparison was not intended to verify the simulations results, but to demonstrate that they were predicting reasonable values within a range of those observed in the groundwater around sites.

The comparison was limited to the most recent year of data, and wells either "mid-gradient" or "down-gradient" of application sites; that is, wells that would be either directly under a waste application site or immediately "downstream" of a site, thus in the direction of travel of potential contamination. The wells were classified by case according to the criterion listed in Part I, Section 4.1.2 of this document.

Of the 77 wells examined, 4% were classified as Case 1, 57% as Case 2, 26% as Case 3, and 13% as other. Most wells classified as "Other" had TDS levels below the groundwater quality objectives.

A histogram of NO_3 in groundwater is shown in Figure 59, along with the results observed from the winery cases. An insufficient number of wells fell into the Case 1 category to make a histogram, but all showed "non-detects" of nitrate. Nitrate concentrations ranged from non-detect to 150 mg-N L^{-1}. This placed the Case 2 results (at 18 mg-N L^{-1}) well within these bounds. The Case 1 and 3 results, both "non-detects", were similar to the Case 3 groundwater measurements, which range from "non-detect" to the limit of 10 mg-N L^{-1}. The concentrations of nitrate in groundwater were likely higher than modeled because of underlying aquifer background contamination.

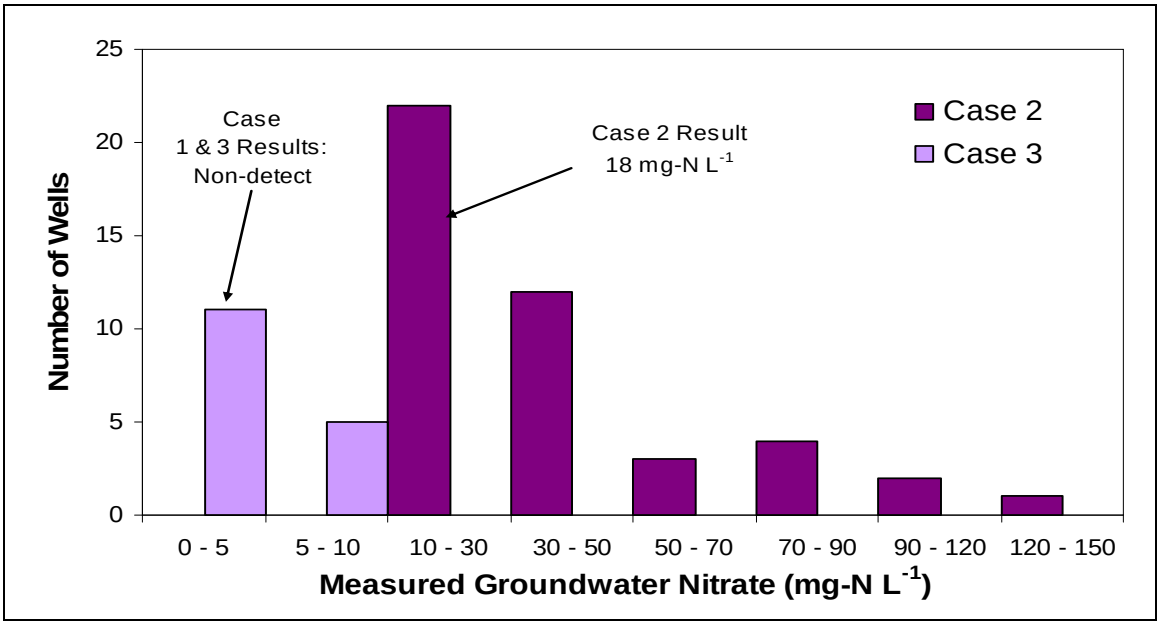

Figure 59

Histogram of Nitrate Concentrations in Groundwater Wells Down-Gradient from Winery Waste Application Sites

A histogram of the FDS concentrations in groundwater (Figure 60) showed a range of "non-detect" to 2100 mg L^{-1}. Most of the simulations showed concentrations that were in the upper end of this range: 1300 mg L^{-1} for Case 3 and 1500 mg L^{-1} for Case 2. Six of the groundwater wells had similar concentrations. Case 1, however, had slightly higher simulated concentrations, 2500 mg L^{-1}. This value is still reasonable close, though, because the modeled concentration is taken at the surface of the groundwater table, while the well measures a much larger portion of the aquifer. Considerable in-aquifer mixing likely occurs, causing dilution of the high TDS concentrations.

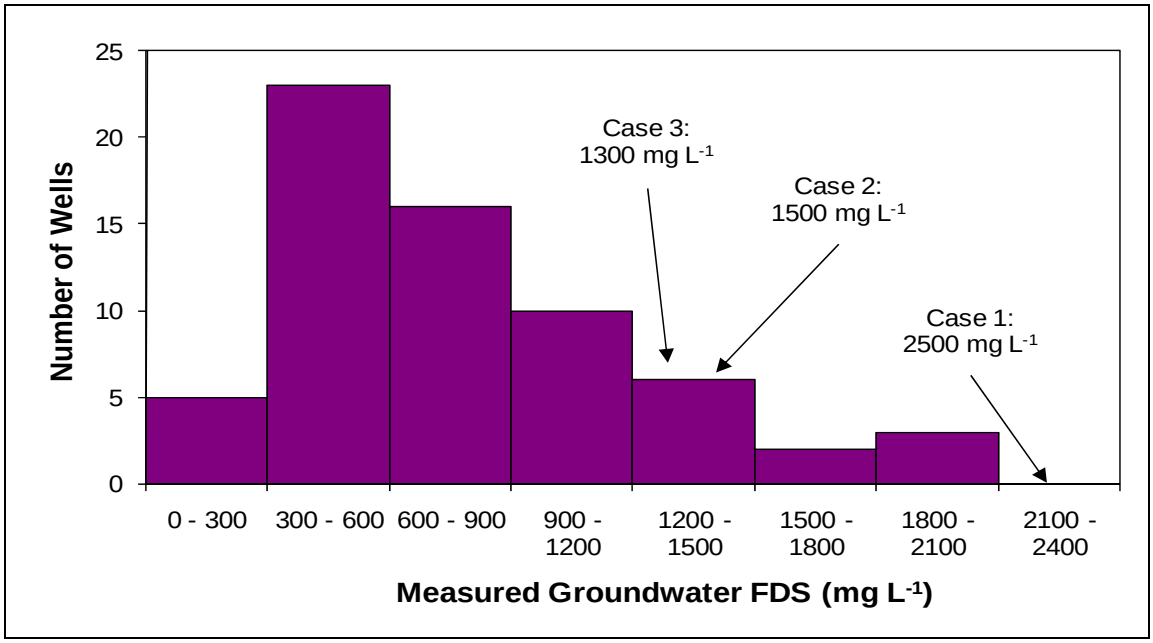

Figure 60

Histogram of FDS Concentration in Groundwater Wells Down-Gradient from Wineries

C. Modesto POTW Scenario

The results of the Modesto POTW simulation indicated that the system followed a similar pattern as that in Case 2 baseline scenario. Nitrate breakthrough occurred with an average concentration of 120 mg L^{-1} (Figure 61). The soil saturation levels remained around 0.6 (Figure 62), keeping the vadose zone aerobic, and leading to 0% of ammonia reaching the water table (Table 50). The degradation of NH_4 led to a nearly four-fold increase between the amounts of NO3 applied at the surface and that reaching the water table. Aerobic conditions also prevented the attenuation of SO4, which reached the water table at a concentration of 110 mg L^{-1}. Breakthrough of organic matter also occurred, with concentrations reaching 1390 mg L^{-1} by year 30; 86% of that applied at the surface reached the water table, indicating that water moved through the system too quickly to allow for its complete microbial consumption.

The FDS concentration reaching the water table was 2500 mg L^{-1}, a 119% increase over that applied at the surface (Table 50). Much of the increase can be attributed to calcite dissolution caused by slightly acidic conditions, which increased levels of Ca and CO_3 in solution.

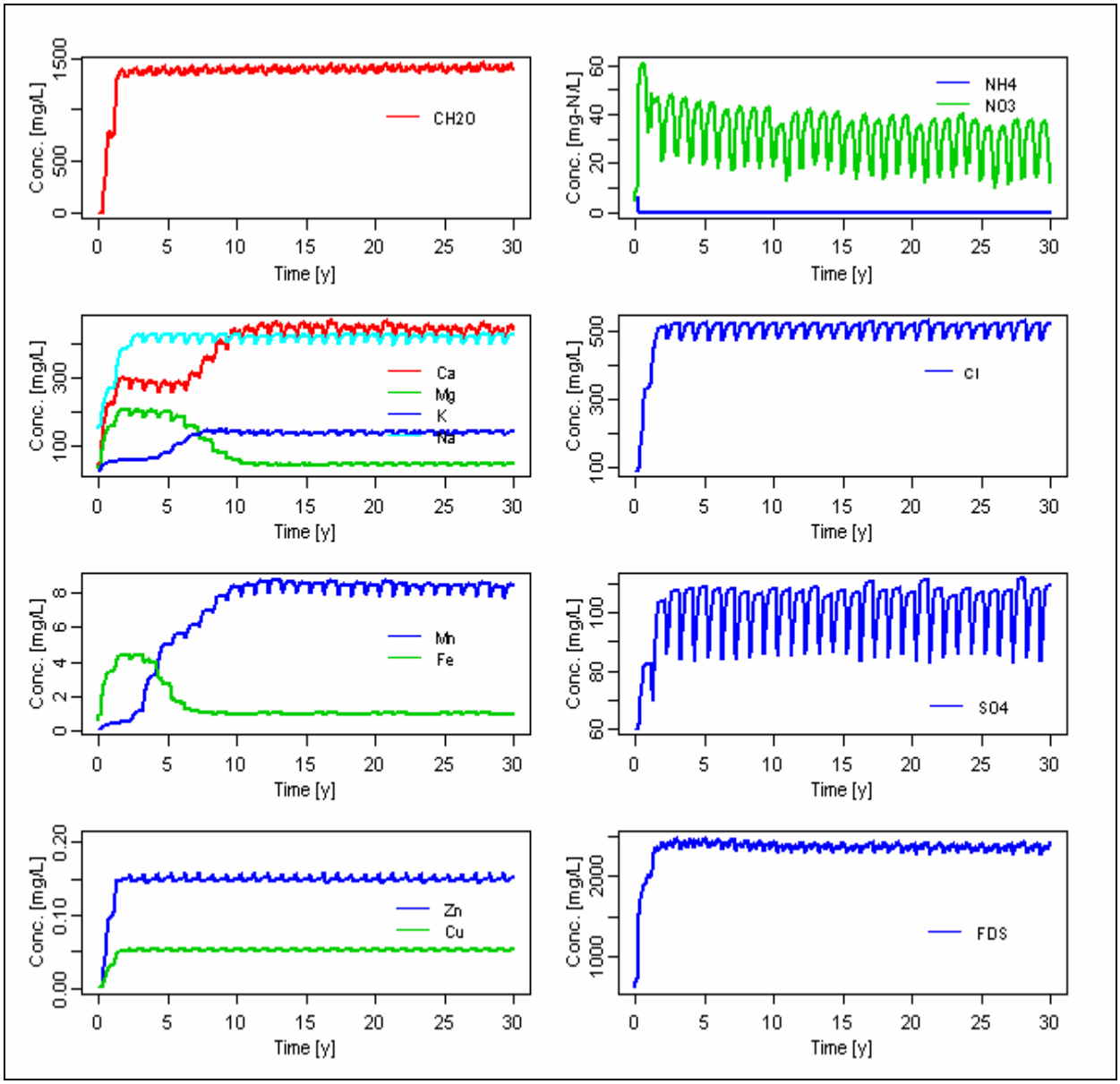

Figure 61

Breakthrough Curves for Modesto POTW Simulation

Table 50: Mass Balance for Modesto POTW

	Surface Loading	Storage	Degassing	Biodegredation (Aqueous)	Biodegredation (Mineral)	Root Uptake	Precipitation	Adsorption	Water Table	Mass Error
CH_2O	8488	-273	0	-980	0	0	0	0	-7262	-26.01
	100%	-3%	0%	-12%	0%	0%	0%	0%	-86%	0%
NH_4	395	0	0	-330	0	-72	0	7	0	-0.77
	100%	0%	0%	-84%	0%	-18%	0%	2%	0%	-0.2%
NO_3	220	-26	0	1011	0	-360	0	0	-846	0.55
	100%	-12%	0%	459%	0%	-163%	0%	0%	-384%	0.2%
O_2	128	0	2030	-2137	0	0	0	0	-21	0.02
	100%	0%	1582%	-1666%	0%	0%	0%	0%	-17%	0.0%
K^+	864	-24	0	0	0	-128	0	-70	-645	-2.03
	100%	-3%	0%	0%	0%	-15%	0%	-8%	-75%	-0.2%
Ca^{2+}	735	-71	0	0	0	-75	1719	-244	-2065	-0.91
	100%	-10%	0%	0%	0%	-10%	234%	-33%	-281%	-0.1%
Mg^{2+}	342	-1	0	0	0	-95	0	170	-416	-0.07
	100%	0%	0%	0%	0%	-28%	0%	50%	-122%	0.0%
Na^+	2229	-51	0	0	0	0	0	-7	-2174	-2.38
	100%	-2%	0%	0%	0%	0%	0%	0%	-98%	-0.1%
Fe^{2+}	59	-2	0	0	0	0	-16	-6	-37	-1.29
	100%	-3%	0%	0%	0%	0%	-26%	-11%	-62%	-2.2%
Mn^{2+}	5	0	0	0	0	0	0	2	-8	0.00
	100%	-1%	0%	0%	0%	0%	0%	43%	-142%	0.1%
CO_3^{2-}	2974	-79	-3770	1959	15	323	2557	0	-3979	-0.24
	100%	-3%	-127%	66%	1%	11%	86%	0%	-134%	0.0%
SO_4^{2-}	557	-7	0	0	0	-45	0	0	-505	0.10
	100%	-1%	0%	0%	0%	-8%	0%	0%	-91%	0.0%
Cl-	2671	-76	0	0	0	0	0	0	-2600	-5.64
	100%	-3%	0%	0%	0%	0%	0%	0%	-97%	-0.2%
PO_4^{3-}	137	0	0	0	0	-127	0	0	-11	-0.31
	100%	0%	0%	0%	0%	-93%	0%	0%	-8%	-0.2%
FDS	11189	-337	-3770	2640	15	-579	4261	-147	-13285	-12.97
	100%	-3%	-34%	24%	0%	-5%	38%	-1%	-119%	-0.1%

Mass balance in pounds per acre per year and percent of total component loading.

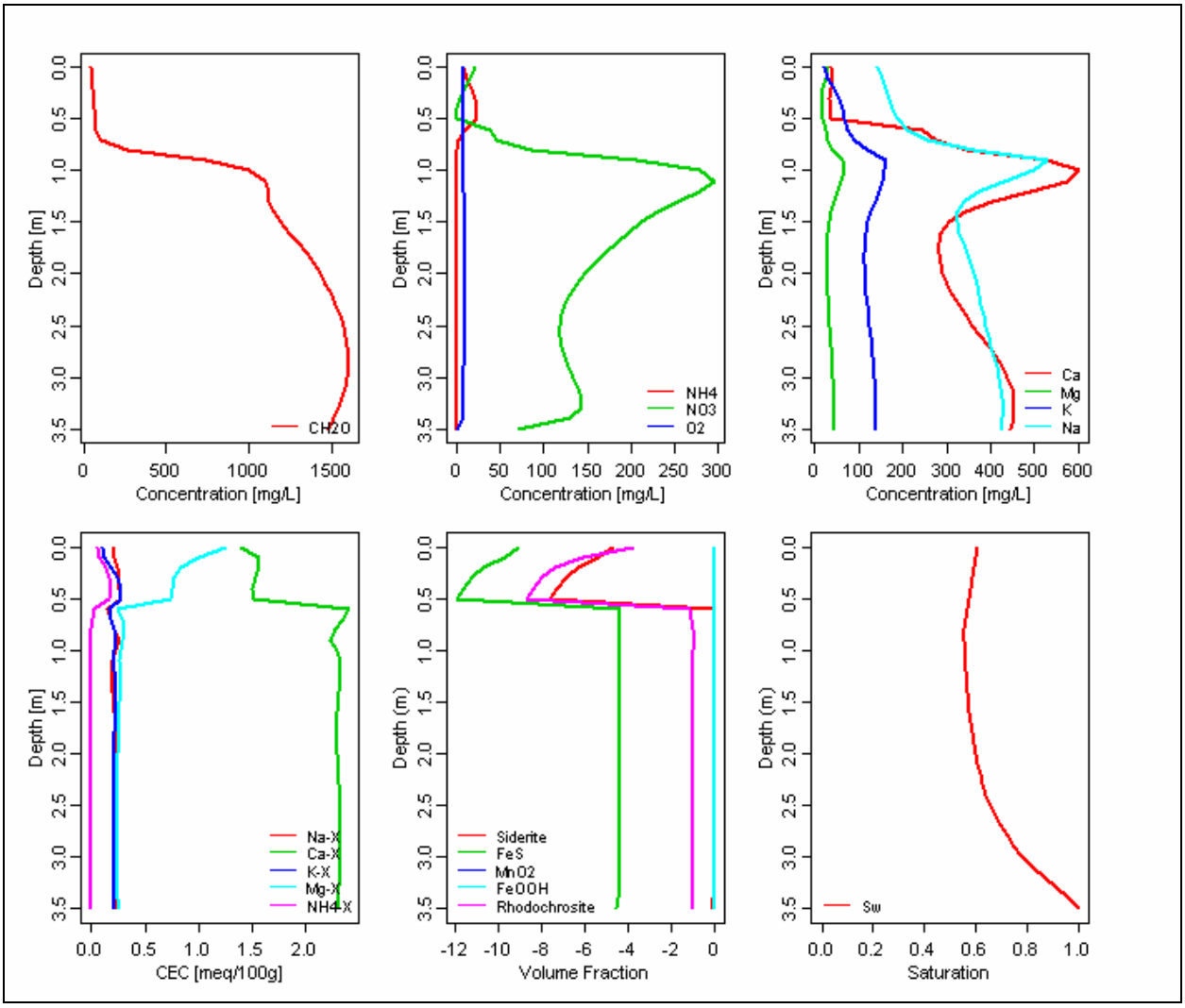

Figure 62

Profiles for Modesto POTW Simulation, Year 30

D. Model Sensitivity Analysis

This section discusses the sensitivity of the modeling results to two assumptions made during the construction of the baseline scenarios. First, a 2-dimensional model with a fluctuating water table is created in Section D.1 in order to address the potential effects of the horizontal and upward transport of FDS and nitrogen compounds, which are ignored in the one-dimensional model. Second, the buildup of salts in the rooting zone is examined, in order to determine its potential impact on crop yield and infiltration reduction. Finally, the potential for microbes and crops to die due to high levels of salinity building up in the vadose zone is addressed, and the impact on the resulting water table concentrations is bracketed.

1. Water Table Fluctuations

A two-dimensional (2-D) model of land application was necessary to investigate the effects of movement of the groundwater at the interface between the saturated and unsaturated zone and the seasonal fluctuations of the water table on the mass transfer into the saturated zone and the concentration profiles in the unsaturated zone. These effects could not be determined with the 1-D column model used in the baseline simulations.

The simulated 2-D domain (see Figure 63) ran 1000 m long (x = 0 to x = 1000) to a depth of 50 m (z = 0 at bottom to z = 50 at surface), discretized into a regular array of 20 m x 1 m cells. Underlying groundwater flow was set to occur in the direction of the positive x direction by creating a constant head (1st type) boundary condition of 33 m at x = 1000. The left boundary (x = 0) was modeled as transient flux condition (2nd type), with a flux of 1.1 x 10-7 m s^{-1} during June through February (Figure 63) and 2.2 x 10-7 m s^{-1} from March to June (Figure 64). The variable boundary condition induced yearly water table fluctuations of approximately 1 m, with the hydraulic gradient varying from 0.001 m m^{-1} to 0.002 m m^{-1}. While these flow conditions do not correspond directly to any location in the GMS groundwater model (Section 6C of the SEP Report), they are consistent with the range of depth to groundwater, hydraulic gradient, water table fluctuation, and horizontal flow found within it.

Wastewater was applied at the surface from x = 200 to x = 500 m. The soil hydraulic conductivity, waste application rate, and evapotranspiration rates were set equal to those in the Winery Case 2 simulations, described in Sections II.2.E.1.b and II.3.A.2. The waste application induced a strong vertical movement of water directly under the site, with little lateral flow in the vadose zone (Figure 63) and seasonally varying saturation levels (Figure 63 and 64).

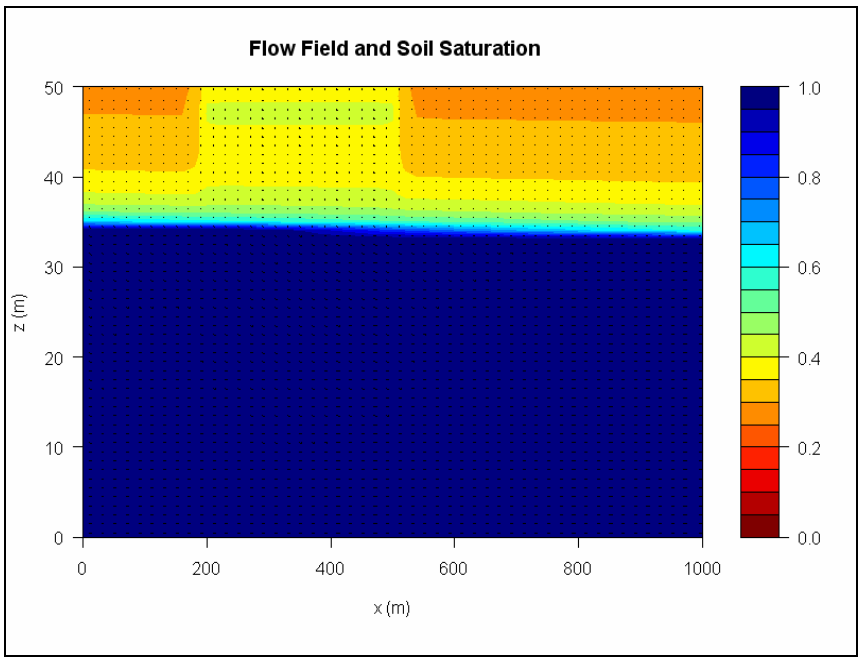

Figure 63

Flow Field at Year 29, February

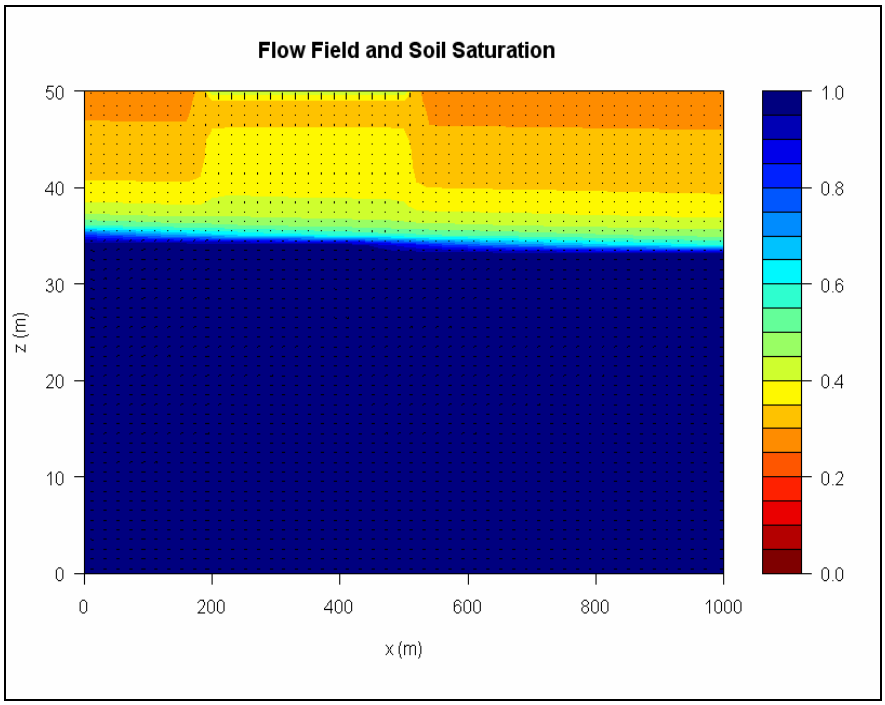

Figure 64

Flow Field at Year 29, June

In order to simplify the chemical system and make the simulations less computationally

intensive, the components were reduced to the following: carbonate, chloride, nitrate, pH, oxygen, nitrogen, carbon dioxide, organic matter, calcium, ammonia, sodium. Microbial reactions including other components were eliminated, leaving only respiration, nitrification, and de-nitrification. Exchangeable species were limited to sodium, calcium, and magnesium and the included minerals were limited to calcite. Crop uptake of calcium, nitrate, and ammonia was also included. Initial concentrations and applied waste concentrations were identical to those used for the Winery Case 2 simulations. A specific mass flux boundary condition (3rd type) was placed at x = 0, with incoming concentrations equal to the initial/background groundwater concentrations. A free outflow (2nd type) boundary condition was placed at x = 1000.

The chloride and carbonate concentration profiles for six time-steps between 99.0 and 100.0 years show dramatic seasonal variation in the vadose zone, but only minute seasonal variation near the water table (Figure 65 and 66). The lack of change in these profiles indicates that the 1 m seasonal fluctuations in water table level are much less important than the near surface seasonal changes induced by precipitation and crop uptake.

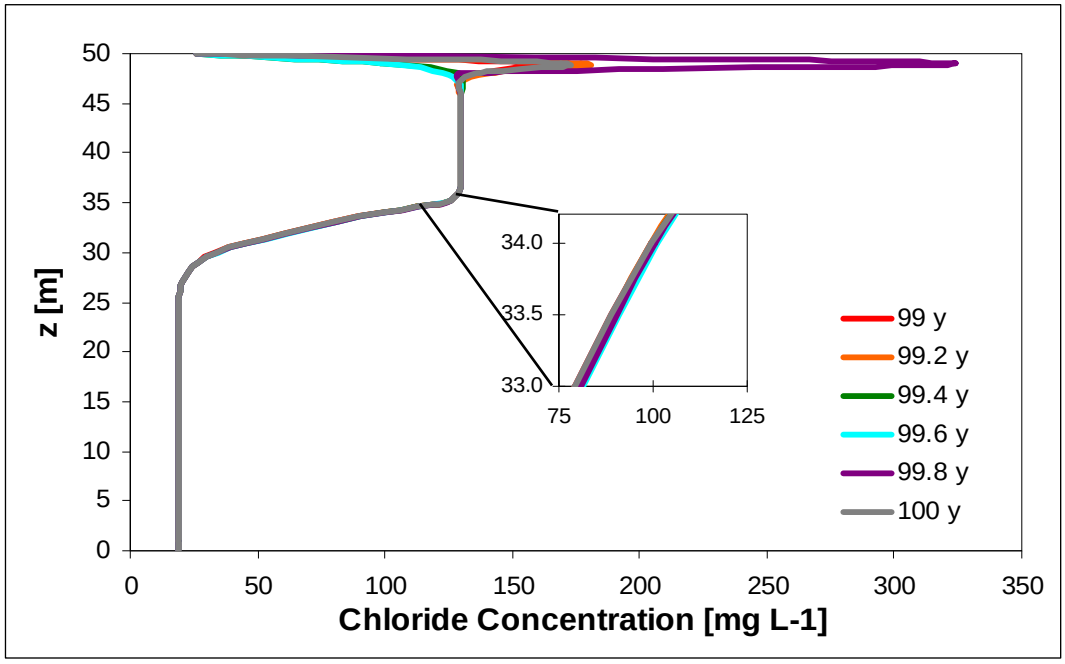

Figure 65

Profile of Chloride Concentration at x = 360 m

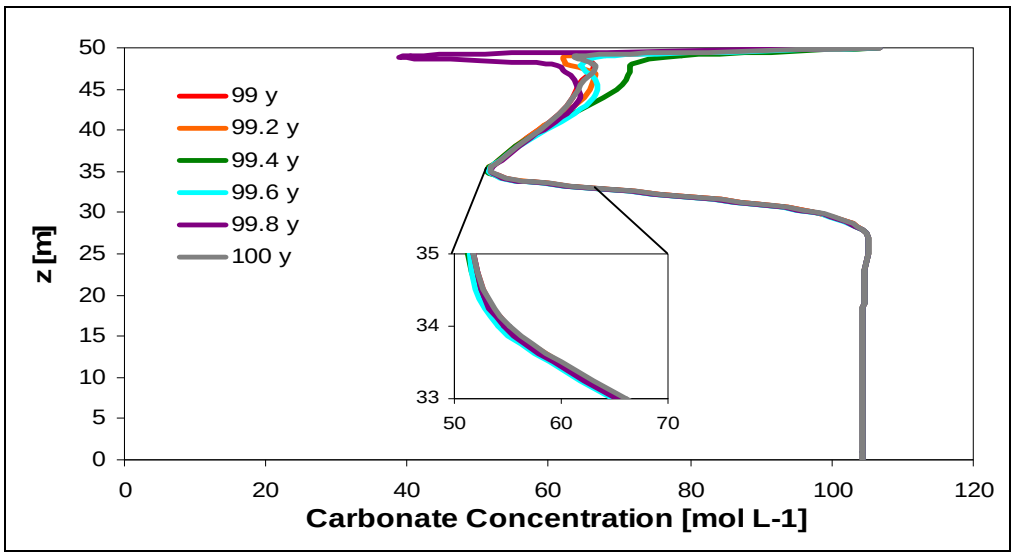

Figure 66

Profile of Carbonate Concentration at x = 360 m

The seasonal variations for nitrate (Figure 67) are less pronounced, in both the near surface and at the water table. The root uptake of nitrate appears to overwhelm the supply, causing the rapid removal noted in the top 1 m. The seasonal variations in water flux do not cause high enough saturation levels to create the anaerobic conditions necessary for nitrate decay, and thus the profile remains fairly steady on a seasonal basis.

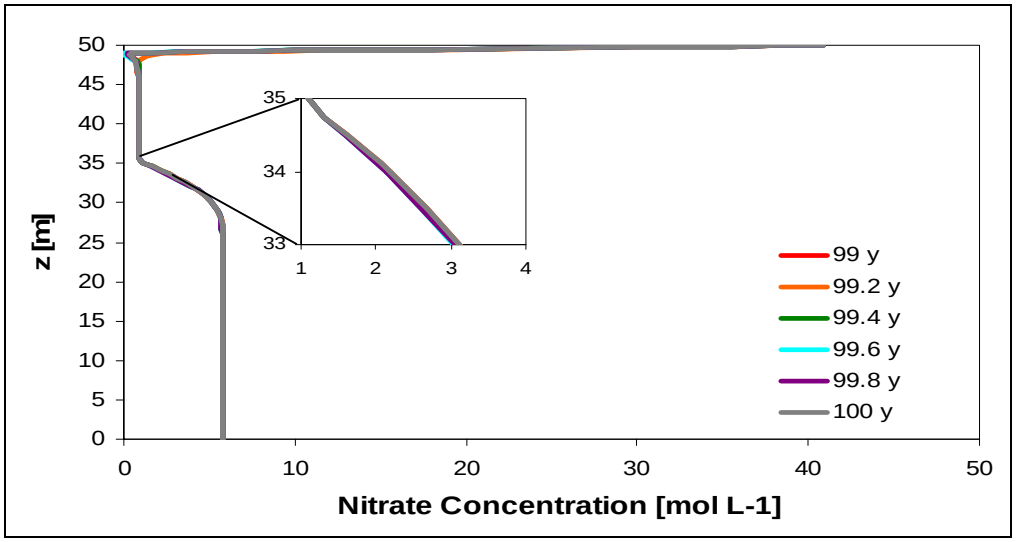

Figure 67

Profile of Nitrate Concentration at x = 360 m

The profiles for the decadal time-steps between 0.1 and 100 years show more variation as the wastewater moves downward through the system. The chloride tracer first reaches the water table between 10 and 20 years (Figure 68), and the profile remains fairly constant between years 60 and 100. Nitrate (Figure 69) and carbonate (Figure 70) concentrations follow similar

temporal behavior. Carbonate concentrations appear to be interacting with the groundwater, with the lowest concentrations noted at x = 35 m (immediately above it) and the highest concentrations at x = 30 m (just below it). This feature was not noted in the 1-D model (Figure 71), likely because a boundary condition was set at the water table in the 1-D model, unlike the 2-D which had no conditions there.

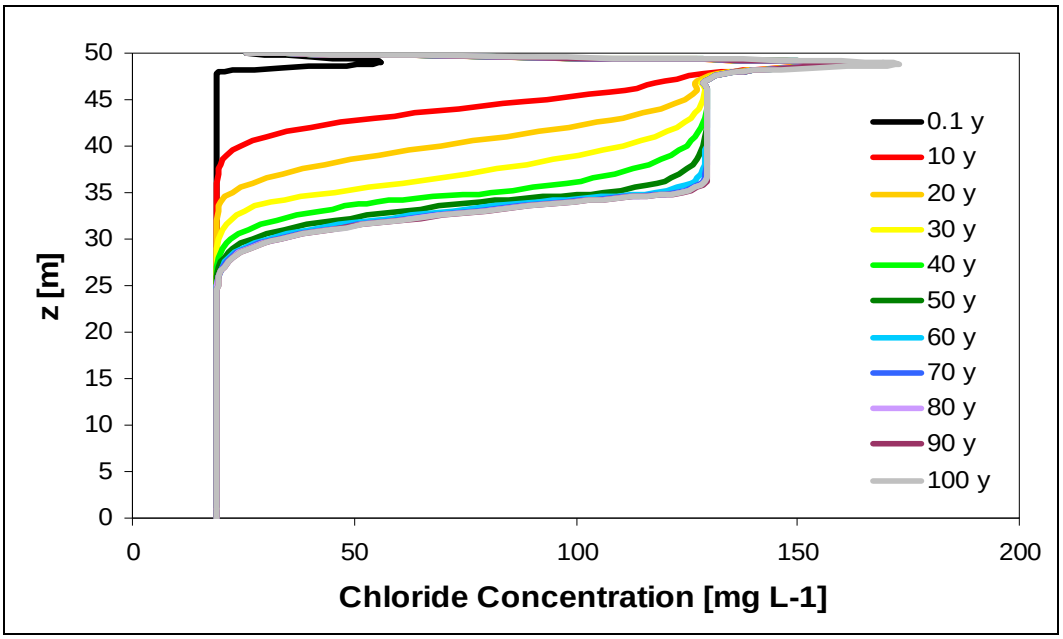

Figure 68

Profile of Chloride Concentration at x = 360 m

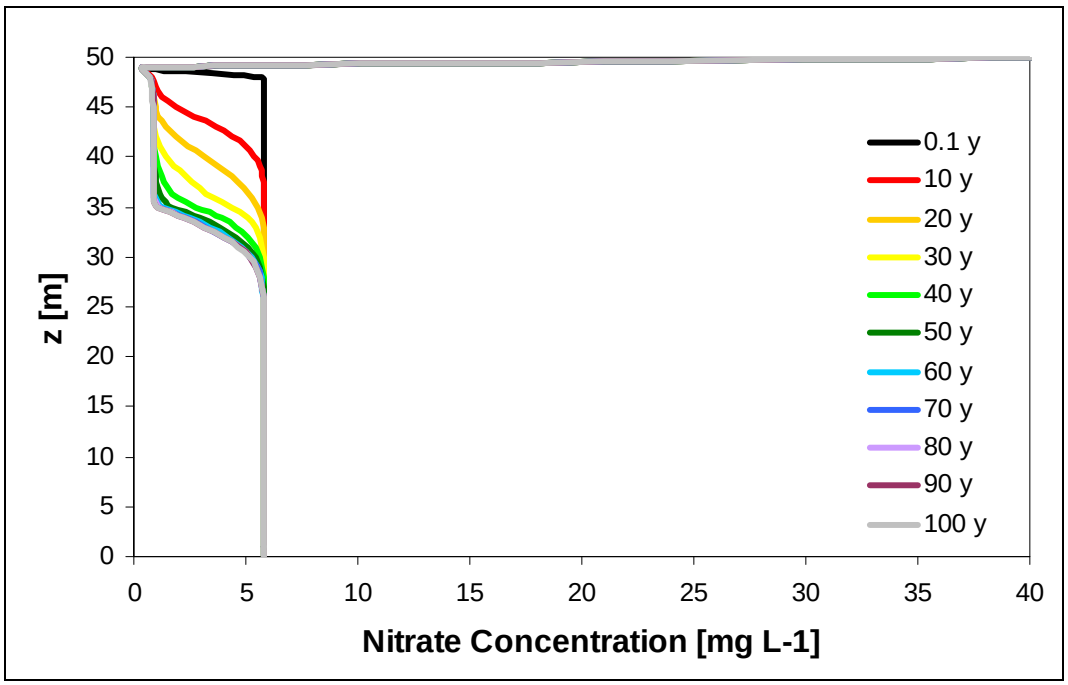

Figure 69

Profile of Nitrate Concentration at x = 360 m

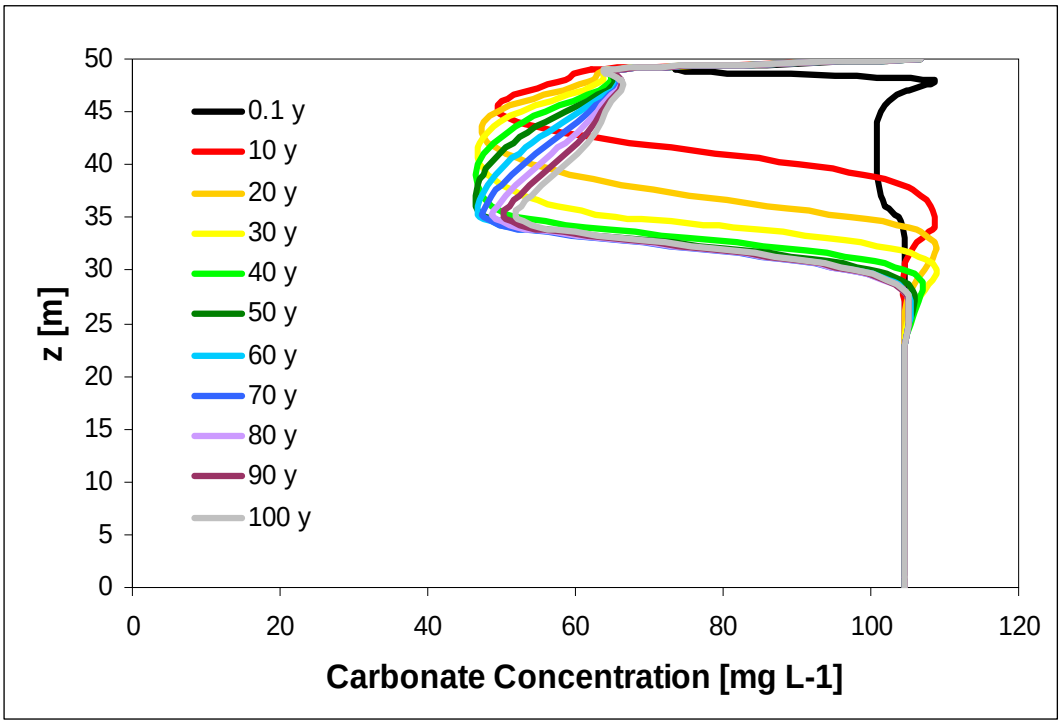

Figure 70

Profile of Carbonate Concentration at x = 360 m

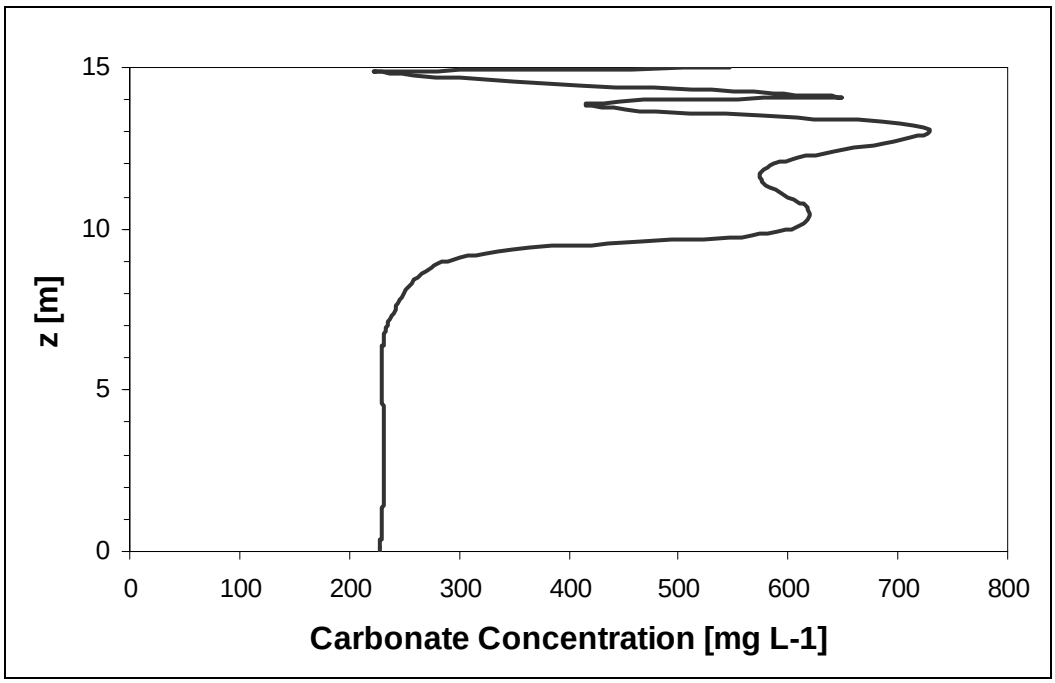

Figure 71

Profile of Carbonate Concentration in 1-D Model at 30y

2. Salinity Buildup in the Root Zone

The primary focus of this study is salinity and nitrogen loading to the groundwater, however, under some conditions, land application may lead to salinity build-up in the rooting zone. This buildup can lower crop yields, reducing ET, and in turn lead to increased levels of wastewater and plant nutrients (N, K, P, Mg, Ca) reaching the groundwater. High levels of salts in the rooting zone can also increase soil sodicity, lowering infiltration rates and increasing the likelihood of wastewater ponding at the ground surface. This section analyzes the salinity concentrations simulated for the rooting zone and estimates how these would impact the crops grown and the water infiltration rates.

a) Leaching Fraction

The leaching fraction (LF) represents the proportion of water applied that is not removed through root uptake. It is calculated using the following equation (Asano et al., 2007):

Eq 28 $$LF = \frac{D_{dw}}{D_{iw}}$$

where D_{dw} is the depth of water leached out of the root zone and D_{iw} is the depth of water applied at the soil surface, both in m.

When the leaching fraction is high, salts and other solutes are transported from the rooting zone to the groundwater below, potentially leading to groundwater degradation. However, low

leaching fractions lead to the buildup of these salts in the soil, which impairs crops and reduces yields if salinity levels become sufficiently high. In land application systems, the ratio is determined by the rate and timing of precipitation, irrigation, and waste application as compared to the rate and timing of evapotranspiration (crop water uptake).

In the Central Valley, precipitation occurs primarily during the winter, when evapotranspiration is low. This leads to low leaching fractions during the spring and summer months (March through August), when crops have the highest ratio of ET to applied water, and high leaching fractions during the fall and winter (November through February). A brief spike in leaching fraction occurs in June, when the wheat is harvested and the corn is planted. This pattern is shown in Figure 72 it consistently repeats throughout the simulated time (Figure 73). Cases 2 and 3 have very similar patterns (Figure 74, Figure 75), although the leaching fraction is much lower in Case 2 (<0.5) likely due to the large difference in hydraulic conductivity.

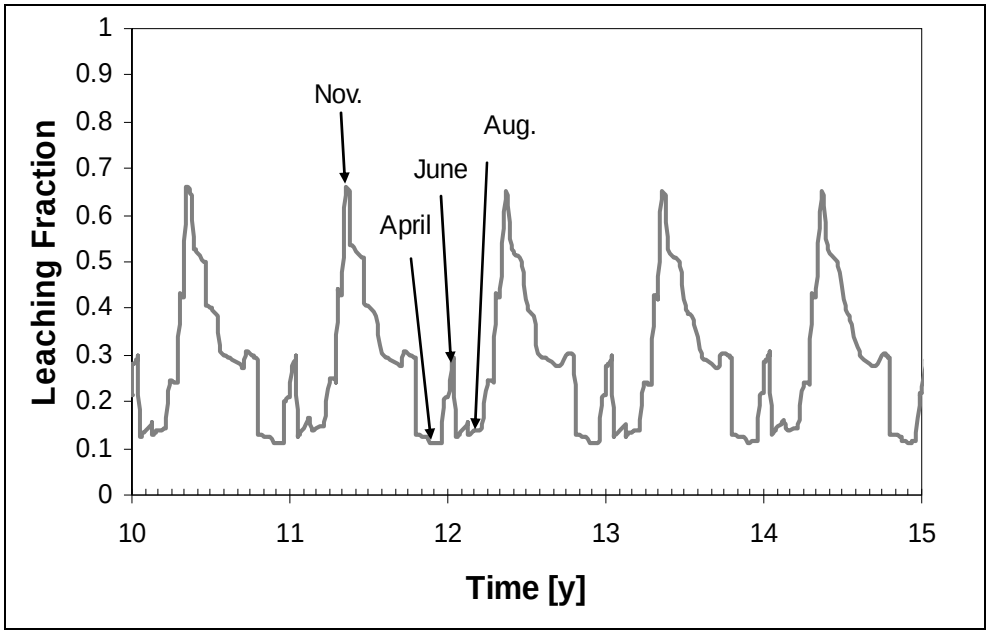

Figure 72

Leaching Fraction for Winery Case 1, Year 10 to 15

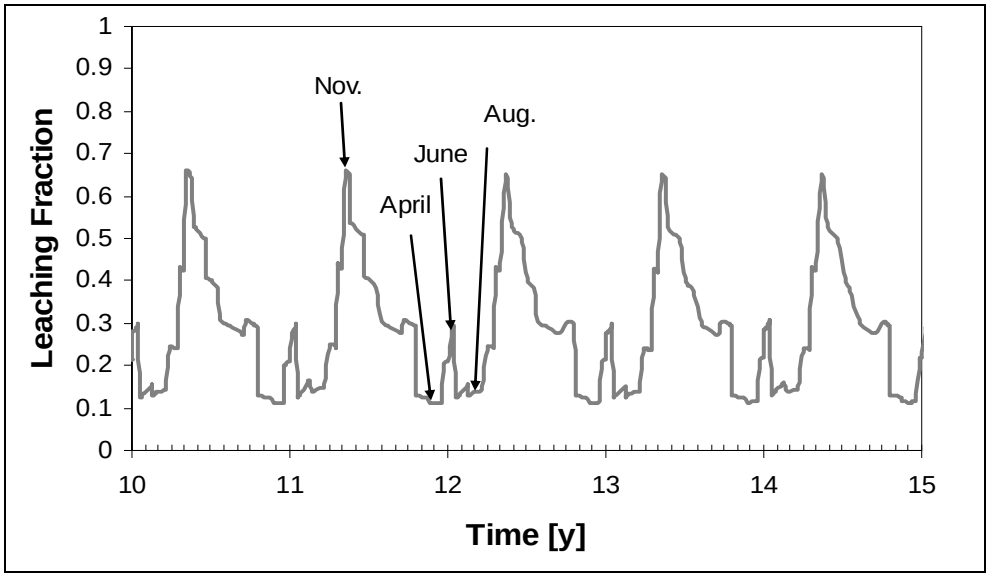

Figure 73

Leaching Fraction for Winery Case 1

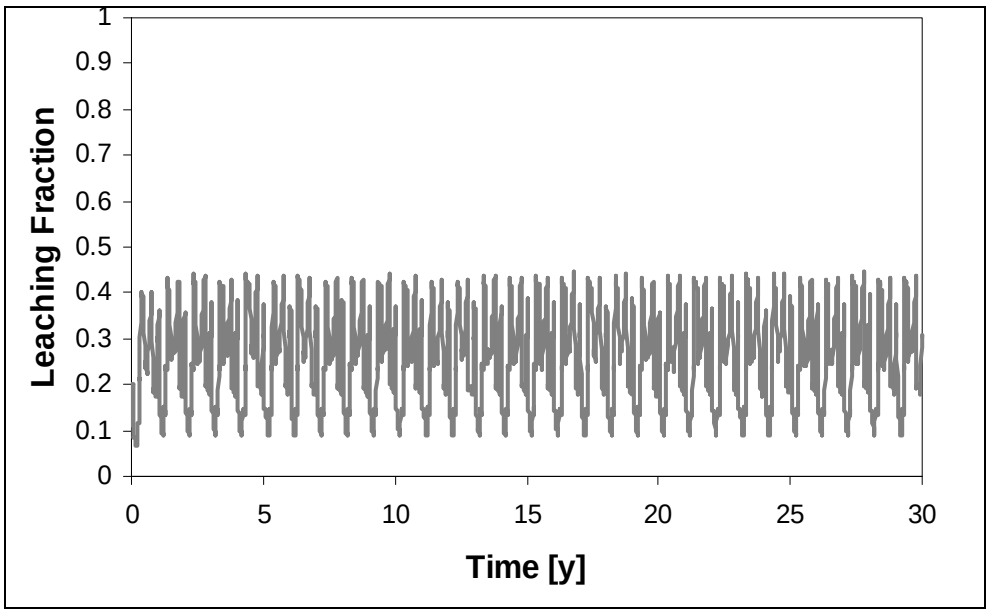

Figure 74

Leaching Fraction for Winery Case 2

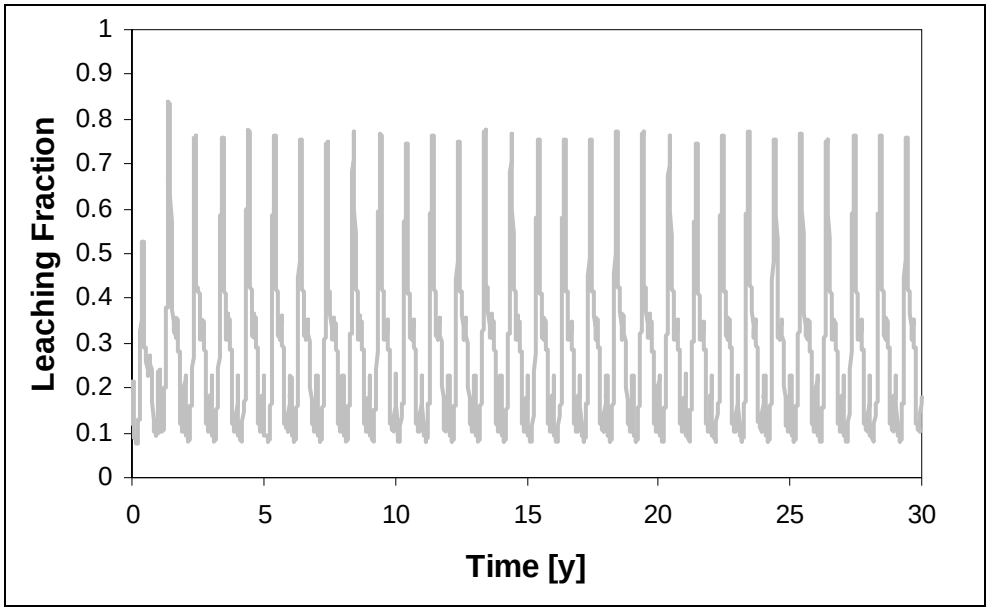

Figure 75

Leaching Fraction for Winery Case 3

While minimizing the leaching fraction is a potential management strategy for lowering groundwater impacts, the pattern of precipitation in the Central Valley prohibits any such solution, since winter rains will almost always be in excess of winter ET rates. Such a management solution is also not advisable, since it could lead to high soil salinity levels which may damage crops.

b) Soil Salinity and Crop Yield

Soil salinity (EC_e) is typically measured by extracting the water contained in a soil sample. Due to the extraction process, the EC measured in the extracted water is approximately half the EC of the soil water itself, known as EC_{sw} (Ayers and Westcot, 1985). MIN3P simulates the FDS concentrations in the soil water itself, so conversion of this value first to EC_{sw} and then to EC_e is necessary, in order to compare it directly to data on crop salinity effects, usually given as EC_e.

To calculate the soil water salinity levels, the following equation was used (Asano et al., 2007; Metcalf & Eddy et al., 1991):

Eq 29 $$EC_{sw} = \frac{FDS}{600}$$

where EC_{sw} is the electrical conductivity of the soil solution, in dS m-1, equivalent to mmhos cm^{-1}, and FDS is fixed dissolved solids calculated by MIN3P, in mg L^{-1}. To convert to soil salinity (EC_e), the soil solution salinity was divided by a factor of two (Asano et al., 2007; Ayers and Westcot, 1985):

Eq 30 $$EC_e = \frac{EC_{sw}}{2}$$

Figure 76 shows the simulated ECe levels for the Winery Case 1. The soil salinity follows a yearly pattern nearly opposite that of the leaching fraction (Figure 77). This pattern is consistent throughout the simulation time for all three cases.

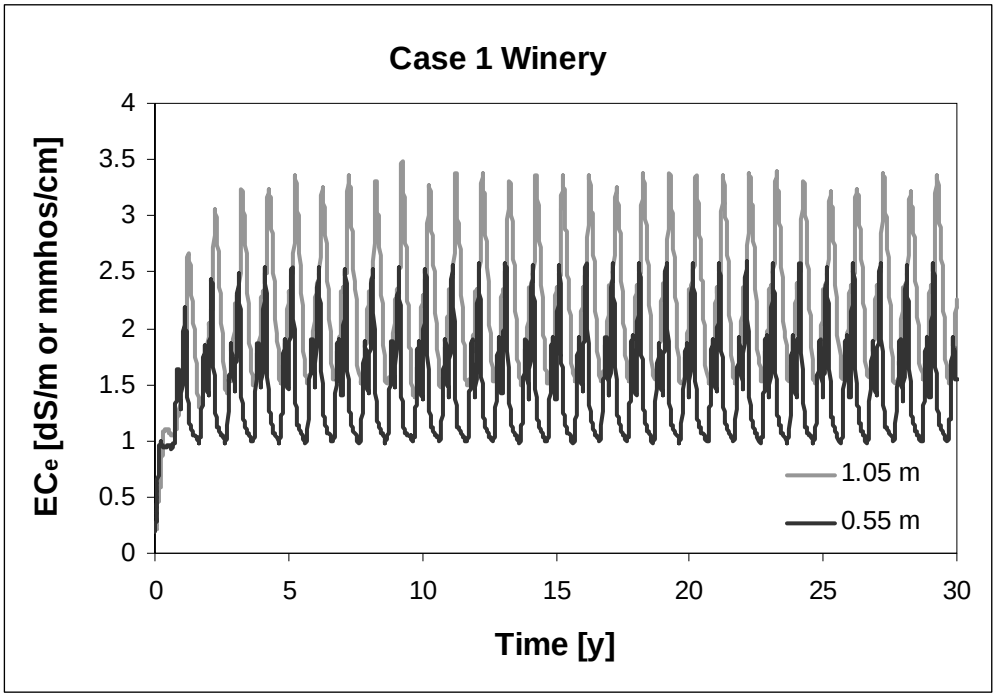

Figure 76

"Soil salinity (EC_e) for Winery Case 1 in the middle of and directly below the rooting zone (0.55 and 1.05 m below ground surface, respectively)."

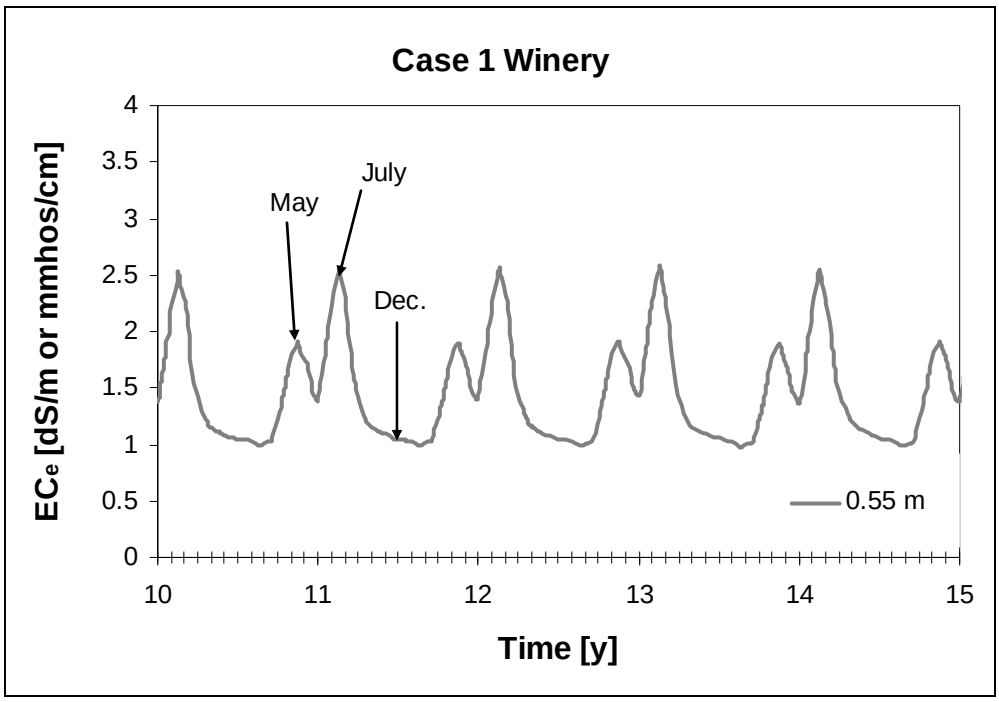

Figure 77

Soil Salinity for Winery Case 1, Years 10 to 15

Periodically elevated soil salinity levels (EC_e>2) were noted in all three winery simulations, shown over the span of one year in Figures 78-80. Significant reduction in plant yield and ET could be possible at these concentrations, but would primarily be limited to the corn crop grown between late June and early October. According to Maas and Hoffman (1977), forage corn is stressed and yields begin to decrease above an EC_e = 1.8 dS m^{-1}. Yields linearly decrease at a rate of 7.4% per 1 dS m^{-1} over this threshold level, meaning that they are reduced by approximately 25% at 5.2 dS m^{-1} and 50% at 8.7 dS m^{-1}. Wheat is more salt tolerant, with an initial threshold of 6.0 dS m^{-1} and a 50% decrease at 13.04 dS m^{-1} (Maas and Hoffman, 1977). The Case 1 simulation (Figure78) shows that the corn crops are subject to considerable salinity stress throughout their entire growing season, while wheat remains almost totally non-stressed. Due to the lower leaching fraction and the higher wastewater salinity levels in Case 2, the wheat becomes significantly stressed during May (Figure 79), while the corn is stressed during July. Both crops remain relatively unstressed in the Case 3 simulations (Figure 80), with slight stresses occurring to the corn crops during July.

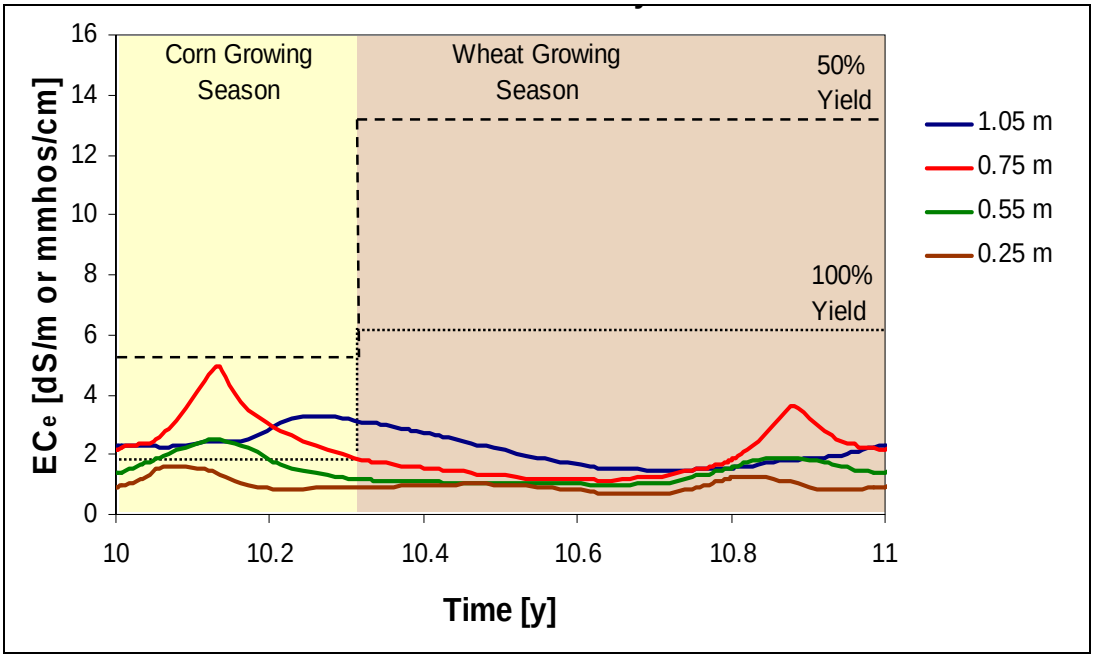

Figure 78

Soil Salinity (EC_e) for Winery Case 1, Yearly Variation and Crop Yield

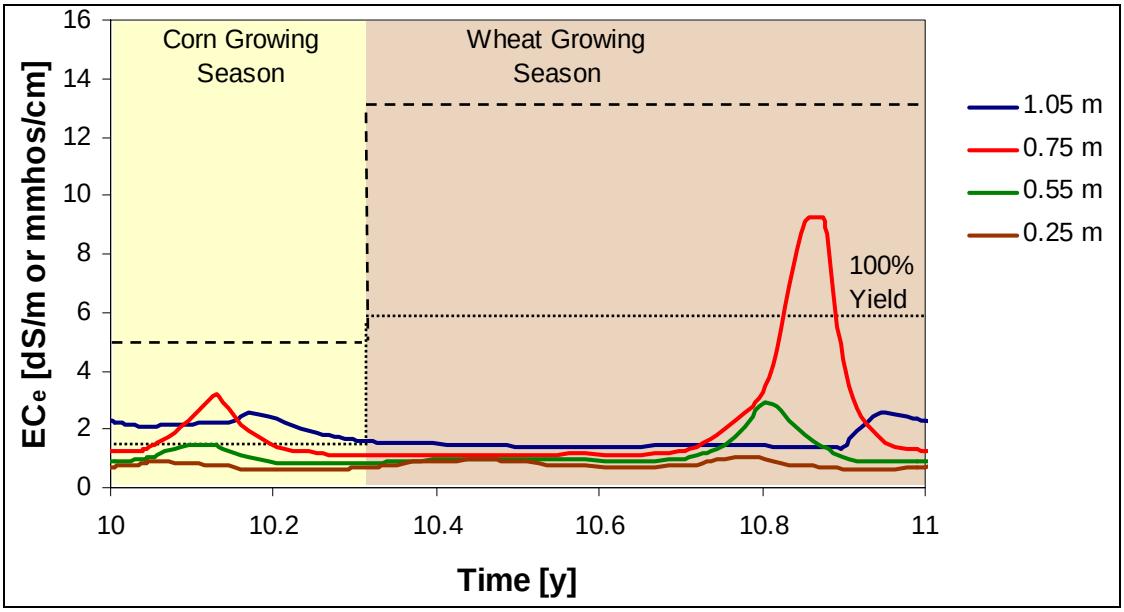

Figure 79

Soil Salinity for Winery Case 2, Yearly Variation and Crop Yield

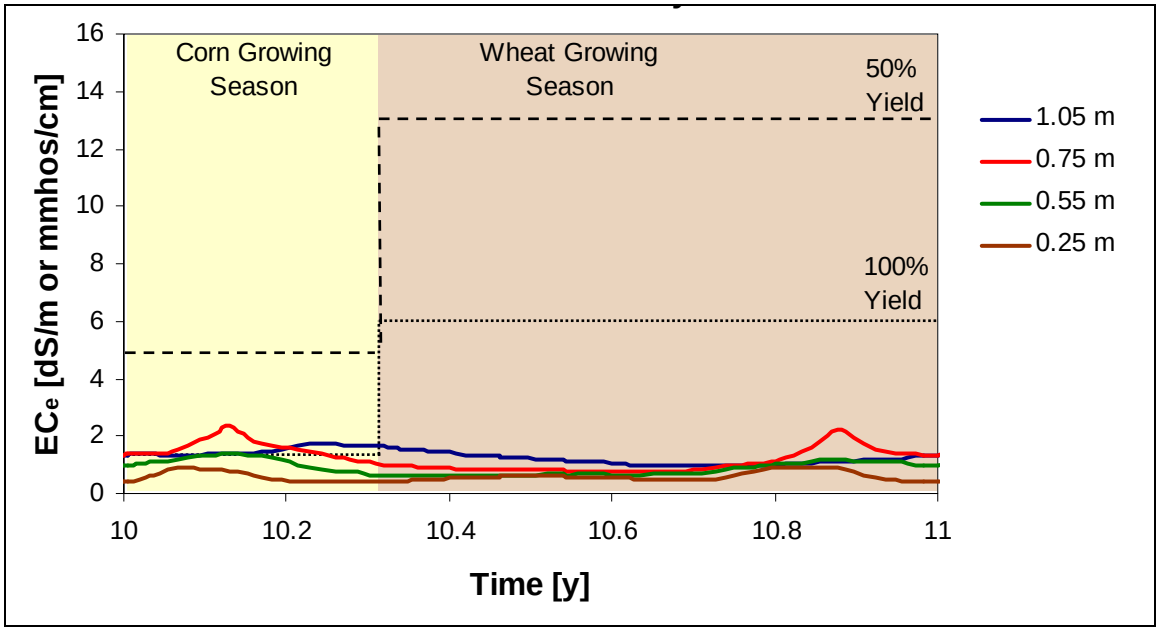

Figure 80

Soil Salinity for Winery Case 3, Yearly Variation and Crop Yield

These simulations show that corn crop yields may be reduced by up to 25 to 50% due to salinity buildup. This reduction could lower the ET and increase the leakage to the groundwater table, altering the FDS concentrations and loading rates to the groundwater table. However, it is unlikely that corn would continue to be grown under these conditions. Likely, farmers using food-processing wastewater would switch to a more salt tolerant crop, such as sorghum, wheatgrass, or barley, which has EC_e thresholds equal to 6.8, 7.5, and 8.0 dS m^{-1}, respectively (Asano et al., 2007; Maas and Hoffman, 1977). Although these crops may have different nutrient uptake rates, this switch is unlikely to result in large changes to FDS reaching the groundwater table.

For Case 2, EC_e levels at a soil depth of 0.75 m during the month of May would significantly lower the yield of most crops (Figure 79). Since the model does not account for changes in plant uptake due to high EC, it may be leading to inaccurate FDS water table loadings during this month, although it is difficult to predict the magnitude and direction of this error. However, conditions such as these may not be allowed to develop in an actual land application situation. In May, modeled irrigation, precipitation, and land application are nearly matched to the crop water uptake rates, leading to a very low leaching fraction. It is unlikely that land owners would permit the soil saturation to be reduced as greatly as the model predicts (0.2 – 0.3). Rather, in order to prevent crop stress, it is likely that additional irrigation water would be provided, leading to higher soil moisture, higher leaching fractions, and lower EC.

The possible impacts of crop productivity loss on salinity loading to the water table are explored further in Section II.3.D.3. An extended discussion on the economical aspects of crop yield losses is provided in Volume III of this study.

c) SAR and Hydraulic Conductivity

Soil sodicity occurs when sodium becomes the dominant cation present in the soil solution. It is usually measured as the sodium adsorption ratio (SAR) and can be found using the following equation (Hillel, 2000):

Eq 31 $$SAR = \frac{\left[Na^{+}\right]}{\sqrt{0.5\left(\left[Ca^{2+}\right]+\left[Mg^{2+}\right]\right)}}$$

where $\left[Na^{+}\right]$ is the sodium concentration, $\left[Ca^{2+}\right]$ is the calcium concentration, and $\left[Mg^{2+}\right]$ is the magnesium concentration, all measured in milliequivalents per liter (meq L^{-1}).

High soil sodicity can cause soil particles to disperse and clays to swell, clogging the pore structure and decreasing hydraulic conductivity, resulting in infiltration problems (Asano et al., 2007). In Winery Cases 1 and 3, root zone SAR remains below 6.0 throughout the simulation time. Figure 81, Figure 83. Case 2 simulations show levels around 15.0 and reaching up to 20.0 (Figure 35), again due to the low leaching fraction.

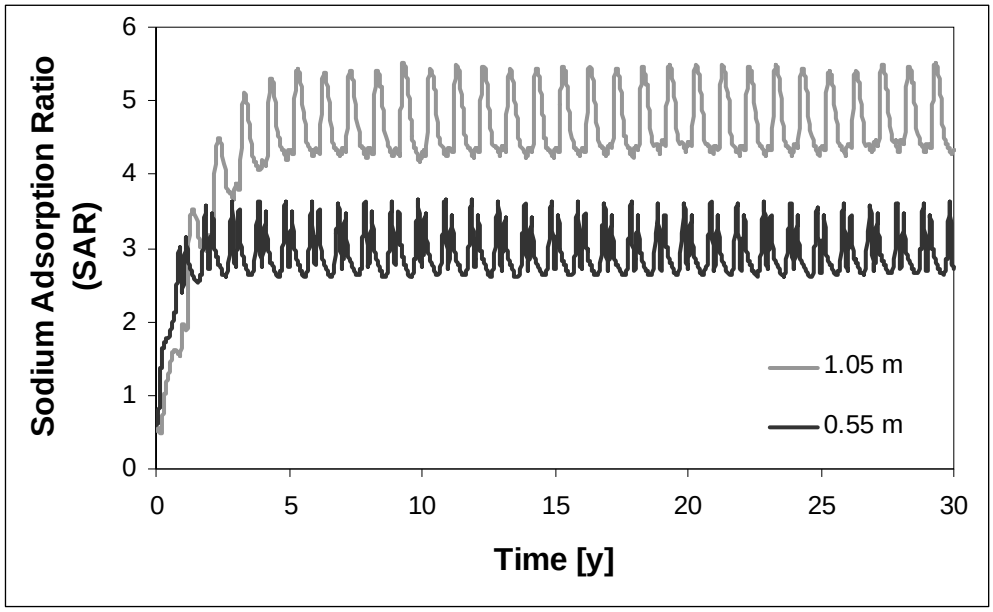

Figure 81

SAR for Winery Case 1

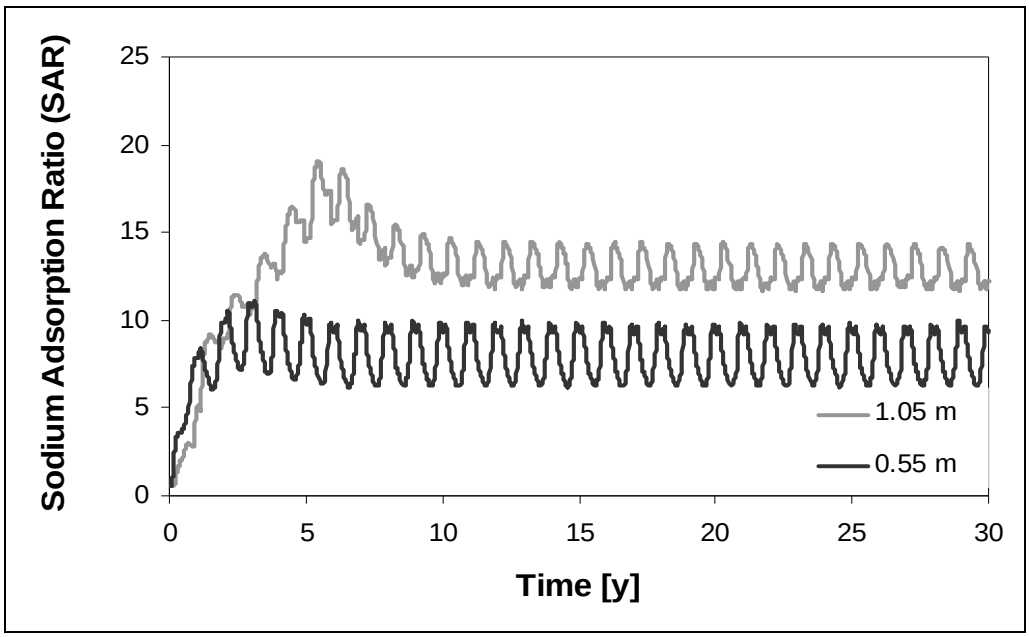

Figure 82

SAR for Winery Case 2

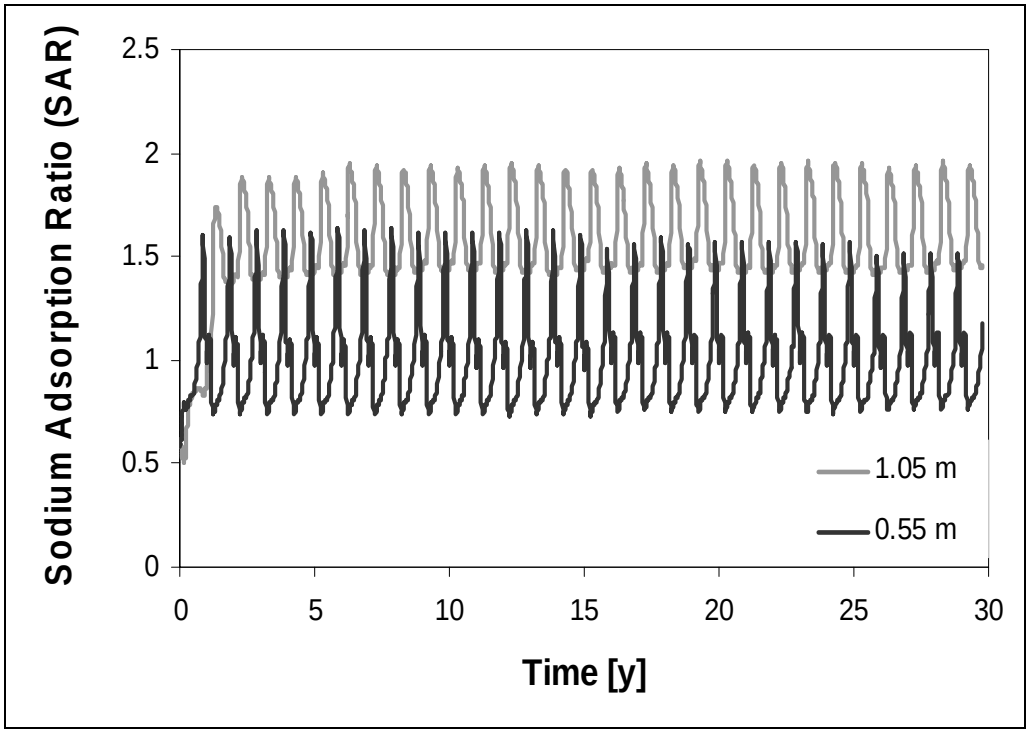

Figure 83

SAR for Winery Case 3

Despite the elevated SAR levels in Cases 1 and 3 and the high SAR levels in Case 2, it is unlikely that infiltration problems will develop. As the EC of the applied water (EC_w) increases, the likelihood of reducing infiltration due to high SAR decreases. Table 51 shows the EC_w for

the wastewater in each simulation, along with the SAR above which infiltration problems can be expected (SAR_{limit}) at that given EC_w. The maximum SAR noted in the simulations is also shown (SAR_{max}). In all cases, the maximum SAR is below the levels expected to cause infiltration problems.

Table 51: ECw and SAR for Winery Simulations

	EC_w	SAR_{limit}	SAR_{max}
Case 1	2.2	11	6.9
Case 2	7.1	>30	19
Case 3	1.2	5	2.7
SAR_{limit}, SAR above which slight to moderate infiltration problems occur; SAR_{max}, maximum SAR noted in simulations. From Ayers and Westcot, 1985.			

3. Salinity Toxicity to Crops and Microbes

As discussed in Section II.3.d.2, high soil salinity concentrations can limit crop productivity (Ludwick et al., 2002) and microbial activity (McClung and Frankenberger, 1985), potentially decreasing the attenuation from crop nutrient uptake and nitrification/ de-nitrification. Following the "best/worst case" approach, three test scenarios were developed to determine how the breakthrough of salinity would be affected. Typically, microbial activity and plant uptake slow as salinity levels increase and cease altogether past a threshold value. These relationships, however, are subject to considerable uncertainty. Rather than attempt to dynamically model changes in uptake rates based on current salinity levels, we instead designed scenarios that would not include attenuation from crops and microbes. These scenarios would demonstrate the upper bounds on FDS.

The first scenario assumed that crops could not be grown on the site, but that microbes were still active. In this, crop transpiration was replaced with soil evaporation in the upper two grid cells of the simulation (15 cm). Evaporation from soil was assumed to be Stage 1 only and follow the equation: $E = Ks*ET_o$, where E is evaporation, K_s is a "crop coefficient" for bare soil ($K_s = 1.22 – 0.04*ET_o$), and ET_o is the reference evapotranspiration (Snyder et al., 2001). Once soil reached the residual saturation, all evaporation stopped. All values of I_{max} (Part I, Section 3.8) were set to zero. This scenario was intended to determine the FDS concentration if no crops could be and/or were grown on a site while land discharge was occurring. The lack of crops was expected to raise levels of nutrients in the soil water, but decrease the amount of carbonate.

The second assumed the opposite: crops could be grown, but microbial processes (respiration,

de-nitrification, nitrification, etc.) ceased. This behavior was achieved by setting the overall reaction rate, k, Part Section II.2 Equation 22 to zero for all microbial reactions. This scenario assumed that all microbial activity had stopped (due to high salinity levels); the levels of nitrate, ammonia, and carbonate reaching the water table were expected to be much in this scenario, while the concentrations of nutrients were lower.

The third scenario assumed that neither microbes nor plants were active, and all values for both k in Part I Equation 22 and I_{max} in Part Section II.2 equation 10 were set to zero. This scenario was anticipated to result in the highest levels of FDS reaching the groundwater table; while carbonate levels would be lower, levels of nutrients and the nitrogen compounds would be higher.

Figure 84 shows the effect of these changes on the FDS breakthrough curve for Winery Case 2. The baseline scenario shows the highest salinity level, with 1600 mg L^{-1}, followed by the "no microbes" scenario at 1500 mg L^{-1}, the "no crops" scenario at 1200 mg L^{-1}, and the "no crops or microbes" scenario at 1100 mg L^{-1}. The higher FDS concentrations occur in the cases with the most evapotranspiration occurring at the surface and in the rooting zone. This increases concentrations of key salinity components, namely Cl, Ca, and Na. The effect is also seen on the mass loading curves.

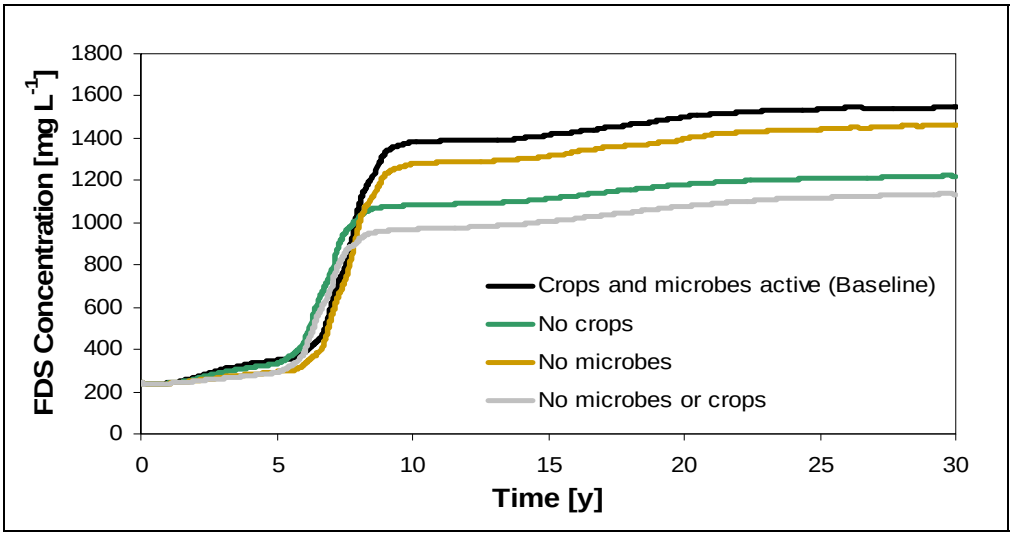

Figure 84

Effect of Salinity Toxicity to Crops and Microbes on FDS Concentration for Winery Case 2

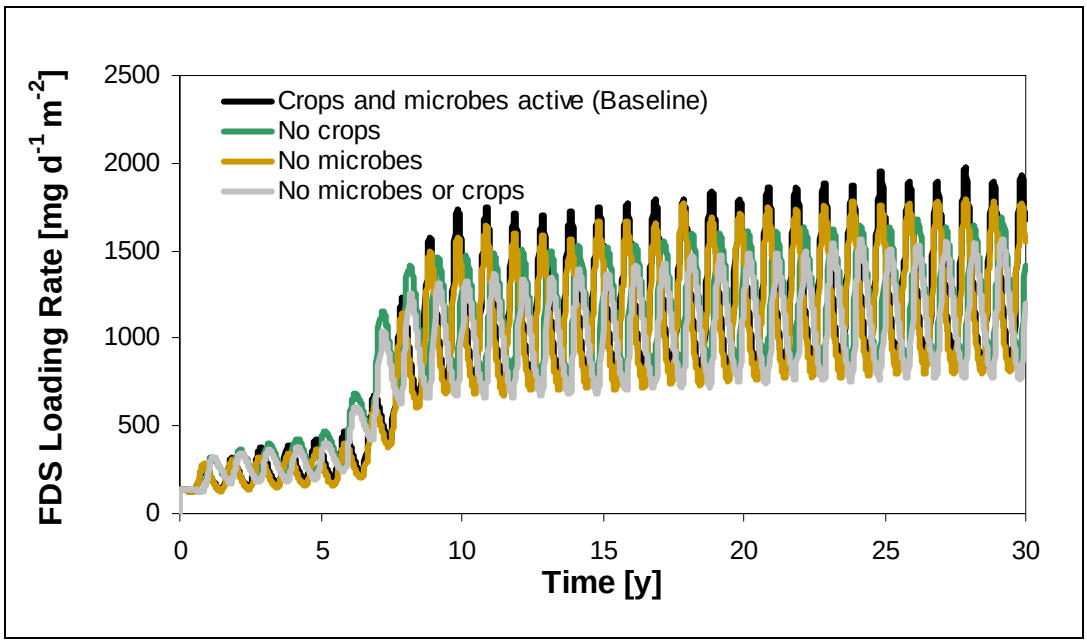

Figure 85

Effect of Salinity Toxicity to Crops and Microbes on FDS Loading Rate for Winery Case 2

The FDS breakthrough of the two "no crops" scenarios also occurs slightly earlier because more water is reaching the water table due to the exclusion of plant transpiration. This can be seen more dramatically in Case 1 (Figure 85), where lower hydraulic conductivity prolongs the time spent in the upper soil layers, increasing evaporation. In this case, the lowest FDS concentrations are predicted for the "no crops" scenario, likely due to the production of carbonate by crops which cannot escape the system due to the high saturation levels and end up enhancing the FDS concentrations. Higher evaporation can also cause salts to accumulate near the surface, decreasing the salinity loading to the water table.

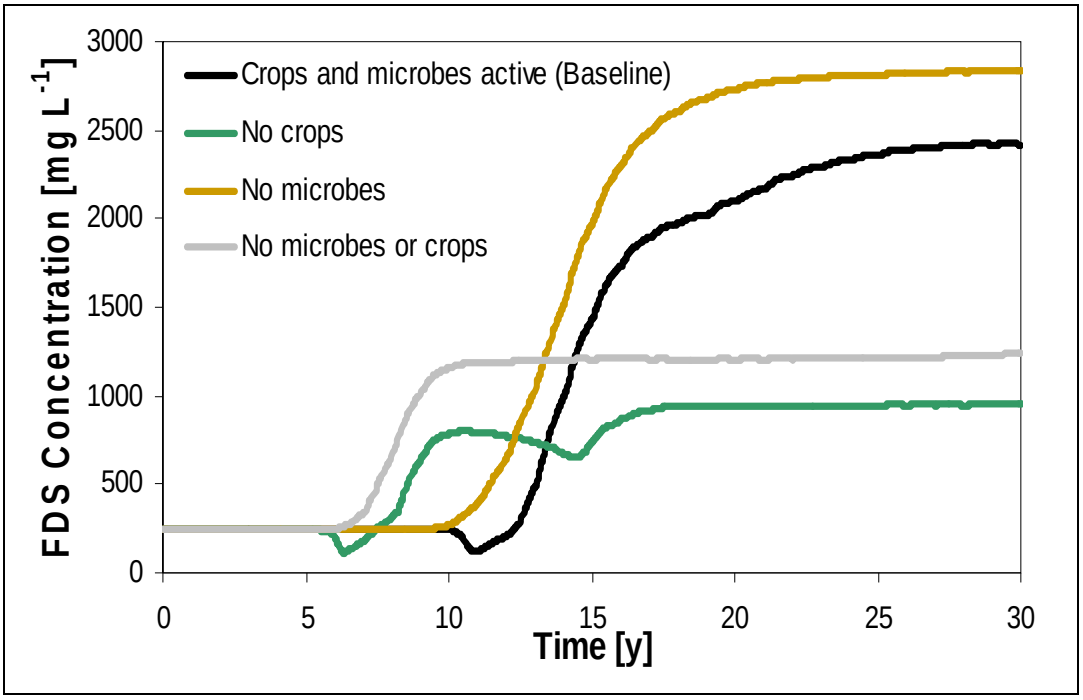

Figure 86

Effect of Salinity Toxicity to Crops and Microbes on FDS Concentration for Winery Case 1

While FDS concentrations may be lower in these scenarios, the lack of crops and microbes is not without consequence for nitrate breakthrough. The baseline scenario predicts breakthrough nitrate concentration around 90 mg L^{-1} in Case 2 (Figure 86). When no microbes are present, this concentration goes down to 36 mg L^{-1}, since no ammonia can be degraded into nitrate and the only nitrate reaching the water table is that originally present in the wastewater. This behavior is different than in Case 1 and Case 3, where the absence of microbes increases the salinity level. The lack of de-nitrification raises nitrate levels to substantially alter the FDS concentration. In Case 2, however, nitrate levels decrease because no ammonia is converted. Since 1 mole of nitrate has roughly 3 times the mass of 1 mole of ammonia, the total FDS mass decreases in Case 2 rather than increasing.

When no crops are present, the nitrate level dramatically increases to 173 mg L^{-1}. In this scenario, ammonia is converted to nitrate which is converted to nitrogen gas, but no plant uptake of nitrate or ammonia occurs, leaving more mass in the system which microbial activity alone cannot attenuate. When neither process is active, nitrate levels (100 mg L^{-1}) resemble the baseline case, however ammonia concentrations increase.

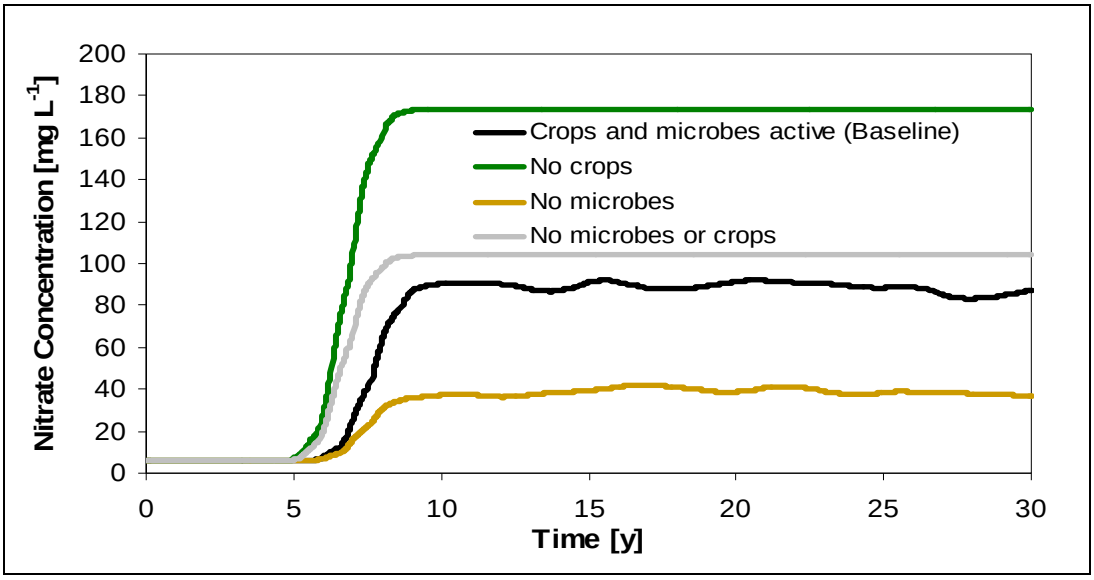

Figure 87

Effect of Salinity Toxicity to Crops and Microbes on Nitrate Breakthrough Concentration for Winery Case 2

Different behavior was observed for Case 3 nitrate concentrations, since stopping microbial activity prevented the case from working as designed for optimal ammonia and nitrate removal. The baseline scenario was the lowest, with no nitrate breakthrough. In the "no-crops" scenario, the concentration eventually reached zero, but nitrate breakthrough occurred during years 15 to 20, when none was detected for the baseline scenario. When no microbes were present, the simulation predicted only slight breakthrough, 1.6 mg L^{-1}, since crop uptake accounted for the rest of the removal and nitrification from ammonia did not occur.

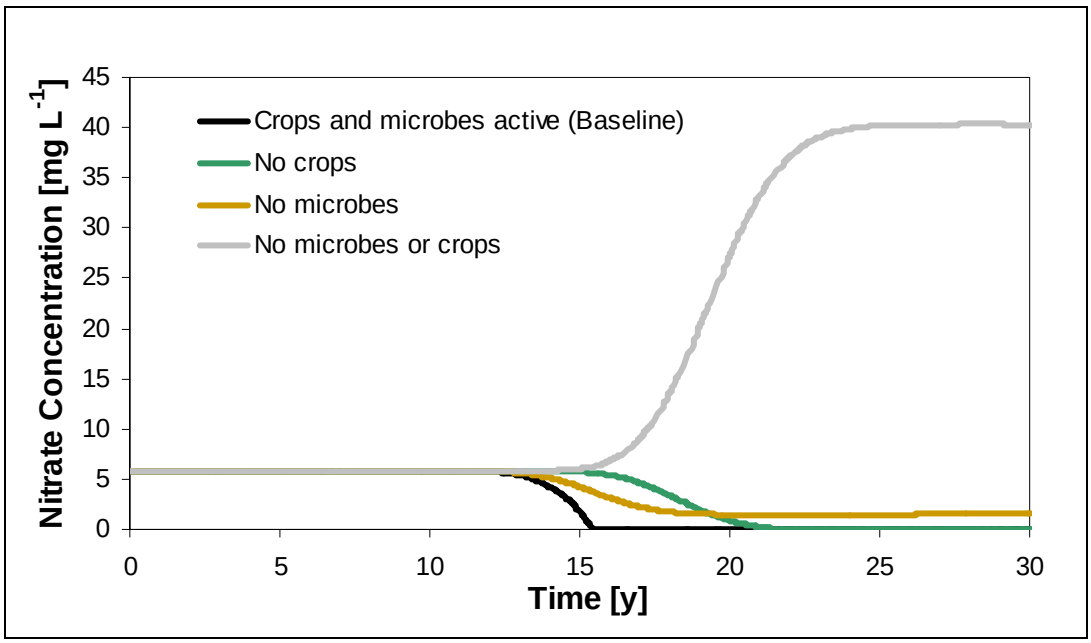

Figure 88

Effect of Salinity Toxicity to Crops and Microbes on Nitrate Breakthrough Concentration for Winery Case 3

Overall, when microbial and crop attenuation processes are removed from the modeling, the FDS levels reaching the water table can either increase or decrease, depending on the wastewater concentrations of ammonia and nitrate and the saturation levels in the soil.

4. Summary of Model Sensitivity Analysis

The numerical experiments discussed in Sections D.1 and D.2 was designed to determine the sensitivity of the model predictions of FDS and nitrogen concentration. The two modeling assumptions tested were: a) that the water table was static, allowing for the use of a 1-D column model, and b) that salinity toxicity to microbes and crops could be neglected.

Using a 2-D model with simplified geochemistry, 1 m seasonal fluctuations in the depth to water table were simulated. No significant increases in salinity or nitrogen compounds due to the fluctuations were noted. However, the profile of carbonate concentrations showed behavior that indicated interaction between the groundwater and the vadose zone that was not resolved in the 2-D model.

By examining the soil salinity concentrations, it was determined that some loss of crop productivity could be expected during the corn growing season. The likely outcome would be the switch from corn to more salt tolerant crops in land application areas, most of which would not be affected by the elevated soil salinity levels. Infiltration problems due to high soil SAR would not likely occur due to the elevated EC levels in the applied water.

Since the functions relating high salinity levels and crop and microbe death are uncertain, a

"worst-case" scenario approach was taken. This assumed that if no microbial reactions or crop nutrient uptake occurred, FDS and nitrogen concentrations would be significantly elevated. This hypothesis was not correct; while ammonia and nitrate concentrations increased under the scenario, FDS values decreased. Without microbial decay and root uptake releasing CO_2, the carbonate levels were lower.

E. Discharge Management Scenarios

This section examines steps which may be taken in order to reduce groundwater degradation associated with waste disposal through land application. These processes fall into three broad categories: actions that alter the characteristics of the waste, decisions that alter how the waste is applied to the disposal site, and the choice of the application site itself.

1. Waste Application Management

The alternate scenarios discussed in this section address site management practices, and how these may be altered to reduce salinity, nitrogen, or organic matter loading to the groundwater.

a) BOD Loading Rate

The EPA recommends a BOD loading rate of 100 lb $acre^{-1}$ d^{-1} in order to reduce nuisance odors (USEPA, 1977). For the winery selected for Case 1 modeling, however, its WDR permits up to 600 lb $acre^{-1}$ d^{-1}, due to the high BOD concentration in the winery's effluent. For the baseline case, the EPA guideline was used. This scenario assesses the impact of changing this limit on salinity release to the water table. In addition to these two rates, a 200 lb $acre^{-1}$ d^{-1} rate was also tested, a value noted in several other WDRs. To achieve these rates, the application area was altered as necessary, from a WDR specified 200 acres (600 lb $acre^{-1}$ d^{-1}) to 600 and 1200 acres (200 and 100 lb $acre^{-1}$ d^{-1}).

The changes in area had the effect of lowering the overall waste application flow rates (q), and thus lowering the BOD and FDS loading rates without changing the waste concentrations of any components. (See Section E.2.a for the effects of changes in concentration). The BOD loading limit had an indirect, but very significant impact on the mass of fixed dissolved solids released to the aquifer. This dramatic difference was not caused by changes in the attenuation processes, but by the loading rate restriction on BOD also restricts the rate of FDS loading.

As a result of the application rate changes, FDS breakthrough occurred more quickly in the 200 and 600 lb $acre^{-1}$ d^{-1} cases compared to the 100 lb $acre^{-1}$ d^{-1} (Figure 89). The FDS concentration at 30 years was not greatly affected, with both the baseline and 600 scenarios at 2400 mg L^{-1}, and the 200 scenario at 2800 mg L^{-1}. When additional water is added to the system, less root zone concentration of Na and Cl occurs, but this is balanced by the increased carbonate production due to the additional degradation of organic matter. Due to the large differences in surface loading rates, the FDS mass loading rates to the water table were very different, however,

ranging from 2500 mg m^{-2} d^{-1} to 26000 mg m^{-2} d^{-1}.

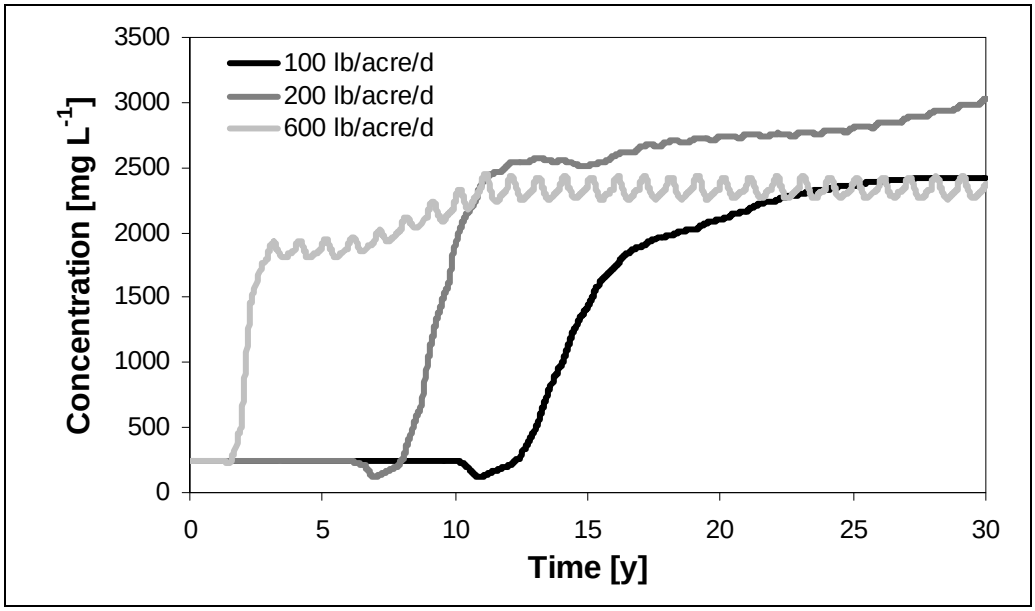

Figure 89

Effect of BOD Loading Rate on FDS Concentration on Case 1 Winery

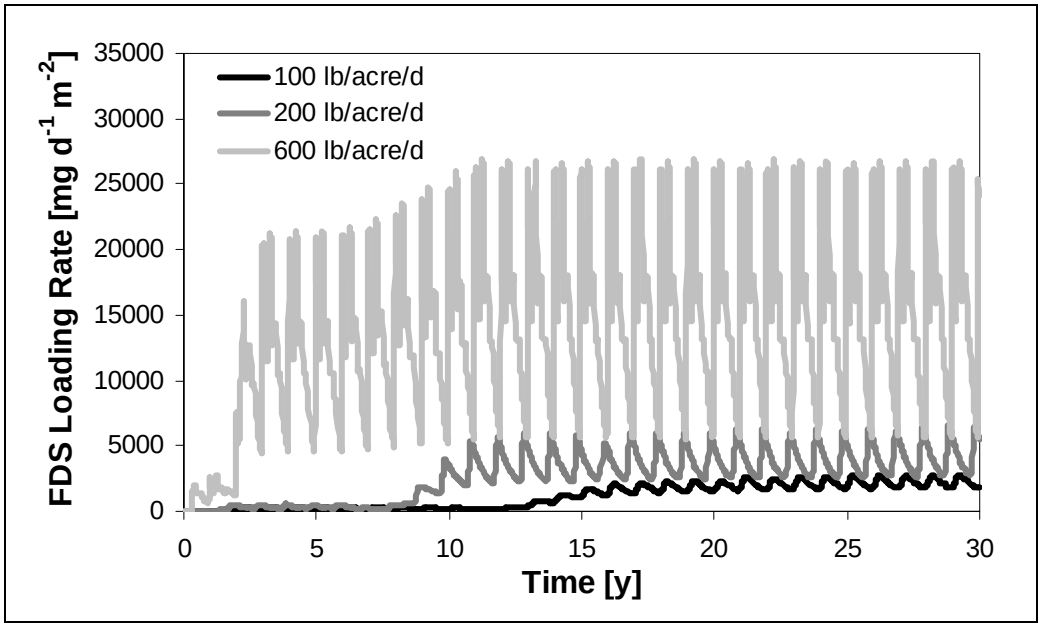

Figure 90

Effect of BOD Loading Rate Limits on FDS Loading on Case 1 Winery

The BOD loading rate should not be the only decision factor when determining the area of land

application. In Winery Cases 2 and 3, the BOD loading rates were much lower than the limit, both less than 15 lb acre^{-1} d^{-1}. If waste was applied at the 100 lb acre-1 d^{-1} limit, the Case 2 FDS concentration at year 30 would go from 1400 to 3800 mg L^{-1} (Figure 91). This increase mirrors the increase in carbonate concentration (Figure 92), produced when the additional organic matter is degraded into carbonate by microbial respiration.

Increased BOD loading rates cause changes in the saturation levels, affecting the ability of carbonate to escape and thus increasing FDS concentrations. The system begins to alternate between aerobic and anaerobic conditions, causing the yearly fluctuations, and the nitrate breakthrough curves support this (Figure 93). During certain periods of the year, nitrate concentrations are lower than in the baseline case, indicating that it is being degraded, which can only happen if anaerobic conditions have developed.

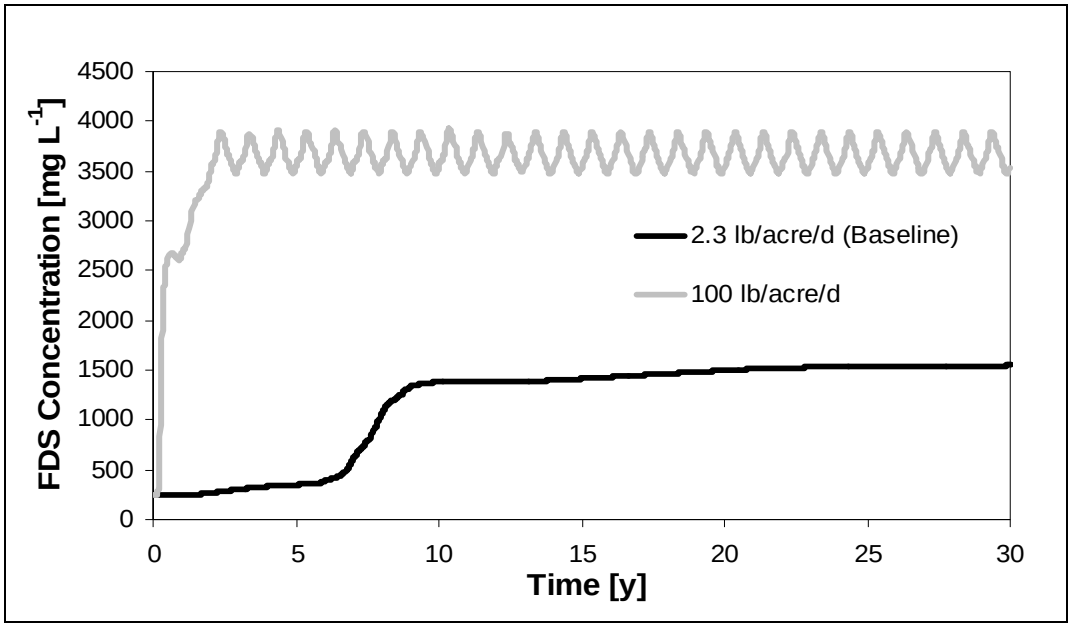

Figure 91

Effect of BOD Limit on FDS Concentration for Case 2 Winery

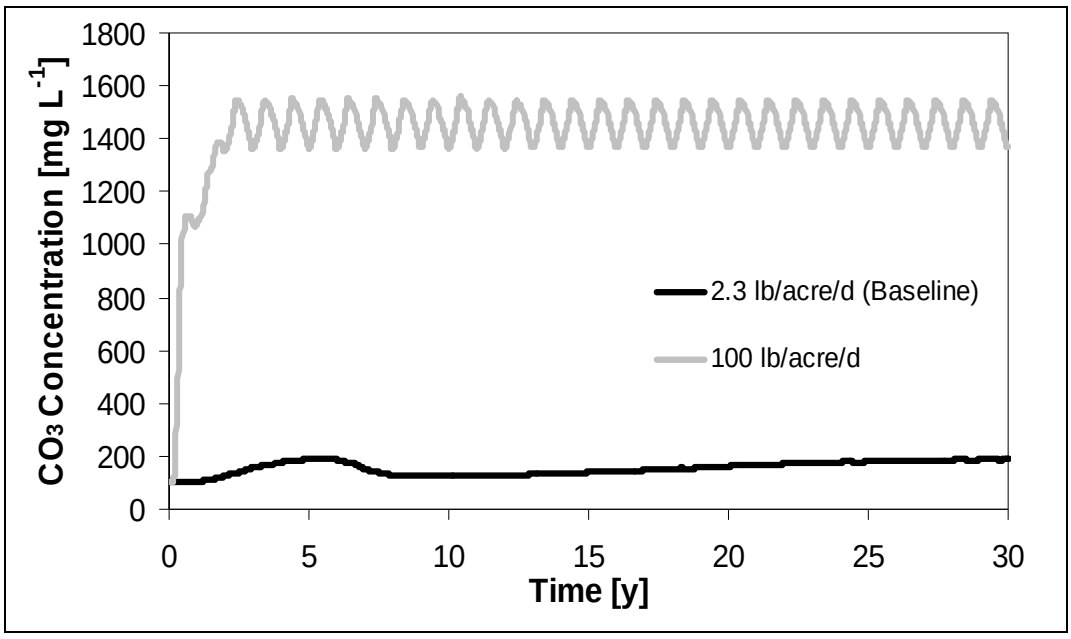

Figure 92

Effect of BOD Limit on Carbonate Concentration for Case 2 Winery

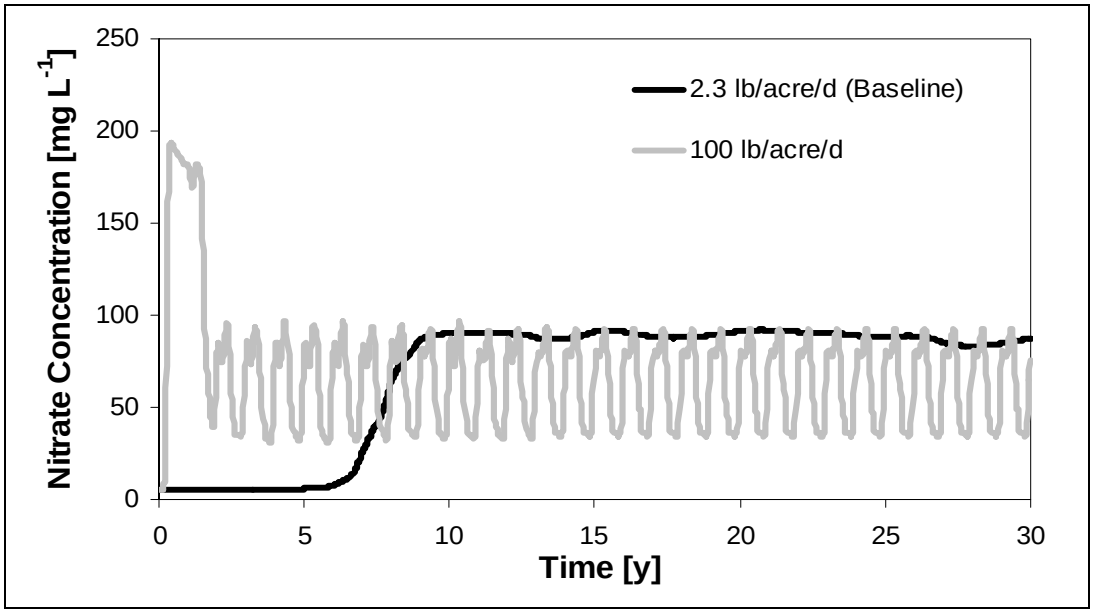

Figure 93

Effect of BOD Limit on Nitrate Concentration for Case 2 Winery

b) NaCl Loading Rate

The CLFP recommends a NaCl loading rate of 835 lb $acre^{-1}$ yr^{-1}, the typical rate of agricultural application from fertilizers (California League of Food Processors, 2007). This alternate

scenario assumes that the characteristics of the waste are not altered, simply that the application acreage is adjusted increased until the loading recommendation is met. This scenario tests whether the recommended loading rate is restrictive enough to prevent FDS concentrations above the water quality standard (500 mg L^{-1}) from reaching the groundwater table. The baseline loading rates were1295 lb $acre^{-1}$ yr^{-1} for Case 1, 2145 lb $acre^{-1}$ yr^{-1} for Case 2, and 490 lb $acre^{-1}$ yr^{-1} for Case 3.

Despite the fact that the baseline Case 3 had a lower loading rate than the maximum recommended, breakthrough above the limit occurred. When the Case 1 and Case 2 application areas were increased to meet the 835 lb $acre^{-1}$ yr^{-1} loading rate, the breakthrough FDS concentration (Figure 94) and loading to the water table (Figure 95) were both lowered.

Even with this limitation, concentrations of up to 1800 mg L^{-1} were noted for Case 1 and 880 mg L^{-1} for Case 2, suggesting that NaCl loading limitation was not strict enough to protect groundwater from FDS. However, the concentrations of Na and Cl were lowered, indicating that the composition of salinity was altered in a way that would be beneficial to consumers of the water.

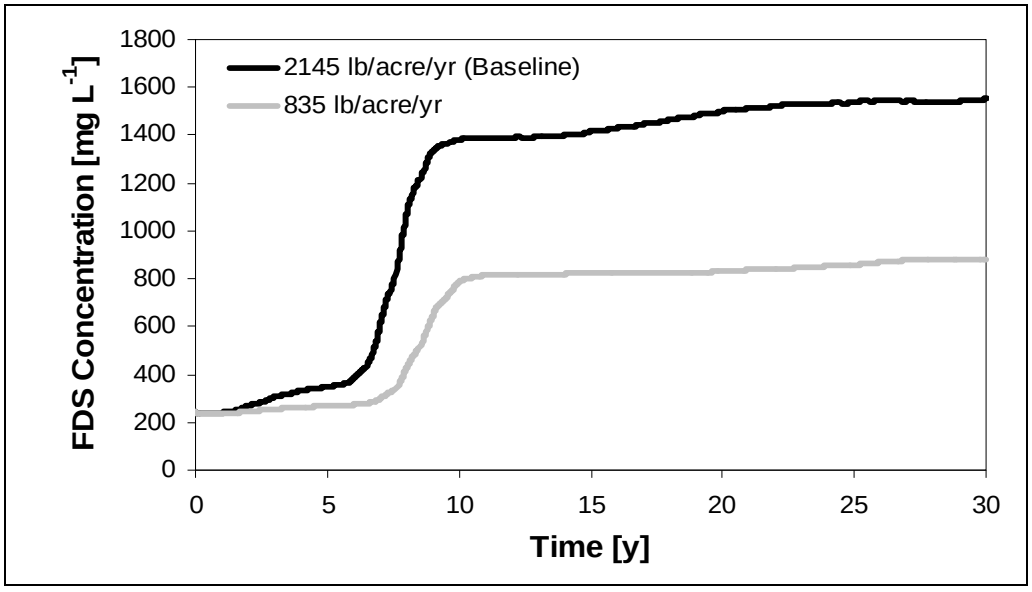

Figure 94

Effect of NaCl Loading Rate Limitations on FDS Concentration on Case 2 Winery

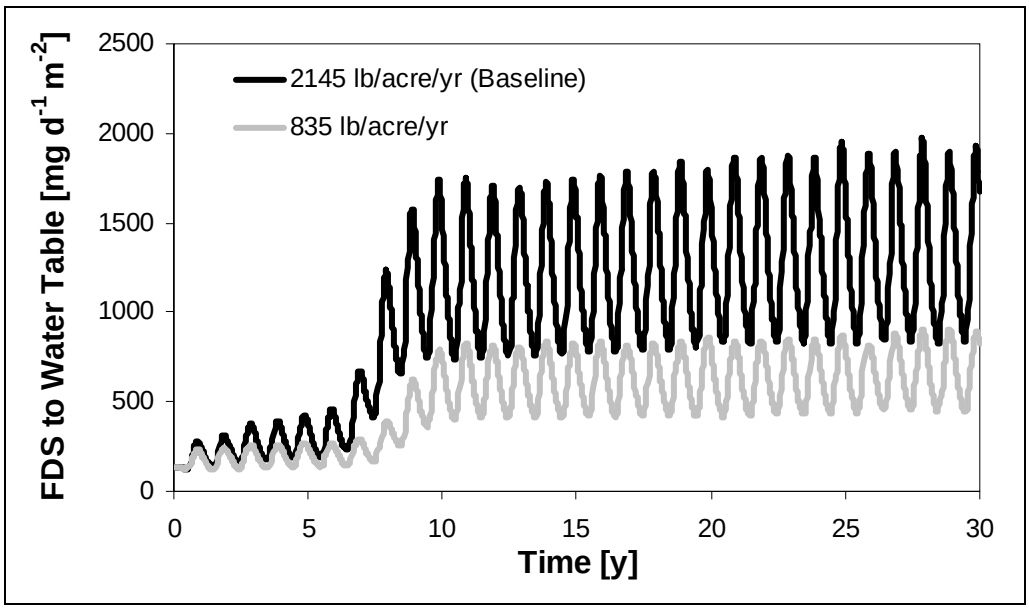

Figure 95

Effect of NaCl Loading Rate Limitations on FDS Water Table Loading on Case 2 Wineries

c) Increased Application Area

One proposed site management strategy is to increase the area of land application in order to reduce the concentration of FDS reaching the groundwater table. In this scenario, the baseline application areas (1244 for Case 1, 15.5 for Case 2, and 14 for Case 3) were increased by 10 and 20%. The resulting breakthrough curves showed that in all cases, FDS concentrations were lowered (Figure 96), by 92 mg L^{-1} for the 10% scenario and 160 mg L^{-1} for the 20% scenario.

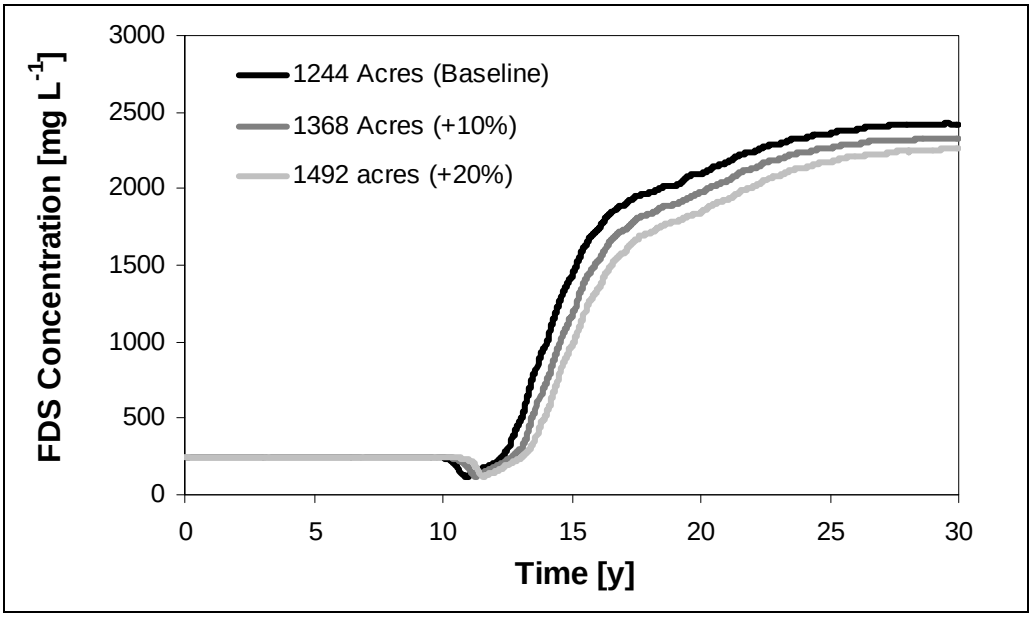

Figure 96

Effect of Application Area Increase on FDS Breakthrough Curves for Case 1 Winery

Increasing the area also did little to reduce the total amount of mass reaching the groundwater (Figure 97), decreasing it by less than 7% in all cases. For Case 1, the baseline case released 3400 g d^{-1}, while the 20% area increase released 3200 g d^{-1}. These results indicate that while an area increase does lead to a slight enhancement of salinity attenuation, the main effects are due solely to dilution. Also, since the main components contributing to salinity (Na, C_l, CO_3) are not taken up by plants or subject to other attenuation processes, the concentration may decrease, but the total loading to the aquifer is only slightly decreased, because of the additional sorption sites available. In certain circumstance, such as areas with high gypsum contents, an increased application area can increase total loading due to an increase in the amount of the mineral available for dissolution.

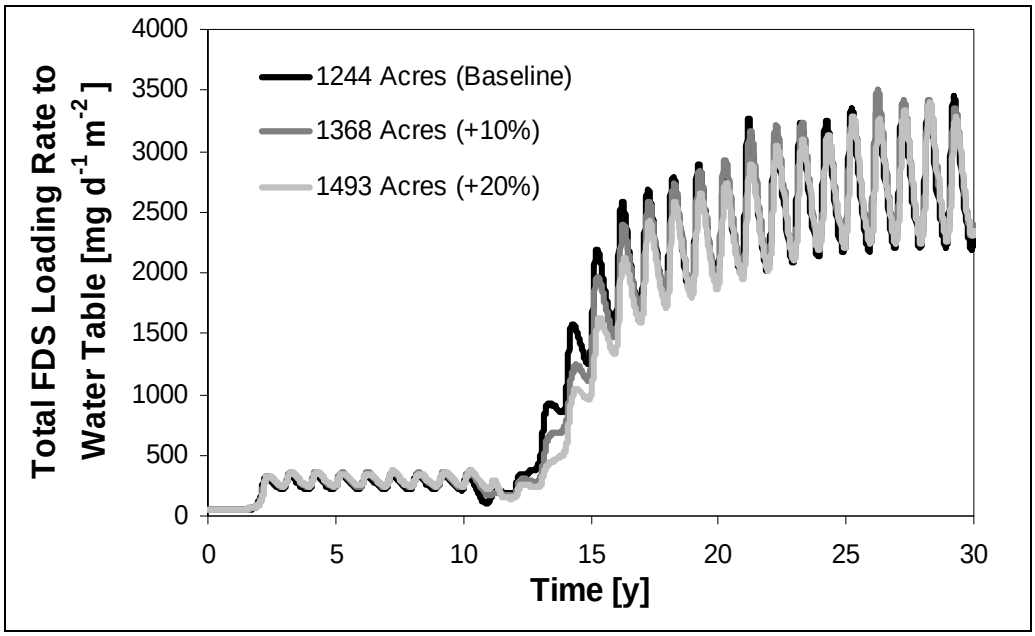

Figure 97

Effect of Area Increase on Total FDS Loading Rate to Water Table for Case 1 Wineries. Fluctuations in the loading rate are caused by seasonal differences in water flow rates.

d) Summary of Loading Rate Experiments

Two wastewater loading rate limits have been propagated: the 100 lb $acre^{-1}$ d^{-1} limit for BOD application specified by the USEPA and the 835 lb $acre^{-1}$ yr^{-1} NaC_l loading recommendation from the CLFP (2007). Often, these rates are met by increasing the application area, rather than reducing the effluent concentrations. The numerical experiments in Sections E.1.a) through E.1.c) were designed to predict if this area increase either reduced the breakthrough concentrations of FDS or nitrogen at the water table or reduced the total mass loading to the water table over the entire application.

While the breakthrough concentrations were generally significantly lowered, the total mass

released to the water table was not. Some mass reduction was noted for ammonia; the added area had more cation exchange sites available for sorption and the lower flows promoted aerobic conditions. Attenuation through sorption is temporary, however, and the reductions in ammonia will not likely last far past the 30 year modeling timeframe. Additionally, the NaC_l loading rate limit did not reliably result in FDS breakthrough concentrations below the groundwater quality objectives.

Large reductions in concentration (50%) required an area increase of at least 50%, likely more. For a large processor, this could mean buying or licensing an additional 1200 acres. Management of the waste-stream, as discussed in the next section (E.2), could be a more economical alternative.

Main Findings:

- The loading rate simulations highlight the need to measure both breakthrough concentration at the water table and mass loading rates to the groundwater.
- The 100 lb $acre^{-1}$ d^{-1} BOD loading rate has little effect on breakthrough concentration of FDS, but a strong impact on FDS loading rate.
- The 835 lb $acre^{-1}$ d^{-1} NaCl loading limit is not protective of groundwater in all circumstances. Site conditions can cause higher than desirable breakthrough concentrations, even at this loading limit.

While increased application area proportionally decreases the concentration reaching the water table by diluting the waste, it does not proportionally decrease the total mass loading. When application area increases, the number of sorption sites for ammonia also increases, leading to lower mass loading of ammonia. However, this process is not sustainable in the long-term.

2. Waste Stream Management

The scenarios in this section address practices that might change the characteristics of the wastewater stream, as it leaves the processing plant. Only a brief mention is made here of the technology needed for implementing such changes, but this aspect of the analysis is discussed in Section III.5: "In-Plant Measures to Reduce Salt Discharges from Food Processing Plants." These are characteristics which may be altered by changes in plant practices or by pre-treatment of applied waste.

a) BOD Concentration

In cases where processors need to lower their BOD loading rate without expanding the land application area, this can be attained by introducing biological pre-treatment of the waste. Such methods include primary sedimentation and activated sludge, which can reduce BOD concentrations by up to 40% and 95%, respectively. These methods remove little ammonia (<15%) and no salts (Metcalf & Eddy et al., 1991). For this alternate scenario, the BOD concentrations were lowered by 50, 95, and 100% of their baseline values. While 100% removal efficiency may not be feasible, it was including in the modeling as a "worst case" scenario.

While lowered BOD is positive from an odor control and waste management perspective, it may negatively impact the subsurface removal mechanisms for nitrogen, most of which rely on a sufficient supply of organic matter. Denitrification (II.2.C.9.a) cannot take place if the microbes involved in the reaction do not have a carbon supply (Eq 17). BOD is assumed to be equivalent to CH_2O (II.2.C), so reducing BOD by 50% reduces the organic matter supply by an equal amount.

In Case 2, BOD removal decreased denitrification rates, increasing nitrate breakthrough. The 30 year concentration went from 82 mg L^{-1} in the baseline case, to 103, 113, and 115 mg L^{-1} for 50, 95, and 100% removal efficiencies. In Case 2, the little nitrate degradation that occurs is due to the aerobic conditions is further inhibited by a lack of organic matter.

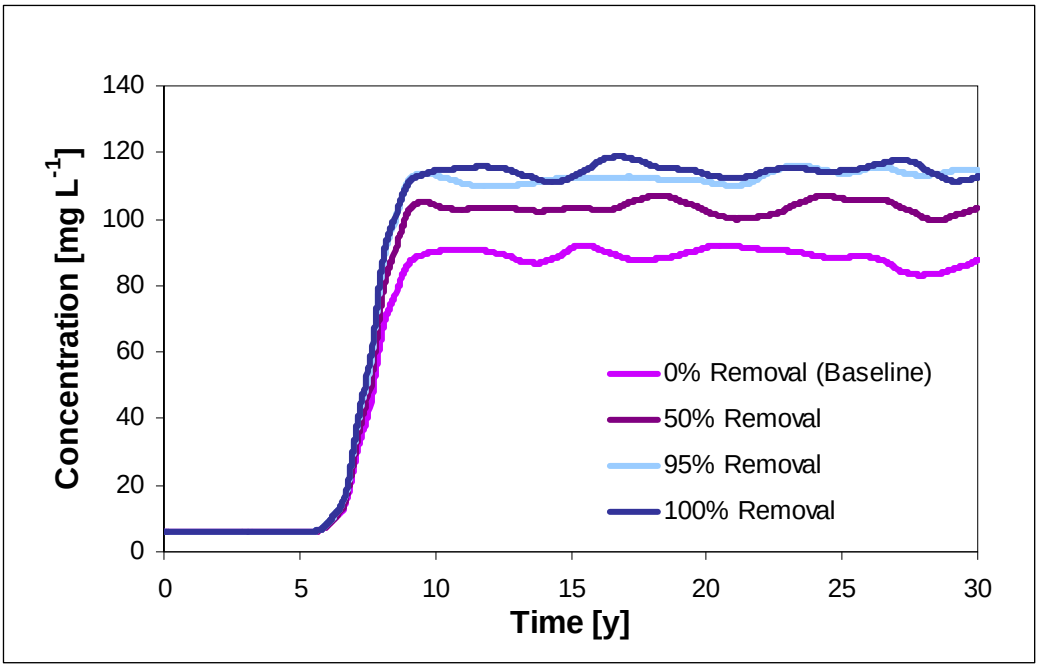

Figure 98

Effect of BOD Removal on Nitrate Breakthrough in Winery Case 2

Case 3, which should be optimal for both nitrate and ammonia removal is also impacted. In the baseline case, all nitrates are consumed and no breakthrough occurs. As BOD is reduced, the curve changes shape. At 100% removal efficiency, nitrate concentrations reach 21 mg L^{-1} at year 30. In Case 3, total removal of organic matter prevented the nitrification and de-nitrification reactions from proceeding and resulted in the breakthrough. Further evidence of this effect can be seen in Figure 99. In the 0 and 50% removal scenarios, excess organic matter reaches the water table, indicating that sufficient amounts are present for microbial reactions. For the 95% removal cases, however, all organic matter is consumed before it reaches the water table.

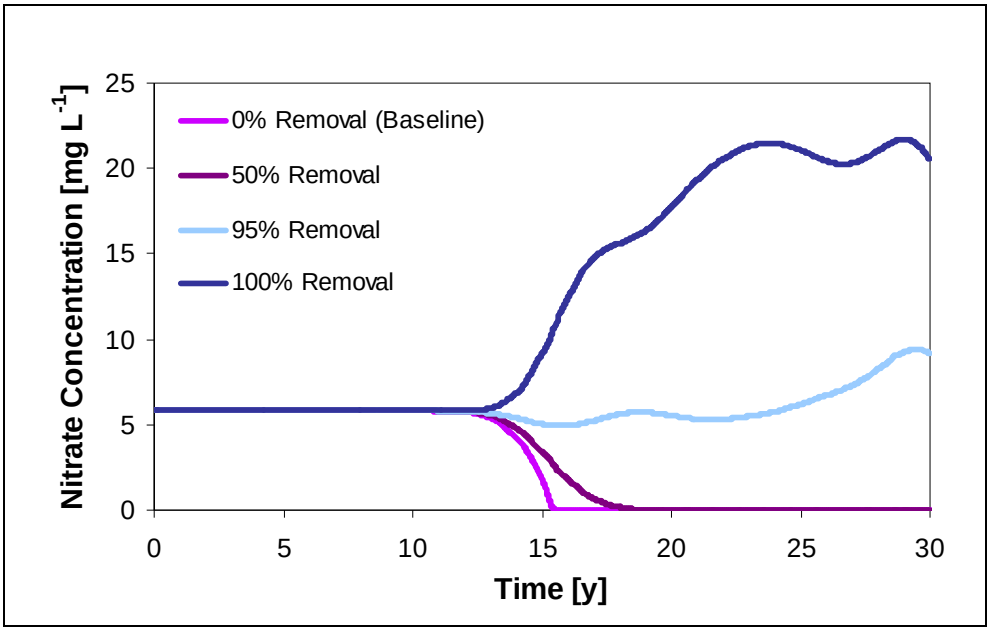

Figure 99

Effect of BOD Removal on Nitrate Breakthrough for Case 3 Winery

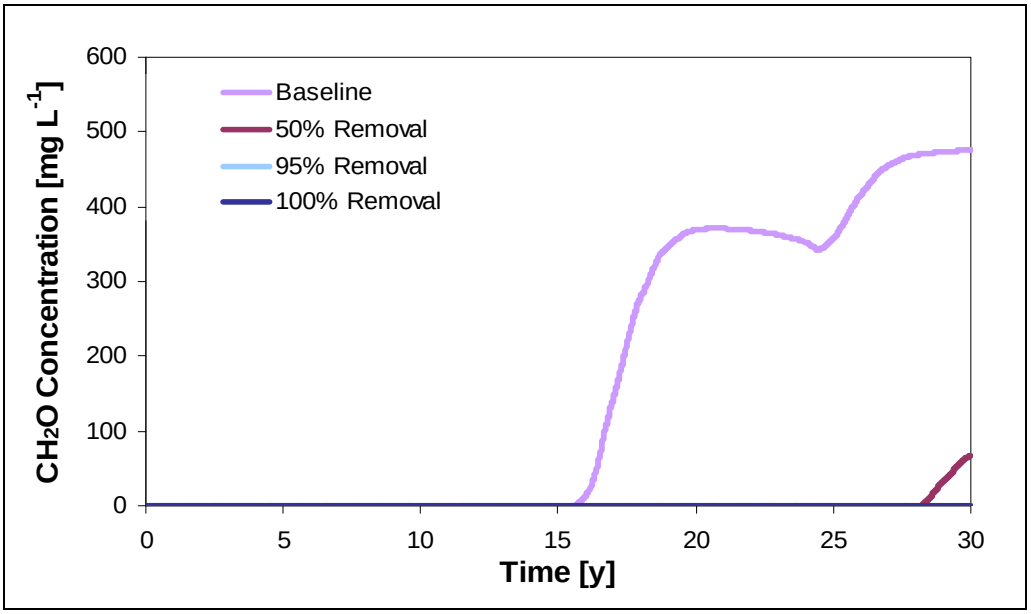

Figure 100

Effect of Pretreatment on Organic Matter Breakthrough for Case 3

In the Case 1 baseline scenario, the BOD loading rate restriction (100 lb acre^{-1} yr^{-1}) had limited the flow rate. When the BOD concentration was reduced, the flow rate could correspondingly be increased. This change lead to quicker breakthrough times for the tracer chloride (Figure 101), as well as increased ammonia concentrations (Figure 102). In the baseline scenario, the ammonia had been retarded by sorption and had only begun to breakthrough to the groundwater table at year 30. When the BOD was reduced by 50%, ammonia concentrations exceeded 400

mg L^{-1} at year 30, and initial breakthrough occurred much earlier, at year 20. For 95 and 100% removal efficiencies, breakthrough occurred at around 5 years, and by year 10, the concentration reached a plateau of 380 mg L^{-1} (Figure 102). While the BOD concentrations in the applied water were lowered, the ammonia concentrations were held constant. By increasing the flow rate, more ammonia mass entered the system, and the exchange/sorption capacity was quickly exhausted.

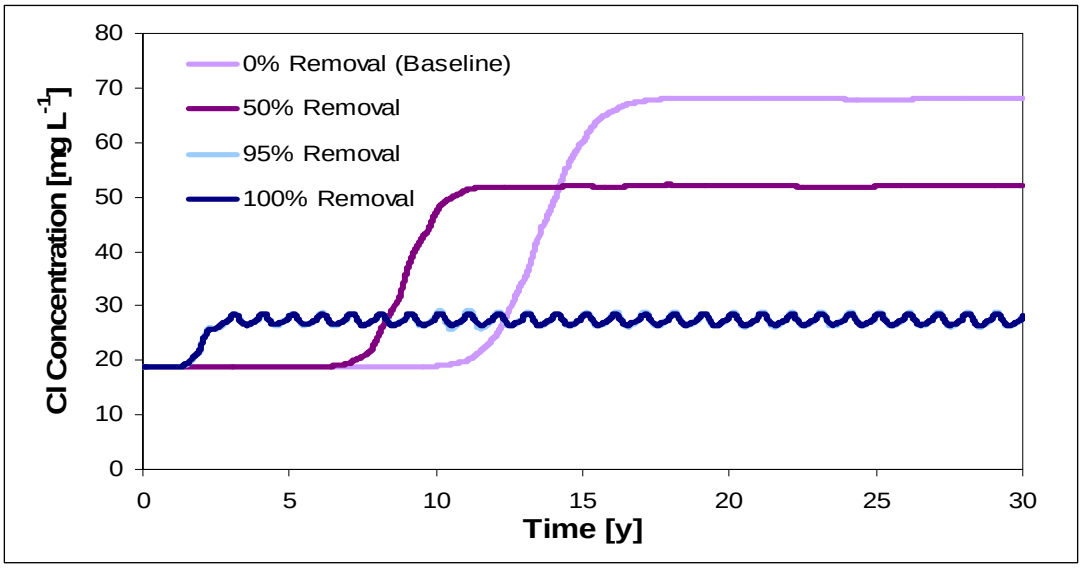

Figure 101

Effect of BOD Removal on Chloride Concentrations for Winery Case 1. In this case, the lower BOD concentrations allow for higher flow rates (based on the 100 lb acre-1 yr-1 limit).

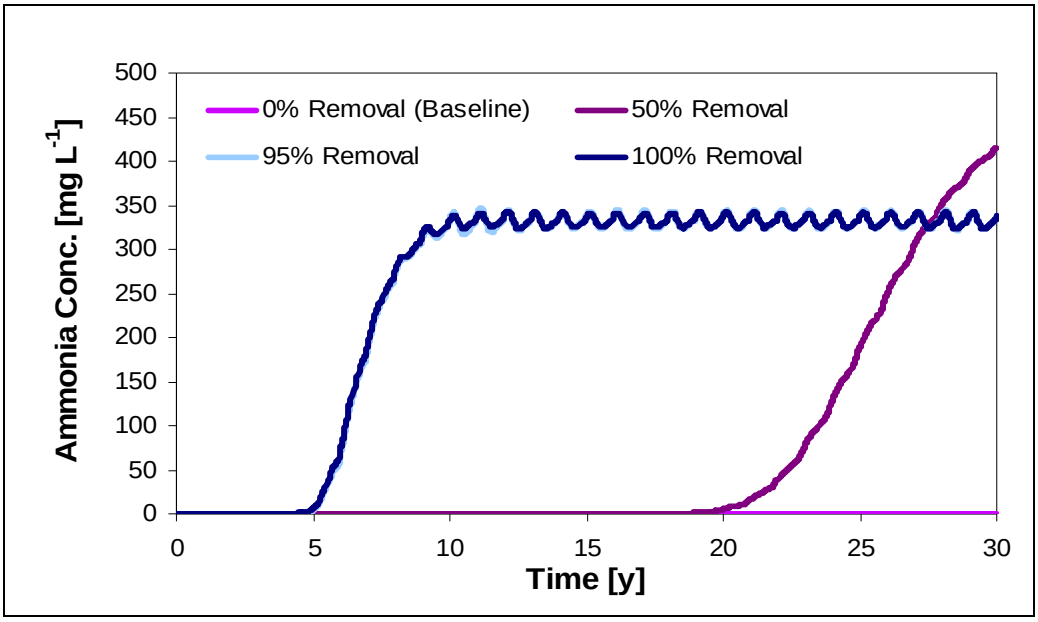

Figure 102

Effect of BOD Removal on Ammonia Breakthrough in Winery Case 1

The overall FDS concentrations were only slightly affected, due solely to the inclusion of nitrate and ammonia in the FDS calculation. The results of these scenarios imply that a certain amount of BOD removal may be positive, reducing odor concerns or organic matter breakthrough, whereas near removal levels of 95 to 100% will likely negatively impact biodegradation in the subsurface.

b) FDS Concentration

The CLFP recommends that for a risk of groundwater degradation that is on-par with that associated with agriculture, the FDS concentration in land applied wastewater should be limited to 640 mg L^{-1} (California League of Food Processors, 2007). This set of scenarios was designed to estimate the reduction in salinity breakthrough that would be achieved if this limitation were applied to the baseline scenarios, assuming that in-plant source control affected all FDS components (Ca^{2+}, Na^{+}, Cl^{-}, etc.) in equal proportion.

In all cases, applying the 640 mg L^{-1} limit served to reduce the FDS concentration reaching the groundwater. Both Case 1 (Figure 103) and Case 2 (Figure 104) saw an approximate 900 mg L^{-1} reduction in FDS concentrations. In Case 1, although the input concentration was limited to 640 mg L^{-1}, the outgoing concentration was higher, 1400 mg L^{-1}, due to the carbonate produced by microorganisms consuming organic matter, concentration of FDS components due to evapotranspiration, and the dissolution of Ca, Mn, and Fe containing minerals This increase was not noted in Case 2 because the unsaturated soil conditions allowed the carbonate to escape the system as carbon dioxide gas. The results of this scenario imply that although a limit on FDS can be set at the surface, the final concentration at the groundwater table may be higher than the input. However, constant, highly saturated conditions like those present in Case 1 are not

necessarily typical of land application, and in most cases, it is unlikely that all CO3 will be retained. Nevertheless, it is important to account for local conditions when changing the concentration profile of the effluents.

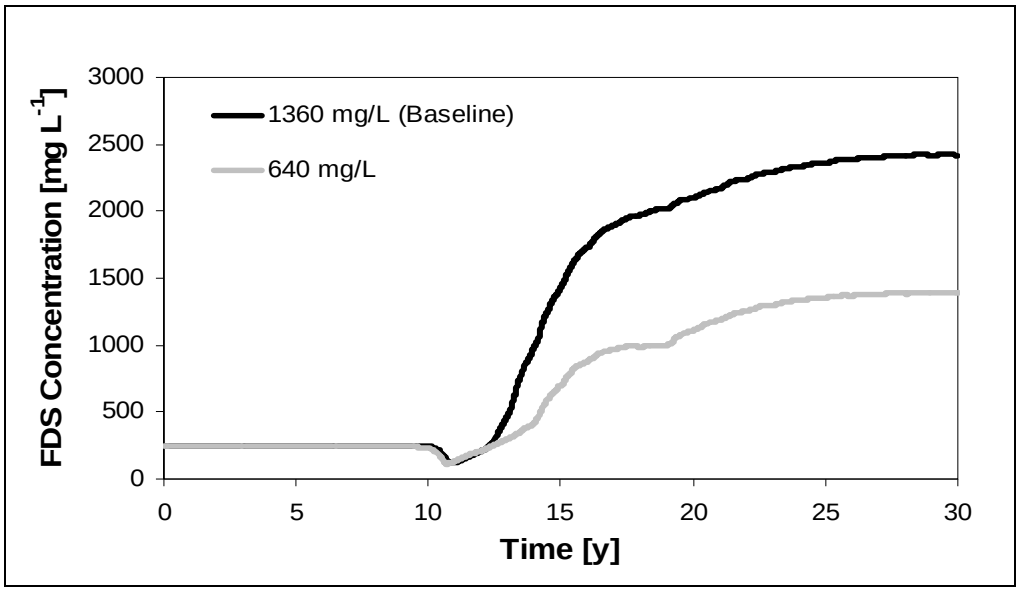

Figure 103

Effect of FDS Concentration Limit on Case 1 Winery

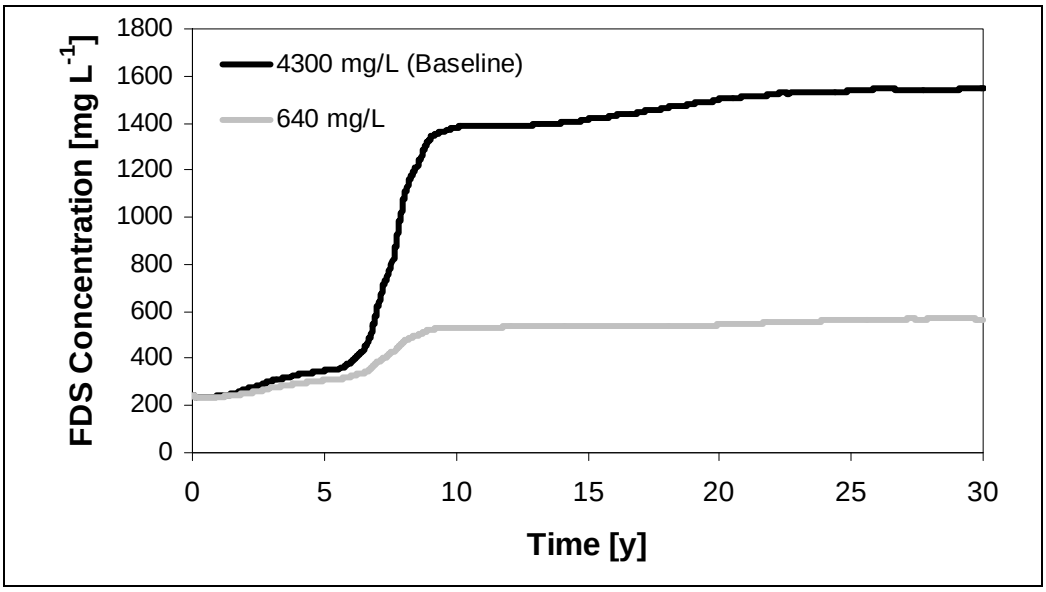

Figure 104

Effect of FDS Concentration Limit on Case 2 Winery

c) In-Plant Chemical Substitution

To reduce salinity reaching the water table, tomato producers have explored switching the chemicals used to remove tomato skins from NaOH to KOH (Das and Barringer, 2006). The goal is to produce wastewater with salinity components that can be more readily consumed by crops, since K is a plant nutrient. To estimate the impact of such actions, this scenario created two sets of simulations, one with 50% of the Na converted to K and one with 100% converted. The baseline scenario has 0% converted.

In Case 2, the conversion decreased the FDS concentration at the groundwater table slightly, by <150 mg L^{-1}. While the concentrations of Na dropped, the concentrations of K did not go up by an equivalent amount, indicating that root uptake was indeed attenuating a portion of the potassium. Ca and Mg concentrations increased above baseline for both scenarios, lessening the improvement in FDS.

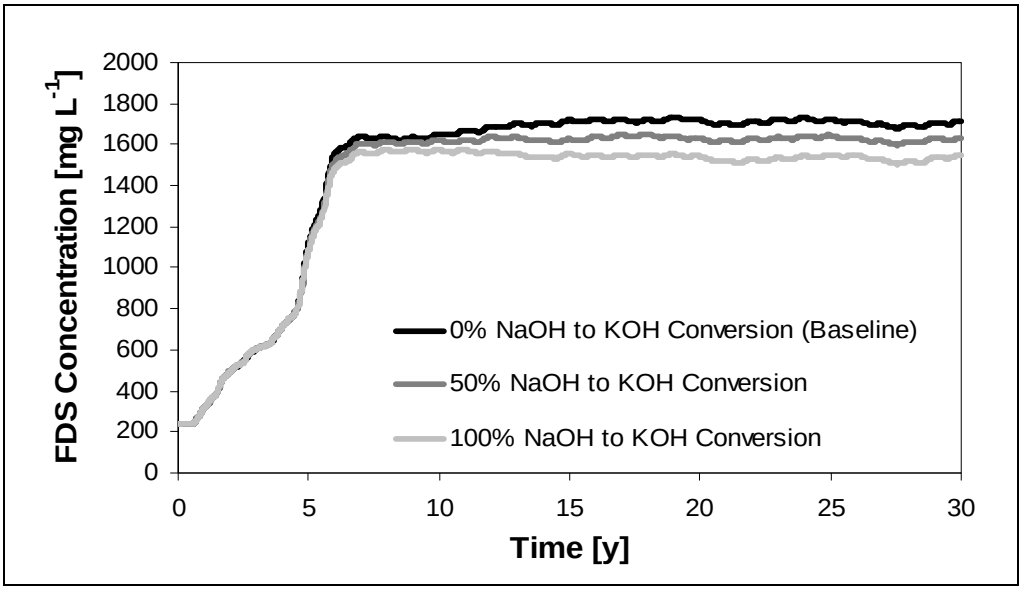

Figure 105

Effect of KOH Substitution on FDS Concentrations for Tomato Case 2

For Case 1, FDS concentrations went up with 100% conversion and down with 50% conversion. The Ca and Mg concentrations showed similar behavior and were likely the case of the difference between scenarios. Again, ion exchange and its timing have a critical role. In this case, ammonia breakthrough occurs earlier with NaOH substitution (Figure 107); potassium follows a similar trend. During years 10 to 25, calcium concentrations increase with KOH substitution (Figure 108). These changes can be attributed to the preference sorption of these ions; for instance, Na has a weaker affinity for clay than K and Ca. The large change in concentration from K to Na affects the cation exchange series, and causes the non-linear behavior in FDS response (Figure 106).

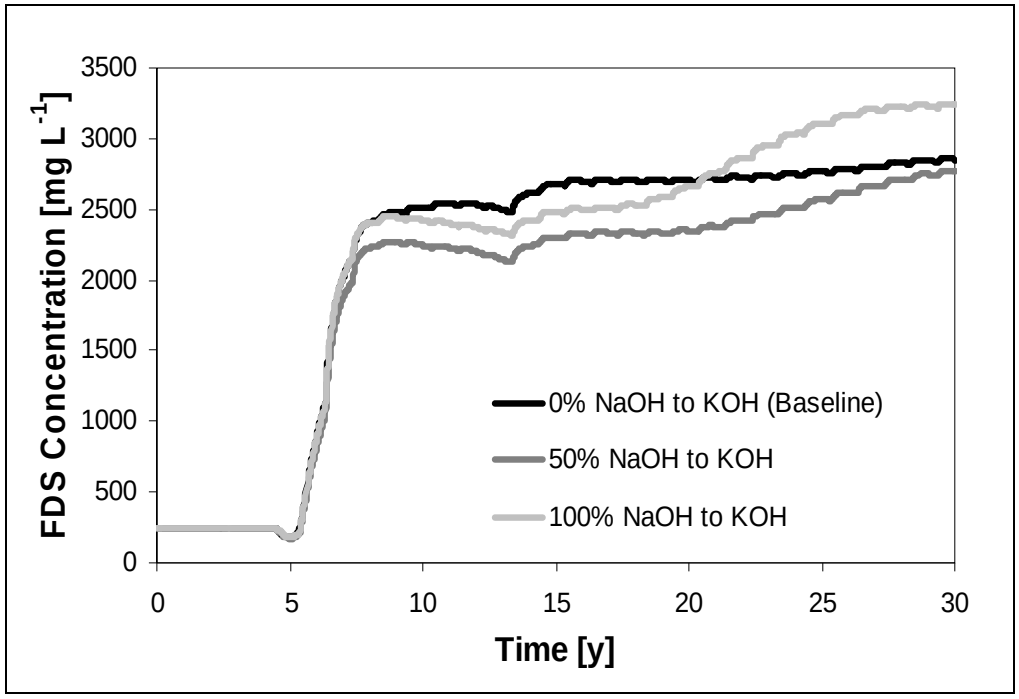

Figure 106

Effect of KOH Substitution on FDS Concentrations for Tomato Case 1

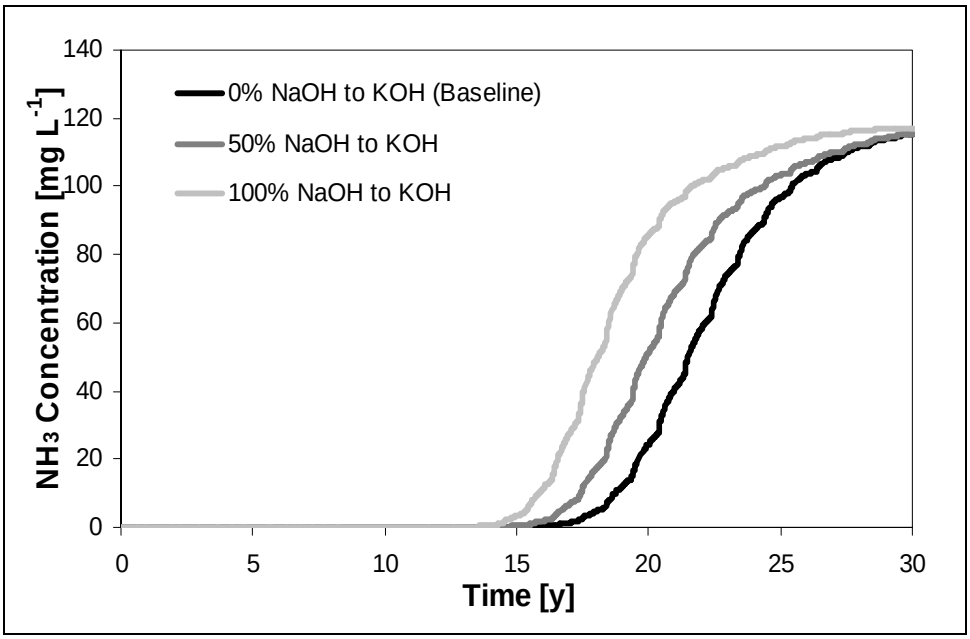

Figure 107

Effect of KOH Substitution on Ammonia Concentrations for Tomato Case 1

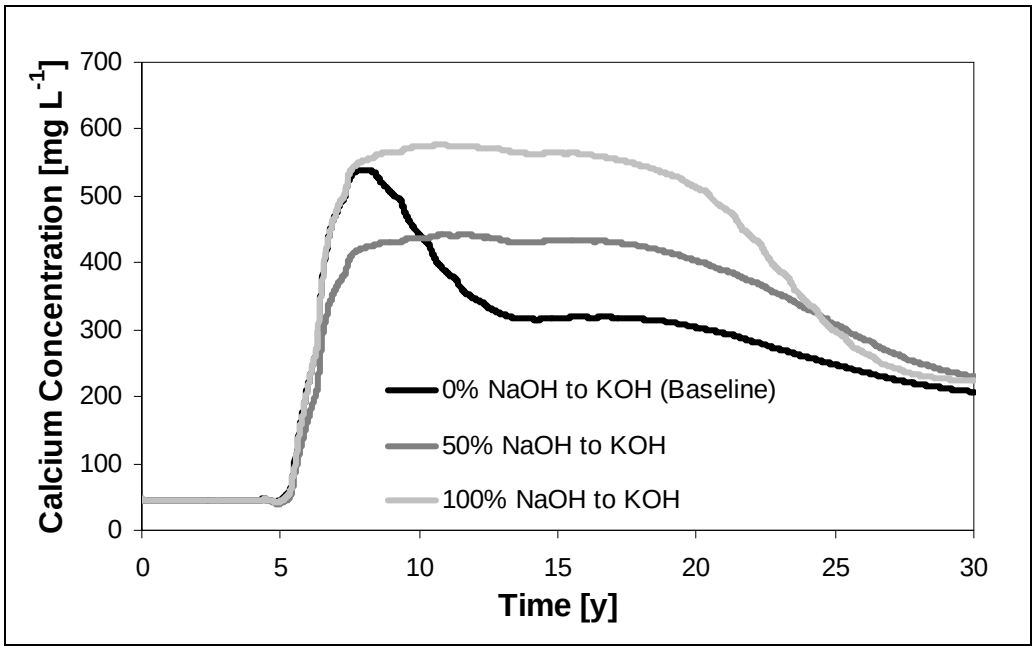

Figure 108

Effect of KOH Substitution on Calcium Concentrations for Tomato Case 1

d) Summary of Waste Stream Management Scenarios

The management or treatment of wastewater before land application can help lower releases to the water table. However, the following concerns were noted:

- BOD removal before application only slightly impacts FDS concentrations reaching the water table but dramatically decreases organic carbon loading. While BOD treatment is beneficial to the groundwater, care should be taken that enough BOD remains to allow the biodegradation of NO_3.
- An FDS concentration limit of 640 mg/L^{-1} in applied will reduce concentrations reaching the water table when imposed on processors with elevated FDS in their waste. However, it is not necessarily protective of the groundwater, due to the effects of waste concentration and carbonate production in the rooting zone.
- Substitution of KOH for NaOH in tomato processing plants can reduce FDS concentrations, but the prediction of the magnitude decrease in complicated by considerations of competition for sorption sites between ammonia and sodium.

3. Site Selection

This section estimates the impact that certain site features may have on the salinity loading to the groundwater table.

a) Depth to Water Table

The depth to the water table varies throughout the study area, from 15 m to 35 m deep (Burow et al., 2004), although local reports show that it can be as low as 2 m near the rivers. As the depth increases, travel time between the ground surface and the water table increases, as well as the volume of soil acting as a buffer between the ground surface and the groundwater table, potentially allowing more waste attenuation. More specifically, we expect that larger depth will increase sorption of salts due to increase in the number of sorption sites. When that depth is comprised of soils close to saturation (Case 1), we expect de-nitrification to be more efficient and complete, with a larger fraction of the nitrates converted to ammonia (see discussion in Section 2.1). In low saturation soils, an increase in depth to the water table is also expected to increase removal through sorption, as well as a more efficient nitrification of ammonia to nitrates.

In the present analysis, a baseline scenario with water table depth of 15 m is compared to depths of 7.5 and 30 m. We found that the impact of depth to water table on FDS breakthrough is strongly dependent on case. For Case 3, as the depth to the water table increased, FDS breakthrough time was prolonged and the 30 yr FDS concentration decreased (Figure 109). Nitrate concentrations remained at background levels until around year 25, when they began to decrease (Figure 110). At the 30 yr mark, the wastewater was just beginning to reach the 30 m water table, so the ultimate concentration may be higher. The differences between the baseline and 7.5m cases were primarily attributable to carbonate and sodium concentrations. The short depth to water table did not allow for much attenuation of either of these compounds.

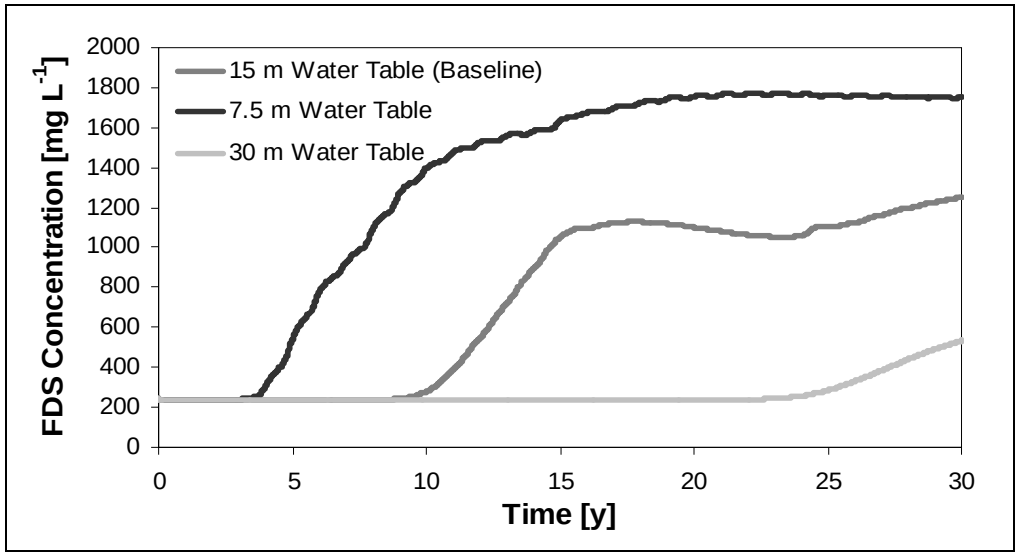

Figure 109

Effect of Water Table Depth on FDS Breakthrough Curves for Winery Case 3

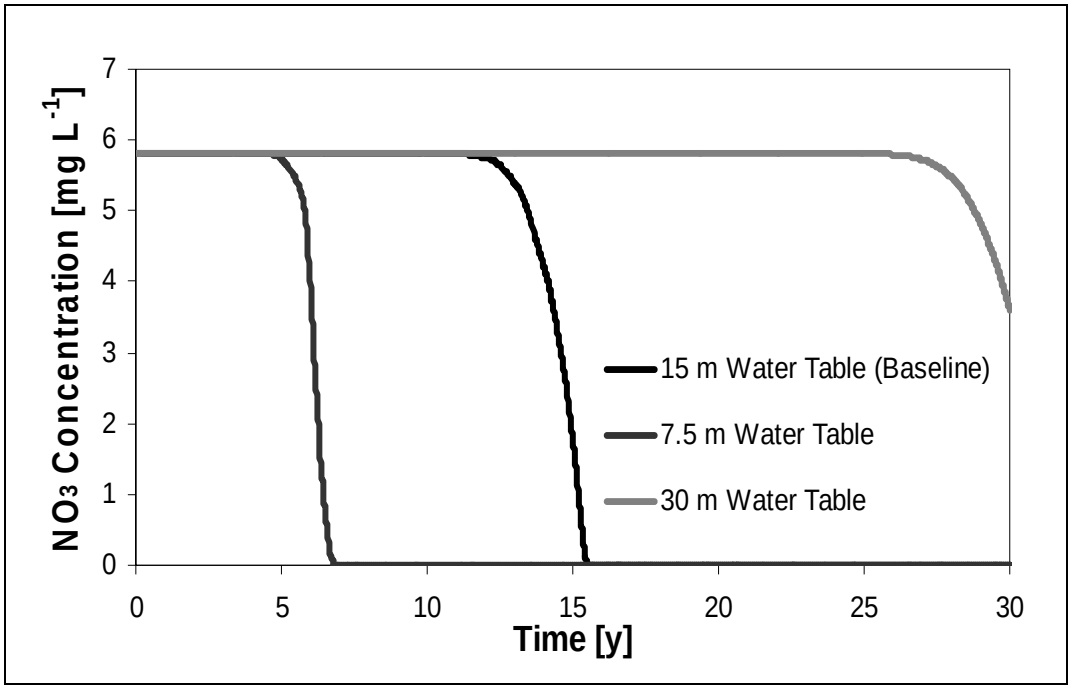

Figure 110

Effect of Water Table Depth on Nitrate Breakthrough for Winery Case 3

Case 2 followed a similar pattern, although breakthrough to the 30m water table was faster due to the higher flow rate. The 30 y concentrations were nearly identical for the 15 and 30 m cases (1420 mg L^{-1}), while the 7.5 m concentration was around 300 mg L^{-1} higher. Nitrate breakthrough also occurred later, but the 30 year concentration was around 85 to 90 mg L^{-1} in all scenarios (Figure 112). In Case 2, all nitrate was removed through crop uptake, which did not vary between scenarios.

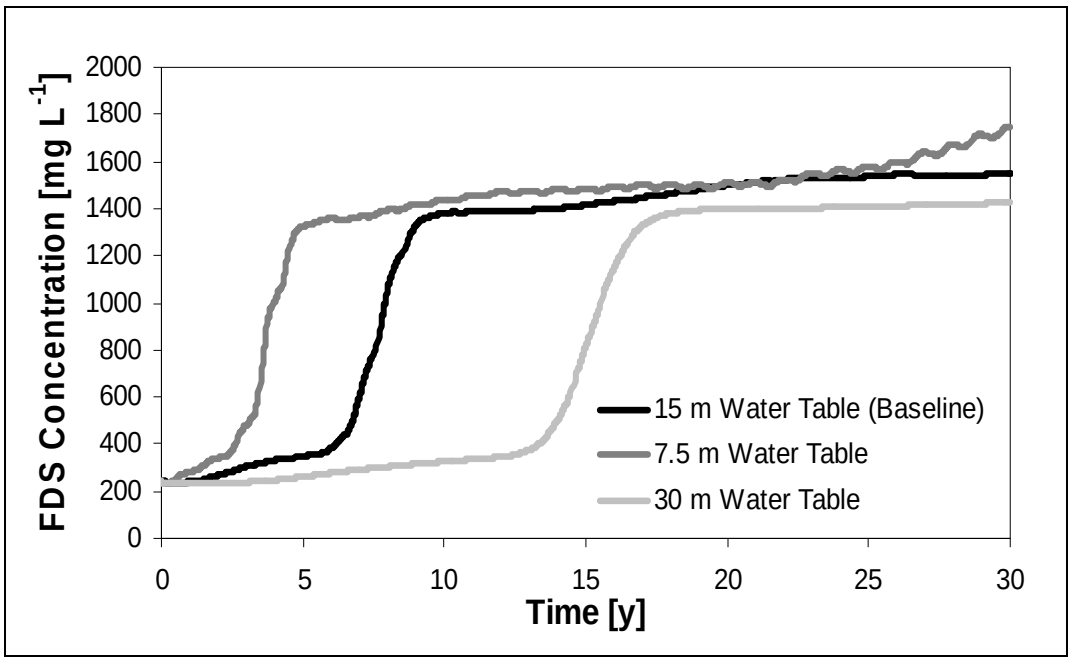

Figure 111

Effect of Water Table on FDS Concentrations for Winery Case 2

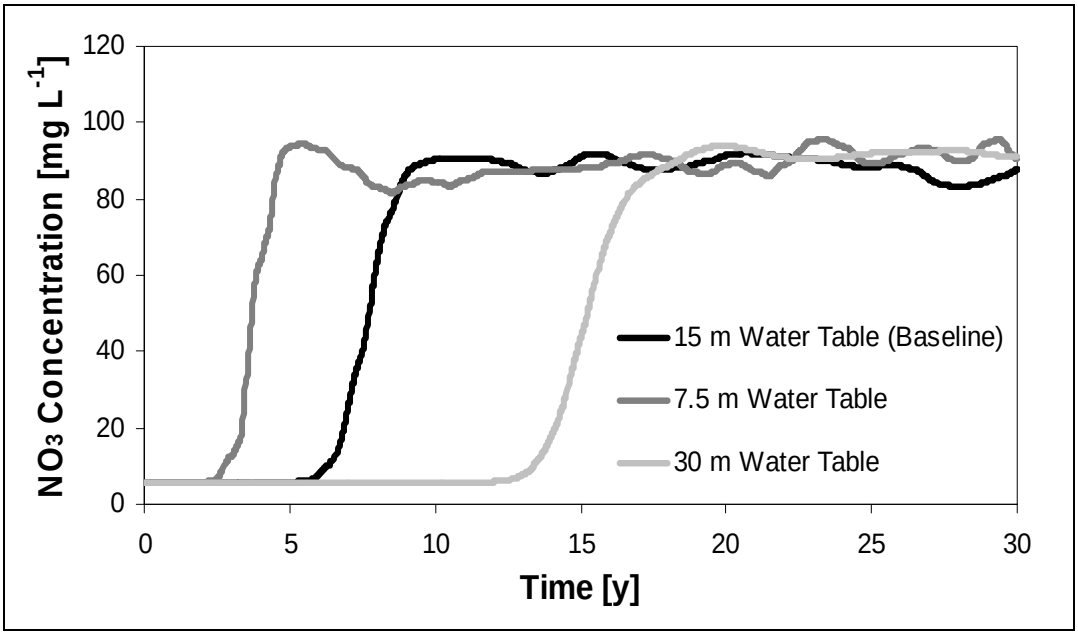

Figure 112

Effect of Water Table on Nitrate Concentrations for Winery Case 2. No ammonia breakthrough was observed.

Case 1 had very earlier breakthrough of the 7.5m FDS concentrations, which then fluctuated between 2000 and 2500 mg L^{-1} (Figure 113). The fluctuations are likely due to seasonally varying water application rate, and are not as apparent in the other curves due to their relatively greater buffering and storage capacity. By Year 30, the FDS concentrations for the 7.5 m water

table and the 15 m water table are nearly identical. The breakthrough curve for the 30 m water table is much lower in concentration, and fluctuates erratically between years 5 and 15. The deeper water table appears to have altered the behavior of carbonate in the system; the FDS and CO3 curves follow nearly identical trends (Figure 113 and 114). Likely, contact with additional soil has allowed calcite precipitation. Ammonia breakthrough occurred quickly for the 7.5 m water table scenario due to the presence of fewer exchange sites, while little breakthrough was noted for the 15 and 30 m scenarios (Figure 115).

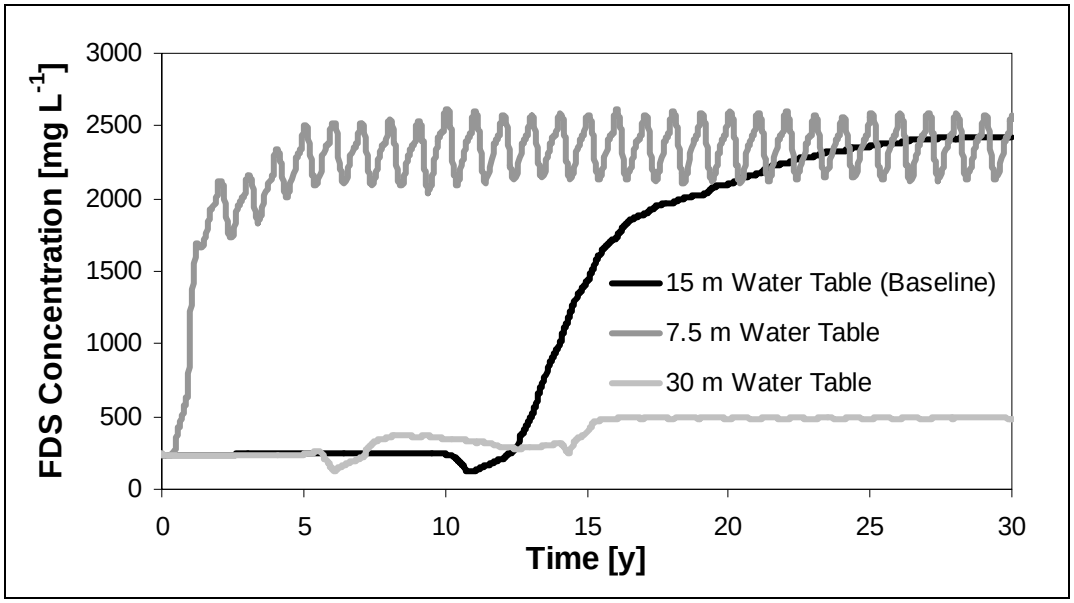

Figure 113

Effect of Water Table on FDS Concentrations for Winery Case 1

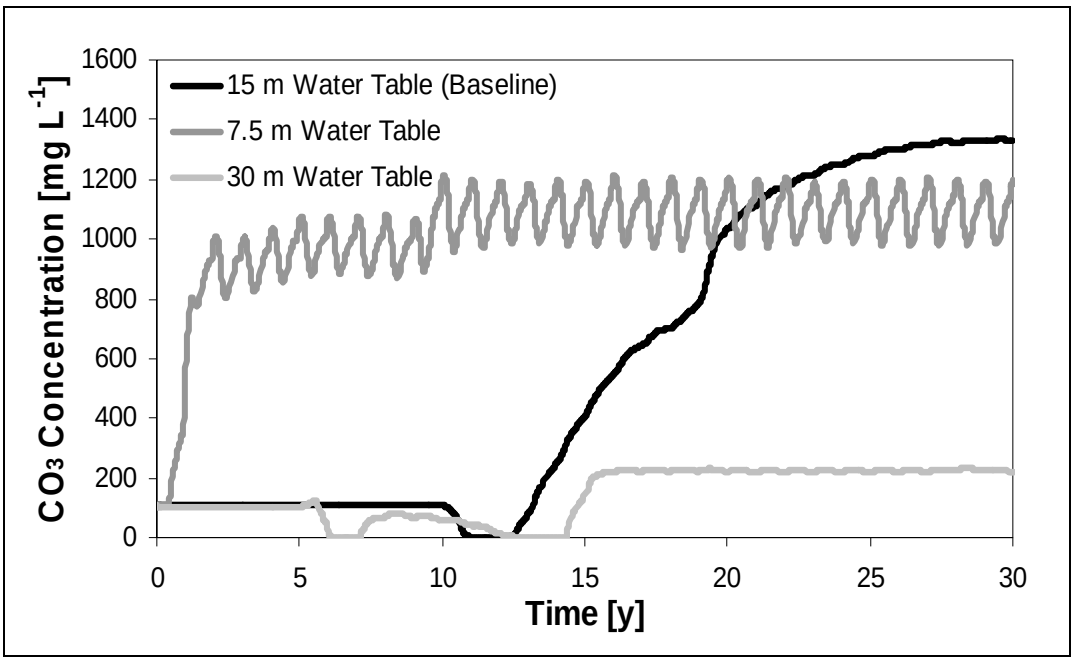

Figure 114

Carbonate Concentration for Case 1 Winery

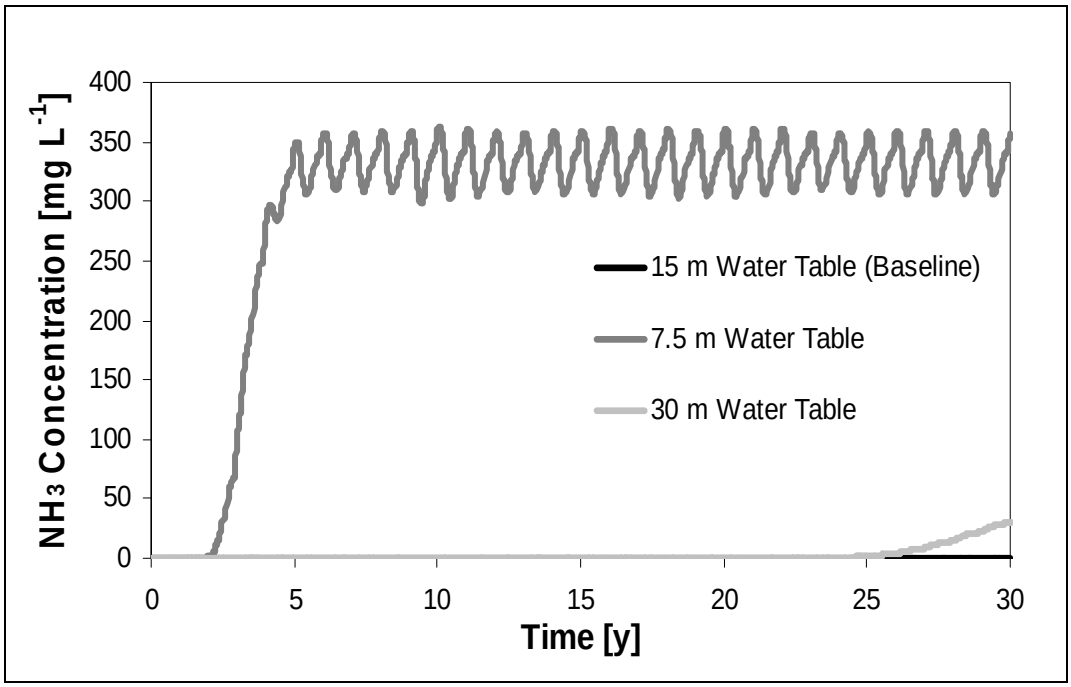

Figure 115

Effect of Water Table Depth on Ammonia Breakthrough in Case 1

Overall, these results indicate that a deeper water table is almost always advantageous to wastewater attenuation.

b) Soil Calcite Concentration

Soil calcite ($CaCO_3$) contents in the study area are typically low and range from 0 to 5% (USDA, 2006). For the baseline case, 1% was modeled, following information provided in Part I, Section 3.9.3. In this scenario, two additional contents at the extremes of the range, 0 and 5% were tested, to determine how this impacted overall salinity.

Dissolution and precipitation of calcite minerals are affected primarily by the pH of soil pore water and the concentration of calcium and carbonate in it. Depending on these conditions, calcite can dissolve, raising FDS by contributing calcium and carbonate ions, or it can precipitate into a solid, lowering FDS. According to Appelo and Postma (2005), degradation of organic matter produces carbon dioxide (CO_2) which reacts with water to dissolve calcite into calcium (Ca^{2+}) and bicarbonate (HCO^{3-}): $CO_2(g) + H_2O + CaCO_3 \rightarrow Ca^{2+} + 2HCO^{3-}$ High CO_2 concentrations enhance dissolution of carbonate while high calcium concentrations enhance precipitation. The pH of the solution influences which of the three carbonate species will predominate: carbonic acid (H_2CO_3) at pH <6.3, bicarbonate (HCO^{3-}) at pH>6.3 and <10.3, and carbonate (CO_3^{2-}) at pH>10.3. As a result, calcite becomes less soluble as pH increases, leading to dissolution in an acidic solution and precipitation in a basic solution.

In Cases 1 and 3, where the soil moisture contents are relatively high (Table 1), an increase in soil calcite content led to additional calcium being released into the soil solution (Figure 117), increasing FDS concentrations (Figure 116). In Case 2, the baseline scenario, 0%, 1%, and 5% calcite simulations produced nearly identical FDS breakthrough curves, with slight differences between 2 and 5 years (Figure 118) brought on by an increase in carbonate around that time (Figure 119) accompanied by a slight difference in pH (Figure 120). In Case 2, little calcite dissolution occurred because carbon dioxide, which increases the solubility of calcite, was allowed to escape from the system due to the low saturation levels. The exact process resulting in the pH elevation has not been determined, but it is likely related to the background water carbonate concentration, which was not equilibrated with the higher calcite content before running the model.

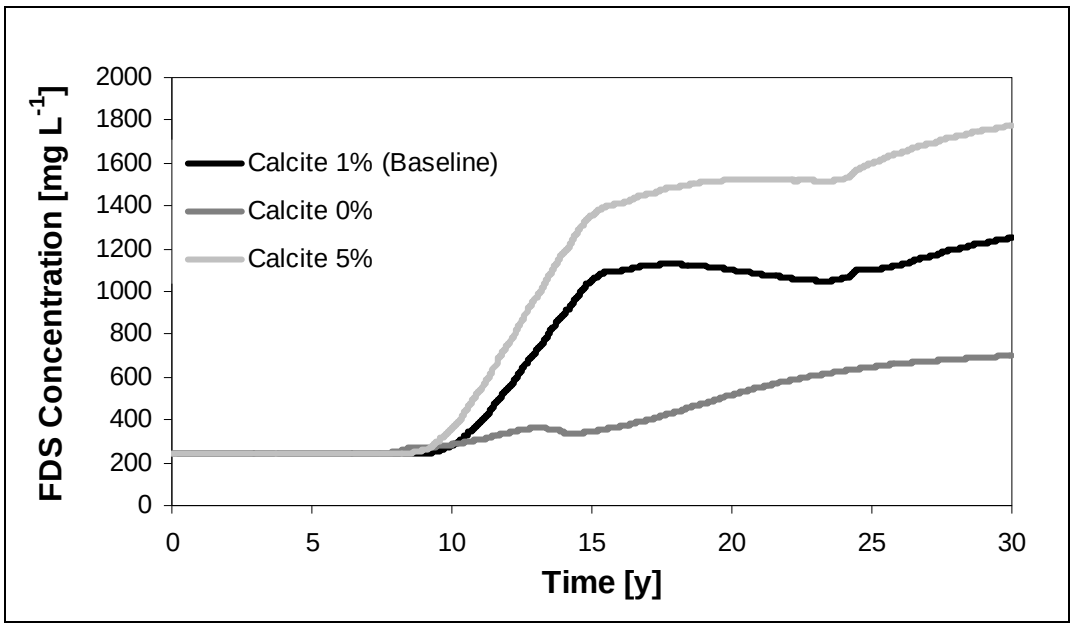

Figure 116

Effect of Soil Calcite Content on FDS for Winery Case 3

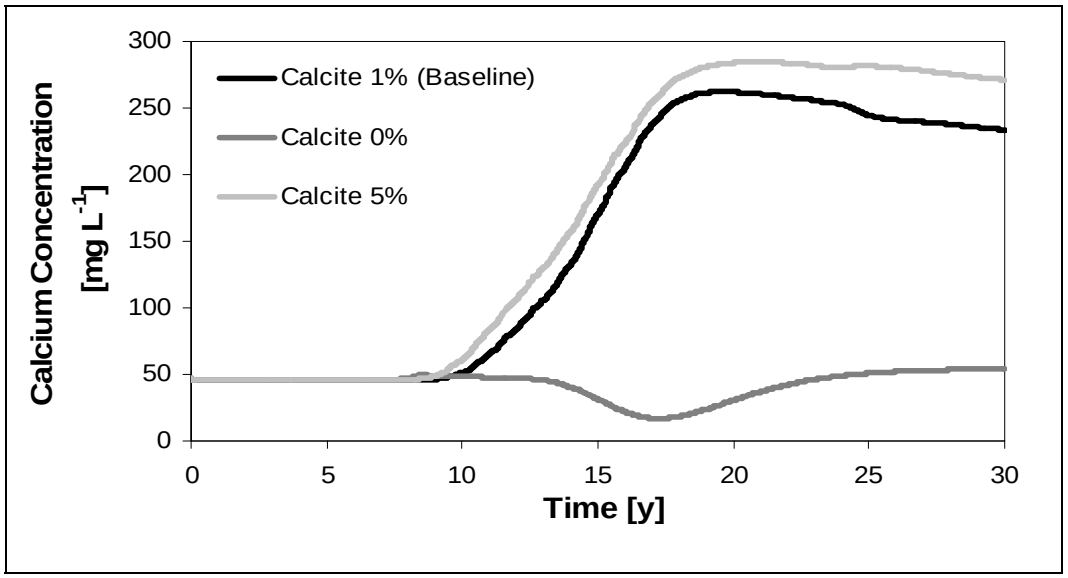

Figure 117

Calcium concentration for Winery Case 3

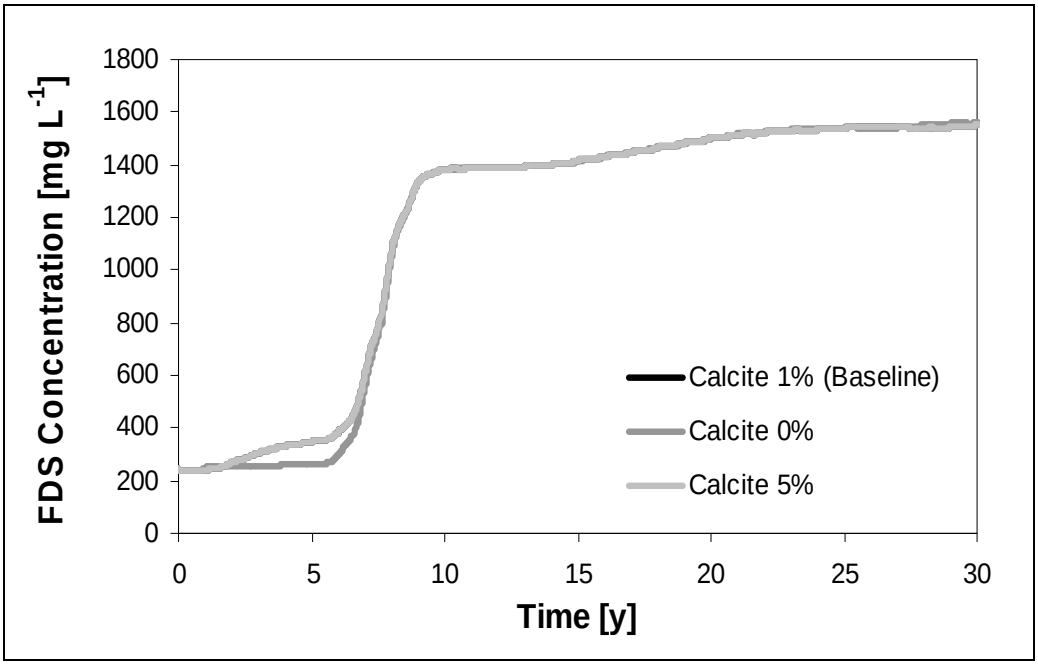

Figure 118

Effect of Calcite Content on FDS Concentration for Winery Case 2

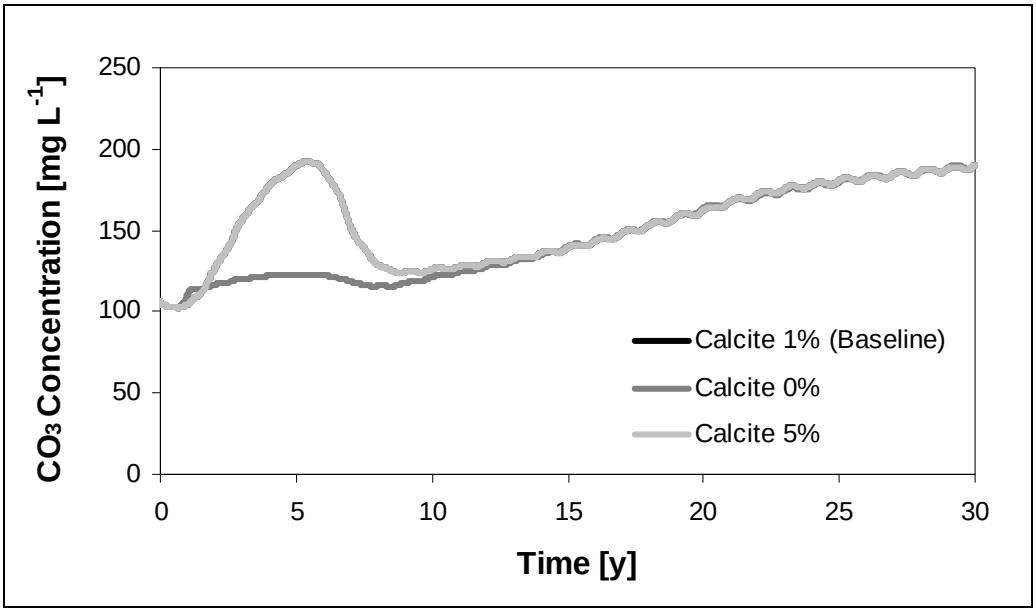

Figure 119

Carbonate Concentration for Winery Case 2

The elevated values found for the 5% calcite scenario between 2 and 7 years are likely an artifact of the background groundwater calcium and carbonate concentrations.

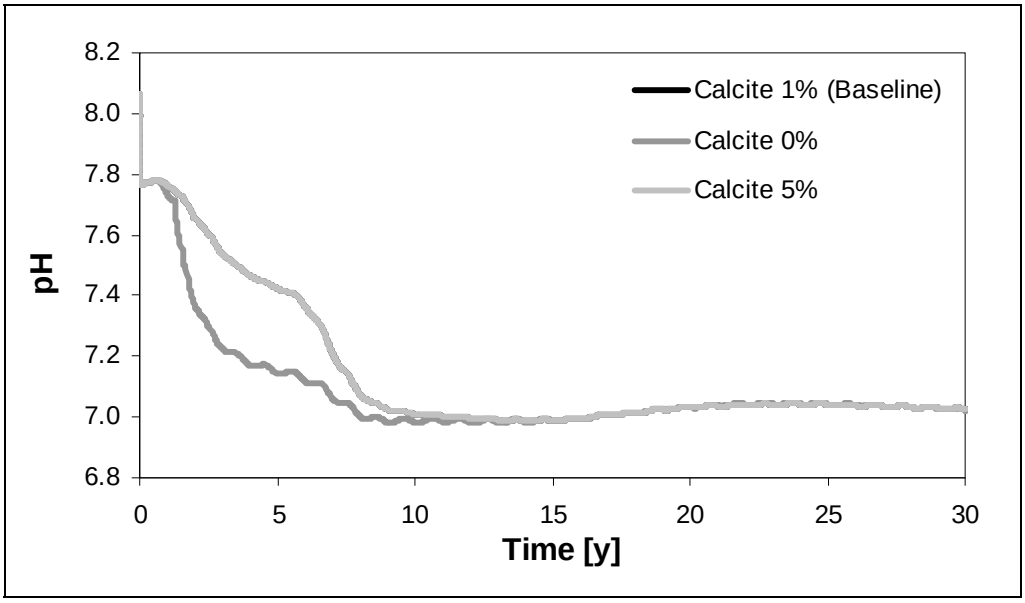

Figure 120

Effect of Calcite Content on pH in Winery Case 2

c) Soil Gypsum Concentration

Soil gypsum ($CaSO_4 \cdot 2H_2O$) is known to contribute to the Central Valley's salinity problems (Schoups et al., 2005), especially in areas of irrigated agriculture, where it is easily dissolved by percolating water. Under most conditions, gypsum has a much higher solubility than calcite. While dissolution of both minerals can increase FDS levels, gypsum dissolution rates are nearly an order of magnitude higher than those for calcite. Additionally, the removal mechanisms for the dissolution products are much different. Calcite dissolution produces both calcium, which can be used by plants, and carbonate, which can escape through degassing of carbon dioxide. Gypsum dissolution produces calcium as well as sulfate, which can be removed through microbial degradation or plant uptake.

Of the site and management scenarios tested in this section, increasing soil gypsum content had the largest impact on FDS reaching the water table. For all cases, the concentrations of both sulfate and calcium in the soil solution immediately increased, due to the dissolving gypsum minerals (Figure 121, Figure 122). The resulting FDS concentrations increased by approximately 2500 mg L^{-1} over the baseline case. Only slight differences were detected between the 2.5 and 5% cases; the extra gypsum content did not increase FDS because the soil solution was already saturated with calcium and sulfate.

Soil saturation had little effect on overall gypsum dissolution; however, the 30 year sulfate concentrations were lower in Cases 1 (1300 mg L^{-1}) and 3 (1730 mg L^{-1}) than in Case 2 (1850 mg L^{-1}). The anaerobic conditions in these cases were favorable for sulfate reduction (Section II.2.C.9.a, Equation 20), and the sulfate levels resulted in lower overall FDS.

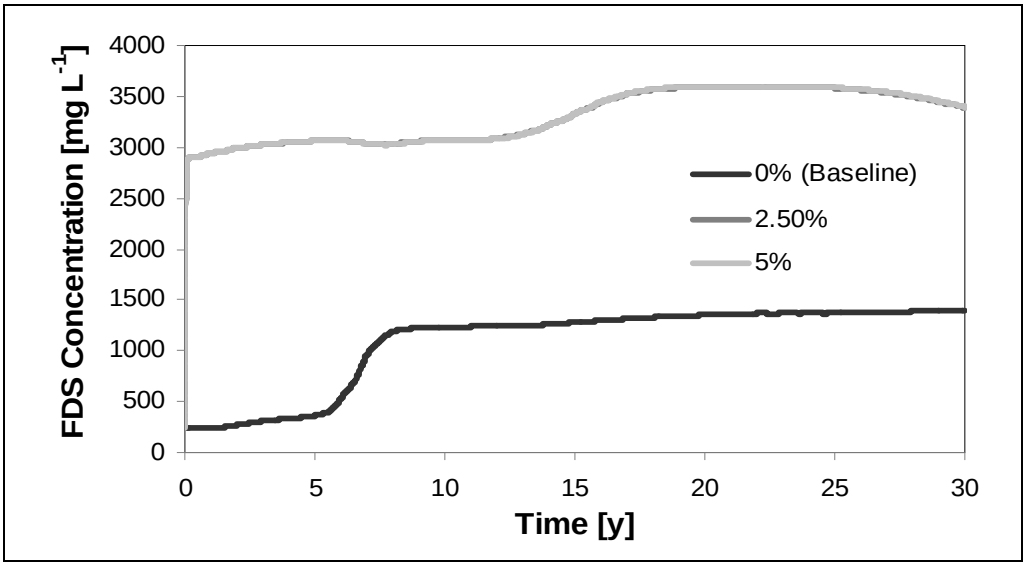

Figure 121

Effect of Soil Gypsum on FDS Concentrations for Wine Case 2

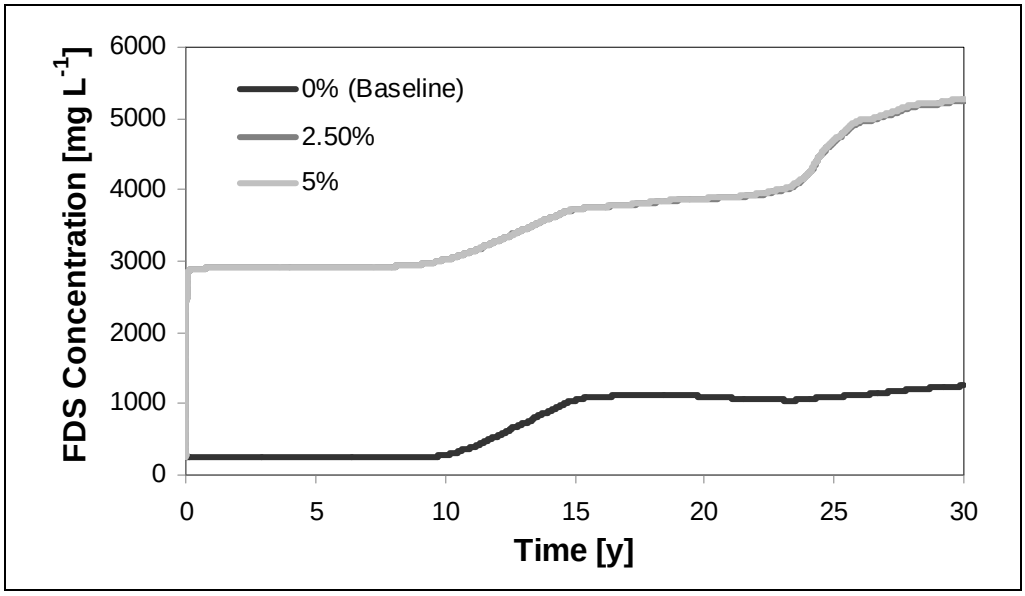

Figure 122

Effect of Soil Gypsum on FDS Concentrations for Wine Case 3

While discharging to soil with large amounts of gypsum could increase salinity levels in groundwater, natural recharge or agricultural activity could have the same effect, and areas under these soils may already have significant natural groundwater degradation. The question, then, on whether to discharge over an area with a high gypsum mineral content may depend entirely on the status of the underlying groundwater prior to discharge.

d) Soil Cation Exchange Capacity

The cation exchange capacity in the study area's soils ranges from 2 to 40 meq $100g^{-1}$ (USDA, 2006). The baseline simulations use a value from the low end of the range, 3 meq $100g^{-1}$. One common misconception is that a higher CEC value will result in lower FDS levels, because more sorption will occur. This assumption is not necessarily correct, because CEC represents an exchange process; when a certain number of moles are sorbed to the soil structure, an equal number of moles are released from the soil. The initial conditions determine which ions are currently occupying exchange sites, but the number of exchanges sites remains constant, i.e. an exchange site is always occupied by an ion. This process can change FDS levels in one of two ways: either by altering the pore water chemistry and inducing other reactions such as precipitation, or by increasing or decreasing the salinity mass. Since FDS is measured in moles, if a heavy ion (Mg = 24.31 g mol^{-1}) is replaced on the soil structure by a lighter one (NH_4 = 18.05 g mol^{-1}), the overall pore water FDS concentration in mg L^{-1} will increase slightly.

To test the effects of CEC on the results, two simulations were run: a moderate CEC (10 meq $100g^{-1}$) scenario and a high CEC (40 meq $100g^{-1}$) scenario. These scenarios are compared to the baseline case, as described in Section II.2. For Case 2, FDS concentrations were very similar for all scenarios (Figure 123), with the baseline scenario slightly higher after 15 years due to a gradual buildup of carbonate. Around the same time, the Ca, K, and Mg concentrations in the baseline scenario decrease, diverging sharply from the other two (Figure 124) and the sodium concentrations increase dramatically (Figure 125). The higher CEC levels were allowing sodium to continuously replace Ca, Mg, and K on the soil structure. Once this capacity was exhausted in the baseline scenario, Na levels started to increase and Ca, Mg, and K levels decreased, since this processes was no longer keeping them elevated. The solution reaching the groundwater table ceased to be altered by this replacement, and began to more closely resemble the incoming wastewater in composition. The precipitation of Ca and CO3 into calcite slowed, since the Ca concentrations decreased, allowing more carbonate to remain in the system and thus increasing FDS.

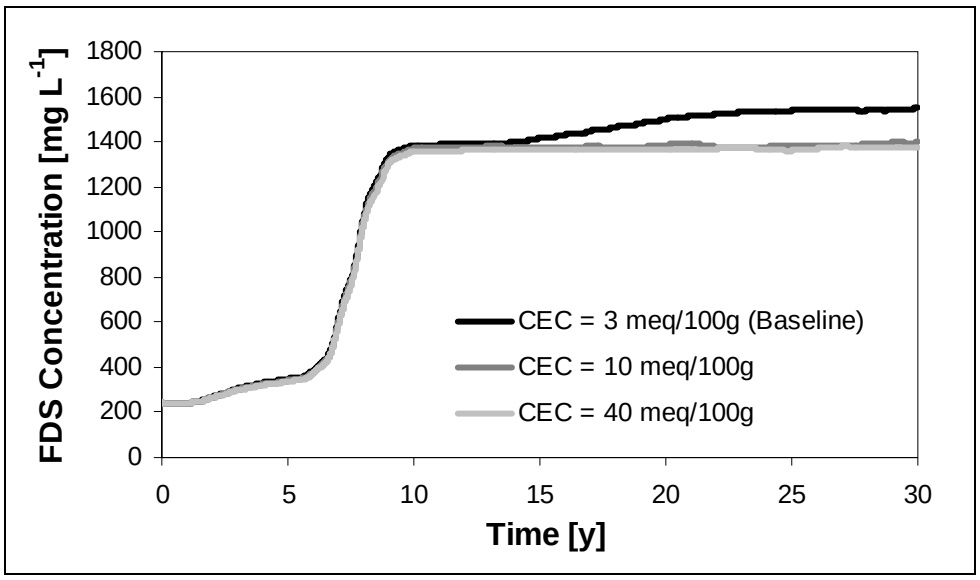

Figure 123

Effect of CEC on FDS Concentration for Winery Case 2

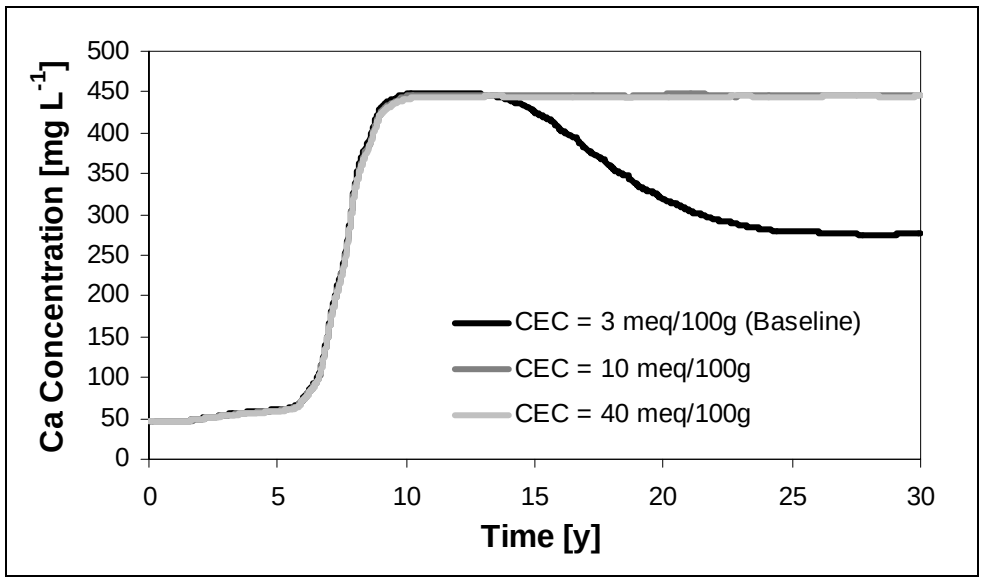

Figure 124

Effect of CEC on Calcium Concentration for Winery Case 2. The concentration curves for Mg and K are of a similar shape, but different magnitude.

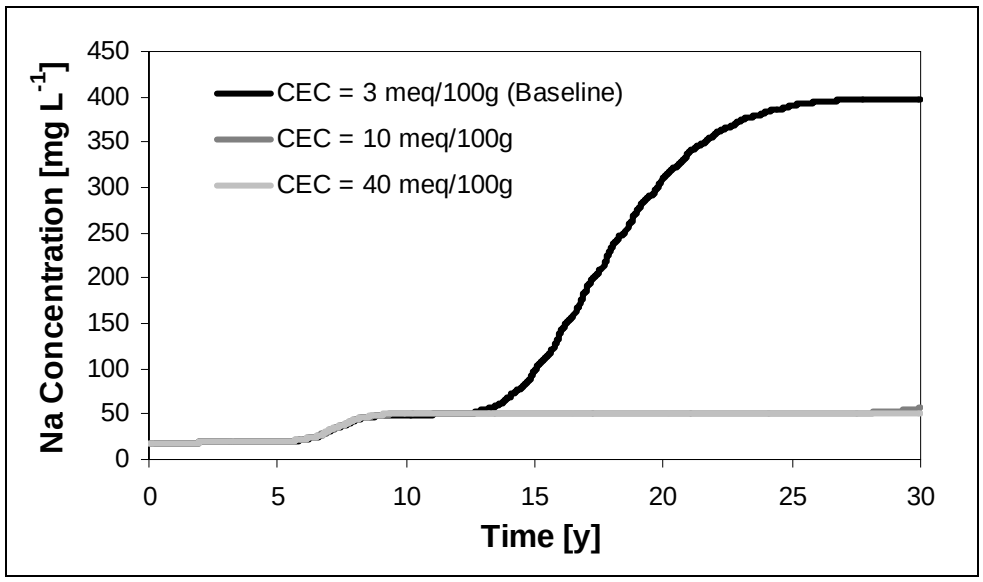

Figure 125

Effect of CEC on Sodium Concentrations in Winery Case 2

The simulation results for Cases 1 and 3 showed increasing FDS levels with increasing CEC values (Figure 126). The ion exchange followed much the same behavior as Case 2; Na levels were higher and Ca, K, and Mg levels were lower in the baseline scenario (Figure 127) due to the exhaustion of the exchange capacity. This occurred less rapidly in Case 3 than in Case 2 due to the lower flow rates and lower wastewater sodium levels. The main difference between the Case 1 and 3 results on one hand and Case 2 results on the other can again be attributed to limit CO_3/CO_2 degassing in the saturated conditions. In the baseline scenario, less calcium is available to precipitate with carbonate, leading to a buildup.

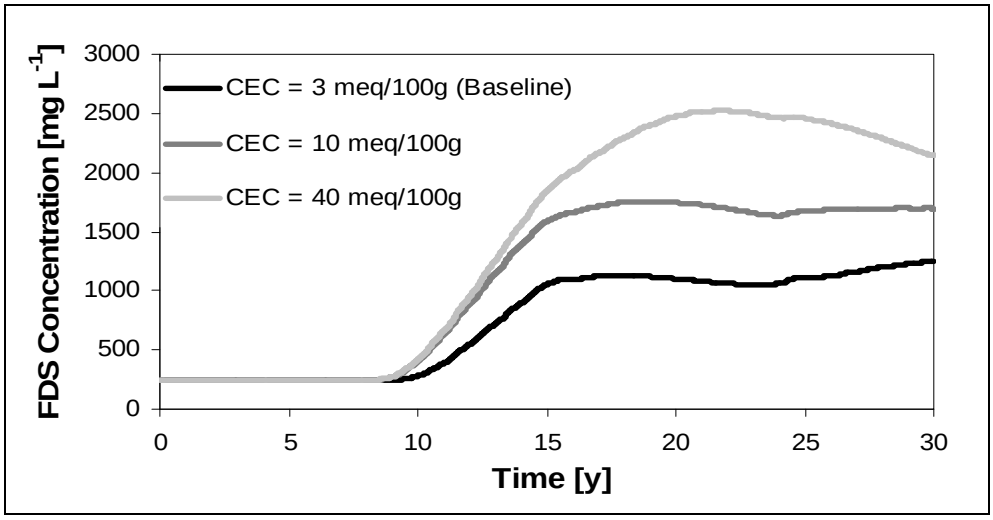

Figure 126

Effect of CEC on FDS Concentrations for Winery Case 3

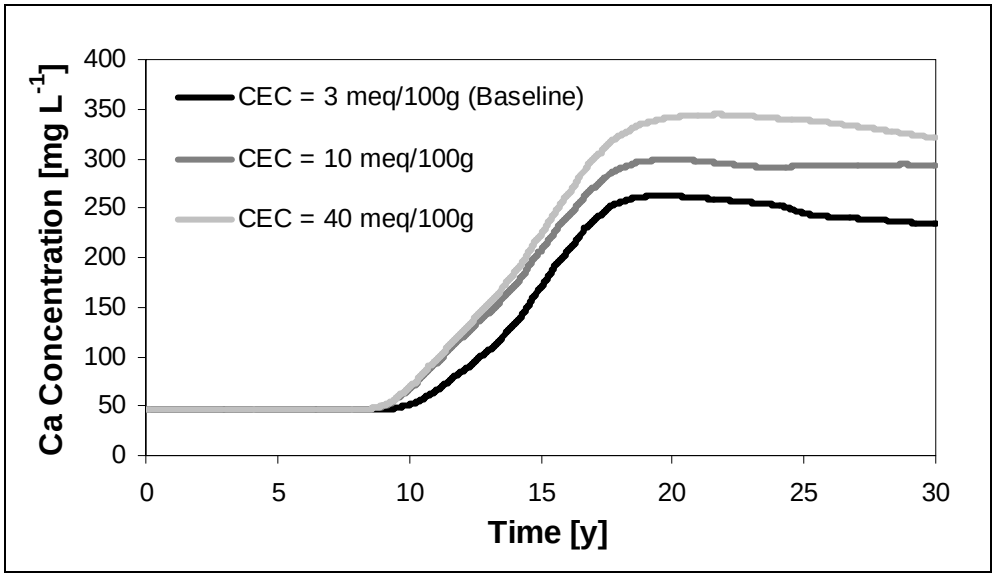

Figure 127

Calcium Concentration for Winery Case 3

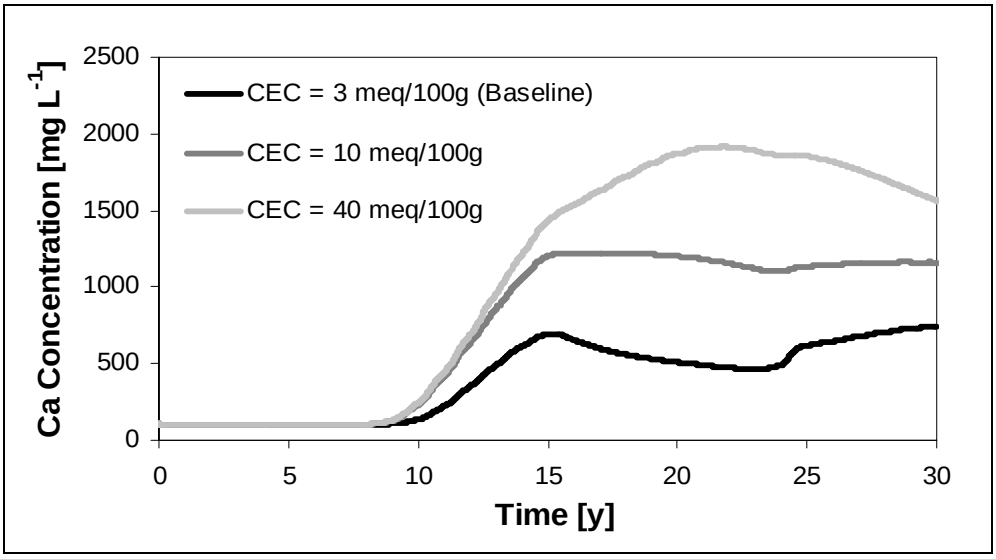

Figure 128

Carbonate Concentrations for Winery Case 3

The results for these simulations are highly dependent on initial condition of the soil. If the pore water initially contains high levels of Na, rather than Mg or Ca, then ion exchange is not likely to take place (since Na has the greatest affinity under most conditions) and the moderate and high CEC scenarios will have results similar to the baseline scenario. The initial conditions estimated in the simulations are highly uncertain since they were not site specific and were based on

Modesto area groundwater concentrations.

e) Site Precipitation

Precipitation in California's Central Valley follows an elevation gradient, with higher levels occurring towards the eastern and western edges of the valley, and lower levels near the center. To determine the effect of precipitation on FDS concentration, two additional precipitation regimes were simulated, one lower (280 mm yr^{-1}) and one higher (406 mm yr^{-1}) than the baseline case (330 yr^{-1}). These were equivalent to the precipitation regimes experienced by the cities Fresno (low precipitation.), Stockton (high precipitation), and Modesto (baseline), and the average monthly precipitation levels for each of these cities were used in the simulations (NOAA Western Regional Climate Center, 2006a; NOAA Western Regional Climate Center, 2006b; NOAA Western Regional Climate Center, 2006c). All cities were selected to be in the same ET zone, in order to keep evapotranspiration values consistent.

In all cases, FDS concentration at Year 30 increased (~400 mg L^{-1}) as precipitation decreased (Figure 129), primarily due to the effect of dilution on the applied wastewater. The increased water flow also caused time to initial breakthrough to be quicker for the higher precipitation scenarios.

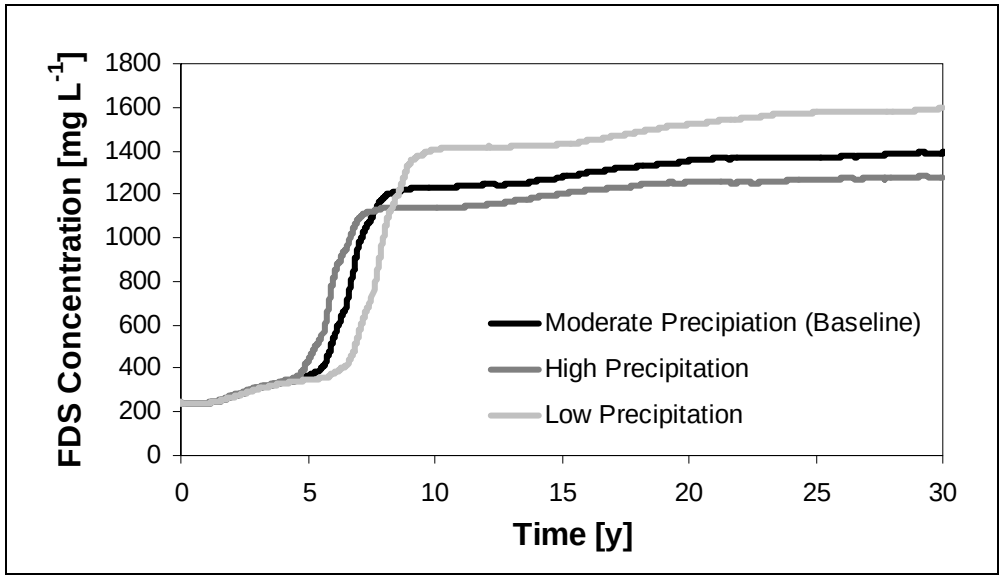

Figure 129

Effect of Precipitation on FDS Concentration for Winery Case 2

f) Site Evapotranspiration

California is divided into 18 evapotranspiration zones, each with different atmospheric and vegetation drivers that contribution to the amount of water lost to the atmosphere. The baseline

scenario uses Zone 12, descriptive of the conditions in the city of Modesto. The broader study area contains two additional zones: 14 (conditions in Holt) and 15 (conditions in the City of Hilmar). Zones 14 and 15 generally have higher evaporative rates. All of these sites are located in the same precipitation zone, so changes to rainfall rates were not necessary. The evaporation rates used in these simulations were taken from the CIMIS system (Cal. Dep. Water Resour., 2006a; Cal. Dep. Water Resour., 2006b; Cal. Dep. Water Resour., 2006c).

The FDS concentration curves in all simulations followed the same pattern (Figure 130); FDS concentrations and times to initial breakthrough increase as evaporation rates increase. The magnitude of the concentration difference (<250 mg L^{-1} in all cases) was small in comparison to other site scenarios.

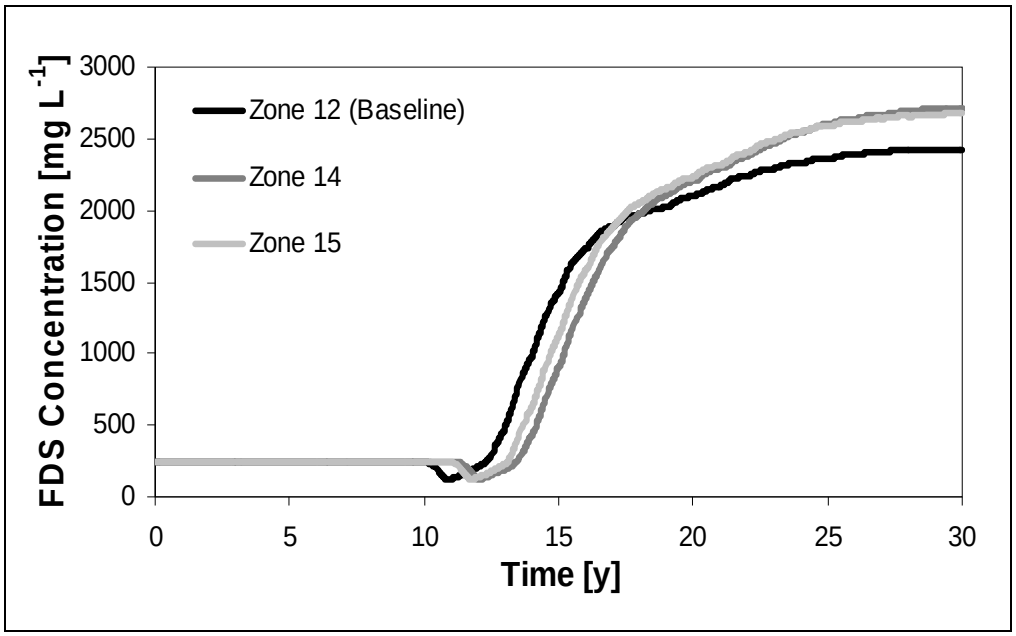

Figure 130

Effect of ET Zone on FDS Concentration Winery Case 1

4. Summary of Management and Site Scenario Results

Table 52 summarizes the results from the numerical experiments performed in Sections E.1 through E.3. The bold values denote scenarios where FDS concentrations were lower than baseline, indicating the change decreased salinity breakthrough to the water table.

Table 52: Summary of Numerical Experiments on Site and Management Options

		FDS Concentration at Year 30		
		Case 1	Case 2	Case 3
Baseline		2418	1551	1249
Site	WT 7	2577	1746	1752
	WT 30	487	1429	534
	Precip H	2002	1280	1052
	Precip L	2592	1595	1306
	Evap Z14	2716	1279	1379
	Evap Z15	2675	1312	1413
	Calcite 0	1844	1560	700
	Calcite 5	3632	1550	1774
	CEC 10	3490	1397	1697
	CEC 40	3466	1370	2140
	Gypsum 2.5	6568	3390	5256
	Gypsum 5	6603	3395	5281
Manage	BOD100	NA	3540	1218
	BOD200	3026	NA	NA
	BOD600	2367	NA	NA
	BOD50	3027	1549	NA
	BOD5	2402	1550	NA
	BOD0	2401	1546	NA
	+10%area	2326	1485	1263
	+20% area	2257	1381	1262
	FDS 640	1388	568	1388
	NaCl 835	1837	881	NA
	150%N	NA	NA	1251
	50% KNa*	2766	1624	1423
	100% KNa*	3238	1550	1379

Bold values indicate those lower than baseline. *Tomato industry specific management strategy and simulation.

F. Demonstration Case (Improved Management Scenario)

To demonstrate how the results of the numerical experiments on site and management options could be possibly applied, a simulation was constructed to represent how improved conditions could be achieved such that the water quality objectives for salinity, nitrate, and ammonia would not be exceeded, and that low amounts of organic matter would reach the water table.

Winery Case 3 was used as a starting point for the demonstration case. The Case 3 combination of hydraulic conductivity, waste application rates, and carbon to nitrogen ratio was originally designed to be "optimal" for the attenuation of nitrogen (Section II.2.B.3) as opposed to Case 1 and Case 2 which were “worst-case” for ammonia and nitrate, respectively Sections II.2.B.1 and 2). Starting with Case 3 allowed us to focus on adjustments that would improve the salinity levels reaching the water table. A winery simulation was chosen because it was examined in

detail in previous sections. The same procedure could be used to show an "improved" scenario for any of the other industries. Additionally, a Case 1 or Case 2 scenario could become an ideal scenario by adjusting the hydraulic conductivity of the soil, increasing it for Case 1 or decreasing it for Case 2.

Next, the site and management parameters needed to be adjusted to achieve FDS concentrations below the groundwater quality objective. Table 48 summarizes how these concentrations varied by test case, showing simulations lower than baseline in bold lettering. Based on this table, the optimal land application site should have a water table at least 30 m below the soil surface (Section E.3.b), have relatively high precipitation (Section E.3.e) , a 0% soil calcite content (Section E.3.b), a low CEC (Section E.3.d), no gypsum (Section E.3.c), and Zone 12 evaporation (Section E.3.f). Although saturation levels were optimal for nitrogen attenuation, they did not allow for CO_3 degassing, so they were decreased slightly by increasing hydraulic conductivity.

The simulations for the optimized case showed much lower FDS concentrations at the water table, 670 mg L^{-1} (Figure 131); somewhat above the groundwater quality objectives but nearly 50% lower than the baseline scenario. Nitrate concentrations were slightly elevated at the water table, 9.3 mg L^{-1} (1.06 mg-N L^{-1}), but no ammonia breakthrough was predicted (Figure 132). Simulated organic matter concentrations were also somewhat high, 226 mg L^{-1} (Figure 133), but lower than the baseline scenario, 477 mg L^{-1}.

The tradeoff between conditions favorable to denitrification and CO_3 degassing makes it difficult to obtain a modeled scenario that has both low FDS and low nitrate concentrations, making source control important. Pre-treatment of the wastewater that would bring applied FDS concentrations would likely be needed to bring the results of this simulated scenario to under the water quality objectives.

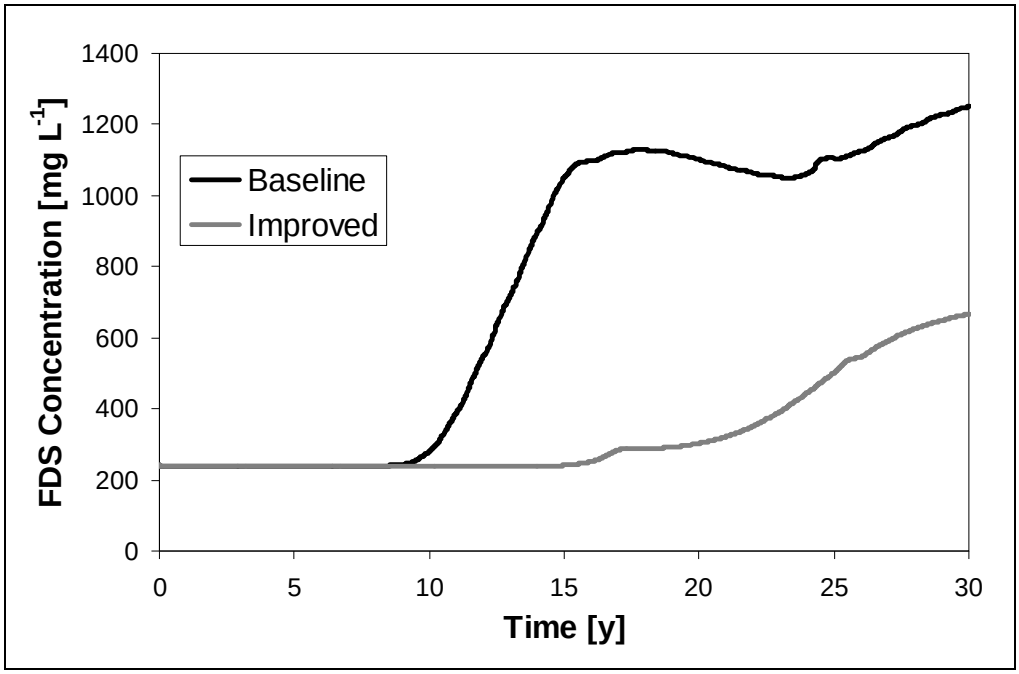

Figure 131

FDS Concentration for Improved Winery Case 3. In the "improved" case, the depth to water table was increased from 15 m to 30 m, the saturated hydraulic conductivity was increased from 2 x 10-7 m s^{-1} to 3.5 x 10-7 m s^{-1}, the BOD concentration was reduced by half, and the precipitation was increased from 330 to 406 mm yr^{-1}

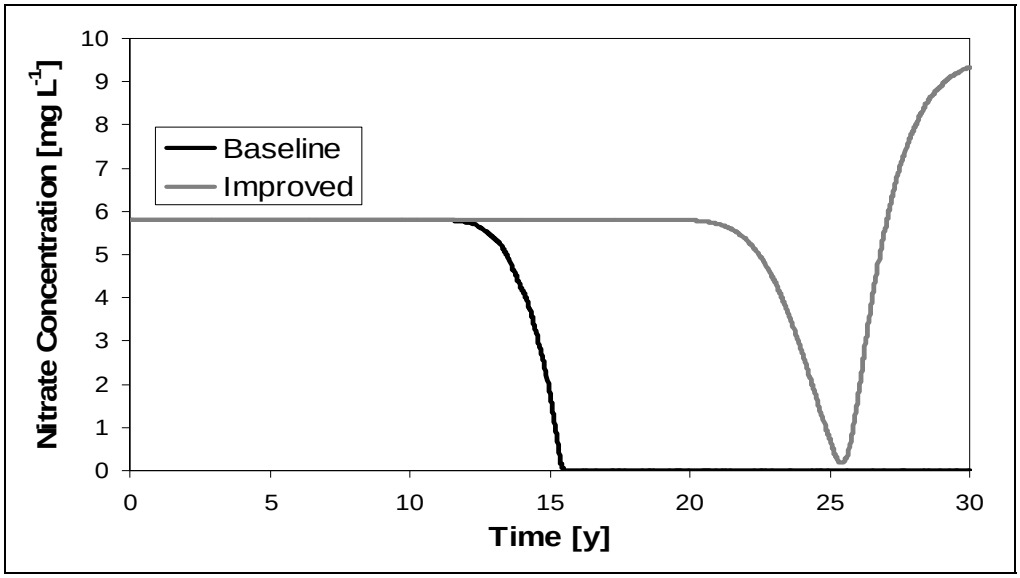

Figure 132

Nitrogen Compound Concentrations for Improved Winery Case 3

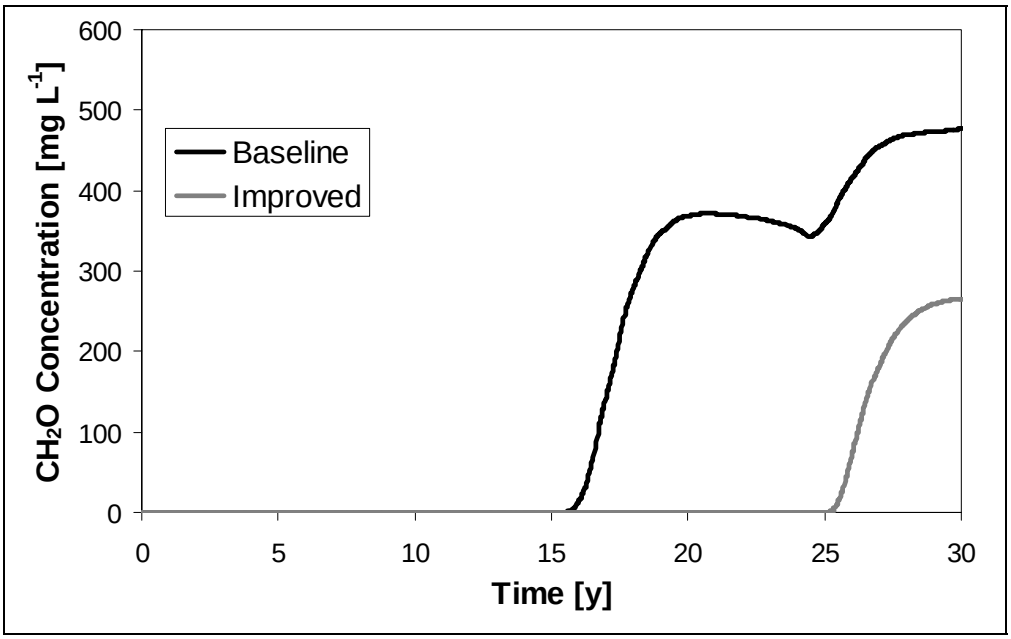

Figure 133

Organic Matter Concentrations for Improved Winery Case 3

G. Summary

We embarked on the study of the unsaturated zone with a list of questions in mind, which we provided in Section II.2. The challenges set forth early on in Section II.2 are addressed through a detailed discussion provided in Sections II.2 and II.3. We start our Summary with a brief summary of these questions and our answers.

Question: What is the capacity of the root zone and the underlying unsaturated sediments to mitigate potential negative impacts of waste water application on groundwater quality? What are the relative contributions of various waste attenuation mechanisms?

Answer: There is only a limited capacity to attenuate salts, and because it is also finite, it is likely to expire with time. The capacity to reduce or even eliminate nitrogen compounds is substantial but it depends on several conditions that cannot always be met.

Question: What is the range of expected, near-source environmental impacts in terms of changes in concentrations of various chemicals at the interface between the saturated and unsaturated zones?

Answer: The evolution of the concentration profiles at the water table (which is the interface between the saturated and unsaturated zone) is provided through a mathematical function known as the breakthrough curve (see for example, Figure 51 of this Section). Our study provides an extensive list of such curves for a wide range of effluents and hydrological conditions. In the case of salts, we expected that over a long term, the salinity at the water table will be equal to the salinity of the effluent, and possibly higher.

Question: What is the effect of site conditions on this attenuation? How do the soil's content of naturally-occurring gypsum and calcite minerals impact attenuation?

Answer: Site conditions have a wide range of effects on attenuation. A summary of our findings is provided at the conclusion of Section E. There is a wide range of site conditions that can be encountered in the Central Valley, in terms of hydrological and geochemical conditions. Site conditions can have favorable or detrimental effects on. A few possibly scenarios, each representing a different set of hydrological and geochemical site conditions are reviewed in Section II.2.B. A detailed discussion of the various site conditions and their effects on the waste stream are provided in Sections II.2 and II.3. We found that site conditions can mitigate and even eliminate the effects of nitrogen compounds on groundwater quality, whereas in the case of salinity, site conditions limited (in magnitude) and finite (in time) capacity to reduce salinity, but they can definitely exacerbate conditions, such as in the presence of gypsum in the soil. The migration of salts in the saturated zone is discussed in Section II.4. The directions of flow in the saturated zone, and in particular, the existence of a vertical gradient, are important site conditions to consider.

Table 52 in Section II.3 summarizes how FDS concentrations at the water table varied under various management practices. Based on this table, the optimal land application site should have a water table at least 30 m below the soil surface (Section E.3.b), have relatively high precipitation (Section E.3.e) , a 0% soil calcite content (Section E.3.b), a low CEC (Section E.3.d), no gypsum (Section E.3.c), and Zone 12 evaporation (Section E.3.f).

The effects of gypsum are discussed in Section II.3.E. Of the site and management scenarios tested in this section, increased soil gypsum content had the largest impact on FDS reaching the water table. For all cases, the concentrations of both sulfate and calcium in the soil solution immediately increased, due to the dissolving gypsum minerals (Figure 62, Figure 63). The resulting FDS concentrations increased by approximately 2500 mg L^{-1} over the baseline case.

Question: What is the worth of discharge management practices? Can careful site selection, in regards to local geological and hydrological conditions, help mitigate environmental impacts? Can controls on discharge rate or area improve attenuation? When designing pre-application source controls for wastewater, what are the most important components to remove from the waste stream?

Answer: Management practices in our discussion includes decisions about site selection, consideration of local conditions and how they might affect the waste stream, as well as proximity to environmentally sensitive sites. Additionally, they include issues such as discharge rates and irrigation regimes, management of the chemical composition of the waste stream. In designing land discharge rates, attention should be given to plant root uptake (see additional discussion below). Additional discussion of this topic is provided in Section II.3.E.

Careful planning needs to include field data acquisition and monitoring of field conditions. Site-specific management practices are as good as the data available to support them. Monitoring will allow assess the discharge practices and to modify them practices as better understanding of the conditions at the site is gained.

The question of reducing impact to groundwater is a question of both spatial scale and timing. The protection offered by site conditions is limited and finite. The protective capacity of the soil and vegetation can be exhausted over a period of the order of 20 years, depending on many factors. It can be much less than that or much longer. This is where management practices can help. There is also the issue of scale. If one considers groundwater degradation at a limited vicinity of the discharge sites as acceptable, then this would allow flexibility in adopting management practices. This can be a slippery slope though, because the spatial containment of salts within a limited area underneath the land discharge zone is multiplicative and temporary. Multiplicative, because there is a need to consider the hundreds of hot spots that will develop due to land discharge as well as from dairies. And temporary, because the containment effects observed in our study and in the field (and explained further below) are affected by the existence of a vertical, downward pointing pressure gradient which curbs lateral migration of solutes at the price of directing it to deeper formations.

Finally, we should mention that proper management is a somewhat elusive concept, because it

depends on what the management goals are. A management goal of reducing impacts to groundwater can translate into a line of action that attempts to limit salts reaching the groundwater but allows accumulation of salts in the vadose zone. This will in turn translate into losses in crop yields. An alternative goal might be to minimize the losses of crop yields by enhancing the leaching of salts from the root zone. This will obviously preserve crop yields, at the price of degradation of groundwater quality.

Question: What are industry-specific issues to consider (e.g., wineries, cheese manufacturers, olive producers, tomato canneries)?

Answer: Section II.1.C discusses salinity loads in the Central Valley, including industry-specific analysis for the tomato, wine and meat industries. These 3 industries were selected for detailed analysis because of their economical dominance in the Central Valley, and the extent of waste stream discharge (see Figure 8 in Section II.1). It discusses the commonality between these industrial groups, and the potential impacts to the environment posed by each of these industrial groups, from the perspective of the chemical composition of the waste stream. This discussion concludes that there is quite a bit of commonality within the various industrial groups, and differences between the various groups. Under similar conditions, this will lead to industry specific issues, such as discussed in Section II.3.3a. For example, tomato processors discharge high loads of fixed dissolved solids (FDS representing inorganics) but much smaller organics (BOD) and nitrogenous compounds (TKN and NO_2+NO_3). In contrast, the discharges from wineries seem to be rich in organics (thus also in total dissolved solids but only moderate in fixed dissolved solids) and in reduced nitrogenous compound (TKN). Their discharges of nitrates vary.

However, the chemical composition of the waste stream is one out of several issues to consider when assessing environmental impacts, as discussed in Section II.2. This includes biogeochemistry at the land application site, hydrological and hydrogeological conditions, and land application practices. For a given set of conditions, industry specific issues can be singled out. However, given the large variability between discharge sites, we believe that singling out particular industries is not warranted. Instead, a holistic approach which integrates all these factors into an advanced numerical analysis modeling tool, such as developed in this study, should be applied to each discharge site under consideration.

Question: Is there a scientific basis for a deterministic "safe agronomic rate" of application of salinity and nitrogen compounds? In determining "safe rates", should we look only at concentrations or also at the loading rate of applications? Is current industry guidance appropriate?

Answer: "Safe Agronomic Rate" (or just agronomic rate) is interpreted here to mean a concentration level in the waste stream that can be applied without causing degradation of groundwater quality. It is a, ambiguous term because the Safe Agronomic Rate may not be safe at all for agriculture: one can design this rate to reduce impacts to groundwater but at the price of increasing salinity at the root zone and thus losses to crop yields. Flushing of salts from soils is a

difficult if not an impossible task. It can lead to abandonment of large agricultural areas. These areas will continue to release salts under the influence of precipitation, which will eventually degrade groundwater quality.

The CLFP (2007, page 7-2) defines agronomic rate as the amount of constituent that meets crop requirement. The concept underlying the safe rate approach is that, if such a rate can be defined, root uptake will eliminate the risk of the chemicals under question reaching the vadose zone underneath the root zone, as well as the water table. As discussed in Sections II.3 and summarized below, there is a limited attenuation capacity for salinity, whether one considers the attenuation capacity offered by root uptake or even when augmenting this with geochemical processes. Attenuation of nitrate compounds, on the other hand, can be significant, especially considering the vertical saturation profile in the vadose zone.

There is a wide range of conditions that affect a "Safe Agronomic Rate". This range includes the chemical profile of the waste stream, the land application process, the type of vegetation, as well as biogeochemical, hydrologic and hydrogeologic conditions. These conditions change over time. There is a large range of variability in these conditions over the Central Valley. Climate is also expected to change over time. Considering all this, we believe that a "safe agronomic rate" is not a viable concept of general applicability, meaning a rate that can be adopted uniformly for an industrial group or several groups or for a region, without site specific investigations. There is no replacement for site investigation and for modeling through advanced modeling tools that are able to consider the wide range of processes.

A different way to consider the viability of the safe rate concept is through long term detailed field experiments. Unfortunately, none exists that we are aware of. If one assumes that application rates at the various land application sites are in line with so-called "safe agronomic rates", the evidence, in terms of ground quality deterioration, suggests that these rates are not applicable universally, as groundwater quality was observed to degrade at many sites (Staff Report, 2006).

Current industry guidance is provided in CLFP (2007). It is not within the scope of this study to provide a detailed review of this manual. What we note, however, is the following. First, the predicting the movement of chemicals in the subsurface requires modeling a long list of processes, some of which need to be modeled simultaneously. This list includes, on the chemical side, complexation, cation exchange, dissolution and precipitation, gas diffusion, chemical uptake by plants, biodegradation reaction including nitrification, denitrification, sulfate, reduction, and respiration, modeling of the transport of NH_4, CH_2O, Cu, Zn, Mn, Fe, PO_4, and the diffusion of N_2, NH_3, O_2. Depending on site conditions, it may be important to model variable crop yield, root growth, and changes in conductivity with higher salinity levels. On the physical side, transient effects in the flow regime due to change in boundary and atmospheric conditions (variable application rates, fluctuations in the water table, changes in soil saturation and biogeochemistry) need to be considered. Modeling of such complexity requires sophisticated numerical tools. No analytical solutions are currently available that can model this range of processes simultaneously, because of the non-linearity of many of the processes, and their

interdependence. CLFP (2007), to our knowledge, does not employ a numerical model to integrate these processes. Furthermore, many of the abovementioned processes are not recognized. Instead, a series of analytical solutions and approximations are used. This can be acceptable if the analytical solutions are successfully compared with and validated against general models that are free of all the assumptions and simplifications that are involved in the derivation of the approximate solutions.

Second, analytical solutions and approximations can also be validated against field data. This is difficult to accomplish, at least in the context of this study, because of the wide range of field conditions that need to be tested. Hence, no data is available to test the models. Based on that, there is no firm basis in our opinion to support a statement that current guidance is appropriate.

To address the above questions, we have adopted and further developed a numerical model (MIN3P) that allows us to simulate in great detail the processes of flow and transport in the unsaturated (vadose) zone. The following discussion enumerates a few of assumptions that were employed in developing our modeling approach: flow and transport were assumed to be one-dimensional in the vertical direction; flow and transport were modeled as transient, with monthly variations allowed in the boundary conditions and in the loading; spatial variability of the hydrogeochemical parameters was neglected based on the assumption that homogenization provides an accurate description of flow and transport for distributed sources such as is the case with land disposal sites

All simulations suggest that the unsaturated zone provides a very limited capacity for the long-term attenuation of salinity loading to the water table. Although ion exchange may affect the composition of the pore water, the salinity front itself cannot be attenuated by this process. This is not unexpected, considering that by definition, ion exchange is an exchange process and not a removal process. Compounds such as Na and C_l, which can be significant constituents of wastewater, are not amenable to precipitation due to the high solubilities of mineral phases that include these components. Furthermore, the concentrations of the compounds may increase beyond concentrations present in the irrigation water due to evapotranspiration processes. All simulations suggest that Ca and Mg are released as a result of land application due to calcite dissolution and displacement from exchange sites, respectively. Although Ca and Mg are not of key concern, they contribute to overall salinity and hardness. Their release is subject to the initial soil conditions, i.e. type of carbonate minerals and Mg content on exchanger. The long term water quality in the aquifer will likely be controlled by idilution processes controlled by soil heterogeneity in the unsaturated and saturated zones.

On the other hand, the simulated attenuation of N-compounds (NH_3 and NO_3) was significant in most simulations considered, but was not enough to prevent breakthrough in some situations. The baseline simulations for Case 1 dairy processors and Case 1 tomato canners showed ammonia levels significantly exceeding the USEPA Draft Health Advisory of 30 mg-N L^{-1} (Marshack, 2003). California's groundwater quality objectives and the EPA's maximum contaminant levels for drinking water specify that nitrate concentrations should not exceed10 mg-N L^{-1}. The baseline simulations for Case 2 dairy processing, tomato canning, and meat

packing all predicted that concentrations above this level would reach the groundwater table.

In this context it must be emphasized that the "worst case" scenarios did not investigate processors or conditions that exceed existing regulations or set limits, and that is because our goal was to study the impacts from land dischargers operating within the conditions specified in the WDR.

It also must be emphasized that the removal of N is highly dependent on the actual nutrient uptake parameters, which are subject to a considerable degree of uncertainty (see discussion below). The simulations also suggest that the microbially mediated conversion of N-compounds may play a role and may have both negative (Case 2, resulting in an increase in nitrate loading) and positive effects (Case 3, resulting in a near complete conversion of N-compounds to N_2). These findings suggest that it may be possible to "design" land application in a manner that promotes microbially-mediated N-removal, although it should be acknowledged that these conditions may be difficult to maintain, because they are affected by a number of interacting parameters including soil hydraulic conductivity and saturation, organic carbon content of the waste water, and reaction rates. It appears that a safer approach is to limit land application rates such that nutrient uptake provides sufficient N-removal.

Our study examined steps which may be taken in order to reduce groundwater degradation associated with waste disposal through land application. These processes fall into three broad categories: actions that alter the characteristics of the waste, decisions that alter how the waste is applied to the disposal site, and the choice of the application site itself. A summary of our findings is provided below.

- Loading limits:
    - Measures that attempt to control the mass loading to the land application site are generally successful at reducing the total mass reaching the water table, but are not necessarily successful with regards to controlling breakthrough concentrations.
    - Loading limits for BOD can indirectly limit salinity loading, a positive side-effect.
    - The 835 lb $acre^{-1}$ yr^{-1} proposed loading limit on NaC_l reduces mass loading to the water table, but does not necessarily result in FDS concentrations meeting the State's groundwater quality objectives.
    - Increases in land application area designed to meet either salinity or BOD loading limits show dimensioning returns; an increase in area does not induce a proportional decrease in total mass loading to the water table.
- Source controls:
    - BOD removal before application only slightly impacts FDS concentrations reaching the water table but dramatically decreases organic carbon loading. While BOD treatment is beneficial to the groundwater, care should be taken that enough BOD remains to allow the biodegradation of NO_3.
    - An FDS concentration limit of 640 mg L^{-1} is not necessarily protective of the groundwater, due to the effects of waste concentration and carbonate production in the rooting zone.

    - Substitution of KOH for NaOH in tomato processing plants can slightly reduce FDS concentrations.
- Site selection:
    - Deeper water tables have an initial protective effect on groundwater, delaying breakthrough and providing additional sorption capacity. This effect is not sustainable; given longer simulation times, the breakthrough concentrations for FDS will likely equal those associated with higher groundwater tables.
    - Soil mineral contents of a site directly affect the FDS breakthrough concentrations, but often in a case dependent manner. Increased calcite contents typically lead to higher FDS levels due to mineral dissolution, but this effect is compounded by CO_2 degassing in Case 2, altering the carbonate/calcite equilibrium. The presence of gypsum always increases the FDS concentrations.
    - Higher CECs do not necessarily lower the FDS concentrations. The effect of CEC changes is highly dependent on the characteristics of the initial soil water and on the saturation conditions.
    - Increased precipitation dilutes the wastewater, leading to slightly lower FDS concentrations, and causes earlier initial breakthrough times.
    - Increased ET concentrates the salts in the rooting zone, leading to higher FDS concentrations at the water table.

Although the simulations presented are process-oriented and consider a significant degree of complexity, several potentially important processes had to be neglected to provide manageability, both in terms of study focus and computational demands. For example, soil heterogeneity and preferential flow were not considered. The occurrence of these processes in the root zone may cause rapid flushing, a decrease in residence time, and may limit the potential for nutrient uptake. This behavior may be enhanced by short term (hourly, daily) peaks in land application rates, which can not be resolved over the 30 year time frame of the simulations. In terms of NH_3-attenuation, it may be possible that electron acceptors other than O_2 affect the persistence of ammonia under anaerobic conditions through the anammox process; however, neglecting this process will provide conservative estimates in terms of NH_3 loading to the aquifer.

Inhibition of root water and solute uptake due to excessive salinity loading and the transient nature of solute uptake due to changes in uptake rates with plant growth were also neglected in the baseline scenarios. Simulations revealed that FDS concentrations were lower when no crops or microbes were present, due to the production of carbonate from organic matter degradation and root solute uptake (Section D.2). However, nitrogen compound release to the water table increased, causing levels exceeding the groundwater quality objectives to be released to the water table. Organic matter concentrations increased and in some cases doubled.

Furthermore, the contribution of gas advection to O_2–ingress was also neglected. This process may either enhance O_2 ingress, if an inward pressure gradient is created by the consumption of O_2 in the sediments, or reduce O_2-ingress, if an outward pressure gradient is generated through the production of CO_2 and N_2. Gas advection is also relevant for describing the displacement of soil gas by changes in soil moisture. These processes may have a limited effect on the

availability of O_2 in the subsurface and therefore affect the transition from aerobic to anaerobic conditions. However, under most conditions, diffusion provides a sufficiently accurate description of gas transport in the unsaturated zone.

Biomass growth and decay have also been excluded and the simulations assume that biomass is at a quasi-steady state. C and N are incorporated into biomass during periods of growth and enhanced microbial activity, which may cause additional removal of N from solution, or in the case of decay, may provide an additional source for these compounds. Bioclogging due to excessive biomass growth or deposition of suspended organic matter present in the waste water was only considered in a very limited fashion (i.e. by reducing the saturated hydraulic conductivity values for Cases 1 and 3). This process may be of importance, because it has the potential to reduce the infiltration capacity into soils and may cause anaerobic conditions, which in turn may affect plant growth, reduce nutrient uptake, and simultaneously limits O_2 ingress and the potential for aerobic degradation reactions.

The baseline simulations assumed that gypsum is not present in the sediments, but that calcite, as a surrogate for carbonate minerals, is available. For soils with accessible gypsum, it can be expected that groundwater quality would be degraded independent of land application due to the dissolution of this mineral phase, which results in an increase in salinity due to high Ca and SO_4-concentrations. When gypsum levels were increased to 2.5% in the site selection scenarios (Section E.3.c), FDS concentrations reaching the water table tripled.

Calcite on the other hand, typically improves groundwater quality due to its significant pH buffering capacity. It should be noted that relatively small fractions of calcite (<< 1vol %) can provide significant and long term pH buffering capacity. However, if carbonate minerals are completely absent, many microbially mediated processes become negatively impacted, thus reducing the attenuation potential. Only select mineral phases have been considered and the dissolution and precipitation of other mineral phases that are likely present in the sediments, e.g. silicate minerals, have been neglected. However, the phases considered here typically provide the main controls on groundwater composition under the conditions investigated. In numerical experiments (Section E.3.b), it was noted that the impact of higher and lower calcite content (0 and 5% as compared to 1% baseline) depended on the saturation status of the soil.

The fate of other contaminants such as phosphate, boron, trace metals, etc may also be of environmental concern due to low MCLs and toxicity at low concentrations. Processes affecting these compounds are not considered here, because the modeling focuses on major ion and redox chemistry, which are not significantly affected by reactions involving these compounds. Once insight has been gained into major ion and redox chemistry, the fate of trace elements can be inferred based on simulated geochemical conditions along the flow-path from ground surface to the water table, or if deemed necessary, additional modeling studies can be undertaken. However, it must be emphasized that for field conditions, geochemical modeling and in particular reactive transport modeling, is of limited use for assessing trace element mobility. Trace elements are affected by a multitude of release and attenuation processes (surface complexation, precipitation, co-precipitation, colloid transport, etc), which are controlled by site-

specific data that is typically unavailable. From a practical point of view, it is impossible to assess the contribution of the various processes on trace element mobility and the predictive value of the modeling is rather restricted.

Despite the simplifications discussed above and the uncertainties regarding some of the key modeling parameters, a number of general conclusions can be drawn from the simulations conducted. The results suggest that the effectiveness of land treatment will benefit from an understanding of soil conditions and the expected geochemical conditions in the root zone and the underlying vadose zone. It may be possible to exploit this understanding to optimize discharge practices for land treatment, in particular for N-compounds. Pretreatment of waste water may have a variety of site-specific effects, which may not necessarily lead to favorable results. For example, the removal of BOD may result in an enhanced potential for nitrification and may limit de-nitrification, which may lead to enhanced NO_3 loading of an aquifer, if root solute uptake is insufficient to remove N. In any case, a distinction between N-loading and salinity-loading must be made. It should be possible to sustain long term and successful N-treatment through land application by N-removal through solute uptake and possibly also microbially mediated conversion to N_2, both processes which provide renewable attenuation capacity. On the other hand, after consideration of evapotranspiration, a conservative transport approach appears to be sufficient and most appropriate to estimate a sustainable long-term salinity loading to the water table. What is a safe agronomic rate remains a hot button issue in the light of the uncertainties, primarily related to solute uptake, as discussed above.

II.4 Saturated Zone Analysis

A. Introduction

Our previous sections presented an extensive analysis of flow and transport of salts in soils underlying land application sites. An important outcome of that section was the computation of the fluxes of salts at the water table under various scenarios. The section below extends the previous analysis into the saturated zone. Here we will analyze the flow and transport of salts in the groundwater aquifer underlying the land application sites. Specifically, we will analyze here the time evolution of the salinity and Chemicals of Concern (COCs) concentration fields in the aquifers.

We do not intend to explore in this section the evolution of the concentration field next to each of the land application sites at the Central Valley. This is unattainable given the scarcity of data, on the one hand, and the large number of land application sites, on the other. Instead, we plan to assess the extent of groundwater contamination under conditions typical to the Central Valley. Our analysis does not intend to replace the role of site specific analysis when evaluating specific sites. Rather, it intends to provide a realistic ensemble of scenarios, that will then be combined together to create a realistic set of expectations in terms of the extent of groundwater contamination. Our scenarios intend to cover extreme conditions. They were designed as a combination of hydrologic conditions and the effluents' chemical profiles that are expected to yield concentration values close to the bounds of the concentrations. The conditions and discharges constituting these worst case scenarios are not representative of actual conditions at the various sites in our model.

We cannot guarantee to have captured the absolute extreme values in concentrations or travel distances from the discharge sites. The range of concentrations and travel distances expected in the field depend on local hydrologic conditions and on the scale of the measurement. Smaller measurement devices will yield increasingly larger concentration values. The concentration values reported in our study should be viewed as averages over the scale of the numerical grid elements (which is of the order of hundreds of meters), and considerable deviations to higher values at smaller scales. The large scale averages are in line with the flux-averaged concentrations, which is the concentration of the water pumped through wells.

We want to emphasize that the tools we developed and presented here are applicable immediately to additional site-specific analyses. The models we developed for this study are comprehensive in terms of the flow and transport processes they cover. Thus, although they are applied here under assumed scenarios, they are immediately applicable.

To create a meaningful ensemble of scenarios, we chose to focus in a limited section of the Central Valley, namely the lower San Joaquin River Basin (see Figure 134). We refer to this area as the Representative Area, or RA. This study area is relatively well-characterized in terms of hydrological and hydrogeological conditions and it has been studied extensively by researchers

from the USGS.

What is the rationale for analyzing an RA? It intends to substitute an analysis of the entire Central Valley, which is an undertaking that is not feasible under the limited budget and time line of the SEP project. For this substitution to be meaningful, the RA needs to be large enough to cover a large number of processors, processes and geological conditions such that findings form the RA can be generalized needs to cover a wide range of conditions to be representative to a large extent of the range of conditions that can possibly be encountered in the Central Valley. Another benefit of working with an RA in our case is that it allowed us to focus on an area that is much better documented in terms of hydrogeological conditions compared to other section of the Central Valley, this eliminating the need to speculate about such conditions over areas that outside of the RA.

The analysis RA includes a development of a numerical model for analyzing flow and solute transport processes. The model is subjected to loading of solute fluxes from a large number of food processing facilities located in the RA. These fluxes were computed in Sections II.2 and II.3.

The study area was subjected to salinity loading at various locations (marked on Figure 134), from facilities large and small. The salt loads we used to test the aquifer are representative of various food processing industrial groups, including the large impact industrial groups, namely, wineries, meat processors and cheese makers. An extended discussion of the rationale leading to the selecting of the salinity loads is provided in the previous section, and is not repeated here for brevity, except to emphasize that the "design loads" used to simulate the salinity loading at the land discharge sites represent extreme conditions. We refer to these loads as our best and worst case scenarios, and the underlying concept are discussed in Section II.2 and again in Section II.3. The rationale behind this choice is that an extreme "design load" would entail an extreme environmental impact to the groundwater and would thus be useful to identify the applicable limits and constraints. Conversely, when an extreme "design load" fails to make a notable impact, this provides an indication that we should not expect significant impacts for loads that are not at the extremes.

Numerical simulations of the transport of salt reaching the groundwater table were carried out over a period of 30 years. This is obviously an arbitrary planning horizon. It was deemed sufficiently length to allow the environmental impacts to groundwater to become noticeable, and at the same time for land use changes to take place, such that the environmental impacts could possibly translate into economical impacts. Numerical simulations over a longer period of time would require the consideration of effects such as climate change, as well as consumer and technological trends, and all this could introduce significant uncertainty as well as a diversion of the discussion away form current issues. Our decision is also supported by the planning horizon of the California water plan, which extends all the way to Year 2030.

An important aspect of our discussion is modeling uncertainty. Spatial viability of hydrological conditions and hydraulic parameters, coupled with scarcity of data, makes our predictions subject

to a large uncertainty. Although our study area is relatively well documented (compared to other regions of the Central Valley), there is still large uncertainty associated with the various parameters away from measurements locations. To capture this uncertainty, we formulated our study in a probabilistic framework. We opted to do that by modeling dependent variables such as the groundwater concentrations at various times and locations as random variables. This implies that they are modeled through their statistical moments such as mean, variances and probability distribution function. We will provide our results using, for example, quantitative assessment the probability for the concentration to exceed a certain threshold value at certain times. It is important to interpret such a statement. An extended discussion on this topic is provided in books such as Rubin (2003). To help our readers, we should just add that a statement such as "the probability for the concentration to exceed a value C_0 is equal to 80% implies that 8 out of ten sites with similar conditions are expected to show concentrations exceeding C_0.

We should comment on why Monte Carlo analysis was deemed appropriate for the saturated zone but not for the unsaturated zone. There are two reasons for that. First, the flow and transport processes are much simpler to grasp and to model compared to the unsaturated zone, and a Monte Carlo, analysis can yield meaningful results. Secondly, the parameters needed for modeling such processes are much better documented, and their statistical distributions are documented in the literature, although not uniquely. This allows for a Monte Carlo simulation. This is unlike the unsaturated zone, where such knowledge is painfully lacking.

Another issue we wish to address in this introduction section is that of subsurface variability of parameters such as the hydraulic conductivity. This subject was explored extensively in the science literature in recent years (*e.g.*, Rubin, 2003, which includes many references). In general, one would like to be able to characterize the flow domain at the highest resolution. This in fact would be a requirement in the case of point sources. Such an undertaking is very demanding in terms of field data acquisition and in terms of numerical modeling. Fortunately, the land application sites cover large areas, much larger compared to the typical length scales of heterogeneity of the relevant properties. In such situations, it is appropriate to use effective properties rather then resorting to detailed subsurface characterization. Effective properties are useful in modeling the mean behavior, or in other words, the large-scale trends of the concentration field. They are not expected to produce the small scale variability of the concentration about such general trends; however, they are successful in their ability to estimate the flux-averaged concentration, which is the concentration that is measurable at the pumping well.

1. Food Processors in the Area

Our numerical study area covers the lower San Joaquin River Basin as shown in Figure 1. This figure also identifies the locations of the food processors modeled in this study. An extended discussion of the food processors is provided in Section 2. Section 2 also includes maps that identify each of these symbols by name.. Each of these facilities was studies through its periodic reports and the documentation related in its permit to operate a land discharge site.

The complete list of food-processing facilities in the study area (Figure 134) includes a wide range of facilities representing the diversity of food processors operating in the Central Valley.

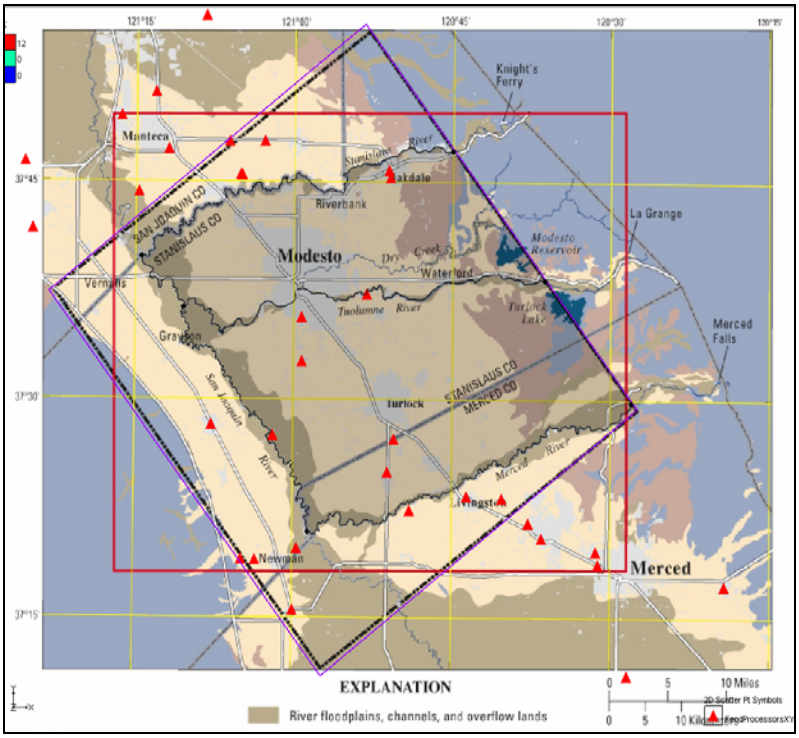

Figure 134

Arial view of our regional study area (black rectangle), and the food processing facilities in the model area (red diamonds). The numerical model's area is shown by the black rectangle. The model does not include the region to the west of the San Joaquin River.

B. Hydrogeologic Setting

The San Joaquin Valley is more than 400 km long, ranging in width from 40 to 90 km, and it makes up the southern two-thirds of the Central Valley. The San Joaquin Valley is bordered on the east by the Sierra Nevada which rises up to elevations of more than 4,200 meters, and on the west by the Coast Range which is of more moderate elevation. The San Joaquin Valley is made up of two sub-regions: the San Joaquin Basin in the north which drains to the Sacramento-San Joaquin Delta and at the southern end an interior drainage called the Tulare Basin named after a

Pleistocene Lake that occupied most of the area (Bertoldi *et al.*, 1991, Burow et al., 2004). Figure 135 shows a generalized geologic section and view of the Central Valley as seen looking Northward along the axis of the valley.

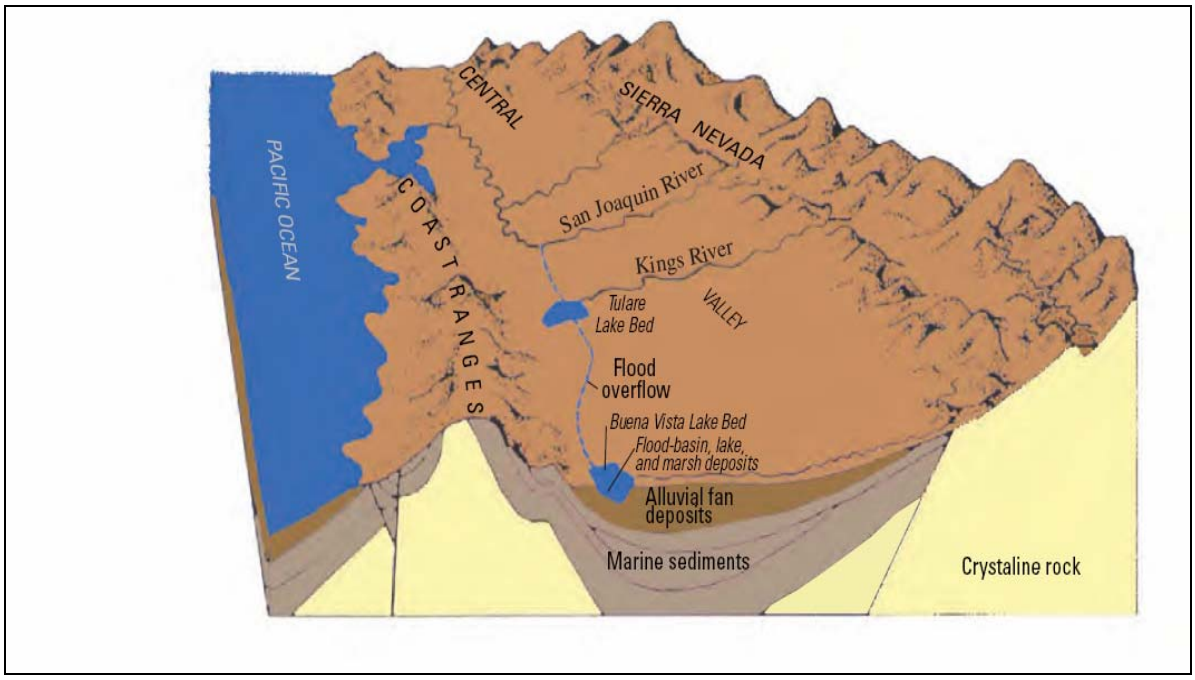

Figure 135

Generalized geologic section and view of the Central Valley as seen looking Northwest along the axis of the valley (from Page, 1986)

Several large overlapping fluvial fans have formed along the eastern margin of the San Joaquin Basin where their rivers exit the Sierra Nevada. Seven of these fans – the Mokelumne, Stanislaus, Tuolumne, Merced, San Joaquin, Kings and Kaweah River fans – have drainage basins that connect to glaciated portions of the Sierra Nevada (Figure 135). The fans in the northern portion are smaller due to the narrower width of the valley compared to the southern area (Weissmann *et al.*, 2005). Smaller fans have formed along the western edge of the valley. Figure 136 indicates that the Central Valley is comprised of a series of fluvial fans. Although no two fluvial fans are identical, they all display a very similar structure. They can generally be divided into three physiographic regions: the western fans, the eastern fans, and the basin deposits as illustrated in Figure 135 (Burow et al., 2004). The sediments on the western side are unconsolidated and have relatively higher hydraulic conductivities. The eastern edge is more consolidated and is characterized by lower hydraulic conductivity. There is a Corcoran clay layer at depths of about 30 to 40 meters that stretches over the western half of the fans (see Figure 143 and 144)

This repeating pattern suggests that studying the transport of salinity over a single or a couple of such fans can provide insight about the transport of salinity at other locations, and that studying salinity transport over a limited section of the Central Valley seems like a reasonable means for obtaining general results.

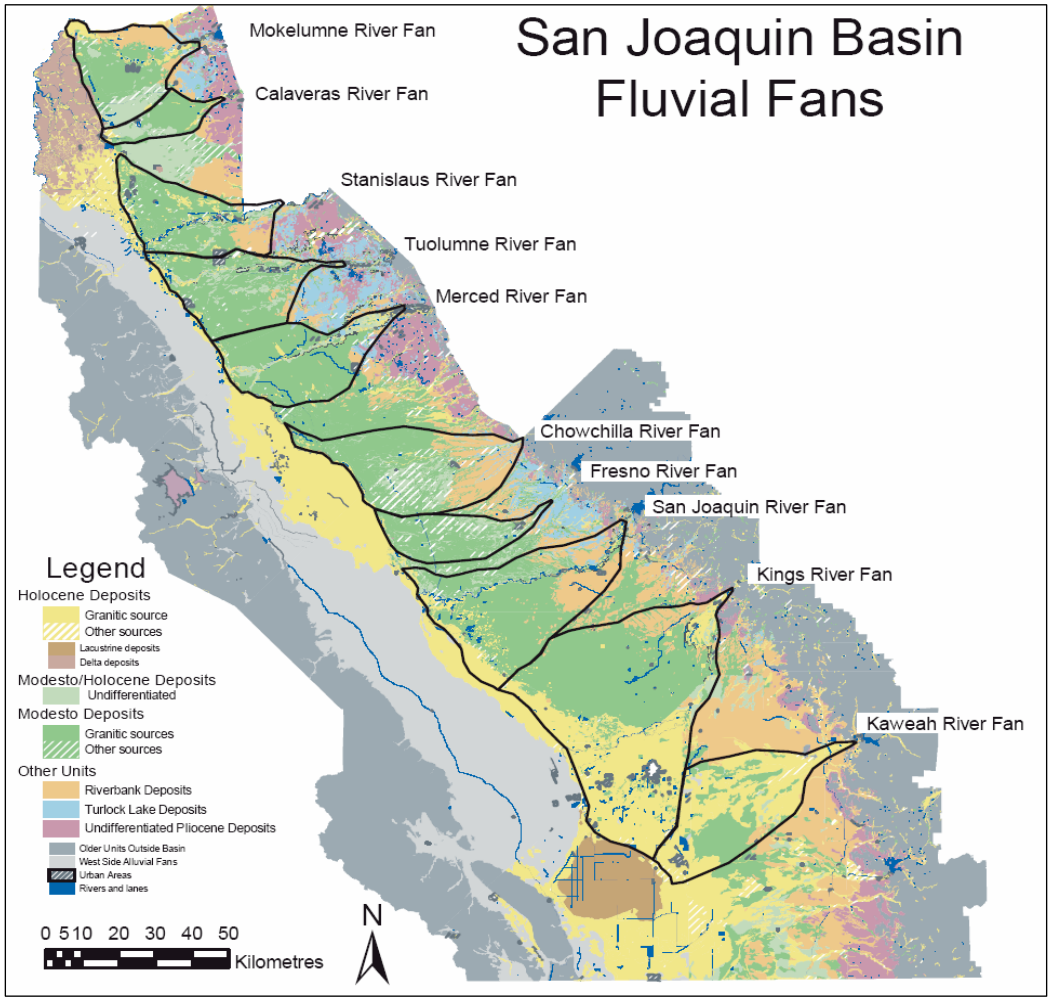

Figure 136

Map showing the structure of overlapping fan systems in the San Joaquin Basin. The study area is shown by the red dashed rectangle and includes the overlapping fans from the Stanislaus, Tuolumne, and Merced Rivers (from Weissmann et al., 2005)

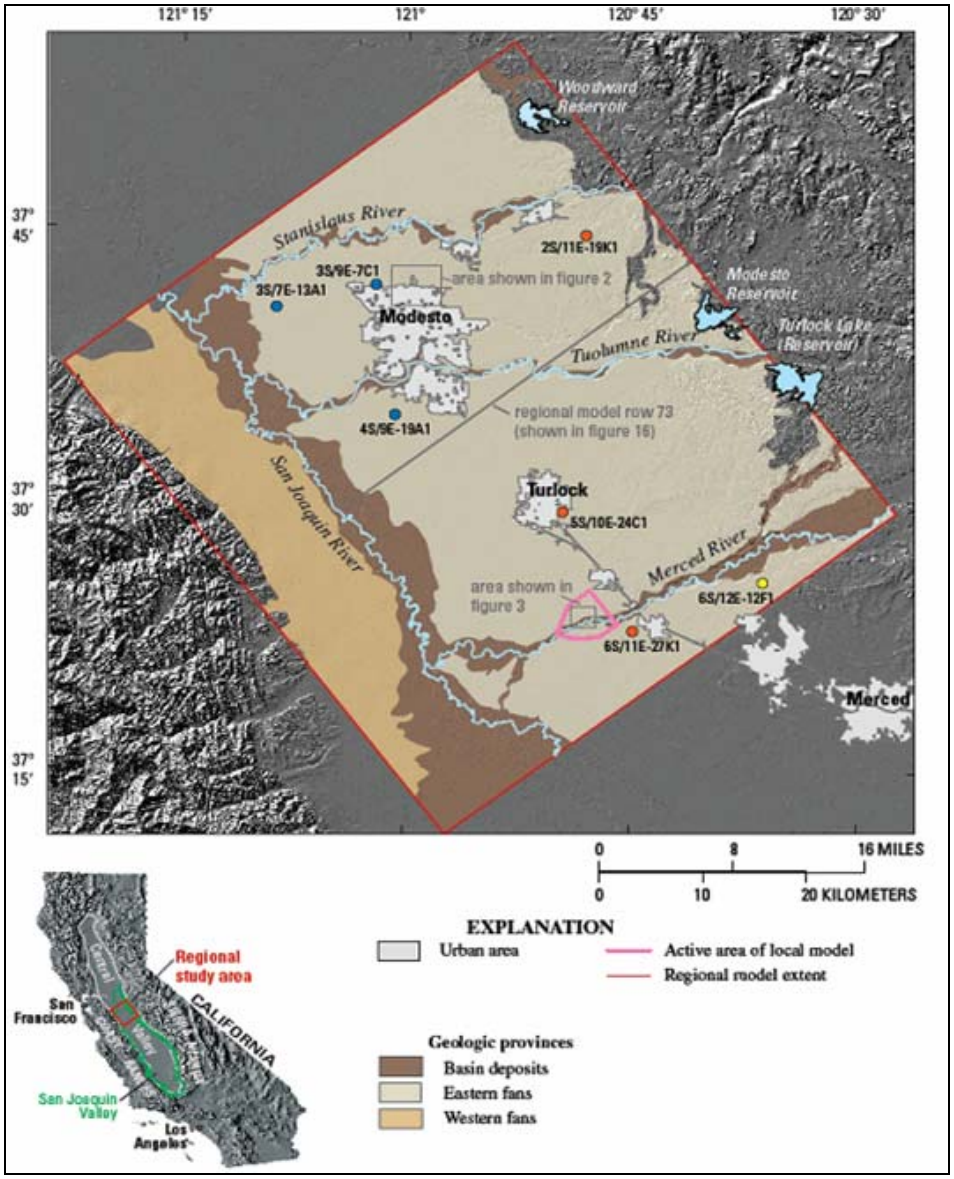

Figure 137

The major physiographic units in the Study Area (Source: Phillips et al. 2007)

1. Regional Hydrology

Under natural conditions prior to intensive agricultural development, ground water in the Central Valley was primarily recharged in the upper parts of alluvial fans where the streams enter the valley (Figure 138 and Figure 139). Ground water flowed followed the dip of the underlying basement rock and flowed southwest towards the San Joaquin River, around which Artesian conditions existed (Bertoldi et al., 1991, Phillips et al, 2007).

Prior to development the Corcoran Clay is believed to have acted as an effective confining layer. The consequent drilling of large diameter wells (see map below showing well locations, different types of wells and different depths in Figure 140) through the Corcoran Clay with well

perforations above and below the clay unit, however, has diminished the effectiveness of the layer as a confined unit (Bertoldi et al., 1991).

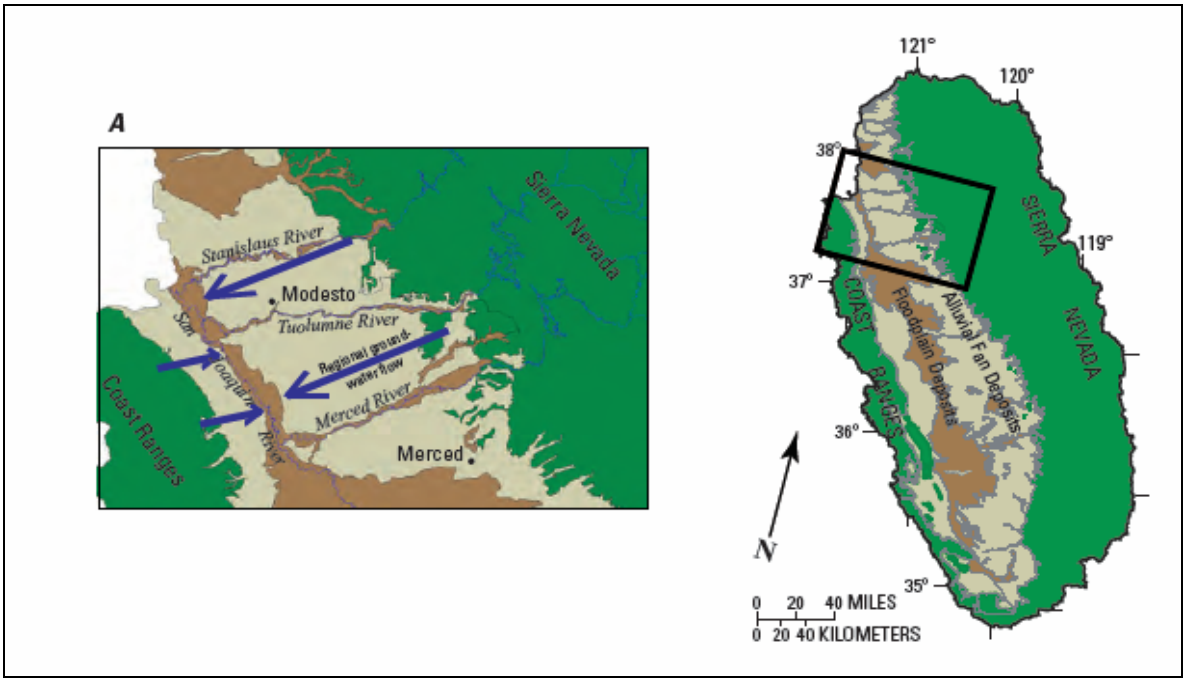

Figure 138

Map view with conceptual diagram, of regional ground water flow (Source: Gronberg & Kratzer, 2006)

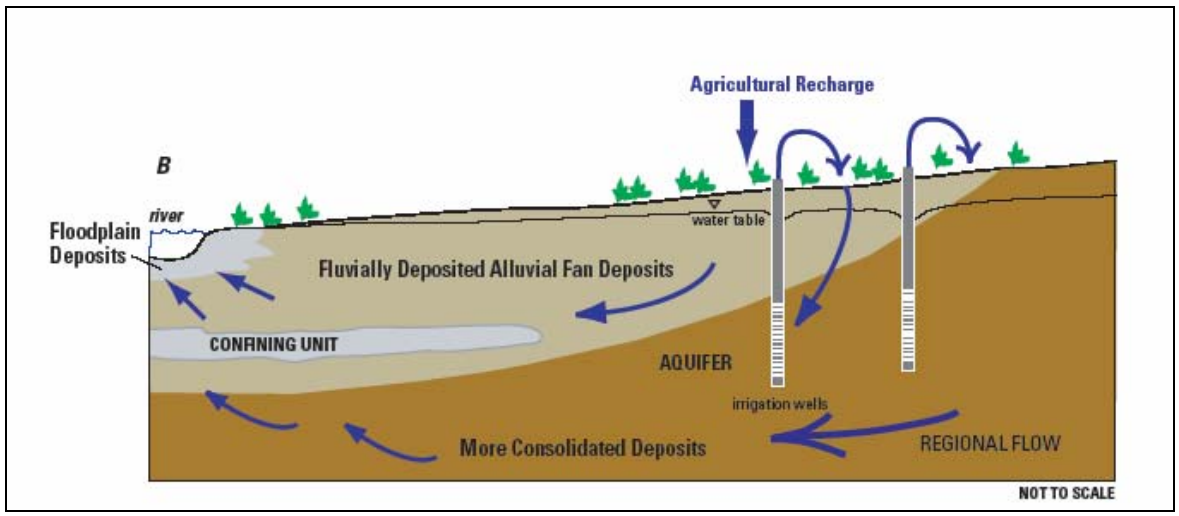

Figure 139

Cross-section with conceptual diagram of the regional ground water flow showing regional flow and vertical components of flow due to agricultural pumping and recharge(Source: Gronberg & Kratzer, 2006)

Extensive groundwater development in the valley (see Figure 140), coupled with the increase in conductivity of the Corcoran Clay layer have greatly altered the regional flow patterns. The current flow regime is strongly affected by agricultural pumping and irrigation, and these local effects lead to strong vertical gradients. The induced gradients in the relatively high pumping zones (see light blue zones in Figure 141) may overwhelm many times the natural gradient by introducing a strong vertical gradient.

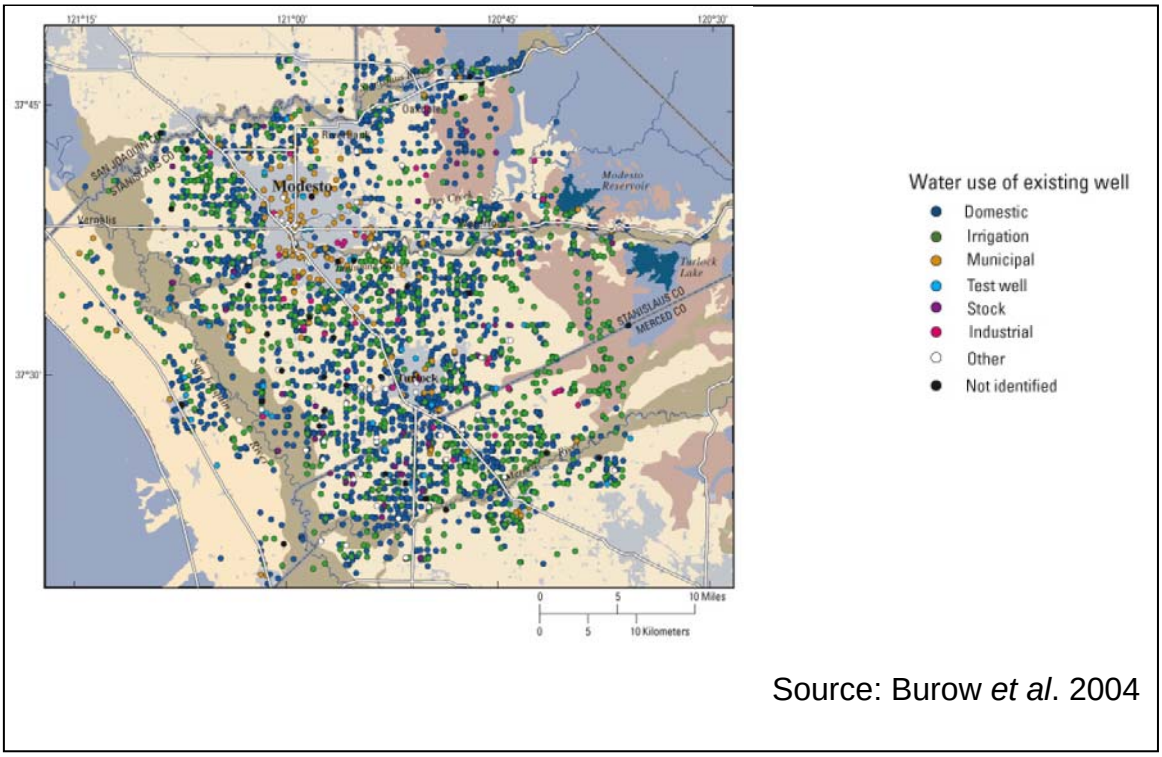

Figure 140

Well types and locations. Irrigation and municipal wells account for the greatest volume of pumping. The median screened depth interval for Irrigation wells is 51 – 74 m below land surface, for municipal wells it is between 59-75m, and for domestic wells it is between 44-47 m (Burow et al., 2004)

C. Water Recharge and Pumping

Water recharge and pumping are modeled following Burow et al. (2004). Evapotranspiration rates were based on data collected by the CIMIS observation network.

Recharge includes water infiltration from irrigation and precipitation. It also includes leakage from reservoirs based on estimates provided in Phillips et al. (2007). Irrigation rates were estimated based on crop type and land use data. Sixty percent of recharge is from irrigation and forty percent is from precipitation. Of the total irrigation, sixty percent is from surface water deliveries and the rest from pumping. This information is important for calculations of the chemical composition of the recharge water which will be discussed later.

Pumping includes municipal and agricultural wells. Pumping rates were determined in Burow et al., (2004) based on data provided by water districts in the study area and by estimates determined from irrigation demands. Domestic wells make a relatively small contribution to the total pumping rates were ignored, following the recommendations of Burow et al. (2004).

Figure 141 shows a color intensity map of the spatially variable recharge to the water table as applied in our model. Figure 142 shows the estimated pumping. This map does not identify depths of the well screens interval, but this data is implemented in our model.

Recharge and pumpage estimates were developed for irrigation districts, which were further broken down into 64 subregions, shown by the various regions in Figure 142.

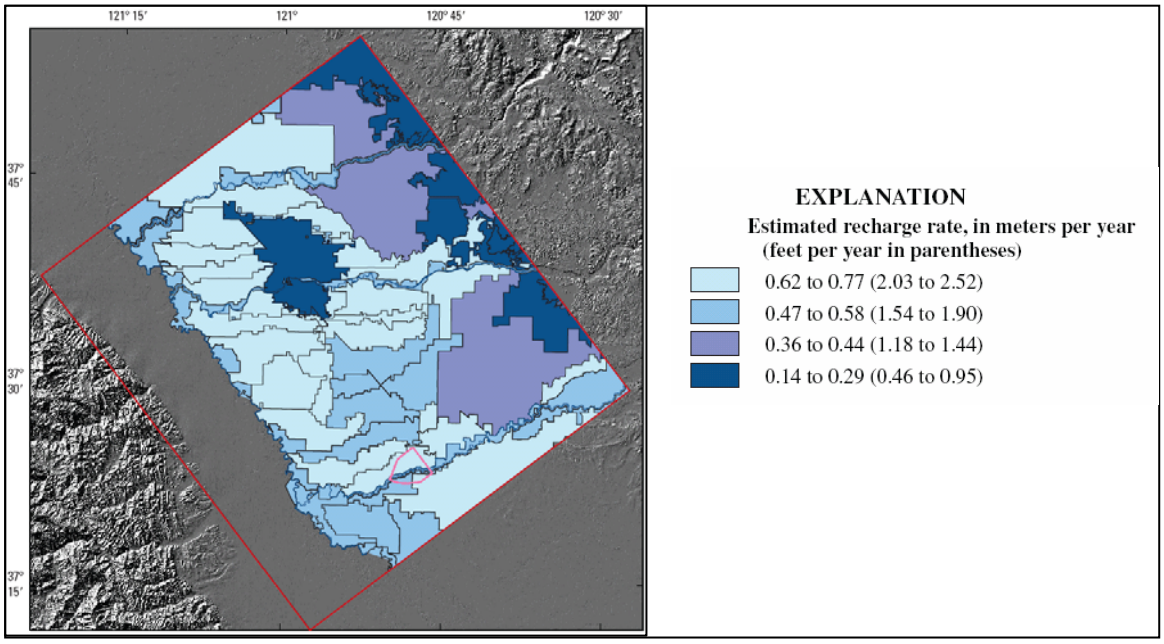

Figure 141

Water-budget: Recharge Map (Source: Phillips et al., 2007)

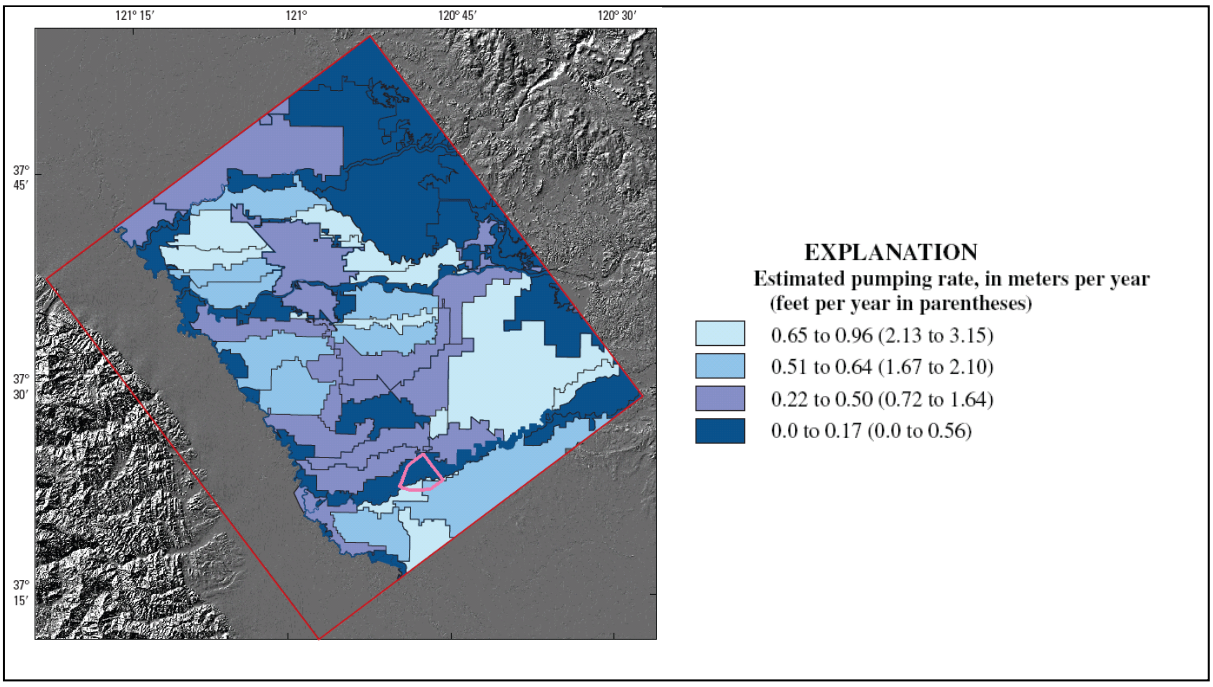

Figure 142

Water Budget: Pumpage map (Source: Phillips et al., 2007)

D. Numerical Modeling of the Study Area

This section provides an overview of the numerical model constructed for the regional study area shown in Figure 134. Our numerical model follows closely the principles and concepts employed in Burow et al. and Phillips et al. (2007), and uses information obtained directly from the USGS numerical model's input files. This section discusses the numerical model's spatial discretization, boundary conditions, sources and sinks, and the hydrogeologic parameters.

Our model is three-dimensional, to allow for modeling the effects of vertical gradients. It is a steady state model based on information from Water Year 2000. Variables such as irrigation, precipitation and pumping were computed on monthly bases, and were then averaged to yield annual rates which were assumed to be constant over time. We are using the GMS (Groundwater Modeling System) pre/post-processor for MODFLOW 2000.

The steady-state modeling strategy is obviously an approximation to a flow regime that is transient in nature. Potential implications of the steady-state flow regime are as follows.

Higher recharge due to reduced pumping rates and increase in infiltration rates would raise the water table and would reduce concentrations. Similarly, a lower water table would increase concentrations. Thus, our model will provide higher or lower estimates of the concentration, depending on the season. It is expected to yield more accurate estimates of annual averages of

the concentration, as these seasonal effects will be wiped out due to averaging.

Another important effect to consider is the variability in flow directions. Rotation of the flow direction due to transients can, under some circumstances, enhances mixing of contaminants in space. This rotation leads to increase in the area affected by the contaminants, but it also leads to dilution and hence reduction in the concentration due to the larger volume of groundwater that mixes with the contaminants. This effect will be noticeable if land discharge occurs in areas with relatively clean ground water. If the groundwater concentrations due to agricultural practices in the areas surrounding the land application sites are of the same order of magnitude, then this effect will be insignificant.

1. Spatial Discretization

The spatial discretization of our model closely follows the strategy implemented in the USGS numerical groundwater model (Phillips et al., 2007). The lateral dimensions of the grid area are 61.20×54.8 kilometers. In plan view, the model area was discretized into a grid of 153×137 blocks with the individual grid block dimensions of 400 meters by 400 meters. This block size is approximately the size of the smallest land discharge area, which is important because it allows us to model accurately the loading of the discharge. In the vertical direction the model area was discretized into five layers, generally of increasing thickness with depth, thus allowing greater resolution at the depths near the water table. The Corcoran clay layer (see Figure 143 and Figure 144) is modeled as a distinct layer because of the large conductivity contrasts with the adjacent layers. The region of the grid to the west of the San Joaquin River was not modeled, so these grid blocks were set as inactive. Figure 143 and Figure 144 provide an aerial view and a vertical cross section of the numerical grid. The elevation of the top layer is taken from digital elevation models developed by the USGS. The thickness of the model ranges between 220 and 430 meters, as shown in a representative cross-section in Figure 144.

The orientation of the model layers follows the dip angle of the sediments. The model axes are generally aligned with the geologic structures of the valley to allow modeling of the hydraulic conductivity and dispersivity as diagonal tensors.

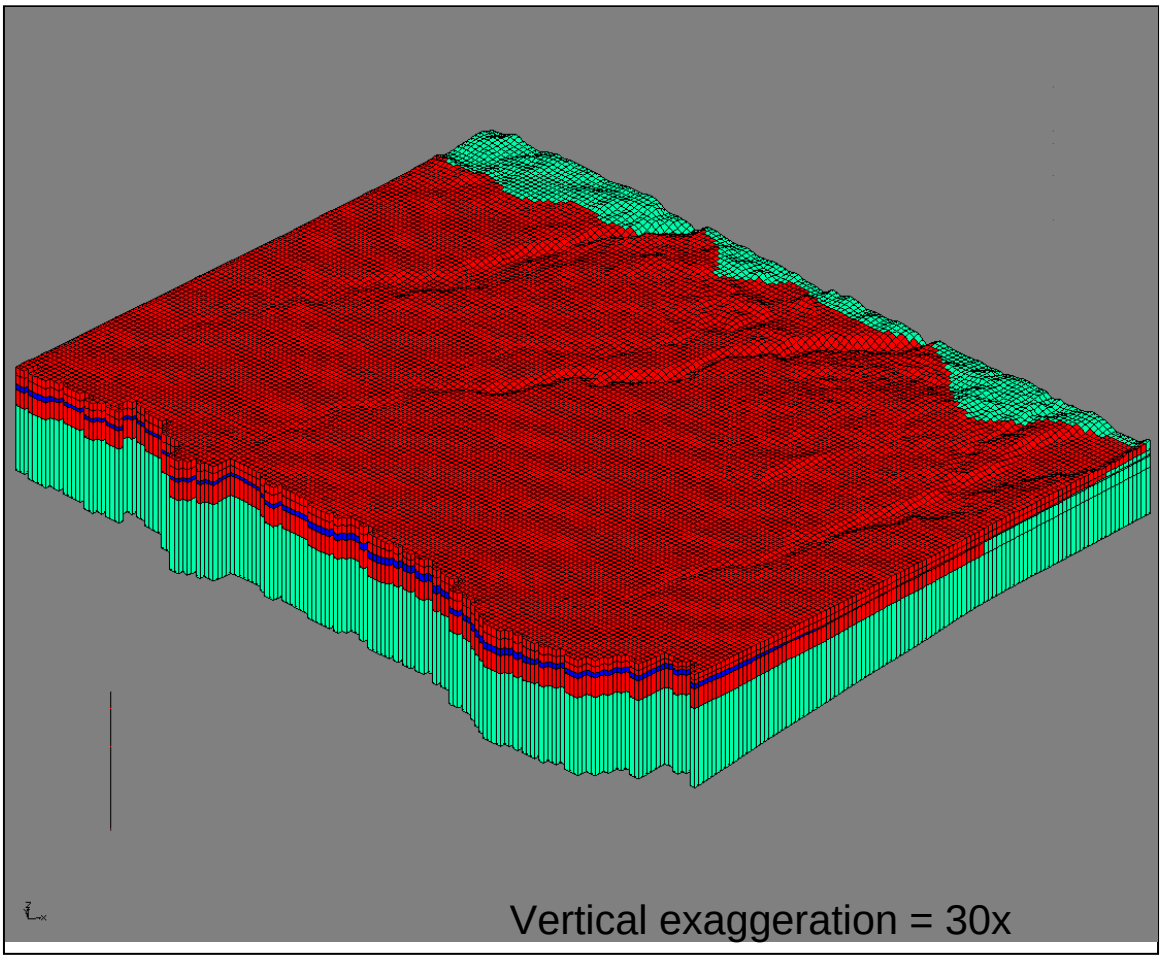

Figure 143

3-D view showing the active portion of the numerical model grid. The Corcoran clay layer is shown in blue, unconsolidated sediments in red and consolidated sediments in green. The elevations of the top of the first layer are derived from the USGS digital elevation model data.

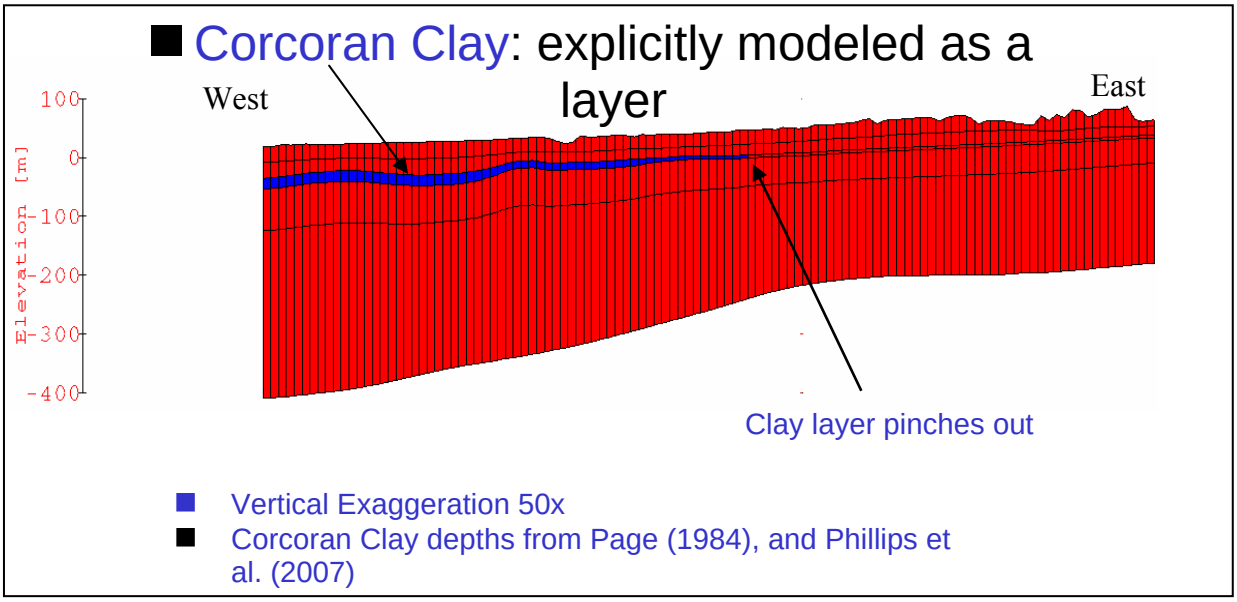

Figure 144

An East-West cross-section showing the five layers of the numerical grid. The cells representing the Corcoran clay are shown in blue. The clay layer pinches out roughly midway through the model area.

2. Boundary Conditions

Boundary conditions are assigned for the lateral boundaries of our study area as well as at the water table, as shown in Figure 145. The easternmost edge of the model at the base of the Sierra foothills was defined as a no-flow boundary. This is based on the assumption that groundwater flow from the foothills is negligible when compared to the flow through the other boundaries. The northern and southern edges were modeled as general-head boundaries using the MODFLOW General Head Boundary package. The western edge of the model along the San Joaquin River was also modeled using the general-head boundary package. This allows for pumping induced cross-flow from under the river. Figure 145 shows a map of the lateral boundary conditions.

The bottom of the aquifer is set at depths determined by the USGS that represent topographic variability and the general dip of the Corcoran Clay and which is assumed to be deep enough to avoid any undesirable modeling effects on the flow regime (Phillips et al., 2007).

The water table was modeled as a flux boundary, based on the spatial distribution of recharge shown in Figure 141. Following the findings of Phillips et al. (2007), the recharge rate for all sub-regions shown Figure 141 had to be reduced by 10 percent in order to achieve numerical convergence in the flow model.

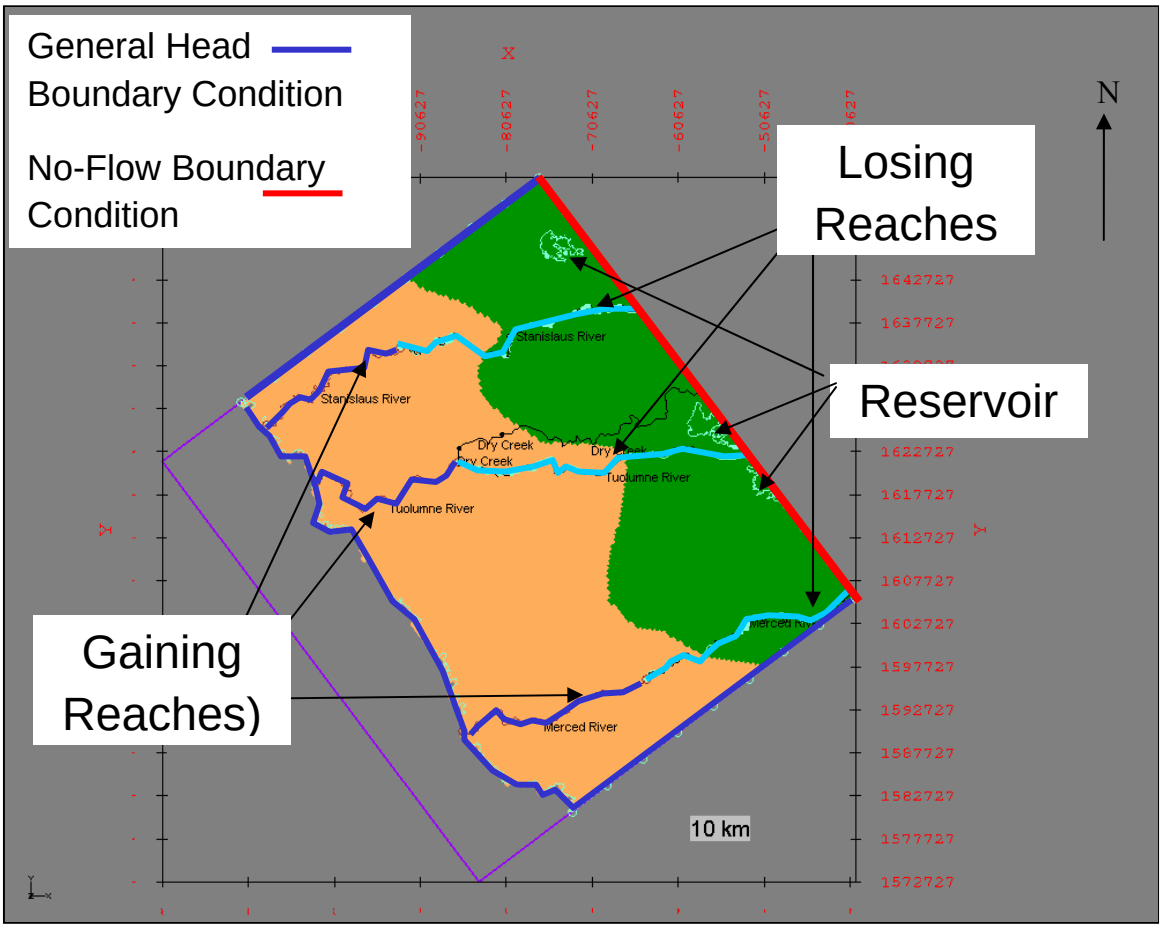

Figure 145

Lateral boundary conditions and included surface water features.

a) Pumping Wells

Pumping wells were modeled using the MODFLOW Well Package. The location and pumping rates of the wells are based on the USGS model (Phillips et al., 2007), as shown in Figure 146 and 147. No grid refinement was carried out around pumping wells. If well locations were not known, then wells were evenly distributed within a sub-region and pumping rates defined to add up to total estimated pumpage for the sub-region, as described in Phillips et al. (2007).

To approximate the depths of the screened intervals the pumping rates were only assigned to the layers of the model that most closely matched the screened intervals. The current model has only 5 layers as compared to the 16 layers in the USGS model, so the depth resolution of the screened intervals is limited by the layer thicknesses.

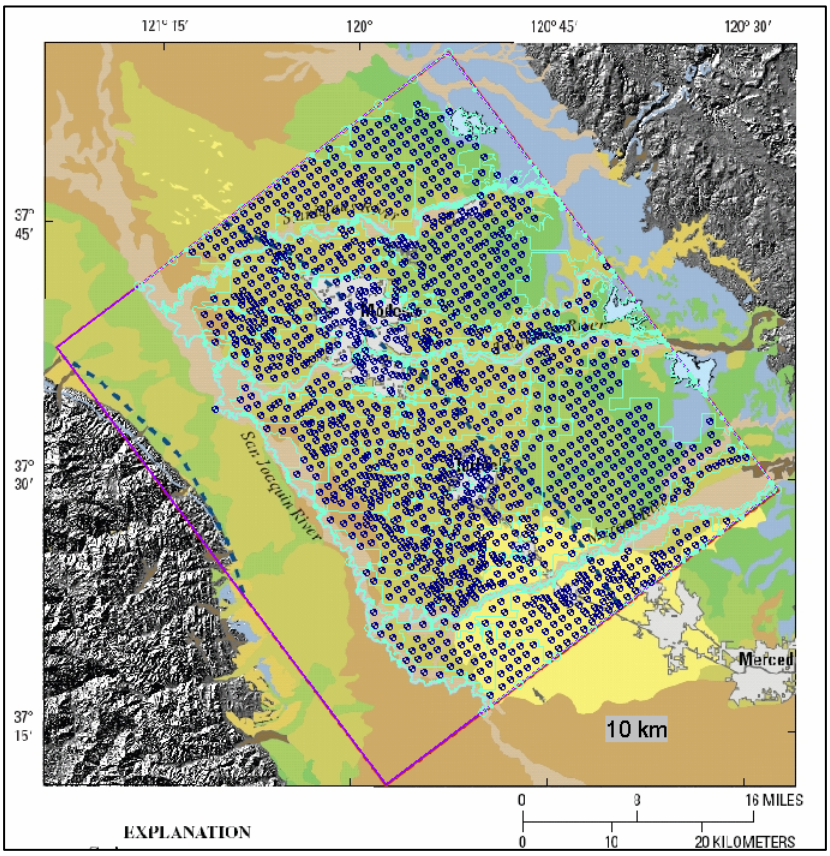

Figure 146

Map showing location of pumping wells (blue circles) in the numerical model (base map from Phillips et al., 2007).

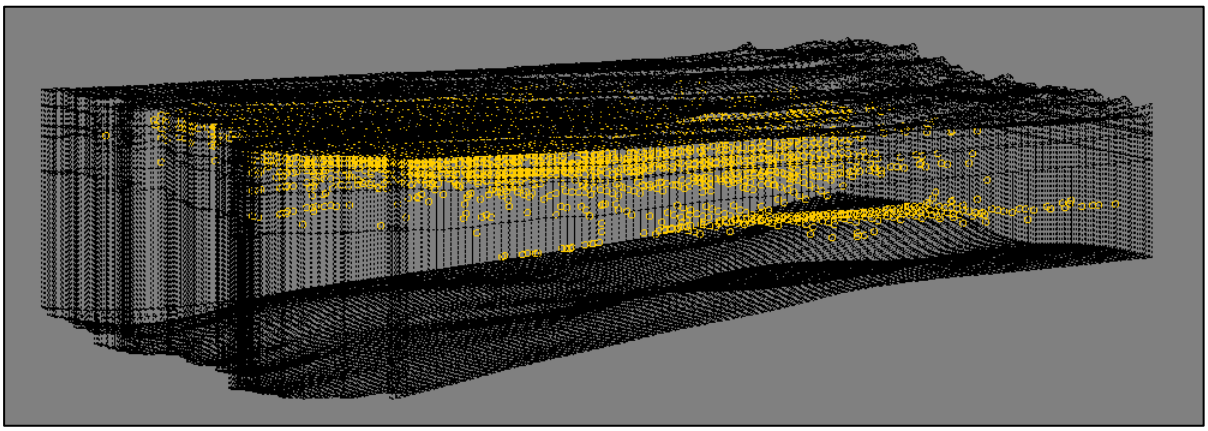

Figure 147

Three dimensional view of the pumping well locations in the model. The yellow circles are located in the center of each grid cell defined as a pumping well. Vertical exaggeration is 30x.

b) Evapotranspiration

Evapotranspiration (ET) was simulated using the MODFLOW Evapotranspiration Package. The evapotranspiration package models ET with a maximum rate of ET_0 at the land surface, decreasing linearly to zero at extinction depth. The USGS value of $ET_0 = 0.043$ m/day was used and is line with the annual average determined from data from the CIMIS website for the water year 2000, $ET_0 = 0.0039$ m/day. The extinction depth of 2.1 meters was also used based on the value used in the USGS model.

c) Ground-Water / Surface Water Interactions

Leakage from the three reservoirs along the eastern edge of the model was simulated by applying an additional recharge based on estimated leakage rates from the reservoirs. The river/groundwater interactions were modeled in the same fashion as in the USGS model. Gaining reaches were modeled with General Head Boundary conditions. The prescribed heads were based on River stage measurements. The losing reaches of the rivers (in the upslope regions) were modeled by applying recharge over the losing reaches [0.005 m/day]. The locations of the different surface water zones are shown in Figure 145.

3. Hydrogeologic Parameters

For a steady-state model, the important parameter to consider is the hydraulic conductivity. Two strategies are commonly pursued in this regard. The first calls for high-resolution modeling the spatial distribution of the hydraulic conductivity, and the second allows modeling the conductivity field through the effective conductivity. Each of these two strategies is suited for different situations, due to their advantages and limitations. An extended discussion of this topic is provided in Rubin (2003, Chapter 5), which includes numerous references to previous works.

We modeled the conductivity field through the effective conductivity. Such an approach is suitable for computing average fluxes in large-scale applications, and when modeling contaminant transport from large, distributed sources, such as is the case for land application sites. The most general definition for the hydraulic conductivity is given by the Batchelor bounds, which are equal to the harmonic and arithmetic averages of the hydraulic conductivity. The geometric mean of the conductivity can be viewed as a convenient choice for an effective conductivity somewhere in the Batchelor bounds range, although it is not rigorous because the geometric mean is the effective conductivity for flow which is essentially two-dimensional and for a symmetrical histogram of the log-conductivity (Rubin, 2003). However, we are going to compensate for this by working with a range of values within those bounds, and we will not limit ourselves to just a single value.

Effective conductivity tensors were computed for each of the 4 lithological units regions shown in Figure 148 and 149. The four units in our model are as follows:

- Corcoran Clay Layer
- Western Area above Corcoran Clay
- Western Area below Corcoran Clay
- Eastern Area (upslope region)

Phillips et al, (2007) provide histograms of calibrated hydraulic conductivities values for all units except the Corcoran clay which is assumed to be of uniform and isotropic conductivity and its value was determined through calibration, and was set equal to 1.3×10^{-3} m/day. This is larger than the core sample values of the clay because of enhanced conductivity due to drilling and possibly fracturing (See Section 9C). Additional discussion is presented in Phillips et al. (2007).

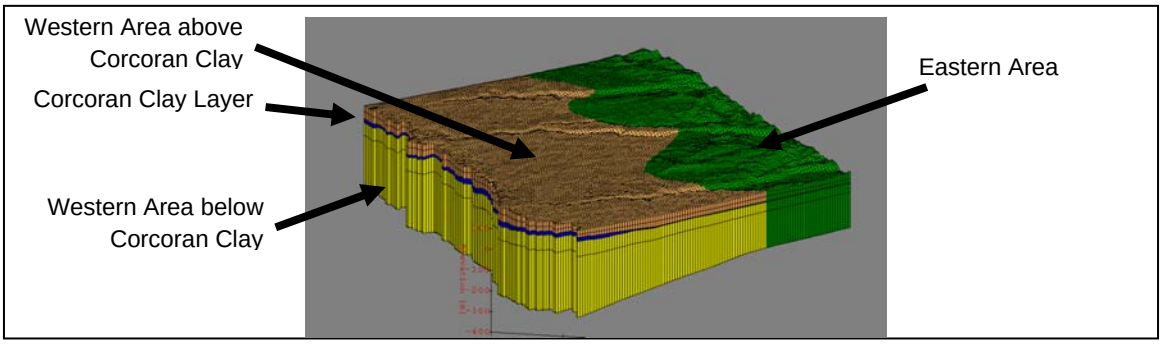

Figure 148

3-D view showing the four different lithologic regions in the numerical model.

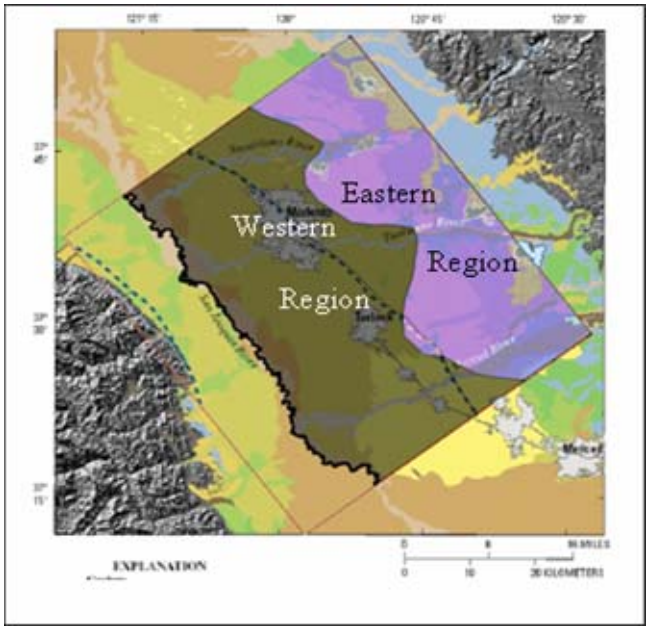

Figure 149

Map view showing the Western and Eastern lithologic regions in the numerical model.

Hydraulic conductivity values were based on the distribution of grid block conductivity values from the USGS model. As stated earlier, the Batchelor bounds for the effective conductivity are defined by the harmonic and arithmetic averages of the conductivities, with the geometric mean lying somewhere next to the middle of this range. All these averages were computed for each zone were used to assign a mean value to each zone in the current model. A variance was also determined for each zone. These will be used to develop different conductivity realizations for Monte Carlo simulations. Table 53 below provides the arithmetic, geometric, and harmonic means of the four lithologic regions, as well as the ratio of horizontal to vertical hydraulic conductivities

Table 53: Table listing the harmonic, K_H, geometric, K_G, and arithmetic,K_A, means of the four lithologic regions shown in Figures 148 and 149, as well as the ratio of horizontal to vertical hydraulic conductivities (K_{hor}/K_{vert})

Lithologic Subregion	K_H [m/day]	K_G [m/day]	K_A [m/day]	K_{hor}/K_{vert}
Western Area above Corcoran Clay	18.80	39.80	84.20	300
Western Area below Corcoran Clay	11.90	25.30	53.50	300
Eastern Area (entire thickness)	11.	23.25	49.20	300
Corcoran Clay	1.3×10^{-3}	1.3×10^{-3}	1.3×10^{-3}	1

4. The Effects of Spatial Variability

As stated earlier, the hydraulic conductivity field is homogenized over large portions of the study area. This modeling decision has two complementary implications with regard to the effects of spatial variability. The first implication is that these effects are lumped into the effective parameters and are modeled only in an average sense, whereas the second one is that these effects are minor in the context of this study. There is an extensive discussion in the scientific literature on this topic, including in Rubin (2003).

Modeling the spatial variability of the conductivity is a decision that depends on the length scales that characterize the flow and transport problem. Modeling its effects depend on the relationship between length scales of heterogeneity (the integral scale) and the dimension of the solute body, travel time and distance. Numerous studies have shown that an integral scale that is small compared to the other length scales justifies the use of effective parameters except for evaluating small scale effect. Larger length scales may have pronounced effects on spatial variability in the concentrations. Such effects may be significant at early travel times (short travel distances), but will peter out with time and travel distance due to the effects of dispersivity.

The purpose of this section is to evaluate the effects of the large scale heterogeneity on the concentration. It follows the investigation of extensive well-logs in the study area by Burow et al. (2004), that indicate the possibility that buried paleo-channels of coarse-grain sediments may exist parallel to the course of the current river channels, as seen for example to the south of the Tuolumne River in Figure 150. These paleo-channels could potentially act as fast pathways of salinity transport. The channeling effect created by contrast between the higher hydraulic conductivity of the channel deposits could lead to sharper concentration fronts.

To study the possible effect that such a channel (or channels) would have on the rate and extent of spread of salt away from the land discharge areas, a synthetic paleo-channel was introduced into the model domain as a narrow band of coarse-grained material with hydraulic conductivity

of 80 m/day, running parallel to the Merced river, as shown in Figure 18, and located directly below the land discharge area for a food processor. This location and the very high value of hydraulic conductivity were chosen to represent what can possibly represent "worst-case" scenario and thus should provide a conservative view of the potential impacts. There is no documentation on the existence of such a paleo channel at this area. The rest of the hydraulic conductivities were kept at the geometric mean for each lithologic zone. The dispersivities were kept the same as in the other runs (α_L =19.2 m, α_L /α_T = 10).

The series of figures below (Figures 152-158) compares the spatial distribution FDS in a homogenized flow field with the distribution in a field with a paleo-channel, emphasizing the differences caused by land discharge. In order to capture the effects of the channel on the spatial distribution of the FDS we calculated the differences in FDS between due land application, in flow domains with and without the channel. Specifically, we computed ΔFDS= FDS (with land Discharge) – FDS (without Land Discharge) in a field without the channel and again in a field with a channel. The difference between these two cases captures the effect of the channel while suppressing all other effects.

What we note from these figures is that the effects of the channel appear to be local. The channel in our simulation enhances the downstream migration of the solutes by a distances of a few hundred meters (corresponding to the dimension of the yellow spot the yellow spot corresponding to X=8 km in Figure 158), but this further downstream migration leads only to a small increase in concentration, of the order of 300 mg/L, and it is limited to Layers 1 and 2. This change can be expected when the channel passes directly underneath the land discharge area, and if its axis is aligned, to a large degree, with the flow direction. Otherwise, it is less noticeable. While the potential exists, in general, for a significant effect on the migration of solutes, our testing shows this effect to be somewhat limited here, primarily due to mitigating action of the lateral dispersivity and the vertical gradient, which act together to divert mass out of the channel, and in this way diminishes significantly its capacity to conduct mass over large distances. This conclusion should be viewed in perspective: a well located a short distance downstream from a land discharge area, pumping its water from the channel, will experience significant effects on the concentration that cannot be predicted using a homogenized conductivity field. Overall, however, given the well locations (Figure 146), the depth to the screened intervals, and the prevalence of channeling (see Figure 150), it appears that only a small number of wells can possibly be affected by the presence of the channels. Thus, it is justified to adopt a uniform conductivity field in the context of this study. For local effects, a more detailed characterization of the conductivity field is needed.

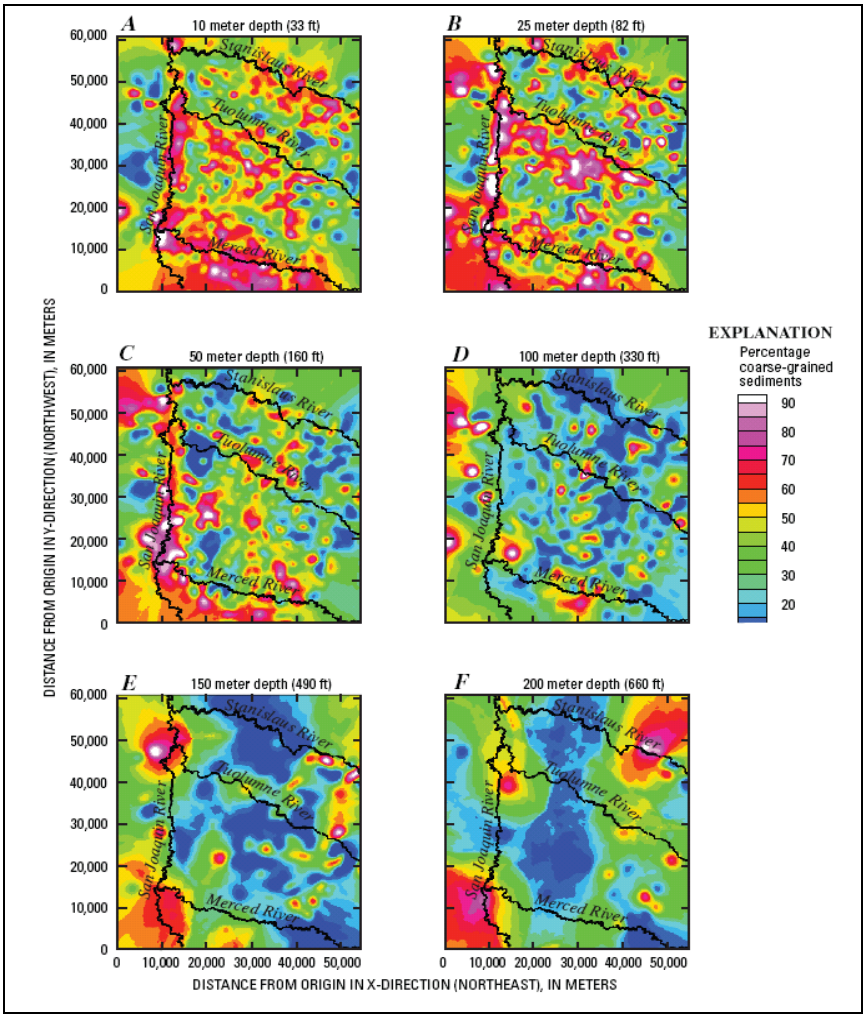

Figure 150

Horizontal planar views through three-dimensional model of percentage coarse-grained sediments in study area (source: Burow et al., 2004). The red, elongated structures at the top maps suggest the presence of paleochannels. These structures disappear at larger depths, suggesting the presence of channels only at shallow formations.

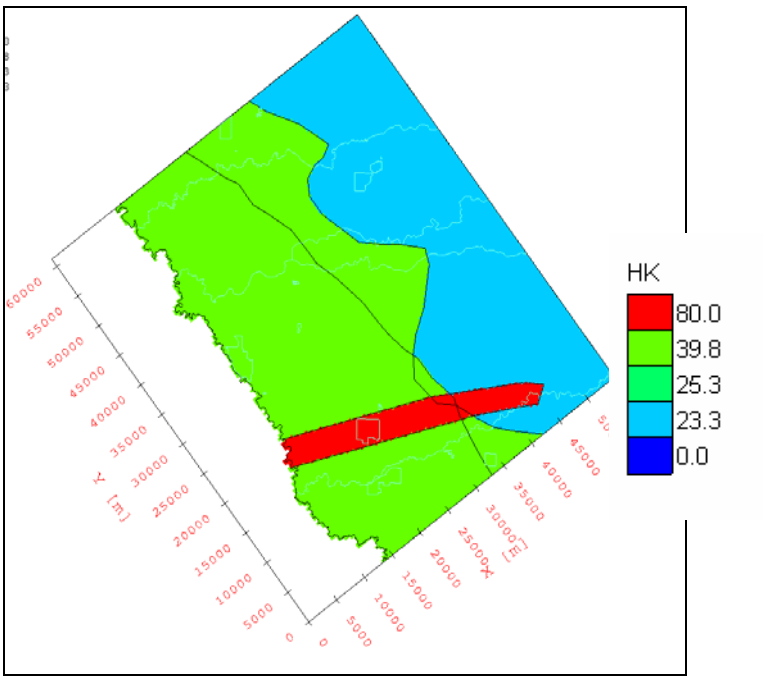

Figure 151

Hypothetical hydraulic conductivity map for layer 1, which is used to analyze the effects of paleo channels on transport of FDS in the saturated zone. Values shown on the color bar are in meters per day. The red area represents a hypothetical paleo-channel with a relatively high conductivity, passing through a land application area in the study area.

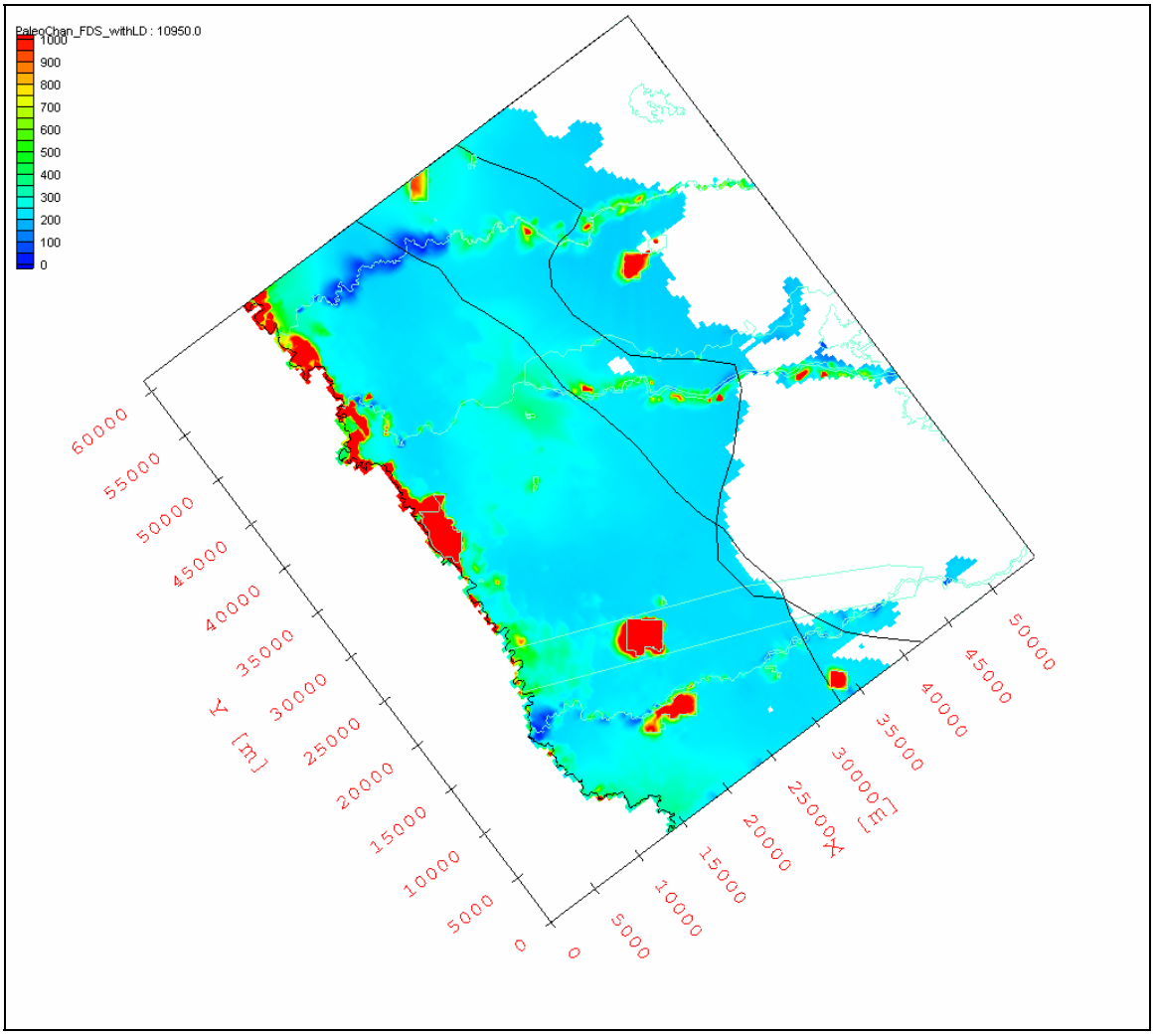

Figure 152

30 year FDS concentration in Layer 01 with paleo-channel. Color bar in mg/L and cutoff at 1000 mg/L.

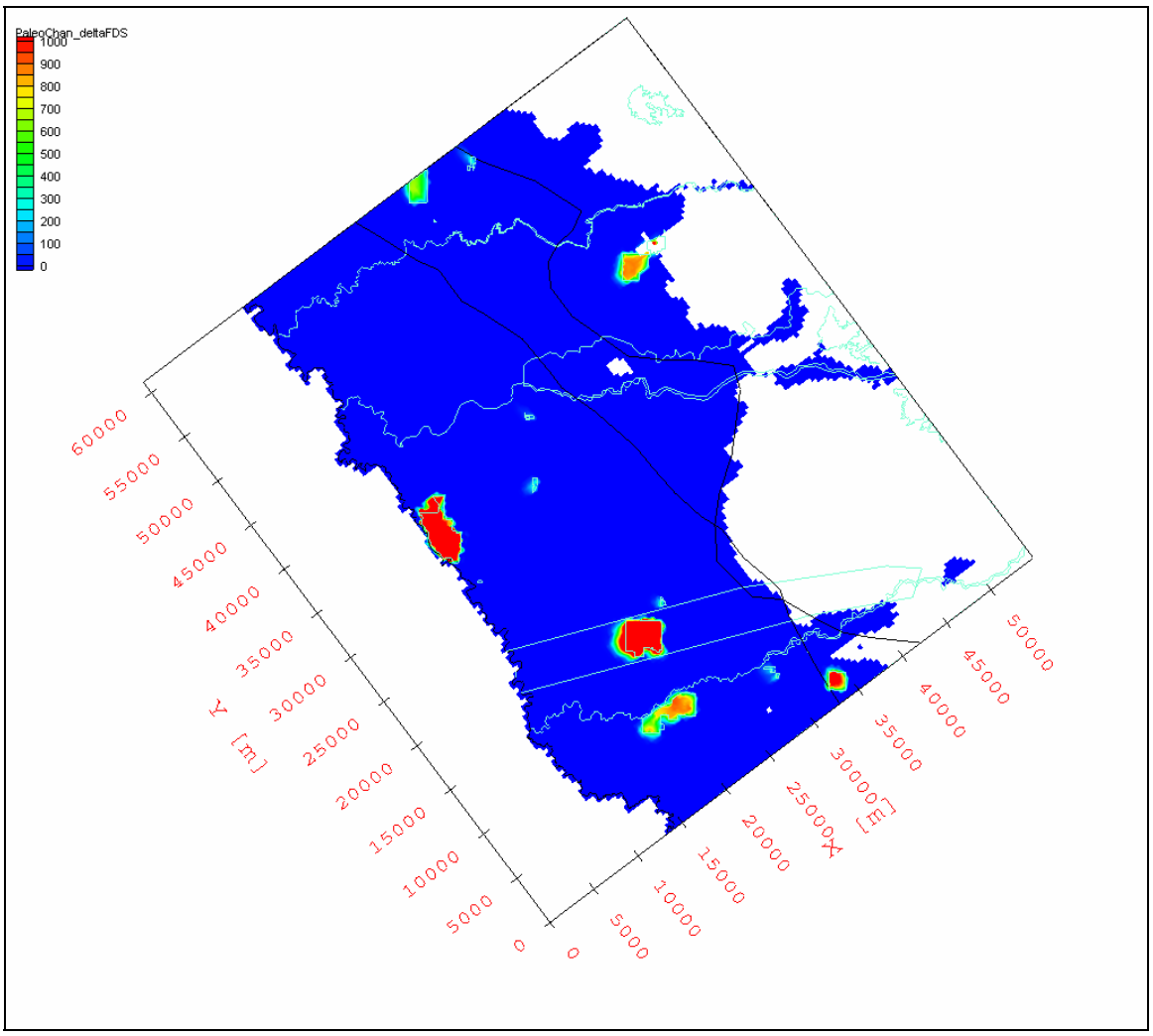

Figure 153

Differences in FDS in Layer 01 with simulated paleo-channel, showing the ΔFDS= FDS (with land Discharge) – FDS (without Land Discharge). Color bar in mg/L and cutoff at 1000 mg/L The outline of the simulated paleo-channel is visible in light blue. This map cannot be used to analyze the significance of the effects of the channel unless compared with a similar one obtained assuming no channel, as shown below.

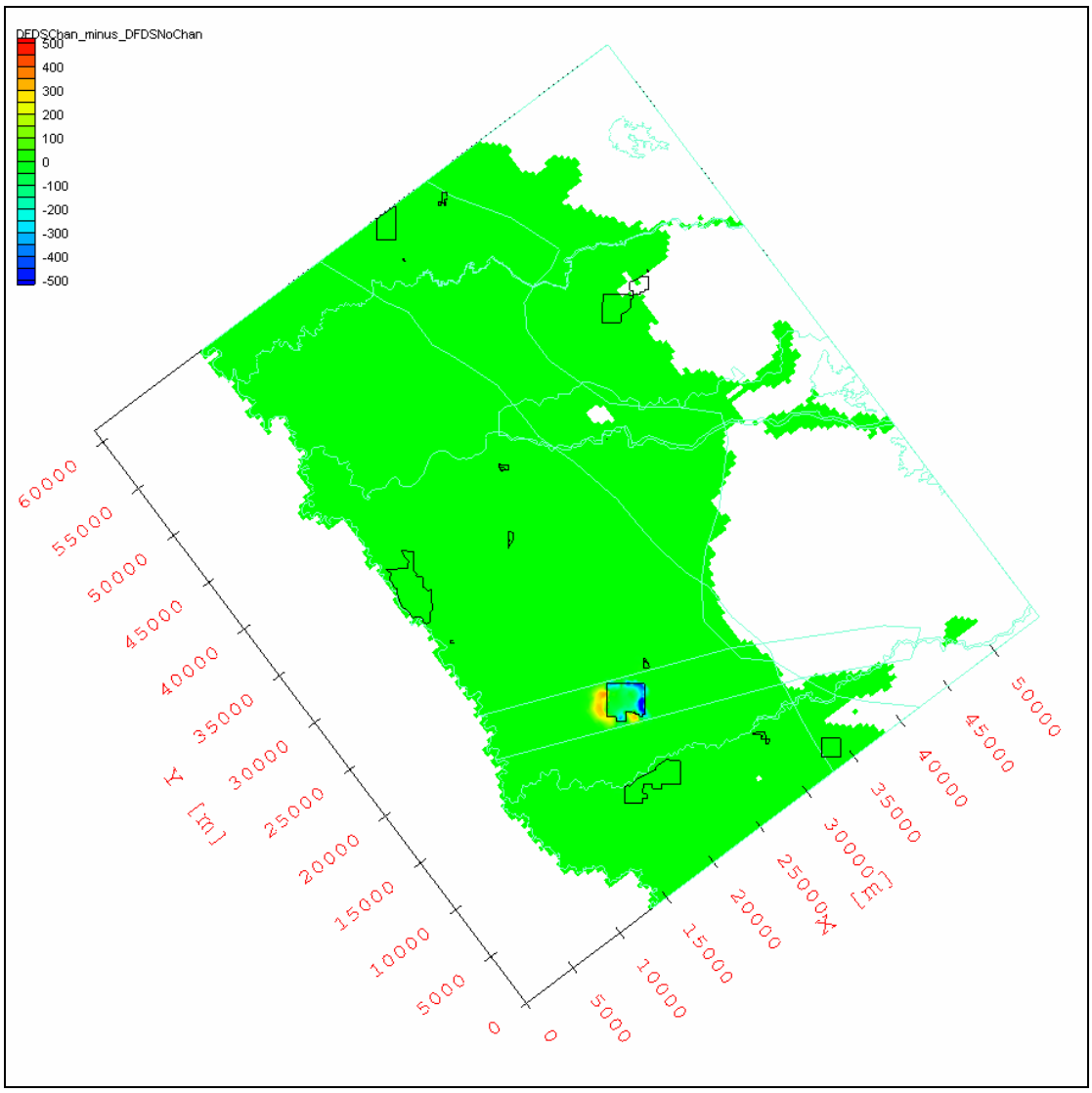

Figure 154

This map shows the difference between ΔFDS= FDS (with land Discharge) – FDS (without Land Discharge), computed with the hypothetical paleo-channel, and ΔFDS without the paleo-channel, in Layer 01. Color bar is in mg/L. This shows the effect a coarse-grained paleo-channel would have as compared to no channel, in the form of differences in concentrations. The plume concentrations are higher at the leading edge of the plume, but are smaller at the tail end.

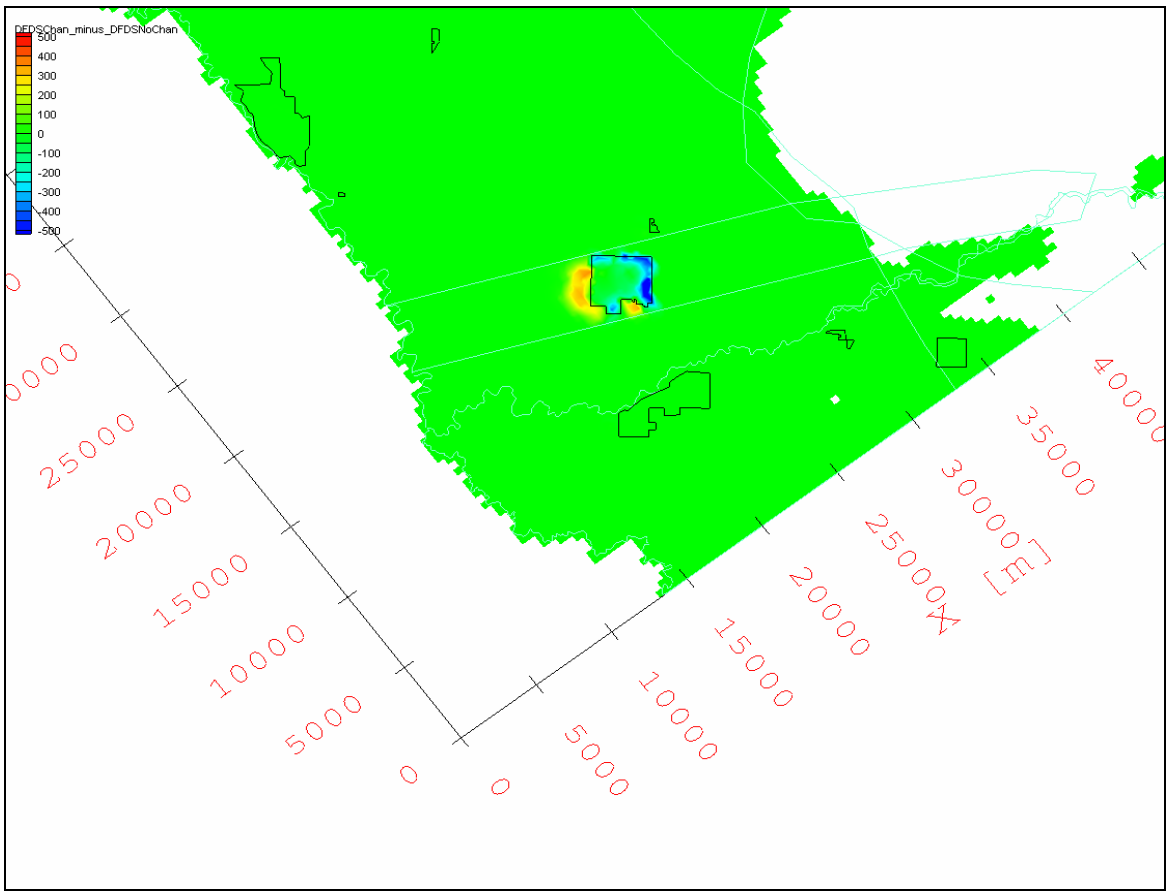

Figure 155

This map shows a zoomed- in view of Figure 154 the difference between ΔFDS with the paleo-channel and ΔFDS without the paleo-channel, in Layer 01. Color bar in mg/L. This shows the effect a coarse-grained paleo-channel would have as compared to no channel. The plume concentrations are higher at the leading edge of the plume, but are smaller at the tail end.

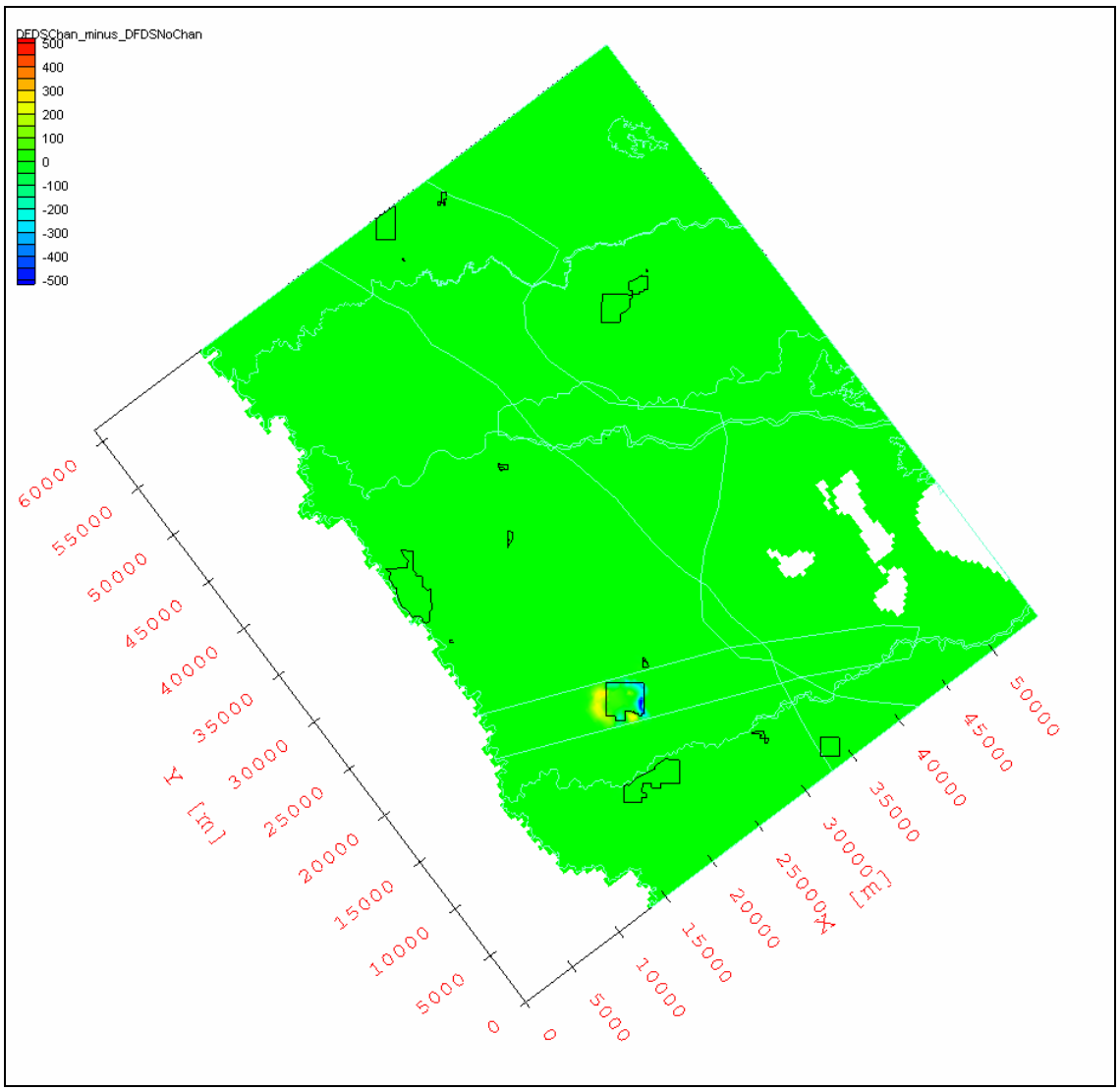

Figure 156

This map shows the difference of ΔFDS with the paleo-channel and ΔFDS with out the paleo-channel, in Layer 02. Color bar in mg/L. This shows the effect a coarse-grained paleo-channel would have as compared to no channel. The plume concentrations are higher at the leading edge of the plume, but are smaller at the tail end.

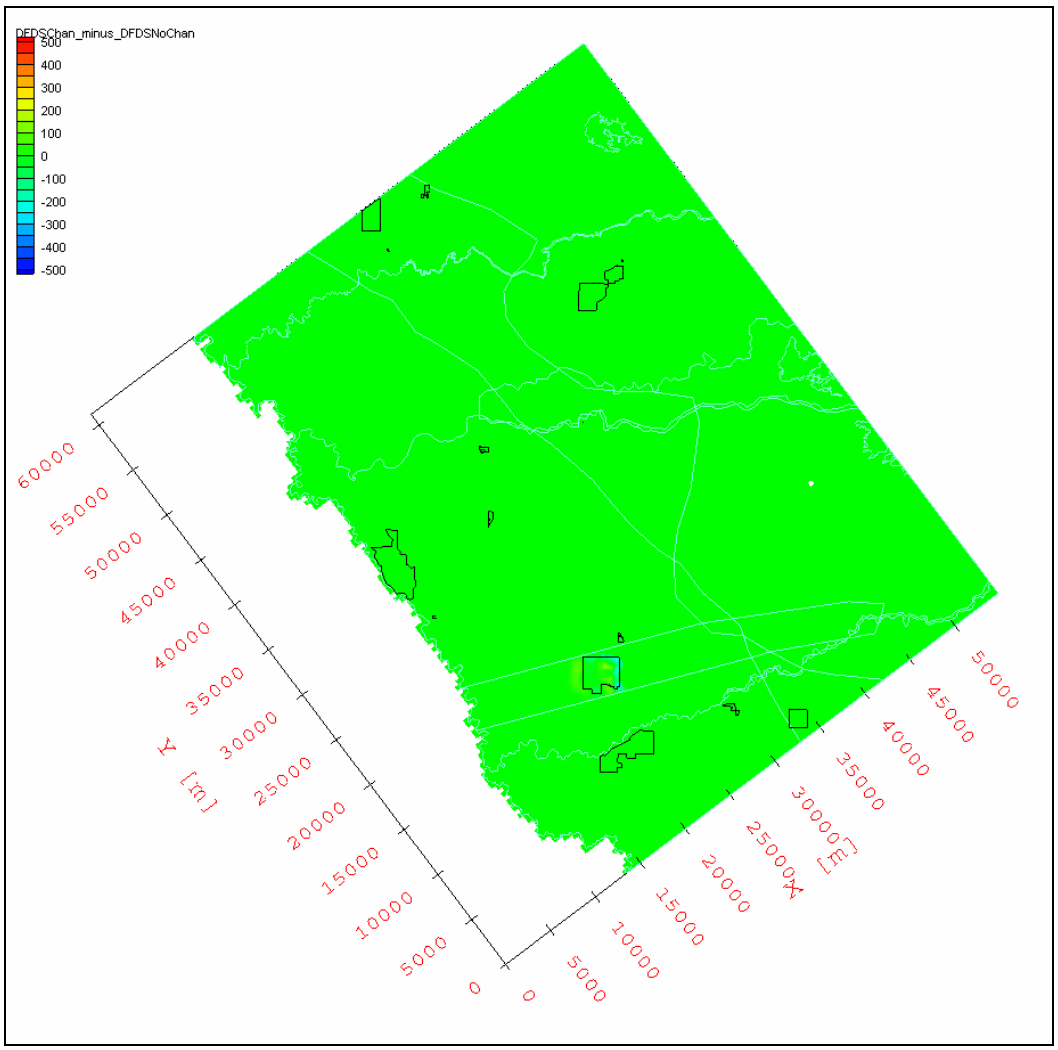

Figure 157

This map shows the difference of ΔFDS with the paleo-channel and ΔFDS with out the paleo-channel, in Layer 03 Color bar in mg/L. It shows the effect a coarse-grained paleo-channel would have as compared to no channel. The effect of the channel is greatly diminished at greater depths.

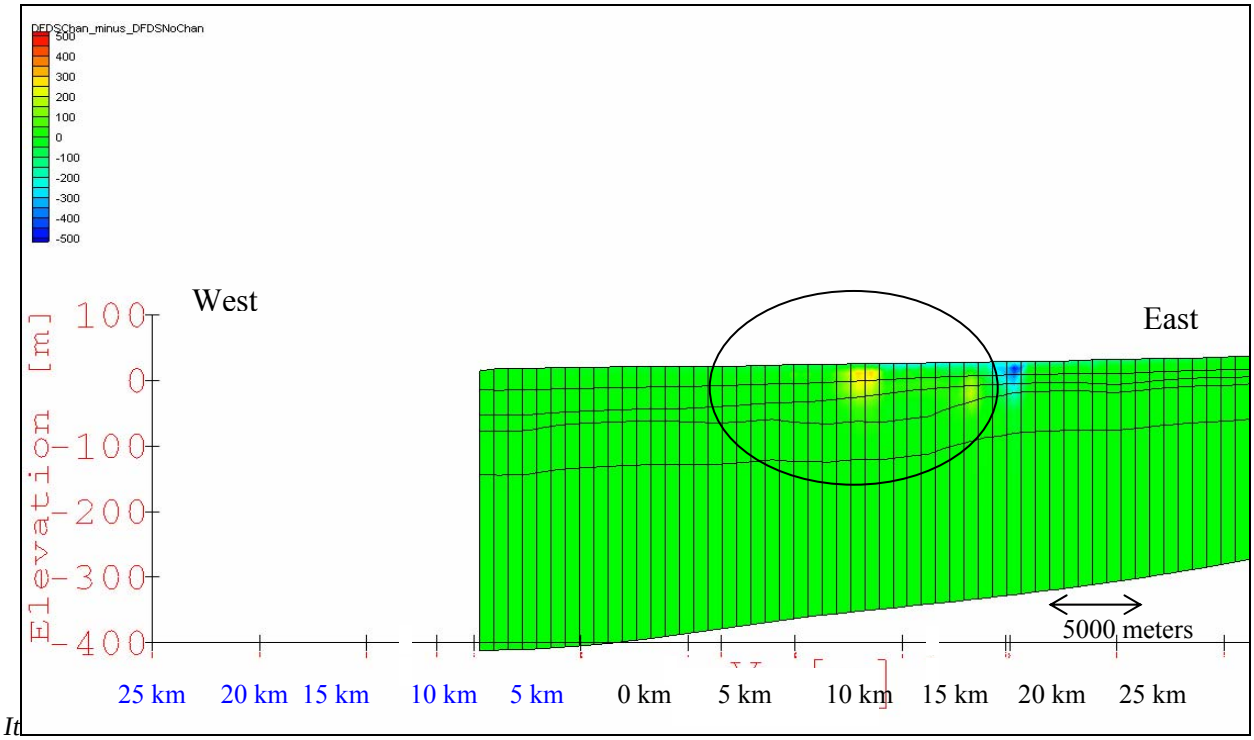

It

Figure 158

This Figure shows a cross-section view with the color scale representing the difference of ΔFDS with the paleo-channel and ΔFDS without the paleo-channel, in Layer 01. Color bar in mg/L. This Figure shows the effect a coarse-grained paleo-channel would have as compared to no channel. The differences in concentrations are positive at the leading edge of the plume, and negative at the tail end. The vertical exaggeration is 30x. In the view below we are seeing projections of the X- and Y axes onto the East-West plane.

E. Results of Flow Model

Our model was built based on the USGS model, which went through extensive testing. We augmented this testing by comparing the numerically computed water table elevations with the observed ones, which is presented here. Figure 159 identifies the location of the observed water table elevations for the spring of 2000 used for our analysis. Figure 160 and 161 show contour maps of the observed and computed water table elevations, respectively.

Figure 162 is a scatter plot of the observed and computed water table elevations. The match between observed and computed values is not perfect (root mean square error of 3.8 m), but it is not expected to be, for several reasons. First, the resolution of the numerical model, basically the numerical grid block size, is different from the actual measurement scale. Second, water table elevations are affected by local variations in hydrologic input and soil properties which cannot be captured by numerical model due to data scarcity of the data needed for fine-scale characterization. Next, our model is steady state whereas the measured water table elevations

reflect the actual conditions at the day of the measurement. The observed values, for example represent spring water levels when the water table would be expected to be higher than the annual average. However, we note the existence of a strong correlation between the computed and observed water table elevations. This is a solid indication with regard to the suitability of our model for the purpose of this analysis.

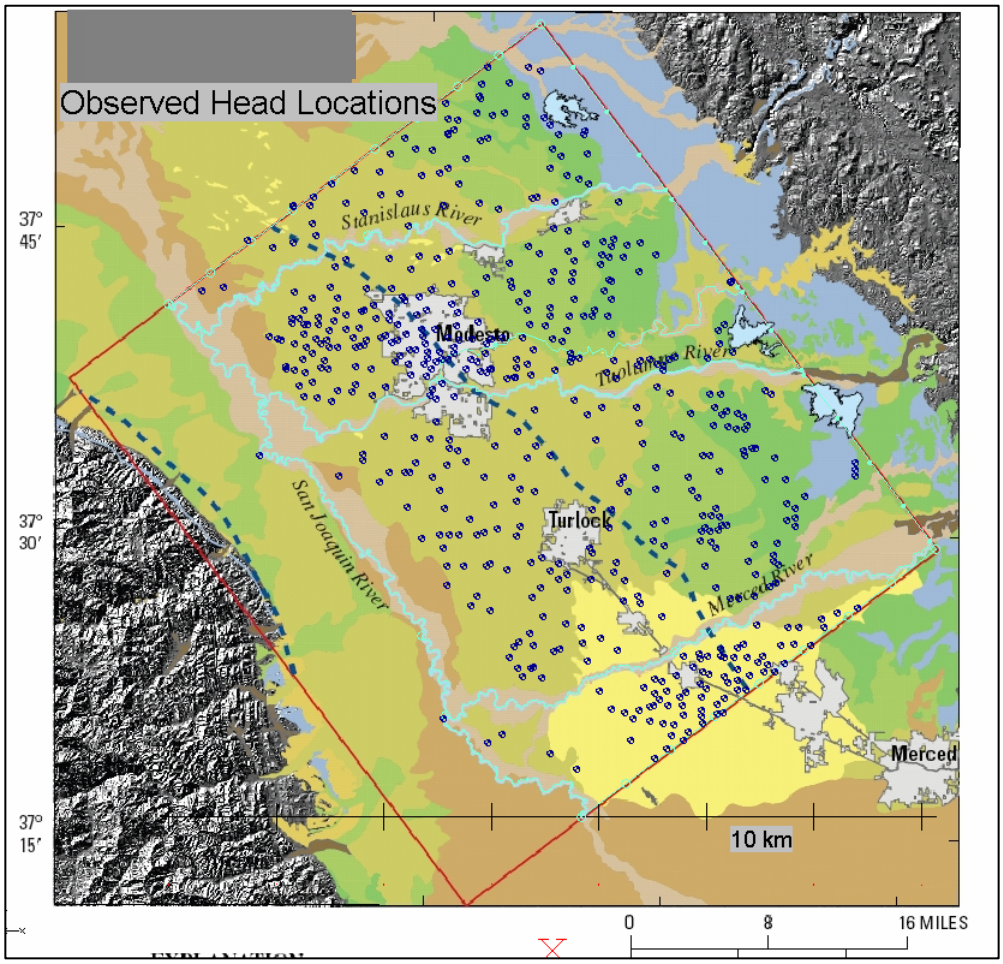

Figure 159

Location of observed water levels for Water Year 2000 from DWR online source [base map from Phillips et al., 2007]. The dashed lines show the lateral extent of the Corcoran clay layer.

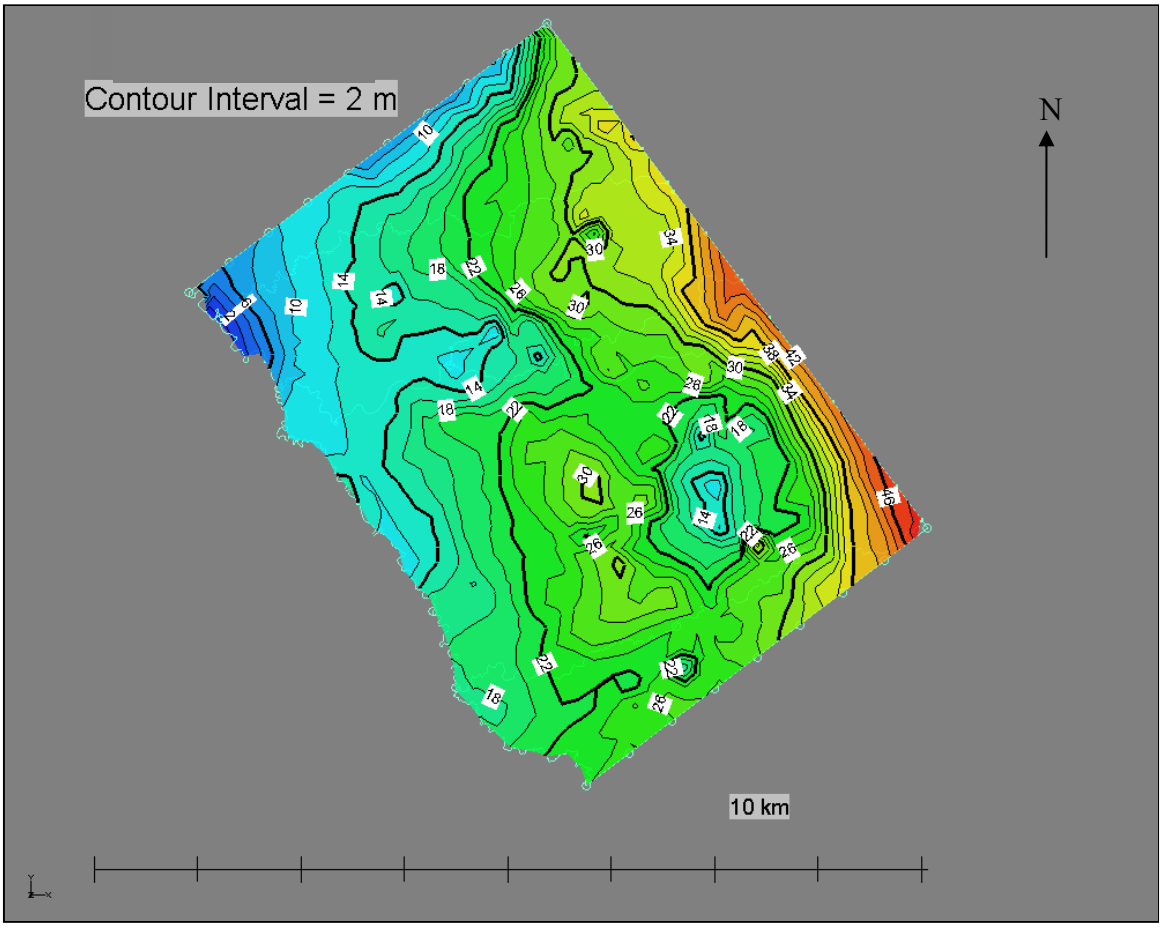

Figure 160

Contour map of the water table for Spring of the Water Year 2000. The contour interval is 2 meters; red corresponds to areas of higher water table elevations and blue to lower water surface elevations.

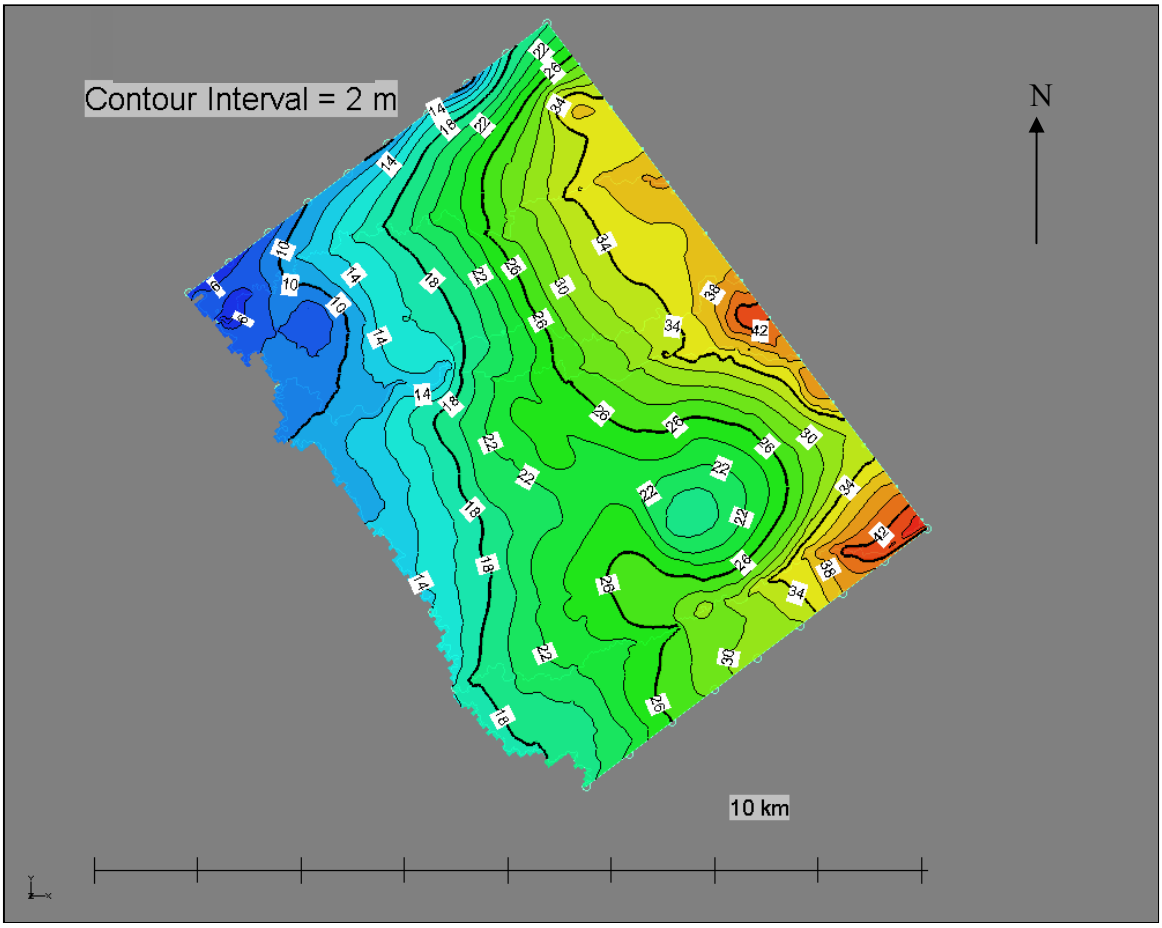

Figure 161

Contour map of computed water table elevations. The contour interval is 2 meters; red corresponds to areas of higher water table elevations and blue to lower water surface elevations.

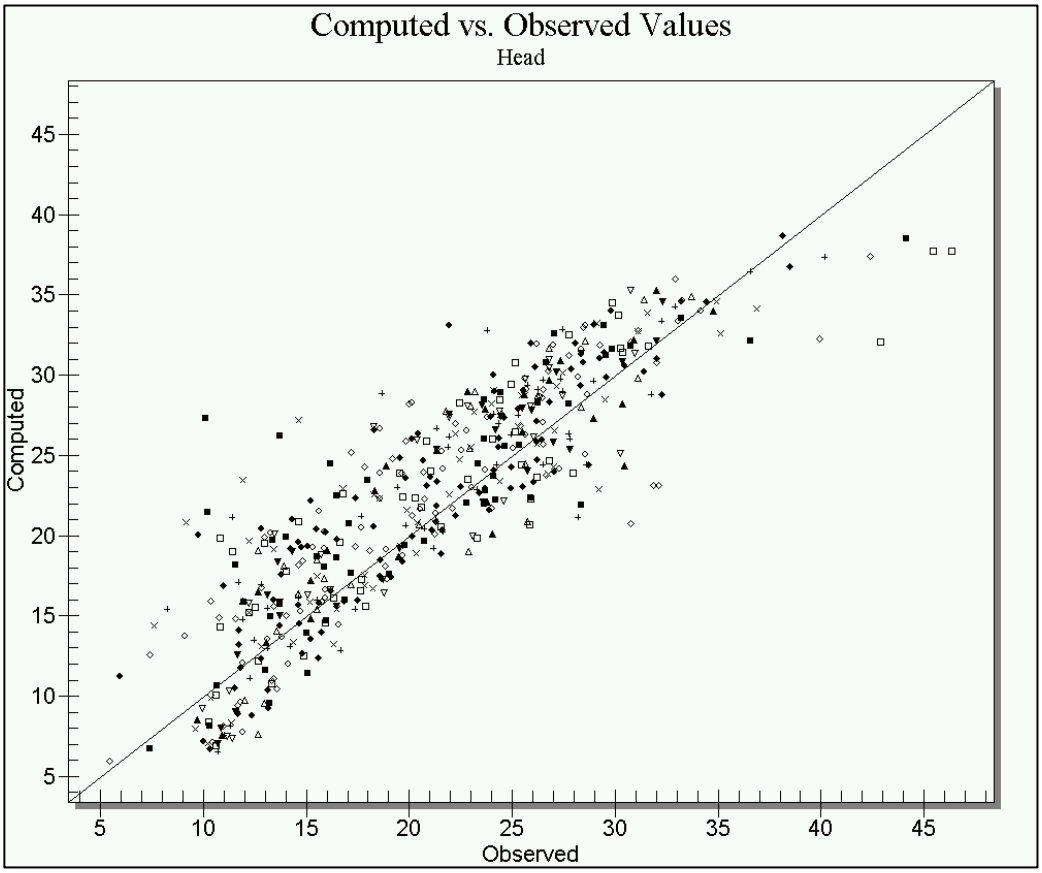

Figure 162

Plot of Computed head values versus observed head values (meters)

F. Salinity Transport Modeling

1. Numerical Model

MT3DMS was used as the numerical engine for the salinity transport modeling. It provides us with the capability to capture the evolution in time and space of the FDS concentration field in the study area under a wide range of conditions. We used the code to numerically solve the transient advection dispersion equation in 3-dimensions. Fixed Dissolved Solids (FDS) is modeled as a non-reactive, non-sorbing tracer. MT3DMS is very well documented and widely in use, and we will not present it here in any detail.

2. Solute Transport Parameters

There are several issues that need to be addressed in this context. The first issue is the adequacy of modeling contaminant transport using large numerical grid blocks. Large numerical grid blocks are not suitable for modeling contaminant transport from point sources. However, the land application sites are of the order of hundred of meters, much larger than the length scale of heterogeneity of the conductivity field. Under these conditions, large blocks are suitable for computing space-averaged concentrations and fluxes.

Large numerical grid blocks are not suitable if high resolution modeling of the concentration field is needed. Such an analysis is needed if one is interested in point values of the concentrations. Such values are of interest from a theoretical point of view, but for applications needed in this study, which involve computing large scale economic impacts, such high resolution modeling is not necessary. Point values of the concentration are of greater concern when dealing with health risks, but again, heath risks are determined based on long-term exposures, which are correlated with space and times averages of the concentration and not with point values.

The second issue is concerned with determining an adequate strategy for modeling the effects of spatial variability. In our approach, the large-scale effects of the spatial variability of the conductivity field on contaminant transport are modeled directly on the numerical grid, by assigning different conductivity values to different regions of the numerical model. The effects of the small scale variability are modeled using macrodispersion coefficients. The macrodispersion coefficients need to account for the effects of sub-grid block scale spatial variability on transport. This is the spatial variability that is characterized by scales of the order of meters in the horizontal directions, and dozens of centimeters in the vertical direction, and it the one that is wiped out due to the uniformity of conductivity over the numerical grid blocks.

An extensive discussion of this topic is provided in Rubin *et al.* (1999, 2003) and in Bellin *et al.* (2004) and our approach in this study follows the strategy outlined in these research papers. To determine the value of the longitudinal dispersivity, we borrow the values of the variance and integral scale of the log-conductivity from the literature (cf., Rubin, 2003, p. 35) corresponding to three-dimensional variability of alluvial fan deposits. To account for uncertainty, we will work with a range of values for the dispersivity ratio, as given below. .

- Alluvial Sediments (Western Area above Corcoran Clay, Western Area Below Corcoran Clay, and Eastern Area)
    - Longitudinal Dispersivity, α_L = 19.2 m
    - Ratio of Longitudinal to Transverse Dispersivity, α_L / α_T = 1 to 20
    - Porosity = 0.30
- Corcoran Clay Layer
    - Longitudinal Dispersivity, aL = 4 m
    - Ratio of Longitudinal toTransverse Dispersivity, α_L / α_T = 1 to 20
    - Porosity = 0.30

3. Initial and Recharge Concentrations

Our transport simulations require that we determine initial concentration for the groundwater. A map for the initial concentration map was generated by interpolating groundwater measurements of total dissolved solids (TDS) from the food processor water well information, and from a USGS water quality data set for the Central Valley compiled in a report by Purkey et al., 2001. A large number of measurements are also available from required reporting by the food processors themselves. To avoid biasing the initial concentrations, we did not include values from source wells immediately down-gradient of the land discharge zones, because these wells represent localized conditions. It is expected that over the large planning horizon, the selection of initial

conditions will be of minor consequence. Furthermore, we will adopt a line of investigation that filters out the effect of initial conditions altogether.

The recharge concentrations of FDS at the areas outside of the land application sites were estimated by calculating a flux-averaged recharge concentration based on the fluxes and compositions of the different sources of recharge water. This is in line with the procedure employed by Schoups (2004)). For each water budget sub-region, a flux averaged recharge concentration, *C*, was calculated using the following equation (based on Schoups (2004) Eq. 4.7)

$$C = \frac{C_{precip} Q_{precip} + C_{gw} Q_{gw} + C_{sw} Q_{sw}}{Q_{tot}} \qquad \text{Eq. 1}$$

where C_{precip} C_{gw}, and C_{sw}, are the source water concentrations for precipitation, groundwater, and surface water, respectively. Q_{tot} is the total recharge flux applied over the model area, and is given by

$$Q_{tot} = Q_{precip} + Q_{gw} + Q_{sw} \; . \qquad \text{Eq. 2}$$

Recharge due to leakage from the three reservoirs shown in Figure 12 was assigned the same concentration as surface water (65 mg/L), as was recharge over the losing reaches of the three rivers. To account for the salinity added due to dissolution of gypsum to the water as it infiltrates through the unsaturated zone (see Schoups 2004), *C* .was increased by about 90 mg/L, to a value of 220 mg/L. This value was found to result in a concentration that more closely matched the initial background concentrations.

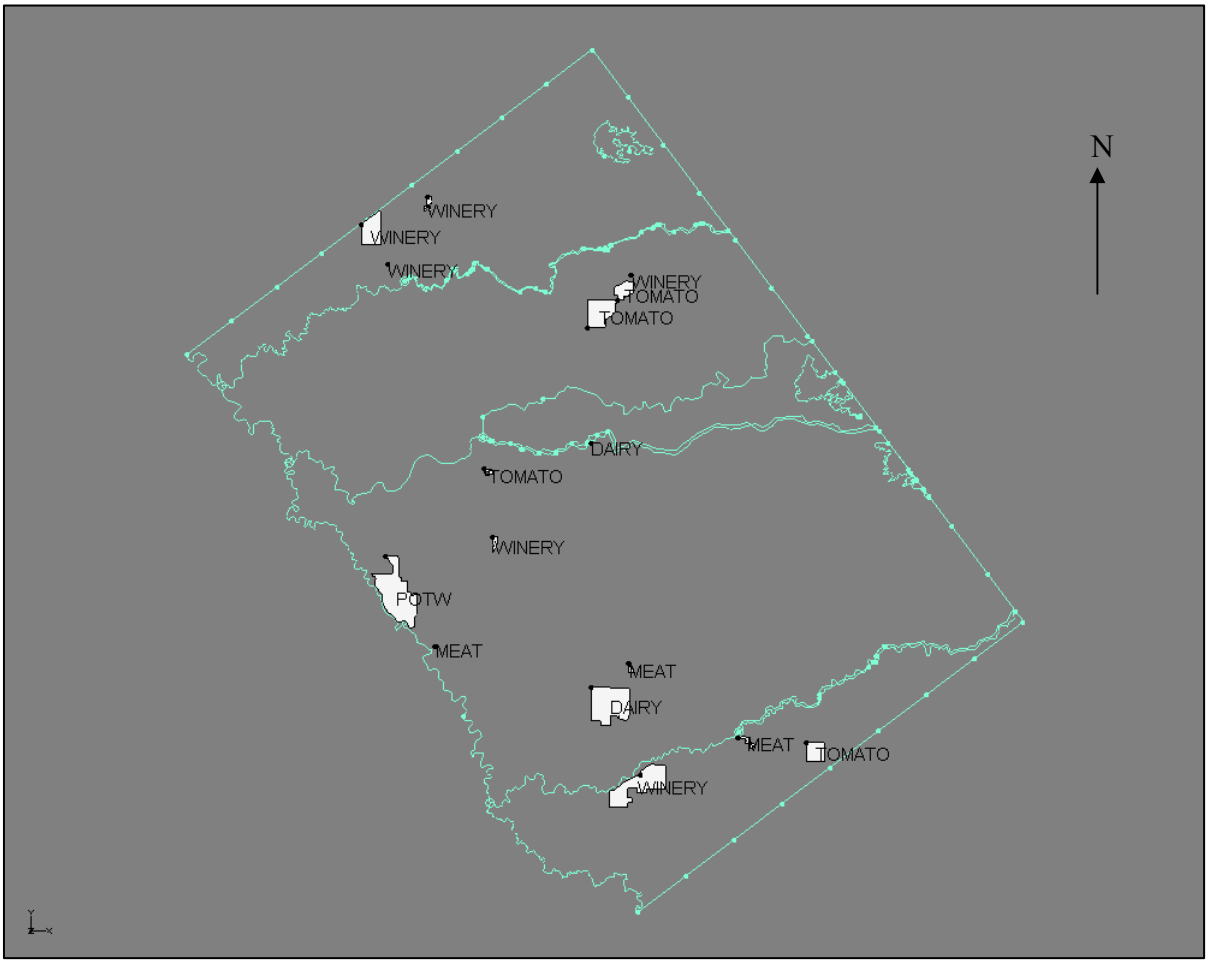

Figure 163

Map showing the land discharge areas (white polygons) for each facility in the regional study area.

4. Food Processor Land Discharge Concentrations

Time-varying salt loads (seasonally averaged over 91.25 day periods) were applied over the total land discharge area for each processor in the model. These salt loadings represent the "transfer functions" from the vadose zone model to the groundwater model, and are the fluxes and loads predicted at the water table by the vadose zone modeling (Section II.2).

Three of the food processing facilities in the model area do not belong to one of the four main industry groups (Meat, Wine, Tomato, Dairy) analyzed in Section II.2. They were assigned salt loads from similar industrial groups.

Land application was assumed to occur over the entire permitted land application area. Our records indicate that it is common practice to apply the effluent over subsections of the total permitted area, rotationally. However, information about the rotation regime is sketchy. The rotation of recharge is expected to reduce concentrations in the groundwater, because it enhances mixing at the edges of the solute body. Hence, our analysis is conservative, in this sense.

Salt Transport Modeling Results

A preliminary perspective on the 30 years design horizon salinity field is shown in the concentration map shown in Figure 164. The parameters used to obtain this perspective are as follows. For the effective conductivity we used the geometric mean conductivity. For macrodispersivity we used 19.2 m and a ratio of 1:10 between both lateral to longitudinal dispersivity and vertical to horizontal dispersivity. This figure shows the evolution of the concentration field due to salinity loading over a period of 30 years, and it suggests that the areas affected are mostly in the close vicinity of the land application sites.

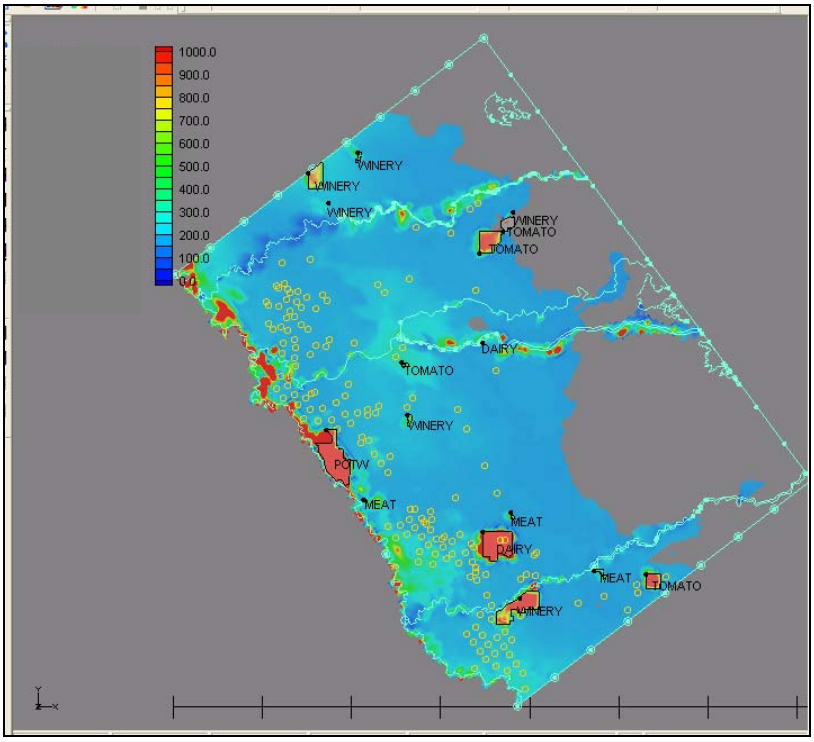

Figure 164

Concentration of FDS (mg/L) at 30yrs in layer 1. Color bar is cutoff at 1000 mg/L (so all red are ≥ 1000 mg/L). The following ratios were employed: $\alpha_L/\alpha_T = 10$ and $\alpha_L/\alpha_V = 10$, where α_L, α_T and α_V denote the longitudinal, transverse and vertical dispersivities. In all our models we assumed $\alpha_V=\alpha_T$.

It is interesting to note in Figure 164 the appearance of concentration's hot spots along several reaches of the Stanislaus and Tuolumne Rivers. These hot spots are unrelated to land discharge operations. They are the result of discharge of saline water from the river into the aquifer at shallow depths and the loss of water due to evapotranspiration, which leads to accumulation of salts. This is confirmed in Figure 165, which identifies (in light blue) the areas where the water table is at less than 2.5 meters below the ground surface, which is assigned as the depth of extinction for evapotranspiration. We note that the light blue areas along the rivers correlate well

with the appearance of concentration's hot spots, and is unrelated to food-processing related land application.

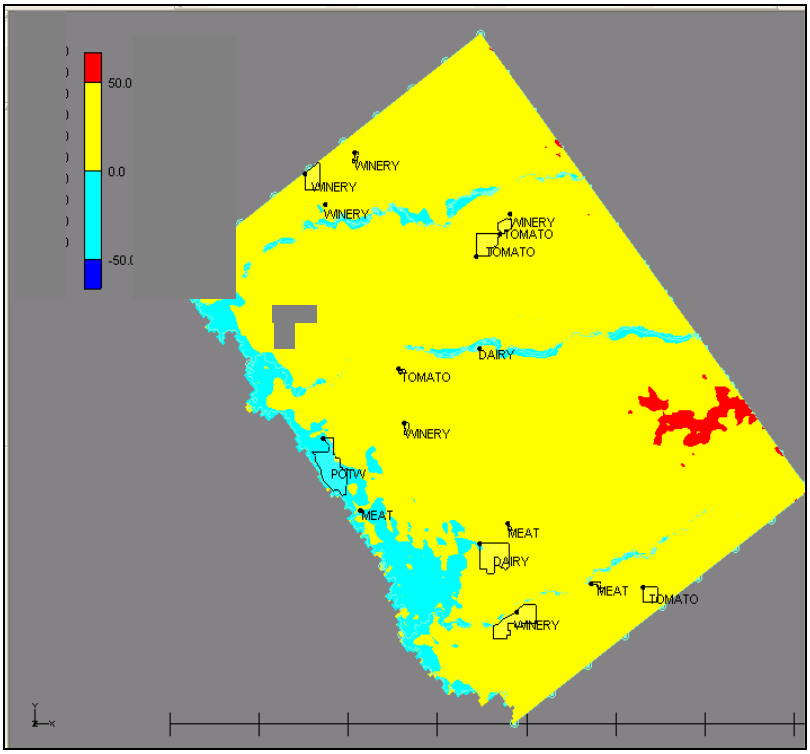

Figure 165

Map of depth to water table less ET's extinction depth (m). Light blue regions show areas where the depth to water table is less than or equal to extinction depth. Such areas are affected by evapotranspiration and are prime candidates for increases in concentrations. This effect is unrelated to food-processing related discharge, unless if taking place in such areas.

Different and complementary perspectives on the effects of land application are provided in Figure 166 and 167. Figure 166 provides an a real view of the difference in concentrations next to the water table at 30 years between the concentration fields with and without land discharge. Figure 167 provides a 3D perspective on that difference. These two figures again confirm the limited spatial extent of the impacts on the concentration due to land discharge.

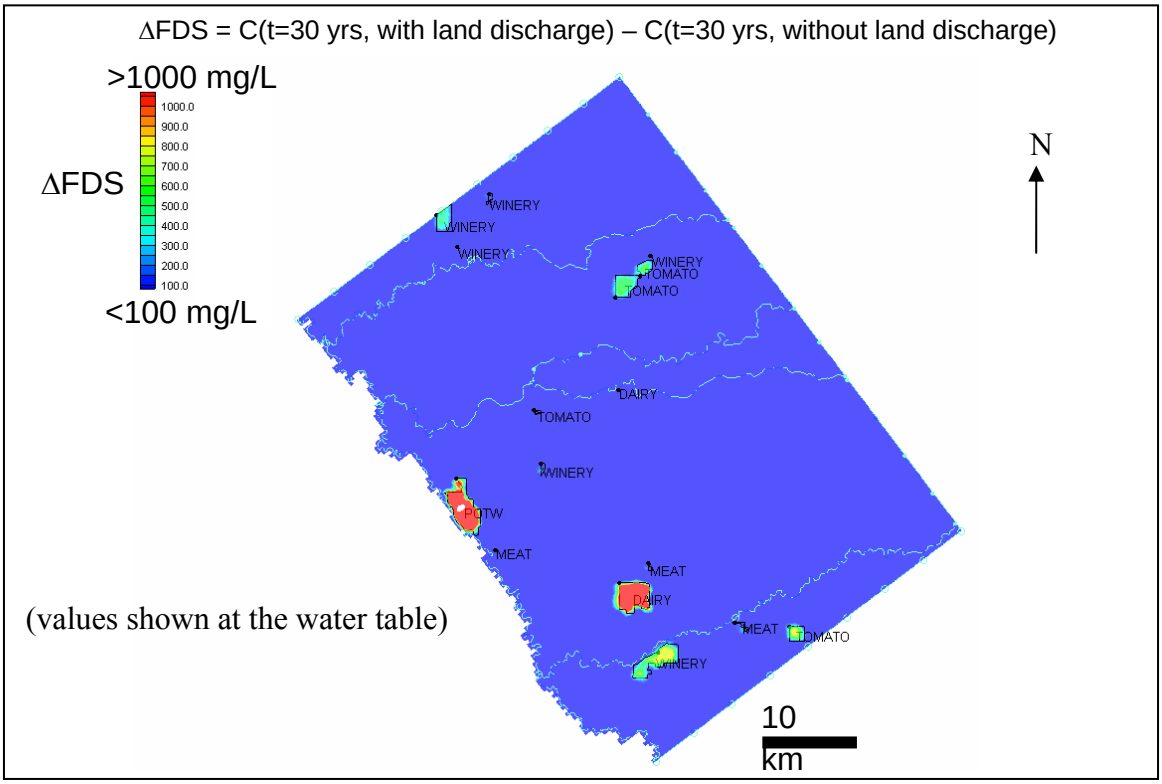

Figure 166

A difference map showing the effect of simulated effluent land discharge after 30 years. ΔFDS = C(t=30 yrs, with land discharge) – C(t=30 yrs, without land discharge). The color intensity scale is cutoff at 1000 mg/l, so anything greater than 1000 mg/L appears as red.

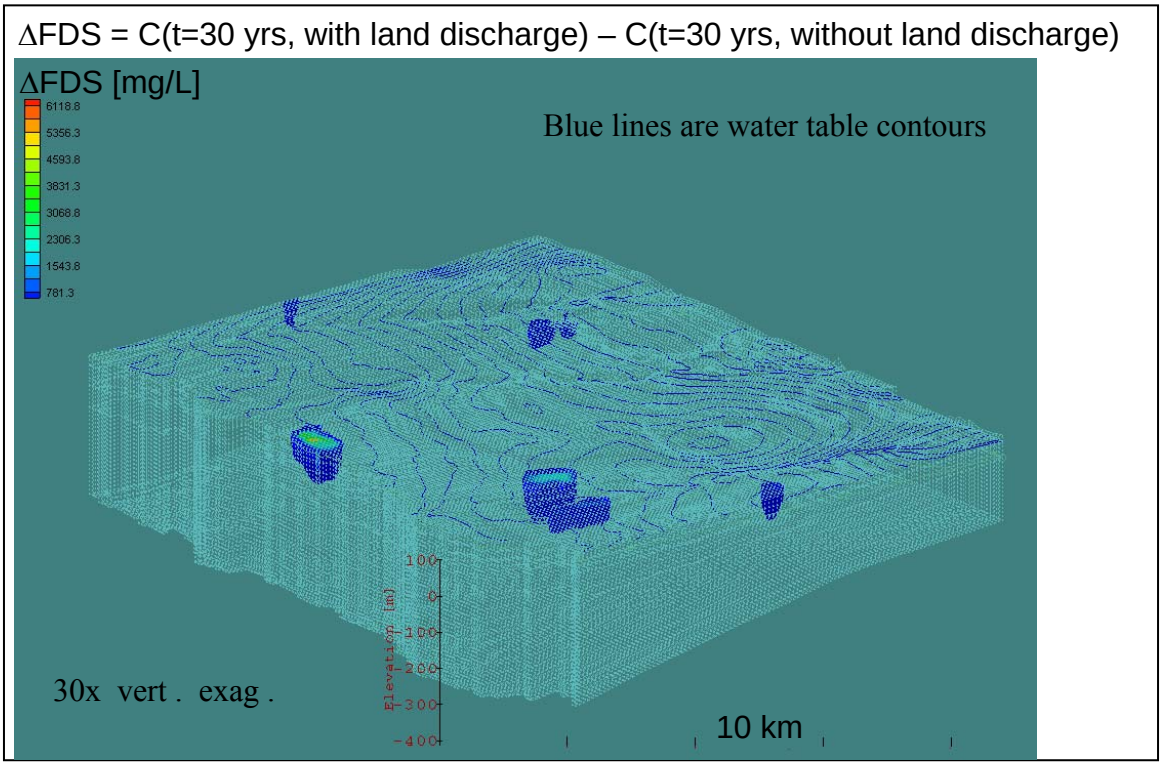

Figure 167

Three-dimensional view of FDS iso-concentrations surfaces. The blue iso-surfaces show the subsurface volumes where ΔFDS ≥ 500 mg/L (relative to 30 yr case with no land discharge).

G. Sensitivity Analysis

This section evaluates the sensitivity of our numerical modeling results to the assumption concerning the ratio between the lateral and longitudinal dispersivities. Let us define α_L α_T as the longitudinal and lateral dispersivities, respectively. The longitudinal dispersivity α_L is used to model the effects of small-scale heterogeneity on the longitudinal spreading of solutes in groundwater, which implies spreading in the flow direction. The lateral dispersivity α_T serves a similar purpose only in the directions orthogonal to the mean flow direction, both in the horizontal and vertical directions. The ratio between α_L and α_T can be determined from field experiments. In the absence of experimental data, it is common to take the ratio α_L/α_T of about 10:1. Our sensitivity analysis explores the effects of this ratio on the concentration field.

In this section we explore the effects of this ratio on the spatial extent of the areas affected by the land discharge. Toward this goal, we will evaluate the evolution of the concentration field in the study area with and without land discharge. We will define $\Delta C(\alpha_L/\alpha_T)$ as the difference at a given point in time between the two concentrations fields (obtained by subtracting the "no land discharge" from the "land discharge" case). For a complete picture, we will look at $\Delta C(\alpha_L/\alpha_T)$ for the ratios α_L/α_T equal to 1, 10, and 20. Towards this goal, we will look at the spatial

distributions of $\Delta C_I(\alpha_L/\alpha_T=1)$, $\Delta C_B(\alpha_L/\alpha_T=10)$, and $\Delta C_{II}(\alpha_L/\alpha_T=20)$, all computed at 30 years. For clarity, note that a positive $\Delta C(\alpha_L/\alpha_T)$ implies an increase in the concentration due to land discharge.

Figure 168 shows the spatial distributions of the differences for the various ratios and at different depths, from a regional perspective. The maps shown cover the entire study area, and are difficult to interpret locally, but they provide the general impression that there is little sensitivity of the spatial extent of contamination to this ratio. In all cases, the effects appear to be localized.

Differences between the various ratios are expected at the local scale. A larger ratio α_L/α_T will enhance longitudinal spreading on account of lateral one. In essence, a larger ratio will lead to cigar-shaped plumes, and smaller ratios will lead to more spherical looking plumes. We will take a closer look at these effects, but from the regional perspective, again, it appears that the effects are limited to the close vicinity of the discharge areas.

Figure 169 provides a closer look at the difference maps for the two ratios α_L/α_T of 1 and 20, which are the two end points of the investigated range of ratios. It can be noticed by looking at the dairy facility at the southern part of the study area that larger $\alpha L/\alpha T$ ratios enhance the longitudinal spread in the westerly direction. We also note that the α_L/α_T =20 case leads to larger differences in concentrations compared to the α_L/α_T =1 case, which are indicated by the prevalence of red hot spots over green, that is particularly visible in the winery located as the southern part of the study area. This is because the solute mass spreads over a smaller volume when moving in geological flow domains of higher α_L/α_T ratios which tend to channelize the solute mass. It is expected that higher ratios will have lower vertical spread as well.

The statistics of the differences in concentrations between the α_L/α_T =20 and α_L/α_T =1 cases are shown in, Table 54 obtained by analyzing close to 104,000 grid nodes. The α_L/α_T =20 leads to the largest differences in absolute value, both positive and negative, with both being the outcome of the channeling effect. The negative differences are somewhat surprising, because land discharge adds solute mass to the aquifer, and one should not expect a reduction in concentration anywhere, but only increases or no changes. However, the negative differences, which are of the order of magnitude of the background concentration, indicate channeling of the initial solute mass in the aquifer away form the high initial concentration areas, which leads to reduction in concentration. The negative values are not real physical effects, but only an artifact of working with a uniform set of initial conditions for all numerical simulations.

In order to filter out this artifact, it is beneficial to evaluate the difference in the differences $\Delta C(\alpha_L/\alpha_T)$, namely ΔC_I-ΔC_B and ΔC_{II}-ΔC_B . This allows evaluating the effects of the land discharge while avoiding any numerical artifacts. Figures 170 and 171 evaluate these differences at the vicinity of the Hilmar Facility, at the southern part of our study area. With blue indicating a decrease in concentration, green indicating near-zero changes and red indicating regions with an increase in concentration, we note that the ratio α_L/α_T =1 leads to larger concentrations going deeper into the aquifer, and to lower concentrations in the shallower portions of the aquifer, closer to the ground surface. This is due to the enhanced lateral spread that characterizes the

α_L/α_T =1 case, that enhances mass transfer in a direction orthogonal to streamlines.

Table 54: Table showing statistics of the concentration differences for each the three scenarios of dispersivity ratios

	Scenario	ΔC_I	ΔC_B	ΔC_{II}
	α_L/α_T	1	10	20
ΔFΔS [mg/L]	Min	-147.4	-356.072	-472.153
	Max	7019.335	10296.12	10926.08
	Range	7166.736	10652.19	11398.23
	Mean	10.72933	12.15585	12.47542
	Median	0.024673	0.00119	0.000641
	Stdev	113.128	151.5622	165.8521
	N	104805	104805	104805

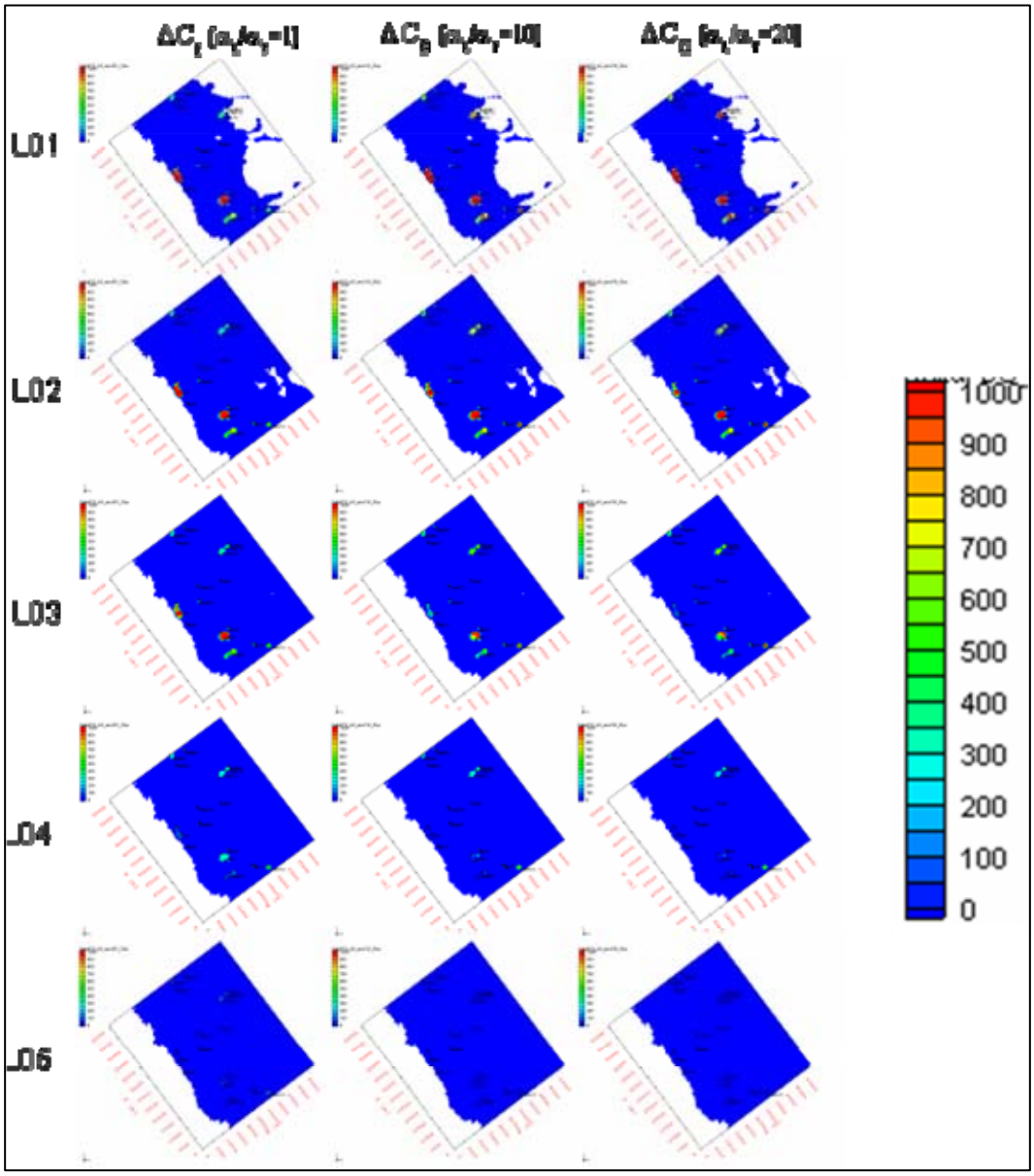

Figure 168

Concentration maps showing the net effect of 30 yrs of land discharge for the three different dispersivity ratio cases. For each dispersivity ratio (columns) the maps shows the concentration difference between 30 yrs with and without land discharge activity for each of the five model layers (L01-L05), starting from top layer (L01) . The color intensity scale is in mg/L and is cutoff at 1000 mg/L (all values greater than 1000 are in red). The white areas on east side the top 2 layers indicate dry cells above water table.

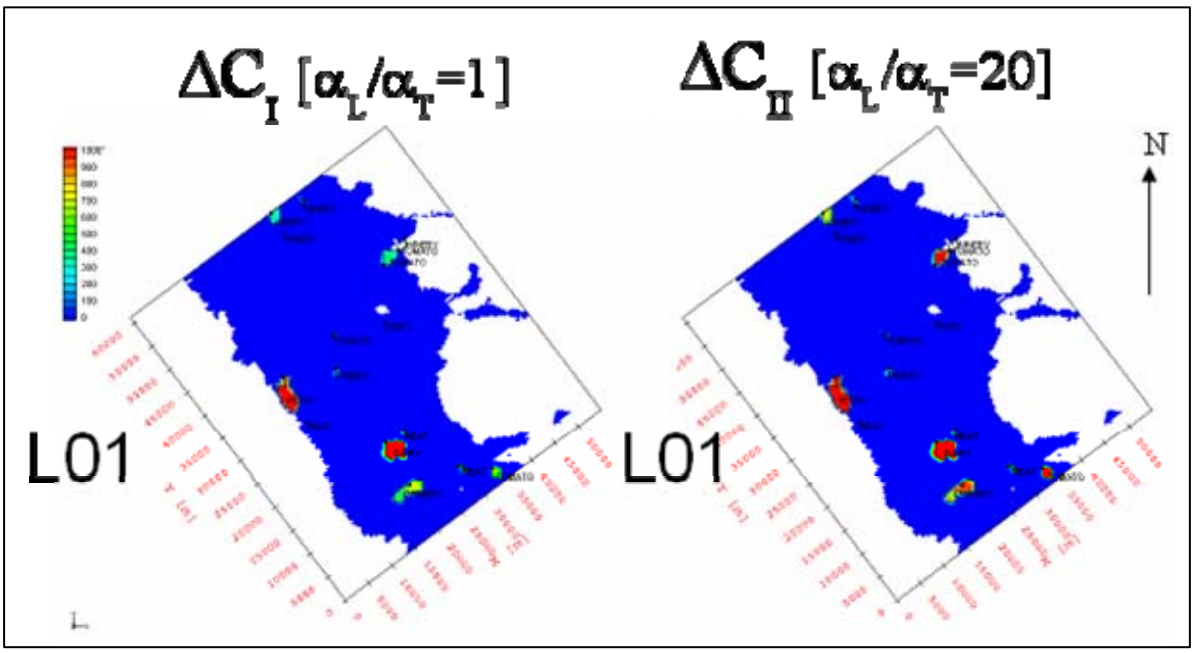

Figure 169

A close-up of the concentration difference maps for the two end points of the dispersivity ratio scenarios, for the top layer of the model. The maps show the concentration difference between 30 yrs with and without land discharge activity for each of the top model layer L01. The color intensity scale is in mg/L and is cutoff at 1000 mg/L (all values greater than 1000 are in red).

H. Monte Carlo Simulations

The sensitivity analyses of the previous section are useful for exploring extreme situations, but they cannot provide probabilities for observing any event (e.g., concentration exceeding certain threshold values). This can be done, however, using Monte Carlo simulations. The process of Monte Carlo simulations (see Rubin, 2003) includes generating alternative, physically plausible images of the flow domain, and analyzing flow and transport in each of them. The differences between the various images represent the uncertainty in the subsurface characterization. The ensemble of images thus analyzed provide an ensemble of plausible values of the dependent variables, such as the concentration of various chemicals of concern at many points and at many time steps, which can then be analyzed statistically. Such an approach is particularly suitable for situations such as we have here, where little information is available in terms of direct measurements, yet there is a reasonable understanding, from previous modeling studies, of the conditions and parameter values' ranges that can be implemented in the Monte Carlo Scheme.

Our sensitivity analyses indicated that the anisotropy ratio of the dispersivity plays a minor role in affecting impacts at a regional scale. The effective conductivity is expected to potentially hold a more significant role. In the Monte Carlo analysis, the effective hydraulic conductivity of each lithologic region is treated as a stochastic random variable, defined by a probability density function (pdf). The hydraulic conductivity for each lithologic region is kept uniform spatially,

but different realizations are randomly generated from a statistical distribution. The pdfs for each zone were defined as uniform distributions with a minimum value equal to the harmonic mean of the conductivity of the i^{th} lithologic region, $K_{H,i}$, and the maximum value equal to the arithmetic mean for that region, $K_{A,i}$. Five random realizations were generated for each lithologic unit, except for the Corcoran Clay layer which was not randomized. Random realizations were generated using the Latin Hypercube method in order to optimize the coverage of the parameter space. Thus a total of 125 (5×5×5) different combinations of effective conductivities for the model domain were generated, each comprised of a different set of effective conductivity. They were then used to run the groundwater flow model and the salinity transport code for the thirty year period. The summary of the parameters used is given below in Table 55.

Table 55: Table showing the parameter values used in the Monte Carlos simulations.

Monte Carlo Simulation Parameters:								
Lithologic Subregion	$K_{min}=K_H$ [m/day]	$K_{max}=K_A$ [m/day]	K_{hor}/K_{vert}	# K-Realiz-ations	Distrib-ution	α_L [m]	α_L/α_T	α_L/α_{vert}
Western Area above Corcoran Clay	18.79	84.22	300	5	uniform	19.2	10	10
Western Area below Corcoran Clay	11.94	53.51	300	5	uniform	19.2	10	10
Eastern Area (entire thickness)	10.98	49.23	300	5	uniform	19.2	10	10
Corcoran Clay	$1.3x10^{-3}$	$1.3x10^{-3}$	1	1	uniform	4	10	10
Total Number of Realizations				125				

The salinity transport model is then run on each of these realizations to get a statistical distribution of salinity concentrations at each point in the model grid. This distribution can be characterized by mean concentrations and standard deviations of the salt concentrations in the model. This probability density function can be used to generate a map which shows the probability of the salt concentration exceeding a given threshold, for example the MCL, at any given point in the model domain

1. Monte Carlo simulation Results

The table below summarizes the statistics of the FDS concentration at 30 years, including minimum, maximum and average concentrations as well as the standard deviation. It shows that the FDS values are characterized by relatively low averages and very high maximum concentration values. The standard deviations are also low, which suggests that most of the domain is characterized by the low FDS values, except for hot spots of very high concentrations.

Table 56: This table shows summary statistics for the values of the ensemble Min, Mean, Max and standard Deviation of the concentration generated in the Monte Carlo Simulations

FDS Summary Statistics [mg/L] over all realizations				
	C_{Min}	C_{Mean}	C_{Max}	C_{stdev}
Min	17.53	31.41	48.87	0.01
Max	9979.36	13045.21	15107.75	12846.75
Range	9961.82	13013.80	15058.87	12846.74
Mean	246.89	259.75	274.24	17.75
Median	222.59	226.73	230.42	1.06
Stdev	169.90	209.38	251.24	185.86
#Cells	104805	104805	104805	104805

The figures below summarize graphically the spatial distribution of the FDS concentration at 30 years at different depths. Figures 170-176 address the concentration means and standard deviations. Figures 177-181 provide the spatial distributions of the probabilities for the FDS concentration to exceed 500 mg/L, which is the non-enforceable guideline based on the cosmetic and aesthetic qualities of water (EPA website, 2001)". These figures show consistently that the spatial extent of the impact on groundwater by land application is limited. These figures include also the impact of water infiltration along the river banks coupled with evaporation.

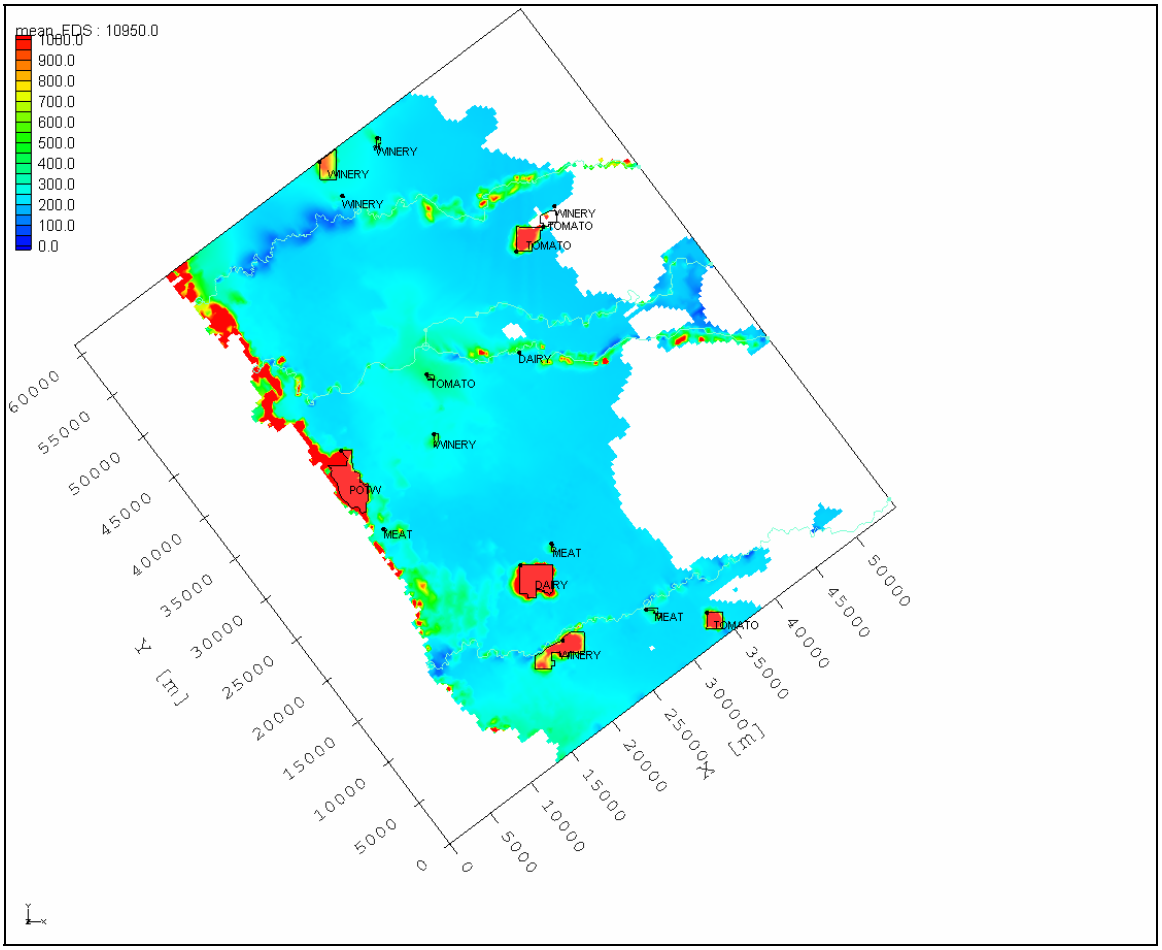

Figure 170

This map shows the ensemble mean concentration, CMean of FDS for each grid block in layer 1 after 30 years. The color scale is in mg/L and is cutoff at 1000 mg/L (red≥1000 mg/l, blue = 0 mg/l). All white areas on the right side indicate dry cell blocks that are above the water table

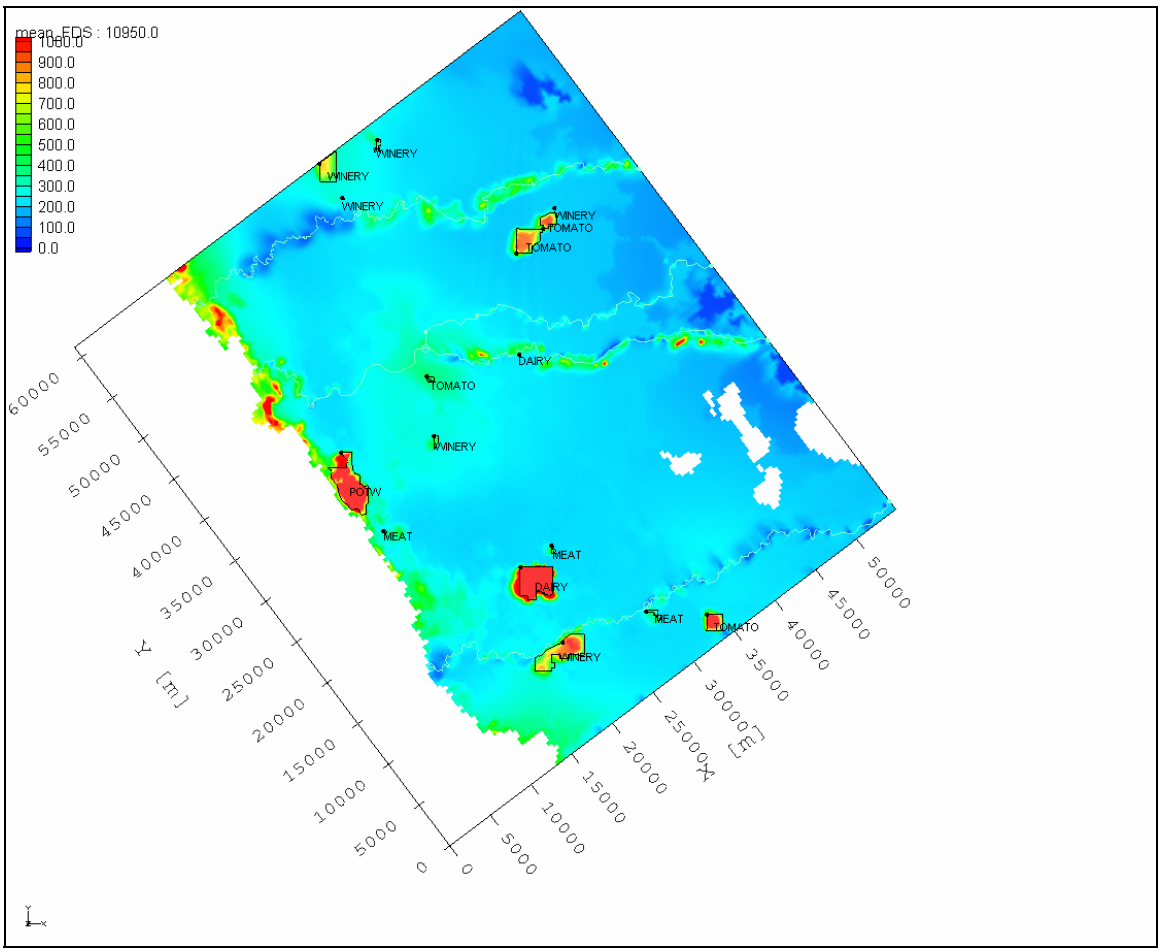

Figure 171

This map shows the ensemble mean concentration, C_{Mean} of FDS for each grid block in layer 2 after 30 years. The color scale is in mg/L and is cutoff at 1000 mg/L (red≥1000 mg/l, blue = 0 mg/l). All white areas on the right side indicate dry cell blocks that are above the water table

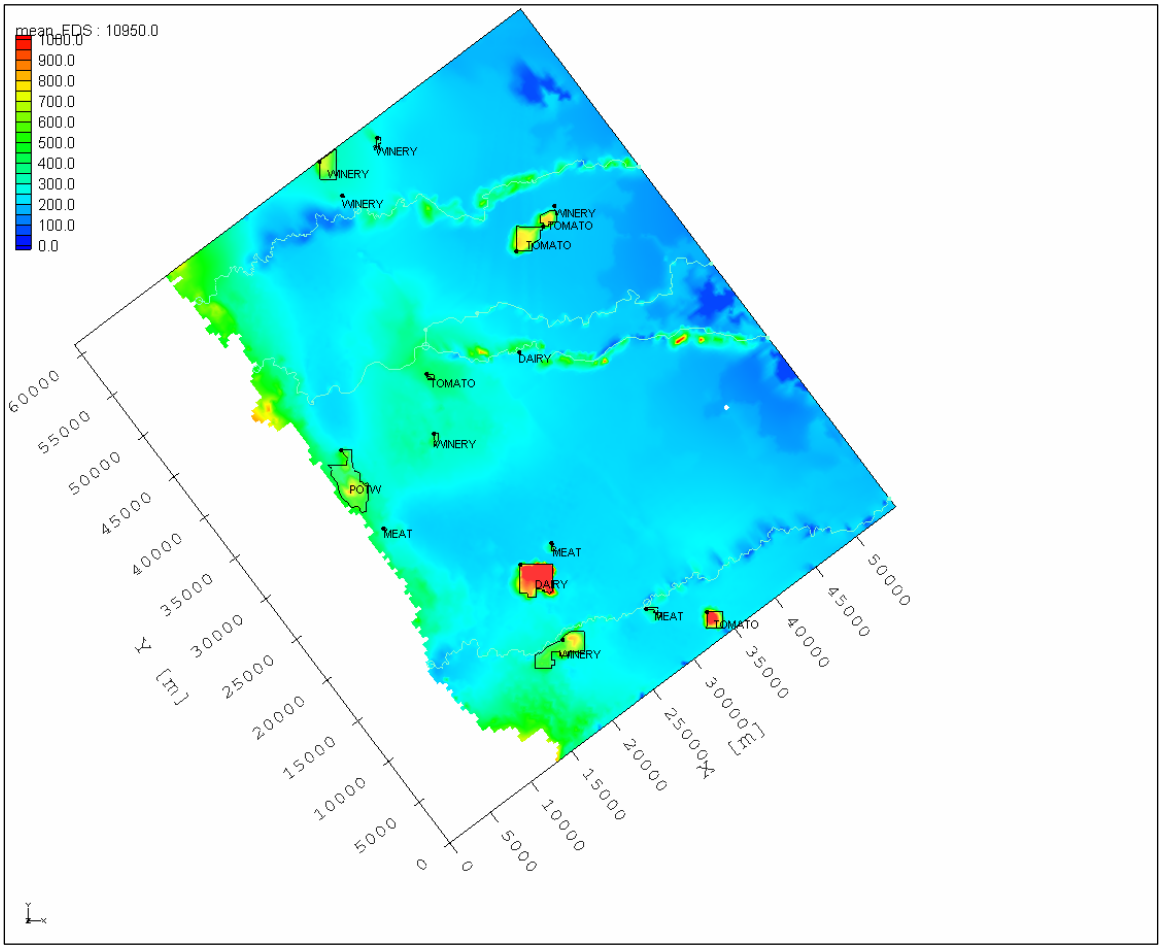

Figure 172

This map shows the ensemble mean concentration, C_{Mean} of FDS for each grid block in layer 3 after 30 years. The color scale is in mg/L and is cutoff at 1000 mg/L (red≥1000 mg/l, blue = 0 mg/l). All white areas on the right side indicate dry cell blocks that are above the water table

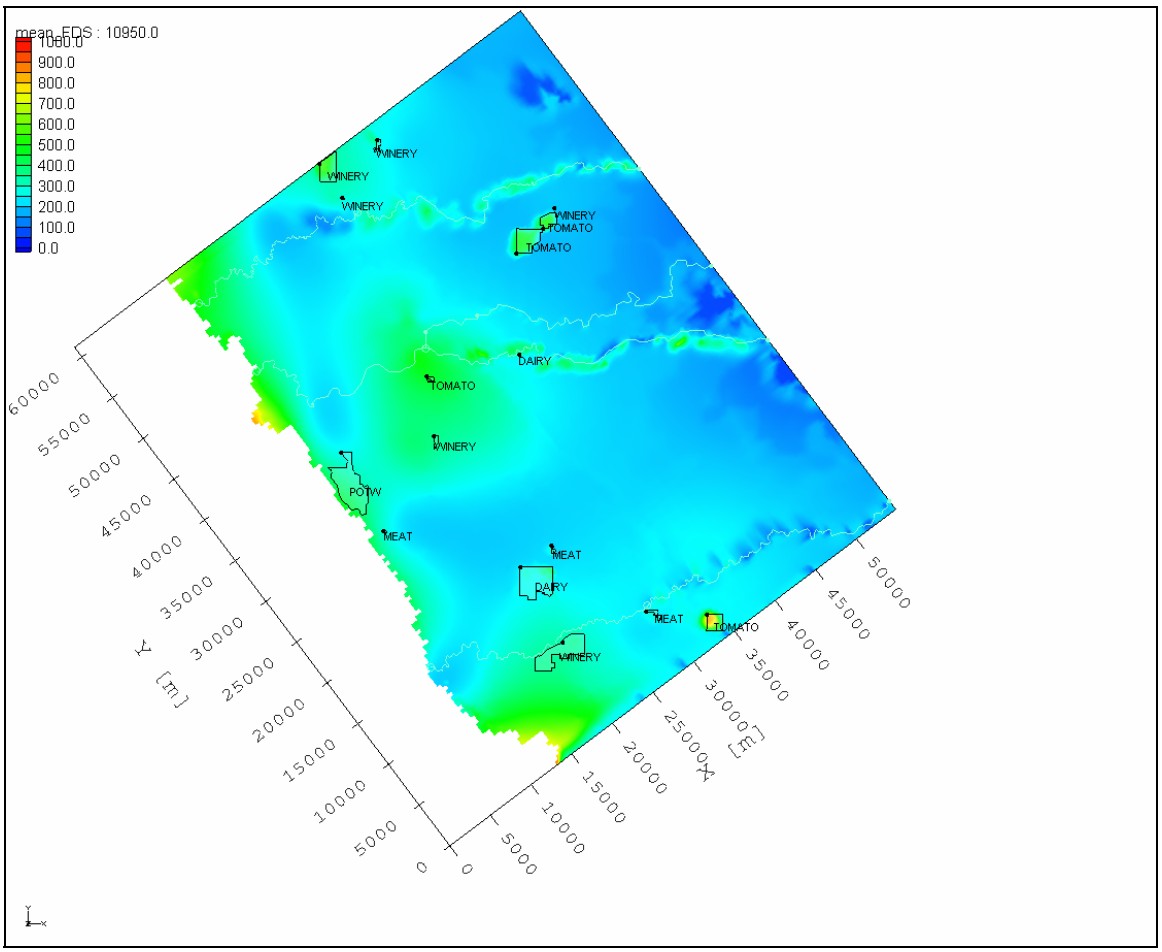

Figure 173

This map shows the ensemble mean concentration, C_{Mean} of FDS for each grid block in layer 4 after 30 years. The color scale is in mg/L and is cutoff at 1000 mg/L (red≥1000 mg/l, blue = 0 mg/l). All white areas on the right side indicate dry cell blocks that are above the water table

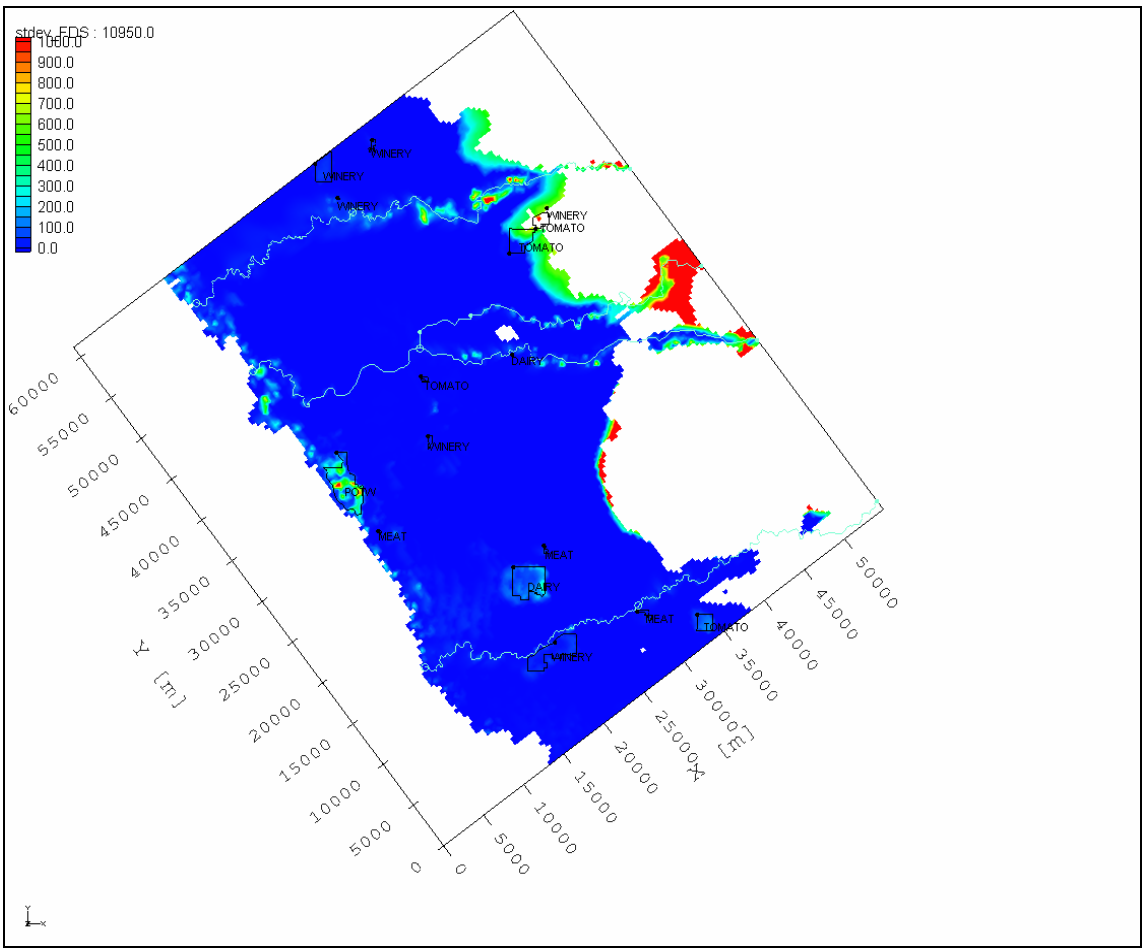

Figure 174

This map shows the concentration standard deviation, C_{Stdev} for the ensemble of all realizations for each grid block in Layer 1 after 30 years. The color scale is in mg/L and is cutoff at 1000 mg/L (red≥1000 mg/l, blue = 0 mg/l). All white areas to on the left side indicate dry cell blocks that are above the water table. The drying out or wetting of different cells as the water table rises and falls with different parameter realizations creates a fringe of artificially high standard deviations along the edge of the grid subject to drying out. This is visible as the red to green colors that follow the "shores" of the dried out cells.

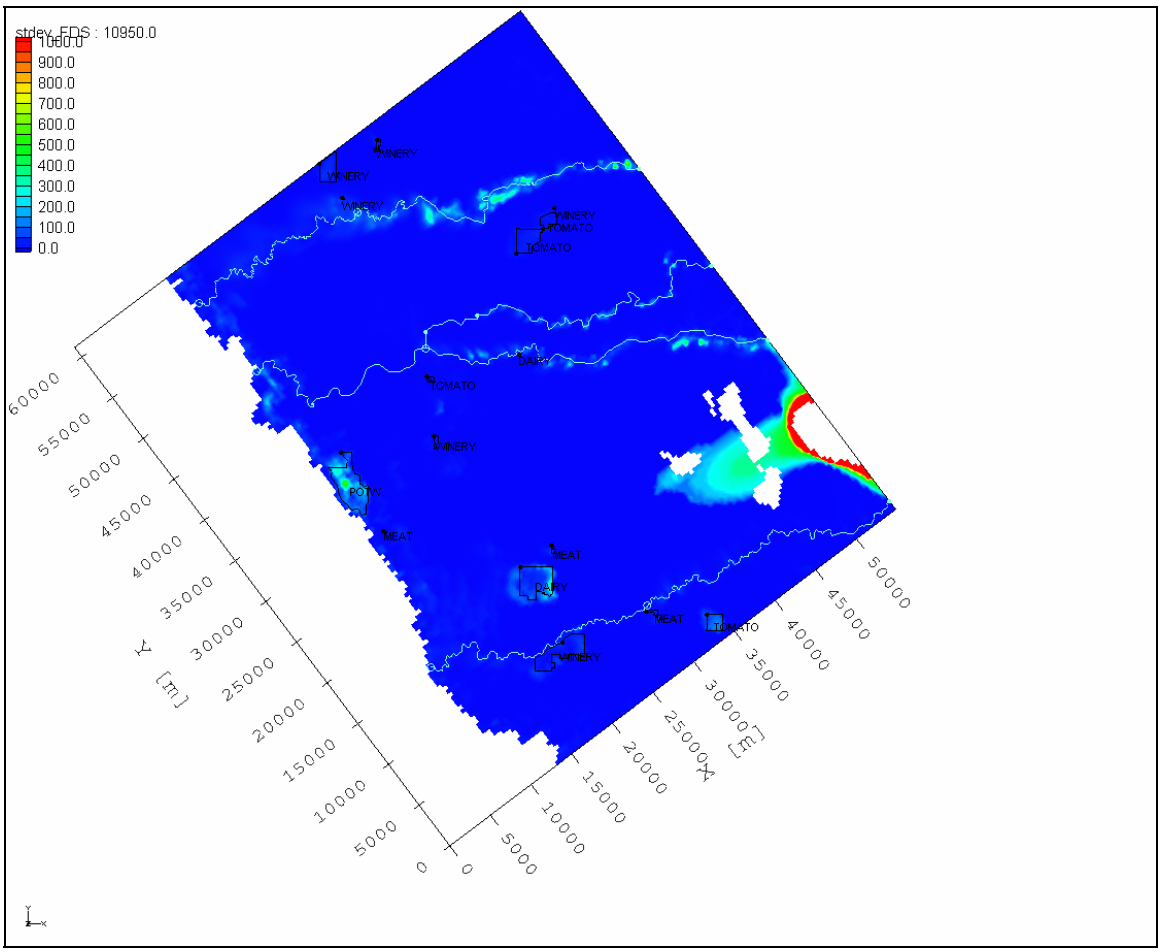

Figure 175

This map shows the concentration standard deviation, C_{Stdev} for the ensemble of all realizations for each grid block in Layer 2 after 30 years. The color scale is in mg/L and is cutoff at 1000 mg/L (red≥1000 mg/l, blue = 0 mg/l). All white areas to on the left side indicate dry cell blocks that are above the water table. The drying out or wetting of different cells as the water table rises and falls with different parameter realizations creates a fringe of artificially high standard deviations along the edge of the grid subject to drying out. This is visible as the red to green colors that follow the "shores" of the dried out cells

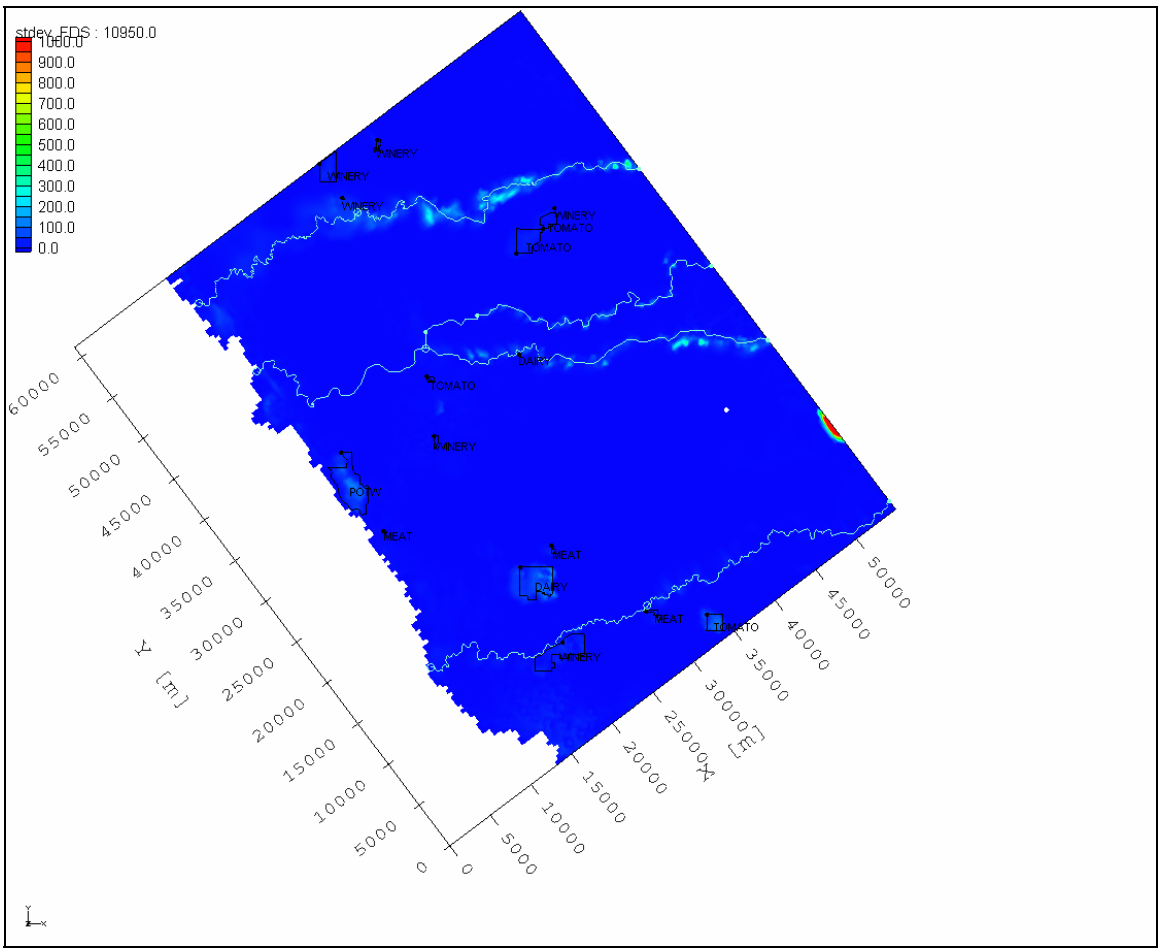

Figure 176

This map shows the concentration standard deviation, C_{Stdev} for the ensemble of all realizations for each grid block in Layer 3 after 30 years. The color scale is in mg/L and is cutoff at 1000 mg/L (red ≥1000 mg/l, blue = 0 mg/l). The standard deviation of the concentration decreases sharply with increasing depth.

Layer 01 Concentration Exceedance Probability Map

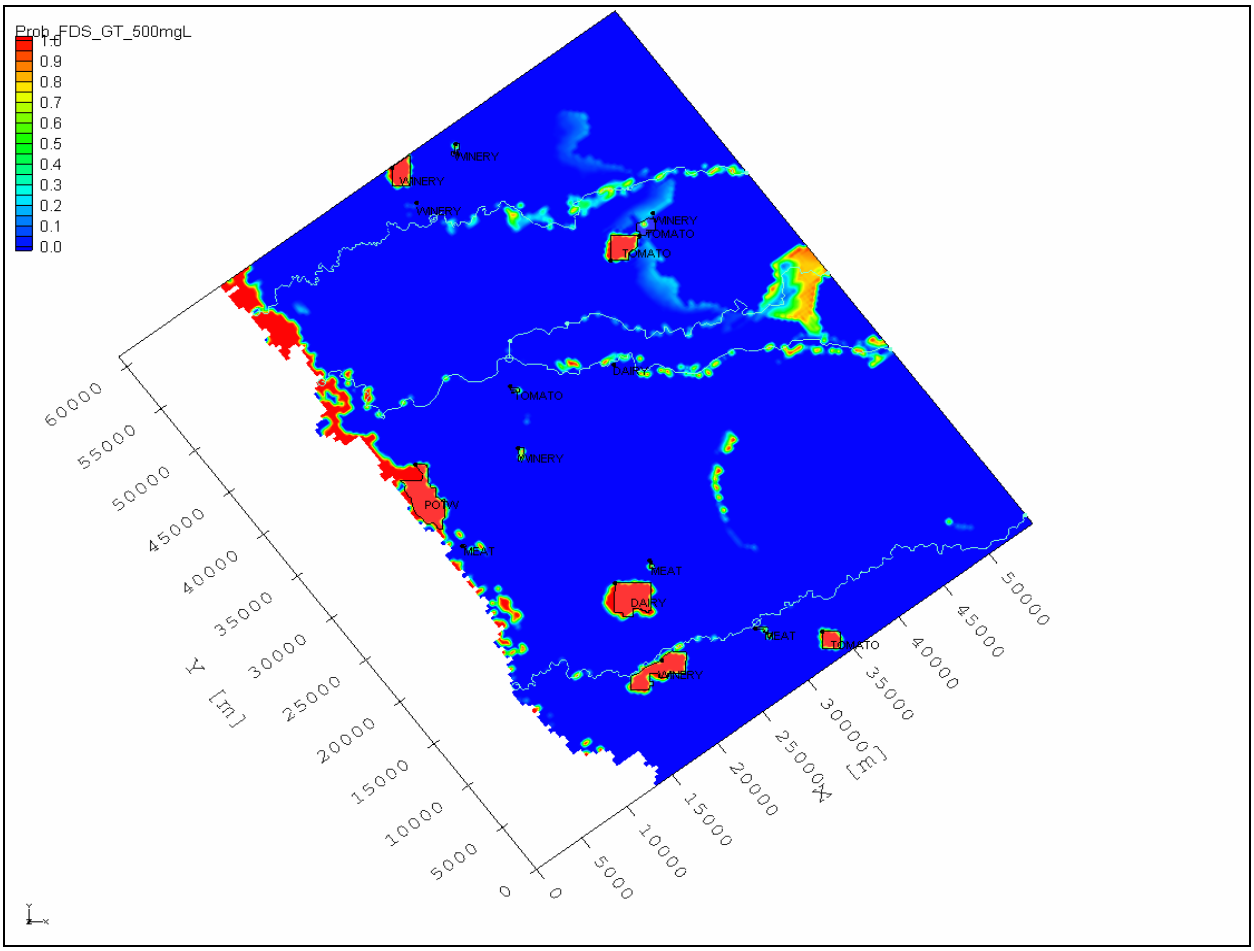

Figure 177

This map shows the probability of FDS>500 mg/L in layer 1 after 30 years. The color scale represents probability with 0 (blue) indicating 0% probability of exceedance, and 1.0 (red) indicating 100% probability of exceeding 500 mg/L. The location of the rivers and major streams are shown as white lines. In addition to the ET hotspots described in the previous section there are a few artifacts associated with grid blocks that border the cells that dry out in (i.e. cells that are entirely above the water table). The large standard deviations associated with these cells prone to drying out causes higher exceedance probabilities to be estimated for these regions.

Layer 02 Concentration Exceedance Probability Map

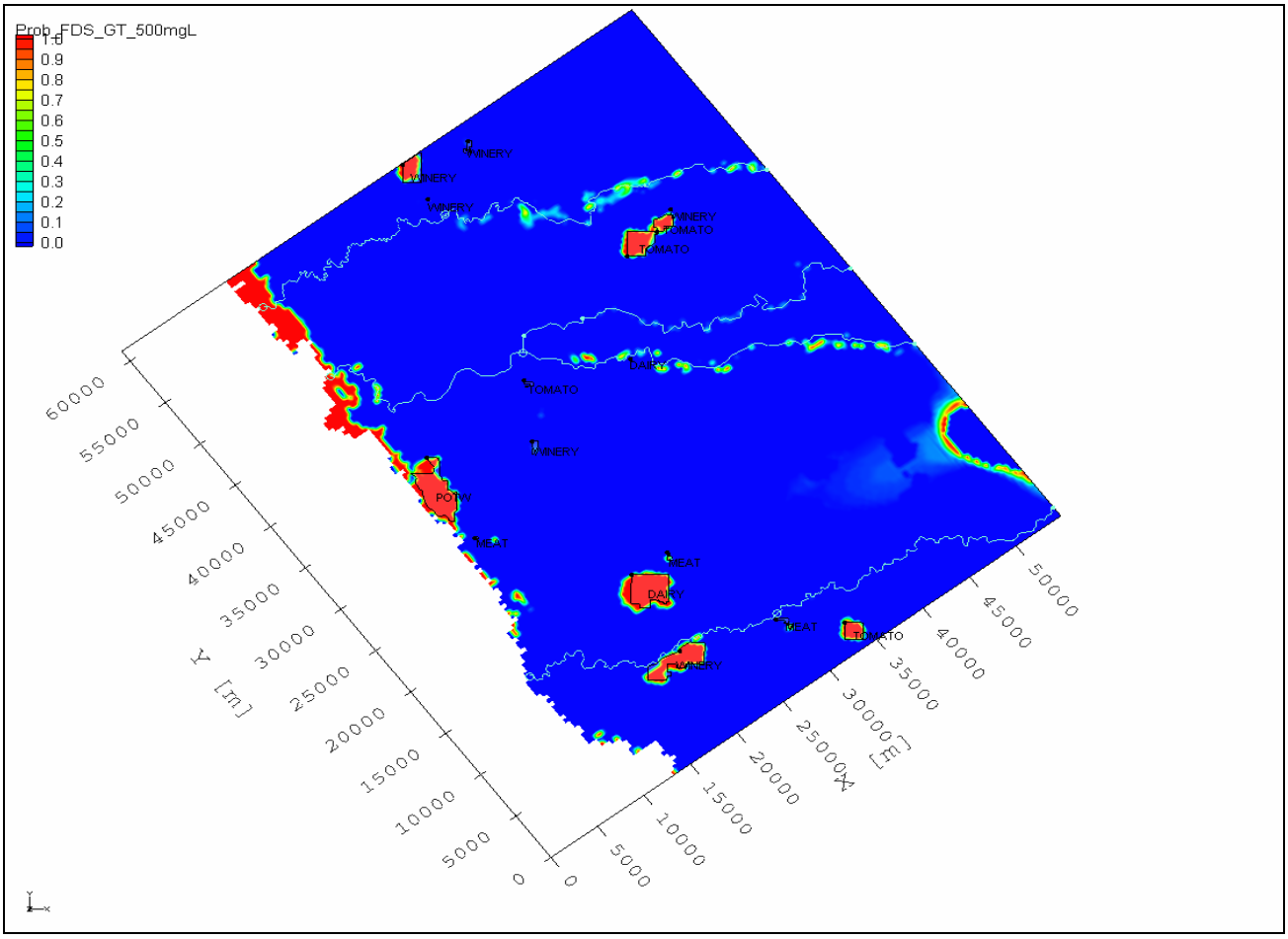

Figure 178

This map shows the probability of FDS>500 mg/L in layer 2 after 30 years. The color scale represents probability with 0 (blue) indicating 0% probability of exceedance, and 1.0 (red) indicating 100% probability of exceeding 500 mg/L. The location of the rivers and major streams are shown as white lines. In addition to the ET hotspots described in the previous section there are a few artifacts associated with grid blocks that border the cells that dry out (i.e. cells that are entirely above the water table). One such artifact is clearly visible in the eastern most corner of the model.

Layer 03 Concentration Exceedance Probability Map

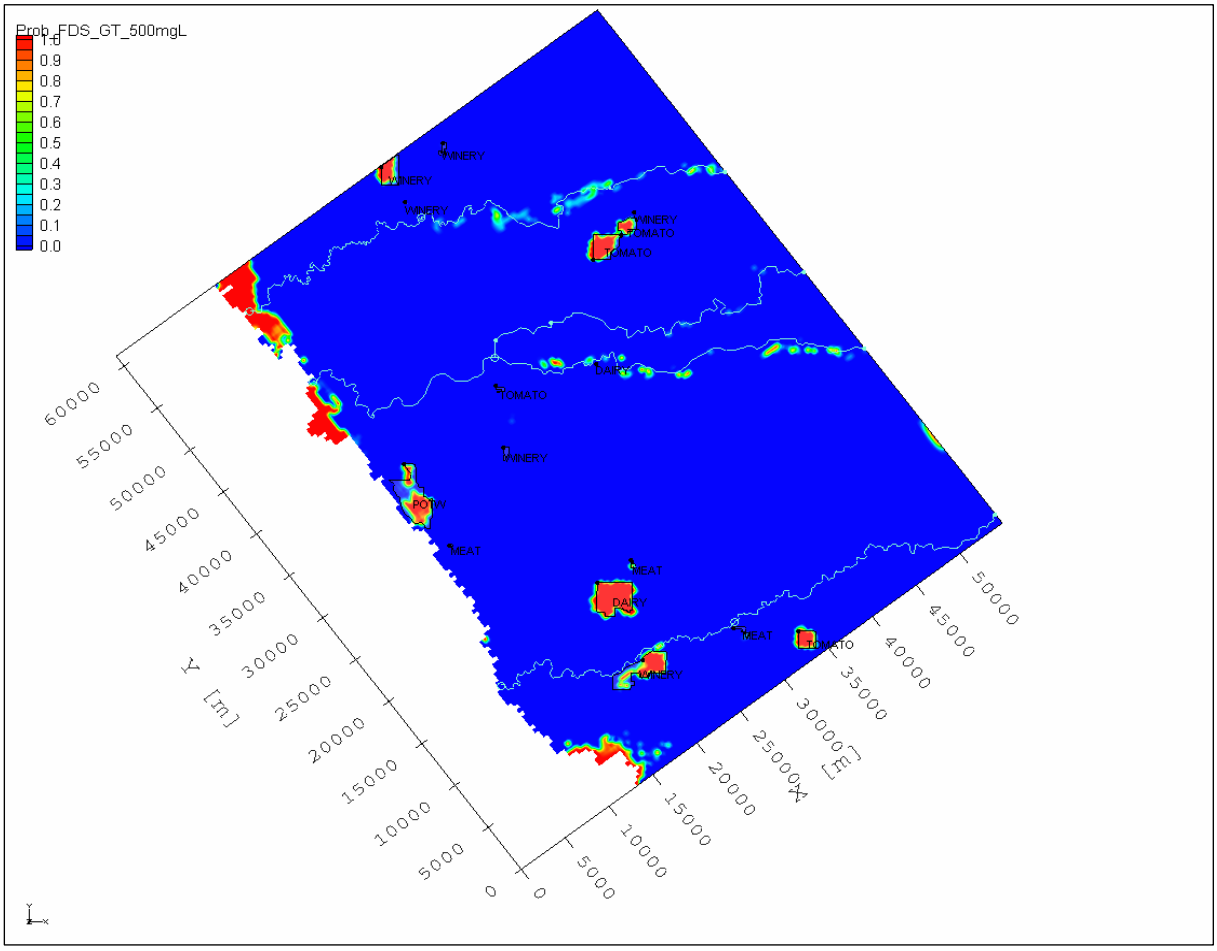

Figure 179

This map shows the probability of FDS>500 mg/L in layer 3 after 30 years. The color scale represents probability with 0 (blue) indicating 0% probability of exceedance, and 1.0 (red) indicating 100% probability of exceeding 500 mg/L. In addition to the ET hotspots described in the previous section there are a few artifacts associated with grid blocks that border the cells that dry out (i.e. cells that are entirely above the water table,). One such artifact is clearly visible in the eastern most corner of the model

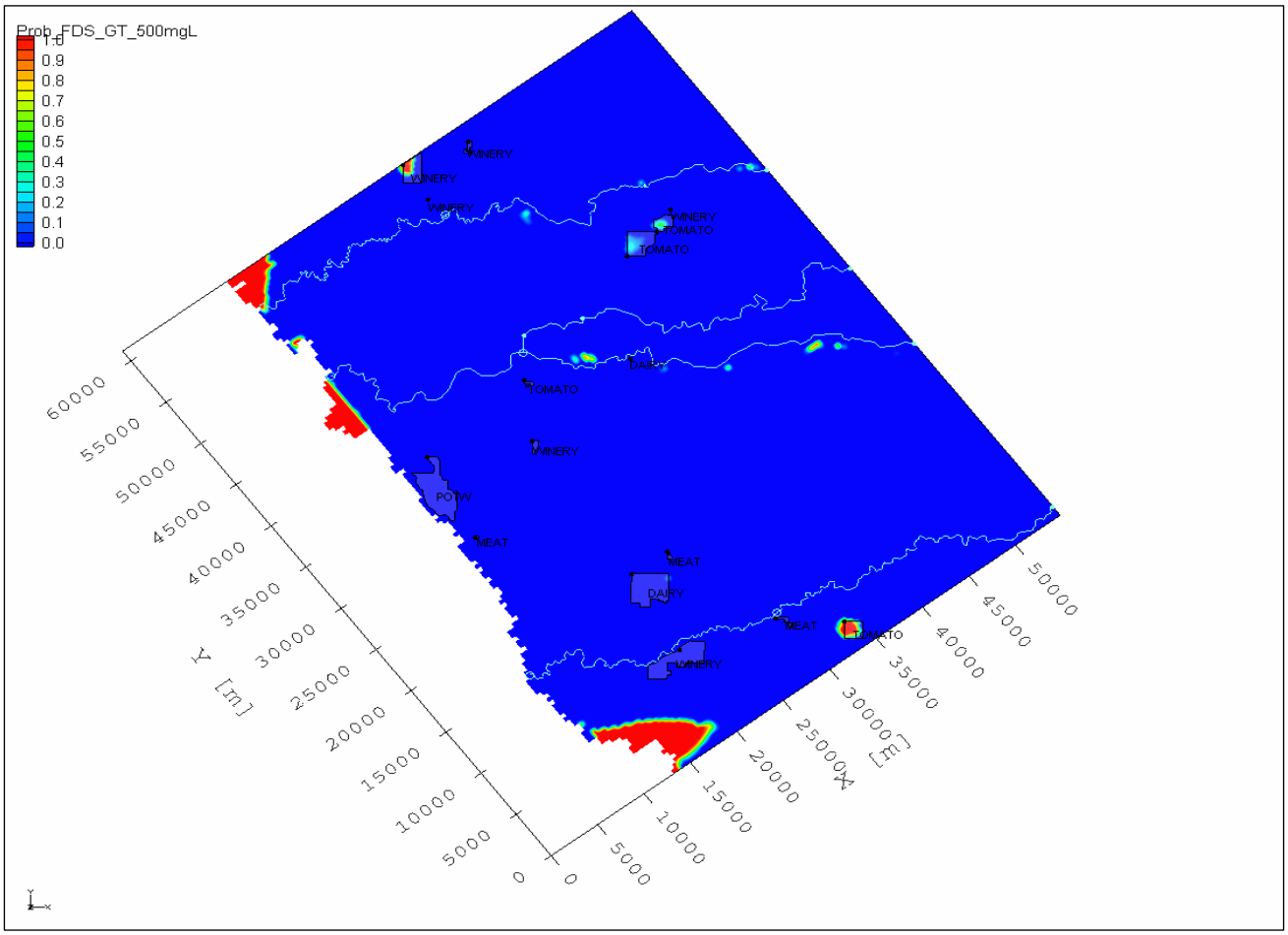

Figure 180

This map shows the probability of FDS>500 mg/L in layer 4 after 30 years. The color scale represents probability with 0 (blue) indicating 0% probability of exceedance, and 1.0 (red) indicating 100% probability of exceeding 500 mg/L. The large “hot spots” that appear along the San Joaquin river edge of the model are due to the initial background concentrations assigned to the model

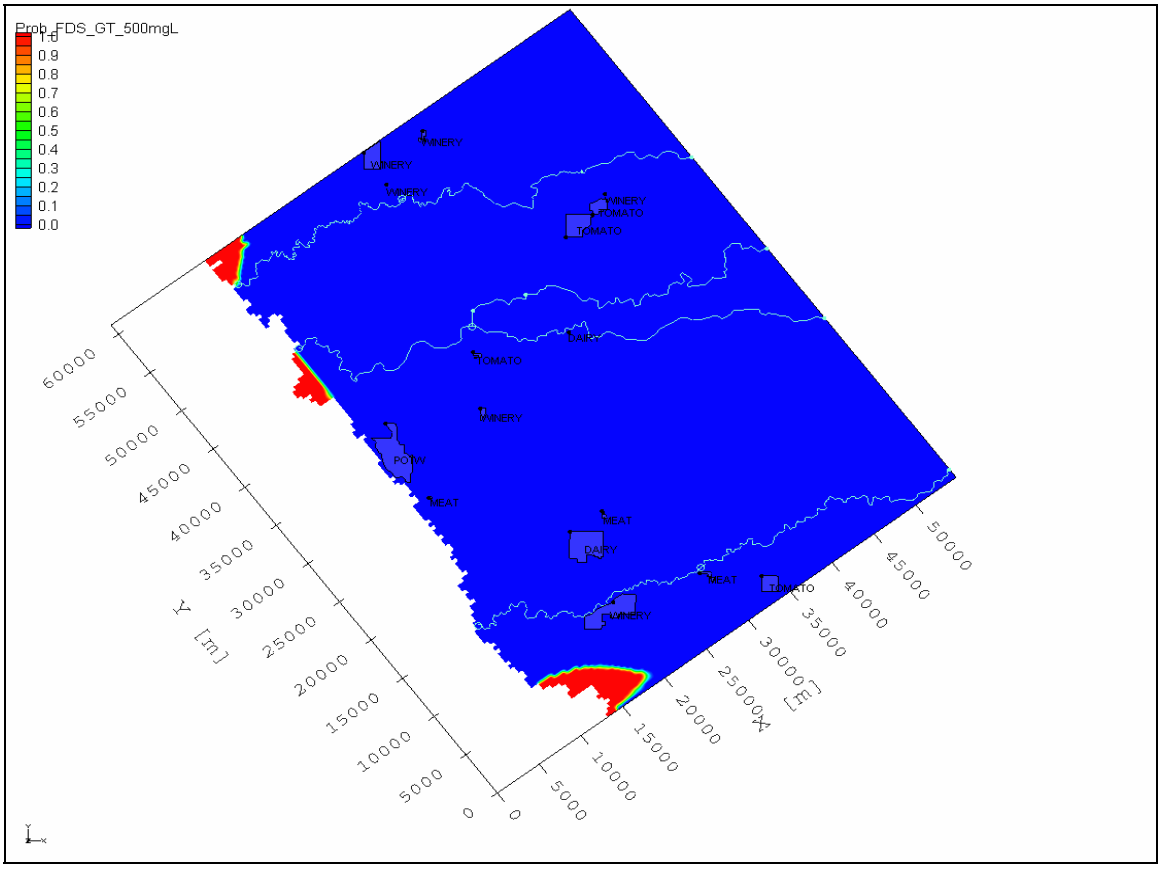

Figure 181

This map shows the probability of FDS>500 mg/L in layer 5 after 30 years. The color scale represents probability with 0 (blue) indicating 0% probability of exceedance, and 1.0 (red) indicating 100% probability of exceeding 500 mg/L. The large "hot spots" that appear along the San Joaquin river edge of the model are due to the initial background concentrations assigned to the model

2. An alternative Monte Carlo analysis

In this Section we pursue an alternative analysis. Rather than assessing the statistics of FDS concentrations, we shall analyze the statistics of the differences in concentrations caused by land discharge. This will allow us to assess directly the impact of land discharge, and to eliminate from the picture important yet unrelated effects such as the hot spots of FDS concentrations along the rivers.

Let us define ΔC as the difference between the FDS concentration with land discharge and the FDS concentration assuming no land discharge. The difference ΔC was calculated using pairs of realizations of the concentration field, each pair including a realization of the concentration field

computed with land discharge and the realization obtained using the same set of parameters, but without land discharge. In the "no land discharge" scenario the land discharge areas were assigned the same recharge fluxes and concentration equal to the corresponding background values.

A large number of pairs were generated, yielding a large ensemble of ΔC. The ensemble of ΔC was then used to calculate statistics, concentration maps, and concentration exceedance probability maps. The FDS concentration at grid blocks that dried out was assumed to be zero. The exceedance probability was estimated by calculating the mean and standard deviation of the ΔC at each grid block and then assuming a lognormal distribution in order to calculate the cumulative density function (CDF). The probability of ΔC > 500 mg/L, is then calculated as 1-CDF(ΔC =500 mg/L).

The table below summarizes the statistics of the ΔC concentration at 30 years, including minimum, maximum and average concentrations as well as the standard deviation. It shows that the ΔC values are characterized by relatively low averages and very high maximum concentration values. The standard deviations are also low, which suggests that most of the domain is characterized by the low ΔC values, except for hot spots of very high concentrations changes.

Table 57: This table shows summary statistics for the values of the ensemble Min, Mean, Max and standard Deviation of the concentration differences (ΔC)

ΔC Summary Statistics [mg/L] over all realizations				
	ΔC_{Min}	ΔC_{Mean}	ΔC_{Max}	ΔC_{Stdev}
Max	7697.59	10086.80	11582.74	915.46
Range	8259.99	10384.07	11653.49	915.46
Mean	7.82	11.34	14.40	1.18
Median	0.00	0.00	0.10	0.03
Stdev	116.86	145.20	166.93	13.48
#Cells	104805	104805	104805	104805

Figures 182-186 depict the spatial distributions of the exceedance probabilities for the 5 model layers. The probability to have ΔC larger than 500 mg/L is very high at most of the land application areas at the 4 top layers, and reduces significantly at larger depths.

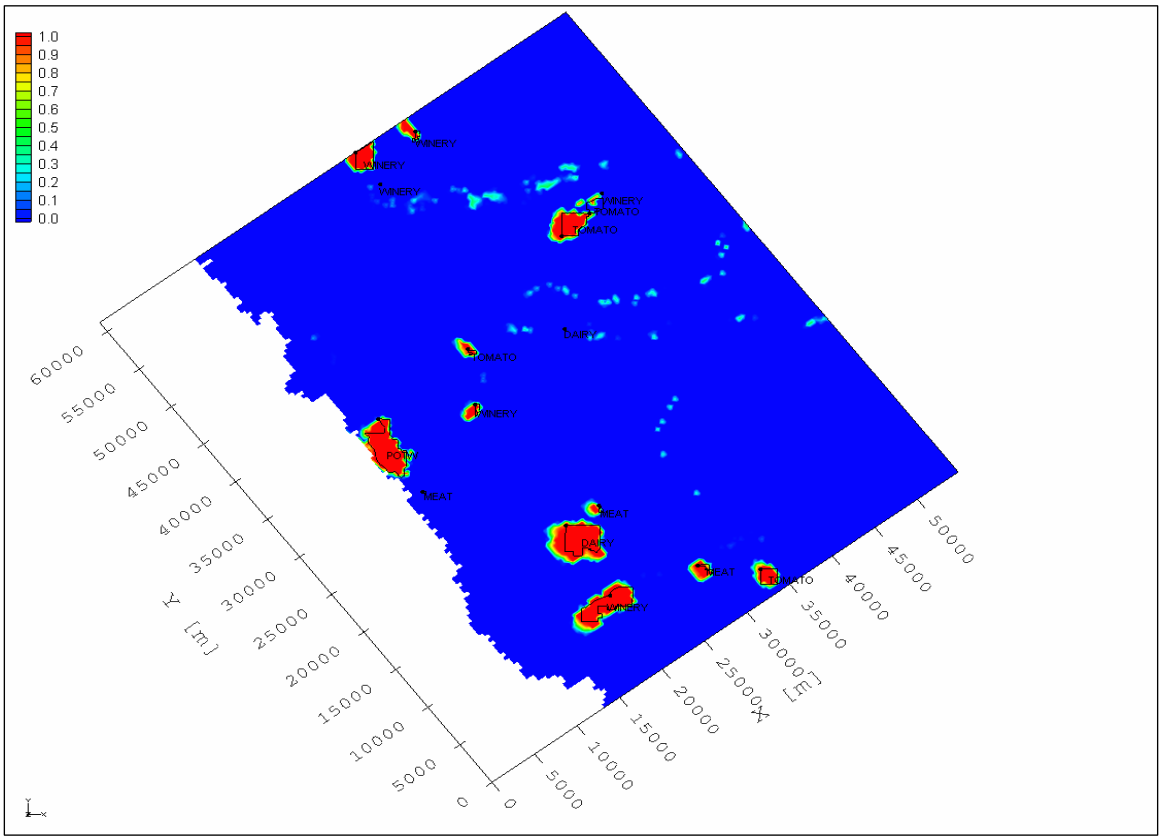

Figure 182

This map shows the probability of ΔC >500 mg/L in layer 1 after 30 years. The color scale represents probability with 0 (blue) indicating 0% probability of exceedance, and 1.0 (red) indicating 100% probability of exceeding 500 mg/L

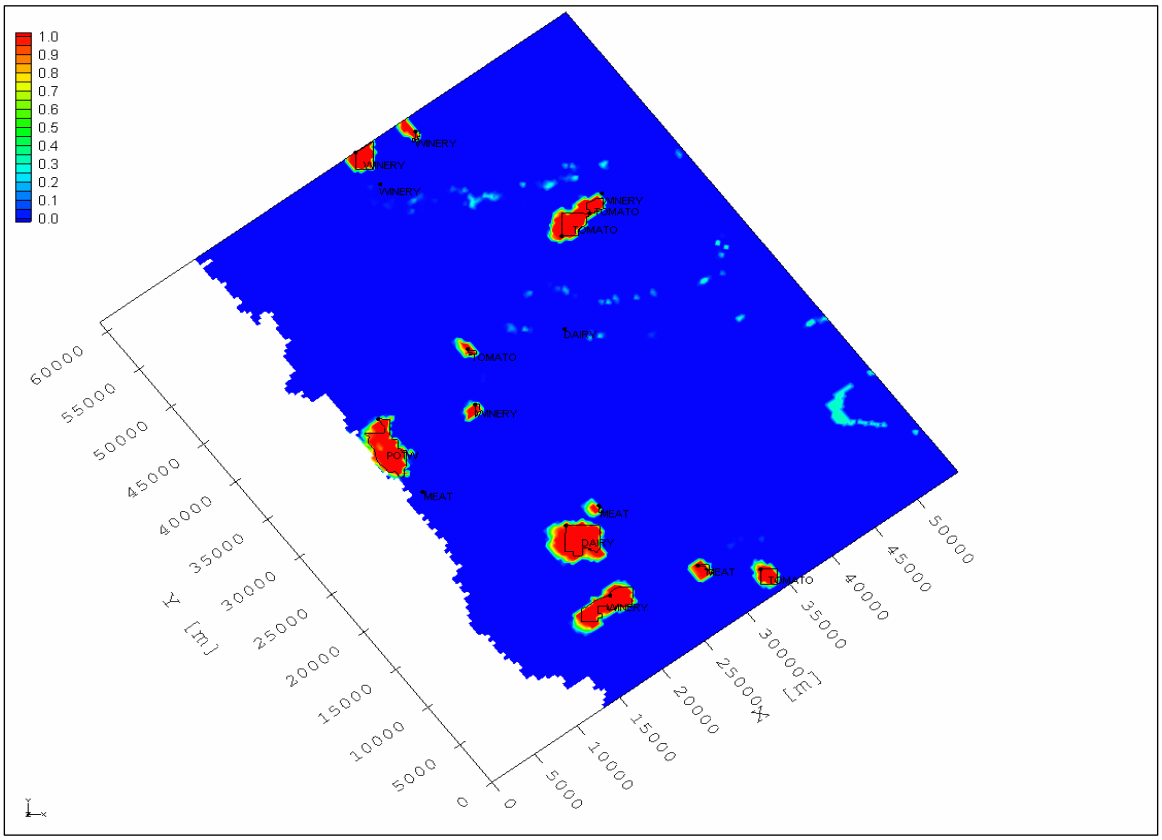

Figure 183

This map shows the probability of ΔC >500 mg/L in layer 2 after 30 years. The color scale represents probability with 0 (blue) indicating 0% probability of exceedance, and 1.0 (red) indicating 100% probability of exceeding 500 mg/L. In addition to the ET hotspots described in the previous section there are a few artifacts associated with grid blocks that border the cells that dry out (i.e. cells that are entirely above the water table,). One such artifact is clearly visible in the eastern most corner of the model

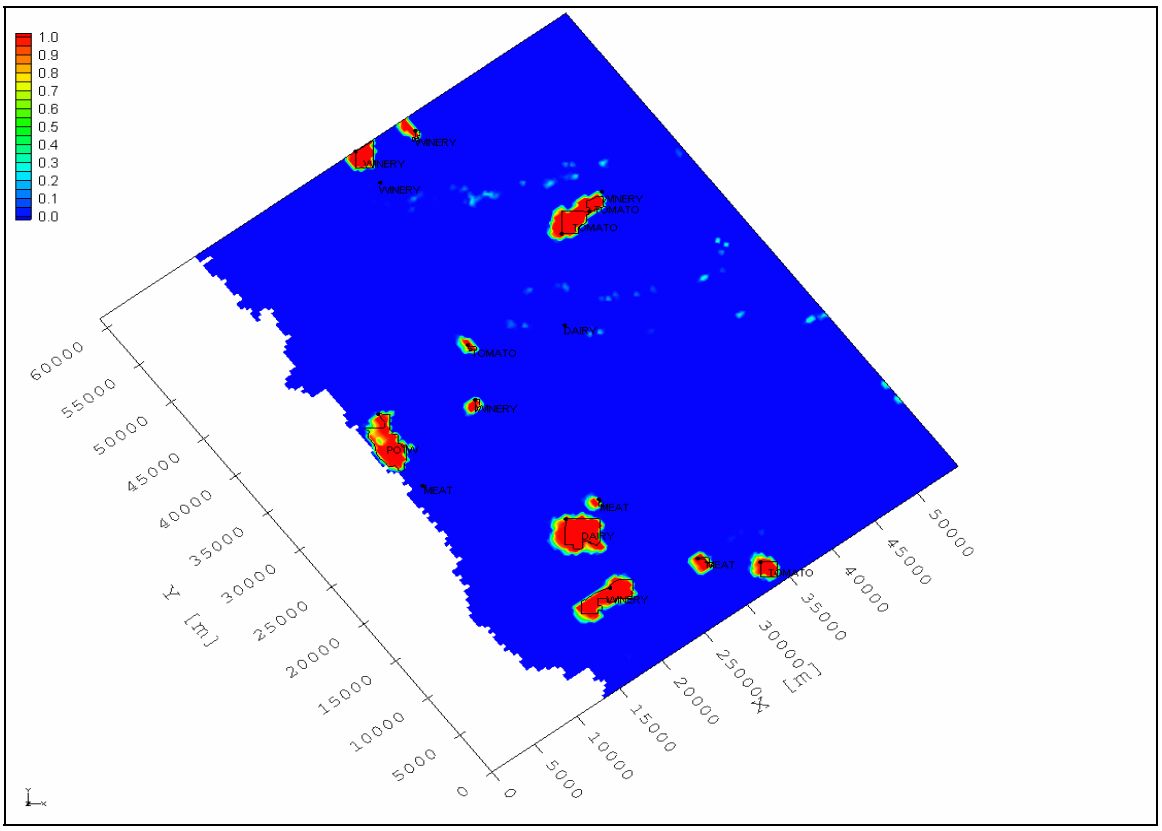

Figure 184

This map shows the probability of ΔC >500 mg/L in layer 3 after 30 years. The color scale represents probability with 0 (blue) indicating 0% probability of exceedance, and 1.0 (red) indicating 100% probability of exceeding 500 mg/L

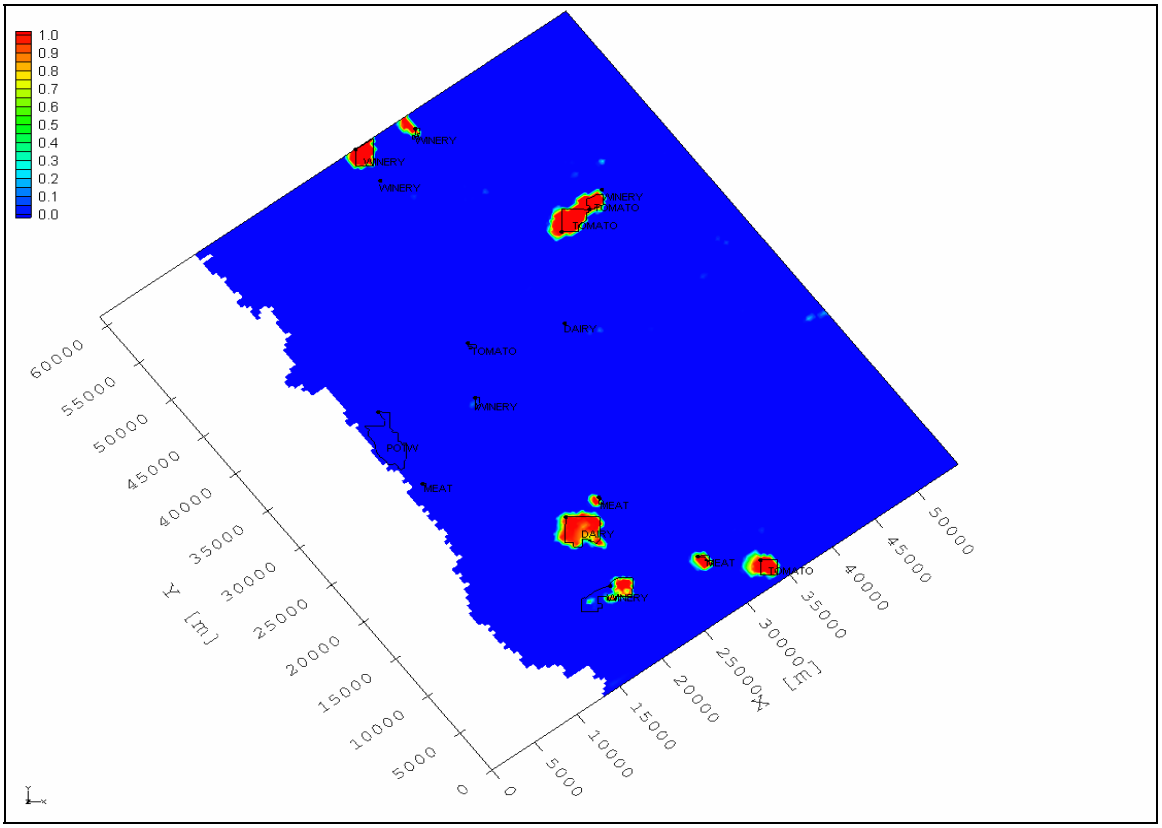

Figure 185

This map shows the probability of ΔC >500 mg/L in layer 4 after 30 years. The color scale represents probability with 0 (blue) indicating 0% probability of exceedance, and 1.0 (red) indicating 100% probability of exceeding 500 mg/L

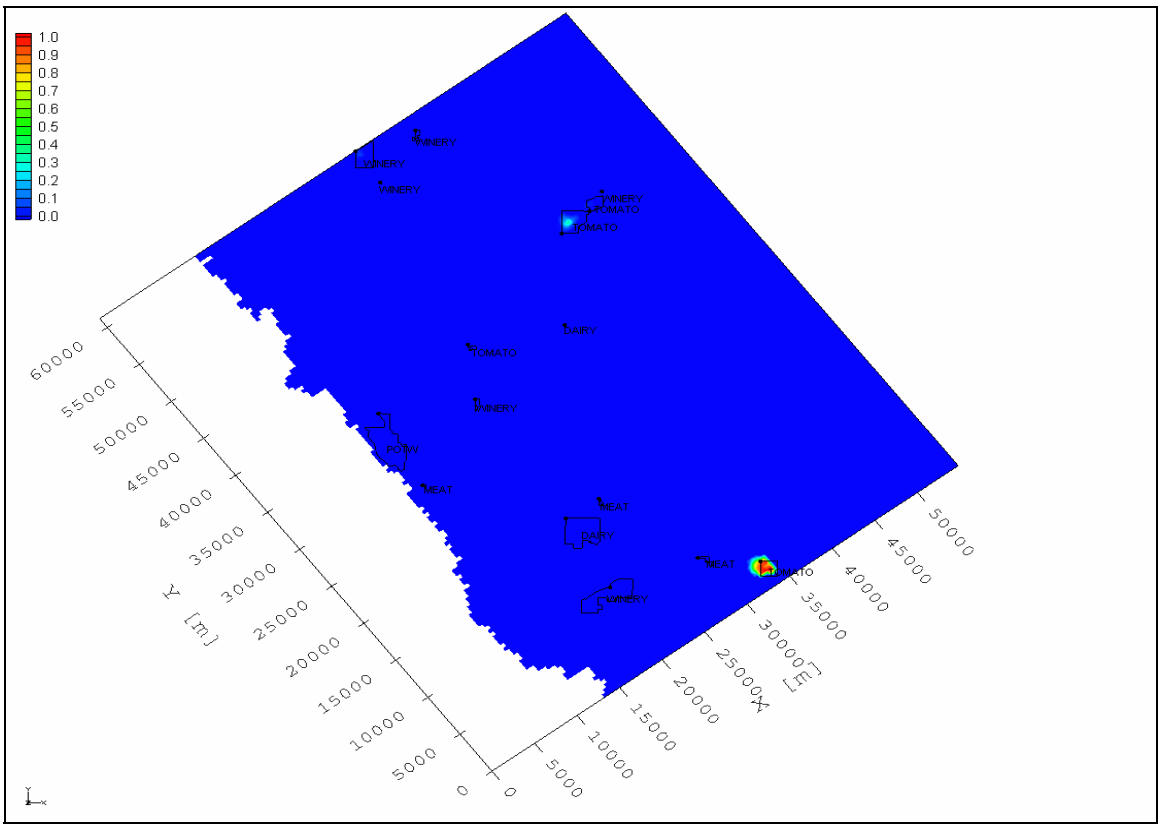

Figure 186

This map shows the probability of ΔC >500 mg/L in layer 5 after 30 years. The color scale represents probability with 0 (blue) indicating 0% probability of exceedance, and 1.0 (red) indicating 100% probability of exceeding 500 mg/L

I. Summary

Section II.4 discusses the development of a groundwater model for the Lower San Joaquin River (LSJR) Basin, and the implementation of the model to investigate the transport of waste water discharged form food processing facilities. This model is part of an integrated saturated-unsaturated system for modeling the fate of the waste water discharge. This system includes an unsaturated zone modeling component that is described in detail in Sections II.2 and II.3. The unsaturated zone modeling component computes the mass (water and solutes) that are discharged into the saturated zone and modeled with the groundwater model.

Our numerical models modeling system can cover a wide range of processes affecting flow and transport in the subsurface, including multi-component chemical reactions. The models are it is suitable and ready for additional large- and small-scale investigations that may be requested as a follow-up to this study, or those that can hopefully become part of the routine monitoring and licensing of industrial and agricultural activities in the Central Valley. Large scale investigation implies a modeling effort that covers a large region with multiple processors, whereas small-

scale investigations can possibly focus, for example, on a single food processor.

Our study of the LSJR basin intends to provide conclusions that are applicable for the entire Central Valley. There are always limitations to such projections due to variations in local hydrological conditions as well as in pumping rates. However, two observations can be made to support the generality of the study's conclusions. First, the geology of the Central Valley is stationary, as is evident from Figure 136, which shows the Central Valley as being comprised of a series of repeating geological units. In this regard, the findings from studying one geological unit can be generalized to other units. Additionally, we modeled the LSJR Basin's hydrologic response (i.e., degradation in groundwater quality) to an ensemble of food processors representing various industrial groups covering the highest impact industrial groups including tomato canners, wineries, meat packers and others. This allows investigating the impacts of various chemical profiles of the waste water discharge.

There are possibly significant differences between the groundwater degradation at specific sites compared to those modeled here. This is primarily because there is no data base currently available to support detailed, site-specific analysis of groundwater degradation, and our model was developed under many assumptions. While these assumptions are based on engineering judgment, they are subject to uncertainty until verified through additional testing.

Another reason why we expect differences between actual impacts and modeled impacts is that our investigation is carried out under assumed worst case scenarios. We thus expect that actual impacts overall (meaning, in most land discharge sites) will be more moderate than those anticipated by the worst case scenario analysis. Worst case scenarios were created by considering several aspects of the modeling effort intended to maximize the groundwater degradation. Worst-case scenarios were constructed by maximize the mass loading from the unsaturated to the saturated zone. For modeling groundwater flow, we consider a broad range of parameters, including the presence of highly-conductive channels. The groundwater is assumed to be at steady state. Transients in the groundwater are known to enhance dispersion (Dagan et al., 1996) which in turn leads to reduction in concentrations. This, steady state leads to larger concentrations.

The motivation behind the modeling decision to work under assumed worst case scenarios is the uncertainty regarding actual site conditions, and the rationale is that worst case scenarios may put brackets to the range of expected impacts to groundwater quality. There can always be surprises, such as the presence of highly conductive channels that connect the land discharge site with water supply well. Surprises can be prevented through site investigation. We tried to minimize surprises through investigating a wide range of conditions, including a hypothetical case of a highly-conductive channel as well as a wide range of hydrologic parameter values, intended to cover the range of parameters expected at the sites.

It should be emphasized that the scenarios modeled do not represent actual conditions imparted by food processors at the specific locations. What we did is identify a "worst case scenario profile" for a particular industry, and then attached it to the various facilities based on their

industrial affiliation. The only modification to local conditions was in matching the total discharge at the site to the one reported by the facility. But again, there is no direct correlation between the chemical composition modeled and the actual one reported at the site. We were not allowed to work with the Hilmar chemical data, based on stipulations made ion the SEP agreement and related regulations. Hence, the chemical profile from the dairy facilities was modeled after data reported in the literature. We cannot comment how close it is to actual conditions at Hilmar.

Our investigation indicates that the degradation to groundwater quality is likely to occur at the close vicinity of the discharge sites. Whereas the solutes can migrate downstream of the discharge sites over distances of thousands of meters, changes (increases) in FDS concentrations larger than 500 mg/L compared to background are limited to the groundwater underneath the discharge sites and over distances of hundreds of meters downstream. The probability for increase in concentrations of such magnitude over larger distances were computed and reported above, and were found to be close to zero. These are the predicted outcomes from our worst-case scenario analyses. Most land discharge sites do not operate under the "worst case scenario", and their impacts on groundwater quality are expected to be milder compared to those predicted by the worst-case scenarios.

The impacts of land discharge on groundwater quality are given in exceedance probabilities. These probabilities represent the probability for the concentration to exceed a threshold at a give placed and time. The statement of impact in terms of probability intends to address the uncertainty in estimating such impact. This uncertainty stems from limited knowledge of actual site conditions, including hydrologic conditions and hydrogeochemical parameters such as the permeability and chemical reaction parameters. To address this uncertainty, we opted to work with a range of values for the uncertain parameters instead of a single value. Each range of values is summarized in the form of a histogram, and values are drawn at random form this range to produce realization. Many realizations are thus produced, each being a physically plausible representation of reality. The underlying assumption is that an ensemble of realizations will create an ensemble of performance that will encapsulate the actual one. This approach follows a well-known procedure in statistics called Monte Carlo simulation. The way to interpret the exceedance probability is as follows. If an exceedance probability at a certain location and time is equal to 90%, this means that 9 out of ten sites are expected to produce a concentration above the threshold at that location and time. As additional data is collected at the discharge site, and as additional information becomes available, the exceedance probabilities will change. Instead of working with large ranges for the unknown parameters, we will be able then to work with narrower ranges. A narrower range can lead to higher or lower number of realizations with concentrations above the threshold values. Additional measurements do not necessarily reduce exceedance probabilities,; they only make predictions more accurate and our prediction closer to reality. The procedure for incorporating measurements into prediction is called conditioning. It is well documented in the statistics literature, and we recommend it for adoption in applications. What can explain this limited spatial extent of the spreading of solutes underneath the discharge sites? plume? It is a combination of effects, including the reduction in concentrations due to

dispersion, and in a few cases due to the buffering effects of the vadose zone (See Summary provided at the end of Section II.3). There is a strong vertical pressure gradient in the shallow aquifers, pointing deeper, which leads to vertical migration of solutes, deeper into the earth, into the deeper aquifer. This limits the spatial extent of the migration of the pollutants, but at the same time to development of hot spots of high concentrations at the areas just underneath and downstream of the land discharge sites. Such hotspots will be sustainable as long as the vertical gradients of sufficient magnitude persist. These gradients, which are created by pumping at the deeper formation, and possibly by other effects such as mountain font recharge. A reversal in the direction of the gradient is possible if the water table in the hydrostratigraphic units surrounding the central Valley increase, for example in high precipitation years or reduction on the deep aquifer pumping.

As the concentration in the hot spots increases, pollutants will continue to migrate into the deeper formations, eventually leading to termination of the deep-formation pumping, as the need arise to drill wells deeper into the aquifer. Once the pumping in the deeper formation ceases or in fact is performed deeper, or the gradient reverses from any other reason, the containment effect will reduce or even vanish, and the pollutants accumulated in the hot spots will migrate and spread over a much larger area. However, this will happen primarily in the upper aquifer, and the FDS hotspots will migrate horizontally. The impact to groundwater quality will become more widespread, but since the pumping wells will be located deeper, the impact on drinking water will not be immediate. If one is willing to write off the water stored in the upper aquifer above the Corcoran layer, then this impact can be considered minor. However, that would imply losing the storage capacity of the upper aquifer. And with time, due to vertical migration of solutes, the contaminants will spread even deeper. Our analysis assumes that the deep formation pumping will continue in its current form into the foreseeable future, which means the 30 years' design horizon for this study. This is a working hypothesis and there is no guarantee that this will be the case. An alternative scenario would be to investigate the effects of pumping termination and gradient reversal at a certain time, and to evaluate this effect on the FDS hot spots. We have not investigated this scenario due to budgetary constraints. But it needs further investigation.

Hydrological conditions, soil parameters, chemical and profiles as well as the magnitude of the waste water discharge vary across land discharge sites. There is no one formula that can be used to predict what the actual impacts to groundwater will be at each of the sites because of the wide range of conditions and parameters that need to be recognized. It is thus imperative that specific site investigation and modeling analysis are conducted at each active and potential land discharge site. Strategies need to be developed to make such studies economic and rapid. The tools we developed and presented here are applicable immediately for such purposes.

II.5 Environmentally Impacted Sites Analysis

A. Introduction

The San Joaquin Valley is unique in both the diversity of flora and fauna found in the region and the extent to which this area has changed due to human influence. Prior to extensive agricultural development, the valley supported extensive wetlands, grasslands, oak savannahs and arid plains, and hosted a myriad of indigenous and migratory species. The floor of this valley is comprised of an ancient seafloor rich in trace elements and heavy metals, and in conjunction with an arid summer climate, serves as an ideal grounds for modern agriculture. Today the Central Valley is a key component in the agricultural infrastructure of the U.S., and correspondingly the extent of wetlands and natural areas has been reduced to roughly 5% of its original size. These islands of natural environment serve as major thoroughfares on the routes of many migratory bird species, and host a diverse assortment of indigenous animals and plants, including multiple threatened and endangered species.

Among the patchwork of national wildlife refuges, state parks and easement areas are lands managed by the U.S. Bureau of Reclamation, U.S. Fish and Wildlife Service, California Department of Parks and Recreation and California Department of Water Resources, all of which involve unique conservation and preservation requirements. Conservation easement areas, which involve a "sale" of land to the federal government, state government or a private interest group, leave the land in private ownership but require specific restrictions dictated in the terms of sale or donation in order to preserve wildlife and natural habitat. Thus the regulatory standards of conservation required in this area vary widely and involve many stakeholders. In addition, the relatively small and sparse conservation areas each host a unique assortment of species. For example, the South Fork Wildlife Area along the Kern River hosts 1/5 of the states remaining natural willow and cottonwood riparian areas. The Tule Elk State Reserve near Bakersfield includes natural grasslands and marshlands and is home to four endangered species, the San Joaquin kit fox, the San Joaquin antelope squirrel, the Tipton kangaroo rat and the blunt-nose leopard lizard, as well as a variety of threatened species. Nearby, the Valley Grasslands in Merced County host 500,000 to 1 million winter migratory birds (www.ceres.ca.gov).

B. Sensitive Sites

For this study, sensitive areas are defined as any area with environmental value in the form of fauna, flora or recreation that could be impacted by salinity discharge. Federal and state parks, easement and protected lands, endangered species critical habitats and surface waters are included. The goal of this study is to catalog those sites that are near Central Valley food processors and need to be considered in future design plans. Impact in this study is defined as a change in salinity concentration of the groundwater or surface water. It does not necessarily imply any violation of applicable regulations or any measurable impact to the natural habitat.

This discussion should be viewed in light of our vadose zone and groundwater studies in other sections of this study. Being included in the list below does not imply any violation of law, or even a realistic chance that this can actually happen. It does imply, however, that additional study or care may beneeded to prevent violations or impacts. The current flow regime in the Central Valley is affected by extensive pumping at the deeper formation. This leads to strong vertical flows and inhibits the lateral migration of solutes from the land discharge sites. However, in the absence of such vertical flows, lateral migration will be enhanced, putting many of the sites enumerated on our list within the reach of salts from the discharge sites.

We are confident that our list is incomplete, in terms of naming of potentially impacted sites, and in terms of assessing all the factors that need to be included in a complete impact analysis. A more detailed analysis needs to account for (1) local hydrological (e.g., precipitation, land cover) and hydrogeological (e.g., soil hydraulic and chemical parameters, depth to water table) factors; (2) eco-toxicological impact studies; (3) contribution from industries other than the food-processing industry (see Discussion in Section II.5D below). Such analysis can change our earlier statement in this section, concerning the risk of environmental impact, materially. All food processor discharges have the potential to impact the groundwater at the discharge site and downstream. Our numerical analyses (Section 6) concluded that such impacts are expected to occur within a 3 mile radius of the discharge site, and most likely at distances much smaller than 3 miles. Our analysis below identifies sites within 3 miles of a food processor discharge that are suspected to be sensitive to salinity discharges. Predicted impacts in addition to local groundwater contamination are summarized in the analysis. It is emphasized that the maps are not exhaustive, and represent the best of our knowledge at the time of preparing this report.

C. Potential Impacts

This study provides an overview of possible impacts to potentially sensitive sites in the Central Valley. The intent is not to exhaustively or specifically catalog environmental impacts of salinity discharges by food processors. The information contained in this section is incomplete and represents the best available information when submitted. Potential impacts have been broken into categories shown in Section II.6.B. Appendix B.1.

Environmentally sensitive sites within 3 miles of food processors and POTWs in the Central Valley are cataloged in II.6.B. Appendix B.2 and B.3, respectively. The Tables also list potential impacts or violations from Appendix B.1 that could occur from salinity discharges, shown in bold.

Central Valley food processors and Publicly Owned Treatment Works (POTWs) are shown in Figures 187 through 192 below. Numbered labels correspond to NAICS industry classifications shown in Table 59 at the end of this section. Many sites potentially sensitive to salinity discharges are also shown in the Figures. Red dots indicate sites that are within 3 miles of an environmentally sensitive site regardless of proximity to urban areas. Yellow dots are within 3 miles of an urban area, but not another environmentally sensitive site and green dots have no

environmentally sensitive sites identified within 3 miles.

Among the potentially sensitive sites close to food processors and POTWs in II.6.B. Appendices B.2 and B.3 are surface water bodies, urban areas, federal and state wildlife areas, endangered species critical habitats and easement lands. The surface water bodies include major rivers such as the San Joaquin, Sacramento, Merced, Kings, Stanislaus and Tuolumne rivers; lakes and reservoirs such as Lake Woollomes, Modesto Reservoir and Ross Reservoir; and smaller water bodies. The wildlife areas include Kesterson National Wildlife Refuge, Mendota Wildlife Area, North Grasslands Wildlife Area, White Slough Wildlife Area, Woodbridge Ecological Reserve and MC Connell State Park. Many cities across the Central Valley using well water are also in close proximity to food processors.

This portion of the study aims to show the widespread potential for impacts to sites across the Central Valley. Section II.6.B Appendix B.1 suggests potential impacts, shown in Section II.6.B B.2 and B.3, to sensitive areas in close proximity to Central Valley food processors. This portion of the study is not meant to be exhaustive. It is emphasized though that there is no indication that there are any impacts that are actually occurring or have occurred to any of the sites enumerated below. This list does not suggest that there is a probability for such impacts to occur. This list is quite speculative in the sense that it is not supported by any evidence to the existence of any effects. As such, it does not form the basis for any action; it only intends to trigger a discussion along this line on this subject and to provide a factual starting point, if such a discussion indeed takes place.

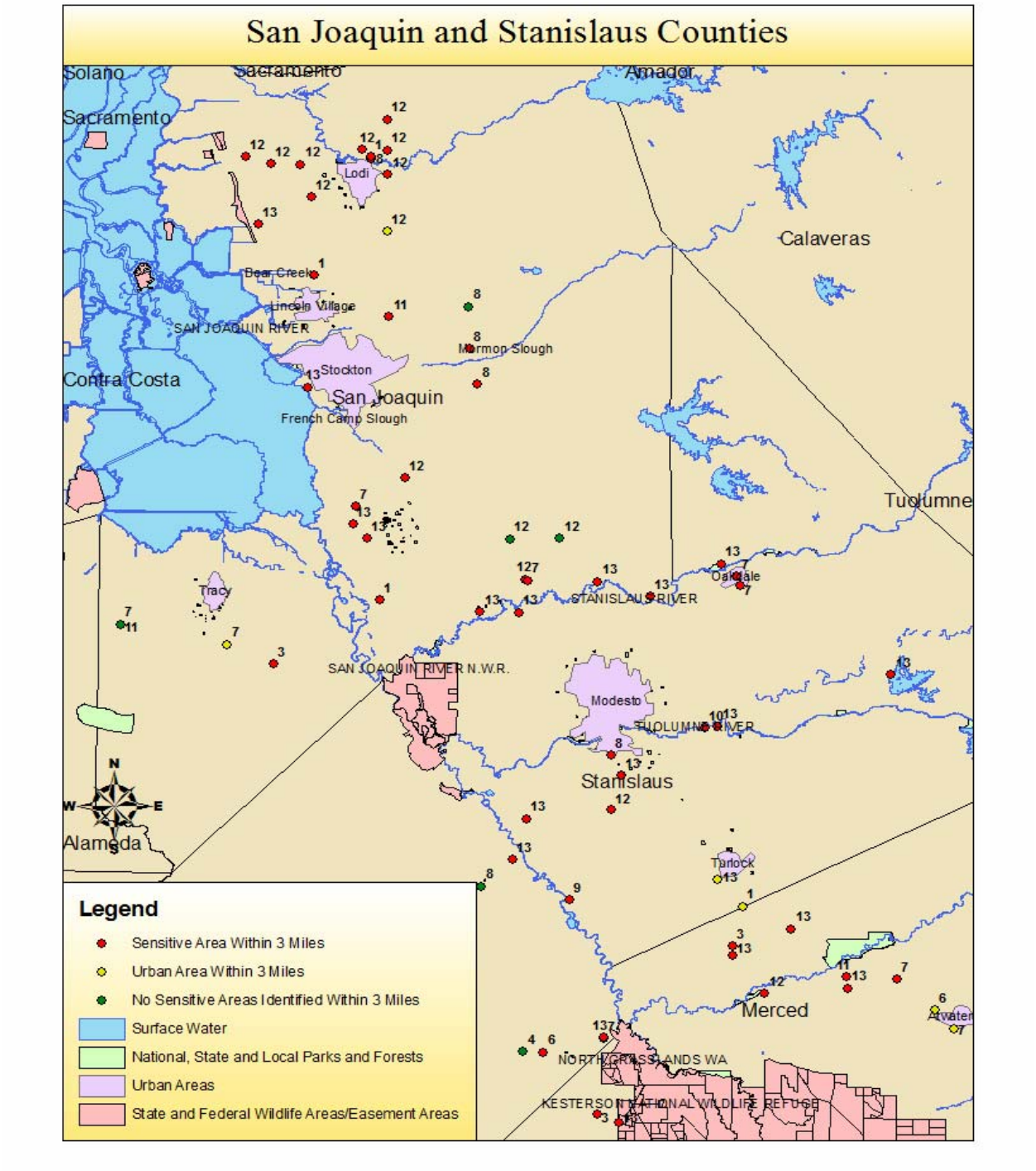

Figure 187

Environmentally sensitive sites in San Joaquin and Stanislaus counties. Numbered labels refer to industry classifications in Table 59. See Appendix B.2 and B.3 in Section II.6.B for more detail.

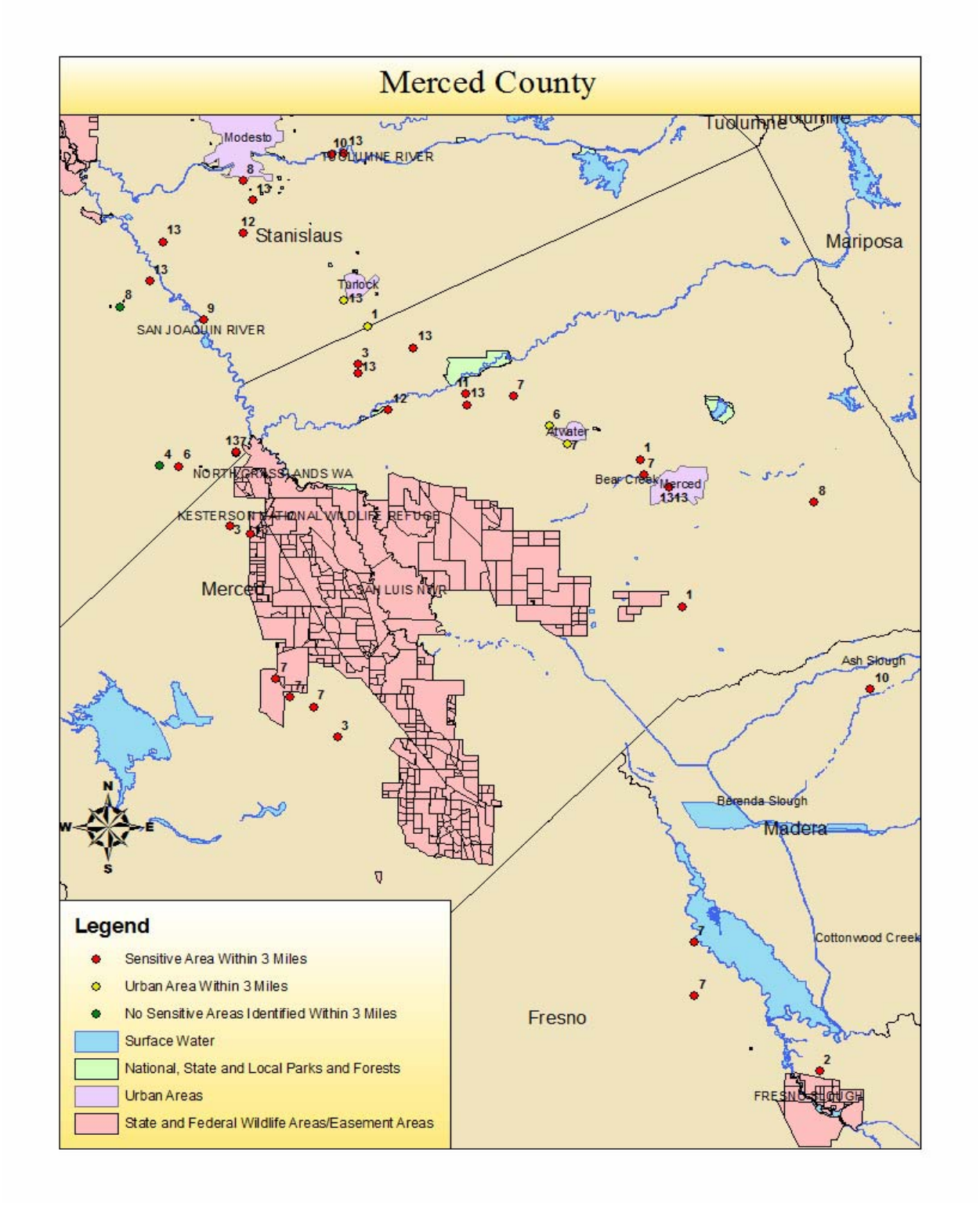

Figure 188

Environmentally sensitive sites in Merced, Madera and Fresno counties. Numbered labels refer to industry classifications in Table 59. See Appendix B.2 and B.3 in Section II.6.B for more detail.

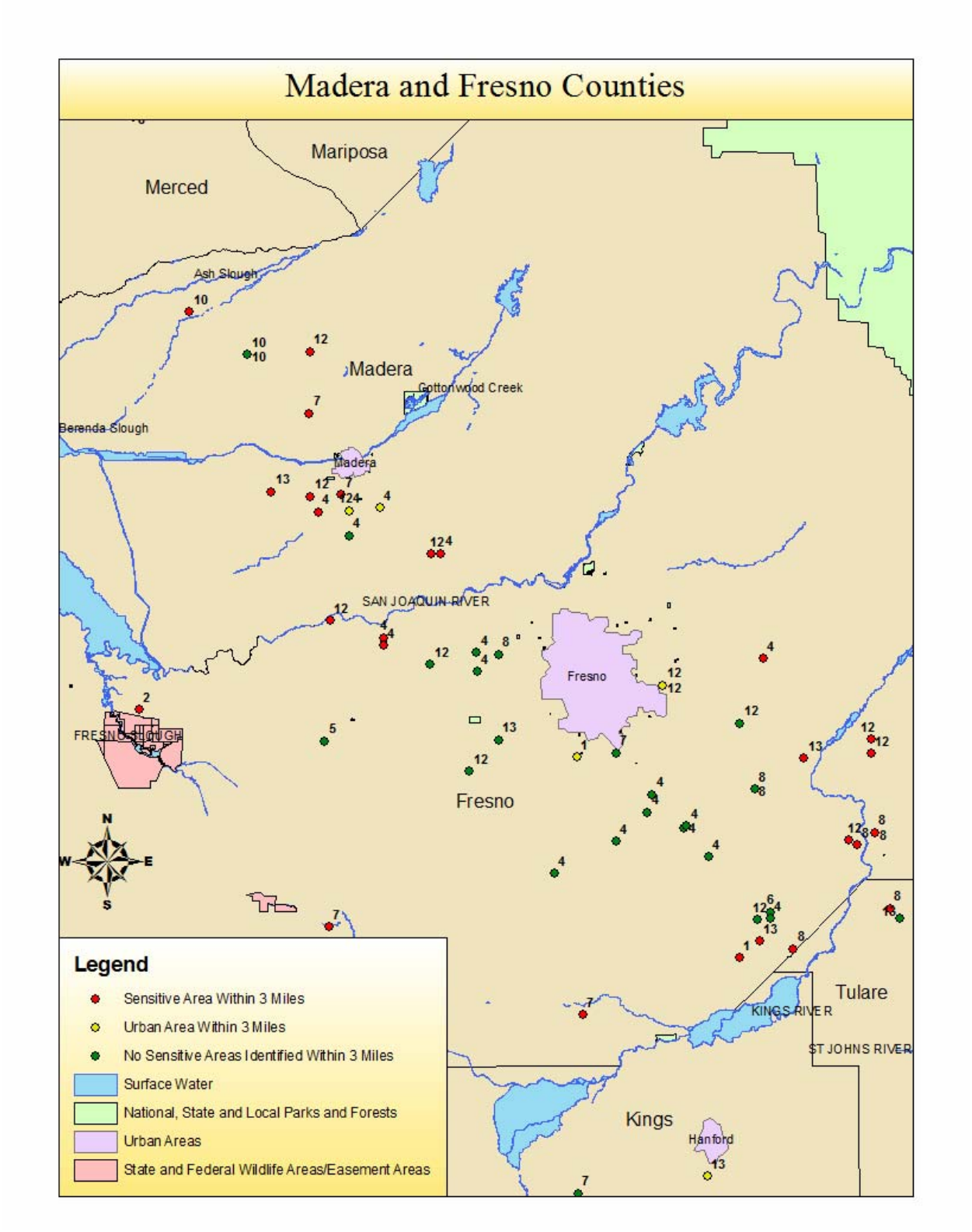

Figure 189

Environmentally sensitive sites in Madera and Fresno counties. Numbered labels refer to industry classifications in Table 59. See Appendix B.2 and B.3 in Section II.6.B for more detail.

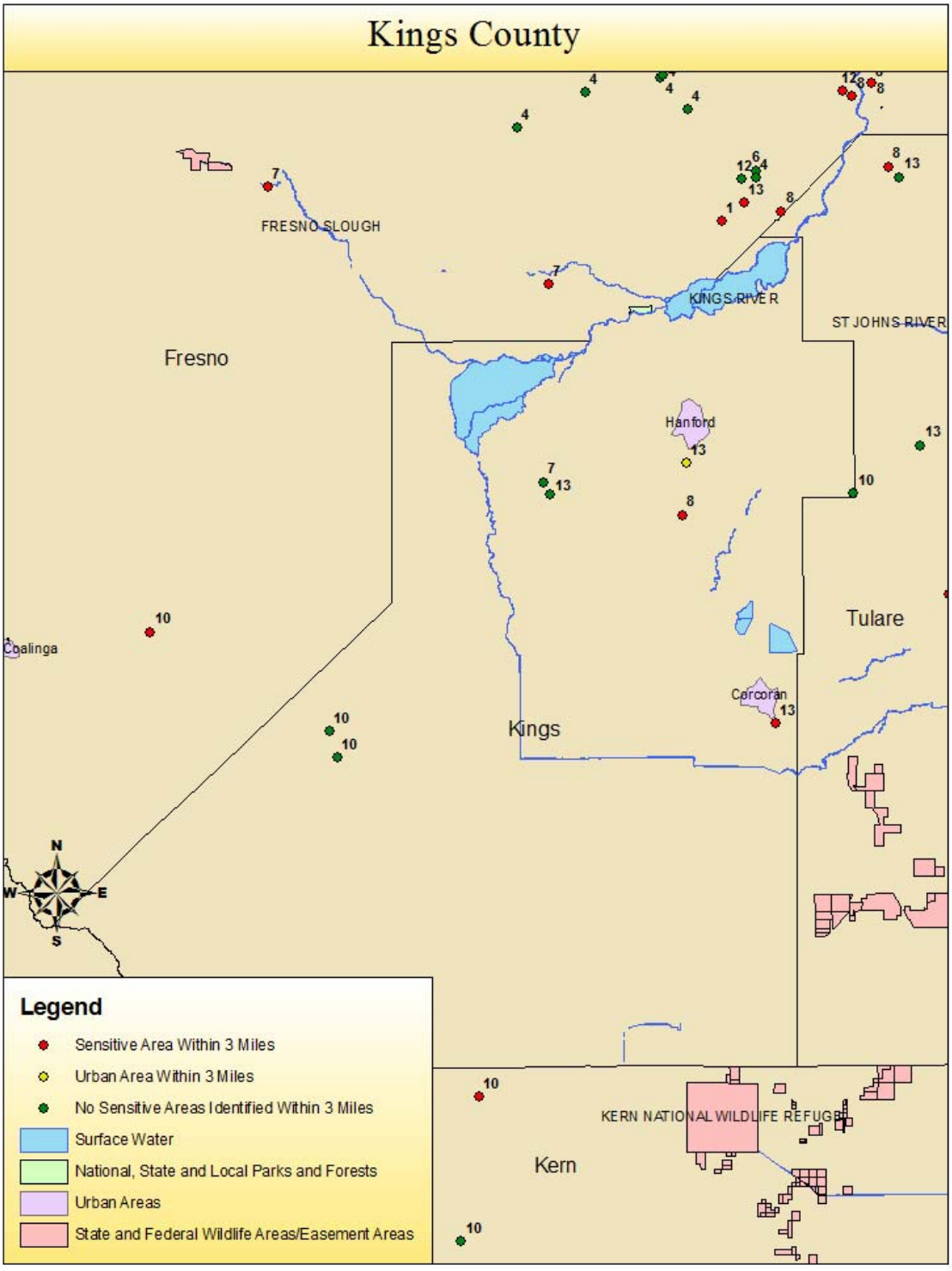

Figure 190

Environmentally sensitive sites in Kings County. Numbered labels refer to industry classifications in Table 59. See Appendix B.2 and B.3 in Section II.6.B for more detail.

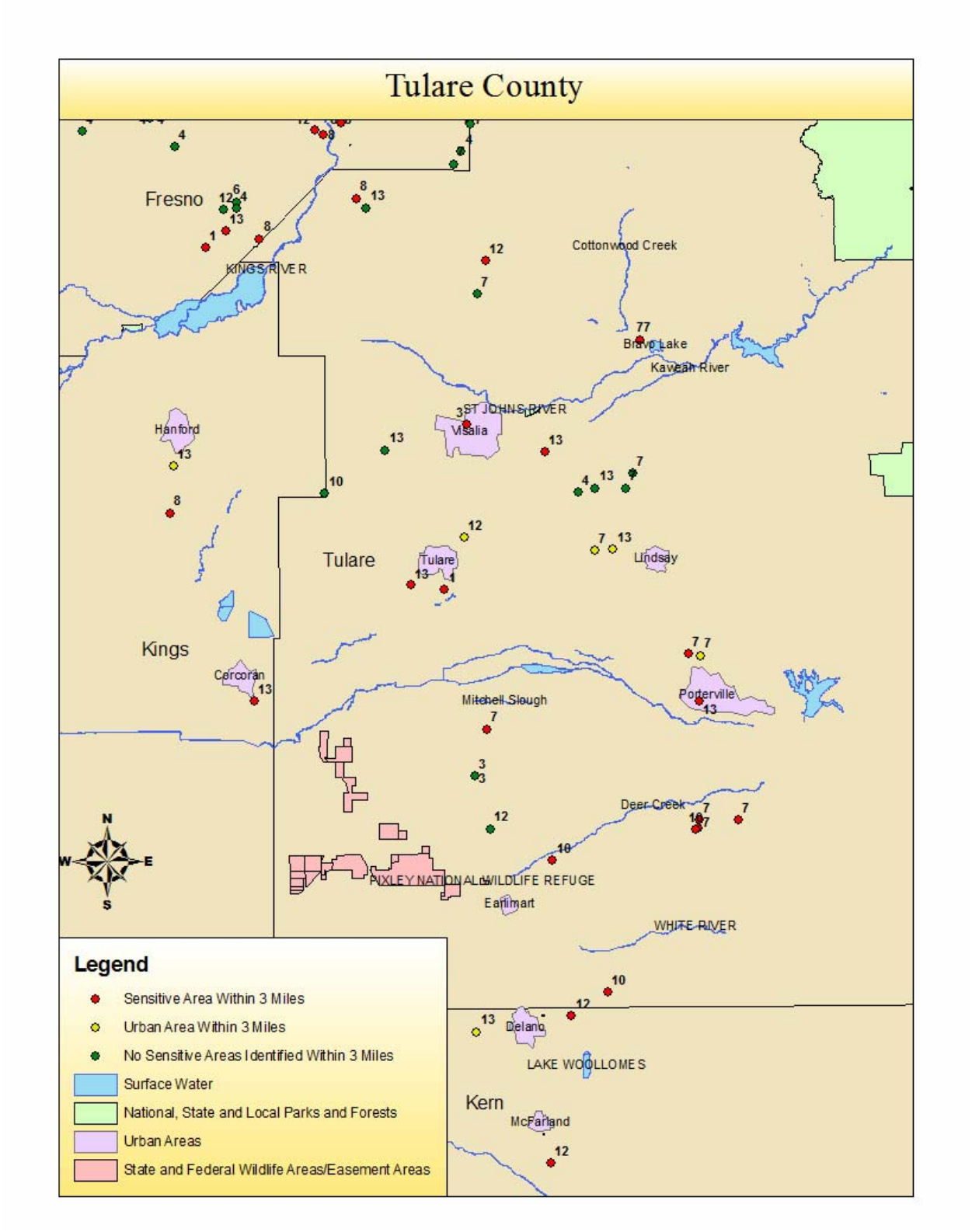

Figure 191

Environmentally sensitive sites in Tulare County. Numbered labels refer to industry classifications in Table 59. See Appendix B.2 and B.3 in Section II.6.B for more detail.

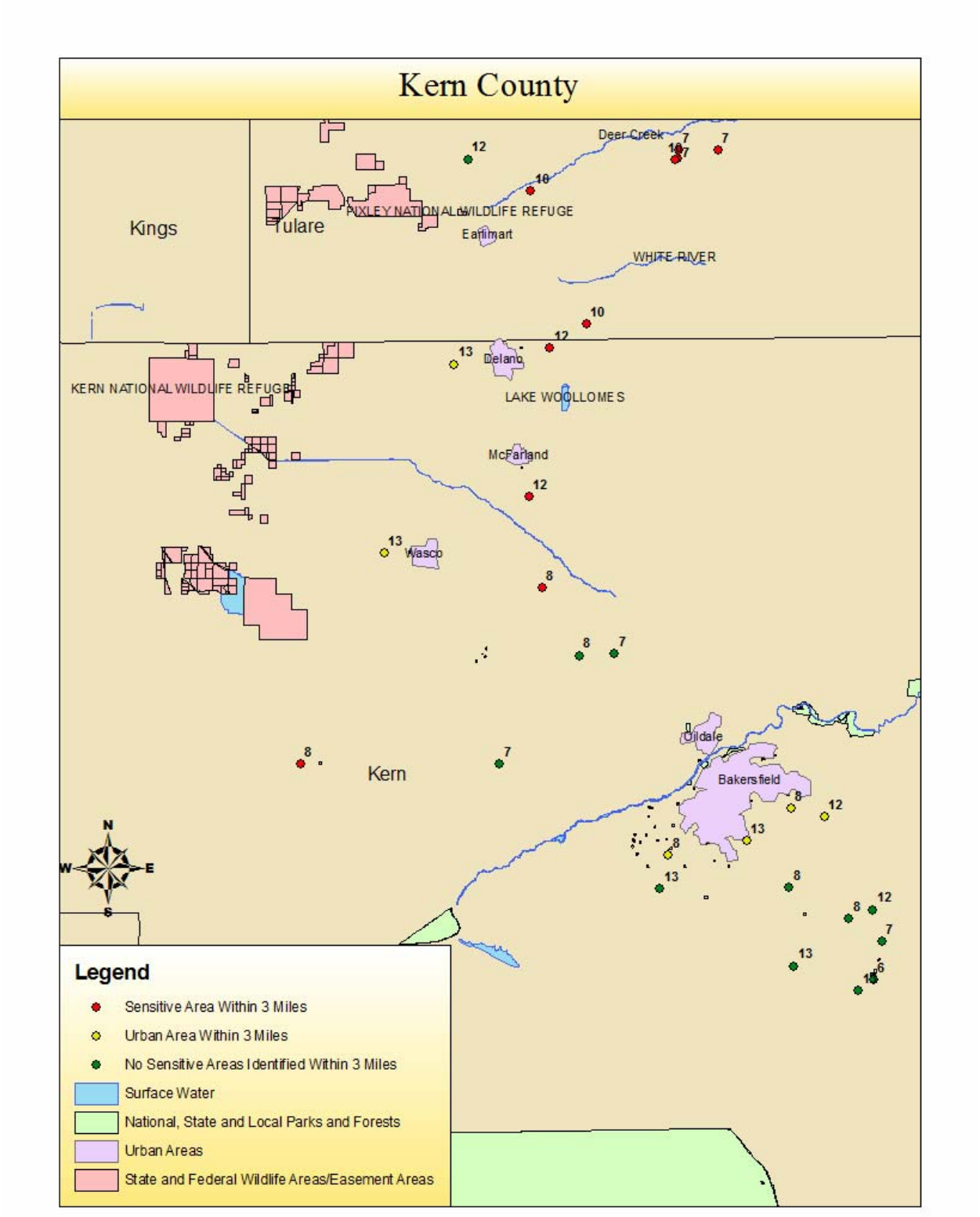

Figure 192

Environmentally sensitive sites in Kern County. Numbered labels refer to industry classifications in Table 59. See Appendix B.2 and B.3 in Section II.6.B for more detail.

1. Endangered Species Critical Habitats

In addition to potentially sensitive areas shown in Figures 187 through 192, there are also several endangered species critical habitats in the Central Valley [3]. Section II.6.B Appendix B.2 and B.3 contain the endangered species critical habitats within 3 miles of processors. Table 58 contains a more complete list of processors in close proximity to endangered species critical habitats. This is not a complete list of California endangered species critical habitats within 10 miles of facilities.

Table 58: Central Valley food processors and POTWs in close proximity to endangered species critical habitats. [1]Labels shown in Appendix II.6.B and on Figures 187-192.

Endangered Species Critical Habitats in Close Proximity to Central Valley Food Processors and POTWs		
Distance (mi)	Buena vista lake shrew	Facility NAICS industry classification and map labels[1]
<3		
3-5	7	Fruit & vegetable canning
5-10	8	Fruit and Vegetable Canning, Pickling, and Drying
	13	Publicly Owned Treatment Works
	8	Fruit and Vegetable Canning, Pickling, and Drying
	13	Publicly Owned Treatment Works
	Delta Smelt	
<3	1	Animal slaughtering & processing
	13	Publicly Owned Treatment Works
	3	Dairy Product Manufacturing
	7	Fruit & vegetable canning
3-5		
5-10		
	CA Tiger Salamander	
<3		

3-5	8	Fruit and Vegetable Canning, Pickling, and Drying
	7	Fruit & vegetable canning
	7	Fruit & vegetable canning
	7	Fruit & vegetable canning
	7	Fruit & vegetable canning
	13	Publicly Owned Treatment Works
5-10	13	Publicly Owned Treatment Works
	7	Fruit & vegetable canning
	13	Publicly Owned Treatment Works
	4	Dried & dehydrated food mfg
	7	Fruit & vegetable canning
	Kecks Checkermallow	
<3		
3-5	7	Fruit & vegetable canning
5-10	7	Fruit & vegetable canning
	7	Fruit & vegetable canning
	10	Roasted Nuts and Peanut Butter Manufacturing
	Large flowered fiddleneck	
5-10	7	Fruit & vegetable canning
	11	Waste & Miscellaneous
	7	Fruit & vegetable canning
	3	Dairy Product Manufacturing
	Vernal Pool	
<3	1	Animal slaughtering & processing

		13	Publicly Owned Treatment Works
		13	Publicly Owned Treatment Works
		8	Fruit and Vegetable Canning, Pickling, and Drying
		4	Dried & dehydrated food mfg
		12	Wineries
		7	Fruit & vegetable canning
		7	Fruit & vegetable canning
		7	Fruit & vegetable canning
		12	Wineries
3-5		7	Fruit & vegetable canning
		13	Publicly Owned Treatment Works
		12	Wineries
		7	Fruit & vegetable canning
		7	Fruit & vegetable canning
		4	Dried & dehydrated food mfg
		12	Wineries
		12	Wineries
		7	Fruit & vegetable canning
		10	Roasted Nuts and Peanut Butter Manufacturing
		10	Roasted Nuts and Peanut Butter Manufacturing
5-10	Many		

Table 59: NAICS industry classification map labels. Numbers correspond to map labels in Figures 187-192 above and Appendices B.2 and B.3 in Section II.6.B.

NAICS Industry Classification	Map Label
Animal slaughtering & processing	1
Beet Sugar Manufacturing	2
Dairy Product Manufacturing	3
Dried & dehydrated food mfg	4
Fat and Oils Refining and Blending	5
Frozen Food Manufacturing	6
Fruit & vegetable canning	7
Fruit and Vegetable Canning, Pickling, and Drying	8
Rendering and Meat Byproduct Processing	9
Roasted Nuts and Peanut Butter Manufacturing	10
Waste & Miscellaneous	11
Wineries	12
Publicly Owned Treatment Works	13

II.6 Appendices

A. Appendix A: List of Dischargers Included in the Screening Analysis (Names and WDID)

Wineries and Related Industries

DELICATO VINEYARDS 5B392039001
GALLO, E & J 5D102022001
GALLO, E & J 5C202017001
GALLO, E & J 5C242004001
GOLDEN STATE VINTNERS 5C10NC00014
GOLDEN STATE VINTNERS 5D102133001
GOLDEN STATE VINTNERS - CUTLER 5D542006001
GOLDEN VALLEY GRAPE JUICE/WINE 5C202033001
GOLDSTONE LAND CO 5B392004003
KAUTZ VINEYARDS INC 5B051019001
LODI VINTNERS, INC. 5B392040001
NONINI, A WINERY 5D102050001
OAK RIDGE WINERY, LLC 5B392001001
O'NEILLS VINTNERS & DISTILLERS 5D102031001
RJM ENTERPRISES 5B392108001
ROBERT MONDAVI CORPORATION 5B392068001
SCHATZ, RODNEY & GAYLA 5B39NC00011
SPENKER RANCH INC 5B39NC00017
SUTTER HOME WINERY, INC. 5B39NC00012
VAN RUITEN-TAYLOR RANCH LTD 5B39NC00036
WINE GROUP, INC. 5D542026001
WINE GROUP, INC. (Sanger) 5D102044002
WINE GROUP, THE (Ripon) 5B392003001

Tomato Processors

CONAGRA GROCERY PRODUCTS CO 5B50NC00011
CONAGRA HELMS 5D102111001
CONOPCO DBA UNILEVER BFNA 5C242022001
INGOMER PACKING (Plant 1) 5c241010001
INGOMER PACKING (Plant 2)
LIBERTY PACKING COMPANY 5C242010001
MORNING STAR PACKING COMPANY 5C241011001
NT GARGIULO & DERRICK ASSOC 5C201027002
OASIS FOODS, INC 5C242013001
SUN GARDEN GANGI CANNING CO. 5C241003002
TRIPLE E PRODUCE CORPORATION 5B392077001

Meat Processors

ALPINE PACKING COMPANY 5B392048001
CLAUSEN MEAT PACKING CO, INC 5C242003001
DAIRYMAN'S MEAT PROCESSING 5C242014001
DARLING INTERNATIONAL INC 5C502027001
FOSTER FARMS 5C241006001
HARRIS FARMS, INC 5D102019001
LONG RANCH, INC. 5B395278001
MOUA YAVA dba ASIAN FARM
RICHWOOD MEAT COMPANY 5C242026001
WOODBRIDGE PARTNERS INC 5B392043001

B. Appendix B: Environmentally Sensitive Areas

1. List of Codes for Potential Impacts

Potential impacts to environmentally sensitive sites within 3 miles of food processor waste water discharge site. Impact codes appear in bold in Appendix B.2 and B.3.

Code	Potential Impact
1	Potential Impact to City Wells
2	Potential Impact to Surface Water: Water Supply A: Municipal Supply B: Agricultural Supply C: Industrial Supply not dependant on water quality D: Industrial Supply that depends on water quality E: Freshwater Replenishment: used to maintain quantity and quality of surface water
3	Potential Impact to Surface Water: Recreational Activities A: Water Contact Recreation B: Non-water Contact Recreation
4	Potential Impact to Surface Water: Fisheries A: Fish Spawning and Early Life B: Migration or Other Temporary Aquatic Activities
5	Potential Impact to Natural Habitat A: Cold Freshwater Habitat B: Warm Freshwater Habitat C: Wildlife Habitat D: Rare, Threatened, or Endangered Species
6	Potential Impacts to Ground Water: Recharge from surface
7	Applicable Federal Regulations
8	Applicable State Regulations

2. List of Environmental Sensitive Areas near Food Processing Facilities

Potentially environmentally sensitive areas within 3 miles of Central Valley food processors. References are in square brackets and the bold codes correspond to impacts in Appendix B.1. Processors are shown in Section II.5.C, Figures 187-192. Map labels corresponding to industry classification are shown in Table 59.

Map Label	NAICS Industry Classification	Sensitive Sites within 3 mi	Impacts (See Table 1 for key)	Notes and Citations
1	Animal slaughtering & processing	City of Lincoln Village		
		Delta Surface Waters	Sacramento San Joaquin Delta – Beneficial uses vary, can include all	[1, p. II-8]
		Delta Smelt Endangered Species Critical Habitat	**5C, 5D**	Critical Habitats [3]
8	Fruit and Vegetable Canning, Pickling, and Drying	City of Bakersfield	**1 (city using well water)**	[8]
7	Fruit & vegetable canning	Dry Creek		

		Vernal Pool Endangered Species Critical Habitat	**5C, 5D**	Critical Habitats [3]
5	Fat and Oils Refining and Blending	None Identified		
8	Fruit and Vegetable Canning, Pickling, and Drying	Kings River	Friant Kern To Peoples Weir: 4 (effluent may be hazardous for fishing and hatching along this segment of the Kings River) **2A,B,D; 3A,B; 5B,C; 6**	[4]

				[2, p. II-4], Basin Plan, 2007, regulations concerning EC of Kings River for Reach IV, limits on EC to less than 200 □mho/cm [2, p. III-5]
12	Wineries	None Identified		
1	Animal slaughtering & processing	City of Fresno	**1 (city using well water)**	[8]
7	Fruit & vegetable canning	None Identified		
4	Dried & dehydrated food mfg	None Identified		

8	Fruit and Vegetable Canning, Pickling, and Drying	Protected/Endangered Habitats	**5C,5D - Native Alkali Scald Habitat, supports endangered/ threatened species through acres of mitigation lands**	[7]
8	Fruit and Vegetable Canning, Pickling, and Drying	City of Bakersfield	**1 (city using well water)**	[8]
7	Fruit & vegetable canning	None Identified		
12	Wineries	Protected/Endangered Habitats	**5C,5D - Vernal Pool and Salt Marsh habitat**	[7]
12	Wineries	None Identified		
8	Fruit and Vegetable Canning, Pickling, and Drying	City of Modesto	**1 (city using well water)**	[8]

		Tuolumne River	Tuolumne River from New Don Pedro Dam to San Joaquin River: 2B; 3A,B; 4A,B; 5A,B,C	[1, p. II-8]
			4 (effluent may be hazardous for fishing and hatching along this segment of the Tuolumne River)	[4]
8	Fruit and Vegetable Canning, Pickling, and Drying	City of Lodi	**1 (city using well water)**	[8]
		Mokelumne River	Mokelumne River from Camanche Reservoir to Delta: 2B; 3A,B; 4A,B; 5A,B,C	[1, p. II-7]
3	Dairy Product Manufacturing	None Identified		
3	Dairy Product Manufacturing	None Identified		

7	Fruit & vegetable canning	Fresno River	Fresno River from Hidden Reservoir to San Joaquin River: 2B; 3A,B; 5B,C	[1, p. II-7]
		City of Madera	**1**	
10	Roasted Nuts and Peanut Butter Manufacturing	None Identified		
3	Dairy Product Manufacturing	Protected/Endangered Habitats	**5C,5D - Alkali Marsh, Sycamore Alluvial Woodland (rare habitat type), Vernal Pools, Duck Clubs**	[7]
7	Fruit & vegetable canning	Delta Surface Waters	Sacramento San Joaquin Delta – Beneficial uses vary, can include all	[1, p. II-8]
		San Joaquin River	San Joaquin River from the Mouth of Merced River to	[1, p. II-8]

			Vernalis (Vernalis is slightly south of the processor) 2B,D; 3A,B; 4A,B; 5B,C	
12	Wineries	Dry Creek		
		Vernal Pool Endangered Species Critical Habitat	**5C,5D**	Critical Habitats [3]
12	Wineries	Cottonwood Creek		
		Fresno River	**4** Fresno River from Hidden Reservoir to San Joaquin River: 2B; 3A,B; 5B,C	[4] [1, p. II-7]
		City of Madera	**1 (city using well water)**	[8]
12	Wineries	Woodbridge Ecological Reserve	**5C**	[5]
		White Slough Wildlife Area	**5C**	[5]
		Delta Surface Waters	Sacramento San Joaquin Delta – Beneficial uses vary,	[1, p. II-8]

			can include all	
6	Frozen Food Manufacturing	Protected/Endangered Habitats	**5C,5D-Main Canal and Sycamore Alluvial Woodland (rare habitat)**	[7]
11	Waste & Miscellaneous	City of Stockton	**1 (city using well water)**	[8]
		Calaveras River	Calaveras River from New Hogan Reservoir to Delta: 2A,B; 3A, B; 4A,B; 5A,B,C	[1, p. II-7]
8	Fruit and Vegetable Canning, Pickling, and Drying	None Identified		
4	Dried & dehydrated food mfg	Vernal Pool Endangered Species Critical Habitat	**5C,5D**	Critical Habitats [3]

10	Roasted Nuts and Peanut Butter Manufacturing	Berenda Slough		
		Ash Slough		
1	Animal slaughtering & processing	City of Turlock	**1 (city using well water)**	[8]
1	Animal slaughtering & processing	City of Tulare	**1 (city using well water)**	[8]
		Bates Slough		
7	Fruit & vegetable canning	Fresno Slough		
		Easement Areas	**5**	
7	Fruit & vegetable canning	City of Oakdale	**1 (city using well water)**	[8]
		Stanislaus River	Stanislaus River from Goodwin Dam to San Joaquin River: 2B,C,D; 3A,B; 4A,B; 5A,B,C	[1, p. II-8]

7	Fruit & vegetable canning	Bear Creek	**3,4**	[4]
		City of Merced	**1 (city using well water)**	[8]
1	Animal slaughtering & processing	Easement Areas	**5**	
		Vernal Pool Endangered Species Critical Habitat	**5C,5D**	Critical Habitats [3]
9	Rendering and Meat Byproduct Processing	San Joaquin River	Mouth of Merced River to Vernalis 2B,D; 3A,B; 4A,B; 5B,C	[1, p. II-8]
8	Fruit and Vegetable Canning, Pickling, and Drying	Guernsey Slough		
8	Fruit and Vegetable Canning, Pickling, and Drying	Kings River	**4**	[4]

			Reach IV: 2A,B,D; 3A,B; 5B,C; 6	[2, p. II-4] Basin Plan, 2007, regulations concerning EC of Kings River for Reach IV, limits on EC to less than 200 □mho/cm [2, p. III-5]
8	Fruit and Vegetable Canning, Pickling, and Drying	None Identified		
8	Fruit and Vegetable Canning, Pickling, and Drying	None Identified		
12	Wineries	City of Delano	**1 (city using well water)**	[8]
		Lake Woollomes	**3,4**	[4]

12	Wineries	French Camp Slough		
10	Roasted Nuts and Peanut Butter Manufacturing	None Identified		
12	Wineries	San Joaquin River	**3,4** Friant Dam to Mendota Pool: 2A,B,D; 3A,B; 4A,B; 5A,B, C	[4] [1, p. II-7] Basin Plan, 2007, regulations concerning EC of San Joaquin from Friant Dam to Mendota Pool, limits on EC to less than 150 □mho/cm (90 percentile) [1, p. III-7]
12	Wineries	Merced River	**3,4** Merced River from McSwain Reservoir to San Joaquin River: 2A,B,C,D; 3A,B; 4A,B; 5A,B,C	[4] [1, p. II-8]
4	Dried & dehydrated food mfg	None Identified		
8	Fruit and Vegetable Canning, Pickling, and Drying	Kings River	**4** Reach IV: 2A,B,D; 3A,B; 5B,C; 6	[4] [2, p. II-4]

				Basin Plan, 2007, regulations concerning EC of Kings River for Reach IV, limits on EC to less than 200 □mho/cm [2, p. III-5]
8	Fruit and Vegetable Canning, Pickling, and Drying	None Identified		
11	Waste & Miscellaneous	Merced River	**3,4**	[4]
		MC Connell State Park	**3**	[6]
4	Dried & dehydrated food mfg	None Identified		
4	Dried & dehydrated food mfg	None Identified		

7	Fruit & vegetable canning	None Identified		
12	Wineries	City of Fresno	**1 (city using well water)**	[8]
12	Wineries	City of Fresno	**1 (city using well water)**	[8]
7	Fruit & vegetable canning	City of Atwater	**1 (city using well water)**	[8]
7	Fruit & vegetable canning	None Identified		
12	Wineries	City of Bakersfield	**1 (city using well water)**	[8]
10	Roasted Nuts and Peanut Butter Manufacturing	Protected/Endangered Habitats	**5C,5D – Chino Creek and Los Gatos Creek (important wildlife corridors)**	[7]
7	Fruit & vegetable canning	Cottonwood Creek		
		St. John's River		
		Bravo Lake		

		Kaweah River	Below Lake Kaweah on Kaweah River: 2A,B,C,D ; 3A, B; 5B,C; 6	[2, p. II-4], Basin Plan, 2007, regulations concerning EC of Kaweah River limits EC to 175 □mho/cm [2, p. III-5]
		Vernal Pool Endangered Species Critical Habitat	**5C,5D**	Critical Habitats [3]
12	Wineries	Vernal Pool Endangered Species Critical Habitat	**5C, 5D**	Critical Habitats [3]
12	Wineries	None Identified		
12	Wineries	City of Madera	**1 (city using well water)**	[8]
12	Wineries	City of Lodi	**1 (city using well water)**	[8]
8	Fruit and Vegetable Canning, Pickling, and Drying	None Identified		

8	Fruit and Vegetable Canning, Pickling, and Drying	None Identified		
6	Frozen Food Manufacturing	None Identified		
8	Fruit and Vegetable Canning, Pickling, and Drying	None Identified		
1	Animal slaughtering & processing	Kings River	Reach V: 2B; 3A, B; 5B,C; 6	[2, p. 13] Basin Plan, 2007, regulations concerning EC of Kings River for Reach V, limits on EC to less than 300 □mho/cm [2, p. III-5]
12	Wineries	None Identified		
7	Fruit & vegetable canning	City of Oakdale	**1 (city using well water)**	[8]

		Stanislaus River	Stanislaus River from Goodwin Dam to San Joaquin River: 2B,C,D; 3A,B; 4A,B; 5A,B,C	[1, p. II-8]
3	Dairy Product Manufacturing	Merced River	Merced River from McSwain Reservoir to San Joaquin River: 2A,B,C,D; 3A,B; 4A,B; 5A,B,C	[1, p. II-8]
6	Frozen Food Manufacturing	None Identified		
10	Roasted Nuts and Peanut Butter Manufacturing	Tuolumne River	Tuolumne River from New Don Pedro Dam to San Joaquin River: 2B; 3A,B; 4A,B; 5A,B,C	[1, p. II-8]
7	Fruit & vegetable canning	Easement Areas	**5**	

8	Fruit and Vegetable Canning, Pickling, and Drying	Kings River	Reach IV: 2A,B,D; 3A,B ; 5B,C, 6	[2, p. II-4] Basin Plan, 2007, regulations concerning EC of Kings River for Reach IV, limits on EC to less than 200 □mho/cm [2, p. III-5]
6	Frozen Food Manufacturing	City of Atwater	**1 (city using well water)**	[8]
4	Dried & dehydrated food mfg	None Identified		
12	Wineries	Ross Reservoir		
10	Roasted Nuts and Peanut Butter Manufacturing	None Identified		
7	Fruit & vegetable canning	None Identified		

3	Dairy Product Manufacturing	City of Visalia St. John's River		
4	Dried & dehydrated food mfg	None Identified		
4	Dried & dehydrated food mfg	None Identified		
4	Dried & dehydrated food mfg	City of Madera	**1 (city using well water)**	[8]
7	Fruit & vegetable canning	Easement Areas	**5**	
4	Dried & dehydrated food mfg	None Identified		
7	Fruit & vegetable canning	None Identified		
12	Wineries	City of Lodi	**1 (city using well water)**	[8]

		Mokelumne River	Mokelumne River from Camanche Reservoir to Delta: 2B; 3A,B; 4A,B; 5A,B,C	[1, p. II-7]
1	Animal slaughtering & processing	San Joaquin River	San Joaquin River from the Mouth of Merced River to Vernalis 2B,D; 3A,B; 4A,B; 5B,C	[1, p. II-8]
7	Fruit & vegetable canning	Murphy Slough		
4	Dried & dehydrated food mfg	San Joaquin River	Friant Dam to Mendota Pool: 2A,B,D; 3A,B; 4A,B; 5A,B, C	[1, p. II-7]

				Basin Plan, 2007, regulations concerning EC of San Joaquin from Friant Dam to Mendota Pool, limits on EC to less than 150 (□mho/cm) (90 percentile) [1, p. III-7]
7	Fruit & vegetable canning	None Identified		
12	Wineries	San Joaquin River	Friant Dam to Mendota Pool:	[1, p. II-7]

			2A,B,D; 3A,B; 4A,B; 5A,B, C	Basin Plan, 2007, regulations concerning EC of San Joaquin from Friant Dam to Mendota Pool, limits on EC to less than 150 (□mho/cm) (90 percentile) [1, p. III-7]
10	Roasted Nuts and Peanut Butter Manufacturing	White River		
8	Fruit and Vegetable Canning, Pickling, and Drying	Mormon Slough		
7	Fruit & vegetable canning	Easement Areas	**5**	

3	Dairy Product Manufacturing	Delta Smelt Endangered Species Critical Habitat	**5C, 5D**	Critical Habitats [3]
11	Waste & Miscellaneous	None Identified		
7	Fruit & vegetable canning	None Identified		
10	Roasted Nuts and Peanut Butter Manufacturing	None Identified		
12	Wineries	None Identified		
12	Wineries	Kings River	Reach IV: 2A,B,D; 3A,B ; 5B,C, 6	[2, p. II-4] Basin Plan, 2007, regulations concerning EC of Kings River for Reach IV, limits on EC to less than 200 m (□mho/cm) [2, p. III-5]

7	Fruit & vegetable canning	San Joaquin River	San Joaquin River from Mendota Dam to Sack Dam: 2B,D; 3A,B; 4A,B; 5B, C	[1, p. II-7]
12	Wineries	City of Lodi	**1 (city using well water)**	[8]
		Mokelumne River	Mokelumne River from Camanche Reservoir to Delta: 2B; 3A,B; 4A,B; 5A,B,C	[1, p. II-7]
8	Fruit and Vegetable Canning, Pickling, and Drying	Bear Creek	**4**	[1, p. II-6]
		Vernal Pool Endangered Species Critical Habitat	**5C, 5D**	Critical Habitats [3]
12	Wineries	Kings River	Reach IV: 2A,B,D; 3A,B ; 5B,C, 6	[2, p. II-4]

				Basin Plan, 2007, regulations concerning EC of Kings River for Reach IV, limits on EC to less than 200 (□mho/cm) [2, p. III-5]
10	Roasted Nuts and Peanut Butter Manufacturing	Protected/Endangered Habitats	**5C,5D – Bitterwater Creek (important riparian habitat)**	[7]
10	Roasted Nuts and Peanut Butter Manufacturing	None Identified		
8	Fruit and Vegetable Canning, Pickling, and Drying	None Identified (San Joaquin river just over 3mi)		
10	Roasted Nuts and Peanut Butter Manufacturing	None Identified		

7	Fruit & vegetable canning	Deer Creek		
1	Animal slaughtering & processing	Bear Creek	**4**	**[1, p. II-6]**
		City of Merced	**1 (city using well water)**	[8]
12	Wineries	Stanislaus River	Stanislaus River from Goodwin Dam to San Joaquin River: 2B,C,D; 3A,B; 4A,B; 5A,B,C	[1, p. II-8]
12	Wineries	City of Lodi		
		Mokelumne River	Mokelumne River from Camanche Reservoir to Delta: 2B; 3A,B; 4A,B; 5A,B,C	**[1, p. II-7]**
4	Dried & dehydrated food mfg	San Joaquin River	Friant Dam to Mendota Pool: 2A,B,D; 3A,B; 4A,B; 5A,B, C	[1, p. II-7] Basin Plan, 2007,

				regulations concerning EC of San Joaquin from Friant Dam to Mendota Pool, limits on EC to less than 150 (□mho/cm) (90 percentile) [1, p. III-7]
4	Dried & dehydrated food mfg	San Joaquin River	San Joaquin River from Friant Dam to Mendota Pool: 2A,B,D; 3A,B; 4A,B; 5A,B,C	[1, p. II-7] Basin Plan, 2007, regulations concerning EC of San Joaquin from Friant Dam to Mendota Pool, limits on EC to less than 150 (□mho/cm) (90 percentile) [1, p. III-7]
12	Wineries	None Identified		
12	Wineries	City of Lodi	**1 (city using well water)**	[8]

		Mokelumne River	Mokelumne River from Camanche Reservoir to Delta: 2B; 3A,B; 4A,B; 5A,B,C	[1, p. II-7]
7	Fruit & vegetable canning	Stanislaus River	Stanislaus River from Goodwin Dam to San Joaquin River: 2B,C,D; 3A,B; 4A,B; 5A,B,C	[1, p. II-8]
7	Fruit & vegetable canning	Merced river	Merced River from McSwain Reservoir to San Joaquin River: 2A,B,C,D; 3A,B; 4A,B; 5A,B,C	[1, p. II-8]
		MC Connell State Park	**3**	[6]
7	Fruit & vegetable canning	Deer Creek		

10	Roasted Nuts and Peanut Butter Manufacturing	Deer Creek		
7	Fruit & vegetable canning	None Identified		
8	Fruit and Vegetable Canning, Pickling, and Drying	Mormon Slough		
12	Wineries	City of Lodi	**1 (city using well water)**	[8]
		Mokelumne River	Mokelumne River from Camanche Reservoir to Delta: 2B; 3A,B; 4A,B; 5A,B,C	[1, p. II-7]
2	Beet Sugar Manufacturing	Fresno Slough		
		Mendota Wildlife Area	**5C,5D**	[5]
		San Joaquin River	Friant Dam to Mendota Pool:	[1, p. II-7]

			2A,B,D; 3A,B; 4A,B; 5A,B, C	Basin Plan, 2007, regulations concerning EC of San Joaquin from Friant Dam to Mendota Pool, limits on EC to less than 150 (□mho/cm) (90 percentile) [1, p. III-7]
7	Fruit & vegetable canning	None Identified		
7	Fruit & vegetable canning	None Identified		
7	Fruit & vegetable canning	Bravo Lake	**3,4**	[4]
		St. John's River		
		Cottonwood Creek		
		Kaweah River	Below Lake Kaweah on Kaweah River:	[2, p. II-4]

			2A,B,C,D ; 3A, B; 5B,C ; 6	Basin Plan, 2007, regulations concerning EC of Kaweah River limits EC to 175 □mho/cm [2, p. III-5]
		Vernal Pool Endangered Species Critical Habitat	**5C, 5D**	Critical Habitats [3]
8	Fruit and Vegetable Canning, Pickling, and Drying	Poso Creek	**2B, E; 3A, B; 5A,B,C; 6**	[2, p. 13]
7	Fruit & vegetable canning	Mitchell Slough		
7	Fruit & vegetable canning	City of Porterville	**1 (city using well water)**	[8]

		Protected/Endangered Habitats	**5C,5D – Vernal Pool Habitat, the Porter Slough, and Hubbs Miner Ditch**	[7]
4	Dried & dehydrated food mfg	None Identified		
4	Dried & dehydrated food mfg	None Identified		
4	Dried & dehydrated food mfg	None Identified		
4	Dried & dehydrated food mfg	City of Madera	**1 (city using well water)**	[8]
8	Fruit and Vegetable Canning, Pickling, and Drying	Kings River	Reach IV: 2A,B,D; 3A,B ; 5B,C, 6	[2, p. II-4]

				Basin Plan, 2007, regulations concerning EC of Kings River for Reach IV, limits on EC to less than 200 (□mho/cm) [2, p. III-5]
12	Wineries	Woodbridge Ecological Reserve	**5C**	[5]
		White Slough Wildlife Area	5C	[5]
		Delta Surface Waters	Sacramento San Joaquin Delta – Beneficial uses vary, can include all	[1, p. II-8]
7	Fruit & vegetable canning	City of Lindsay	**1 (city using well water)**	[8]
7	Fruit & vegetable canning	North Grasslands Wildlife Area	**5C**	[5]
		Easement Areas	**5**	
7	Fruit & vegetable canning	City of Porterville	**1 (city using well water)**	[8]

12	Wineries	City of McFarland		
		Poso Creek	Poso Creek: 2B,E; 3A, B; 5A,B,C; 6	[2, p. II-4]
7	Fruit & vegetable canning	San Joaquin River	San Joaquin River from Mendota Dam to Sack Dam: 2B,D; 3A,B; 4A,B; 5B, C	[1, p. II-7]
10	Roasted Nuts and Peanut Butter Manufacturing	Deer Creek		
7	Fruit & vegetable canning	None Identified		
7	Fruit & vegetable canning	City of Tracy	**1 (city using well water)**	[8]
		Delta Smelt Endangered Species Critical Habitat	**5C, 5D**	Critical Habitats [3]

3	Dairy Product Manufacturing	Easement Areas	**5**	
4	Dried & dehydrated food mfg	None Identified		
12	Wineries	City of Lodi	**1 (city using well water)**	[8]
		Mokelumne River	Mokelumne River from Camanche Reservoir to Delta: 2B; 3A,B; 4A,B; 5A,B,C	[1, p. II-7]
7	Fruit & vegetable canning	None Identified		
4	Dried & dehydrated food mfg	City of Madera	**1 (city using well water)**	[8]
		Cottonwood Creek		
12	Wineries	None Identified		
7	Fruit & vegetable canning	Deer Creek		

4	Dried & dehydrated food mfg	None Identified		
12	Wineries	City of Tulare	**1 (city using well water)**	[8]
12	Wineries	None Identified		
12	Wineries	Kings River	Reach IV: 2A,B,D; 3A,B ; 5B,C, 6	[2, p. II-4] Basin Plan, 2007, regulations concerning EC of Kings River for Reach IV, limits on EC to less than 200 (□mho/cm) [2, p. III-5]
1	Animal slaughtering & processing	Lodi City	**1 (city using well water)**	[8]

		Mokelumne River	Mokelumne River from Camanche Reservoir to Delta: 2B; 3A,B; 4A,B; 5A,B,C	[1, p. II-7]
4	Dried & dehydrated food mfg	None Identified		

3. Potentially Environmentally Sensitive Areas Near POTWs

Potentially environmentally sensitive areas within 3 miles of Central Valley POTWs. References are in square brackets and bold codes correspond to impacts in Appendix B.1. POTWs are shown in Section II.5.C, Figures 187-192. Map labels corresponding to industry classification are shown in Table 59.

Map Label	Industry Classification	Sensitive Sites within 3 mi	Impacts (See Table 1 for key)	Notes and Citations
13	Publicly Owned Treatment Works	City of Corcoran	1 (city using well water)	[8]
		Tule River	Below Lake Success on Tule River: 2A,B,C,D ; 3A, B; 5B,C ; 6	[2, p. II-4] Basin Plan, 2007, regulations concerning EC of Tule River limits EC to 450 µmho/cm [2, p. III-5]
		Vernal Pool Endangered	5C, 5D	Critical Habitats [3]

		Species Critical Habitat		
13	Publicly Owned Treatment Works	City of Delano	1 (city using well water)	[8]
13	Publicly Owned Treatment Works	None Identified		
13	Publicly Owned Treatment Works	Stanislaus River	Stanislaus River from Goodwin Dam to San Joaquin River: 2B,C,D; 3A,B; 4A,B; 5A,B,C	[1, p. II-8]
13	Publicly Owned Treatment Works	None Identified		
13	Publicly Owned Treatment Works	None Identified		
13	Publicly Owned Treatment Works	Kesterson National Wildlife Refuge	5C	
		Easement Areas	5	
13	Publicly Owned Treatment Works	Tuolumne River	Tuolumne River from New Don Pedro Dam to San Joaquin River: 2B; 3A,B; 4A,B; 5A,B,C	[1, p. II-8]

13	Publicly Owned Treatment Works	Merced River	Merced River from McSwain Reservoir to San Joaquin River: 2A,B,C,D; 3A,B; 4A,B; 5A,B,C	[1, p. II-8]
		MC Connell State Park	3	[6]
13	Publicly Owned Treatment Works	White Slough Wildlife Area	5C	[5]
		Delta Surface Waters	Sacramento San Joaquin Delta – Beneficial uses vary, can include all	[1, p. II-8]
		White Slough		
13	Publicly Owned Treatment Works	Bear Creek	4	[1,22]
		City of Merced	1 (city using well water)	[8]
13	Publicly Owned Treatment Works	Delta Surface Water	Sacramento San Joaquin Delta – Beneficial uses vary, can include all	[1, p. II-8]

		San Joaquin River	San Joaquin from the mouth of Merced River to Vernalis: 2B,D; 3A,B; 4A,B; 5B,C	[1, p. II-8]
13	Publicly Owned Treatment Works	Bear Creek	4	[1, p. II-6]
		City of Merced	1 (city using well water)	[8]
13	Publicly Owned Treatment Works	Brush Lake		
		San Joaquin River	San Joaquin River from mouth of Merced River to Vernalis 2B,D; 3A,B; 4A,B; 5B,C	[1, p. II-8]
13	Publicly Owned	San Joaquin River		

	Treatment Works	Merced River	Merced River from McSwain Reservoir to San Joaquin River: 2A,B,C,D; 3A,B; 4A,B; 5A,B,C	[1, p. II-8]
		North Grasslands Wildlife Area	5C	
		Easement Areas	5	
13	Publicly Owned Treatment Works	Stanislaus River	Stanislaus River from Goodwin Dam to San Joaquin River: 2B,C,D; 3A,B; 4A,B; 5A,B,C	[1, p. II-8]
		City of Oakdale	1 (city using well water)	[8]
13	Publicly Owned Treatment Works	San Joaquin River	Mouth of Merced River to Vernalis 2B,D; 3A,B; 4A,B; 5B,C	[1, p. II-8]

13	Publicly Owned Treatment Works	Stanislaus River	Stanislaus River from Goodwin Dam to San Joaquin River: 2B,C,D; 3A,B; 4A,B; 5A,B,C	[1, p. II-8]
13	Publicly Owned Treatment Works	Stanislaus River	Stanislaus River from Goodwin Dam to San Joaquin River: 2B,C,D; 3A,B; 4A,B; 5A,B,C	[1, p. II-8]
13	Publicly Owned Treatment Works	Stanislaus River	Stanislaus River from Goodwin Dam to San Joaquin River: 2B,C,D; 3A,B; 4A,B; 5A,B,C	[1, p. II-8]
13	Publicly Owned	Kings River	2A,B,D; 3A,B ;	[2, p. II-4]

	Treatment Works		5B,C, 6	Basin Plan, 2007, regulations concerning EC of Kings River for Reach IV, limits on EC to less than 200 μmho/cm [2, p. III-5]
13	Publicly Owned Treatment Works	Kings River	Reach IV: 2A,B,D; 3A,B; 5B,C; 6 Reach V: 2B; 3A,B; 5B,C; 6	[2, p. 13] [2, p. 13]

				Basin Plan, 2007, regulations concerning EC of Kings River for Reach IV & V, limits on EC to less than 200 and 300 μmho/cm respectively [2, p. III-5]
13	Publicly Owned Treatment Works	City of Tulare	1 (city using well water)	[8]
		Bates Slough		
13	Publicly Owned Treatment Works	City of Turlock	1 (city using well water)	[8]
13	Publicly Owned Treatment Works	None Identified		
13	Publicly Owned Treatment Works	City of Bakersfield	1 (city using well water)	[8]
13	Publicly Owned Treatment Works	None Identified		
13	Publicly Owned Treatment Works	Tuolumne River	Tuolumne River from New Don Pedro Dam to San Joaquin River: 2B; 3A,B; 4A,B; 5A,B,C	[1, p. II-8]
		City of Modesto	1 (city using well water)	[8]

13	Publicly Owned Treatment Works	Sacramento River	Sacramento River at Big Chico Creek: 2B; 3A,B; 4A,B; 5A,B,C	[1, p. II-5]
		Mud Creek		
13	Publicly Owned Treatment Works	Sacramento River	Sacramento from Shasta Dam to Colusa Basin Drain: 2A,B,C; 3A,B; 4A,B; 5A,B,C	[1, p. II-5]
13	Publicly Owned Treatment Works	Merced River	Merced River from McSwain Reservoir to San Joaquin River: 2A,B,C,D; 3A,B; 4A,B; 5A,B,C	[1, p. II-8]
		MC Connell State Park	3	[6]
13	Publicly Owned Treatment Works	St. John's River		
13	Publicly Owned Treatment Works	None Identified		
13	Publicly Owned Treatment Works	City of Gridley	1 (city using well water)	[8]
		Feather River	Feather River from	[1, p. II-6]

			Fish Barrier Dam to Sacramento River: 2A,B; 3A,B; 4A,B; 5A,B,C	Basin Plan, 2007, regulations concerning EC of Feather River limits EC to 150 μmho/cm [1, p. III-7]
		Easement Areas	5	
13	Publicly Owned Treatment Works	City of Hanford	1 (city using well water)	[8]
13	Publicly Owned Treatment Works	Merced River	Merced River from McSwain Reservoir to San Joaquin River: 2A,B,C,D; 3A,B; 4A,B; 5A,B,C	[1, p. II-8]
13	Publicly Owned Treatment Works	None Identified		
13	Publicly Owned Treatment Works	Delta Surface Waters	Sacramento San Joaquin Delta – Beneficial uses vary, can include all	[1, p. II-8]

		San Joaquin River	San Joaquin from the mouth of Merced River to Vernalis (Vernalis is slightly south of the processor) 2B,D; 3A,B; 4A,B; 5B,C	[1, p. II-8]
13	Publicly Owned Treatment Works	None Identified		
13	Publicly Owned Treatment Works	City of Lindsay	1 (city using well water)	[8]
13	Publicly Owned Treatment Works	Fresno River	Fresno River from Hidden Reservoir to San Joaquin River: 2B; 3A,B; 5B,C [1, p. 23]	
13	Publicly Owned Treatment Works	City of Porterville	1 (city using well water)	[8]
		Tule River	Below Lake Success on Tule River: 2A,B,C,D ; 3A,B; 5B,C; 6	[2, p. II-4] Basin Plan, 2007, p. 22, regulations concerning EC of Tule River limits EC to 450 µmho/cm [2, p. III-5]

13	Publicly Owned Treatment Works	City of Stockton	1 (city using well water)	[8]
		Delta Surface Water	Sacramento San Joaquin Delta – Beneficial uses vary, can include all	[1, p. II-8]
		Calaveras River	Calaveras River from New Hogan Reservoir to Delta: 2A,B; 3A,B; 4A,B; 5A,B,C	[1, p. II-7]
		French Camp Slough		
		Delta Smelt Endangered Species Critical Habitat	5C, 5D	Critical Habitats [3]
13	Publicly Owned Treatment Works	None Identified		
13	Publicly Owned Treatment Works	City of Wasco	1 (city using well water)	[8]
13	Publicly Owned	Modesto Reservoir		

	Treatment Works	Tuolumne River	Tuolumne River from New Don Pedro Dam to San Joaquin River: 2B; 3A,B; 4A,B; 5A,B,C	[1, p. II-8]
		Dry Creek		
13	Publicly Owned Treatment Works	City of Woodland	1 (city using well water)	[8]
		Willow Slough		
		Cache Creek		
13	Publicly Owned Treatment Works	City of Yuba City		
		City of Olivehurst		
		Feather River	Feather River from Fish Barrier Dam to Sacramento River: 2A,B; 3A,B; 4A,B; 5A,B,C	[1, p. II-6] Basin Plan, 2007, regulations concerning EC of Feather River limits EC to 150 µmho/cm [1, p. III-7]

		Yuba River	Yuba River from Englebright Dam to Feather River: 2B,D; 3A,B; 4A,B; 5A,B,C	[1, p. II-6]
		Vernal Pool Endangered Species Critical Habitat	5C 5D	Critical Habitats [3]

C. Appendix C: SEP Study Management of Salinity in Wastewater from the California Food Processing Industry – Unsaturated Zone Modeling

1. Tomato Canning Baseline Simulations

FIGURE 1
TOMATO CASE 1 BREAKTHROUGH CURVES

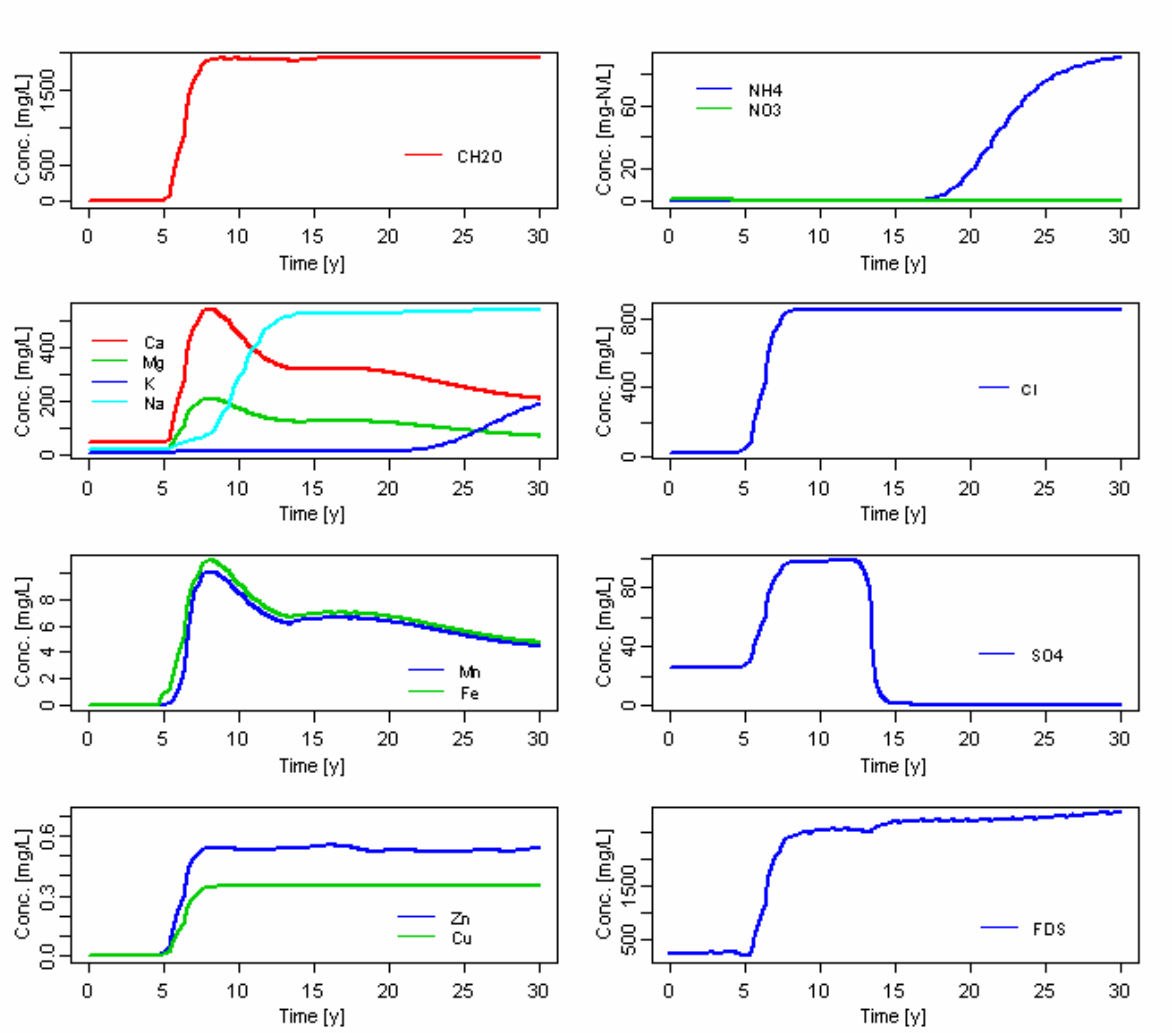

FIGURE 2
TOMATO CASE 1 PROFILES, YEAR 30

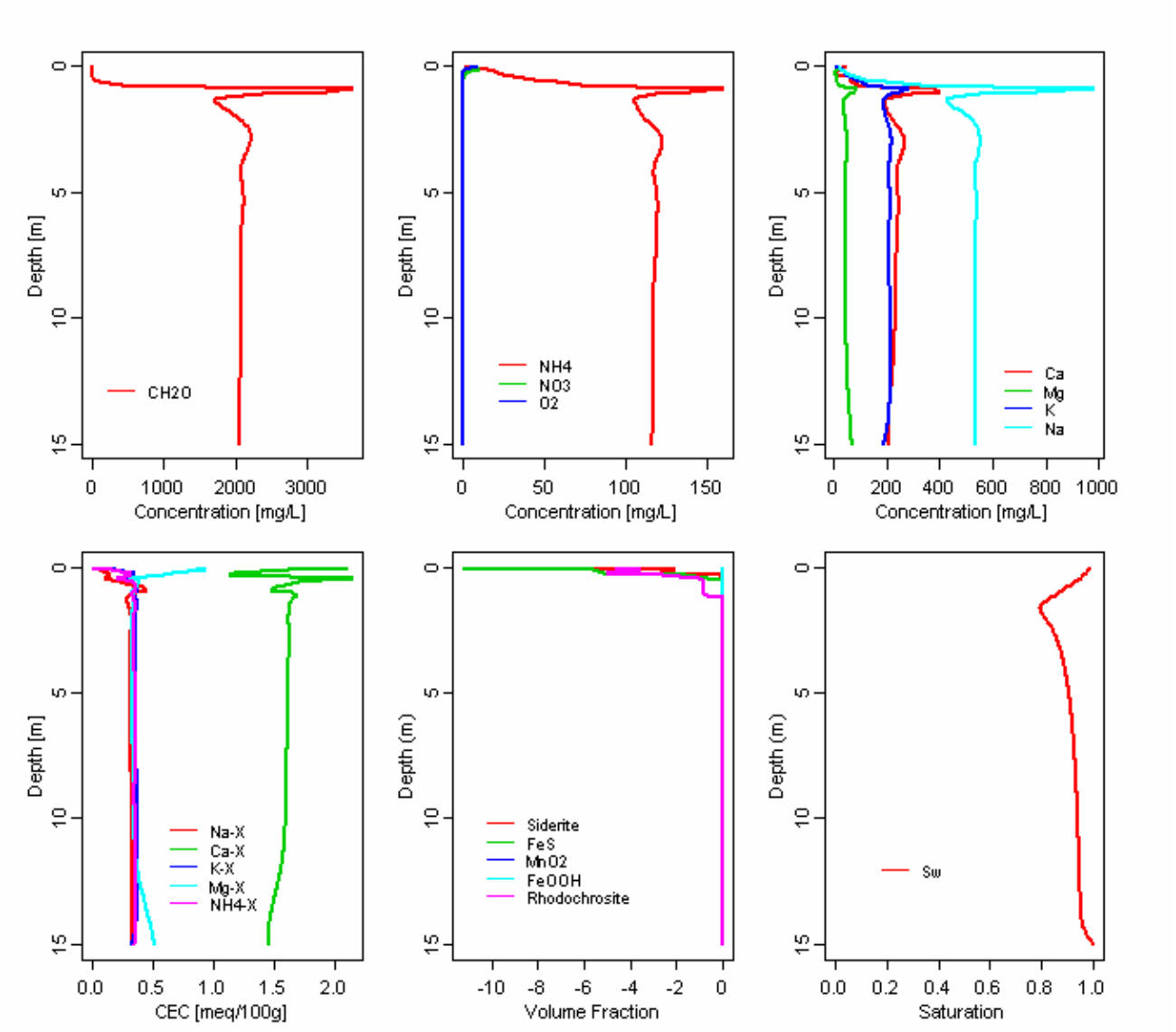

Table 1
Tomato Case 1 Mass Balance Table

	Surface Loading	Storage	Degassing	Biodegredation (Aqueous)	Biodegredation (Mineral)	Root Uptake	Precipitation	Adsorption	Water Table	Mass Error
CH_2O	13468	-2667	0	-497	-346	0	0	0	-9961	-3.17
	100%	-20%	0%	-4%	-3%	0%	0%	0%	-74%	0%
NH_4	990	-162	0	-70	0	-146	0	-417	-195	-0.09
	100%	-16%	0%	-7%	0%	-15%	0%	-42%	-20%	0.0%
NO_3	192	7	0	-67	0	-128	0	0	-4	0.16
	100%	4%	0%	-35%	0%	-67%	0%	0%	-2%	0.1%
O_2	140	0	133	-272	0	0	0	0	0	0.08
	100%	0%	95%	-195%	0%	0%	0%	0%	0%	0.1%
K^+	1521	-283	0	0	0	-130	0	-895	-213	-0.36
	100%	-19%	0%	0%	0%	-9%	0%	-59%	-14%	0.0%
Ca^{2+}	802	-259	0	0	0	-81	583	701	-1747	-0.39
	100%	-32%	0%	0%	0%	-10%	73%	87%	-218%	0.0%
Mg^{2+}	408	-45	0	0	0	-95	0	388	-656	-0.16
	100%	-11%	0%	0%	0%	-23%	0%	95%	-161%	0.0%
Na^+	3521	-715	0	0	0	0	0	-444	-2362	-0.87
	100%	-20%	0%	0%	0%	0%	0%	-13%	-67%	0.0%
Fe^{2+}	168	-7	0	0	1255	0	-1357	-26	-34	-0.77
	100%	-4%	0%	0%	749%	0%	-810%	-15%	-20%	-0.5%
Mn^{2+}	5	-7	0	0	649	0	-595	-17	-37	-1.96
	100%	-150%	0%	0%	13849%	0%	-12702%	-357%	-782%	-41.9%
CO_3^{2-}	4175	-1131	-74	994	698	339	-958	0	-4041	0.31
	100%	-27%	-2%	24%	17%	8%	-23%	0%	-97%	0.0%
SO_4^{2-}	688	5	0	-463	0	-45	0	0	-186	-1.06
	100%	1%	0%	-67%	0%	-7%	0%	0%	-27%	-0.2%
Cl-	5602	-1144	0	0	0	0	0	0	-4460	-1.48
	100%	-20%	0%	0%	0%	0%	0%	0%	-80%	0.0%
PO_4^{3-}	323	-13	0	0	0	-262	0	0	-49	-0.09
	100%	-4%	0%	0%	0%	-81%	0%	0%	-15%	0.0%
FDS	18394	-3753	-74	394	2601	-549	-2328	-710	-13983	-6.77
	100%	-20%	0%	2%	14%	-3%	-13%	-4%	-76%	0.0%

Mass balance in pounds per acre per year and percent of total component loading.

FIGURE 3
TOMATO CASE 2 BREAKTHROUGH CURVES

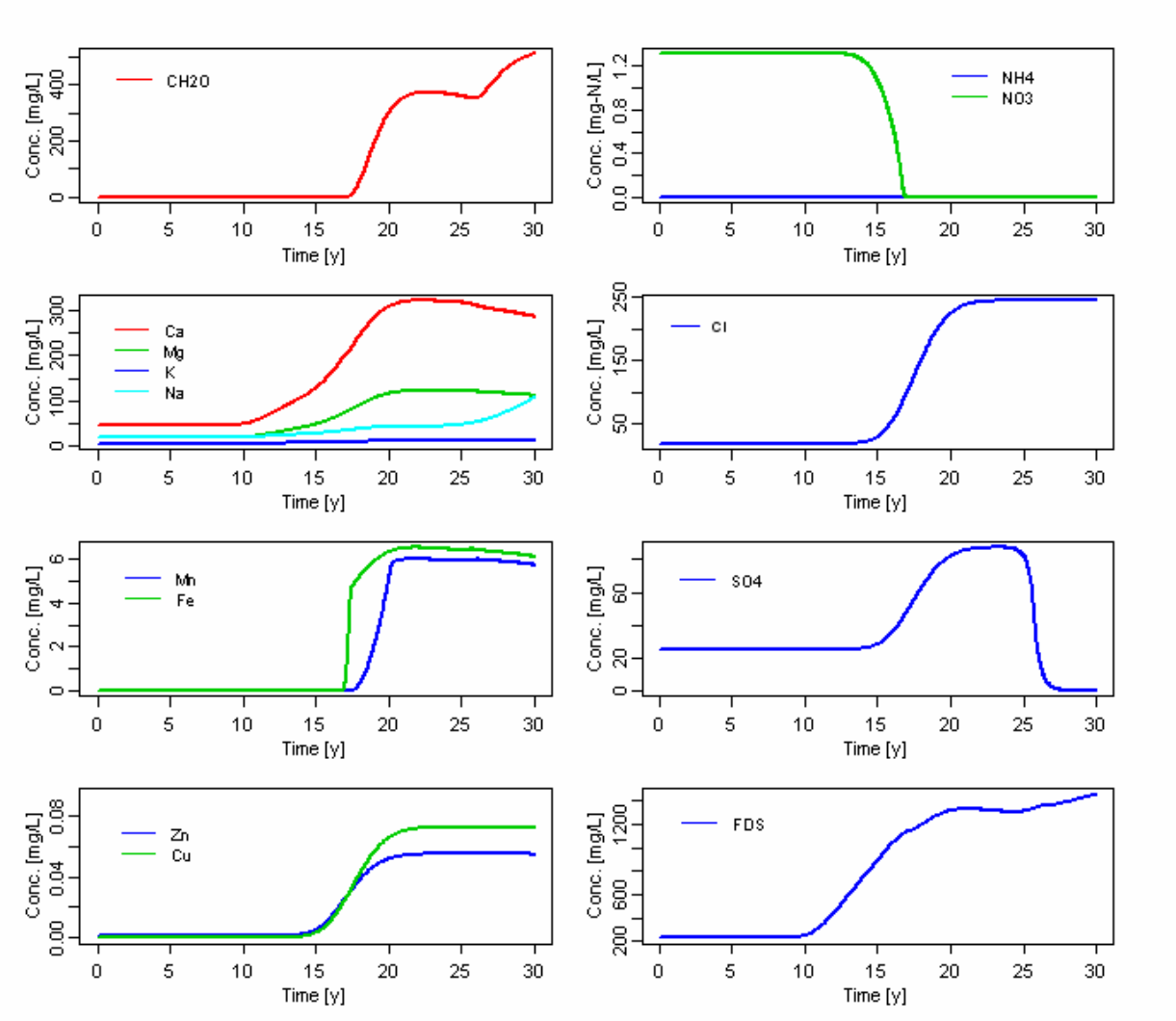

FIGURE 4
TOMATO CASE 2 PROFILES, YEAR 30

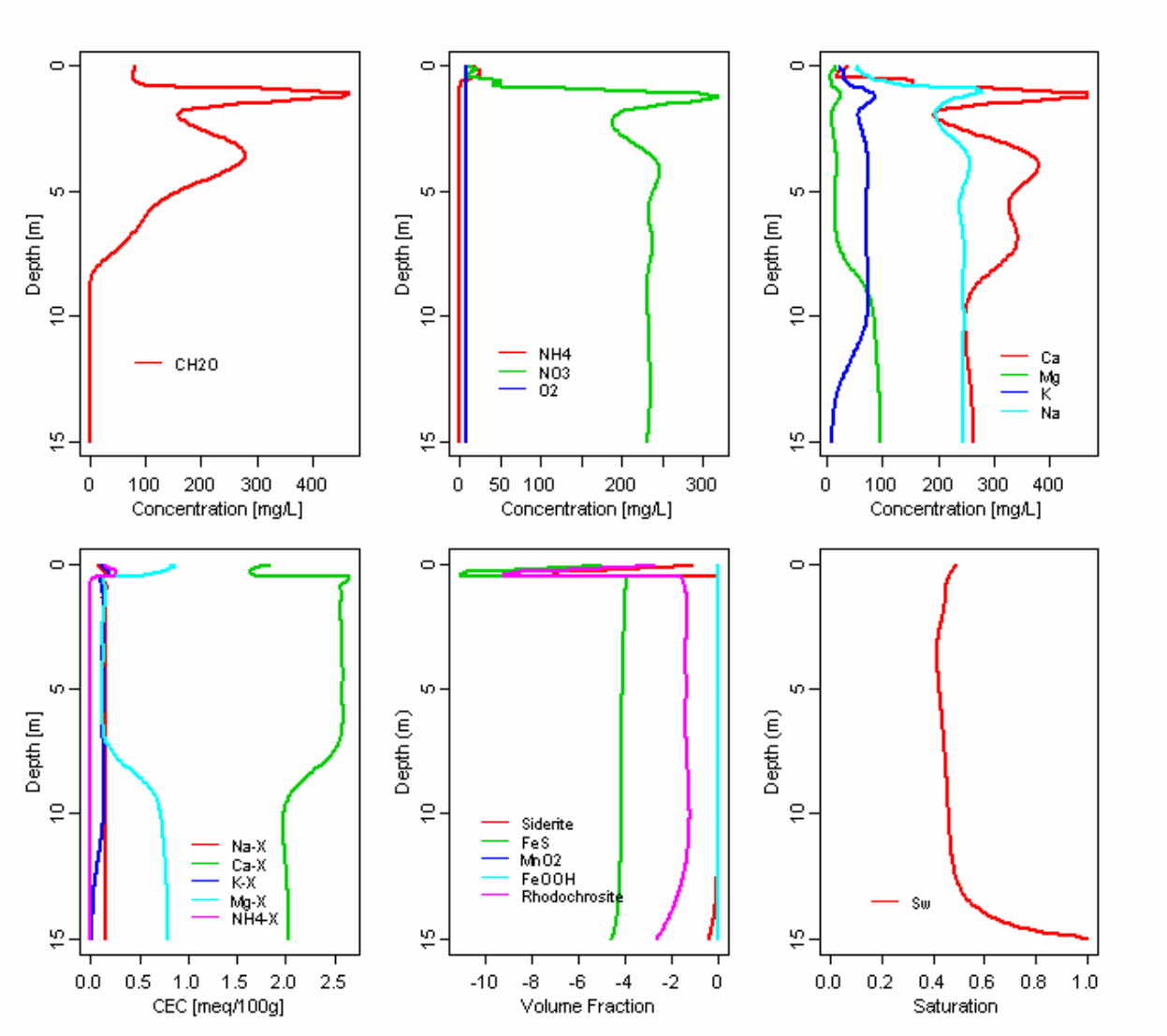

Table 2
Tomato Case 2 Mass Balance Table

	Surface Loading	Storage	Degassing	Biodegredation (Aqueous)	Biodegredation (Mineral)	Root Uptake	Precipitation	Adsorption	Water Table	Mass Error
CH_2O	1720	-56	0	-1663	0	0	0	0	0	0.31
	100%	-3%	0%	-97%	0%	0%	0%	0%	0%	0%
NH_4	466	0	0	-390	0	-68	0	-7	0	0.23
	100%	0%	0%	-84%	0%	-15%	0%	-2%	0%	0.0%
NO_3	214	-159	0	1177	0	-385	0	0	-845	0.22
	100%	-75%	0%	551%	0%	-180%	0%	0%	-396%	0.1%
O_2	120	1	2964	-3053	0	0	0	0	-32	-0.09
	100%	1%	2465%	-2539%	0%	0%	0%	0%	-27%	-0.1%
K^+	436	-36	0	0	0	-129	0	-233	-38	0.04
	100%	-8%	0%	0%	0%	-29%	0%	-53%	-9%	0.0%
Ca^{2+}	365	-173	0	0	0	-80	1218	-248	-1082	-0.44
	100%	-47%	0%	0%	0%	-22%	334%	-68%	-297%	-0.1%
Mg^{2+}	167	-26	0	0	0	-90	0	340	-392	-0.15
	100%	-15%	0%	0%	0%	-54%	0%	203%	-234%	-0.1%
Na^+	1033	-160	0	0	0	0	0	-192	-682	-0.01
	100%	-15%	0%	0%	0%	0%	0%	-19%	-66%	0.0%
Fe^{2+}	47	-4	0	0	0	0	-21	-24	-1	-2.18
	100%	-8%	0%	0%	0%	0%	-45%	-51%	-1%	-4.7%
Mn^{2+}	1	0	0	0	0	0	0	-1	0	0.00
	100%	-12%	0%	0%	0%	0%	0%	-87%	-1%	0.0%
CO_3^{2-}	1542	-200	-5110	3326	11	283	1800	0	-1654	-0.46
	100%	-13%	-331%	216%	1%	18%	117%	0%	-107%	0.0%
SO_4^{2-}	267	-20	0	0	0	-45	0	0	-202	-0.22
	100%	-8%	0%	0%	0%	-17%	0%	0%	-76%	-0.1%
Cl-	1614	-254	0	0	0	0	0	0	-1360	0.08
	100%	-16%	0%	0%	0%	0%	0%	0%	-84%	0.0%
PO_4^{3-}	90	-3	0	0	0	-72	0	0	-15	0.01
	100%	-3%	0%	0%	0%	-80%	0%	0%	-17%	0.0%
FDS	6241	-1035	-5110	4113	11	-586	2997	-365	-6270	-2.88
	100%	-17%	-82%	66%	0%	-9%	48%	-6%	-100%	0.0%

Mass balance in pounds per acre per year and percent of total component loading.

FIGURE 5
TOMATO CASE 3 BREAKTHROUGH CURVES

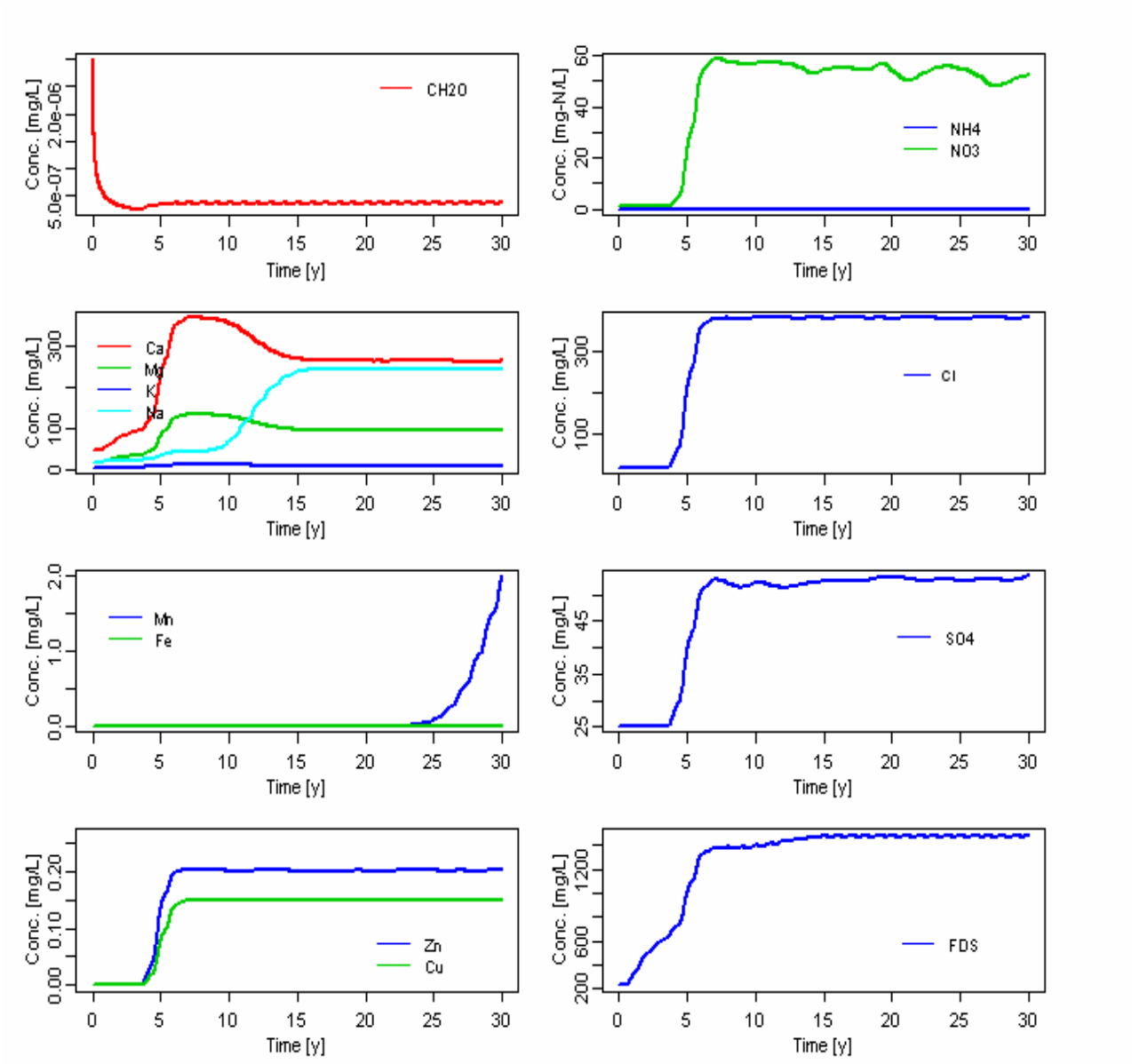

FIGURE 6
TOMATO CASE 3 PROFILES, YEAR 30

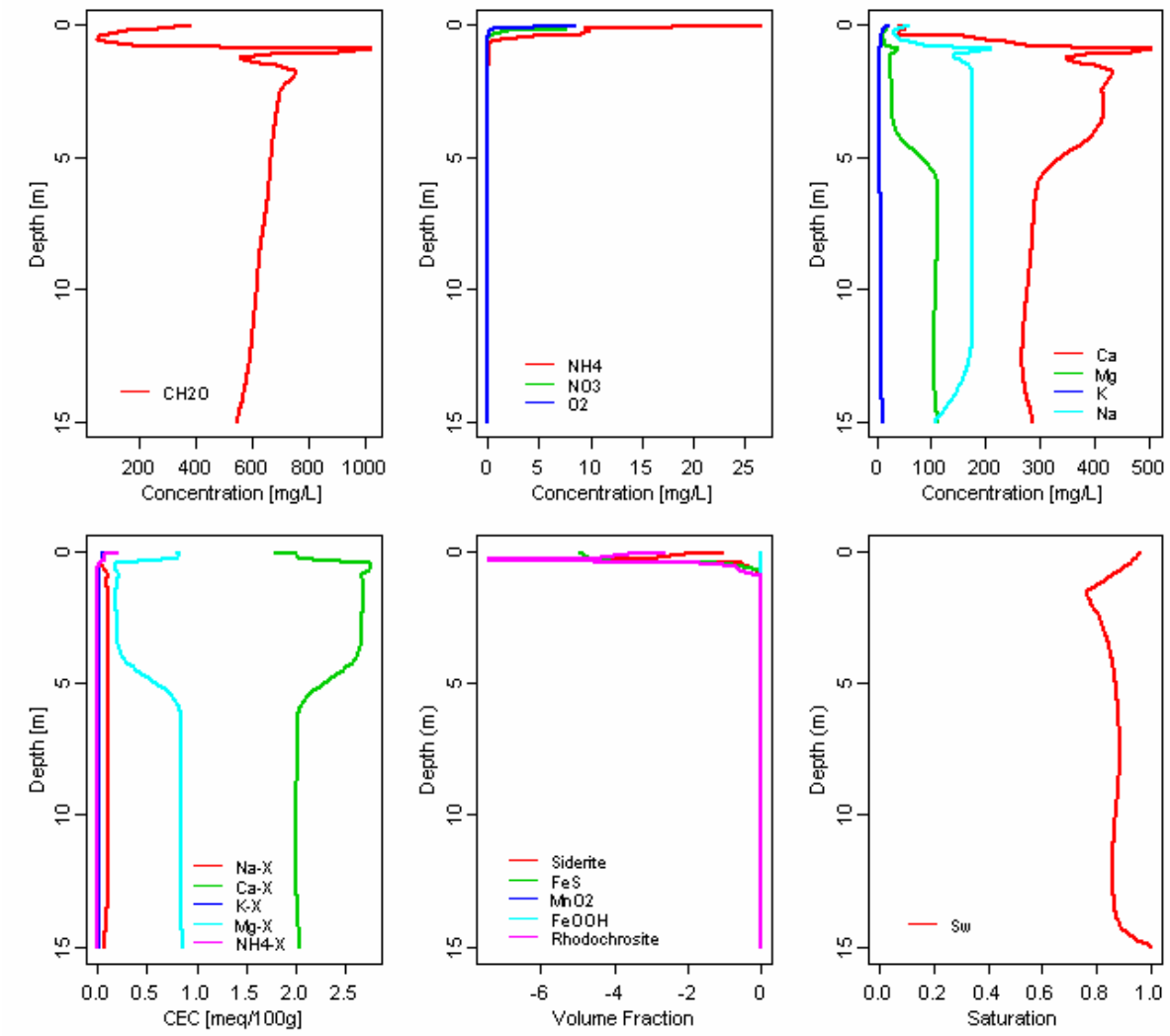

Table 3
Tomato Case 3 Mass Balance Table

	Surface Loading	Storage	Degassing	Biodegredation (Aqueous)	Biodegredation (Mineral)	Root Uptake	Precipitation	Adsorption	Water Table	Mass Error
CH_2O	1802	-762	0	-449	-269	0	0	0	-314	8.93
	100%	-42%	0%	-25%	-15%	0%	0%	0%	-17%	0%
NH_4	180	0	0	-121	0	-57	0	-2	0	0.74
	100%	0%	0%	-67%	0%	-32%	0%	-1%	0%	0.4%
NO_3	129	8	0	78	0	-208	0	0	-7	0.03
	100%	6%	0%	61%	0%	-162%	0%	0%	-5%	0.0%
O_2	103	11	495	-603	0	0	0	0	-7	-0.03
	100%	11%	481%	-586%	0%	0%	0%	0%	-6%	0.0%
K^+	139	-5	0	0	0	-126	0	8	-16	0.51
	100%	-3%	0%	0%	0%	-91%	0%	6%	-11%	0.4%
Ca^{2+}	410	-350	0	0	0	-84	533	-139	-370	-0.30
	100%	-85%	0%	0%	0%	-21%	130%	-34%	-90%	-0.1%
Mg^{2+}	162	-88	0	0	0	-94	0	161	-141	-0.07
	100%	-54%	0%	0%	0%	-58%	0%	99%	-87%	0.0%
Na^+	382	-193	0	0	0	0	0	-111	-76	1.05
	100%	-51%	0%	0%	0%	0%	0%	-29%	-20%	0.3%
Fe^{2+}	12	-9	0	0	683	0	-661	-19	-5	0.77
	100%	-74%	0%	0%	5882%	0%	-5695%	-167%	-40%	6.7%
Mn^{2+}	0	-9	0	0	647	0	-611	-24	-6	-1.75
	100%	-2714%	0%	0%	196162%	0%	-185187%	-7146%	-1743%	-528.8%
CO_3^{2-}	1148	-1152	-258	897	540	150	-501	0	-823	1.27
	100%	-100%	-22%	78%	47%	13%	-44%	0%	-72%	0.1%
SO_4^{2-}	237	22	0	-130	0	-46	0	0	-84	-0.96
	100%	9%	0%	-55%	0%	-19%	0%	0%	-35%	-0.4%
Cl-	532	-287	0	0	0	0	0	0	-243	1.82
	100%	-54%	0%	0%	0%	0%	0%	0%	-46%	0.3%
PO_4^{3-}	22	0	0	0	0	-22	0	0	0	0.12
	100%	0%	0%	0%	0%	-99%	0%	0%	0%	0.5%
FDS	3353	-2062	-258	725	1870	-488	-1240	-126	-1770	3.24
	100%	-62%	-8%	22%	56%	-15%	-37%	-4%	-53%	0.1%

Mass balance in pounds per acre per year and percent of total component loading.

2. Wineries and Grape Processing Baseline Simulations

FIGURE 7
CASE 1 WINE BREAKTHROUGH CURVES

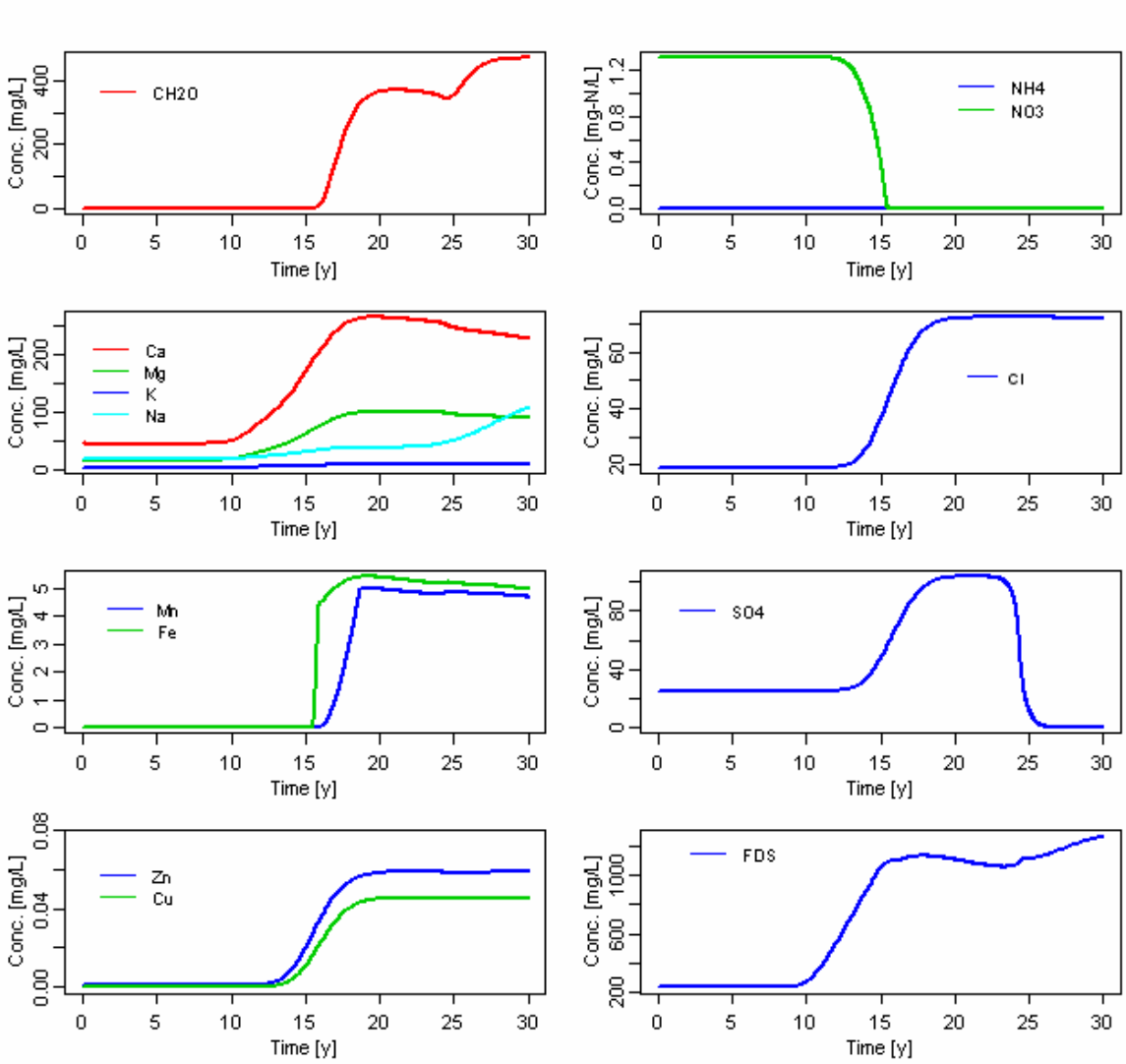

FIGURE 8
WINE CASE 1 PROFILES, YEAR 30

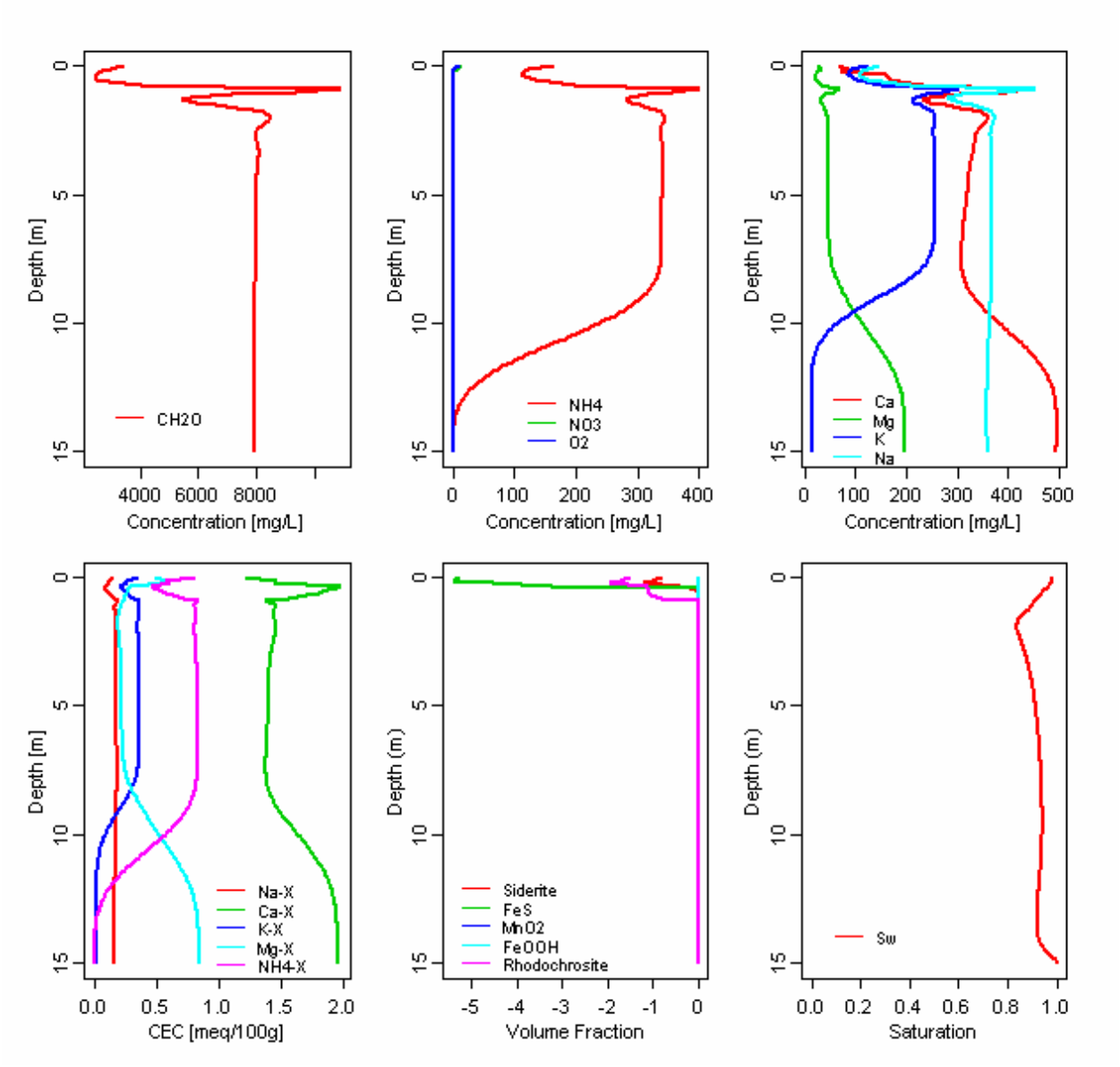

Table 4
Winery Case 1 Mass Balance Table

	Surface Loading	Storage	Degassing	Biodegredation (Aqueous)	Biodegredation (Mineral)	Root Uptake	Precipitation	Adsorption	Water Table	Mass Error
CH_2O	22865	-10269	0	-473	-337	0	0	0	-11750	37.27
	100%	-45%	0%	-2%	-1%	0%	0%	0%	-51%	0%
NH_4	1203	-325	0	-45	0	-146	0	-685	0	1.97
	100%	-27%	0%	-4%	0%	-12%	0%	-57%	0%	0.2%
NO_3	187	7	0	-108	0	-82	0	0	-4	0.16
	100%	4%	0%	-58%	0%	-44%	0%	0%	-2%	0.1%
O_2	110	0	70	-180	0	0	0	0	0	-0.02
	100%	0%	64%	-164%	0%	0%	0%	0%	0%	0.0%
K^+	895	-208	0	0	0	-132	0	-526	-28	1.42
	100%	-23%	0%	0%	0%	-15%	0%	-59%	-3%	0.2%
Ca^{2+}	633	-462	0	0	0	-85	165	689	-940	0.08
	100%	-73%	0%	0%	0%	-14%	26%	109%	-148%	0.0%
Mg^{2+}	239	-112	0	0	0	-97	0	339	-368	0.02
	100%	-47%	0%	0%	0%	-41%	0%	142%	-154%	0.0%
Na^+	1093	-477	0	0	0	0	0	-222	-392	1.44
	100%	-44%	0%	0%	0%	0%	0%	-20%	-36%	0.1%
Fe^{2+}	11	-12	0	0	1180	0	-1147	-14	-18	0.85
	100%	-101%	0%	0%	10269%	0%	-9986%	-121%	-154%	7.4%
Mn^{2+}	2	-12	0	0	652	0	-609	-17	-19	-1.84
	100%	-518%	0%	0%	28558%	0%	-26654%	-744%	-822%	-80.6%
CO_3^{2-}	3520	-2041	-137	945	678	134	-1361	0	-1734	4.03
	100%	-58%	-4%	27%	19%	4%	-39%	0%	-49%	0.1%
SO_4^{2-}	673	-11	0	-472	0	-46	0	0	-145	-1.13
	100%	-2%	0%	-70%	0%	-7%	0%	0%	-22%	-0.2%
Cl-	202	-70	0	0	0	0	0	0	-133	-0.06
	100%	-34%	0%	0%	0%	0%	0%	0%	-66%	0.0%
PO_4^{3-}	71	-1	0	0	0	-69	0	0	-1	0.12
	100%	-1%	0%	0%	0%	-97%	0%	0%	-2%	0.2%
FDS	8729	-3722	-137	321	2510	-524	-2952	-435	-3782	7.06
	100%	-43%	-2%	4%	29%	-6%	-34%	-5%	-43%	0.1%

Mass balance in pounds per acre per year and percent of total component loading.

Figure 9
Case 2 Wine Breakthrough Curves

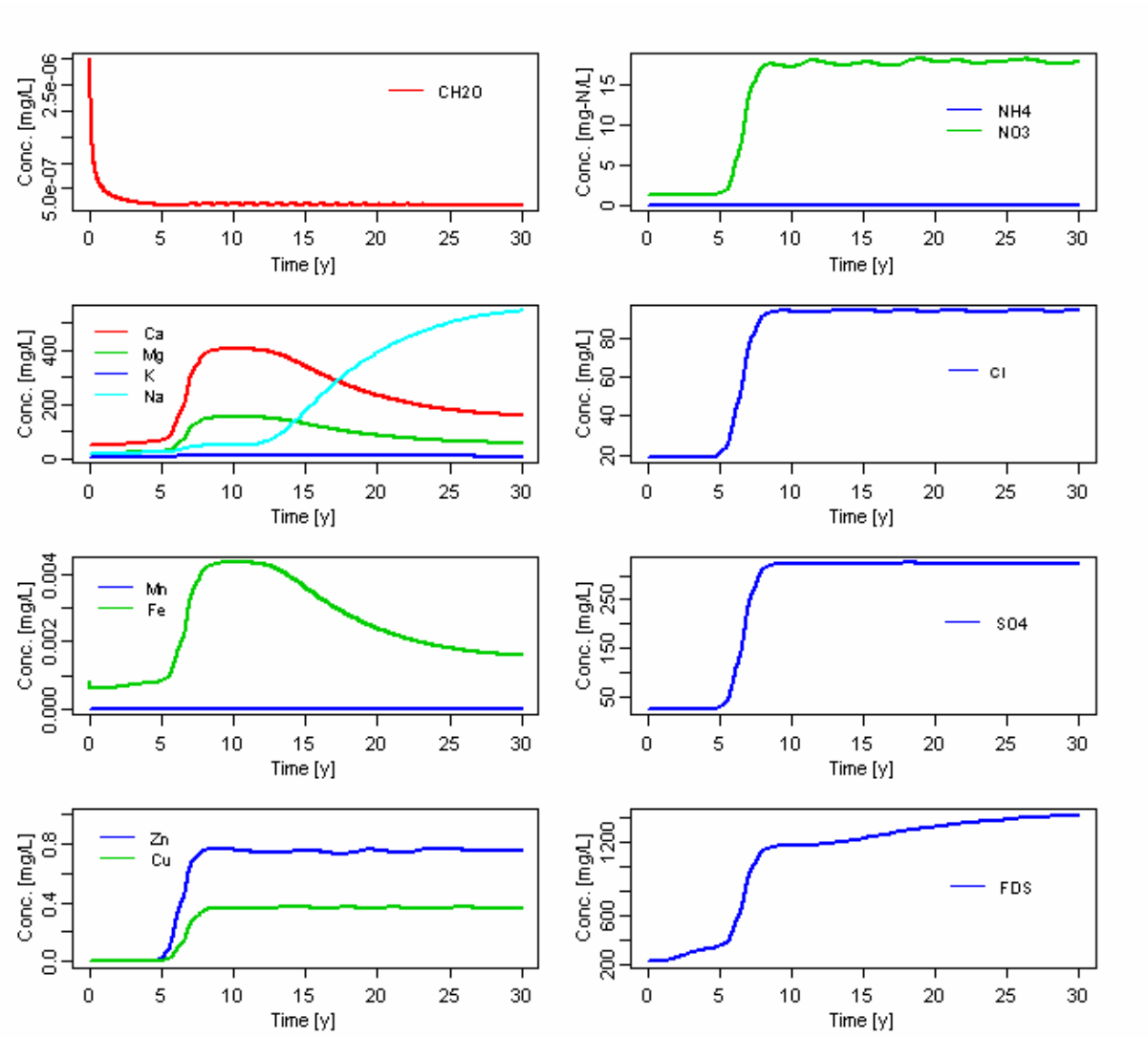

FIGURE 10
WINE CASE 2 PROFILES, YEAR 30

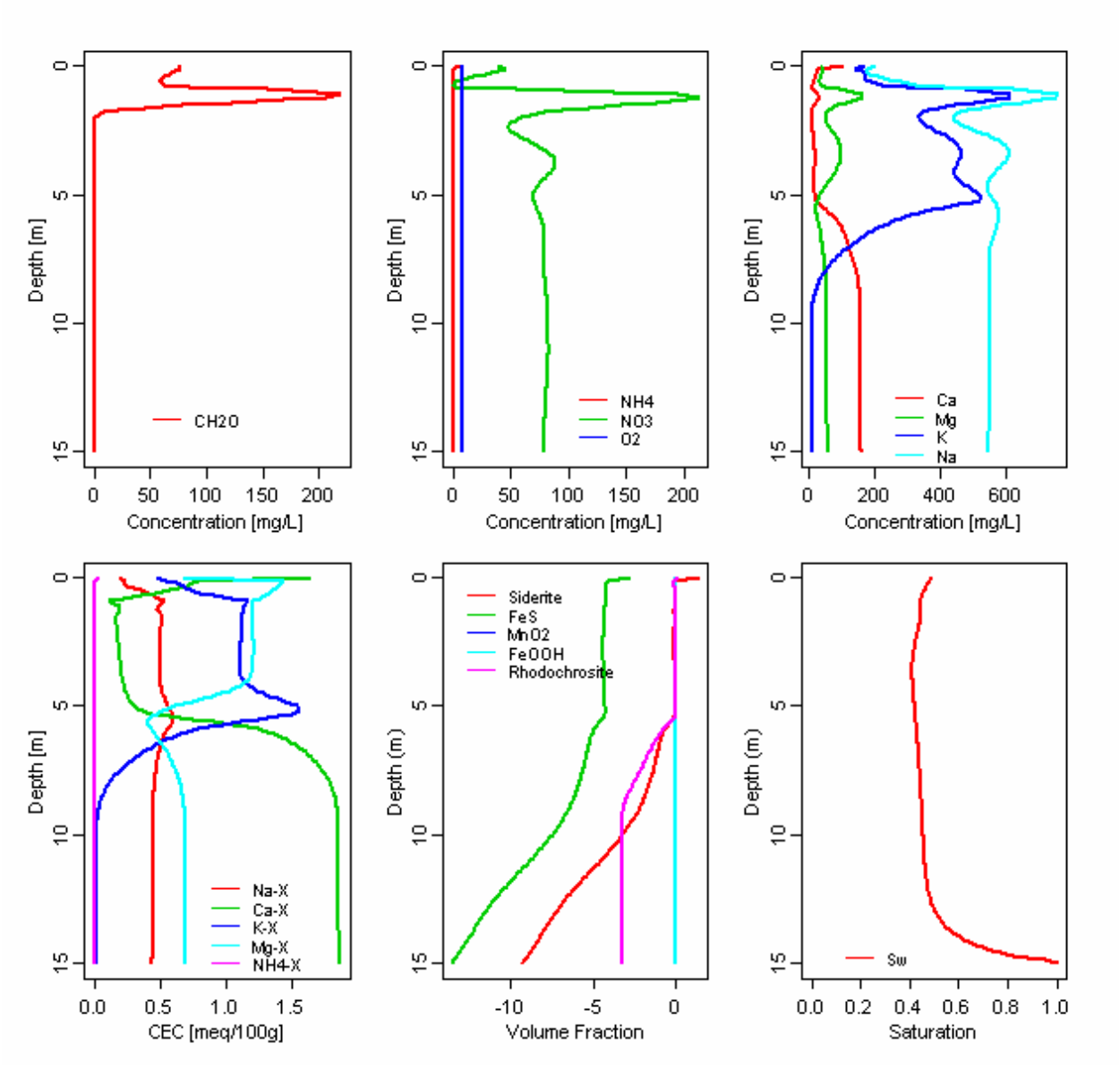

Table 5
Winery Case 2 Mass Balance Table

	Surface Loading	Storage	Degassing	Biodegredation (Aqueous)	Biodegredation (Mineral)	Root Uptake	Precipitation	Adsorption	Water Table	Mass Error
CH_2O	654	-6	0	-647	0	0	0	0	0	1.77
	100%	-1%	0%	-99%	0%	0%	0%	0%	0%	0%
NH_4	92	0	0	-74	0	-18	0	0	0	0.22
	100%	0%	0%	-81%	0%	-19%	0%	0%	0%	0.2%
NO_3	435	-53	0	195	0	-373	0	0	-203	0.94
	100%	-12%	0%	45%	0%	-86%	0%	0%	-47%	0.2%
O_2	109	0	832	-915	0	0	0	0	-27	-0.03
	100%	0%	761%	-836%	0%	0%	0%	0%	-25%	0.0%
K^+	1528	-115	0	0	0	-129	0	-1252	-26	4.08
	100%	-8%	0%	0%	0%	-8%	0%	-82%	-2%	0.3%
Ca^{2+}	985	-39	0	0	0	-66	-1328	1194	-745	1.23
	100%	-4%	0%	0%	0%	-7%	-135%	121%	-76%	0.1%
Mg^{2+}	371	-28	0	0	0	-95	0	27	-275	0.43
	100%	-8%	0%	0%	0%	-26%	0%	7%	-74%	0.1%
Na^+	1839	-379	0	0	0	0	0	-684	-772	4.49
	100%	-21%	0%	0%	0%	0%	0%	-37%	-42%	0.2%
Fe^{2+}	20	0	0	0	0	0	-19	-1	0	-0.01
	100%	0%	0%	0%	0%	0%	-94%	-5%	0%	0.0%
Mn^{2+}	4	0	0	0	0	0	-3	-1	0	-0.15
	100%	-3%	0%	0%	0%	0%	-70%	-31%	0%	-3.8%
CO_3^{2-}	5139	-166	-4008	1293	0	312	-2010	0	-549	10.38
	100%	-3%	-78%	25%	0%	6%	-39%	0%	-11%	0.2%
SO_4^{2-}	1101	-211	0	0	0	-44	0	0	-843	2.21
	100%	-19%	0%	0%	0%	-4%	0%	0%	-77%	0.2%
Cl-	305	-53	0	0	0	0	0	0	-253	0.20
	100%	-17%	0%	0%	0%	0%	0%	0%	-83%	0.1%
PO_4^{3-}	123	-3	0	0	0	-109	0	0	-10	0.34
	100%	-2%	0%	0%	0%	-89%	0%	0%	-9%	0.3%
FDS	11942	-1047	-4008	1415	0	-523	-3359	-717	-3677	24.38
	100%	-9%	-34%	12%	0%	-4%	-28%	-6%	-31%	0.2%

Mass balance in pounds per acre per year and percent of total component loading.

FIGURE 11
CASE 3 WINE BREAKTHROUGH CURVES

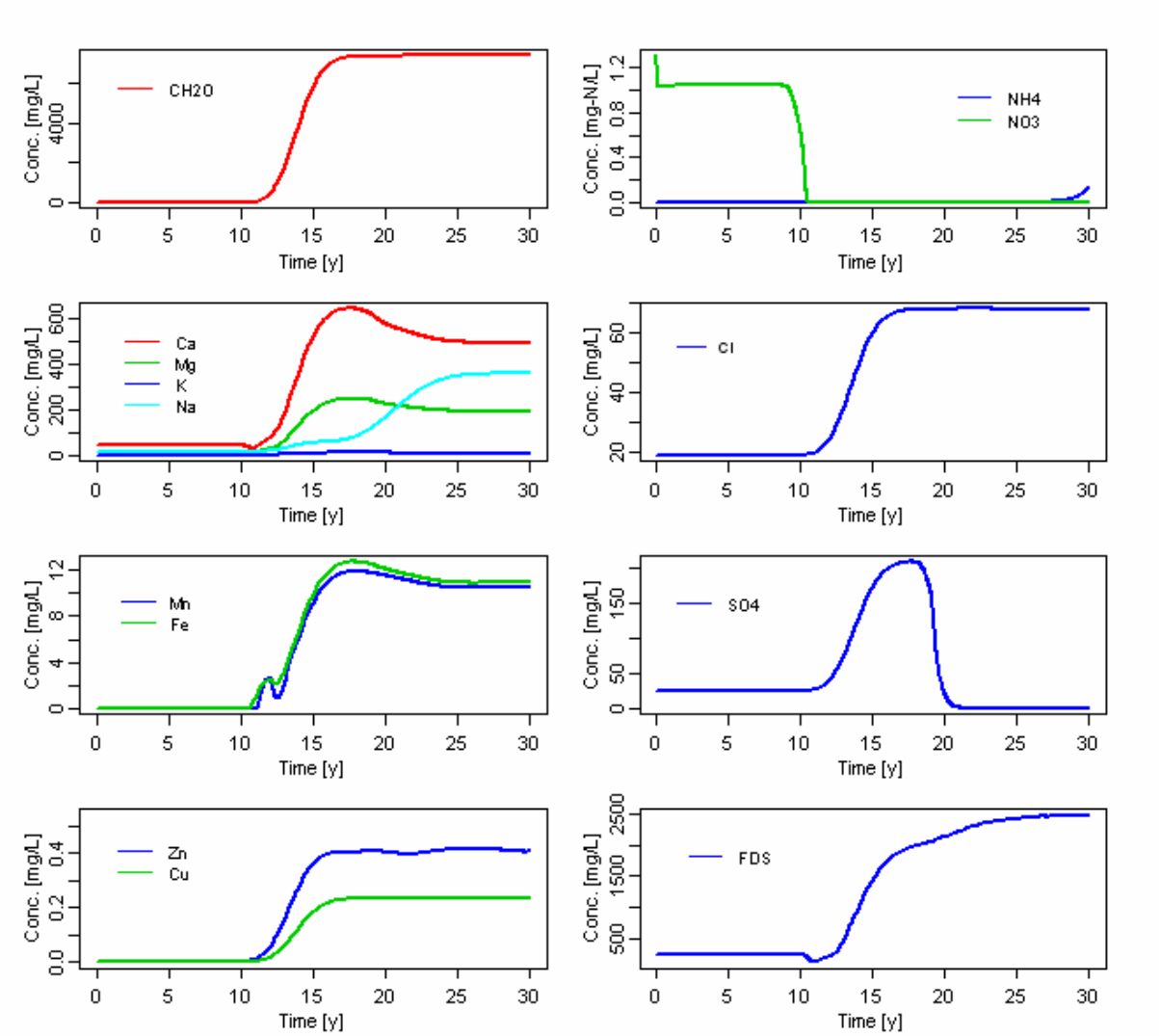

FIGURE 12
WINE CASE 3 PROFILES, YEAR 30

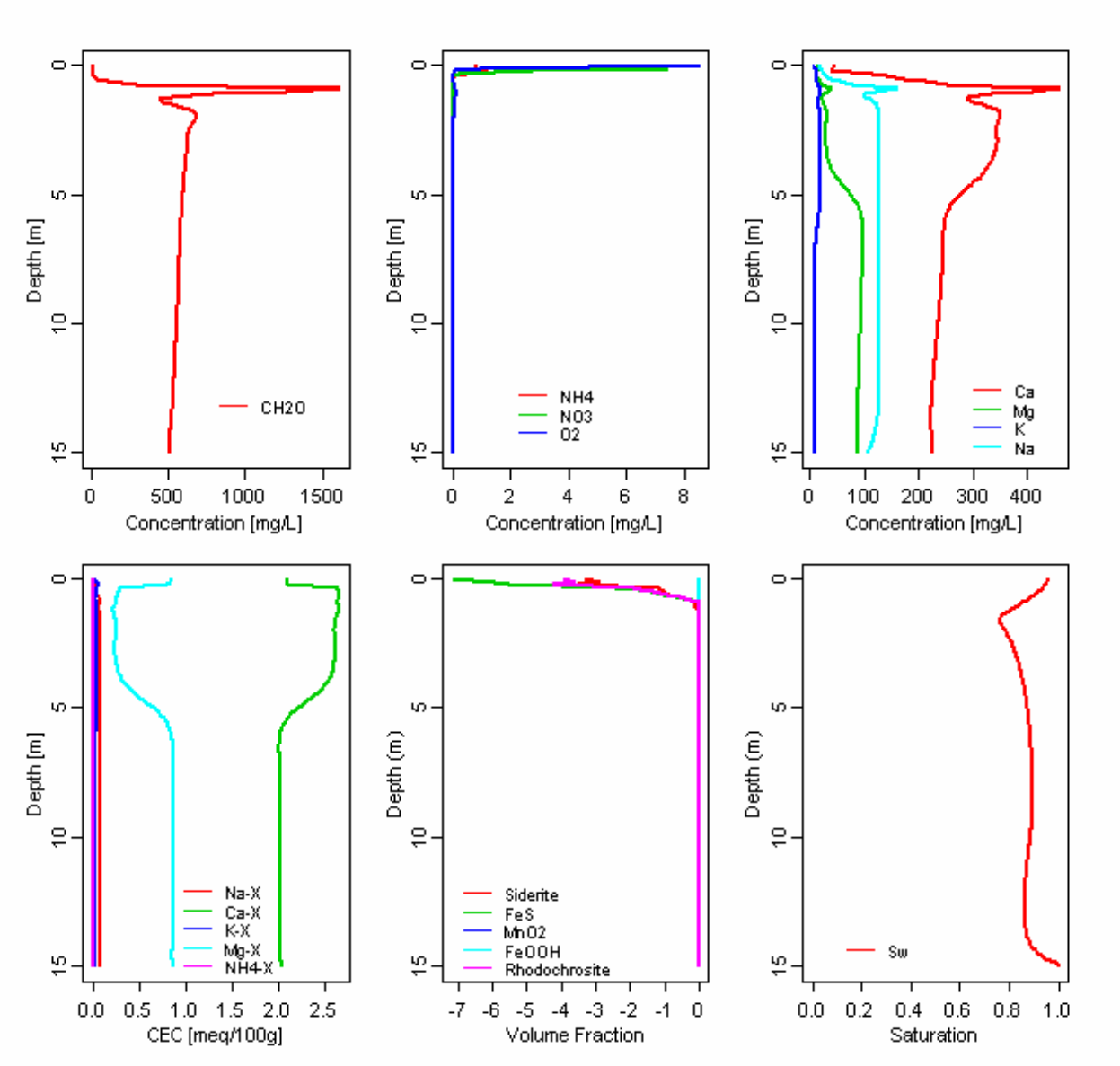

Table 6
Winery Case 3 Mass Balance Table

	Surface Loading	Storage	Degassing	Biodegredation (Aqueous)	Biodegredation (Mineral)	Root Uptake	Precipitation	Adsorption	Water Table	Mass Error
CH_2O	1880	-700	0	-501	-266	0	0	0	-405	7.40
	100%	-37%	0%	-27%	-14%	0%	0%	0%	-22%	0%
NH_4	74	0	0	-57	0	-17	0	0	0	0.17
	100%	0%	0%	-77%	0%	-23%	0%	0%	0%	0.2%
NO_3	144	8	0	9	0	-154	0	0	-7	0.11
	100%	5%	0%	7%	0%	-107%	0%	0%	-5%	0.1%
O_2	105	11	396	-505	0	0	0	0	-8	0.00
	100%	11%	376%	-480%	0%	0%	0%	0%	-7%	0.0%
K^+	176	-11	0	0	0	-128	0	-19	-17	0.57
	100%	-6%	0%	0%	0%	-73%	0%	-11%	-10%	0.3%
Ca^{2+}	457	-286	0	0	0	-85	403	-115	-375	-0.17
	100%	-63%	0%	0%	0%	-19%	88%	-25%	-82%	0.0%
Mg^{2+}	172	-76	0	0	0	-90	0	138	-144	-0.06
	100%	-44%	0%	0%	0%	-52%	0%	80%	-83%	0.0%
Na^+	313	-141	0	0	0	0	0	-83	-89	0.52
	100%	-45%	0%	0%	0%	0%	0%	-26%	-29%	0.2%
Fe^{2+}	2	-7	0	0	673	0	-644	-18	-5	0.73
	100%	-396%	0%	0%	36771%	0%	-35169%	-1000%	-267%	39.7%
Mn^{2+}	0	-8	0	0	642	0	-607	-23	-6	-1.54
	100%	-2079%	0%	0%	173663%	0%	-164153%	-6324%	-1624%	-416.2%
CO_3^{2-}	1352	-1176	-191	1001	533	113	-649	0	-982	1.79
	100%	-87%	-14%	74%	39%	8%	-48%	0%	-73%	0.1%
SO_4^{2-}	297	17	0	-167	0	-44	0	0	-104	-0.94
	100%	6%	0%	-56%	0%	-15%	0%	0%	-35%	-0.3%
Cl-	177	-69	0	0	0	0	0	0	-108	-0.10
	100%	-39%	0%	0%	0%	0%	0%	0%	-61%	-0.1%
PO_4^{3-}	11	0	0	0	0	-11	0	0	0	0.05
	100%	-1%	0%	0%	0%	-98%	0%	0%	-1%	0.4%
FDS	3176	-1749	-191	787	1848	-416	-1496	-121	-1838	1.13
	100%	-55%	-6%	25%	58%	-13%	-47%	-4%	-58%	0.0%

Mass balance in pounds per acre per year and percent of total component loading.

3. Daily Processing Baseline Simulations

FIGURE 13
CASE 1 DAIRY BREAKTHROUGH CURVES

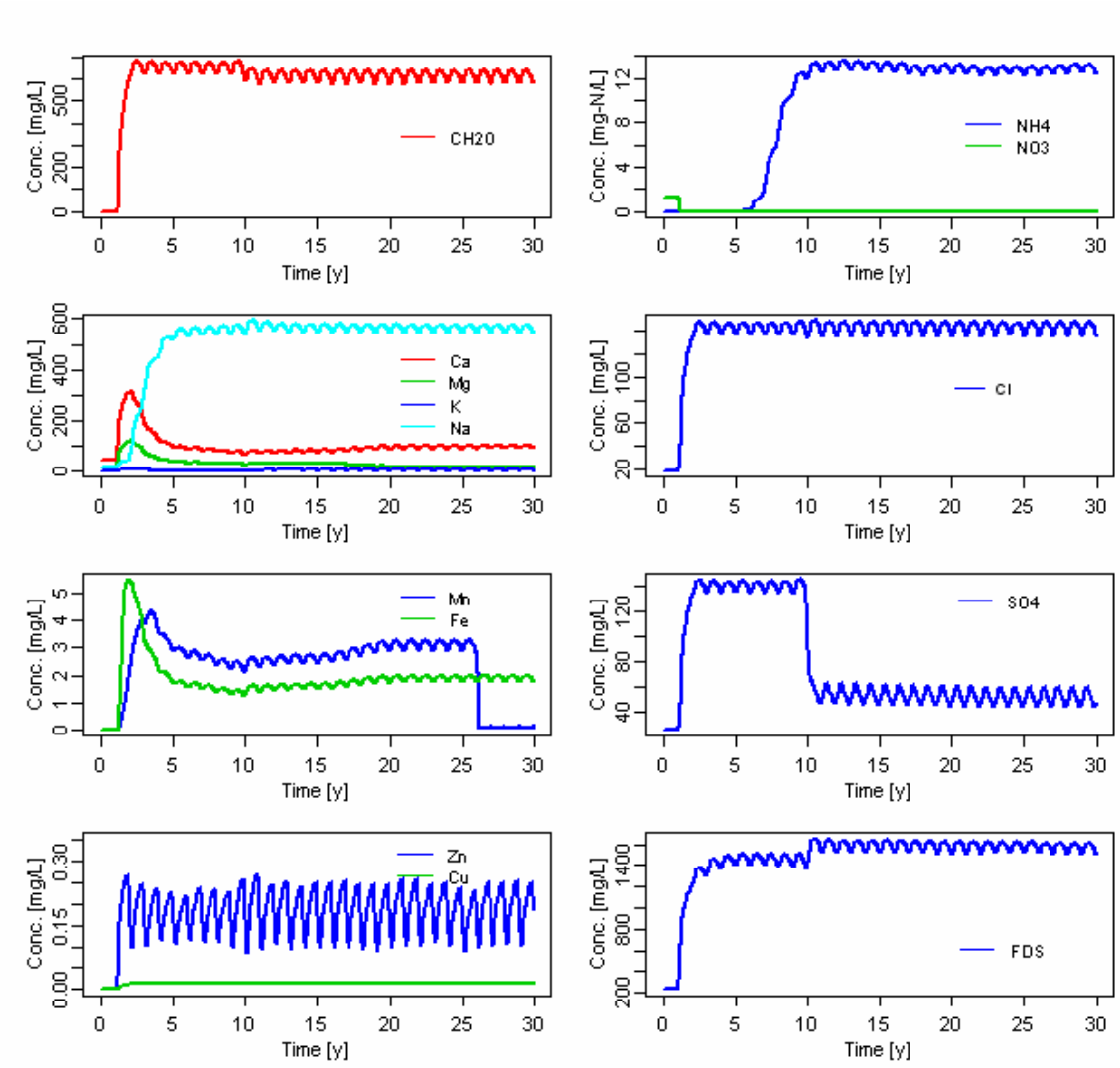

FIGURE 14
DAIRY CASE 1 PROFILES, YEAR 30

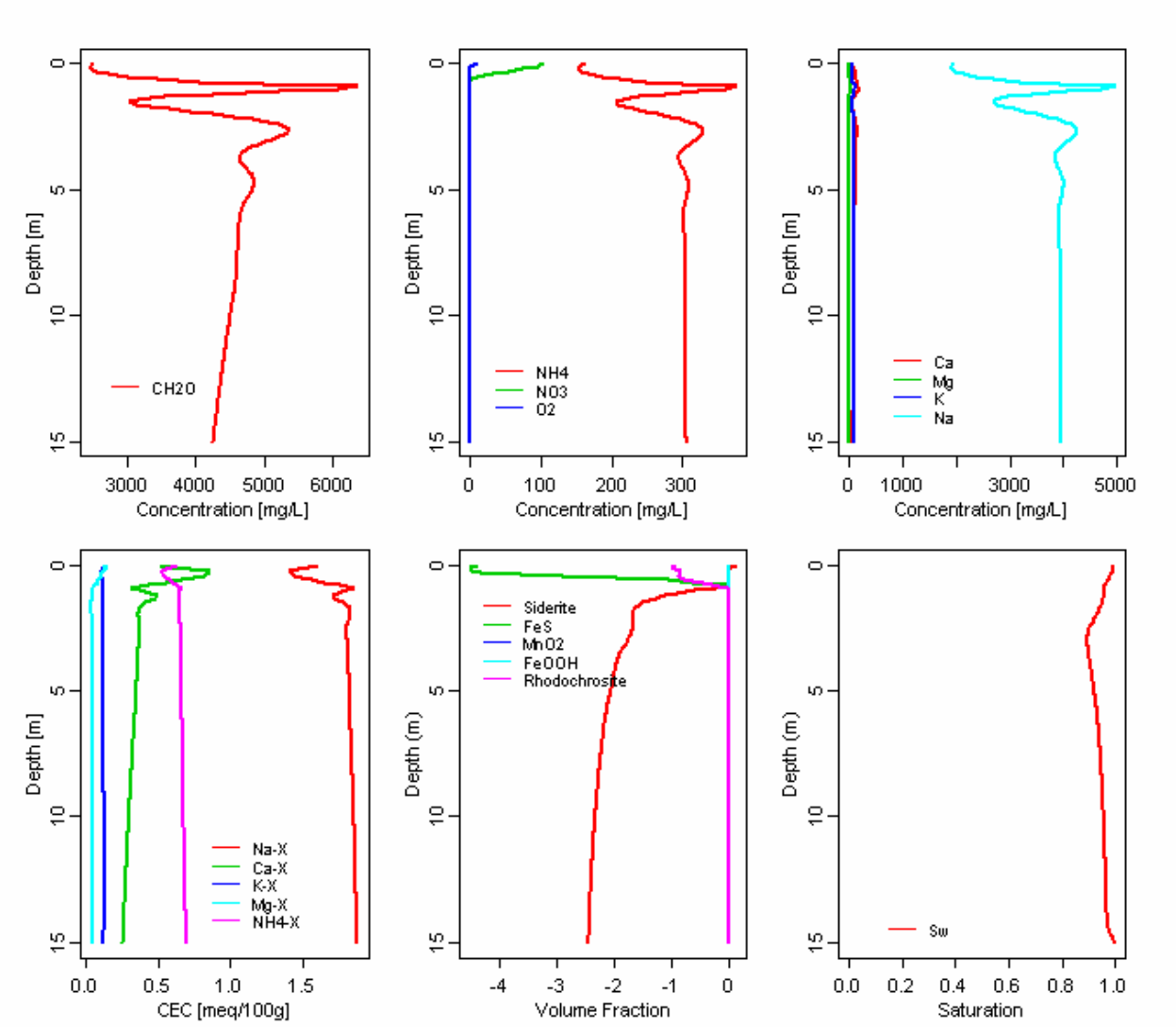

Table 7
Dairy Case 1 Mass Balance

	Surface Loading	Storage	Degassing	Biodegredation (Aqueous)	Biodegredation (Mineral)	Root Uptake	Precipitation	Adsorption	Water Table	Mass Error
CH_2O	26634	-6174	0	-2835	-342	0	0	0	-17284	-0.72
	100%	-23%	0%	-11%	-1%	0%	0%	0%	-65%	0%
NH_4	1870	-434	0	-33	0	-147	0	-796	-461	0.11
	100%	-23%	0%	-2%	0%	-8%	0%	-43%	-25%	0.0%
NO_3	1252	5	0	-1015	0	-238	0	0	-4	0.06
	100%	0%	0%	-81%	0%	-19%	0%	0%	0%	0.0%
O_2	130	0	4	-134	0	0	0	0	0	0.05
	100%	0%	3%	-103%	0%	0%	0%	0%	0%	0.0%
K^+	657	-130	0	0	0	-131	0	-274	-122	0.01
	100%	-20%	0%	0%	0%	-20%	0%	-42%	-19%	0.0%
Ca^{2+}	683	-94	0	0	0	-82	-764	2362	-2105	0.01
	100%	-14%	0%	0%	0%	-12%	-112%	346%	-308%	0.0%
Mg^{2+}	162	2	0	0	0	-86	0	647	-724	-0.03
	100%	1%	0%	0%	0%	-53%	0%	399%	-447%	0.0%
Na^+	22020	-5620	0	0	0	0	0	-2752	-13647	0.82
	100%	-26%	0%	0%	0%	0%	0%	-12%	-62%	0.0%
Fe^{2+}	48	-2	0	0	1252	0	-1264	0	-41	-7.39
	100%	-4%	0%	0%	2611%	0%	-2636%	-1%	-86%	-15.4%
Mn^{2+}	4	-4	0	0	637	0	-589	-3	-45	-1.74
	100%	-114%	0%	0%	17579%	0%	-16266%	-96%	-1251%	-48.0%
CO_3^{2-}	8722	-3552	-71	5669	695	723	-1828	0	-10354	3.72
	100%	-41%	-1%	65%	8%	8%	-21%	0%	-119%	0.0%
SO_4^{2-}	8388	-1394	0	-3418	0	-45	0	0	-3533	-2.68
	100%	-17%	0%	-41%	0%	-1%	0%	0%	-42%	0.0%
Cl-	8393	-2127	0	0	0	0	0	0	-6266	0.32
	100%	-25%	0%	0%	0%	0%	0%	0%	-75%	0.0%
PO_4^{3-}	1188	-155	0	0	0	-611	0	0	-422	0.05
	100%	-13%	0%	0%	0%	-51%	0%	0%	-36%	0.0%
FDS	53387	-13504	-71	1203	2583	-618	-4445	-818	-37725	-6.75
	100%	-25%	0%	2%	5%	-1%	-8%	-2%	-71%	0.0%

Mass balance in pounds per acre per year and percent of total component loading.

FIGURE 15
CASE 2 DAIRY BREAKTHROUGH CURVES

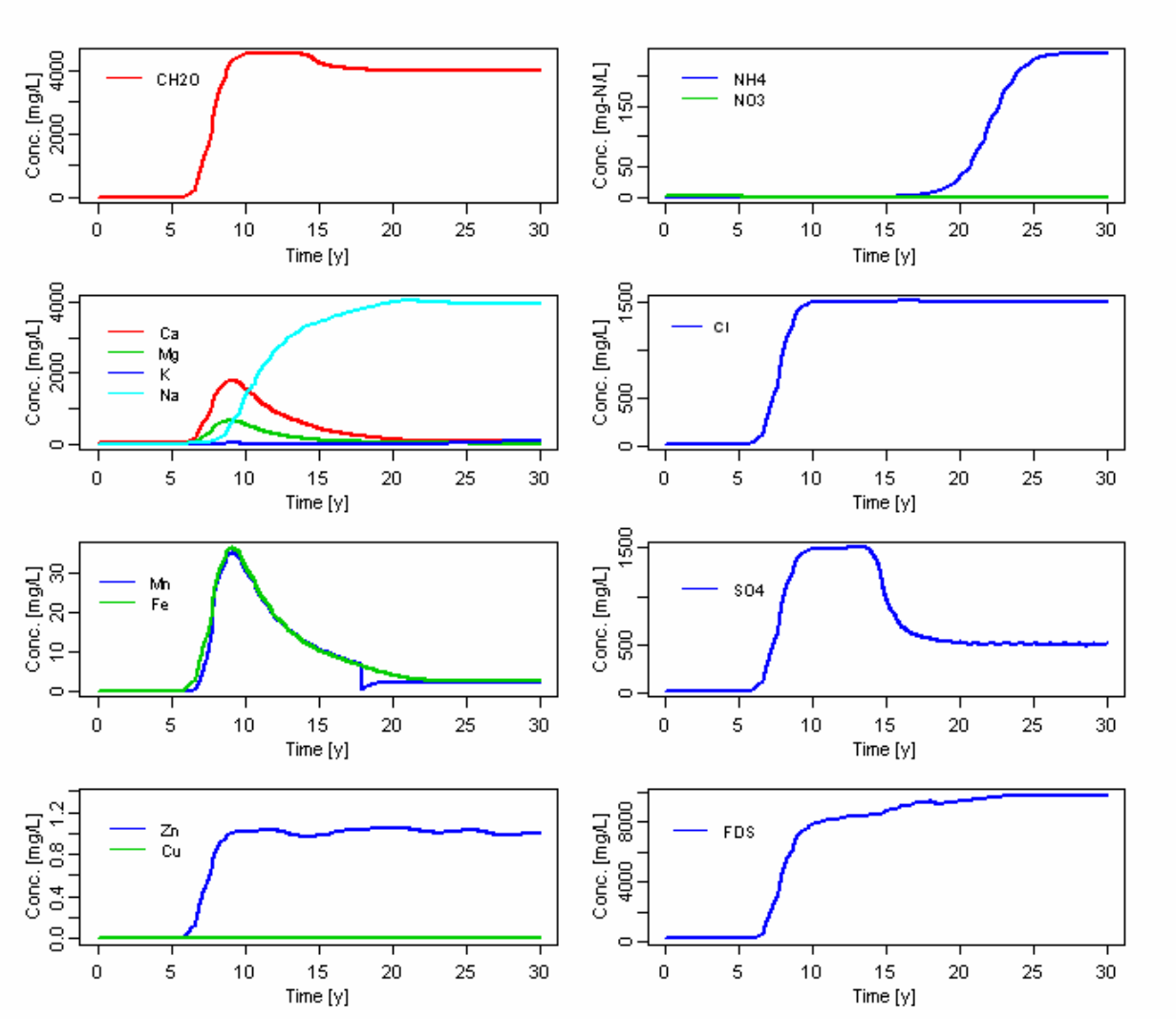

FIGURE 16
DAIRY CASE 2 PROFILES, YEAR 30

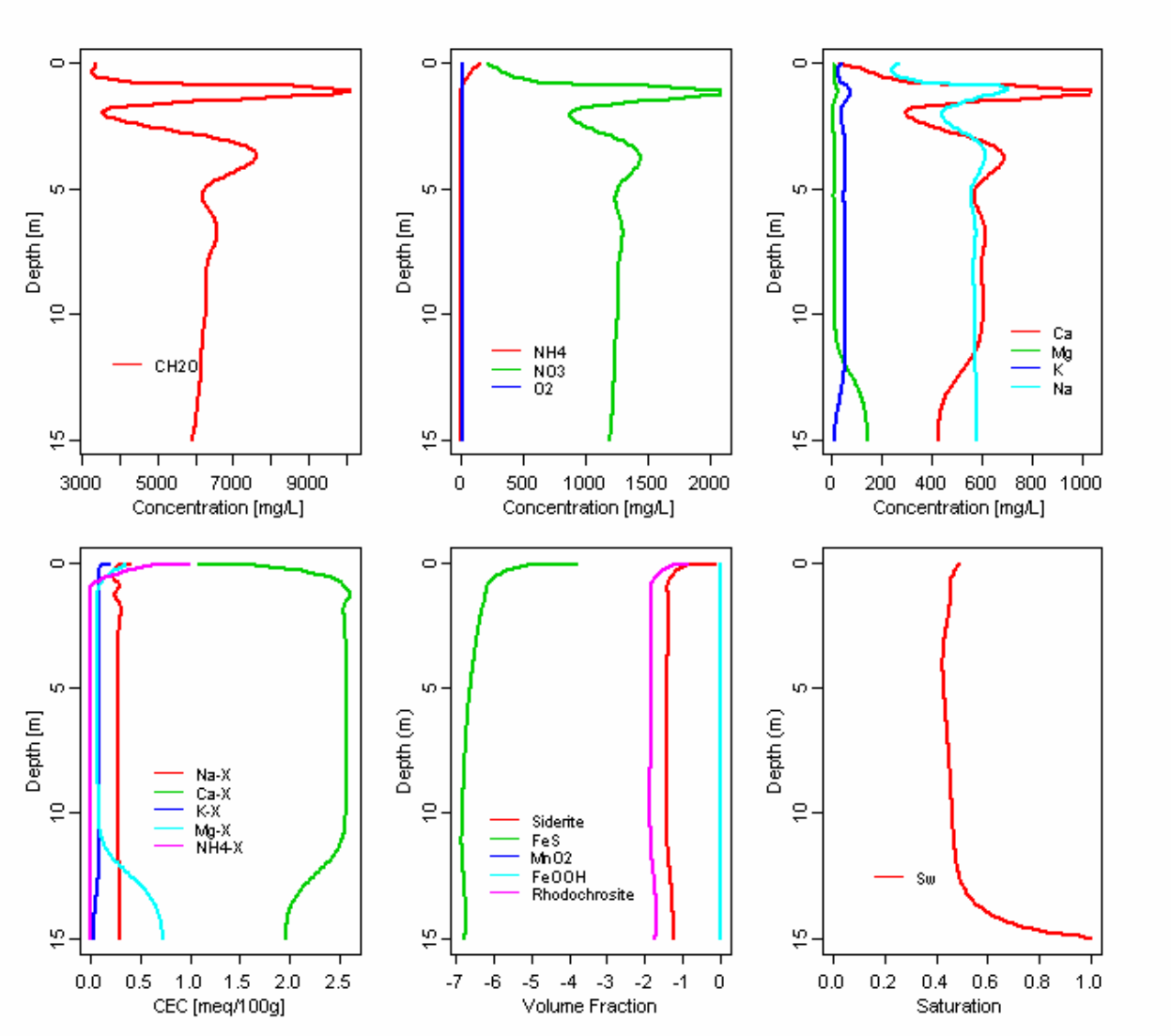

Table 8
Dairy Case 2 Mass Balance

	Surface Loading	Storage	Degassing	Biodegredation (Aqueous)	Biodegredation (Mineral)	Root Uptake	Precipitation	Adsorption	Water Table	Mass Error
CH_2O	25345	-4279	0	-3408	0	0	0	0	-17636	22.28
	100%	-17%	0%	-13%	0%	0%	0%	0%	-70%	0%
NH_4	1265	-1	0	-1111	0	-134	0	-17	0	1.15
	100%	0%	0%	-88%	0%	-11%	0%	-1%	0%	0.1%
NO_3	1724	-902	0	3306	0	-400	0	0	-3726	1.46
	100%	-52%	0%	192%	0%	-23%	0%	0%	-216%	0.1%
O_2	118	2	7135	-7249	0	0	0	0	-6	0.04
	100%	2%	6054%	-6151%	0%	0%	0%	0%	-5%	0.0%
K^+	354	-33	0	0	0	-131	0	-146	-43	0.25
	100%	-9%	0%	0%	0%	-37%	0%	-41%	-12%	0.1%
Ca^{2+}	425	-368	0	0	0	-86	2089	-451	-1611	-0.18
	100%	-86%	0%	0%	0%	-20%	491%	-106%	-379%	0.0%
Mg^{2+}	146	-20	0	0	0	-86	0	534	-574	-0.13
	100%	-14%	0%	0%	0%	-59%	0%	367%	-394%	-0.1%
Na^+	2247	-399	0	0	0	0	0	-385	-1461	1.74
	100%	-18%	0%	0%	0%	0%	0%	-17%	-65%	0.1%
Fe^{2+}	2	0	0	0	0	0	0	-1	-1	0.00
	100%	-19%	0%	0%	0%	0%	0%	-46%	-35%	0.1%
Mn^{2+}	1	0	0	0	0	0	0	0	0	0.00
	100%	-18%	0%	0%	0%	0%	0%	-67%	-14%	0.1%
CO_3^{2-}	1739	-240	-9902	6816	0	773	3127	0	-2314	0.00
	100%	-14%	-569%	392%	0%	44%	180%	0%	-133%	0.0%
SO_4^{2-}	459	-58	0	0	0	-46	0	0	-356	0.04
	100%	-13%	0%	0%	0%	-10%	0%	0%	-77%	0.0%
Cl-	1266	-217	0	0	0	0	0	0	-1048	0.91
	100%	-17%	0%	0%	0%	0%	0%	0%	-83%	0.1%
PO_4^{3-}	1090	-98	0	0	0	-581	0	0	-410	0.98
	100%	-9%	0%	0%	0%	-53%	0%	0%	-38%	0.1%
FDS	10717	-2336	-9902	9010	0	-691	5217	-466	-11543	6.21
	100%	-22%	-92%	84%	0%	-6%	49%	-4%	-108%	0.1%

Mass balance in pounds per acre per year and percent of total component loading.

FIGURE 17
CASE 3 DAIRY BREAKTHROUGH CURVES

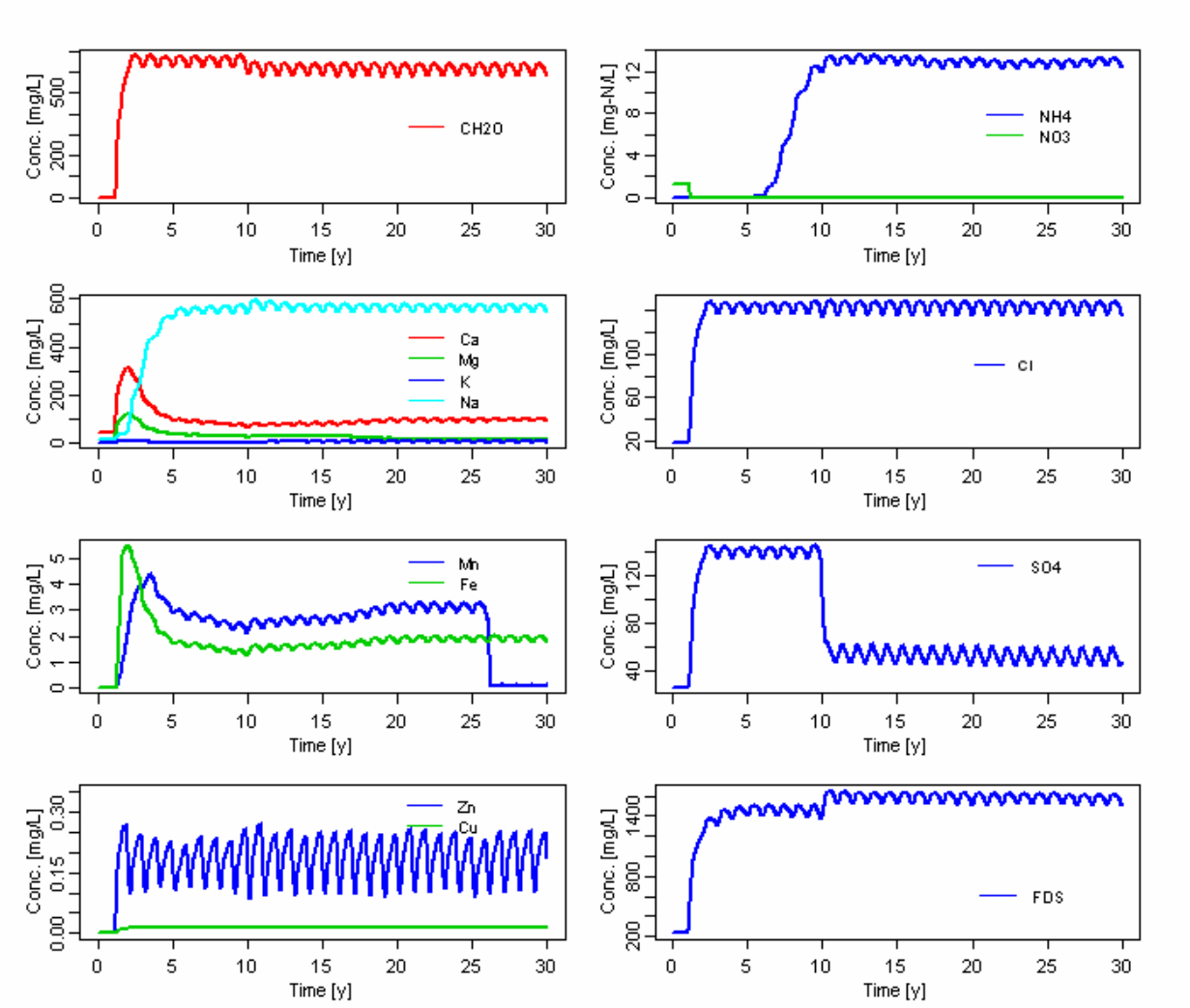

FIGURE 18
DAIRY CASE 3 PROFILES, YEAR 30

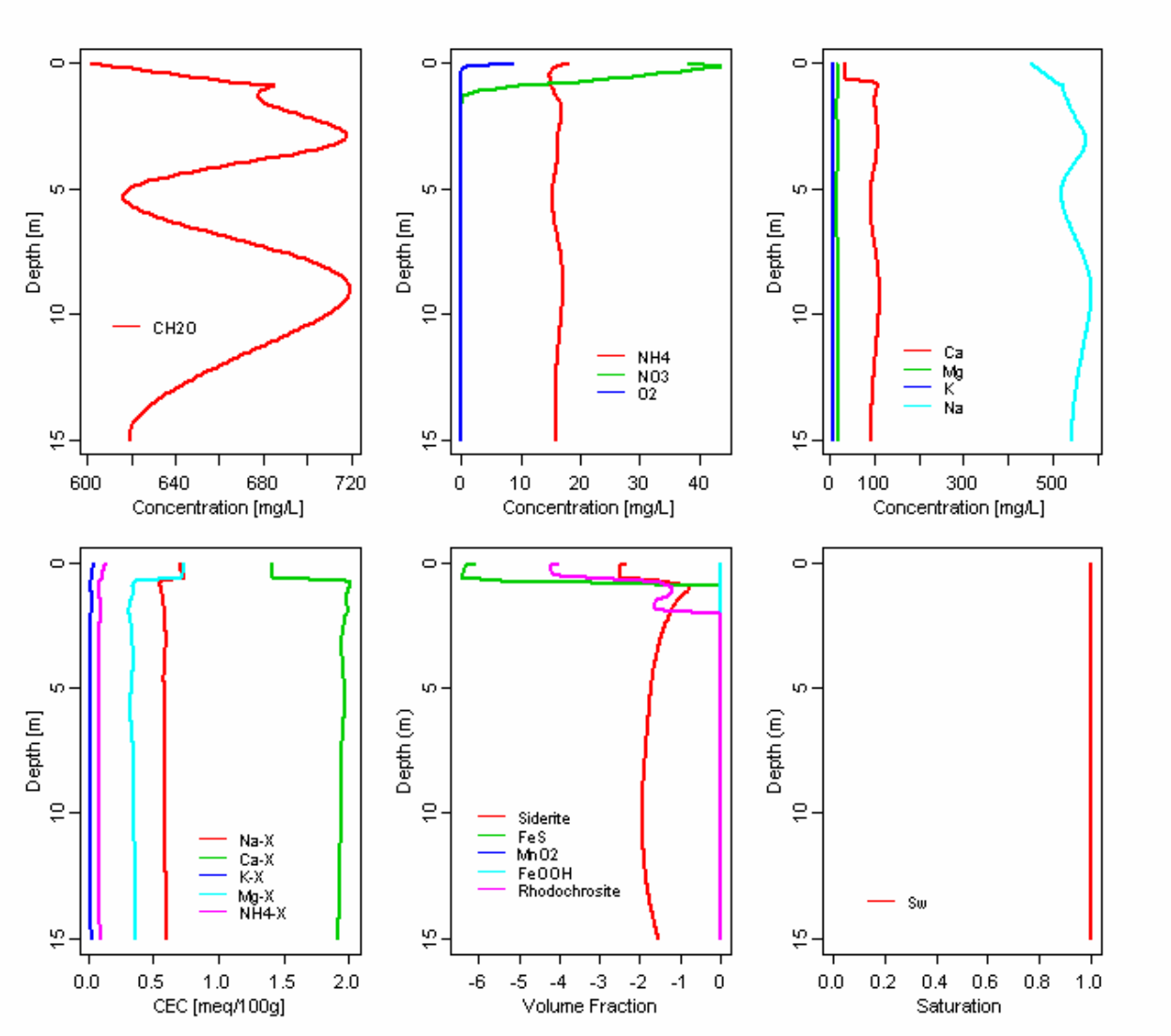

Table 9
Dairy Case 3 Mass Balance

	Surface Loading	Storage	Degassing	Biodegredation (Aqueous)	Biodegredation (Mineral)	Root Uptake	Precipitation	Adsorption	Water Table	Mass Error
CH_2O	21466	-975	0	-2118	-324	0	0	0	-18050	-1.43
	100%	-5%	0%	-10%	-2%	0%	0%	0%	-84%	0%
NH_4	730	-25	0	-88	0	-140	0	-104	-373	-0.04
	100%	-3%	0%	-12%	0%	-19%	0%	-14%	-51%	0.0%
NO_3	1522	5	0	-1192	0	-329	0	0	-6	-0.01
	100%	0%	0%	-78%	0%	-22%	0%	0%	0%	0.0%
O_2	343	11	60	-371	0	0	0	0	-44	0.04
	100%	3%	18%	-108%	0%	0%	0%	0%	-13%	0.0%
K^+	327	-4	0	0	0	-124	0	-7	-191	-0.01
	100%	-1%	0%	0%	0%	-38%	0%	-2%	-58%	0.0%
Ca^{2+}	1272	-90	0	0	0	-70	1708	241	-3061	-0.08
	100%	-7%	0%	0%	0%	-6%	134%	19%	-241%	0.0%
Mg^{2+}	640	-3	0	0	0	-85	0	395	-947	0.00
	100%	-1%	0%	0%	0%	-13%	0%	62%	-148%	0.0%
Na^+	17156	-833	0	0	0	0	0	-871	-15452	0.21
	100%	-5%	0%	0%	0%	0%	0%	-5%	-90%	0.0%
Fe^{2+}	3	0	0	0	1114	0	-1066	0	-72	-21.32
	100%	-5%	0%	0%	32326%	0%	-30946%	-14%	-2080%	-618.9%
Mn^{2+}	0	-3	0	0	638	0	-565	-19	-56	-3.66
	100%	-6765%	0%	0%	1672313%	0%	-1479191%	-50195%	-145849%	-9586.9%
CO_3^{2-}	4405	-442	0	4236	683	759	1918	0	-11557	1.32
	100%	-10%	0%	96%	16%	17%	44%	0%	-262%	0.0%
SO_4^{2-}	4321	-107	0	-1855	0	-44	0	0	-2317	-0.99
	100%	-2%	0%	-43%	0%	-1%	0%	0%	-54%	0.0%
Cl-	4339	-191	0	0	0	0	0	0	-4148	0.00
	100%	-4%	0%	0%	0%	0%	0%	0%	-96%	0.0%
PO_4^{3-}	7535	-351	0	0	0	-604	0	0	-6581	0.17
	100%	-5%	0%	0%	0%	-8%	0%	0%	-87%	0.0%
FDS	42250	-2043	0	1101	2435	-637	1996	-366	-44759	-24.41
	100%	-5%	0%	3%	6%	-2%	5%	-1%	-106%	-0.1%

Mass balance in pounds per acre per year and percent of total component loading.

4. Meat Packing Baseline Simulations

FIGURE 19
CASE 1 MEAT BREAKTHROUGH CURVES

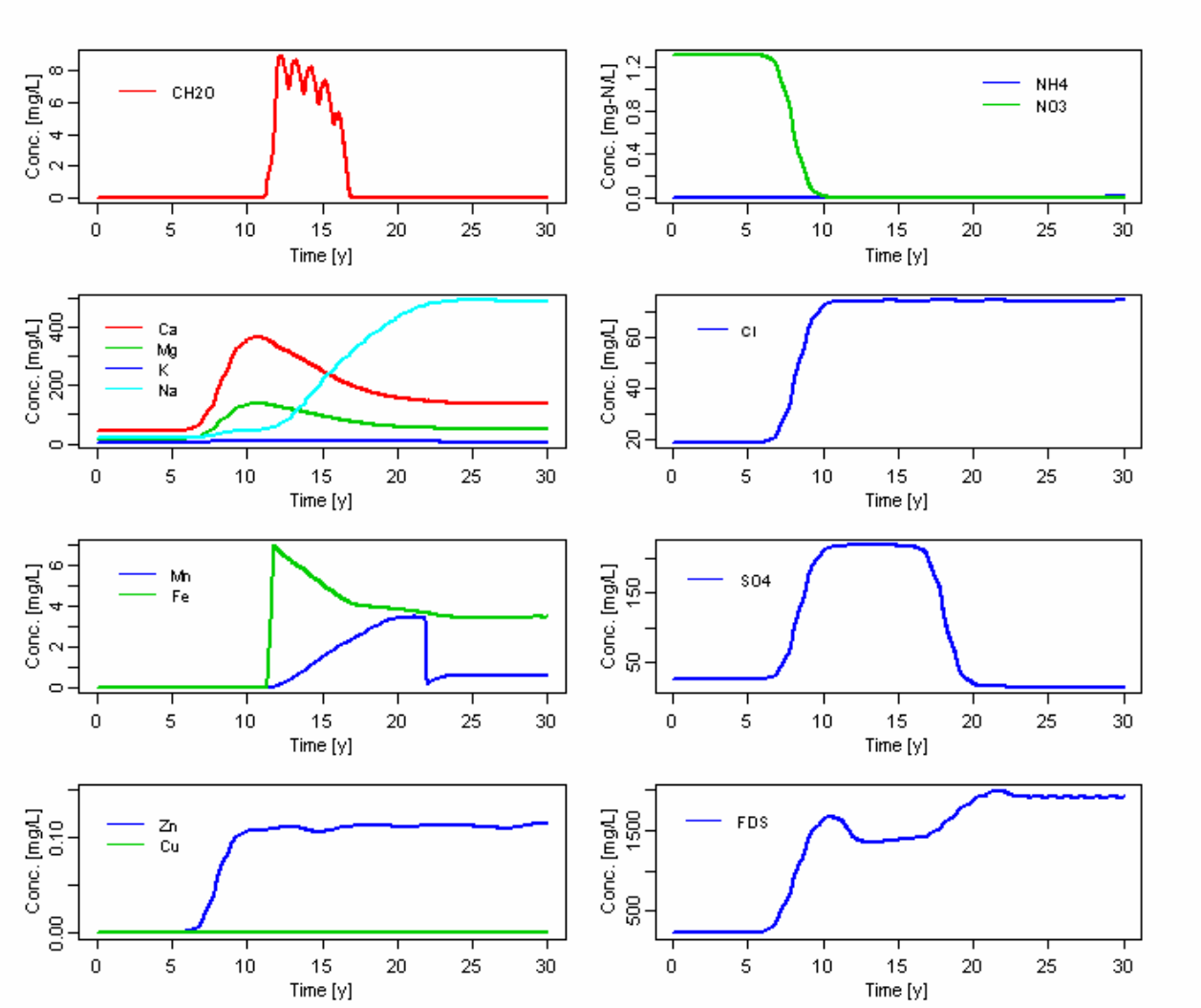

FIGURE 20
MEAT CASE 1 PROFILES, YEAR 30

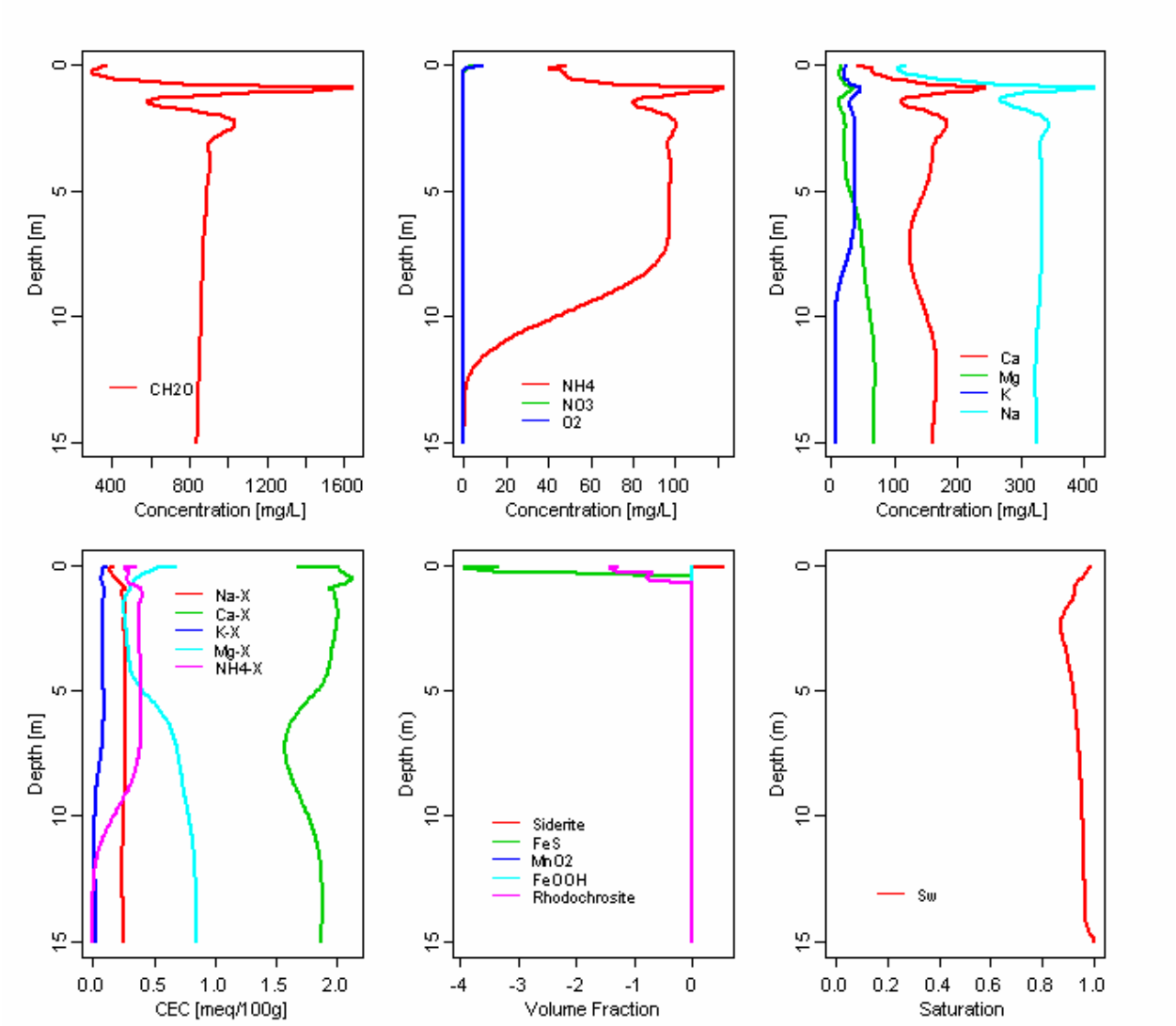

Table 10
Meat Case 1 Mass Balance

	Surface Loading	Storage	Degassing	Biodegredation (Aqueous)	Biodegredation (Mineral)	Root Uptake	Precipitation	Adsorption	Water Table	Mass Error
CH_2O	3838	-1168	0	-423	-319	0	0	0	-1925	2.91
	100%	-30%	0%	-11%	-8%	0%	0%	0%	-50%	0%
NH_4	570	-87	0	-37	0	-149	0	-297	0	0.60
	100%	-15%	0%	-7%	0%	-26%	0%	-52%	0%	0.1%
NO_3	117	7	0	-72	0	-48	0	0	-4	0.01
	100%	6%	0%	-62%	0%	-41%	0%	0%	-4%	0.0%
O_2	118	0	34	-151	0	0	0	0	0	0.06
	100%	0%	28%	-128%	0%	0%	0%	0%	0%	0.1%
K^+	280	-27	0	0	0	-131	0	-94	-28	0.24
	100%	-10%	0%	0%	0%	-47%	0%	-33%	-10%	0.1%
Ca^{2+}	476	-159	0	0	0	-82	-21	379	-593	-0.14
	100%	-33%	0%	0%	0%	-17%	-4%	80%	-125%	0.0%
Mg^{2+}	180	-47	0	0	0	-93	0	198	-238	-0.05
	100%	-26%	0%	0%	0%	-52%	0%	110%	-132%	0.0%
Na^+	1315	-442	0	0	0	0	0	-346	-526	1.18
	100%	-34%	0%	0%	0%	0%	0%	-26%	-40%	0.1%
Fe^{2+}	35	-5	0	0	1046	0	-1049	-16	-10	0.98
	100%	-14%	0%	0%	3013%	0%	-3021%	-46%	-29%	2.8%
Mn^{2+}	1	-5	0	0	654	0	-620	-20	-11	-1.89
	100%	-904%	0%	0%	116772%	0%	-110771%	-3517%	-2017%	-337.6%
CO_3^{2-}	2698	-1203	-41	846	639	168	-1554	0	-1549	3.68
	100%	-45%	-2%	31%	24%	6%	-58%	0%	-57%	0.1%
SO_4^{2-}	673	-1	0	-454	0	-46	0	0	-173	-1.52
	100%	0%	0%	-67%	0%	-7%	0%	0%	-26%	-0.2%
Cl-	259	-68	0	0	0	0	0	0	-190	0.01
	100%	-26%	0%	0%	0%	0%	0%	0%	-74%	0.0%
PO_4^{3-}	136	-5	0	0	0	-123	0	0	-8	0.14
	100%	-3%	0%	0%	0%	-90%	0%	0%	-6%	0.1%
FDS	6738	-2042	-41	283	2339	-503	-3244	-195	-3331	3.22
	100%	-30%	-1%	4%	35%	-7%	-48%	-3%	-49%	0.0%

Mass balance in pounds per acre per year and percent of total component loading.

FIGURE 21
CASE 2 MEAT BREAKTHROUGH CURVES

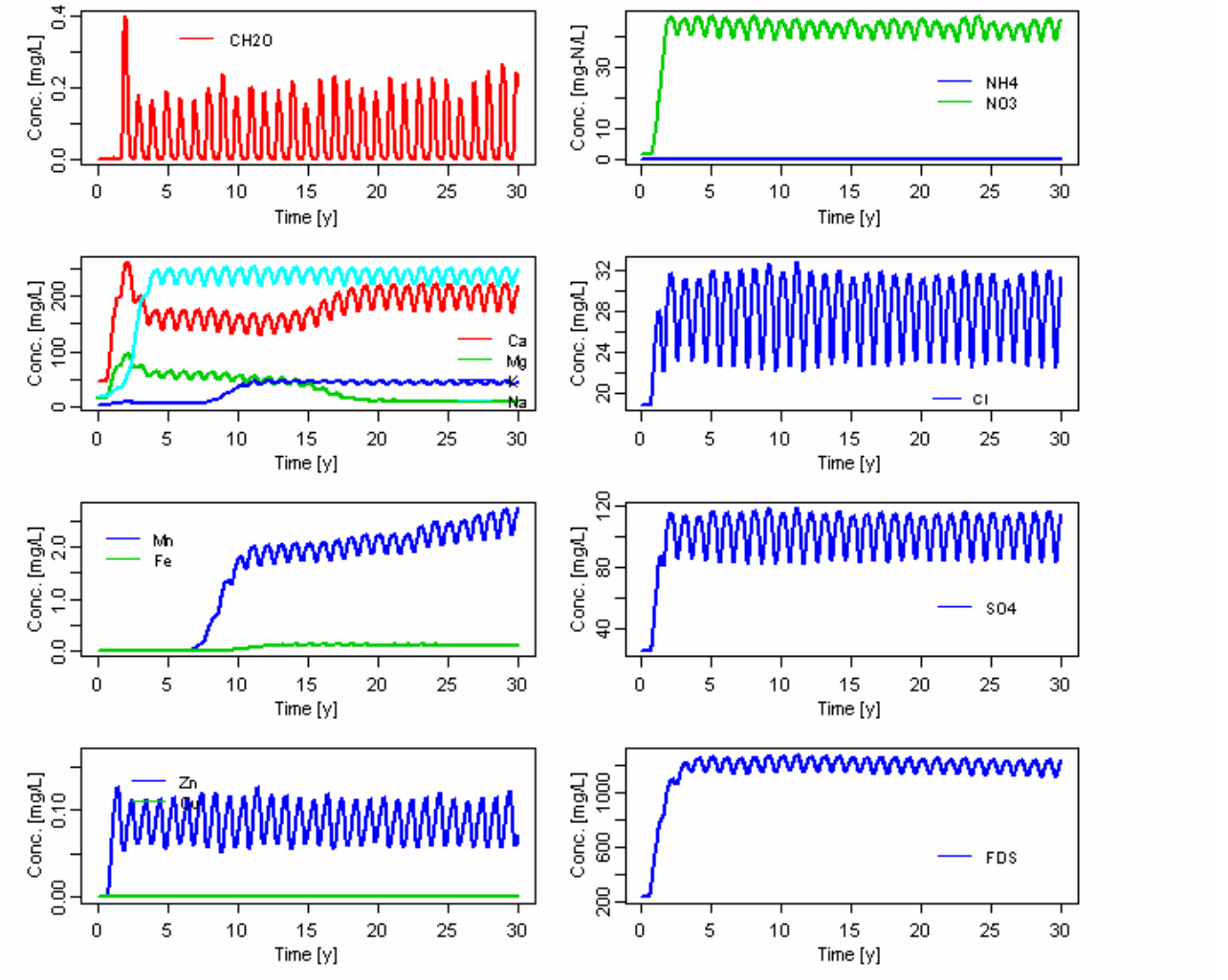

FIGURE 22
MEAT CASE 2 PROFILES, YEAR 30

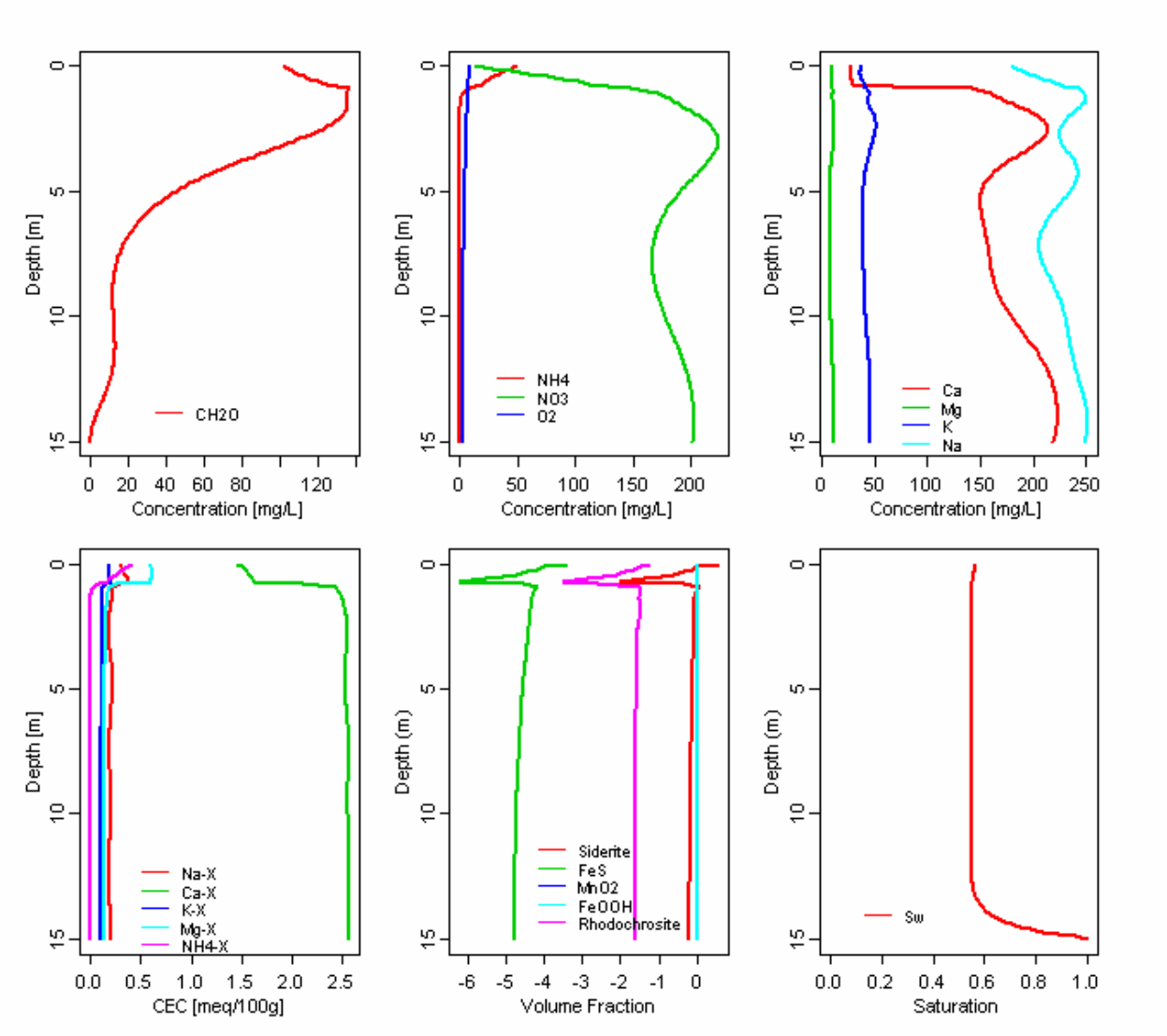

Table 11
Meat Case 2 Mass Balance

	Surface Loading	Storage	Degassing	Biodegredation (Aqueous)	Biodegredation (Mineral)	Root Uptake	Precipitation	Adsorption	Water Table	Mass Error
CH_2O	3022	-36	0	-2985	0	0	0	0	-2	-0.06
	100%	-1%	0%	-99%	0%	0%	0%	0%	0%	0%
NH_4	1587	-1	0	-1431	0	-140	0	-15	0	-0.03
	100%	0%	0%	-90%	0%	-9%	0%	-1%	0%	0.0%
NO_3	471	-159	0	4383	0	-389	0	0	-4306	0.03
	100%	-34%	0%	930%	0%	-83%	0%	0%	-913%	0.0%
O_2	287	3	7703	-7920	0	0	0	0	-74	0.14
	100%	1%	2680%	-2755%	0%	0%	0%	0%	-26%	0.0%
K^+	1188	-35	0	0	0	-127	0	-240	-786	0.03
	100%	-3%	0%	0%	0%	-11%	0%	-20%	-66%	0.0%
Ca^{2+}	852	-123	0	0	0	-60	4024	-524	-4169	0.01
	100%	-14%	0%	0%	0%	-7%	472%	-61%	-490%	0.0%
Mg^{2+}	321	4	0	0	0	-71	0	555	-809	-0.02
	100%	1%	0%	0%	0%	-22%	0%	173%	-252%	0.0%
Na^+	5657	-191	0	0	0	0	0	-270	-5196	-0.09
	100%	-3%	0%	0%	0%	0%	0%	-5%	-92%	0.0%
Fe^{2+}	164	-2	0	0	0	0	-107	-21	-35	-2.02
	100%	-1%	0%	0%	0%	0%	-65%	-13%	-22%	-1.2%
Mn^{2+}	3	0	0	0	0	0	0	-1	-2	0.00
	100%	-3%	0%	0%	0%	0%	0%	-33%	-64%	0.0%
CO_3^{2-}	8291	-333	-7188	5971	31	488	5908	0	-13169	-0.25
	100%	-4%	-87%	72%	0%	6%	71%	0%	-159%	0.0%
SO_4^{2-}	2427	-68	0	0	0	-41	0	0	-2318	-0.04
	100%	-3%	0%	0%	0%	-2%	0%	0%	-96%	0.0%
Cl-	655	-10	0	0	0	0	0	0	-645	-0.02
	100%	-2%	0%	0%	0%	0%	0%	0%	-98%	0.0%
PO_4^{3-}	639	-13	0	0	0	-289	0	0	-337	-0.01
	100%	-2%	0%	0%	0%	-45%	0%	0%	-53%	0.0%
FDS	22254	-930	-7188	8923	31	-629	9825	-516	-31772	-2.41
	100%	-4%	-32%	40%	0%	-3%	44%	-2%	-143%	0.0%

Mass balance in pounds per acre per year and percent of total component loading.

FIGURE 23
CASE 3 MEAT BREAKTHROUGH CURVES

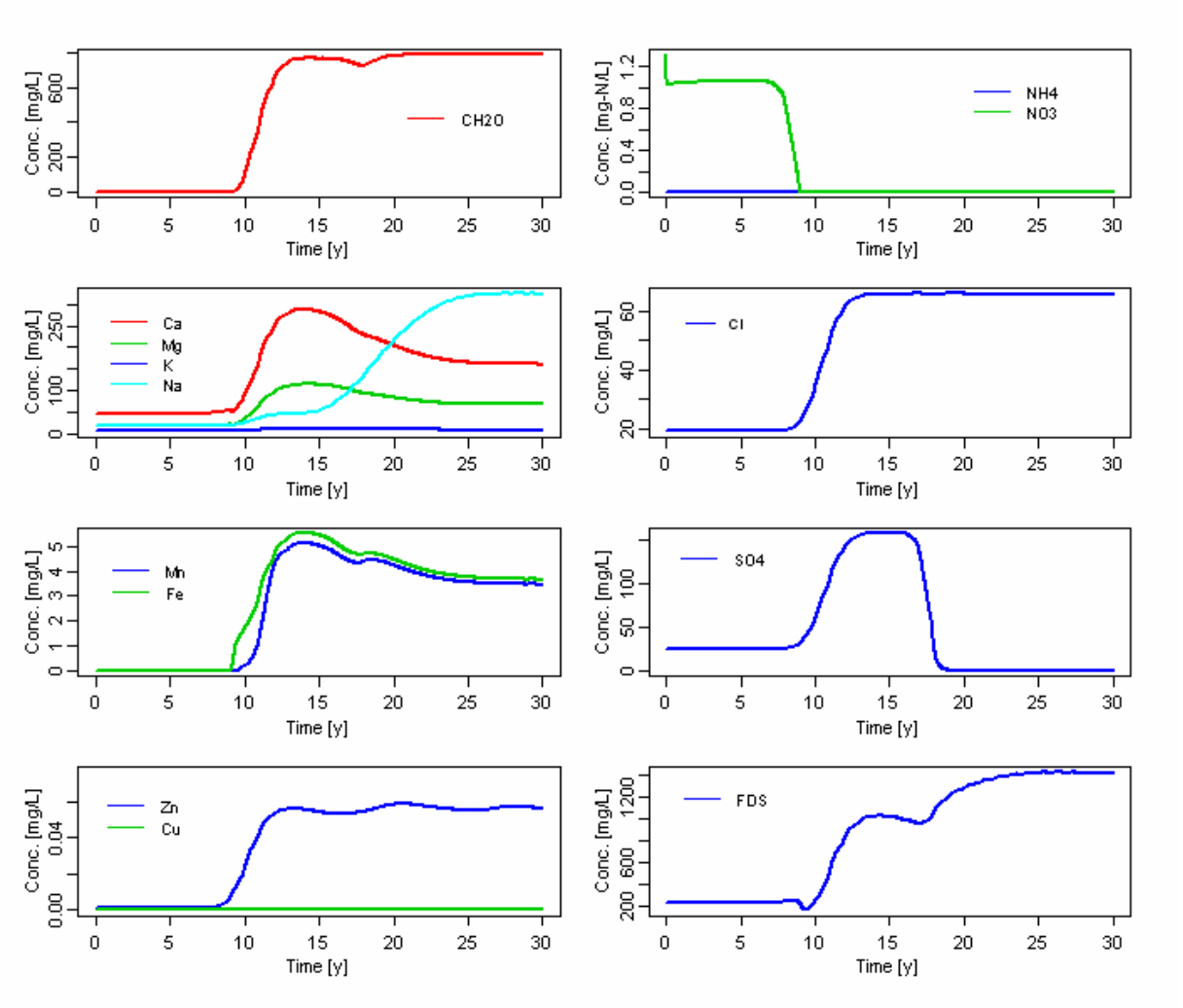

FIGURE 24
MEAT CASE 3 PROFILES, YEAR 30

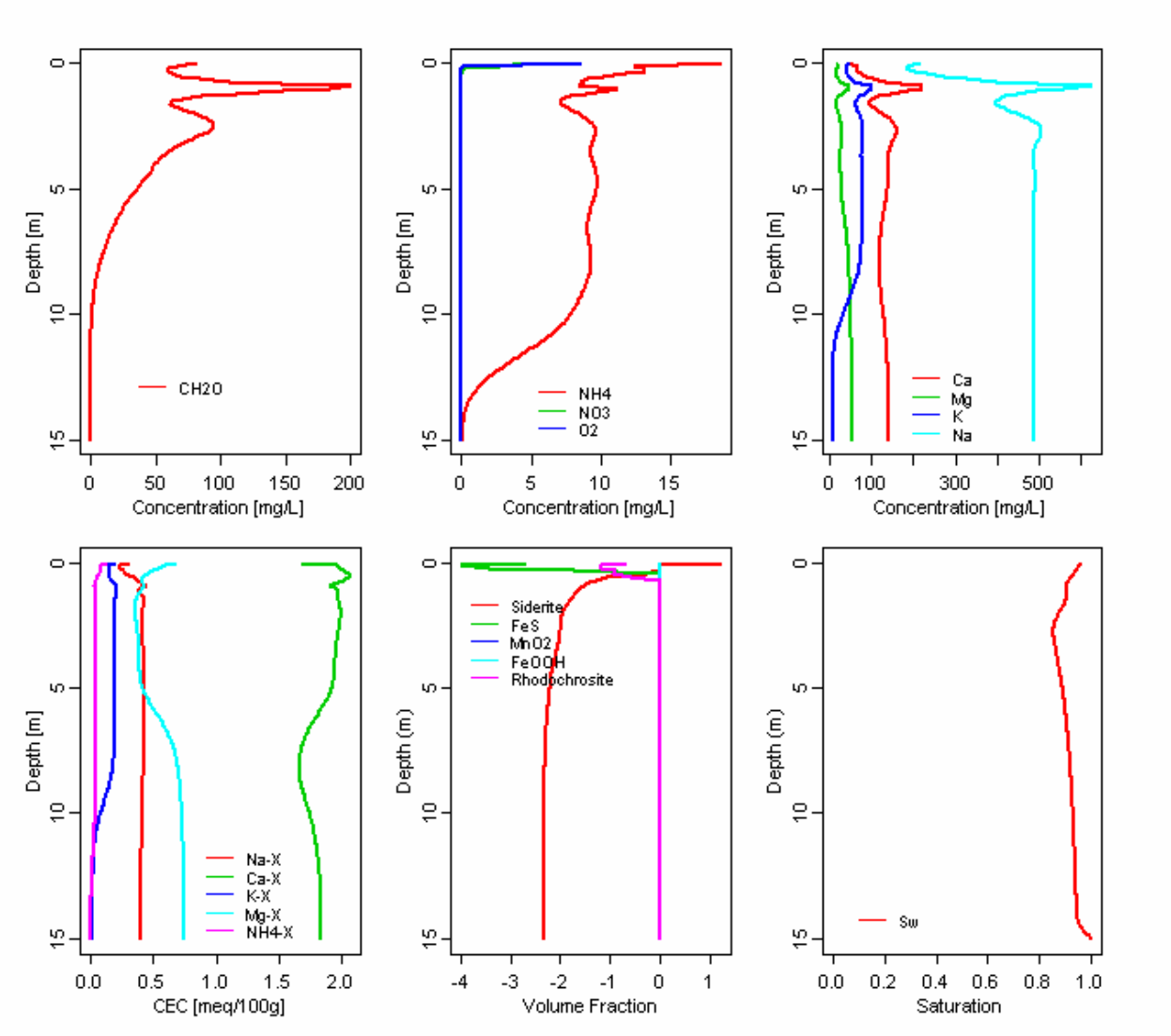

Table 12
Meat Case 3 Mass Balance

	Surface Loading	Storage	Degassing	Biodegredation (Aqueous)	Biodegredation (Mineral)	Root Uptake	Precipitation	Adsorption	Water Table	Mass Error
CH_2O	850	-37	0	-620	-187	0	0	0	-6	0.24
	100%	-4%	0%	-73%	-22%	0%	0%	0%	-1%	0%
NH_4	247	-10	0	-57	0	-142	0	-37	0	0.23
	100%	-4%	0%	-23%	0%	-58%	0%	-15%	0%	0.1%
NO_3	131	8	0	-63	0	-69	0	0	-7	0.00
	100%	6%	0%	-48%	0%	-52%	0%	0%	-5%	0.0%
O_2	126	11	160	-277	0	0	0	0	-21	-0.03
	100%	9%	127%	-219%	0%	0%	0%	0%	-16%	0.0%
K^+	511	-63	0	0	0	-132	0	-281	-34	0.48
	100%	-12%	0%	0%	0%	-26%	0%	-55%	-7%	0.1%
Ca^{2+}	591	-124	0	0	0	-82	72	359	-816	-0.02
	100%	-21%	0%	0%	0%	-14%	12%	61%	-138%	0.0%
Mg^{2+}	223	-33	0	0	0	-94	0	211	-307	-0.01
	100%	-15%	0%	0%	0%	-42%	0%	95%	-138%	0.0%
Na^+	2415	-647	0	0	0	0	0	-582	-1184	2.32
	100%	-27%	0%	0%	0%	0%	0%	-24%	-49%	0.1%
Fe^{2+}	67	-1	0	0	182	0	-248	-1	-4	-4.20
	100%	-1%	0%	0%	271%	0%	-369%	-1%	-6%	-6.2%
Mn^{2+}	1	-4	0	0	596	0	-561	-20	-13	-1.22
	100%	-416%	0%	0%	55222%	0%	-52008%	-1843%	-1168%	-113.0%
CO_3^{2-}	3454	-1344	-72	1240	380	256	-564	0	-3347	3.34
	100%	-39%	-2%	36%	11%	7%	-16%	0%	-97%	0.1%
SO_4^{2-}	1124	-39	0	-630	0	-46	0	0	-409	-0.21
	100%	-3%	0%	-56%	0%	-4%	0%	0%	-36%	0.0%
Cl-	367	-77	0	0	0	0	0	0	-290	0.13
	100%	-21%	0%	0%	0%	0%	0%	0%	-79%	0.0%
PO_4^{3-}	263	-16	0	0	0	-205	0	0	-42	0.28
	100%	-6%	0%	0%	0%	-78%	0%	0%	-16%	0.1%
FDS	9393	-2349	-72	490	1157	-513	-1301	-350	-6454	1.11
	100%	-25%	-1%	5%	12%	-5%	-14%	-4%	-69%	0.0%

Mass balance in pounds per acre per year and percent of total component loading.

5. POTW Baseline Simulation

FIGURE 25
POTW BREAKTHROUGH CURVES

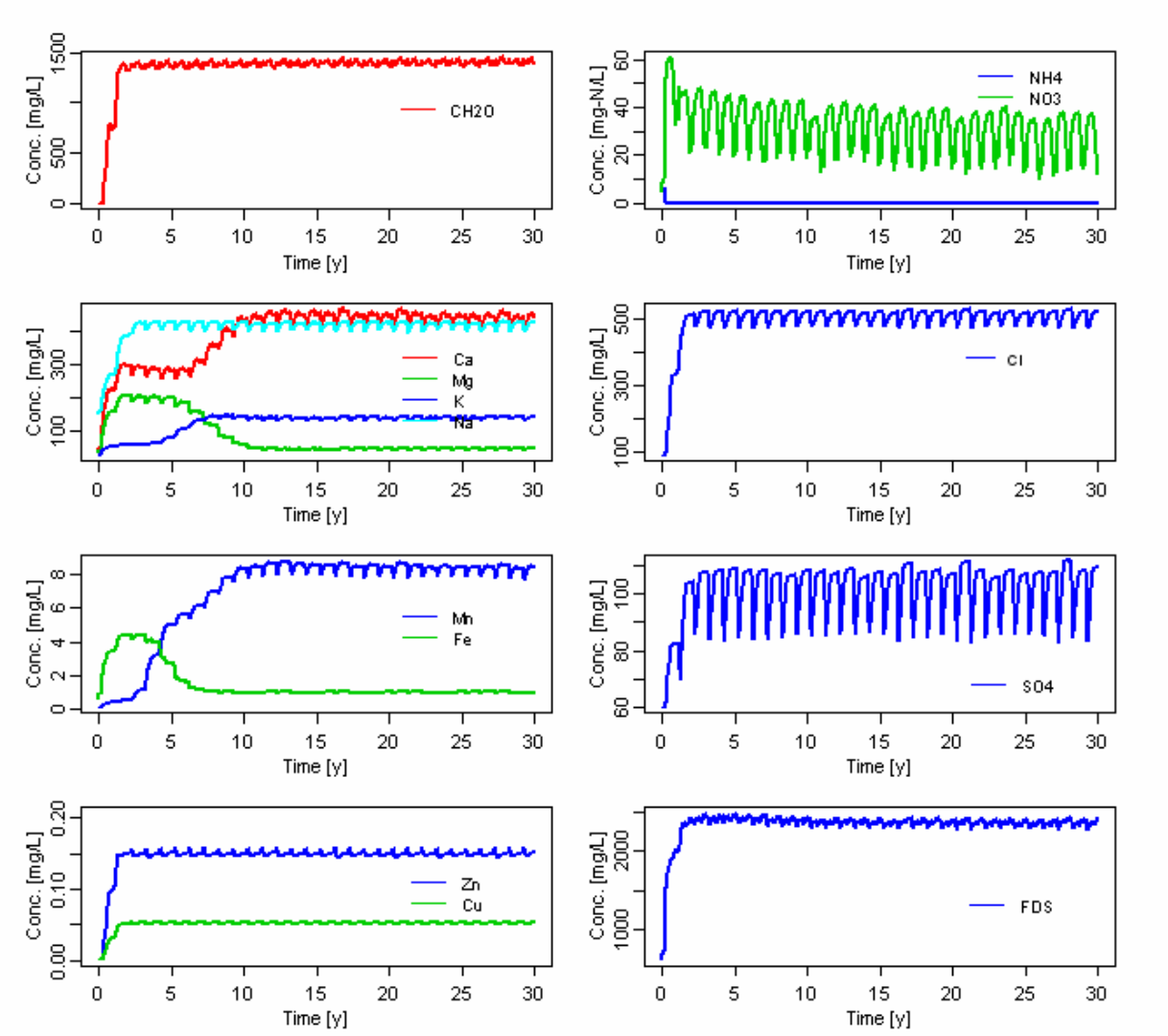

FIGURE 26
POTW PROFILES, YEAR 30

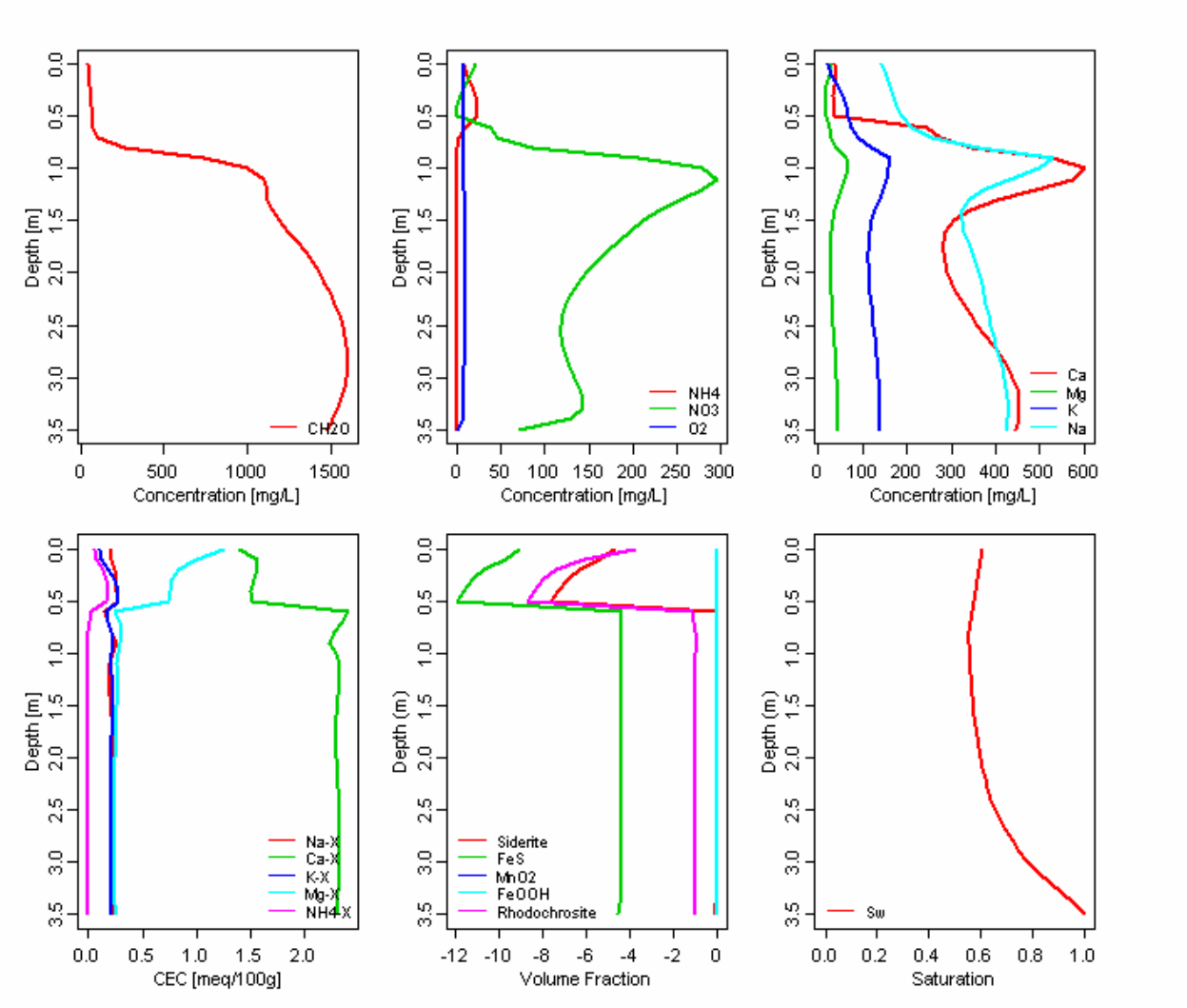

Table 13
POTW Mass Balance

	Surface Loading	Storage	Degassing	Biodegredation (Aqueous)	Biodegredation (Mineral)	Root Uptake	Precipitation	Adsorption	Water Table	Mass Error
CH_2O	8488	-273	0	-980	0	0	0	0	-7262	-26.01
	100%	-3%	0%	-12%	0%	0%	0%	0%	-86%	0%
NH_4	395	0	0	-330	0	-72	0	7	0	-0.77
	100%	0%	0%	-84%	0%	-18%	0%	2%	0%	-0.2%
NO_3	220	-26	0	1011	0	-360	0	0	-846	0.55
	100%	-12%	0%	459%	0%	-163%	0%	0%	-384%	0.2%
O_2	128	0	2030	-2137	0	0	0	0	-21	0.02
	100%	0%	1582%	-1666%	0%	0%	0%	0%	-17%	0.0%
K^+	864	-24	0	0	0	-128	0	-70	-645	-2.03
	100%	-3%	0%	0%	0%	-15%	0%	-8%	-75%	-0.2%
Ca^{2+}	735	-71	0	0	0	-75	1719	-244	-2065	-0.91
	100%	-10%	0%	0%	0%	-10%	234%	-33%	-281%	-0.1%
Mg^{2+}	342	-1	0	0	0	-95	0	170	-416	-0.07
	100%	0%	0%	0%	0%	-28%	0%	50%	-122%	0.0%
Na^+	2229	-51	0	0	0	0	0	-7	-2174	-2.38
	100%	-2%	0%	0%	0%	0%	0%	0%	-98%	-0.1%
Fe^{2+}	59	-2	0	0	0	0	-16	-6	-37	-1.29
	100%	-3%	0%	0%	0%	0%	-26%	-11%	-62%	-2.2%
Mn^{2+}	5	0	0	0	0	0	0	2	-8	0.00
	100%	-1%	0%	0%	0%	0%	0%	43%	-142%	0.1%
CO_3^{2-}	2974	-79	-3770	1959	15	323	2557	0	-3979	-0.24
	100%	-3%	-127%	66%	1%	11%	86%	0%	-134%	0.0%
SO_4^{2-}	557	-7	0	0	0	-45	0	0	-505	0.10
	100%	-1%	0%	0%	0%	-8%	0%	0%	-91%	0.0%
Cl-	2671	-76	0	0	0	0	0	0	-2600	-5.64
	100%	-3%	0%	0%	0%	0%	0%	0%	-97%	-0.2%
PO_4^{3-}	137	0	0	0	0	-127	0	0	-11	-0.31
	100%	0%	0%	0%	0%	-93%	0%	0%	-8%	-0.2%
FDS	11189	-337	-3770	2640	15	-579	4261	-147	-13285	-12.97
	100%	-3%	-34%	24%	0%	-5%	38%	-1%	-119%	-0.1%

Mass balance in pounds per acre per year and percent of total component loading.